frontiers | Research Topics

Mitochondrial plasticity and quality control in health and disease

Edited by
Milena Rizzo, Francesca Forini, Emilia Bramanti, Elena Levantini, Filippo M. Santorelli, Azhar Ali and Vincenzo Lionetti

Published in
Frontiers in Cell and Developmental Biology
Frontiers in Molecular Biosciences

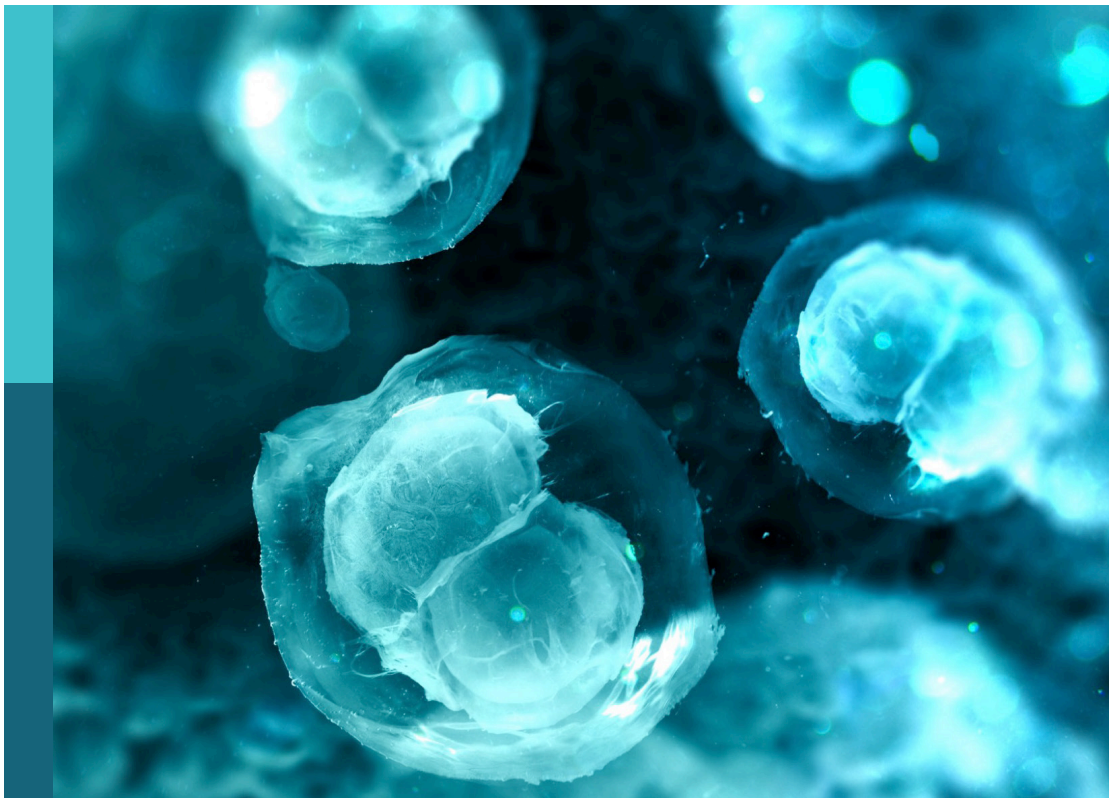

ISSN 1664-8714
ISBN 978-2-8325-5317-6
DOI 10.3389/978-2-8325-5317-6

About Frontiers

Frontiers is more than just an open access publisher of scholarly articles: it is a pioneering approach to the world of academia, radically improving the way scholarly research is managed. The grand vision of Frontiers is a world where all people have an equal opportunity to seek, share and generate knowledge. Frontiers provides immediate and permanent online open access to all its publications, but this alone is not enough to realize our grand goals.

Frontiers journal series

The Frontiers journal series is a multi-tier and interdisciplinary set of open-access, online journals, promising a paradigm shift from the current review, selection and dissemination processes in academic publishing. All Frontiers journals are driven by researchers for researchers; therefore, they constitute a service to the scholarly community. At the same time, the *Frontiers journal series* operates on a revolutionary invention, the tiered publishing system, initially addressing specific communities of scholars, and gradually climbing up to broader public understanding, thus serving the interests of the lay society, too.

Dedication to quality

Each Frontiers article is a landmark of the highest quality, thanks to genuinely collaborative interactions between authors and review editors, who include some of the world's best academicians. Research must be certified by peers before entering a stream of knowledge that may eventually reach the public - and shape society; therefore, Frontiers only applies the most rigorous and unbiased reviews. Frontiers revolutionizes research publishing by freely delivering the most outstanding research, evaluated with no bias from both the academic and social point of view. By applying the most advanced information technologies, Frontiers is catapulting scholarly publishing into a new generation.

What are Frontiers Research Topics?

Frontiers Research Topics are very popular trademarks of the *Frontiers journals series*: they are collections of at least ten articles, all centered on a particular subject. With their unique mix of varied contributions from Original Research to Review Articles, Frontiers Research Topics unify the most influential researchers, the latest key findings and historical advances in a hot research area.

Find out more on how to host your own Frontiers Research Topic or contribute to one as an author by contacting the Frontiers editorial office: frontiersin.org/about/contact

Mitochondrial plasticity and quality control in health and disease

Topic editors

Milena Rizzo — Institute of Clinical Physiology, National Research Council (CNR), Italy

Francesca Forini — Institute of Clinical Physiology, National Research Council (CNR), Italy

Emilia Bramanti — Institute of Chemistry of Organometallic Compounds, National Research Council (CNR), Italy

Elena Levantini — Pisa Research Area, National Research Council (CNR), Italy

Filippo M. Santorelli — Stella Maris Foundation (IRCCS), Italy

Azhar Ali — National University of Singapore, Singapore

Vincenzo Lionetti — Sant'Anna School of Advanced Studies, Italy

Citation

Rizzo, M., Forini, F., Bramanti, E., Levantini, E., Santorelli, F. M., Ali, A., Lionetti, V., eds. (2024). *Mitochondrial plasticity and quality control in health and disease*. Lausanne: Frontiers Media SA. doi: 10.3389/978-2-8325-5317-6

Table of contents

05 Editorial: Mitochondrial plasticity and quality control in health and disease
Francesca Forini, Elena Levantini, Emilia Bramanti, Filippo Maria Santorelli, Azhar Ali, Vincenzo Lionetti and Milena Rizzo

09 Investigation of FGF21 mRNA levels and relative mitochondrial DNA copy number levels and their relation in nonalcoholic fatty liver disease: a case-control study
Massoud Houshmand, Vahide Zeinali, Amirhossein Hosseini, Atena Seifi, Bardia Danaei and Sharareh Kamfar

18 Regulation of mitochondrial morphology and cristae architecture by the TLR4 pathway in human skeletal muscle
Mauricio Castro-Sepulveda, Mauro Tuñón-Suárez, Giovanni Rosales-Soto, Ronald Vargas-Foitzick, Louise Deldicque and Hermann Zbinden-Foncea

27 Targeting mitochondrial dynamics proteins for the treatment of doxorubicin-induced cardiotoxicity
Rui Chen, Mengwen Niu, Xin Hu and Yuquan He

46 The mitochondrial protein Sod2 is important for the migration, maintenance, and fitness of germ cells
Katsiaryna Tarbashevich, Laura Ermlich, Julian Wegner, Jana Pfeiffer and Erez Raz

58 Mesenchymal stromal/stem cells and bronchopulmonary dysplasia
Shuqing Zhang, Cassidy Mulder, Suzette Riddle, Rui Song and Dongmei Yue

71 Mitochondrial quality control in health and cardiovascular diseases
Asli E. Atici, Timothy R. Crother and Magali Noval Rivas

96 Cardioprotective effects of Moku-boi-to and its impact on AngII-induced cardiomyocyte hypertrophy
Hideaki Tagashira, Fumiha Abe, Kaori Sato-Numata, Karen Aizawa, Kei Hirasawa, Yoshinobu Kure, Daiki Iwata and Tomohiro Numata

113 Impact of platelet-derived mitochondria transfer in the metabolic profiling and progression of metastatic MDA-MB-231 human triple-negative breast cancer cells
Lucas Cereceda, J. Cesar Cardenas, Maroun Khoury, Eduardo Silva-Pavez and Yessia Hidalgo

127 The genetic landscape of mitochondrial diseases in the next-generation sequencing era: a Portuguese cohort study
C. Nogueira, C. Pereira, L. Silva, Mateus Laranjeira, A. Lopes, R. Neiva, E. Rodrigues, T. Campos, E. Martins, A. Bandeira, M. Coelho, M. Magalhães, J. Damásio, A. Gaspar, P Janeiro, A. Levy Gomes, A. C. Ferreira, S. Jacinto, J. P. Vieira, L. Diogo, H. Santos, C. Mendonça and L. Vilarinho

140 Mitochondrial stress response and myogenic differentiation
Fu Lin, Liankun Sun, Yu Zhang, Weinan Gao, Zihan Chen, Yanan Liu, Kai Tian, Xuyu Han, Ruize Liu, Yang Li and Luyan Shen

154 Spatial detection of mitochondrial DNA and RNA in tissues
Michelle Giarmarco, Jordan Seto, Daniel Brock and Susan Brockerhoff

frontiers | Frontiers in Cell and Developmental Biology

TYPE Editorial
PUBLISHED 02 August 2024
DOI 10.3389/fcell.2024.1468818

OPEN ACCESS

EDITED AND REVIEWED BY
Graça Soveral,
University of Lisbon, Portugal

*CORRESPONDENCE
Milena Rizzo,
milena.rizzo@cnr.it
Francesca Forini,
francesca.forini@cnr.it

RECEIVED 22 July 2024
ACCEPTED 24 July 2024
PUBLISHED 02 August 2024

CITATION
Forini F, Levantini E, Bramanti E, Santorelli FM, Ali A, Lionetti V and Rizzo M (2024), Editorial: Mitochondrial plasticity and quality control in health and disease.
Front. Cell Dev. Biol. 12:1468818.
doi: 10.3389/fcell.2024.1468818

Editorial: Mitochondrial plasticity and quality control in health and disease

Francesca Forini[1]*, Elena Levantini[2], Emilia Bramanti[3], Filippo Maria Santorelli[4], Azhar Ali[5], Vincenzo Lionetti[6,7] and Milena Rizzo[1]*

[1]Institute of Clinical Physiology (IFC), National Research Council (CNR), Pisa, Italy, [2]Institute of Biomedical Technologies (ITB), National Research Council (CNR), Pisa, Italy, [3]Institute of Chemistry of Organometallic Compounds (ICCOM), National Research Council (CNR), Pisa, Italy, [4]Molecular Medicine & Neurobiology, IRCCS Fondazione Stella Maris, Pisa, Italy, [5]Cancer Science Institute Singapore, Singapore, Singapore, [6]Interdisciplinary Research Center "Health Science", Scuola Superiore Sant'Anna, Pisa, Italy, [7]UOSVD Anesthesia and Resuscitation, Pisa, Italy

KEYWORDS

mitochondria quality control, mitochondrial genome, mitochondrial disorders, mitochondrial dysfunction in pathologies, mitochondria in development and differentiation

Editorial on the Research Topic
Mitochondrial plasticity and quality control in health and disease

1 Introduction

Mitochondria play a multifaceted role in cellular physiology extending from the regulation of energy production and cell metabolism to calcium buffering and the modulation of intracellular signaling. Given that mitochondrial dysfunctions are involved in a spectrum of complex human pathologies and inheritable disorders, preserving a functional mitochondrial network is crucial for health and disease status and it has become a focal point of innovative therapeutic strategies.

This Research Topic compiles articles focused on two primary areas of mitochondrial research: i) the investigation of mitochondrial dysfunction in various pathological conditions (including mitochondrial diseases) and the exploration of therapeutic interventions that target and/or exploit mitochondria; and ii) the elucidation of the crucial role of mitochondria in development and differentiation. Finally, this issue introduces a novel methodology that employs commercially available tools for the quantification of mitochondrial DNA and RNA within intact and complex tissues.

2 Mitochondrial disfunction in pathological conditions

2.1 Cardiovascular diseases

Preservation of mitochondrial homeostasis through mitochondrial quality control (MQC) is fundamental for organs with high energy demands, such as the heart. The

comprehensive review by Atici et al. underscores the significance of MQC in the context of cardiovascular physiology and various disease states, including myocardial ischemia-reperfusion injury, atherosclerosis, heart failure (HF), cardiac hypertrophy (CH), hypertension, and both diabetic and genetic cardiomyopathies, as well as Kawasaki Disease. Enhancing mitochondrial function holds promise for mitigating tissue remodeling, preventing the onset of cardiovascular disease, regenerating the myocardium and potentially extending lifespan. Cardioprotection might be achieved through the application of either synthetic or natural mitochondria-targeted compounds that promote balanced mitochondrial fusion and fission, mitophagy, bioenergetics, ROS detoxification, replenishment of the mitochondria pool, and enhancement of inter-organelle communication.

Among the natural compounds, Moku-boi-to (MBT), a Japanese medical herbal concoction, has demonstrated promising protective effects in both *in vivo* and *in vitro* models of CH by restoring mitochondrial dynamics (Tagashira et al.). Altered mitochondrial fragmentation, which leads to excessive mitophagy and decreased ATP production, thus favoring ROS generation, can be addressed by MBT treatment (Quiles and Gustafsson, 2022; Yang et al., 2022). The authors demonstrated that in a mouse model of HF, MBT treatment improved heart contractility and mitigated CH (Tagashira et al.). Mechanistically, MBT prevents the accumulation of the mitochondrial pro-fission protein Dynamin 1 Like (DRP1) and the resultant mitochondrial fragmentation induced by hypertrophic stimuli, while concurrently reducing mitochondrial dysfunction, ROS production, intracellular Ca^{2+} dysregulation, and cell death.

The dynamic balance of mitochondrial fission and fusion ensures a prompt adaptation to the cell's rapidly changing metabolic demands (Tilokani et al., 2018). Metabolic reprogramming, favoring glucose utilization over fatty acid oxidation, is a hallmark of both heart disease and malignant cell growth, shapes the epigenetic landscape of cardiomyocytes enabling heart regeneration (Li et al., 2023) and making mitochondria strategic targets in the cardio-oncology field (Karlstaedt et al., 2022). In a comprehensive review, Chen et al. provide insights into the complex processes that involve mitochondrial impairments in doxorubicin (DOX)-induced cardiotoxicity, with an emphasis on the metabolic consequences. Rebalancing mitochondrial dynamics by inhibiting DRP1-mediated mitochondrial fission and enhancing Mitofusin 2 (MFN2)-mediated mitochondrial fusion, could promote chromatin reconfiguration that is correlated to the shift in cellular energy metabolism from glycolysis to fatty acid oxidation with maintenance of oxidative phosphorylation. This dual-action has the potential to decrease the cardiac adverse effects of DOX, while enhancing its anti-cancer efficacy.

2.2 Metabolic diseases

In the skeletal muscle (SkM), a reduction in the elongated mitochondrial phenotype, indicative of dysregulated mitochondrial dynamics, is a feature of metabolic disorders such as type 2 diabetes mellitus (T2DM). Using SkM biopsies from T2DM patients, Castro-Sepulveda et al. showed that the activation of toll-like receptor 4 (TLR4), a mediator of both infectious and non-infectious inflammatory diseases (Wei et al., 2023), contributes to significant changes in mitochondrial morphology and cristae density. This effect is mediated by a reduction in the levels of the pro-fusion protein Mitochondrial Dynamin like GTPase (Opa1). Given the critical role of SkM in the pathophysiology of T2DM (DeFronzo, 2009), this mitochondrial-related signaling cascade may contribute to insulin resistance in T2DM thus exacerbating hyperglycemia-induced multiple organ failure.

Non-alcoholic fatty liver disease (NAFLD) represents another metabolic condition where mitochondrial remodeling plays a key role (Zheng et al., 2023). A recent observational case-control study highlighted that NAFLD patients (Houshmand et al.) present with an increased hepatic mitochondrial DNA copy number, a surrogate marker of mitochondrial functionality (Castellani et al., 2020). This finding correlated with increased expression of Fibroblast Growth Factor 21 (FGF21), a regulator of glucose and lipid metabolism, energy homeostasis, and insulin sensitivity (Cuevas-Ramos et al., 2009). These findings suggest an adaptive response aimed at increasing the liver's capacity to metabolize fat. However, this compensatory response may ultimately turn detrimental by causing uncontrolled oxidative stress and progressive mitochondrial dysfunction.

2.3 Mitochondrial diseases

Mitochondrial dysfunctions are not only confined to complex-diseases; they can also arise from pathological variants in genes crucial for mitochondrial function and MQC. Given the genetic heterogeneity of mitochondrial disorders (MDs) and the current lack of effective therapeutic options, establishing a precise genetic diagnosis can significantly enhance our understanding of the disease. This, in turn, may lead to an improved ability to manage it.

The innovative use of next-generation sequencing (NGS) approaches, coupled with comprehensive analysis of the entire mitochondrial genome, as demonstrated by Nogueira et al., 2024 helped achieve genetic diagnoses across a wide demographic, encompassing both pediatric and adult cases. Notably, variants in mtDNA are predominantly associated with adult-onset MDs, while nuclear DNA variants are more frequently linked to early-onset forms of MDs.

2.4 Intercellular mitochondrial transfer in pathology and therapy

Mitochondrial transfer has been recently recognized as a crucial process for MCQ (Liu et al., 2023) and has emerged as a novel therapeutic approach in disease treatment (Clemente-Suárez et al., 2023). In their seminal review, Zhang et al., explored the role of mesenchymal stromal/stem cells (MSCs) in pulmonary development and their dysfunction's contribution to bronchopulmonary dysplasia (BPD). The review focuses on the efficacy of MSC therapy in treating BPD, a condition linked to defects in mitochondrial structure, dynamics, and oxidative metabolism. MSC treatment has been shown to decrease

mitochondrial dysfunction by i) stimulating mitochondrial replication in injured lung cells and by ii) restoring mitochondrial function through the direct transfer of healthy mitochondria from MSCs to the damaged primary cells of the lung. It is conceivable that tissue repair is mediated by mitochondria transferred from MSC-derived cells, similar to the observations obtained following transplantation of mitochondria-rich extracellular vesicles in the heart (Ikeda et al., 2021).

However, mitochondrial transfer can promote adverse effects favoring pathological conditions. For instance, Cereceda et al. suggested that the uptake of platelet-derived mitochondria by triple-negative breast cancer cell lines increases mitochondrial respiration, ATP production, cell proliferation, and metabolic adaptability. This enhancement in cellular functions may contribute to tumor progression, underscoring the multifaceted nature of mitochondrial transfer in the context of diseases.

3 Mitochondrial function in differentiation and development

Myogenic differentiation, a key step in skeletal muscle regeneration, is characterized by significant changes in both the quantity and functionality of mitochondria to meet the increased energy demand. Throughout this process, transient and mild cellular stress triggers a variety of mitochondrial response pathways, collectively termed mitochondrial stress responses (MSRs), which favor cellular homeostasis. The review by Lin et al., described MSRs and their involvement in the regulation of physiological myogenic differentiation, providing new perspectives into potential treatments for muscle diseases associated to impaired myogenic differentiation.

Superoxide dismutase 2 (Sod2) is a key mitochondrial enzyme involved in MSR, which plays a primary role in ROS detoxification. Tarbashevich et al., using zebrafish models, demonstrated that Sod2 is also involved in the "purifying selection" of primordial germ cells (PGMs). Such process safeguards mitochondrial integrity across generations, ensuring the propagation of mtDNA devoid of deleterious mutations (Schwartz et al., 2022). Results by Tarbashevich et al. suggest that PGCs deficient in Sod2 are less competitive in generating gametes compared to their wild-type counterparts, due to the selective disadvantage imposed by higher levels of ROS-induced damage.

4 Genome quantitation

Finally, Giarmarco et al. introduced a new method for the spatial quantification of both mtDNA and mtRNA within fixed frozen tissue sections. This method employs a dual-probe strategy that combines RNAscope™ *in situ* hybridization (ISH) with immunohistochemistry (IHC) for precise labeling of mitochondria. Such a technique could prove to accurately quantify mtDNA copy numbers and expression levels, while preserving the integrity of cell morphology within its native microenvironment. The authors applied this methodology in a complex tissue like the retina, with the aim to evaluate circadian variations in mtDNA and mtRNA levels in zebrafish cone and rod photoreceptors, at an individual cells' resolution.

5 Conclusion

Mitochondria are metabolic hubs, essential for cellular homeostasis, whose dysregulation is associated with a broad range of diseases. Targeting mitochondria is therefore an attractive strategy, and precision medicine based on mitochondria is emerging as a rapidly evolving field. The multi-layered research presented in this Research Topic emphasizes the crucial impact of this organelle in both health and disease. The studies highlight our increased understanding of mitochondrial dynamics within their cellular milieu and suggest the feasibility of targeting mitochondrial dysfunctions as a viable strategy for a range of pathologies, from cardiovascular diseases to metabolic disorders. Additionally, advancements in genetic diagnostics promise to refine our ability to manage mitochondrial disorders more effectively. Last, the exploration of mitochondrial transfer as a therapeutic intervention will require careful consideration of its dichotomous effects, offering benefits in regenerative medicine while posing challenges in cancer treatment. We anticipate a future where mitochondrial parameters emerge as pivotal biomarkers and therapeutic targets. The insights gained from these studies will inform the next-generation of mitochondrial researchers, propelling us towards more precise interventions.

Author contributions

FF: Conceptualization, Writing–original draft, Writing–review and editing. EL: Writing–original draft, Writing–review and editing. EB: Writing–review and editing. FS: Writing–review and editing. AA: Writing–review and editing. VL: Writing–review and editing. MR: Conceptualization, Writing–original draft, Writing–review and editing.

Funding

The author(s) declare that no financial support was received for the research, authorship, and/or publication of this article.

Acknowledgments

FF acknowledges the Italian Ministry of Health, PRIN 2022-LANTERN, protocol n° 20227LC4SK; EL acknowledges AIRC Investigator Grant 2021 ID 25734; FS acknowledges the Italian Ministry of Health "Ricerca Corrente 2023" and "Ricerca Corrente 5X1000"; VL acknowledges PRIN 2022–EXTREMEHEART, European Union–Next Generation EU; MR acknowledges Fondazione Pisa project number 309/22.

Conflict of interest

The authors declare that the research was conducted in the absence of any commercial or financial relationships that could be construed as a potential conflict of interest.

The author(s) declared that they were an editorial board member of Frontiers, at the time of submission. This had no impact on the peer review process and the final decision.

Publisher's note

References

Castellani, C. A., Longchamps, R. J., Sun, J., Guallar, E., and Arking, D. E. (2020). Thinking outside the nucleus: mitochondrial DNA copy number in health and disease. *Mitochondrion* 53, 214–223. doi:10.1016/j.mito.2020.06.004

Clemente-Suárez, V. J., Martín-Rodríguez, A., Yáñez-Sepúlveda, R., and Tornero-Aguilera, J. F. (2023). Mitochondrial transfer as a novel therapeutic approach in disease diagnosis and treatment. *Int. J. Mol. Sci.* 24, 8848. doi:10.3390/ijms24108848

Cuevas-Ramos, D., Almeda-Valdes, P., Aguilar-Salinas, C., Cuevas-Ramos, G., Cuevas-Sosa, A., and Gomez-Perez, F. (2009). The role of Fibroblast growth factor 21 (FGF21) on energy balance, glucose and lipid metabolism. *Curr. Diabetes Rev.* 5, 216–220. doi:10.2174/157339909789804396

DeFronzo, R. A. (2009). Banting Lecture. From the triumvirate to the ominous octet: a new paradigm for the treatment of type 2 diabetes mellitus. *Diabetes* 58, 773–795. doi:10.2337/db09-9028

Ikeda, G., Santoso, M. R., Tada, Y., Li, A. M., Vaskova, E., Jung, J.-H., et al. (2021). Mitochondria-rich extracellular vesicles from autologous stem cell-derived cardiomyocytes restore energetics of ischemic myocardium. *J. Am. Coll. Cardiol.* 77, 1073–1088. doi:10.1016/j.jacc.2020.12.060

Karlstaedt, A., Moslehi, J., and de Boer, R. A. (2022). Cardio-onco-metabolism: metabolic remodelling in cardiovascular disease and cancer. *Nat. Rev. Cardiol.* 19, 414–425. doi:10.1038/s41569-022-00698-6

Li, X., Wu, F., Günther, S., Looso, M., Kuenne, C., Zhang, T., et al. (2023). Inhibition of fatty acid oxidation enables heart regeneration in adult mice. *Nature* 622, 619–626. doi:10.1038/s41586-023-06585-5

Liu, Y., Fu, T., Li, G., Li, B., Luo, G., Li, N., et al. (2023). Mitochondrial transfer between cell crosstalk - an emerging role in mitochondrial quality control. *Ageing Res. Rev.* 91, 102038. doi:10.1016/j.arr.2023.102038

Nogueira, C., Pereira, C., Silva, L., Laranjeira, M., Lopes, A., Neiva, R., et al. (2024). The genetic landscape of mitochondrial diseases in the next-generation sequencing era: a Portuguese cohort study. *Front. Cell Dev. Biol.* 12, 1331351. doi:10.3389/fcell.2024.1331351

Quiles, J. M., and Gustafsson, Å. B. (2022). The role of mitochondrial fission in cardiovascular health and disease. *Nat. Rev. Cardiol.* 19, 723–736. doi:10.1038/s41569-022-00703-y

Schwartz, A. Z. A., Tsyba, N., Abdu, Y., Patel, M. R., and Nance, J. (2022). Independent regulation of mitochondrial DNA quantity and quality in *Caenorhabditis elegans* primordial germ cells. *Elife* 11, e80396. doi:10.7554/eLife.80396

Tilokani, L., Nagashima, S., Paupe, V., and Prudent, J. (2018). Mitochondrial dynamics: overview of molecular mechanisms. *Essays Biochem.* 62, 341–360. doi:10.1042/EBC20170104

Wei, J., Zhang, Y., Li, H., Wang, F., and Yao, S. (2023). Toll-like receptor 4: a potential therapeutic target for multiple human diseases. *Biomed. Pharmacother.* 166, 115338. doi:10.1016/j.biopha.2023.115338

Yang, D., Liu, H.-Q., Liu, F.-Y., Guo, Z., An, P., Wang, M.-Y., et al. (2022). Mitochondria in pathological cardiac hypertrophy research and therapy. *Front. Cardiovasc Med.* 8, 822969. doi:10.3389/fcvm.2021.822969

Zheng, Y., Wang, S., Wu, J., and Wang, Y. (2023). Mitochondrial metabolic dysfunction and non-alcoholic fatty liver disease: new insights from pathogenic mechanisms to clinically targeted therapy. *J. Transl. Med.* 21, 510. doi:10.1186/s12967-023-04367-1

frontiers | Frontiers in Molecular Biosciences

TYPE Original Research
PUBLISHED 06 June 2023
DOI 10.3389/fmolb.2023.1203019

OPEN ACCESS

EDITED BY
Filippo M. Santorelli,
Stella Maris Foundation (IRCCS), Italy

REVIEWED BY
Jogendra Singh Pawar,
The Ohio State University, United States
Vaibhav Deshmukh,
Washington University in St. Louis, United States
Rosalba Carrozzo,
Bambino Gesù Children's Hospital (IRCCS), Italy

*CORRESPONDENCE
Sharareh Kamfar,
kamfarshareareh@gmail.com

RECEIVED 10 April 2023
ACCEPTED 22 May 2023
PUBLISHED 06 June 2023

CITATION
Houshmand M, Zeinali V, Hosseini A, Seifi A, Danaei B and Kamfar S (2023), Investigation of FGF21 mRNA levels and relative mitochondrial DNA copy number levels and their relation in nonalcoholic fatty liver disease: a case-control study. *Front. Mol. Biosci.* 10:1203019. doi: 10.3389/fmolb.2023.1203019

Investigation of FGF21 mRNA levels and relative mitochondrial DNA copy number levels and their relation in nonalcoholic fatty liver disease: a case-control study

Massoud Houshmand[1], Vahide Zeinali[2], Amirhossein Hosseini[3], Atena Seifi[4], Bardia Danaei[5] and Sharareh Kamfar[6]*

[1]Department of Medical Genetics, National Institute for Genetic Engineering and Biotechnology, Tehran, Iran, [2]Research Institute for Children's Health, Shahid Beheshti University of Medical Sciences, Tehran, Iran, [3]Pediatric Gastroenterology, Hepatology, and Nutrition Research Center, Research Institute for Children's Health, Shahid Beheshti University of Medical Sciences, Tehran, Iran, [4]Pediatric Nephrology Research Center, Research Institute for Children's Health, Shahid Beheshti University of Medical Science, Tehran, Iran, [5]Department of Microbiology, School of Medicine, Shahid Beheshti University of Medical Sciences, Tehran, Iran, [6]Pediatric Congenital Hematologic Disorders Research Center, Research Institute for Children's Health, Shahid Beheshti University of Medical Sciences, Tehran, Iran

Background: Although the exact mechanisms of nonalcoholic fatty liver disease (NAFLD) are not fully understood, numerous pieces of evidence show that the variations in mitochondrial DNA (mtDNA) level and hepatic Fibroblast growth factor 21 (FGF21) expression may be related to NAFLD susceptibility.

Objectives: The main objective of this study was to determine relative levels of mtDNA copy number and hepatic FGF21 expression in a cohort of Iranian NAFLD patients and evaluate the possible relationship.

Methods: This study included 27 NAFLD patients (10 with nonalcoholic fatty liver (NAFL) and 17 with non-alcoholic steatohepatitis (NASH)) and ten healthy subjects. Total RNA and genomic DNA were extracted from liver tissue samples, and then mtDNA copy number and FGF21 expression levels were assessed by quantitative real-time PCR.

Results: The relative level of hepatic mtDNA copy number was 3.9-fold higher in patients than in controls ($p < 0.0001$). NAFLD patients showed a 2.9-fold increase in hepatic FGF21 expression compared to controls ($p < 0.013$). Results showed that hepatic FGF21 expression was positively correlated with BMI, serum ALT, and AST levels ($p < 0.05$). The level of mitochondrial copy number and hepatic FGF21 expression was not significantly associated with stages of change in hepatic steatosis. Finally, there was a significant correlation between FGF21 expression and mitochondrial copy number in NAFLD patients ($p = 0.027$).

Conclusion: Our findings suggest a considerable rise of hepatic FGF21 mRNA levels and mtDNA-CN and show a positive correlation between them in the liver tissue of NAFLD patients.

KEYWORDS

fibroblast growth factor 21, mitochondrial DNA, nonalcoholic fatty liver disease, FGF21, NAFLD

Introduction

Chronic liver diseases are rapidly growing as health priorities globally. Fatty liver disease can occur in the setting of both nonalcoholic fatty liver disease (NAFLD) and alcoholic liver disease (ALD) (Toshikuni et al., 2014). NAFLD is among the most prevalent chronic liver disorders worldwide, with a pooled global prevalence of 25.24% and over the past 2 decades there has been a steady increase in its incidence across many populations. (Mitra et al., 2020). NAFLD is characterized by steatosis affecting more than 5% of hepatocytes in individuals who do not consume excessive amounts of alcohol, do not have other liver diseases, and do not take steatogenic drugs. The histological spectrum of NAFLD comprises nonalcoholic fatty liver (NAFL), which involves steatosis without hepatocellular injury, and steatohepatitis (NASH), which involves inflammation and hepatocyte ballooning degeneration in addition to steatosis. Patients with NAFLD can progress to fibrosis, and ultimately, cirrhosis (Chalasani et al., 2012; Younossi et al., 2018). Patients with cirrhosis are at risk of potentially life-threatening liver-related complications such as portal hypertension, hepatic failure, and hepatocellular carcinoma (Ascha et al., 2010; Bhala et al., 2011; Nusrat et al., 2014). Knowledge about the mechanisms that are potentially involved in the pathogenesis of NAFLD is still incomplete. However, new evidence suggests that the pathogenesis of NAFLD involves complex mechanisms collectively referred to as the "multiple parallel hits hypothesis". This theory proposes that multiple components act in parallel to contribute to the development of NAFLD, rather than in a linear series (Lonardo et al., 2017; Caturano et al., 2021). According to this theory, these factors are believed to play role in the development of NAFLD: insulin resistance (IR), genetic and epigenetic factors, mitochondrial dysfunction, endoplasmic reticulum stress, microbiota, chronic low-grade inflammation, and dysfunction of adipose tissue (Acierno et al., 2020).

The pathogenesis of NAFLD is impacted by changes in the mitochondria, such as mitochondrial DNA depletion, as well as modifications in the beta-oxidation and respiratory chain functions. (Pessayre and Fromenty, 2005). If mitochondrial and peroxisomal functions are unable to handle the increased lipid flow, it can cause respiratory oxidation to collapse, leading to disruption in lipid balance, production of harmful metabolites, and an excess of reactive oxygen species (ROS) (Begriche et al., 2006; Wang et al., 2020). These events contribute to oxidative stress, hepatic necro-inflammatory processes, and worsening of mitochondrial damage. In fact, it has been proven that mitochondrial dysfunction is directly associated with IR, obesity, and the release of pro-inflammatory cytokines levels like tumor necrosis factor-alpha (TNF-α) (Paradies et al., 2014). Furthermore, ROS and oxidized low-density lipoprotein (LDL) cholesterol particles can activate Kupffer and hepatic stellate cells, leading to the deposition of collagen and the progression of liver fibrosis (Cusi, 2009).

In addition, endoplasmic reticulum (ER) malfunction probably leads to accumulation of unfolded proteins inside the ER, increased protein synthesis, reduction of Adenosine triphosphate (ATP), and activation of the unfolded protein response (UPR). UPR is a compensatory response to decrease protein synthesis, increase protein trafficking capacity through the ER, and increase protein degradative pathways (Wang and Kaufman, 2014). UPR failure to solve the protein-folding defect, may induce hepatocytes apoptosis.

Based on the mentioned multi-hit hypothesis, and factors like ATP deficiency, increased lipid flow, and dysfunction of beta-oxidation which are directly linked to mitochondria, several studies have suggested that NAFLD might be a mitochondrial disease (Begriche et al., 2006; Dornas and Schuppan, 2020; Xu et al., 2021). This condition leads to mitochondrial damage and mitochondrial DNA copy number (mtDNA-CN) variations in hepatocytes (Pirola et al., 2015; Kamfar et al., 2016).

Circulating fibroblast growth factor 21 (FGF21), a member of the FGF family, is predominantly liver-derived and is involved in the hormonal regulation of glucose and lipid metabolism, energy homeostasis, insulin sensitivity, and other metabolic functions (Cuevas-Ramos et al., 2009). Numerous preclinical and clinical evidence suggested that aberrant FGF21 signaling may play a role in the pathogenesis and progression of NAFLD (Liu et al., 2015; Rusli et al., 2016; Tucker et al., 2019). Both FGF21 serum levels and FGF21 expression were discussed to be indicators of NAFLD (Falamarzi et al., 2022). It has been shown that FGF21 stimulates lipolysis by decreasing fat stores leading to reducing hepatic steatosis and lipotoxicity (Xu et al., 2009; Tanaka et al., 2015; Bao et al., 2018). Moreover, several studies have also reported that FGF21 reduces oxidative stress and endoplasmic reticulum stress (Ye et al., 2014; Boparai et al., 2015) and enhances mitochondrial function (Lee et al., 2016).

In this observational case-control study, considering the role of FGF21 and mitochondria in NAFLD pathogenesis, our first aim was to assess FGF21 expression and mtDNA-CN in Iranian NAFLD patients in different stages of the disease and compare those to healthy control group. Our second objective was to investigate the possible relation between the levels of FGF21 expression and mtDNA-CN in liver samples from Iranian NAFLD patients.

Methods

Study population

Over one and a half years, this study was carried out on NAFLD patients identified from a sub-specialist tertiary NAFLD clinic at the Khatam Ol-Anbia Hospital, Tehran, Iran. Participants were selected based on liver ultrasonography, clinical, and laboratory findings. Patients with other liver problems, cancer, family history of diabetes, history of alcohol drinking, viral hepatitis (B or C), steatogenic medications, and glucocorticoid therapy were carefully excluded. Control group consisted of healthy volunteers who did not have any history of liver and metabolic related disorders. A liver needle biopsy was used to obtain liver samples. two to three samples were obtained from each participant which were used for histological assessment and nucleic acid extraction. Relevant clinical and laboratory data were collected from the time of liver biopsy. Patients with NAFLD were classified into NAFL and NASH based on the histologic findings and were approved by at least two pathologists. The same method was used for control group classification and individuals with pathologic findings in their samples were excluded from the control group. The medical ethics committee

approved the Protocol of Hamadan University of Medical Sciences (P/16/35/9/3481), and all the participants signed Written Informed Consent before participating in this research study. The study protocol conformed to the ethical guidelines of the World Medical Association Declaration of Helsinki.

Anthropometric assessment and results of biochemical analysis

Relevant clinical details such as age, gender, weight, and height were obtained from all patients at the time of liver biopsy. The body mass index (BMI) was calculated by the formula: weight (kg)/height^2 (m^2). Blood tests taken at the time of liver biopsy were used to determine related paraclinical parameters. An automated enzymatic procedure assayed with alanine transaminase (ALT), aspartate transaminase (AST), cholesterol, triglyceride, HDL cholesterol, and fasting blood glucose (FBS) levels. The Friedewald formula was used for calculation of LDL-cholesterol levels.

Histological assessment

Percutaneous liver biopsies were performed using a Menghini needle. Liver biopsies were all >15 mm in length and were read by two experienced hepatopathologists. And any disagreement was resolved with discussion between them. "NASH" was defined as steatosis with hepatocyte ballooning degeneration and inflammation with or without fibrosis (Yeh and Brunt, 2014). "NAFL" was defined as steatosis only, or steatosis with mild inflammation without hepatocyte ballooning degeneration.

DNA/RNA extraction

Genomic DNA and total RNA were extracted simultaneously from fresh liver samples using the AllPrep DNA/RNA Micro (Qiagen, Dubai, United Arab Emirates). According to the manufacturer's instructions, hepatic tissue samples were first lysed and homogenized in a buffer for inhibition of DNases and RNases to obtain intact DNA and RNA. The lysate was passed through an AllPrep DNA spin column to selectively and efficiently isolate DNA. The column was then washed and DNA was eluted. Ethanol was added to the flow-through from the AllPrep DNA spin column to allow proper binding conditions for RNA, and the sample was then applied to RNeasy MinElute spin column, where total RNA binds into the membrane and contaminants were effectively washed away. Finally, RNA was then eluted in water.

Mitochondrial DNA copy number

Quantification of mtDNA-CN was assessed using quantitative real-time PCR (qPCR). According to the manufacturer's Protocol, this assay was carried out using the SYBR master mix (Real qPCR 2x Mix, Amplicon, Wrocław, Poland). Amplification was done with two pair primers: ONP86/ONP89 and B-actin (Shakhssalim et al., 2013; Kamfar et al., 2016; Zabihi Diba et al., 2016). The first set of primers (86/89) was used to amplify a normal fragment in mtDNA, and the second set (B-actin) was used as an internal control for nucleic DNA. Primer-BLAST was used to check the primer specificity (Ye et al., 2012). The amplification was done for 40 cycles using the following conditions: 95°C for 15 min, then 95°C for 30 s, and 58°C for 1 min. All samples were run in triplicate. Relative levels of mtDNA-CN were measured by using the $2^{-\Delta\Delta CT}$ method (Jensen, 2012).

Hepatic mRNA expression of FGF21

RNA isolated from liver biopsy was reverse transcripted using the cDNA Synthesis Kit (Thermo Fisher Scientific, Waltham, MA, United States of America) and the obtained cDNA was used as template in the qPCR reaction. According to the manufacturer's Protocol, the quantitative real-time PCR assay was carried out using specific primers in a 20 µL reaction volume containing SYBR Green master mix (Real QPCR 2x Mix, Amplicon, Wrocław, Poland). Each reaction was run in duplicate, and the accuracy of qPCR product size was confirmed by gel electrophoresis. Two primer pairs were designed to analyze FGF21 and B-actin as housekeeping genes (Table 1).

Statistical analysis

Analyses were performed using SPSS 18.0 software package (SPSS Inc., United States). Data were presented as means ± standard deviation (SD). The student's t-test was used for comparing normally distributed variables. Logistic regression was used to adjust for age, BMI, and lipid level confounders. Pearson correlation coefficient was carried out to describe the relationship of FGF21 expression and mtDNA-CN with variables related to NAFLD. In all statistical tests, $p < 0.05$ was regarded as statistically significant.

Results

Baseline characteristics of participants, including 27 patients with NAFLD (17 NASH, 10 NAFL) and ten healthy control subjects, are presented in Table2. The mean TG, ALT, AST, and BMI in NAFLD patients were significantly higher than in the control group ($p < 0.05$). No statistically significant difference was found in the other parameters between these two groups. According to the results, we observed a 3.9-fold increase in relative mtDNA-CN in the livers of NAFLD patients compared to healthy controls ($p < 0.0001$) (Figure1). A comparison of mtDNA-CN showed a 4.3 ($p < 0.008$) and 3.5-fold ($p < 0.013$) increase in patients with NAFL and NASH compared to control subjects, respectively. No substantial differences were observed in mtDNA-CN between the NAFL and NASH patients ($p < 0.615$) (Supplementary Table S1). No relation was observed after adjustment for age and BMI between mtDNA-CN and variables such as lipid levels and blood pressure ($p > 0.05$). In addition, no significant association was found between mtDNA-CN and age ($p > 0.05$) (Supplementary Table S2).

TABLE 1 Sequences of primers used for quantitative real-time PCR.

B-actin	Forward	5′- AGACGCAGGATGGCATGGG-3′	161bp	P60709	Accession number
	Reverse	5′- GAGACCTTCAACACCCCAGCC-3			
FGF21	Forward	5′-TCAAGACATCCAGGTTCC-3′	109 bp	Q9NSA1	
	Reverse	5′-TATCCGTCCTCAAGAAGC-3′			

TABLE 2 Anthropometrics parameters and biochemical indexes among control and NAFLD group.

Parameter	NAFLD (n = 27)	Control (n = 10)	P value[a]
Gender (Male/Female)	(11/16)	(2/8)	0.440
Age (year)	43.19 ± 9.60	38.00 ± 8.96	0.143
Body Mass Index (kg/m2)	44.21 ± 9.90	26.90 ± 2.56	<0.001[a]
Systolic blood pressure (mmHg)	120.37 ± 10.37	115.0 ± 7.07	0.141
Diastolic blood pressure (mmHg)	75.07 ± 5.99	74.00 ± 5.16	0.620
LDL-Cholesterol (mmol/L)	100.14 ± 32.59	110.50 ± 24.36	0.381
HDL-Cholesterol (mmol/L)	46.04 ± 9.70	54.80 ± 6.07	0.012
Triglycerides (mmol/L)	193.0 ± 80.27	129.8 ± 36.13	0.023[a]
Total Cholesterol (mmol/L)	187.85 ± 29.87	188.3 ± 28.04	0.967
FBS (mmol/L)	112.30 ± 28.94	115.1 ± 34.72	0.806
ALT (U/L)	38.65 ± 23.72	16.00 ± 3.80	<0.001[a]
AST (U/L)	25.68 ± 12.24	17.30 ± 1.57	0.002[a]
ALP (U/L)	189.74 ± 65.38	175.50 ± 34.86	0.519

p values were computed by t-test.
Abbreviations: FBS: fasting blood glucose; HDL: high-density lipoprotein; LDL: low-density lipoprotein; ALT: Alanine transaminase, AST: Aspartate Aminotransferase, ALP: Alkaline Phosphatase Test.
[a]Statistically significant.
[b]Values are presented as mean±SD, or median (interquartile range).

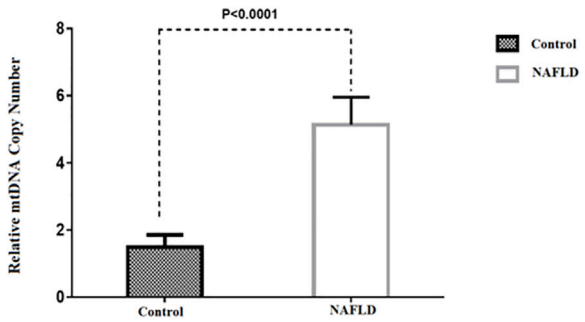

FIGURE 1
Comparison of the relative mtDNA copy number between NAFLD and control group. *p-value was computed t-test and data are shown as Mean ± SEM.

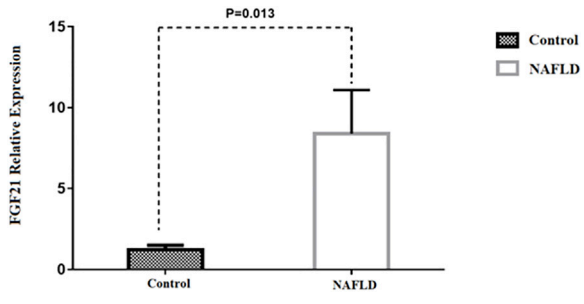

FIGURE 2
Comparison of the FGF21 relative expression between NAFLD and control group. *p-value was computed by t-test and data are shown as Mean ± SEM.

Our findings also indicated that FGF21 expression in hepatic tissue was 2.9-fold higher in patients with NAFLD than in control subjects (p = 0.013) (Figure 2). No significant difference was observed between patients with NAFL and NASH (p = 0.843) (Supplementary Table S1). Our results also showed a positive correlation between FGF21 expression and BMI (p = 0.035), AST (p = 0.02), and ALT (p < 0.01) levels (Supplementary Table S2). We found no sex difference in the expression of FGF21 between NAFL and NASH groups (p > 0.05). In addition, there was no significant relation between FGF21 expression and other anthropometric and

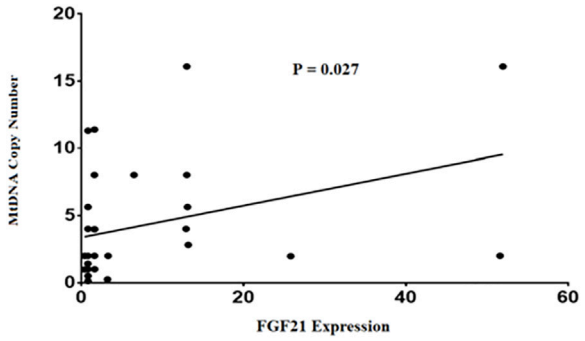

FIGURE 3
Comparison of the relative mtDNA copy number and FGF21 expression in NAFLD patients.

biochemical measurements after adjusting for age and BMI in these groups.

Finally, our findings in this study demonstrated a positive correlation between mtDNA-CN and FGF21expression levels in NAFLD patients ($p = 0.027$) (Figure 3). This comparison remained statistically significant after adjusting for age and BMI ($p = 0.035$).

Discussion

Recent studies have shown that NAFLD can be classified as a mitochondrial disease, in fact mitochondrial malfunction leads to abnormal hepatic fatty acid oxidation causing fat accumulation and hepatic steatosis. In addition to that, such mitochondria produce more ROS and less ATPs which cause more damages to mitochondria and hepatic cells making a destructive cycle (Koroglu et al., 2016; Dornas and Schuppan, 2020; Dabravolski et al., 2021). Thus, measuring relative mtDNA-CN as determining factor for mitochondrial damage and activity rate can be helpful for identifying the stage and prognosis of the disease (Cao et al., 2020; Filograna et al., 2021). On the other hand, in some stages of different mitochondrial disorders mtDNA-CN can be within the normal range and its changes should be interpreted along with clinical, histological, and other laboratory findings (Mavraki et al., 2023). However, despite its flows, mtDNA-CN is widely accepted among researchers as a useful method to assess mitochondrial function (Castellani et al., 2020; Zhang et al., 2022). Our results showed significant elevation in relative mtDNA-CN in NAFLD patients' liver which were in accordance with our previous work (Kamfar et al., 2016). Also, Malik et al. demonstrated a rise in hepatic mtDNA content during the initial stages of hepatic steatosis in mice models (Malik et al., 2019). Chiappini et al. also found that the mtDNA to nuclear DNA (nDNA) ratio was higher in hepatic steatosis than in normal liver tissues (Chiappini et al., 2006). However, in contrast to these results Sookian et al. and Pirola et al. reported significant lower mtDNA/nDNA ratio in the liver of NAFLD patients compared to that of healthy control group (Sookoian et al., 2010; Pirola et al., 2015). Studies suggested that mtDNA-CN upregulation in humans with mitochondrial diseases, mostly concomitant with an overall rise in mitochondrial biogenesis, is regularly occurring and typically considered as a compensatory mechanism to support cellular bioenergetics (Hsin-Chen et al., 2000; Lee et al., 2018; Skuratovskaia et al., 2019; Filograna et al., 2021). We assumed that in NAFL patients this compensatory mechanism leads to mtDNA-CN upregulation and when this mechanism fails, due to disease progression and significant higher oxidative stress in NASH patients, the mtDNA-CN falls down. On the other hand, an increase in defective mitochondria can be considered detrimental rather than protective because of ROS accumulation as byproducts of the defective mitochondria (Sanyal et al., 2001; Shami et al., 2021). So, the precise involvement of mitochondrial biogenesis in these patients remains a topic of debate. In the present study we investigate NAFL and NASH patients separately in this regard. Although in our results relative mtDNA-CN was higher in NASH samples compared to NAFL ones, the difference was not significant. Thus, the interpretation of this data can be challenging, partly due to method-, specimen- and study design-related issues.

Some studies reported substantial depletion of mtDNA-CN in hepatic cells with aging in animal models (Barazzoni et al., 2000; Hartmann et al., 2011). Wachsmuth et al. suggested that mtDNA-CN decreased with age in human muscle tissue (Wachsmuth et al., 2016). However, Frahm et al. reported no age-related increase of mtDNA amount in brain, skeletal muscle and human heart (Frahm et al., 2005). Their result was in accordance with our present and previous studies (Kamfar et al., 2016) on human liver cells. This can have several reasons, for example, beside limited number of samples, our studies had a case-control design and we did not investigate liver mtDNA-CN in individuals through long duration of time. Also, evidence indicated that mtDNA-CN can vary between different cell types and answer differently to various physiologic and pathologic states including NAFLD (Tapia et al., 2018; Ma et al., 2020; Filograna et al., 2021) suggesting a dynamic nature for this parameter.

In the current study, we detected a significant increase in FGF21 expression in patients with higher BMI. This results were in concordance to many previous studies conducted on children (Reinehr et al., 2012) and adults (Dushay et al., 2010; Tyynismaa et al., 2011). According to our results, FGF21 expression rise was also significantly correlated to high AST and high ALT. Nakanishi et al. supported this result in their study which showed that FGF21 level was remarkably associated with AST and ALT elevation (Nakanishi et al., 2021). This emphasizes FGF21 role as an ameliorating agent which its production increases in liver injuries.

Numerous evidence showed that circulatory FGF21 rise in NAFLD patients and discussed its role as a protective factor (Tucker et al., 2019; Tillman and Rolph, 2020). FGF21 elevation can be seen as another compensatory mechanism in these patients. However, we do not fully understand the molecular regulatory mechanisms behind its function yet (Watanabe et al., 2020; Tan

et al., 2023). In our study we detected remarkable increase in its expression in liver tissue of NAFLD patients compared to of control group. This result was supported by other previous works (Kamfar et al., 2016; Liu et al., 2023). Li et al. suggested that FGF21 may mirror the severity and progression of NAFLD due to its association with obesity, triglyceride, and gama-glutamyltransferase (Li et al., 2010). They reported that hepatic FGF21 mRNA expression in NAFLD patients with grade 1 was 4-fold higher than that in grade 0 ($p < 0.01$), and grade 2–3 was 14.71-fold higher than that in grade 0 ($p < 0.01$). In another study conducted by Flisiak-Jackiewicz et al. serum FGF21 levels were higher significantly in obese children with NAFLD compared to obese children without the disease and had a positive correlation with steatosis grades in biopsies (Flisiak-Jackiewicz et al., 2019). However, we did not detect any significant difference in its expression between NAFL and NASH patients. This can be due to the failure of FGF21 related compensatory mechanisms in more advanced stages of the disease. In this regard Alisi et al. found that FGF21 levels increased progressively with the increase of hepatic steatosis, but when hepatic fat content reached the fourth quartile, FGF21 levels tended to decline (Alisi et al., 2013). The authors of that study suggested that decreased production of this molecule by hepatocytes due to their injury or death caused by lipotoxicity and hepatic inflammation may be the cause of its decline in adult patients with severe liver steatohepatitis. Their results were also in accordance with the study conducted by Dushay et al. who reported lower hepatic FGF21 expression in NASH compared to NAFLD and suggested it may reflect more advanced hepatic injury (Dushay et al., 2010).

Finally, we reported a positive correlation between mtDNA-CN and FGF21 expression levels in liver tissue samples of patients with NAFLD which as mentioned before might be a mitochondrial disease. Based on current results, these two factors may play critical roles at the early stages of disease in inhibiting NAFLD development to NASH. In a recent systematic review, Lin et al. reported that FGF21 is highly sensitive and specific for diagnosis of mitochondrial diseases (Lin et al., 2020). According to a study conducted by Ji et al. FGF21 expression in mitochondrial diseases increases as a compensatory mechanism in energy metabolism. Furthermore, they showed that FGF21 regulates energy homeostasis by increasing expression of mitochondrial genes and mtDNA-CN (Ji et al., 2015). A more accurate explanation of the relation between these two factors in NAFLD remains to be investigated. Despite the importance of this matter, there are currently no approved therapies for treating NAFLD or NASH globally (Francque and Vonghia, 2019). Exercise prescription is considered a central strategy in treatment (van der Windt et al., 2018). In confirmation of this proposed option, in one study, J Henkel et al. showed that exercise improved glucose tolerance in NAFLD by inducing FGF21 production by the liver (Henkel et al., 2019).

Our study holds some limitations. Firstly, limited number of participants is an important barrier for making a reliable conclusion that needed to be noticed. Secondly, because of the dangers of sample collection in this study we could not match our controls with patients perfectly. We tried to minimize the effect of this bias by adjusting for some confounding factors like age and BMI in our analysis. Thirdly, we did not collect data during the progression of the disease in individuals hence our results regarding changes in parameters during disease progression are subject to error. Finally, like any study using liver biopsy as a standard, miss-diagnosis of disease stage at biopsy can be caused by sampling error (Ratziu et al., 2005). The potential for sampling error in this study was minimized by collecting 2 to 3 biopsies >15 mm from each participant and consulting two hepatopathologists to examine each sample.

In the present study we did not collect data on FGF21 protein levels in liver tissues and blood samples of patients and just reported and analyzed FGF21 mRNA levels. It has been shown that the protein levels can be independent of associated mRNA levels in tissues and blood (Greenbaum et al., 2003; Silva and Vogel, 2016). This can be caused by several factors affecting FGF21 production like mRNA degradation, translation, and protein degradation (Battle et al., 2015; Bayoumi et al., 2021). Hence, making it challenging to find a direct cause-and-effect relationship between different gene expressions. We tried to tackle this issue by measuring mRNA levels which become affected prior to changes in protein levels and to help clarifying ambiguities. More studies with larger number of participants and measuring protein levels through disease progression are needed to track the changes more specifically.

As for studying mitochondrial changes we only collected data on mtDNA-CN in liver tissues of participants as previous literature suggested it to be a biomarker of mitochondrial function (Castellani et al., 2020; Zhang et al., 2022). However, further studies on mitochondrial changes with different methods like electron microscopy and evaluation of consequences of mtDNA-CN changes are needed.

Taken together, in this case-control study, we have shown a considerable rise in FGF21 expression and mtDNA-CN in NAFLD patients compared to healthy control group. While the data presented here suggest that mitochondrial dysfunction and FGF21 expression are involved in the disease mechanism, they are not conclusive in predicting prognosis or progression of the disease. Furthermore, our results suggested a positive correlation between hepatic FGF21 expression and mtDNA-CN in the liver tissue of NAFLD patients. Further research is needed to determine the exact relationship between mtDNA-CN and FGF21 with NAFLD susceptibility.

Data availability statement

The original contributions presented in the study are included in the article/Supplementary Materials, further inquiries can be directed to the corresponding author.

Ethics statement

The studies involving human participants were reviewed and approved by the Hamadan University of Medical Sciences (P/16/35/9/3481). The patients/participants provided their written informed consent to participate in this study.

Author contributions

All authors listed have made a substantial, direct, and intellectual contribution to the work and approved it for publication.

Funding

This study was supported by the Shahid Beheshti University of Medical Sciences, Tehran, Iran.

Acknowledgments

We are all very thankful to all generous donors for research purposes.

Conflict of interest

The authors declare that the research was conducted in the absence of any commercial or financial relationships that could be construed as a potential conflict of interest.

Publisher's note

All claims expressed in this article are solely those of the authors and do not necessarily represent those of their affiliated organizations, or those of the publisher, the editors and the reviewers. Any product that may be evaluated in this article, or claim that may be made by its manufacturer, is not guaranteed or endorsed by the publisher.

Supplementary material

The Supplementary Material for this article can be found online at: https://www.frontiersin.org/articles/10.3389/fmolb.2023.1203019/full#supplementary-material

SUPPLEMENTARY TABLE S1
Comparison of mtDNA-CN between NAFL and NASH patients and controls.

SUPPLEMENTARY TABLE S2
Correlations of serum fgf21 expression with copy number anthropometric parameters and biochemical indexes.

References

Acierno, C., Caturano, A., Pafundi, P. C., Nevola, R., Adinolfi, L. E., and Sasso, F. C. (2020). Nonalcoholic fatty liver disease and type 2 diabetes: Pathophysiological mechanisms shared between the two faces of the same coin. *Explor. Med.* 1 (5). doi:10.37349/emed.2020.00019

Alisi, A., Ceccarelli, S., Panera, N., Prono, F., Petrini, S., De Stefanis, C., et al. (2013). Association between serum atypical fibroblast growth factors 21 and 19 and pediatric nonalcoholic fatty liver disease. *PLoS One* 8 (6), e67160. doi:10.1371/journal.pone.0067160

Ascha, M. S., Hanouneh, I. A., Lopez, R., Tamimi, T. A-R., Feldstein, A. F., and Zein, N. N. (2010). The incidence and risk factors of hepatocellular carcinoma in patients with nonalcoholic steatohepatitis. *Hepatology* 51 (6), 1972–1978. doi:10.1002/hep.23527

Bao, L., Yin, J., Gao, W., Wang, Q., Yao, W., and Gao, X. (2018). A long-acting FGF21 alleviates hepatic steatosis and inflammation in a mouse model of non-alcoholic steatohepatitis partly through an FGF21-adiponectin-IL17A pathway. *Br. J. Pharmacol.* 175 (16), 3379–3393. doi:10.1111/bph.14383

Barazzoni, R., Short, K. R., and Nair, K. S. (2000). Effects of aging on mitochondrial DNA copy number and cytochromec oxidase gene expression in rat skeletal muscle, liver, and heart. *J. Biol. Chem.* 275 (5), 3343–3347. doi:10.1074/jbc.275.5.3343

Battle, A., Khan, Z., Wang, S. H., Mitrano, A., Ford, M. J., Pritchard, J. K., et al. (2015). Genomic variation. Impact of regulatory variation from RNA to protein. *Science* 347 (6222), 664–667. doi:10.1126/science.1260793

Bayoumi, A., Elsayed, A., Han, S., Petta, S., Adams, L. A., Aller, R., et al. (2021). Mistranslation drives alterations in protein levels and the effects of a synonymous variant at the fibroblast growth factor 21 locus. *Adv. Sci.* 8 (11), 2004168. doi:10.1002/advs.202004168

Begriche, K., Igoudjil, A., Pessayre, D., and Fromenty, B. (2006). Mitochondrial dysfunction in NASH: Causes, consequences and possible means to prevent it. *Mitochondrion* 6 (1), 1–28. doi:10.1016/j.mito.2005.10.004

Bhala, N., Angulo, P., van der Poorten, D., Lee, E., Hui, J. M., Saracco, G., et al. (2011). The natural history of nonalcoholic fatty liver disease with advanced fibrosis or cirrhosis: An international collaborative study. *Hepatology* 54 (4), 1208–1216. doi:10.1002/hep.24491

Boparai, R. K., Arum, O., Miquet, J. G., Masternak, M. M., Bartke, A., and Khardori, R. K. (2015). Resistance to the beneficial metabolic effects and hepatic antioxidant defense actions of fibroblast growth factor 21 treatment in growth hormone-overexpressing transgenic mice. *Int. J. Endocrinol.* 2015, 282375. doi:10.1155/2015/282375

Cao, K., Wang, K., Yang, M., Liu, X., Lv, W., and Liu, J. (2020). Punicalagin improves hepatic lipid metabolism via modulation of oxidative stress and mitochondrial biogenesis in hyperlipidemic mice. *Food Funct.* 11 (11), 9624–9633. doi:10.1039/d0fo01545h

Castellani, C. A., Longchamps, R. J., Sun, J., Guallar, E., and Arking, D. E. (2020). Thinking outside the nucleus: Mitochondrial DNA copy number in health and disease. *Mitochondrion* 53, 214–223. doi:10.1016/j.mito.2020.06.004

Caturano, A., Acierno, C., Nevola, R., Pafundi, P. C., Galiero, R., Rinaldi, L., et al. (2021). Non-alcoholic fatty liver disease: From pathogenesis to clinical impact. *Processes* 9 (1), 135. doi:10.3390/pr9010135

Chalasani, N., Younossi, Z., Lavine, J. E., Diehl, A. M., Brunt, E. M., Cusi, K., et al. (2012). The diagnosis and management of non-alcoholic fatty liver disease: Practice guideline by the American association for the study of liver diseases, American college of gastroenterology, and the American gastroenterological association. *Hepatology* 55 (6), 2005–2023. doi:10.1002/hep.25762

Chiappini, F., Barrier, A., Saffroy, R., Domart, M-C., Dagues, N., Azoulay, D., et al. (2006). Exploration of global gene expression in human liver steatosis by high-density oligonucleotide microarray. *Lab. Investig.* 86 (2), 154–165. doi:10.1038/labinvest.3700374

Cuevas-Ramos, D., Almeda-Valdes, P., Aguilar-Salinas, C. A., Cuevas-Ramos, G., Cuevas-Sosa, A. A., and Gomez-Perez, F. J. (2009). The role of fibroblast growth factor 21 (FGF21) on energy balance, glucose and lipid metabolism. *Curr. diabetes Rev.* 5 (4), 216–220. doi:10.2174/157339909789804396

Cusi, K. (2009). Nonalcoholic fatty liver disease in type 2 diabetes mellitus. *Curr. Opin. Endocrinol. Diabetes Obes.* 16 (2), 141–149. doi:10.1097/MED.0b013e3283293015

Dabravolski, S. A., Bezsonov, E. E., Baig, M. S., Popkova, T. V., Nedosugova, L. V., Starodubova, A. V., et al. (2021). Mitochondrial mutations and genetic factors determining NAFLD risk. *Int. J. Mol. Sci.* 22 (9), 4459. doi:10.3390/ijms22094459

Dornas, W., and Schuppan, D. (2020). Mitochondrial oxidative injury: A key player in nonalcoholic fatty liver disease. *Am. J. Physiology-Gastrointestinal Liver Physiology* 319 (3), G400–G11. doi:10.1152/ajpgi.00121.2020

Dushay, J., Chui, P. C., Gopalakrishnan, G. S., Varela-Rey, M., Crawley, M., Fisher, F. M., et al. (2010). Increased fibroblast growth factor 21 in obesity and nonalcoholic fatty liver disease. *Gastroenterology* 139 (2), 456–463. doi:10.1053/j.gastro.2010.04.054

Falamarzi, K., Malekpour, M., Tafti, M. F., Azarpira, N., Behboodi, M., and Zarei, M. (2022). The role of FGF21 and its analogs on liver associated diseases. *Front. Med. (Lausanne)* 9, 967375. doi:10.3389/fmed.2022.967375

Filograna, R., Mennuni, M., Alsina, D., and Larsson, N-G. (2021). Mitochondrial DNA copy number in human disease: The more the better? *FEBS Lett.* 595 (8), 976–1002. doi:10.1002/1873-3468.14021

Flisiak-Jackiewicz, M., Bobrus-Chociej, A., Wasilewska, N., Tarasow, E., Wojtkowska, M., and Lebensztejn, D. M. (2019). Can hepatokines be regarded as novel non-invasive serum biomarkers of intrahepatic lipid content in obese children? *Adv. Med. Sci.* 64 (2), 280–284. doi:10.1016/j.advms.2019.02.005

Frahm, T., Mohamed, S. A., Bruse, P., Gemünd, C., Oehmichen, M., and Meissner, C. (2005). Lack of age-related increase of mitochondrial DNA amount in brain, skeletal muscle and human heart. *Mech. ageing Dev.* 126 (11), 1192–1200. doi:10.1016/j.mad.2005.06.008

Francque, S., and Vonghia, L. (2019). Pharmacological treatment for non-alcoholic fatty liver disease. *Adv. Ther.* 36 (5), 1052–1074. doi:10.1007/s12325-019-00898-6

Greenbaum, D., Colangelo, C., Williams, K., and Gerstein, M. (2003). Comparing protein abundance and mRNA expression levels on a genomic scale. *Genome Biol.* 4 (9), 117. doi:10.1186/gb-2003-4-9-117

Hartmann, N., Reichwald, K., Wittig, I., Dröse, S., Schmeisser, S., Lück, C., et al. (2011). Mitochondrial DNA copy number and function decrease with age in the short-lived fish Nothobranchius furzeri. *Aging Cell* 10 (5), 824–831. doi:10.1111/j.1474-9726.2011.00723.x

Henkel, J., Buchheim-Dieckow, K., Castro, J. P., Laeger, T., Wardelmann, K., Kleinridders, A., et al. (2019). Reduced oxidative stress and enhanced FGF21 formation in livers of endurance-exercised rats with diet-induced NASH. *Nutrients* 11 (11), 2709. doi:10.3390/nu11112709

Hsin-Chen, L., Pen-Hui, Y., Ching-You, L., Chin-Wen, C., and Yau-Huei, W. (2000). Increase of mitochondria and mitochondrial DNA in response to oxidative stress in human cells. *Biochem. J.* 348 (2), 425–432. doi:10.1042/bj3480425

Jensen, E. C. (2012). Real-time reverse transcription polymerase chain reaction to measure mRNA: Use, limitations, and presentation of results. *Anatomical Rec.* 295 (1), 1–3. doi:10.1002/ar.21487

Ji, K., Zheng, J., Lv, J., Xu, J., Ji, X., Luo, Y. B., et al. (2015). Skeletal muscle increases FGF21 expression in mitochondrial disorders to compensate for energy metabolic insufficiency by activating the mTOR-YY1-PGC1α pathway. *Free Radic. Biol. Med.* 84, 161–170. doi:10.1016/j.freeradbiomed.2015.03.020

Kamfar, S., Alavian, S. M., Houshmand, M., Yadegarazari, R., Seifi Zarei, B., Khalaj, A., et al. (2016). Liver mitochondrial DNA copy number and deletion levels may contribute to nonalcoholic fatty liver disease susceptibility. *Hepat. Mon.* 16 (12), e40774. doi:10.5812/hepatmon.40774

Koroglu, E., Canbakan, B., Atay, K., Hatemi, I., Tuncer, M., Dobrucali, A., et al. (2016). Role of oxidative stress and insulin resistance in disease severity of non-alcoholic fatty liver disease. *Turk J. Gastroenterol.* 27 (4), 361–366. doi:10.5152/tjg.2016.16106

Lee, J. H., Kang, Y. E., Chang, J. Y., Park, K. C., Kim, H-W., Kim, J. T., et al. (2016). An engineered FGF21 variant, LY2405319, can prevent non-alcoholic steatohepatitis by enhancing hepatic mitochondrial function. *Am. J. Transl. Res.* 8 (11), 4750–4763.

Lee, K., Haddad, A., Osme, A., Kim, C., Borzou, A., Ilchenko, S., et al. (2018). Hepatic mitochondrial defects in a nonalcoholic fatty liver disease mouse model are associated with increased degradation of oxidative phosphorylation subunits*. *Mol. Cell. Proteomics* 17 (12), 2371–2386. doi:10.1074/mcp.RA118.000961

Li, H., Fang, Q., Gao, F., Fan, J., Zhou, J., Wang, X., et al. (2010). Fibroblast growth factor 21 levels are increased in nonalcoholic fatty liver disease patients and are correlated with hepatic triglyceride. *J. Hepatol.* 53 (5), 934–940. doi:10.1016/j.jhep.2010.05.018

Lin, Y., Ji, K., Ma, X., Liu, S., Li, W., Zhao, Y., et al. (2020). Accuracy of FGF-21 and GDF-15 for the diagnosis of mitochondrial disorders: A meta-analysis. *Ann. Clin. Transl. Neurol.* 7 (7), 1204–1213. doi:10.1002/acn3.51104

Liu, C., Schönke, M., Spoorenberg, B., Lambooij, J. M., van der Zande, H. J. P., Zhou, E., et al. (2023). FGF21 protects against hepatic lipotoxicity and macrophage activation to attenuate fibrogenesis in nonalcoholic steatohepatitis. *eLife* 12, e83075. doi:10.7554/eLife.83075

Liu, J., Xu, Y., Hu, Y., and Wang, G. (2015). The role of fibroblast growth factor 21 in the pathogenesis of non-alcoholic fatty liver disease and implications for therapy. *Metabolism* 64 (3), 380–390. doi:10.1016/j.metabol.2014.11.009

Lonardo, A., Nascimbeni, F., Maurantonio, M., Marrazzo, A., Rinaldi, L., and Adinolfi, L. E. (2017). Nonalcoholic fatty liver disease: Evolving paradigms. *World J. Gastroenterology* 23 (36), 6571–6592. doi:10.3748/wjg.v23.i36.6571

Ma, C., Liu, Y., He, S., Zeng, J., Li, P., Ma, C., et al. (2020). Association between leukocyte mitochondrial DNA copy number and non-alcoholic fatty liver disease in a Chinese population is mediated by 8-oxo-2'-deoxyguanosine. *Front. Med. (Lausanne)* 7, 536. doi:10.3389/fmed.2020.00536

Malik, A. N., Simões, I. C. M., Rosa, H. S., Khan, S., Karkucinska-Wieckowska, A., and Wieckowski, M. R. (2019). A diet induced maladaptive increase in hepatic mitochondrial DNA precedes OXPHOS defects and may contribute to non-alcoholic fatty liver disease. *Cells* 8 (10), 1222. doi:10.3390/cells8101222

Mavraki, E., Labrum, R., Sergeant, K., Alston, C. L., Woodward, C., Smith, C., et al. (2023). Genetic testing for mitochondrial disease: The United Kingdom best practice guidelines. *Eur. J. Hum. Genet.* 31 (2), 148–163. doi:10.1038/s41431-022-01249-w

Mitra, S., De, A., and Chowdhury, A. (2020). Epidemiology of non-alcoholic and alcoholic fatty liver diseases. *Transl. Gastroenterol. Hepatol.* 5, 16. doi:10.21037/tgh.2019.09.08

Nakanishi, K., Ishibashi, C., Ide, S., Yamamoto, R., Nishida, M., Nagatomo, I., et al. (2021). Serum FGF21 levels are altered by various factors including lifestyle behaviors in male subjects. *Sci. Rep.* 11 (1), 22632. doi:10.1038/s41598-021-02075-8

Nusrat, S., Khan, M. S., Fazili, J., and Madhoun, M. F. (2014). Cirrhosis and its complications: Evidence based treatment. *World J. Gastroenterol.* 20 (18), 5442–5460. doi:10.3748/wjg.v20.i18.5442

Paradies, G., Paradies, V., Ruggiero, F. M., and Petrosillo, G. (2014). Oxidative stress, cardiolipin and mitochondrial dysfunction in nonalcoholic fatty liver disease. *World J. gastroenterology WJG* 20 (39), 14205–14218. doi:10.3748/wjg.v20.i39.14205

Pessayre, D., and Fromenty, B. (2005). Nash: A mitochondrial disease. *J. hepatology* 42 (6), 928–940. doi:10.1016/j.jhep.2005.03.004

Pirola, C. J., Scian, R., Gianotti, T. F., Dopazo, H., Rohr, C., Martino, J. S., et al. (2015). Epigenetic modifications in the biology of nonalcoholic fatty liver disease: The role of DNA hydroxymethylation and TET proteins. *Medicine* 94 (36), e1480. doi:10.1097/MD.0000000000001480

Ratziu, V., Charlotte, F., Heurtier, A., Gombert, S., Giral, P., Bruckert, E., et al. (2005). Sampling variability of liver biopsy in nonalcoholic fatty liver disease. *Gastroenterology* 128 (7), 1898–1906. doi:10.1053/j.gastro.2005.03.084

Reinehr, T., Woelfle, J., Wunsch, R., and Roth, C. L. (2012). Fibroblast growth factor 21 (FGF-21) and its relation to obesity, metabolic syndrome, and nonalcoholic fatty liver in children: A longitudinal analysis. *J. Clin. Endocrinol. Metabolism* 97 (6), 2143–2150. doi:10.1210/jc.2012-1221

Rusli, F., Deelen, J., Andriyani, E., Boekschoten, M. V., Lute, C., van den Akker, E. B., et al. (2016). Fibroblast growth factor 21 reflects liver fat accumulation and dysregulation of signalling pathways in the liver of C57BL/6J mice. *Sci. Rep.* 6 (1), 30484. doi:10.1038/srep30484

Sanyal, A. J., Campbell-Sargent, C., Mirshahi, F., Rizzo, W. B., Contos, M. J., Sterling, R. K., et al. (2001). Nonalcoholic steatohepatitis: Association of insulin resistance and mitochondrial abnormalities. *Gastroenterology* 120 (5), 1183–1192. doi:10.1053/gast.2001.23256

Shakhssalim, N., Houshmand, M., Kamalidehghan, B., Faraji, A., Sarhangnejad, R., Dadgar, S., et al. (2013). The mitochondrial C16069T polymorphism, not mitochondrial D310 (D-loop) mononucleotide sequence variations, is associated with bladder cancer. *Cancer Cell Int.* 13 (1), 120. doi:10.1186/1475-2867-13-120

Shami, G. J., Cheng, D., Verhaegh, P., Koek, G., Wisse, E., and Braet, F. (2021). Three-dimensional ultrastructure of giant mitochondria in human non-alcoholic fatty liver disease. *Sci. Rep.* 11 (1), 3319. doi:10.1038/s41598-021-82884-z

Silva, G. M., and Vogel, C. (2016). Quantifying gene expression: The importance of being subtle. *Mol. Syst. Biol.* 12 (10), 885. doi:10.15252/msb.20167325

Skuratovskaia, D., Zatolokin, P., Vulf, M., Mazunin, I., and Litvinova, L. (2019). Interrelation of chemerin and TNF-α with mtDNA copy number in adipose tissues and blood cells in obese patients with and without type 2 diabetes. *BMC Med. Genomics* 12 (2), 40. doi:10.1186/s12920-019-0485-8

Sookoian, S., Rosselli, M. S., Gemma, C., Burgueño, A. L., Gianotti, T. F., Castaño, G. O., et al. (2010). Epigenetic regulation of insulin resistance in nonalcoholic fatty liver disease: Impact of liver methylation of the peroxisome proliferator-activated receptor γ coactivator 1α promoter. *Hepatology* 52 (6), 1992–2000. doi:10.1002/hep.23927

Tan, H., Yue, T., Chen, Z., Wu, W., Xu, S., and Weng, J. (2023). Targeting FGF21 in cardiovascular and metabolic diseases: From mechanism to medicine. *Int. J. Biol. Sci.* 19 (1), 66–88. doi:10.7150/ijbs.73936

Tanaka, N., Takahashi, S., Zhang, Y., Krausz, K. W., Smith, P. B., Patterson, A. D., et al. (2015). Role of fibroblast growth factor 21 in the early stage of NASH induced by methionine-and choline-deficient diet. *Biochimica Biophysica Acta (BBA)-Molecular Basis Dis.* 1852 (7), 1242–1252. doi:10.1016/j.bbadis.2015.02.012

Tapia, M. A. P., Fragoso-Bargas, N., Rodríguez-Ríos, D., Lazo-de-la-Vega-Monroy, M. L., del Rocío Ibarra-Reynoso, L., Ruíz-Noa, Y., et al. (2018). Peripheral blood mitochondrial DNA copy number, a potential marker of non-alcoholic fatty liver disease? *FASEB J.* 32 (S1), lb112–lb. doi:10.1096/fasebj.2018.32.1_supplement.lb112

Tillman, E. J., and Rolph, T. (2020). FGF21: An emerging therapeutic target for non-alcoholic steatohepatitis and related metabolic diseases. *Front. Endocrinol.* 11, 601290. doi:10.3389/fendo.2020.601290

Toshikuni, N., Tsutsumi, M., and Arisawa, T. (2014). Clinical differences between alcoholic liver disease and nonalcoholic fatty liver disease. *World J. Gastroenterol.* 20 (26), 8393–8406. doi:10.3748/wjg.v20.i26.8393

Tucker, B., Li, H., Long, X., Rye, K. A., and Ong, K. L. (2019). Fibroblast growth factor 21 in non-alcoholic fatty liver disease. *Metabolism* 101, 153994. doi:10.1016/j.metabol.2019.153994

Tyynismaa, H., Raivio, T., Hakkarainen, A., Ortega-Alonso, A., Lundbom, N., Kaprio, J., et al. (2011). Liver fat but not other adiposity measures influence circulating FGF21 levels in healthy young adult twins. *J. Clin. Endocrinol. Metab.* 96 (2), E351–E355. doi:10.1210/jc.2010-1326

van der Windt, D. J., Sud, V., Zhang, H., Tsung, A., and Huang, H. (2018). The effects of physical exercise on fatty liver disease. *Gene Expr.* 18 (2), 89–101. doi:10.3727/105221617X15124844266408

Wachsmuth, M., Huebner, A., Li, M., Madea, B., and Stoneking, M. (2016). Age-related and heteroplasmy-related variation in human mtDNA copy number. *PLoS Genet.* 12 (3), 1005939. doi:10.1371/journal.pgen.1005939

Wang, J., He, W., Tsai, P-J., Chen, P-H., Ye, M., Guo, J., et al. (2020). Mutual interaction between endoplasmic reticulum and mitochondria in nonalcoholic fatty liver disease. *Lipids Health Dis.* 19, 72–19. doi:10.1186/s12944-020-01210-0

Wang, M., and Kaufman, R. J. (2014). The impact of the endoplasmic reticulum protein-folding environment on cancer development. *Nat. Rev. Cancer* 14 (9), 581–597. doi:10.1038/nrc3800

Watanabe, M., Risi, R., Camajani, E., Contini, S., Persichetti, A., Tuccinardi, D., et al. (2020). Baseline homa IR and circulating FGF21 levels predict NAFLD improvement in patients undergoing a low carbohydrate dietary intervention for weight loss: A prospective observational pilot study. *Nutrients* 12 (7), 2141. doi:10.3390/nu12072141

Xu, J., Lloyd, D. J., Hale, C., Stanislaus, S., Chen, M., Sivits, G., et al. (2009). Fibroblast growth factor 21 reverses hepatic steatosis, increases energy expenditure, and improves insulin sensitivity in diet-induced obese mice. *Diabetes* 58 (1), 250–259. doi:10.2337/db08-0392

Xu, J., Shen, J., Yuan, R., Jia, B., Zhang, Y., Wang, S., et al. (2021). Mitochondrial targeting therapeutics: Promising role of natural products in non-alcoholic fatty liver disease. *Front. Pharmacol.* 12, 796207. doi:10.3389/fphar.2021.796207

Ye, D., Wang, Y., Li, H., Jia, W., Man, K., Lo, C. M., et al. (2014). Fibroblast growth factor 21 protects against acetaminophen-induced hepatotoxicity by potentiating peroxisome proliferator-activated receptor coactivator protein-1α-mediated antioxidant capacity in mice. *Hepatology* 60 (3), 977–989. doi:10.1002/hep.27060

Ye, J., Coulouris, G., Zaretskaya, I., Cutcutache, I., Rozen, S., and Madden, T. L. (2012). Primer-BLAST: A tool to design target-specific primers for polymerase chain reaction. *BMC Bioinforma.* 13 (1), 134. doi:10.1186/1471-2105-13-134

Yeh, M. M., and Brunt, E. M. (2014). Pathological features of fatty liver disease. *Gastroenterology* 147 (4), 754–764. doi:10.1053/j.gastro.2014.07.056

Younossi, Z., Anstee, Q. M., Marietti, M., Hardy, T., Henry, L., Eslam, M., et al. (2018). Global burden of NAFLD and NASH: Trends, predictions, risk factors and prevention. *Nat. Rev. Gastroenterology hepatology* 15 (1), 11–20. doi:10.1038/nrgastro.2017.109

Zabihi Diba, L., Mohaddes Ardebili, S. M., Gharesouran, J., and Houshmand, M. (2016). Age-related decrease in mtDNA content as a consequence of mtDNA 4977 bp deletion. *Mitochondrial DNA Part A* 27 (4), 3008–3012. doi:10.3109/19401736.2015.1063046

Zhang, Z., Yang, D., Zhou, B., Luan, Y., Yao, Q., Liu, Y., et al. (2022). Decrease of MtDNA copy number affects mitochondrial function and involves in the pathological consequences of ischaemic stroke. *J. Cell. Mol. Med.* 26 (15), 4157–4168. doi:10.1111/jcmm.17262

frontiers | Frontiers in Cell and Developmental Biology

TYPE Brief Research Report
PUBLISHED 26 June 2023
DOI 10.3389/fcell.2023.1212779

OPEN ACCESS

EDITED BY
Francesca Forini,
National Research Council (CNR), Italy

REVIEWED BY
Naresh Chandra Bal,
KIIT University, India
Yuko Ono,
Kobe University, Japan

*CORRESPONDENCE
Mauricio Castro-Sepulveda,
mcastro@uft.cl
Hermann Zbinden-Foncea,
hzbinden@uft.cl

†PRESENT ADDRESS
Giovanni Rosales-Soto, Laboratorio de Fisiología del Ejercicio y Metabolismo, Escuela de Kinesiología, Facultad de Medicina,Universidad Finis Terrae, Santiago, Chile

RECEIVED 26 April 2023
ACCEPTED 12 June 2023
PUBLISHED 26 June 2023

CITATION
Castro-Sepulveda M, Tuñón-Suárez M, Rosales-Soto G, Vargas-Foitzick R, Deldicque L and Zbinden-Foncea H (2023), Regulation of mitochondrial morphology and cristae architecture by the TLR4 pathway in human skeletal muscle.
Front. Cell Dev. Biol. 11:1212779.
doi: 10.3389/fcell.2023.1212779

Regulation of mitochondrial morphology and cristae architecture by the TLR4 pathway in human skeletal muscle

Mauricio Castro-Sepulveda[1]*, Mauro Tuñón-Suárez[1], Giovanni Rosales-Soto[2†], Ronald Vargas-Foitzick[1], Louise Deldicque[3] and Hermann Zbinden-Foncea[1,3,4]*

[1]Laboratorio de Fisiología del Ejercicio y Metabolismo, Escuela de Kinesiología, Facultad de Medicina, Universidad Finis Terrae, Santiago, Chile, [2]Facultad de Ciencias de la Educación, Universidad San Sebastián, Sede Bellavista, Santiago, Chile, [3]Institute of Neuroscience, UCLouvain, Ottignies-Louvain-la-Neuve, Belgium, [4]Facultad de Ciencias de la Salud, Universidad Francisco de Vitoria, Madrid, España

In skeletal muscle (SkM), a reduced mitochondrial elongate phenotype is associated with several metabolic disorders like type 2 diabetes mellitus (T2DM). However, the mechanisms contributing to this reduction in mitochondrial elongate phenotype in SkM have not been fully elucidated. It has recently been shown in a SkM cell line that toll-like receptor 4 (TLR4) contributes to the regulation of mitochondrial morphology. However, this has not been investigated in human SkM. Here we found that in human SkM biopsies, TLR4 protein correlated negatively with Opa1 (pro-mitochondrial fusion protein). Moreover, the incubation of human myotubes with LPS reduced mitochondrial size and elongation and induced abnormal mitochondrial cristae, which was prevented with the co-incubation of LPS with TAK^{242}. Finally, T2DM myotubes were found to have reduced mitochondrial elongation and mitochondrial cristae density. Mitochondrial morphology, membrane structure, and insulin-stimulated glucose uptake were restored to healthy levels in T2DM myotubes treated with TAK^{242}. In conclusion, mitochondrial morphology and mitochondrial cristae seem to be regulated by the TLR4 pathway in human SkM. Those mitochondrial alterations might potentially contribute to insulin resistance in the SkM of patients with T2DM.

KEYWORDS

mitochondrial dynamics, skeletal muscle function, mitochondrial nanotunnels, Lipopolysaccharide, TAK^{242}, type 2 diabetes

1 Introduction

Skeletal muscle (SkM) contributes to a large proportion of whole-body fatty acid uptake and oxidation, as well as to 80% of insulin-stimulated glucose disposal (Baron et al., 1988). Therefore, SkM plays an important role in whole-body metabolic regulation (Pedersen and Febbraio, 2012). In this sense, the mitochondrial function plays an important role in the cell energy supply. In humans, mitochondria occupy >5% of SkM fiber volume (Castro-Sepulveda et al., 2020), and their function has been associated with SkM metabolism and function (Islam et al., 2018).

Mitochondria are dynamic organelles whose morphology (fragmented or elongated) is determined by fusion and fission events (Castro-Sepulveda el al., 2023). SkM mitochondria

of subjects with type 2 diabetes mellitus (T2DM) display a fragmented phenotype (Kelley et al., 2002). Moreover, we showed that in human SkM, a mitochondrial connected phenotype was negatively correlated with lipid droplet density and positively correlated with whole-body lipid oxidation (Castro-Sepulveda et al., 2020), which are two variables associated with insulin resistance. In agreement with those *in vivo* results, an *in vitro* study showed that myotubes from insulin resistant patients presented a fragmented mitochondrial phenotype. Treatment of those myotubes with Mdivi-1 drug, a specific inhibitor of mitochondrial fission, restored the mitochondrial connected phenotype, and insulin-stimulated glucose uptake to control levels from healthy volunteers (Kugler et al., 2021). Therefore, mitochondrial morphology plays a role in SkM insulin sensitivity. Elucidating the mechanisms that regulate SkM mitochondrial morphology may reveal important therapeutic targets for metabolic disorders including T2DM.

Toll-like receptor 4 (TLR4), a classical cell pro-inflammatory receptor, is found in the SkM and when activated with LPS induces a local inflammatory response (Reyna et al., 2008; Liang et al., 2013). Increased TLR4 protein expression has been reported in the SkM of subjects with obesity and T2DM, which in turn was associated with insulin resistance (Reyna et al., 2008; Dasu et al., 2010). Therefore, T2DM patients present both fragmented mitochondria phenotype and increased expression of components of the TLR4 pathway in the SkM. However, to date, no study has clearly established any interaction between inflammation and mitochondrial dynamics in the context of insulin resistance. A recent study has shown that incubation of mouse myogenic C2C12 cells with LPS induced fragmented mitochondrial phenotype (Eggelbusch et al., 2022). A similar TLR4-induced fragmented mitochondrial phenotype was found in murine cardiomyocytes (Wu et al., 2018). Together, those results suggest that TLR4 regulates mitochondrial morphology. However, this has not been studied in human SkM. Therefore, we hypothesize that TLR4 regulates mitochondrial morphology in human SkM, which would be involved in the regulation of insulin sensitivity in the context of T2DM.

2 Methods

2.1 *In vivo* study in healthy human SkM

2.1.1 Subjects

Twelve nondiabetic, nonsmoker men (mean [standard deviation], age, 24.7 [1.5] y; Weight, 75.7 [11.1] kg; body mass index, 24.4 [2.6] $kg{\cdot}m^{-2}$; glucose, 86.9 [6.8] $mg{\cdot}dl^{-1}$ insulin, 8.9 [7.6] $\mu UI{\cdot}ml^{-1}$; HOMA-IR 2.0 [2.0]; triglycerides, 102 [53] $mg{\cdot}dl^{-1}$; total cholesterol, 185 [38] $mg{\cdot}dl^{-1}$; LDL-C, 114 [35] $mg{\cdot}dl^{-1}$; HDL-C, 51 [14] $mg{\cdot}dl^{-1}$; VLDL-C, 21 [11] $mg{\cdot}dl^{-1}$.), without history of cardiovascular, respiratory, or thyroid disease, were included. The sample size was calculated using G-power software, considering the study by Castro-Sepulveda et al. (2020), using the correlation (r = 0.69) between human SKM mitochondrial size (TEM) with whole-body resting RQ, with a power (1—β) of 0.95. The calculated samples size was 10. A 20% of desertion rate or technical problem with the muscle was taken into account for a final sample size of 12 subjects per group. Volunteers were recruited through posters placed at the Finis Terrae University and on massive social media. The volunteers were summoned to a brief interview during which the study protocol was explained to them. In this interview, the inclusion criteria were evaluated and the informed consent was given to and signed by the volunteers. Biopsies from the vastus lateralis of the dominant leg were obtained at the middle point between the anterior superior iliac spine and the patella. The modified Bergström needle technique with suction was used. After local anesthesia (2% lidocaine) was applied, a small incision was made into the skin and fascia, and the biopsy needle was inserted into the muscle. About 100 mg of tissue was withdrawn through manual suction. Excess blood, visible fat, and connective tissue were removed from the tissue. All biopsies were obtained at rest between 8:00 and 9:00 AM. Half of the muscle tissue was immediately frozen in liquid nitrogen and stored at −80°C for Western blotting; the other half was fixed in 2.5% glutaraldehyde for transmission electron microscopy analyses (Castro-Sepulveda et al., 2020). After the biopsies, the doctor gave the health recommendations to the volunteers to treat the incision during the following 56 h. None of the volunteers reported inconveniences. All subjects signed a written informed consent form in accordance with the Helsinki Declaration, and it was approved by the Institutional Review Board at the Universidad Finis Terrae (22-077)-Accredited by SEREMI of Health Exempt Resolution No. 002681/2021.

2.1.2 SkM preparation for transmission electron microscopy (TEM) and image analyses

The SkM biopsies were fixed, and dissected into fiber bundles, washed with 0.1 M sodium cacodylate buffer, stained with 2% osmium tetroxide in 0.1 M sodium cacodylate buffer for 2 h and embedded in Epon resin. Finally, 80-nm sections were examined using a TEM (Tecnai T12 at 80 kV, Philips; Microscopy Facility, Pontificia Universidad Católica de Chile). Mitochondrial morphology was assessed using Fiji/ImageJ software.

2.1.3 Western blotting

SkM samples were homogenized in a lysis buffer as described previously (Castro-Sepulveda et al., 2020). Proteins were separated by SDS-PAGE and transferred to PVDF membranes. The following antibodies were used: Mfn1 (sc-166644-Santa Cruz Biotechnology), Mfn2 (ab56889-Abcam), Opa1 (612606-BD-Biosciences), TLR4 (sc-293072-Santa-Cruz-Biotechnology), Drp1 (sc-101270-Santa-Cruz-Biotechnology), pDrp1 (Ser616, 3455-Cell-Signaling-Technology), Fis1 (ALX-210-1037-Enzo-Life-Sciences), total OXPHOS cocktail (ab110413-Abcam) and GAPDH (2118-Cell-Signaling-Technology). Representative pictures of the blots can be found in Supplementary Figure S1. The Western blotting data for Mfn1-2, Opa1, GAPDH, and TEM images has been previously published (Castro-Sepulveda et al., 2020), but herein we re-analyzed those data differently.

2.1.4 Blood analyses and maximal oxygen uptake

Serum levels of insulin were determined by chemiluminescence and triglycerides, total cholesterol, low-density lipoprotein cholesterol (LDL-C), and high-density lipoprotein cholesterol (HDL-C) by dry chemistry (Bionet, Santiago, Chile). Blood samples were taken ~7 days prior to the muscle biopsy. Maximal oxygen uptake (VO2max) was determined during an incremental

cycle ergometer as previously described (Castro-Sepulveda et al., 2020).

2.2 *In vitro* study in human primary myotubes

2.2.1 SkM tissue explants and satellite cell isolation

For this study, the inclusion criteria for the healthy volunteers were: BMI between 18 and 25 kg·m^{-2} and no diagnosis of metabolic syndrome, insulin resistance, or T2DM. For the T2DM group, the inclusion criteria was: having a fasting glycaemia over 126 mg·dl^{-1} or over 200 mg·dl^{-1}, 2 h following a 75 g glucose challenge. All subjects signed a written informed consent form in accordance with the Helsinki Declaration. The study was approved by the Institutional Review Board at the Universidad Finis Terrae (22-076)-Accredited by SEREMI of Health Exempt Resolution No. 002681/2021. SkM biopsies of the vastus lateralis were obtained from healthy males (n = 3; age, 31.0 ± 3.6 years; body mass index, 25.2 ± 1.8 kg·m^{-2}; HOMA-IR, 1.1 ± 0.3), and T2DM patients (n = 3; age, 42.5 ± 7.5 years; body mass index, 31.5 ± 4.2 kg·m^{-2}; HOMA-IR, 3.6 ± 0.2). After the biopsies, the doctor gave the health recommendations to the volunteers to treat the incision with ice gel pack during the following 56 h. None of the volunteers reported inconveniences. A part of the muscle biopsy (~20 mg) was placed in a 35-mm plate coated with Matrigel and maintained in a growth medium (DMEM, Sigma-Aldrich). Cells were harvested using dispase (BD Biosciences), sub-cultured in growth medium, and then sorted using magnetic activated cell sorting (MACS©; Miltenyi Biotec) with magnetic microbeads directly linked to CD56 (purified mouse, anti-human CD56, BD-Biosciences) to isolate satellite cells from other cell populations (Valero-Breton et al., 2020).

2.2.2 Myoblast transfection, differentiation to myotubes, and image analysis

For transfection with mtDsRed plasmid, myoblasts from three healthy and three T2DM volunteers were evenly pooled and incubated at 37°C. The myoblast pool were transfected with mtDsRed plasmid (1 µg) using Lipofectamine 2000 (2 µg, Thermo Fisher Scientific). Healthy myotubes were incubated with DMSO (vehicle, CTRL), LPS (10 µg·ml-1, activator of TLR4) and LPS + TAK^{242} (1 µM, inhibitor of TLR4) for 24 h. Confocal images were captured in live myotubes (Zeiss LSM 880 with Airyscan detection, Microscopy Facility, Pontificia Universidad Católica de Chile). Mitochondrial number and density were quantified using Fiji/ImageJ software.

2.2.3 Myotube preparation for TEM and image analysis

After 24 h of treatment, the myotubes were dissociated with trypsine (Thermo Fisher Scientific), centrifuged, and pellefixed in 2% glutaraldehyde. The fixed pellet was dissected into fiber bundles and analyzed by TEM (Tecnai T12 at 80 kV, Philips; Microscopy Facility, Pontificia Universidad Católica de Chile). Mitochondrial morphology was evaluated as previously described (Vincent et al., 2016; Castro-Sepúlveda et al., 2021a). Example of morphometric analyses in Supplementary Figure S2.

2.2.4 Oxygen consumption

Live myotubes were resuspended in PBS (500 µL) and placed in a gas-tight chamber. Basal oxygen consumption rate (OCR) was measured at 37°C using a Clark electrode (Yellow Springs Instruments) (Castro-Sepúlveda et al., 2021b).

2.2.5 Single-cell fluorescent hexose uptake assay

Myotubes were treated with insulin (100 nM, Actrapid, Novo-Nordisk, Denmark) for 20 min. After, the myotubes were washed and incubated with 2-NBDG (Molecular Probes, Invitrogen, Carlsbad; 300 µM) for 15 min, and transferred to a confocal microscope (Carl Zeiss Pascal 5; Universidad de Chile). Hexose uptake was estimated by comparing intracellular fluorescence with the extracellular signal of live myotubes (Rosales-Soto et al., 2020). The images were quantified by Fiji/ImageJ software.

2.3 Statistics

Data are presented as means and standard deviations. Correlations were analyzed using Pearson test. Comparisons between groups were performed using Kruskal–Wallis test and Dunn´s *post hoc* test for multiple comparisons. A two-way ANOVA was used (after logarithmic transformation) to compare 2-NBDG myotube uptake between groups. $p < 0.05$ was considered significant. Prism 7 (GraphPad Software, La Jolla, CA) was used for analyses.

3 Results

TLR4 protein expression did not correlate with age, body mass index, or metabolic parameters (Table 1).

The protein expression of TLR4 did not correlate with outer mitochondrial membrane pro-fusion Mfn1 and Mfn2 (Figure 1A), nor with pro-fission Fis1, Drp1 and Drp1Ser616 (Figure 1B). A negative correlation was detected between the protein expression of TLR4 and the inner mitochondrial membrane pro-fusion Opa1 (r = −0.61; p = 0.03; Figure 1A). TLR4 protein expression was negatively correlated with SDHB (complex II; r = −0.55; p = 0.06; Figure 1C), UQCRC2 (complex III; r = −0.70; p = 0.01; Figure 1C), and ATP5A protein expression (r = −0.62; p = 0.03; Figure 1C). Morphometric analysis revealed a negative correlation between TLR4 protein expression and mitochondrial size (r = −0.55; p = 0.06; Figures 1D, F), but not with mitochondrial density (r = −0.06; p = 0.85; Figures 1E, D).

LPS treatment led to a higher mitochondrial number (p = 0.008; Figures 2A, B), but did not modify mitochondrial density (Figures 2A, C) nor myotube basal respiration (Figure 2D), compared to CTRL. When myotubes were co-treated with LPS and TAK^{242}, no differences were found in mitochondrial number (Figure 2B) compared to CTRL. We confirmed by TEM that LPS altered the mitochondrial morphology (Figures 2E–H). As mitochondrial fusion/fission imbalances may alter mitochondrial cristae structure (Otera et al., 2016; Castro-Sepúlveda et al., 2021a), we evaluated the effects of LPS and TAK^{242} treatment on cristae structure in human myotubes (Figures 2E, I–K). LPS reduced the mitochondrial cristae number (p = 0.012; Figure 2I) and increased

TABLE 1 Correlation of TLR4 protein expression with age, body mass index, and metabolic parameters.

n = 12	r value	*p*-value
Age (y)	−0.27	0.39
Body mass index (kg·m^{-2})	−0.21	0.51
Glucose (mg·dl^{-1})	−0.30	0.34
Insulin (μUl·ml^{-1})	−0.26	0.42
HOMA-IR	−0.25	0.44
VO_{2max} (ml·kg^{-1}·min^{-1})	0.09	0.77

HOMA-IR, homeostasis model assessment of insulin resistance; VO2max, maximal oxygen uptake.

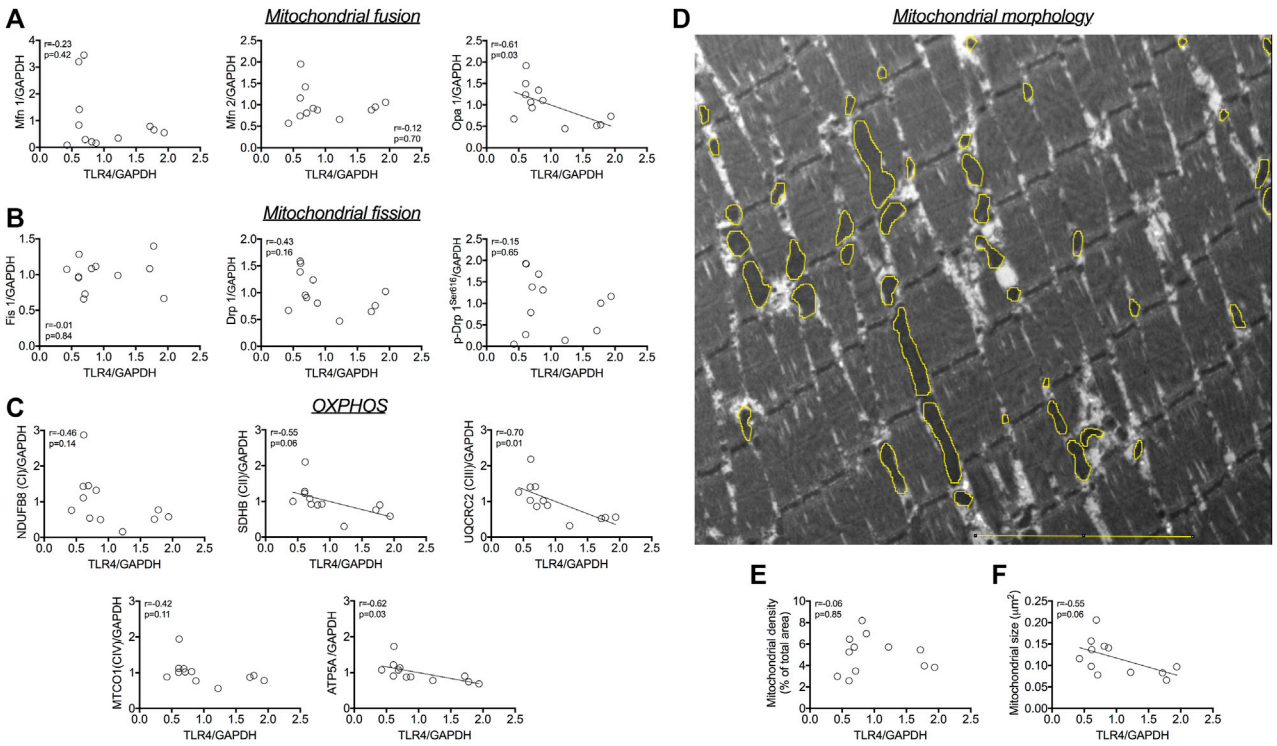

FIGURE 1
Association between TLR4 protein and **(A)** pro-fusion mitochondrial protein expression (Mfn1, Mfn2 and Opa 1). Association between TLR4 protein and **(B)** pro-fission mitochondrial protein expression (Fis1, Drp1 and Drp1Ser616). Association between TLR4 protein expression and **(C)** OXPHOS proteins **(D)** Representative image of mitochondria in skeletal muscle; in yellow, example of masks drawing over outer mitochondrial membrane to evaluate mitochondrial morphology. Correlation between TLR4 protein expression and **(E)** mitochondrial size, and **(F)** mitochondrial density. Associations were tested using Pearson tests (n = 12). Bar, 5 μm. Associations were tested using Pearson tests (n = 12).

the percentage of mitochondrial nanotunnels (p = 0.011; Figure 2J) and abnormal mitochondrial cristae (p = 0.019; Figure 2K), which were all mitigated by the addition of TAK^{242} to LPS.

The role of TLR4 in mitochondrial disturbances was then investigated in a clinical model of inflammation such as myotubes from T2DM patients. T2DM myotubes had less elongated mitochondria (p = 0.028; Figures 3A–D), a higher percentage of abnormal mitochondria cristae (p = 0.047; Figures 3A, E), and a lower number of mitochondrial cristae (p = 0.008; Figures 3A, F) than health CTRL myotubes, which were reversed when T2DM myotubes were treated with TAK^{242}. As it has previously been evidenced that restoration of the connected mitochondrial phenotype in myotubes from insulin-resistant patients by a mitochondrial anti-fission drug restored insulin-stimulated glucose uptake (Kugler et al., 2021), we evaluated whether restoration of the connected mitochondrial phenotype by TAK^{242} contributed to insulin-stimulated glucose uptake in myotubes of patients with T2DM. As expected, we found that insulin increased 2-NBDG uptake in CTRL (p = 0.022) but not in T2DM myotubes (Figures 3G, H). TAK^{242} treatment restored

10.3389/fcell.2023.1212779

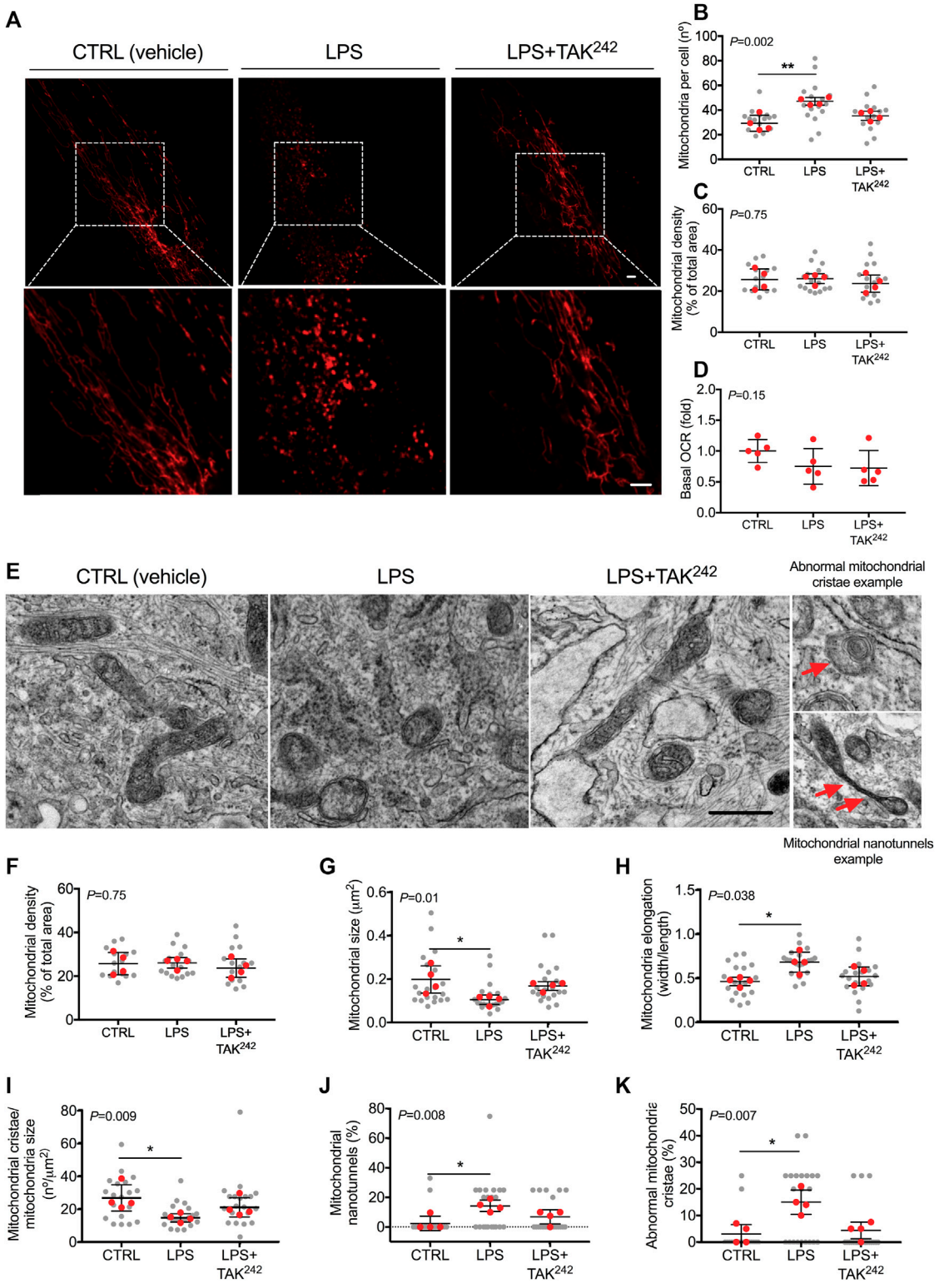

FIGURE 2
(A) Representative image of mitochondria in live human myotubes transfected with mtDsRed (Red) and treated with DMSO (vehicle, CTRL), LPS and LPS + TAK^{242}, Bar, 20 µm **(B)** Mitochondrial number per cell **(C)** mitochondrial density and **(D)** basal OCR in live human myotubes treated with vehicle, LPS, and LPS + TAK^{242} **(E)** Representative electron microscopy image of mitochondria in human myotubes treated with DMSO (vehicle, CTRL), LPS, and LPS + TAK^{242}, Bar, 1 µm **(E)** Representative image of mitochondria morphology, abnormal mitochondrial cristae and nanotunnels (red arrows) in TEM. Mitochondrial **(F)** density, **(G)** size, **(H)** elongation, **(I)** cristae number, **(J)** nanotunnels and **(K)** abnormal cristae in human myotubes treated with vehicle, LPS and LPS + TAK^{242}. n = 4 independent experiments per group; 4-7 myotubes per experiment. The red points in the graphs indicate the mean of the 4 independent experiments. The gray points indicate technical replicates. Data shown in the graphs are means and SD. p-value of the Kruskal–Wallis test is given at the top left of each graph. **, $p < 0.01$, *, $p < 0.05$ from the Dunn's test.

10.3389/fcell.2023.1212779

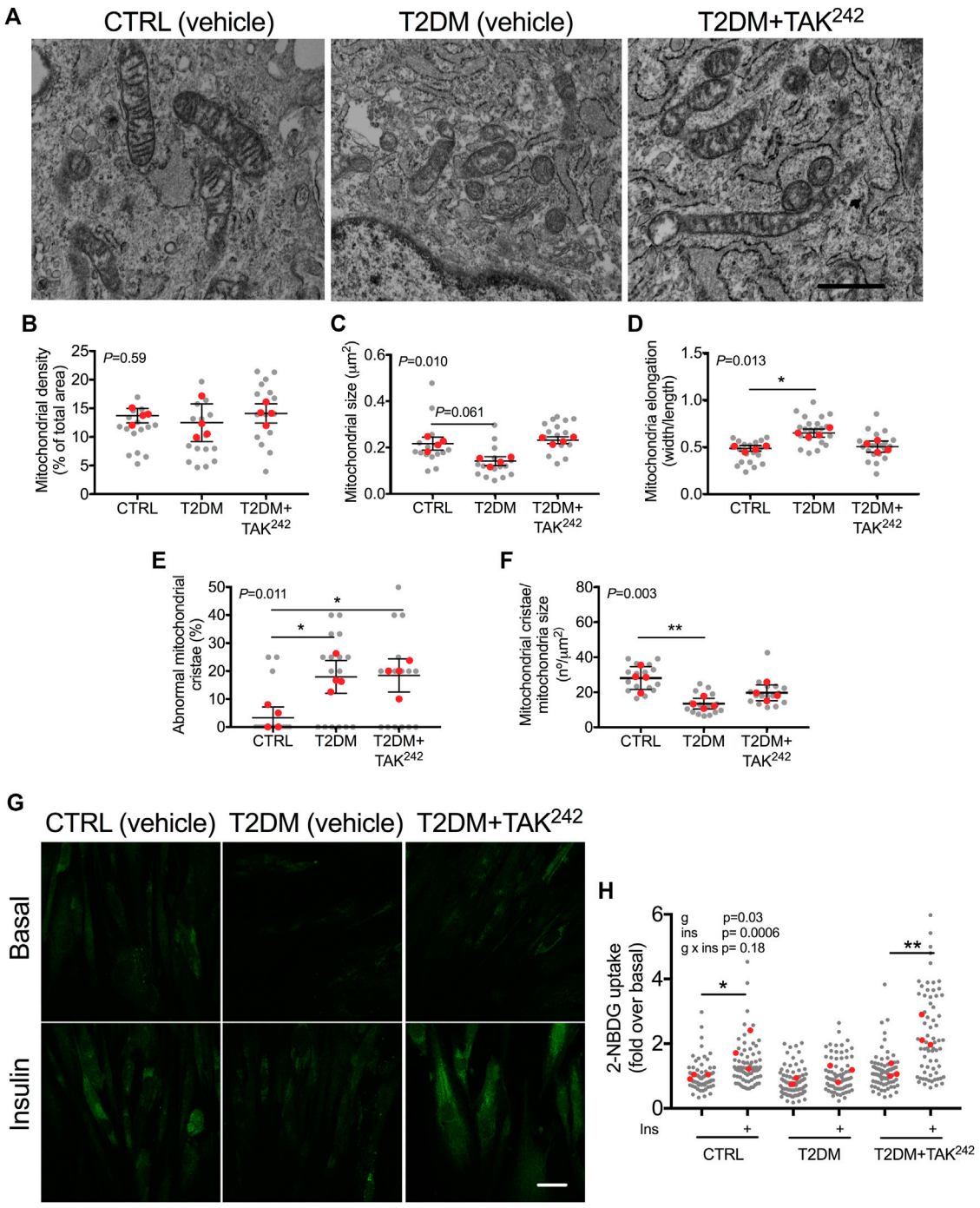

FIGURE 3
(A) Representative image of mitochondria in human myotubes treated with DMSO (vehicle, CTRL), myotubes from people with type 2 diabetes mellitus (T2DM) and T2DM myotubes treated with TAK^{242}. Mitochondrial **(B)** density **(C)** size **(D)** elongation **(E)** abnormal cristae and **(F)** cristae number in CTRL, T2DM and T2DM + TAK^{242} myotubes. *p*-value of the Kruskal–Wallis test is given at the top left of each graph. *, $p < 0.05$ and **, $p < 0.01$ from the Dunn's test. **(G)** Representative image of 2-NBDG (green) and **(H)** 2-NBDG uptake in CTRL, T2DM and T2DM + TAK^{242} myotubes in basal and insulin-stimulated conditions. *p*-values of the 2-way ANOVA are given at the top left. *, $p < 0.05$ and **, $p < 0.01$ from the *post hoc* Dunn's test. n = 3-4 independent experiments per group; 4–10 myotubes per experiment. The red points in the graphs indicate the mean of the 4 independent experiments. The gray points indicate technical replicates. Data shown in the graphs are means and SD. Bar in A, 1 µm; Bar in F, 10 µm.

insulin-stimulated 2-NBDG uptake in T2DM myotubes ($p = 0.006$; Figures 3G, H). We found no differences between the CTRL, T2DM, nor T2DM + TAK^{242} groups in basal conditions (-Ins). In insulin-stimulated conditions (+Ins), we found differences between CTRL and T2DM ($p = 0.052$), T2DM and TAK^{242} ($p = 0.02$), but not between CTRL and TAK^{242} ($p = 0.26$).

4 Discussion

We hypothesized in this study that in human SkM, mitochondrial morphology could be regulated by the TLR4 pathway, which could in turn contribute to changes in insulin resistance. The main findings were that: 1) in human SkM *in vivo*, TLR4 protein expression was negatively correlated to Opa1 protein expression and mitochondrial size; 2) in human myotubes, LPS-induced activation of TLR4 increased mitochondrial fragmented phenotype and increased the percentage of abnormal mitochondrial cristae and nanotunnels, which was reversed when TAK^{242} was added to LPS; and 3) T2DM myotubes displayed a mitochondrial fragmented phenotype, and abnormal mitochondrial cristae structure compared to healthy myotubes, which was partially rescued when T2DM myotubes were treated with TAK^{242}; 4) TAK^{242} restored the lower insulin-stimulated glucose uptake in T2DM compared to healthy myotubes; potentially due to restoration of the connected mitochondrial phenotype as previously evidenced (Jheng et al., 2012; Kugler et al., 2021).

Previous studies have shown that the TLR4 pathway may regulate mitochondrial morphology in *vitro* muscle models and in murine cardiac muscle. C2C12 cells treated with LPS for 24 h increased the mitochondrial fragmented phenotype (Eggelbusch et al., 2022). In mice, intraperitoneal injection of LPS twice a week for 5 weeks induced a mitochondrial fragmented phenotype in the cardiac muscle and lower Opa1 and Mfn1 protein expression (Wu et al., 2018). In line with this, we found a positive correlation between TLR4 protein expression in skeletal muscle and the mitochondrial fragmented phenotype. Interestingly, we found that higher TLR4 protein expression was associated with lower Opa1 protein expression in human SkM, as was found in murine cardiomyocytes treated with LPS (Wu et al., 2018). Opa1 is a pro-fusion mitochondrial protein and plays a role in mitochondrial cristae morphology (Cartes-Saavedra et al., 2023). Therefore, Opa1 might mediate TLR4-induced inflammation to regulate mitochondrial fusion and mitochondrial cristae. Finally, TLR4 protein expression was negatively correlated with OXPHOS (CII, CIII and CV) protein expression. This suggests that TLR4 could regulate the oxidative capacity in human SkM through the regulation of mitochondrial morphology. Regarding the mechanism by which the activation of TLR4 by LPS regulates Opa1 and OXPHOS, it has recently been shown in renal tubular epithelial cells that LPS decreased deacetylation of i-AAA protease (YME1L1), an upstream regulatory molecule of OPA1 (Jian et al., 2023). Therefore, we speculate that chronic low-grade inflammation in young subjects could decrease the OPA1 protein expression through YMEIL1. The chronic low-grade inflammation-induced decrease in Opa1 may be an initial step in the development of metabolic alterations in the SkM of young subjects, but this requires further investigation. Another potential mediator of LPS-induced changes in mitochondrial structure alterations in SkM is sarcopilin, however, more studies are needed to confirm this (Bal et al., 2021).

In SkM, mitochondrial cristae density is associated with metabolic capacity in humans (Castro-Sepulveda et al., 2023) and thermogenesis in mice (Bal et al., 2017). However, it is not fully understood how mitochondrial cristae density or architecture is regulated. A potential regulator is inflammation, as we showed that COVID-19 patients with severe infection, characterized by higher systemic inflammation, had a lower mononuclear cell mitochondrial cristae density (Castro-Sepulveda et al., 2022). Our study in human myotubes is the first to evaluate the effects of LPS on mitochondrial cristae architecture. Our results showed that LPS treatment induced abnormal mitochondrial cristae, mitochondrial nanotunnels, and reduced mitochondrial cristae density, which was reversed upon LPS co-treatment with TAK^{242}. Mitochondrial nanotunnels were previously described in human SkM myopathy (Vincent et al., 2016), and inflammation is one of the characteristics of myopathies. Emerging evidence suggests that mitochondrial nanotunnels are generated by immobilized mitochondria (Vincent et al., 2017). One could hypothesize that TLR4-induced inflammation could immobilize mitochondria, but this must be investigated and confirmed in future studies. Calcium release from the endoplasmic reticulum and shuttle to mitochondria could contribute to the regulation of mitochondrial cristae by TLR4 (Swalsingh et al., 2022). In summary, our results show that LPS induced a mitochondrial fragmented phenotype and induced alterations in mitochondrial cristae, which was reversed upon LPS co-treatment with TAK^{242} in human myotubes.

Cultured human myotubes from T2DM patients maintain the same phenotype characteristics as the donor with diabetes, such as the inflammatory state (Gaster et al., 2002; Hansen et al., 2004). Hence, we evaluated the effects of TAK^{242} on mitochondrial morphology and cristae, and insulin resistance in myotubes from T2DM patients. Our study is the first to evaluate mitochondrial morphology and mitochondrial cristae in human T2DM myotubes. T2DM human myotubes had a fragmented mitochondrial phenotype, and abnormal mitochondrial cristae structure, which was partially rescued upon TAK^{242} treatment. Our study in T2DM myotubes confirmed the role of TLR4 and inflammation in the regulation of mitochondrial morphology and mitochondrial cristae architecture. Indeed, the treatment with TAK^{242}, a specific inhibitor of TLR4 with anti-inflammatory effect, restored the mitochondrial morphology and partially the architecture of the mitochondrial cristae in T2DM myotubes. Interestingly, the reduced insulin-stimulated glucose uptake in T2DM vs. control myotubes was restored as well after TAK^{242} treatment, together with the restoration of the connected mitochondrial phenotype. A previous study in human myotubes from healthy subjects showed that LPS treatment for 12 h reduced insulin-stimulated glucose uptake (Liang et al., 2013). With respect to the role of mitochondrial morphology in insulin resistance, it has previously been found that both genetic and pharmacological inhibition of mitochondrial fission restored insulin-stimulated glucose uptake in several models of insulin resistance such as lipotoxicity in C2C12, high-fat diet in mice and myotubes from humans with insulin resistance (Jheng et al., 2012; Kugler et al., 2021). Finally, the activation of TLR4 might reduce insulin-stimulated glucose uptake by dysregulation of mitochondrial morphology in primary cardiomyocytes from rats (Parra et al., 2014), which our results confirm in human myotubes. Together those results strongly suggest that activation of the TLR4 pathway induces a mitochondrial fragmented phenotype, which decreases insulin sensitivity.

We based the choice of the concentration and duration for LPS and TAK^{242} on a previous study in a cardiomyocyte cell line using a concentration of 10 μg LPS·ml^{-1} and a duration of incubation of 24 h, conditions that were able to induce a fragmented mitochondrial

phenotype (Wu et al., 2018). In a recent study in C2C12 myotubes, lower LPS concentrations together with a shorter incubation duration (100 ng LPS·ml^{-1} for 2 h) induced a fragmented mitochondrial phenotype as well (Eggelbusch et al., 2022). Finally, in human myotubes, incubation of 50 pg LPS·ml^{-1} and 500 ng·ml^{-1} for 2, 6, 12, and 24 h all induced a similar decrease in fatty acid oxidation (Frisard et al., 2010). Altogether, those results suggest that a wide range of LPS concentrations have similar effects on muscle metabolism *in vitro*. For TAK^{242} concentrations, it seems that a consensus has been reached in the literature for using 1 μM as it is consistently efficient at reducing the harmful effects of LPS or other toxins *in vitro* and *in vivo* (Takashima et al., 2009; Ono and Sakamoto, 2017; Ono et al., 2020).

In conclusion, mitochondrial morphology and mitochondrial cristae seem to be regulated by the TLR4 pathway in human SkM. Those mitochondrial alterations might potentially contribute to insulin resistance in the SkM of patients with T2DM. Both the TLR4 pathway and downstream mitochondrial alterations could therefore be of potential interest in the development of pharmacological treatments against insulin resistance.

Data availability statement

The original contributions presented in the study are included in the article/Supplementary Material, further inquiries can be directed to the corresponding authors.

Ethics statement

The studies involving human participants were reviewed and approved by Finis Terrae. The patients/participants provided their written informed consent to participate in this study.

Author contributions

MC-S contributed to the study conceptualization, methodology, investigation, writing the original draft, review, and editing of the manuscript, and visualization. MT-S, GR-S, and RV-F contributed to the study methodology and investigation. MC-S, LD, and HZ-F contributed to the study conceptualization, methodology, resources, reviewing and editing of the manuscript, supervision, and funding acquisition. MC-S, and HZ-F are the guarantor of this work and, as such, had full access to all the data in the study and takes responsibility for the integrity of the data and the accuracy of the data analysis. All authors contributed to the article and approved the submitted version.

Funding

This work was supported by funding CAI 2021, and CICI 2022 to MC-S, by ANID/CONICYT FONDECYT Iniciación 11230548 to MC-S, and by ANID/CONICYT FONDECYT regular 1231633 to HZ-F. This work was supported by the Unidad de Microscopía Avanzada UC (UMA UC).

Acknowledgments

We sincerely thank all study participants, and Francisco Diaz for technical assistance. We also extend our thanks to Dr. Alvaro Elorza for providing the mtDsRed plasmid.

Conflict of interest

The authors declare that the research was conducted in the absence of any commercial or financial relationships that could be construed as a potential conflict of interest.

Publisher's note

Supplementary material

The Supplementary Material for this article can be found online at: https://www.frontiersin.org/articles/10.3389/fcell.2023.1212779/full#supplementary-material

References

Bal, N. C., Gupta, S. C., Pant, M., Sopariwala, D. H., Gonzalez-Escobedo, G., Turner, J., et al. (2021). Is upregulation of sarcolipin beneficial or detrimental to muscle function? *Front. physiology* 12, 633058. doi:10.3389/fphys.2021.633058

Bal, N. C., Maurya, S. K., Pani, S., Sethy, C., Banerjee, A., Das, S., et al. (2017). Mild cold induced thermogenesis: Are BAT and skeletal muscle synergistic partners? *Biosci. Rep.* 37 (5), BSR20171087. doi:10.1042/BSR20171087

Baron, A. D., Brechtel, G., Wallace, P., and Edelman, S. V. (1988). Rates and tissue sites of non-insulin- and insulin-mediated glucose uptake in humans. *Am. J. physiology* 255 (1), E769–E774. doi:10.1152/ajpendo.1988.255.6.E769

Cartes-Saavedra, B., Lagos, D., Macuada, J., Arancibia, D., Burté, F., Sjöberg-Herrera, M. K., et al. (2023). OPA1 disease-causing mutants have domain-specific effects on mitochondrial ultrastructure and fusion. *Proc. Natl. Acad. Sci. U. S. A.* 120 (12), e2207471120. doi:10.1073/pnas.2207471120

Castro-Sepulveda, M., Fernández-Verdejo, R., Tuñón-Suárez, M., Morales-Zúñiga, J., Troncoso, M., Jannas-Vela, S., et al. (2021b). Low abundance of Mfn2 protein correlates with reduced mitochondria-SR juxtaposition and mitochondrial cristae density in human men skeletal muscle: Examining organelle measurements from TEM images. *FASEB* 35 (4), e21553. doi:10.1096/fj.202002615RR

Castro-Sepulveda, M., Fernández-Verdejo, R., Zbinden-Foncea, H., and Rieusset, J. (2023). Mitochondria-SR interaction and mitochondrial fusion/fission in the regulation of skeletal muscle metabolism. *Metabolism Clin. Exp.* 144, 155578. doi:10.1016/j.metabol.2023.155578

Castro-Sepulveda, M., Jannas-Vela, S., Fernández-Verdejo, R., Ávalos-Allele, D., Tapia, G., Villagrán, C., et al. (2020). Relative lipid oxidation associates directly with mitochondrial fusion phenotype and mitochondria-sarcoplasmic reticulum interactions in human skeletal muscle. *Am. J. physiology. Endocrinol. metabolism* 318 (6), E848–E855. doi:10.1152/ajpendo.00025.2020

Castro-Sepúlveda, M., Morio, B., Tuñón-Suárez, M., Jannas-Vela, S., Díaz-Castro, F., Rieusset, J., et al. (2021a). The fasting-feeding metabolic transition regulates mitochondrial dynamics. *FASEB* 35 (10), e21891. doi:10.1096/fj.202100929R

Castro-Sepulveda, M., Tapia, G., Tuñón-Suárez, M., Diaz, A., Marambio, H., Valero-Breton, M., et al. (2022). Severe COVID-19 correlates with lower mitochondrial cristae density in PBMCs and greater sitting time in humans. *Physiol. Rep.* 10 (14), e15369. doi:10.14814/phy2.15369

Dasu, M. R., Devaraj, S., Park, S., and Jialal, I. (2010). Increased toll-like receptor (TLR) activation and TLR ligands in recently diagnosed type 2 diabetic subjects. *Diabetes care* 33 (4), 861–868. doi:10.2337/dc09-1799

Eggelbusch, M., Shi, A., Broeksma, B. C., Vázquez-Cruz, M., Soares, M. N., de Wit, G. M. J., et al. (2022). The NLRP3 inflammasome contributes to inflammation-induced morphological and metabolic alterations in skeletal muscle. *J. cachexia, sarcopenia muscle* 13 (6), 3048–3061. doi:10.1002/jcsm.13062

Frisard, M. I., McMillan, R. P., Marchand, J., Wahlberg, K. A., Wu, Y., Voelker, K. A., et al. (2010). Toll-like receptor 4 modulates skeletal muscle substrate metabolism. *Am. J. physiology. Endocrinol. metabolism* 298 (5), E988–E998. doi:10.1152/ajpendo.00307.2009

Gaster, M., Petersen, I., Højlund, K., Poulsen, P., and Beck-Nielsen, H. (2002). The diabetic phenotype is conserved in myotubes established from diabetic subjects: Evidence for primary defects in glucose transport and glycogen synthase activity. *Diabetes* 51 (4), 921–927. doi:10.2337/diabetes.51.4.921

Hansen, L., Gaster, M., Oakeley, E. J., Brusgaard, K., Damsgaard Nielsen, E. M., Beck-Nielsen, H., et al. (2004). Expression profiling of insulin action in human myotubes: Induction of inflammatory and pro-angiogenic pathways in relationship with glycogen synthesis and type 2 diabetes. *Biochem. biophysical Res. Commun.* 323 (2), 685–695. doi:10.1016/j.bbrc.2004.08.146

Islam, H., Edgett, B. A., and Gurd, B. J. (2018). Coordination of mitochondrial biogenesis by PGC-1α in human skeletal muscle: A re-evaluation. *Metabolism Clin. Exp.* 79, 42–51. doi:10.1016/j.metabol.2017.11.001

Jheng, H. F., Tsai, P. J., Guo, S. M., Kuo, L. H., Chang, C. S., Su, I. J., et al. (2012). Mitochondrial fission contributes to mitochondrial dysfunction and insulin resistance in skeletal muscle. *Mol. Cell. Biol.* 32 (2), 309–319. doi:10.1128/MCB.05603-11

Jian, Y., Yang, Y., Cheng, L., Yang, X., Liu, H., Li, W., et al. (2023). Sirt3 mitigates LPS-induced mitochondrial damage in renal tubular epithelial cells by deacetylating YME1L1. *Cell Prolif.* 56 (2), e13362. doi:10.1111/cpr.13362

Kelley, D. E., He, J., Menshikova, E. V., and Ritov, V. B. (2002). Dysfunction of mitochondria in human skeletal muscle in type 2 diabetes. *Diabetes* 51 (10), 2944–2950. doi:10.2337/diabetes.51.10.2944

Kugler, B. A., Deng, W., Duguay, A. L., Garcia, J. P., Anderson, M. C., Nguyen, P. D., et al. (2021). Pharmacological inhibition of dynamin-related protein 1 attenuates skeletal muscle insulin resistance in obesity. *Physiol. Rep.* 9 (7), e14808. doi:10.14814/phy2.14808

Liang, H., Hussey, S. E., Sanchez-Avila, A., Tantiwong, P., and Musi, N. (2013). Effect of lipopolysaccharide on inflammation and insulin action in human muscle. *PloS one* 8 (5), e63983. doi:10.1371/journal.pone.0063983

Ono, Y., Maejima, Y., Saito, M., Sakamoto, K., Horita, S., Shimomura, K., et al. (2020). TAK-242, a specific inhibitor of Toll-like receptor 4 signalling, prevents endotoxemia-induced skeletal muscle wasting in mice. *Sci. Rep.* 10 (1), 694. doi:10.1038/s41598-020-57714-3

Ono, Y., and Sakamoto, K. (2017). Lipopolysaccharide inhibits myogenic differentiation of C2C12 myoblasts through the Toll-like receptor 4-nuclear factor-κB signaling pathway and myoblast-derived tumor necrosis factor-α. *PloS one* 12 (7), e0182040. doi:10.1371/journal.pone.0182040

Otera, H., Miyata, N., Kuge, O., and Mihara, K. (2016). Drp1-dependent mitochondrial fission via MiD49/51 is essential for apoptotic cristae remodeling. *J. Cell. Biol.* 212 (5), 531–544. doi:10.1083/jcb.201508099

Parra, V., Verdejo, H. E., Iglewski, M., Del Campo, A., Troncoso, R., Jones, D., et al. (2014). Insulin stimulates mitochondrial fusion and function in cardiomyocytes via the Akt-mTOR-NFκB-Opa-1 signaling pathway. *Diabetes* 63 (1), 75–88. doi:10.2337/db13-0340

Pedersen, B. K., and Febbraio, M. A. (2012). Muscles, exercise and obesity: Skeletal muscle as a secretory organ. *Nat. Rev. Endocrinol.* 8 (8), 457–465. doi:10.1038/nrendo.2012.49

Reyna, S. M., Ghosh, S., Tantiwong, P., Meka, C. S., Eagan, P., Jenkinson, C. P., et al. (2008). Elevated toll-like receptor 4 expression and signaling in muscle from insulin-resistant subjects. *Diabetes* 57 (10), 2595–2602. doi:10.2337/db08-0038

Rosales-Soto, G., Diaz-Vegas, A., Casas, M., Contreras-Ferrat, A., and Jaimovich, E. (2020). Fibroblast growth factor-21 potentiates glucose transport in skeletal muscle fibers. *J. Mol. Endocrinol.* 65, 85–95. JME-19-0210.R2. Advance online publication. doi:10.1530/JME-19-0210

Swalsingh, G., Pani, P., and Bal, N. C. (2022). Structural functionality of skeletal muscle mitochondria and its correlation with metabolic diseases. *Clin. Sci.* 136 (24), 1851–1871. doi:10.1042/CS20220636

Takashima, K., Matsunaga, N., Yoshimatsu, M., Hazeki, K., Kaisho, T., Uekata, M., et al. (2009). Analysis of binding site for the novel small-molecule TLR4 signal transduction inhibitor TAK-242 and its therapeutic effect on mouse sepsis model. *Br. J. Pharmacol.* 157 (7), 1250–1262. doi:10.1111/j.1476-5381.2009.00297.x

Valero-Breton, M., Warnier, G., Castro-Sepulveda, M., Deldicque, L., and Zbinden-Foncea, H. (2020). Acute and chronic effects of high frequency electric pulse stimulation on the akt/mTOR pathway in human primary myotubes. *Front. Bioeng. Biotechnol.* 8, 565679. doi:10.3389/fbioe.2020.565679

Vincent, A. E., Ng, Y. S., White, K., Davey, T., Mannella, C., Falkous, G., et al. (2016). The spectrum of mitochondrial ultrastructural defects in mitochondrial myopathy. *Sci. Rep.* 6, 30610. doi:10.1038/srep30610

Vincent, A. E., Turnbull, D. M., Eisner, V., Hajnóczky, G., and Picard, M. (2017). Mitochondrial nanotunnels. *Trends Cell. Biol.* 27 (11), 787–799. doi:10.1016/j.tcb.2017.08.009

Wu, B., Li, J., Ni, H., Zhuang, X., Qi, Z., Chen, Q., et al. (2018). TLR4 activation promotes the progression of experimental autoimmune myocarditis to dilated cardiomyopathy by inducing mitochondrial dynamic imbalance. *Oxidative Med. Cell. Longev.* 2018, 3181278. doi:10.1155/2018/3181278

frontiers | Frontiers in Molecular Biosciences

TYPE Review
PUBLISHED 03 August 2023
DOI 10.3389/fmolb.2023.1241225

OPEN ACCESS

EDITED BY
Vincenzo Lionetti,
Sant'Anna School of Advanced Studies, Italy

REVIEWED BY
Francisco O. Silva,
University of Texas Southwestern Medical Center, United States
Vaibhav Deshmukh,
Washington University in St. Louis, United States

*CORRESPONDENCE
Yuquan He,
heyq@jlu.edu.cn
Xin Hu,
huxin@jlu.edu.cn

†These authors have contributed equally to this work

RECEIVED 16 June 2023
ACCEPTED 24 July 2023
PUBLISHED 03 August 2023

CITATION
Chen R, Niu M, Hu X and He Y (2023), Targeting mitochondrial dynamics proteins for the treatment of doxorubicin-induced cardiotoxicity. *Front. Mol. Biosci.* 10:1241225. doi: 10.3389/fmolb.2023.1241225

Targeting mitochondrial dynamics proteins for the treatment of doxorubicin-induced cardiotoxicity

Rui Chen[1], Mengwen Niu[2], Xin Hu[1*†] and Yuquan He[1*†]

[1]Department of Cardiology, China-Japan Union Hospital of Jilin University, Changchun, China, [2]Department of Rheumatology and Immunology, China-Japan Union Hospital of Jilin University, Changchun, China

Doxorubicin (DOX) is an extensively used chemotherapeutic agent that can cause severe and frequent cardiotoxicity, which limits its clinical application. Although there have been extensive researches on the cardiotoxicity caused by DOX, there is still a lack of effective treatment. It is necessary to understand the molecular mechanism of DOX-induced cardiotoxicity and search for new therapeutic targets which do not sacrifice their anticancer effects. Mitochondria are considered to be the main target of cardiotoxicity caused by DOX. The imbalance of mitochondrial dynamics characterized by increased mitochondrial fission and inhibited mitochondrial fusion is often reported in DOX-induced cardiotoxicity, which can result in excessive ROS production, energy metabolism disorders, cell apoptosis, and various other problems. Also, mitochondrial dynamics disorder is related to tumorigenesis. Surprisingly, recent studies show that targeting mitochondrial dynamics proteins such as DRP1 and MFN2 can not only defend against DOX-induced cardiotoxicity but also enhance or not impair the anticancer effect. Herein, we summarize mitochondrial dynamics disorder in DOX-induced cardiac injury. Furthermore, we provide an overview of current pharmacological and non-pharmacological interventions targeting proteins involved in mitochondrial dynamics to alleviate cardiac damage caused by DOX.

KEYWORDS

doxorubicin (Dox), cardiotoxicity, anticancer effect, mitochondrial dynamics, pharmacological and non-pharmacological interventions

1 Introduction

Due to population growth and improvements in the early identification and treatment of cancers, the number of cancer survivors is increasing, but the survivors often encounter adverse cardiovascular events linked to their cancer therapy or as a result of the worsening of underlying cardiovascular disease (Curigliano et al., 2016), such as arrhythmia, treatment-induced hypertension, thromboembolic ischemia, or heart failure (Narezkina and Nasim, 2019).

It is well established that anthracyclines are usually highly efficacious in the treatment of solid tumors and hematological malignancies but may cause cardiac damage, usually irreversible, which can affect prognosis (Felker et al., 2000; Octavia et al., 2012; Mitry and Edwards, 2016). Doxorubicin (DOX), an antibiotic anthracycline, is frequently used in the treatment of various cancers, including breast cancer, leukemia, and pediatric cancer. There have been documented cases of heart failure that were shown to be closely related to

cumulative DOX dosing. When a cumulative lifetime dose of DOX reached 400 mg/m^2, congestive heart failure was 5% more likely to occur, and heart failure had a 48% probability of occurring at 700 mg/m^2 (Swain et al., 2003). It is because of its tendency to cause severe cardiotoxicity that the use of DOX in the treatment of cancer is limited.

To date, several processes have been proposed as potential causes of DOX cardiotoxicity, including DNA damage, mitochondrial dysfunction, oxidative stress, and various types of cell death such as apoptosis (Zhang et al., 2012; Kalyanaraman, 2020; Wallace et al., 2020; Wu et al., 2022a). But effective targeted treatments for DOX cardiotoxicity are still insufficient. Given that cardiac mitochondrial damage is predicted to occur within a few hours after DOX administration (Renu et al., 2018), abnormality of mitochondrial morphology and dysfunction are drawing increasing attention. And amounts of studies demonstrate that the imbalance of mitochondrial dynamics tends to enhance mitochondrial fission and weaken mitochondrial fusion underlying DOX treatment in cardiomyocytes and hearts. Now, a thorough report on the role of mitochondrial dynamics proteins in cardiomyocytes countering DOX treatment is showed in this paper, and the pharmacological and non-pharmacological interventions targeting impaired mitochondrial dynamics is presented. This information can aid in the development of additional cardioprotective measures.

2 Current mechanisms of DOX-induced cardiotoxicity: oxidative stress and DNA damage

Mitochondria are a major cellular target of DOX. It has been previously demonstrated that mitochondrial damage is strongly linked to DOX-induced cardiotoxicity (Wallace et al., 2020; Schirone et al., 2022). By accumulation in mitochondria of cardiomyocytes, DOX increase ROS production and decrease energy production, causing cell apoptosis (Songbo et al., 2019). Excessive accumulation of intracellular ROS is associated with the modification of mitochondrial dynamics, which play an important role in maintaining mitochondrial function and mediating mitophagy (Songbo et al., 2019). It is widely accepted that the generation of reactive oxygen species (ROS) via redox cycling is a significant source of dose-dependent cardiotoxicity caused by DOX (Varga et al., 2015; Mitry and Edwards, 2016). Anthracyclines can be converted into semiquinone doxorubicin (SQ-DOX), which is catalyzed by nicotinamide adenine dinucleotide phosphate oxidase and nitric oxide synthases in the cytoplasm (Songbo et al., 2019). Due to its unstable structural properties and a high affinity between DOX and cardiolipin at the inner mitochondrial membrane, SQ-DOX can be easily oxidized in the mitochondria, causing the release and accumulation of ROS (Songbo et al., 2019). Excessive ROS production can cause various types of cellular damage and, eventually, cell death. Because the cardiomyocytes have a higher concentration of mitochondria and the heart has lower levels of antioxidant enzymes such as superoxide dismutase (SOD) than other organs, it makes sense that the heart is more susceptible to damage by anthracycline-induced ROS generation (Songbo et al., 2019). Excessive amounts of ROS can cause the opening of mitochondrial permeability transition pores (mPTP) and lead to irreversible loss of mitochondrial membrane potential (MMP), causing mitochondrial damage and cell death (Zorov et al., 2000). Therefore, previous studies initially used antioxidants to combat the cardiotoxicity of anthracyclines. However, the cardioprotective effects of the antioxidants did not result in therapeutic advantages in avoiding or repairing myocardial dysfunction and heart failure in DOX-treated patients (Broeyer et al., 2014; Yeh and Chang, 2016).

Topoisomerase II (Top2), found in eukaryotic cells, is involved in DNA metabolism. This enzyme plays crucial roles in chromosome organization and segregation to support cell growth by unwinding, unknotting, and untangling genetic material by creating momentary double-stranded breaks in DNA (McClendon and Osheroff, 2007). There are two forms of topoisomerase II (Top2): Top2α and Top2β. TOP2α, undetectable in adult cardiomyocytes, is overexpressed in tumor cells, and DOX exerts cytotoxicity in tumor cells by forming Top2α-DOX-DNA complex, responsible for DNA breakage and tumor cell death (Kalyanaraman, 2020). Unexpectedly, TOP2β in adult cardiomyocytes is also a target of DOX, resulting in a Top2β-DOX-DNA ternary complex that causes DNA breakage, cell death and damages in the heart eventually. So, Top2β in cardiomyocytes is also thought to mediate DOX-induced cardiotoxicity (Kalyanaraman, 2020). By the cardiomyocyte-specific deletion of *Top2β* (encoding Top2β), progressive heart failure caused by DOX can be prevented (Zhang et al., 2012). In addition, during DOX exposure, iron metabolism may be directly disrupted by the interruption of key iron-binding and transporter proteins, resulting in iron accumulation in the mitochondria and ferroptosis, which is a type of iron-dependent programmed cell death (Huang et al., 2022). Several previous studies have demonstrated that DOX-induced mitochondrial iron overload and subsequent mitochondria-dependent ferroptosis are major contributing factors in the cardiotoxicity of anthracyclines (Quagliariello et al., 2021; Shan et al., 2021; Huang et al., 2022). Further investigation is warranted to investigate whether ferroptosis inhibitors can be used as cardiac protectors against anthracycline cardiotoxicity. At present, dexrazoxane (DEX) is the only drug recognized by the FDA as being effective in preventing cardiomyopathy and heart failure brought on by anthracycline anticancer drugs (Zamorano et al., 2017). DEX prevents cardiac Top2β from binding to DOX, thus avoiding the formation of DNA double-strand breaks that can result from anthracycline-TOP2β-DNA cleavage complex (Deng et al., 2014; Bures et al., 2017; Corremans et al., 2019; Hasinoff et al., 2020). Also, DEX acts as an iron chelator, alleviating iron accumulation in mitochondria and subsequent ferroptosis (Xu et al., 2005; Hasinoff et al., 2020). However, it can unexpectedly bind to Top2α, which can result in a disruption of the form of Top2α-DOX-DNA, and thus DEX can reduce the anticancer effect of DOX and even increase the risk of secondary malignancies (Tebbi et al., 2007; Vejpongsa and Yeh, 2014).

Recent studies have demonstrated increased mitochondrial fission and inhibited fusion in cardiomyocytes under DOX treatment, resulting in mitochondrial morphological abnormality and dysfunction, accompanied by excessive ROS production, energy metabolism disorders, cell apoptosis, and cardiac dysfunction

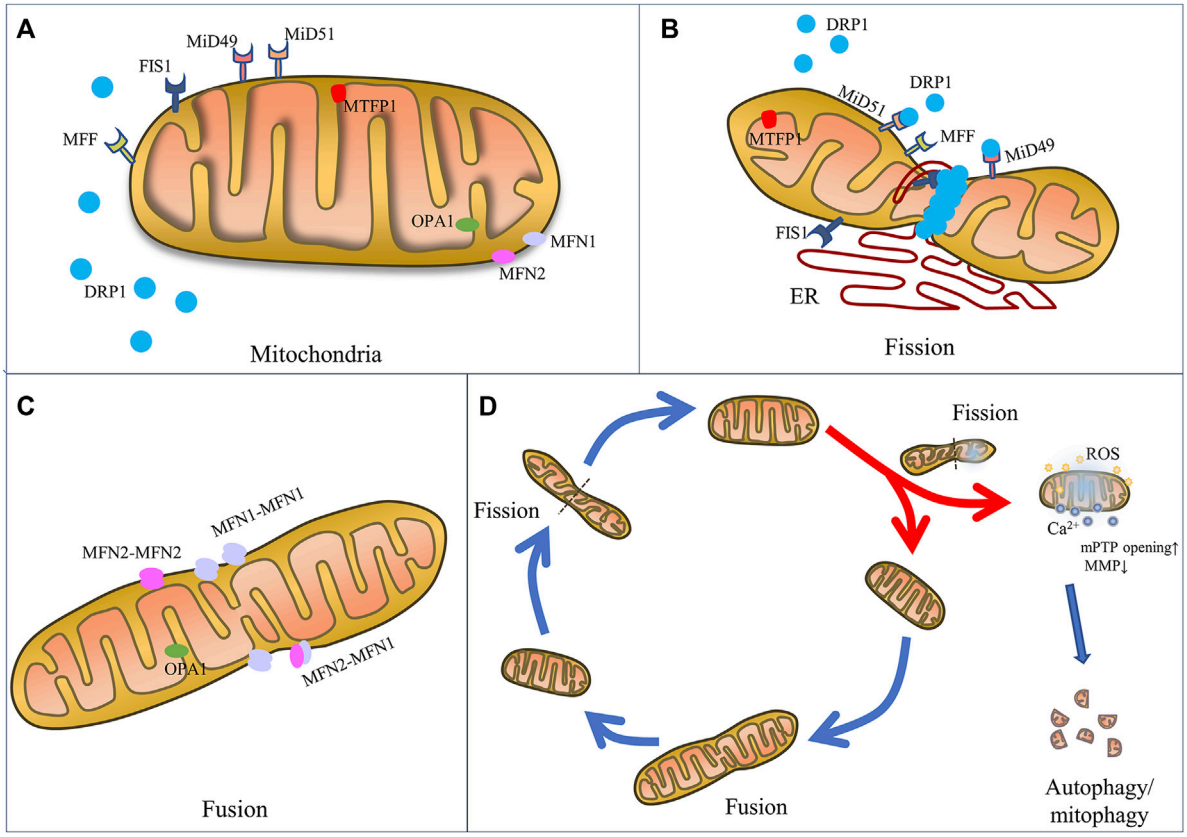

FIGURE 1
The mechanics of mitochondrial fission and fusion. Schematic representation of mitochondrial fusion and fission machinery and related cell function. **(A)** Mitochondrial dynamics-associated key mediators including pro-fission proteins (DRP1, FIS1, MFF, MiD49, MiD51, and MTF18) and pro-fusion proteins (MFN1, MFN2, and OPA1). **(B)** Mitochondrial fission is mainly regulated by the key player DRP1, OMM receptors (MFF, MiD49, MiD51 and FIS1), which are responsible for the recruitment of DRP1 from the cytosol to mitochondria. And ER wraps mitochondria and identifies the fission site, where DRP1 oligomerizes and induces mem-brane constriction. **(C)** Mitochondrial fusion relies on MFN1 and MFN2 located on the OMM to tether the OMMs of mitochondria, and on OPA1 to mediate fusion of IMM. **(D)** Mitochondrial fate is regulated by fission and fusion to adapt mitochondrial morphology to different stresses. Fission constricts and severs one mitochondrion to daughter mitochondria for cell division or fragmented mitochondria for removal by mitophagy and renewal by fusion into an elongated organelle.

(Carvalho et al., 2014; Catanzaro et al., 2019; Huang et al., 2022). What's more, some compounds have been proven to reduce DOX cardiotoxicity by rebalancing mitochondrial fission and fusion (Osataphan et al., 2020; Wu et al., 2022b), implying the regulation of mitochondrial dynamics imbalance may serve as a potent therapeutic strategy for the reduction of DOX-induced cardiotoxicity.

3 Mitochondrial dynamics

3.1 Mechanics of mitochondrial dynamics

Composed of an inner membrane (IMM) and an outer membrane (OMM) which constantly undergo fusion and fission process, mitochondrial dynamics are finely regulated by a class of dynamin superfamilies known as big GTPases, which are recognized for their capacity to self-assemble and hydrolyze GTP and for their intracellular membrane remodeling activities (Antonny et al., 2016). For example, mitochondrial fission is mainly mediated by a 100 kDa GTPase called dynamin-related protein 1 (DRP1) (Antonny et al., 2016), while mitochondrial fusion is regulated by several specific GTPases, including mitofusin1 (MFN1), mitofusin2 (MFN2) and optic atrophy 1 (OPA1) (Chan, 2020; Giacomello et al., 2020) (Figure 1).

Specifically, mitochondrial fission is the constriction and severance of one mitochondrion to produce fragmented organelles, while mitochondrial fusion is the merging of two or more mitochondria, creating an elongated organelle. The function of mitochondrial fission is to produce two or more daughter mitochondria or mitochondrial fragmentations, which can often be distinguished by varying membrane potentials (Tilokani et al., 2018). In fact, during the mitochondrial life cycle, mitochondrial biogenesis is triggered, causing the formation of new mitochondria, and the mitophagy process occurs, causing the removal of dysfunctional mitochondria or mitochondrial fragmentations generated by mitochondrial fission (Kleele et al., 2021). Fusion is the process by which mitochondria merge to generate a larger organelle, with the fused mitochondria sharing matrix components such as mitochondrial DNA (mtDNA), lipids,

proteins, metabolites, and ions (Tilokani et al., 2018). The distribution and integrity of the mitochondria are preserved by these dynamic morphological changes, thereby maintaining function in order to produce sufficient energy and coordinate cellular biological processes, such as calcium homeostasis, redox equilibrium, and apoptosis, in order to achieve cell homeostasis during physiological changes and resist metabolic and environmental stresses (Giacomello et al., 2020).

3.1.1 Mitochondrial fission

The mitochondrial fission process is regulated by various fission factors, including DRP1, mitochondrial fission 1 protein (FIS1), mitochondrial fission factor (MFF), and mitochondrial dynamics proteins 49 kDa and 51 kDa (known as MiD49 and MiD51). In fact, when DRP1 is recruited into the OMM, endoplasmic reticulum (ER) moves toward the mitochondrial periphery and encircles the mitochondria, causing them to tighten (Kraus and Ryan, 2017). In this stage, the diameter of the mitochondrion is decreased from 300–500 nm–150 nm, which causes the development of DRP1–oligo rings (Kamerkar et al., 2018).

As the main mediator of mitochondrial fission, the DRP1 protein has a GTPase effector domain (GED) that is necessary for the conformational changes in DRP1 helices and their constrictive functions in the OMM (Frohlich et al., 2013). Located in cytosol, DRP1 is recruited by receptors to the OMM and induces membrane constriction through oligomerization, forming a ring structure. Because DRP1 lacks a domain that directly binds to phospholipids in the membrane, its recruitment to the outer membrane at sites of contact with ER requires mitochondrial receptors, including the MID49, MID51, and MFF (Loson et al., 2013; Kalia et al., 2018) receptors. When mitochondrial dysfunction and the intracellular AMP/ATP ratio increase, MiD49 and MiD51 recruit DRP1 to the outer membrane, thus promoting DRP1 oligomerization, and MFF specifically recruits DRP1 oligomers with active forms (Kalia et al., 2018). During fission, the enzyme activity of DRP1 is as important as its expression level. The activity of DRP1 is primarily regulated by serine phosphorylation. Phosphorylation at the serine 616 site enhances the activity of DRP1 to promote mitochondrial fission, while phosphorylation at the serine 637 site decreases DRP1 enzyme activity as well as mitochondrial translocation. The phosphorylation ratio between the serine 616 site and the 637 site determines the activity of DRP1 (Chang and Blackstone, 2007; Cribbs and Strack, 2007; Taguchi et al., 2007). DRP1 activity is also post-translationally modified by S-nitrosylation (Lee and Kim, 2018), SUMOylation (Yamada et al., 2021), O-GlcNAcylation (Park et al., 2021), and ubiquitination (Wang et al., 2011; Jin et al., 2021).

FIS1, on the mitochondrial OMM, mediates the translocation of DRP1 from the cytoplasm to the OMM (Macdonald et al., 2014). DRP1 gathers at the mitochondrial division site, forming a lock-lock structure and is then combined with FIS1 to form a complex. The distance and angle between molecules are changed by hydrolysis of GTP and gradually compressed until the mitochondrion transforms into two separate mitochondria. When mitochondrial division is complete, DRP1 is phosphorylated and exfoliates into the cytoplasm (Macdonald et al., 2014). However, FIS1 has recently been implicated in the induction of mitochondrial fragmentation even in the absence of DRP1, a newly discovered function that prevents the fusion process by inhibiting the GTPase activity of MFN1/2 and OPA1 (Yu et al., 2019). Accordingly, by lowering FIS1's interaction with MFN1/2 and OPA1, the overexpression of MID49 and MID51 has been demonstrated to encourage fission in a DRP1-independent manner (Yu et al., 2021).

In addition, a novel mitochondrial inner membrane protein, mitochondrial fission protein 1 (MTFP1), also known as MTP18, has been discovered to be essential for maintaining mitochondrial integrity, and has consequently been implicated in the regulation of mitochondrial fragmentation in cardiac myocytes and cancer cells (Tondera et al., 2005; Aung et al., 2017). According to Tondera, when MTP18 was overexpressed in COS-7 cells transfected with MTP18-myc expression construct, the shape of the mitochondria changed from filamentous to punctate structures, indicating excessive mitochondrial fragmentation (Tondera et al., 2005). Additionally, RNA interference induced loss of endogenous MTP18 function leads to an increase in fused mitochondria. Furthermore, MTP18 appears to be necessary for mitochondrial fission as it is prevented in cells that have had MTP18 knocked down by RNA interference despite the overexpression of FIS1 (Tondera et al., 2005). And in HL-1 cardiac myocytes, the MTP18 expression was upregulated upon DOX treatment, according to Aung. But knockdown of MTP18 prevented cardiac myocytes from excessive mitochondrial fission by alleviating the DRP1 translocation to the mitochondria and accumulation in the mitochondria, which improved cell apoptosis (Aung et al., 2017). Consistent with the above, it was also found an aberrant overexpression of MTP18 in hepatocellular carcinoma (HCC) cell lines and tumor tissues, and MTP18 promoted tumor growth and metastasis by inducing the progression of cell cycle, epithelial to mesenchymal transition (EMT) and production of MMP9 and suppressing cell apoptosis, which was involved in increased mitochondrial fission and subsequent ROS production (Zhang et al., 2018b).

3.1.2 Mitochondrial fusion

As mitochondria is composed of OMM and IMM, mitochondrial fusion requires two steps. First, the process is initialized by OMM fusion, which is carried out by MFN1 and MFN2. After conformational activation, MFNs from nearby mitochondria oligomerize to form homotypic (MFN1-MFN1 or MFN2-MFN2) or heterotypic (MFN1-MFN2) complexes, which subsequently aid in tethering the OMMs of nearby mitochondria (Rojo et al., 2002; Chen et al., 2003). The GTPase domain on MFN1/2 regulates the outer membranes of the mitochondria to fuse (Chen et al., 2003). MFN1 and MFN2 are highly homologous, but have different hydrolytic activity and fusion efficiency. MFN1 demonstrates stronger hydrolytic activity and pro-fusion efficiency. MFN2 plays a greater role in the formation of the fusion network between mitochondria and ER, as well as in regulating Ca^{2+} homeostasis (Inagaki et al., 2023).

Following OMM fusion, OPA1, located in the IMM, has been proven to be necessary for IMM fusion (Cipolat et al., 2004). In order to mediate the fusion of the IMM, OPA1 creates homotypic (OPA1-OPA1) and heterotypic (OPA1-cardiolipin) complexes after the OMM fuses (Frezza et al., 2006; Yu et al., 2020). Under the control of two mitochondrial metalloproteinases (OMA1 and Yme1L), it can produce short soluble fragments (Wai et al., 2015). OPA1 is divided into at least five fragments, of which the

two forms with the highest molecular weight are called L-OPA1, and the other three S-OPA1. In contrast to S-OPA1, which is found in the cristae (pleomorphic invaginations of IMM) of the intermembrane space (IMS), L-OPA1 is fixed on the IMM. Also, OPA1 has been shown to play a role in the modification of the cristae during apoptosis as well as the release of cytochrome c from the cristae (Frezza et al., 2006).

The fission or fusion process is also regulated by interactions between fission proteins and fusion proteins. For example, without DRP1, FIS1 hinders fusion by directly controlling the GTPase activity of MFN1/2 and OPA1 and reducing their interaction with FIS1. Also, it has been demonstrated that overexpression of MID49 and MID51 increases fusion in a DRP1-independent way (Yu et al., 2019; Yu et al., 2021). Therefore, further research is merited in order to determine if fusion and fission function separately and in opposition to each other or whether they work in harmony to modify mitochondrial morphology.

3.2 Mitochondrial dynamics and cell function

Changes in mitochondrial morphology are related to key cellular functions, including ROS and Ca^{2+} signaling, energy metabolism, apoptosis, autophagy/mitophagy, inflammation, senescence, and various others (Lee et al., 2004; Yu et al., 2006; Hom et al., 2010; Giacomello et al., 2020). Here, energy metabolism, mitophagy, and cell apoptosis are discussed.

It has been proven that mitochondrial fission is the basis of apoptosis. Pro-apoptotic pore-forming proteins BAX and BAK promote the stabilization of DRP1 at the fission site, leading to mitochondrial fission and network disruption. The above-mentioned changes are accompanied by a transfer of Ca^{2+} signals from the ER to the mitochondria and increased release of cytochrome c, which leads to mitochondrial apoptosis (Wasiak et al., 2007; Prudent et al., 2015). Also, the inhibition of mitochondrial fusion is involved in the process of apoptosis. For example, non-oligomerized MFN1 contributes to promoting BAK oligomerization, which in turn promotes mitochondrial permeability during apoptosis (Ferreira et al., 2019). In addition, OPA1-dependent cristae remodeling is required for the effective release of cytochrome c (Campanella et al., 2008; Landes et al., 2010), and permeability transition pore opening with Ca^{2+} overload in mitochondria contributes to mitochondrial osmotic expansion and cristae dilatation (Bernardi et al., 2015; Prudent et al., 2015).

Mitochondrial dynamics also play an important role in the control of energy metabolism. The IMM is one of the primary sites of oxidative phosphorylation (OXPHOS), and OPA1 overexpression is conducive to the assembly and stabilization of mitochondrial respiratory chain complexes that produce energy (Cogliati et al., 2013). Loss of OPA1 results in mitochondrial malfunction, reduced oxidative phosphorylation and ATP generation, faulty mitochondrial Ca^{2+} signaling, and pro-apoptotic effects (Kushnareva et al., 2013). YME1L and OMA1, specific OPA1-targeting proteases that can cleaved OPA1, increase mitochondrial ATP function leading to enhanced fusion (Mishra and Chan, 2016). And by controlling MFN2 expression, PGC-1 modifies mitochondrial shape, oxygen consumption, and membrane potential, illuminating an intriguing connection between mitochondrial dynamics and biogenesis (Peng et al., 2017). Mitochondrial fission is also related to the energy state of the cell. As a receptor of cell energy, AMPK can directly phosphorylate MFF (one of the OMM receptors of DRP1) during mitochondrial respiratory suppression, promote mitochondrial fission, and then clear damaged mitochondria through autophagy or eventually induce apoptosis (Toyama et al., 2016). PKA also phosphorylates DRP1 at Ser637 during starvation, promoting unwanted mitochondrial fusion, thereby avoiding autophagy and promoting cell survival (Gomes et al., 2011; Rambold et al., 2011).

As we know, mitophagy is an indispensable process, removing damaged or senescent mitochondria in order to maintain mitochondrial function and cell homeostasis, and the fission event is required for mitophagy (Li et al., 2022). Classically, mitophagy is performed in the parkin-dependent mechanism. The phosphatase and tensin homologue (PTEN)-induced kinase 1 (PINK1) accumulates on the OMM and recruits Parkin and promotes its translocation into the mitochondria (Yin et al., 2018). And then, Parkin ubiquitinates several targets such as MFN1, which marks defective mitochondria, and that is a trigger signal for the mitophagy process (Ziviani et al., 2010; Sarraf et al., 2013). Parkin ubiquitinates MFN2, thus affecting ER-mitochondrial binding, as well as mitochondrial dynamics and mitophagy (Sugiura et al., 2013). The resulting action on mitophagy adaptors p62/sequestosome 1/LC3 (microtubule-associated protein 1 light chain 3) facilitates the absorption of damaged mitochondria into autophagosomes and the ensuing autolysosomal digesting (Yamada et al., 2019).

4 Mitochondrial dynamics disorder in DOX-induced cardiac injury

Cardiomyocyte, which contains up to 6000 mitochondria and fills 30%–40% of the cell's volume, is one of the highest ATP-consuming cell types, in which mitochondria are largely found under the serosa, around the nucleus, and between the sarcomeres, allowing them to continually supply energy for cardiac contraction (Cao and Zheng, 2019). Due to their heavy reliance on energy production, cardiomyocytes are particularly susceptible to harmful substances that can affect the mitochondria (Varga et al., 2015). Impairment of mitochondrial dynamics has been observed in many cases of heart disease, including cardiac hypertrophy, heart failure, ischemia/reperfusion (I/R) damage, atherosclerosis (Cao and Zheng, 2019), and metabolic and genetic cardiomyopathies, as well as DOX-induced cardiomyopathy (Osataphan et al., 2020). Under circumstances of stress or disease, cardiac mitochondria undergo structural alterations, mitochondrial dysfunction, cell apoptosis, and various other changes (Li et al., 2020a).

DOX-stimulated cardiomyocytes display mitochondrial structural abnormalities (such as mitochondrial fragmentation, cristae loss, and matrix destruction), which increase the production of ROS, decrease the MMP, increase the opening of mPTP, disrupt energy metabolism, overburden mitophagy, and cause mitochondrial dysfunction, which results in cardiomyocyte apoptosis (Varga et al., 2015; Wallace et al., 2020). Eventually, dilated cardiomyopathy, heart failure, and ultimately death are possible outcomes of DOX exposure. It is therefore evident that abnormalities in mitochondrial dynamics, characterized by an increase in mitochondrial fission and a decrease in mitochondrial

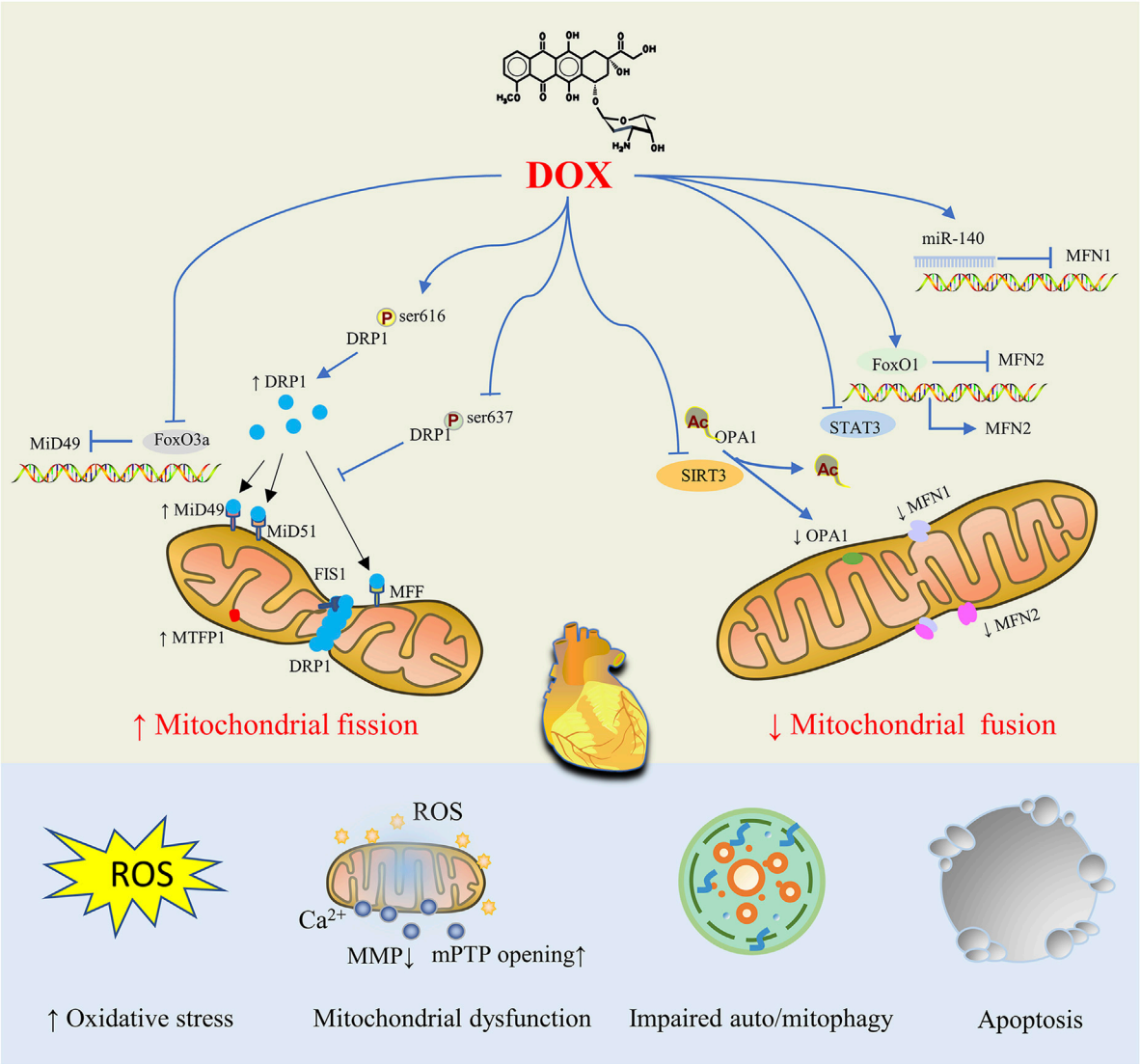

FIGURE 2
Mitochondrial Dynamics Disorders in doxorubicin (DOX)-induced Cardiac Injury. By controlling proteins involved in mitochondrial fission and fusion, DOX treatment tilts the mitochondrial dynamic balance toward fission, resulting in abnormal mitochondrial structure that ultimately causes oxidative stress, mitochondrial dysfunction, impaired auto/mitophagy, cardiomyocyte apoptosis and cardiac injury.

fusion, are the most prominent causes of DOX-induced myocardial injury. For DOX-induced dysregulated mitochondrial dynamics, a number of regulatory mechanics have been proposed, such as changes in the protein expression level of key proteins, post-translational modification and enzyme activity, the process of protein oligomerization, and various possible interactions between these proteins (Figure 2).

4.1 Disorders of mitochondrial fission proteins

Previous studies have demonstrated that patients with dilated cardiomyopathy (DCM) have higher levels of DRP1 expression and ser 616 phosphorylation, and that DRP1 may also have a role in mediating mitochondrial fission in Dox-induced cardiotoxicity (Catanzaro et al., 2019). In fact, according to numerous preclinical studies *in vitro* and *in vivo*, DRP1 inhibition had a cardioprotective effect, countering cardiotoxicity caused by DOX. Using siRNA to silence DRP1, mitochondrial fission was inhibited while mitochondrial fusion was increased (Lee et al., 2004). In a DOX-treated H9c2 cardiomyocytes model, excess mitochondrial fission was observed, which was reversed by siRNA-mediated DRP1 knockout (Catanzaro et al., 2019). It was also demonstrated that a DRP1 heterozygous deletion in mice protected against DOX-induced cardiotoxicity, indicating the role of DRP1-dependent mitochondrial dysfunction in DOX-induced cardiotoxicity (Catanzaro et al., 2019). So it was in neonatal rat cardiomyocytes exposed to DOX (Wang et al., 2015).

In response to cellular stress, the phosphorylation of DRP1 at Ser616 increased mitochondrial fission, while the phosphorylation of Ser637 reduced both the enzyme activity of DRP1 and its translocation to mitochondria (Tsushima et al., 2018). Moreover, treatment with DOX in mouse hearts increased Ser616 phosphorylation of DRP1, thus promoting mitochondrial fission (Xia et al., 2017; Miyoshi et al., 2022), which was improved by the administration of LCZ696, a novel angiotensin receptor neprilysin inhibitor (Miyoshi et al., 2022). Also, the inhibition of miR-23a diminished Ser616 phosphorylation of DRP1 and attenuated cardiomyocyte damage caused after DOX administration by directly targeting PGC-1α/p-DRP1 (Du et al., 2019).

It was reported by Aung et al. that MTP18, another mitochondrial fission-associated protein, participated in DOX-induced cardiotoxicity through pro-mitochondrial fission and pro-apoptotic actions (Aung et al., 2017). In HL-1 cardiac myocytes, DOX upregulated the MTP18 expression, and knockdown of MTP18 prevented cardiac myocytes from excessive mitochondrial fission by interfering with the DRP1 translocation to the mitochondria and accumulation in the mitochondria, leading to improved apoptosis (Aung et al., 2017). On the other hand, an inadequate amount of DOX may cause a considerable proportion of cells to suffer mitochondrial fission and death when MTP18 is overexpressed (Aung et al., 2017).

Also, the recruitment of DRP1 to the mitochondrial OMM can be directly mediated by MiD49 (encoded by gene mitochondrial elongation factor 2, MIEF2). Accordingly, knockdown of MIEF2 reduced its association with DRP1, and thus enhanced mitochondrial fusion (Palmer et al., 2011), suggesting that MIEF2 plays a vital role in regulating mitochondrial morphology. Foxo3a, a transcription factor encoded by gene forkhead box O3A, belonging to the Forkhead family, regulates DNA repair, carcinogenesis, cell differentiation, and oxidative stress (Accili and Arden, 2004). When encountering DOX, Foxo3a was downregulated in cardiomyocytes, and cardio-specific Foxo3a transgenic mice showed a reduction of mitochondrial fission, prevention of cardiomyocyte apoptosis, and reversal of cardiac dysfunction according to a study by Luyu Zhou et al. (Zhou et al., 2017). Mechanically, Foxo3a directly targeted MIEF2, and inhibited its expression at the transcriptional and translational levels. MIEF2 and Foxo3a show potential as interesting therapeutic targets that can improve both cancer therapy and cardio-protection.

4.2 Disorders of mitochondrial fusion proteins

In addition to the enhancement of mitochondrial fission during DOX treatment, it has been observed that mitochondrial fusion is inhibited, resulting in cardiotoxicity. And the restoration of mitochondrial fusion proteins and the fusion process may help alleviate DOX-induced mitochondrial dysfunction and myocardial injury.

In primary rat cardiomyocytes induced by DOX, it was noted that the expression of MFN2 decreased, leading to decreased fusion and increased ROS generation and cell apoptosis (Tang et al., 2017). In addition, overexpression of MFN2 by transfection of cardiomyocytes with MFN2 CRISPR activation plasmid restored mitochondrial fusion and cell apoptosis (Tang et al., 2017). Furthermore, a recent study conducted by Ding found that MFN2 overexpression promoted mitochondrial fusion and prevented oxidative stress, apoptosis, and cardiac dysfunction caused by DOX (Ding et al., 2022a). DOX exposure led to upregulation of FoxO1 (encoded by gene forkhead box O1), which belongs to the Forkhead family of transcription factors and acts as a key regulator of myocardial homeostasis, thus negatively regulating MFN2 transcription (Ding et al., 2022a). And FoxO1 RNAi dramatically boosted MFN2 mRNA and protein expression, restoring mitochondrial fusion and cell apoptosis (Ding et al., 2022a). Furthermore, treatment with Paeonal, a phenol derived from plants, by activating Stat3, a transcription factor which directly binds to the promoter of MFN2 and upregulates MFN2's expression at the transcriptional level, enhanced MFN2-mediated mitochondrial fusion, protecting the heart from DOX-induced damage (Ding et al., 2022b).

Several previous studies have demonstrated that miRNA plays a role in regulating key mitochondrial fusion proteins. For example, miR-140 can suppress the expression of MFN1 by targeting the 3′-untranslated region (3′-UTR) and subsequently the knockdown of miR-140 attenuated mitochondrial fission and apoptosis caused by DOX treatment (Li et al., 2014).

It is well known that the cardio-protective inducible enzyme heme oxygenase-1 (HO-1) plays an important role in protecting against DOX induced cardiomyopathy in mice (Hull et al., 2016). While preventing the elevation of the mitochondrial fission mediator Fis1, HO-1 overexpression increased the expression of the fusion mediators MFN1 and MFN2. In summary, the targeting of mitochondrial dynamics proteins was one of the mechanics by which HO-1 played a positive role in cardio-protection against DOX.

In addition to MFN1/2, abnormal expression of OPA1 was also seen in DOX myocardial toxicity. By normalizing expression levels of mitochondrial fusion proteins MFN2, Opa1, and Fis1 (with no change in DRP1 expression), cyclosporine A maintained mitochondrial fusion and preserved mitochondrial function, thereby improving cardiac function and survival in acute and chronic models of cardio-toxicity induced by DOX (Marechal et al., 2011).

And OPA1 was hyperacetylated under stress conditions such as those caused by DOX, and this reduced the GTPase activity of OPA1 and inhibited mitochondrial fusion. A study conducted by Sadhana and co-researchers demonstrated that OPA1 was a direct target of SIRT3, a type of mammalian sirtuin located in mitochondria which deacetylates and modifies the enzymatic activities of several mitochondrial proteins (Bell and Guarente, 2011), and OPA1 can be deacetylated at lysine 926 and 931 residues by SIRT3 (Samant et al., 2014). That is, SIRT3-dependent activation of OPA1 can help protect the mitochondrial network of cardiomyocytes and prevent cell death from DOX.

In summary, numerous studies have demonstrated that exposure to DOX causes the upregulation of mitochondrial fission proteins such as DRP1 and the downregulation of the mitochondrial fusion proteins MFN1, MFN2 and Opa1, resulting

in mitochondrial fragmentation and a damaged mitochondrial network. Further understanding of the mechanics of mitochondrial imbalance in DOX-induced cardiotoxicity will help confirm mitochondrial fusion and fission associated proteins as prospective therapeutic targets for reducing DOX-induced cardiotoxicity.

5 Mitochondrial dynamics disorder in cancer

Numerous studies have revealed that the balance of mitochondrial dynamics affects cellular biochemical processes like apoptosis and metabolism. During tumorigenesis, mitochondrial dynamic imbalance is also frequently reported (Yin et al., 2022). It has been shown that mitochondrial fission enhancement mediated by upregulation of DRP1 and mitochondrial fusion attenuation mediated by downregulation of MFN2 are associated with multiple cancers and promote tumor cell metastasis and drug tolerance, thus tumor progression (Ma et al., 2020; Ding et al., 2022a). Compared with non-metastatic breast cancer cells, metastatic breast cancer cells have higher expression of DRP1 and lower expression of MFN1 (Zhao et al., 2013). Overexpression of Mfn-2, inhibition of Drp-1, or knockdown of Drp-1 can reduce the proliferation of cancer cells and induce increased apoptosis of tumor cells, thereby shrinking tumors in lung, breast, and colon cancer (Inoue-Yamauchi and Oda, 2012; Rehman et al., 2012; Zhao et al., 2013). The DRP1 inhibitor Mdivi-1 chemically sensitizes tumor cells to the cytotoxic effects of chemotherapeutic drugs by inhibiting mitochondrial fission, leading to the accumulation of defective mitochondria, and ultimately causing dose-dependent death of tumor cells (Courtois et al., 2021).

To date, targeting MFN2-mediated mitochondrial fusion has received increasing attention. Mitochondrial dynamics is constantly changing as energy demand. Unlike cardiomyocytes, whose energy is mainly derived from OXPHOS, tumor cells are infinitely proliferating, and even under normal oxygen conditions, their energy is mainly derived from aerobic glycolysis, supplying crucial metabolites for the biosynthetic requirements of prolonged cell growth as well as enough ATP for cancer cells, which is called the Warburg effect (Lunt and Vander Heiden, 2011). Mitochondrial fusion is often associated with the enhancement of OXPHOS in cardiomyocytes (Ding et al., 2022a), while the mitochondrial fission in tumor cells helps to inhibit OXPHOS and enhance aerobic glycolysis (Gao et al., 2020). According to recent research conducted by Ding and co-workers, promoting MFN2 mediated mitochondrial fusion induces a similar metabolic transition from glycolysis to OXPHOS in cardiomyocytes and tumor cells (Ding et al., 2022a), charactered by decrease in the oxygen consumption rate (OCR)-to-extracellular acidification rate (ECAR) ratio. Mechanically, DOX exposure significantly inhibits mitochondrial complex activity and several OXPHOS enzymes, and also inhibits aerobic glycolytic capacity and related glycolytic enzymes in cardiomyocytes and tumor cells, exhibiting greater effect on OXPHOS compared to glycolysis. Due to their different metabolic patterns, enhanced mitochondrial fusion promotes cardiomyocyte survival and induces tumor cell death. Moreover, overexpression of DRP1 promotes mitochondrial fission and significantly weakens the inhibitory effect of MFN2 on DOX-induced cardiac injury (Ding et al., 2022a). In summary, in-depth study of mitochondrial dynamics regulating cell metabolism will provide us with novel therapeutic strategies for alleviating tumor treatment-related cardiotoxicity without sacrificing anticancer effects (Figure 3).

6 Modulating the balance of mitochondria dynamics

Given that DOX impairs mitochondrial dynamics, alleviating mitochondrial fission activation and promoting fusion seem to be effective ways to reduce cardiac function disturbances caused by DOX treatment. Indeed, several studies have confirmed this through gene therapy, pharmacological approaches, and even drug compounds and herbal medicines used in combination in DOX administration (Figure 4). However, there is a need for further research into the application of mitochondrial-targeted agent candidates in clinical DOX cardiotoxicity prevention and treatment without changing the antitumor effect of DOX. Next, we provide an overview of current pharmacological and non-pharmacological interventions targeting mitochondrial dynamics proteins for cardiac damage caused by DOX (Table 1).

6.1 Pharmacological strategies targeting mitochondrial dynamics disorders

Due to their potential as therapeutic strategies for the targeting of mitochondrial disorders, pharmacological strategies that directly regulate mitochondrial fission and fusion processes are being researched intently. According to Emmanouil (Zacharioudakis and Gavathiotis, 2023), based on advancements in uncovering structure-function correlations, protein-protein interaction of effector proteins and regulation mechanics, and development of pharmacological regulators, targeting fusion and fission associated proteins demonstrate a great therapeutic potential in, for example, cancer, cardiovascular disease, and neurological diseases by reversing the imbalanced mitochondrial dynamics in the onset and progression of these pathologies. Specially, the regulation of protein-protein interactions for oligomers formation of DRP1, OPA1, and MFN1/2, as well as the selective regulation of the effects of the OPA1, MFN1/2, and DRP1 GTPase domains, show great potential for the regulation of mitochondrial fusion and fission.

Mitochondrial Division Inhibitor (Mdivi-1), a quinazolinone derivative, selectively inhibits the main regulator of mitochondrial fission DRP1, making it the most effective inhibitor discovered during the chemical screening of mitochondrial division inhibitors (Cassidy-Stone et al., 2008). According to previous studies, Mdivi-1 reduced mitochondrial fission and can play a crucial role in ameliorating heart failure (Givvimani et al., 2012). Mdivi-1 has been shown to provide cytoprotection in DOX-induced cardiomyopathy in *ex vivo* experiments and in Langendorff perfused heart models by reducing ROS formation, lowering intracellular calcium overload, maintaining mitochondrial function, and avoiding cardiac myocyte hypercontractility (Gharanei et al.,

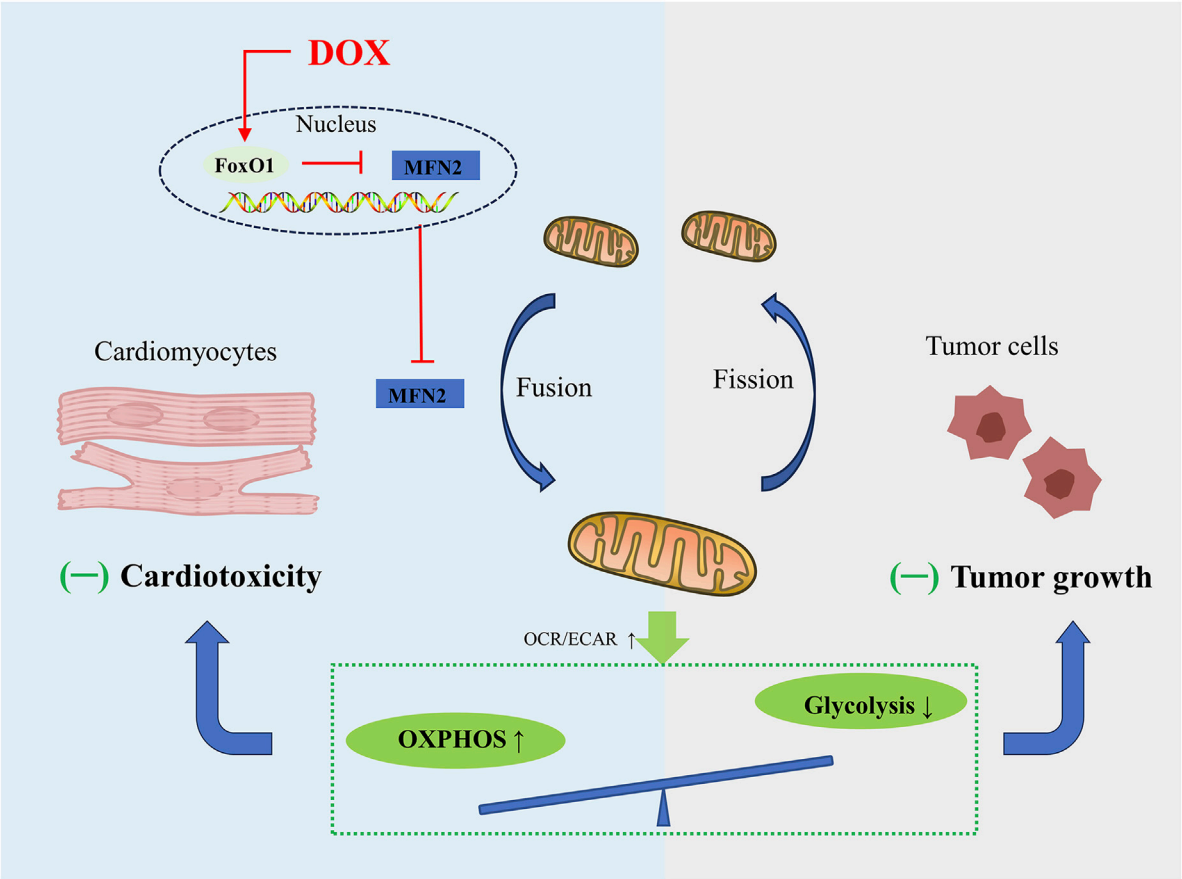

FIGURE 3
Schematic figure showing that promoting MFN2-mediated mitochondrial fusion induces a similar metabolic transition from glycolysis to OXPHOS in cardiomyocytes and tumor cells, alleviating DOX-induced cardiotoxicity while increasing tumor cell death.

2013). Mdivi-1 not only restored DOX-induced cardiac myocyte depolarization and decreased myocardial infarction size (Gharanei et al., 2013), but also affected the anticancer properties of DOX. A study in a rat model showed that DRP1 and p-DRP1 (Ser616) levels were significantly increased in tissues with mitochondrial damage, while expression levels of MFN1/2 and Opa1 were decreased in DOX-induced myocardial tissues (Xia et al., 2017). By preventing cardiac mitochondrial DRP1 accumulation and cytosolic p-DRP1 (Ser616) activation, Mdivi-1 provided strong protection against excessive mitochondrial fission and fragmentation caused by DOX in an *in vivo* environment, thus reversing changes in mitochondrial morphology and improving mitochondrial function (Xia et al., 2017).

There has been very little research into pharmacological regulators targeting mitochondrial fusion molecules. As a cell-permeable phenylhydrazone compound, M1 was the most effective compound in promoting mitochondrial fusion, according to earlier investigations utilizing different models of cardiac injury. Due to selective upregulation of fusion proteins like MFN1/2 and Opa1 (proteins required for mitochondrial fusion), the protective effects of M1 were demonstrated in models of MPP + or staurosporine-induced cytotoxicity, in diabetic cardiomyopathy hearts, and in cases of cardiac I/R damage (Maneechote et al., 2019). According to another study, M1 reestablished the development of the mitochondrial tubular network via the fragmented mitochondria in MFN1 knockout mice or MFN2 knockout mice (Wang et al., 2012). However, M1 treatment had no effect on the mitochondrial elongation activity of MFN1/2 double KO or Opa1 KO embryonic fibroblasts (MEFs) (Wang et al., 2012). This suggests that basal fusion activity is necessary for M1 to elongate mitochondria, as the formation of the mitochondrial network tubules require interaction with the mitochondrial fusion proteins (MFN1/2 and OPA1).

Treatment with M1 or the combination of Mdivi-1 with M1 may be able to protect the heart from the cardiotoxicity caused by DOX, however this is uncertain. In a study recently performed by Maneechote and his co-researchers, the effects of Mdivi-1, M1, and the combination treatment for cardiomyopathy using DOX-treated rats as a model were examined (Maneechote et al., 2022). The study illustrated for the first time that M1 was potent in preventing the cardiotoxic effects of DOX and encouraging mitochondrial fusion by upregulating MFN1/2 and Opa1. This indicates that Mdivi-1 and M1 may have some protective effects against the cardiotoxicity caused by DOX (Maneechote et al., 2022). The process relies on fission/fusion protein expression. Though

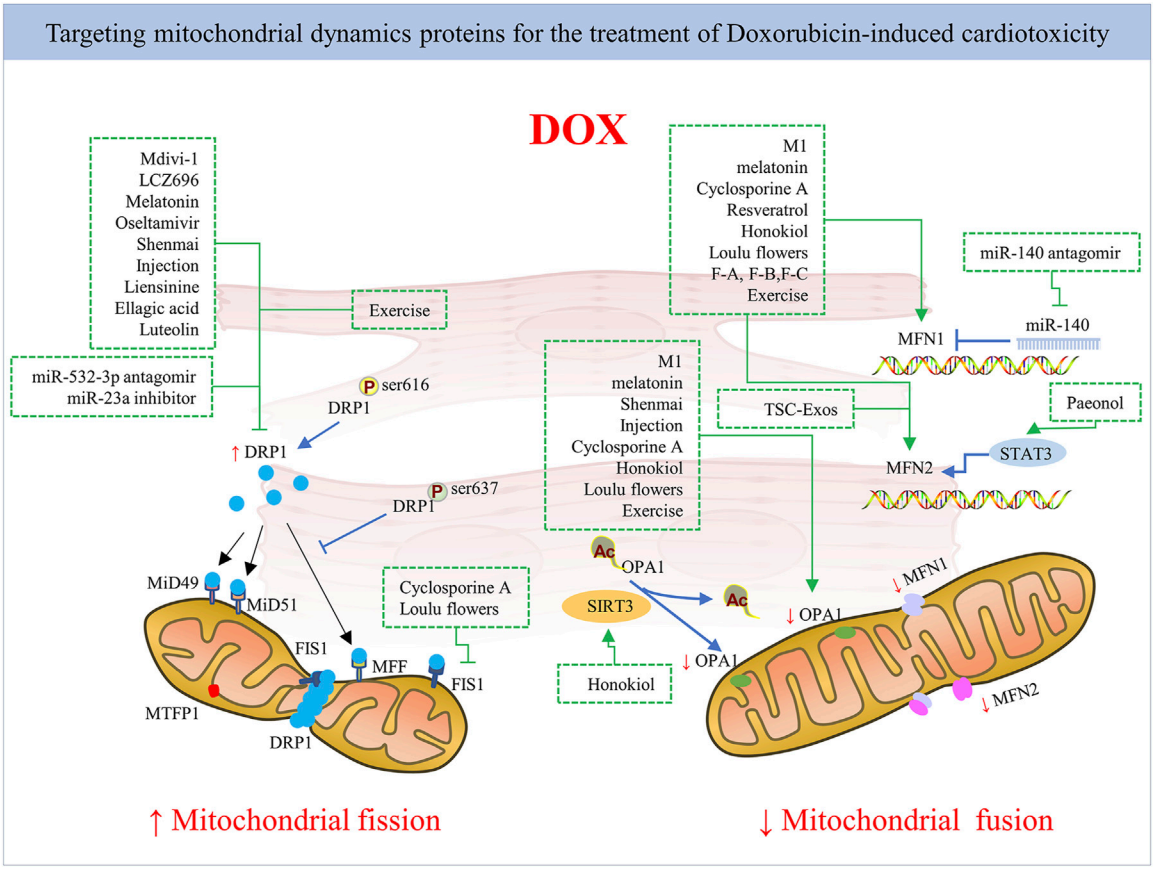

FIGURE 4
The mechanism of pharmacological strategies and exercise targeting mitochondrial dynamics proteins for DOX-induced cardiotoxicity. Inhibiting mitochondrial fission by targeting mitochondrial fission protein DRP1 mainly or promoting mitochondrial fusion by targeting mitochondrial fusion proteins like MFN1/2 and Opa1 via pharmacological and non-pharmacological strategies exerts cardioprotection against DOX.

reduced cardiomyocyte death and improved contractile properties have been achieved by Mdivi-1 and M1, there was no synergistic advantage from the combination of Mdivi-1 and M1 treatment. The effect of the fusion promoter and the fission inhibitor might coincide at this stage, where mitochondrial fission-mediated fragmentation acts as a downstream natural process. Hence, no great advantages were evident when either medication had already reached its peak effectiveness. It is noteworthy that neither Mdivi-1 nor M1 exhibited any negative effects on DOX's anticancer activities in breast cancer cell lines. These results can provide some knowledge of the potential therapeutic role of mitochondrial dynamic regulation in DOX-induced cardiotoxicity without sacrificing the effectiveness of the treatment's anti-cancer properties.

However, it is been found that Mdivi-1 also inhibits the activity of complex I, reducing mitochondrial respiration and increasing the production of ROS (Bordt et al., 2017). This unfavorable target effect may limit the clinical application of Mdivi-1. Also, because of *in silico* screens combined with structure-guided drug generation employing the DRP1 GTPase domain, Drpitor and its optimized variant Drpitor1a were found to be more effective and specific than Mdivi-1 in inhibiting DRP1's GTPase activity (Wu et al., 2020; Zacharioudakis and Gavathiotis, 2023). Additionally, they improved cardioprotective properties against cardiac I/R injury while demonstrating anticancer actions by lowering cell proliferation and triggering lung cancer cell apoptosis (Wu et al., 2020). P110 is receiving increasing attention as another peptide inhibitor that inhibits the interaction between DRP1 and Fis1. By blocking DRP1/Fis1 connections in models of septic cardiomyopathy both *in vivo* and *in vitro*, P110 can lower septic cardiomyopathy's morbidity and mortality (Haileselassie et al., 2019). Also, by preventing DRP1 activation and mitochondrial translocation, P110 plays a neuroprotective role (Filichia et al., 2016). Further research is merited to determine whether Drpitor and Drpitor1a, as well as P110, play an important role in DOX-induced cardiac damage.

6.2 Drug compounds

In addition to pharmacological regulators, recent research suggests that several drug compounds may attenuate DOX cardiotoxicity by operating on mitochondrial dynamics. These compounds are already registered drugs for the treatment of other diseases, and can easily be repurposed for use in cardio-protection from DOX exposure.

TABLE 1 An overview of current pharmacological and non-pharmacological interventions targeting mitochondrial dynamics proteins for cardiac damage caused by DOX.

Intervention	Agent	Model	Molecular action in mitochondrial dynamics	Effects on cardiac phenotype	Changes in anticancer effects	Reference
Pharmaceutical modulators	Mdivi-1 (1/5/10/20 μM, respectively 30 min before DOX)	H9C2 (5 μM DOX)	↓DRP1 ser 616 phosphorylation	suppress mitochondrial fission and fragmentation	/	Xia et al. (2017)
			↓DRP1 accumulation in mitochondrial	preserve cardiac function		
	M1 (2 mg/kg/day for 30 days) (Mdivi-1, 1.2 mg/kg daily for 30 days)	rat/H9C2 (3 mg/kg DOX on days 0, 4, 8, 15, 22 and 29)	↑expression of MFN1/2 and Opa1	promote mitochondrial fusion	not reduce the anti-cancer efficacy of DOX in MCF7 and MDA-MB231 breast cancer cell lines	Maneechote et al. (2022)
				alleviate mitochondrial fragmentation and apoptosis		
				preserve cardiac function		
Drug compounds	LCZ696 (60 mg/kg/day for 4 weeks, beginning on the day after DOX injection)	mice/H9C2 (15 mg/kg, three times/week for 2 weeks in mice)	↓DRP1 ser 616 phosphorylation	alleviate mitochondrial fragmentation and cell apoptosis	/	Xia et al. (2017)
	Metformin (10 mg/ kg/day) and melatonin (250 mg/ kg/ day for 30 consecutive days)	rat/H9C2 (3 mg/kg DOX on days 0, 4, 8, 15, 22 and 29)	↓DRP1 ser 616 phosphorylation	improve cardiac mitochondrial dynamic balance, mitophagy and mitochondrial function	synergistic anti-cancer effects with Dox in MCF7 and MDA-MB231	Arinno et al. (2021)
			↑expression of MFN1/2 and OPA1	alleviate cell apoptosis		
	Oseltamivir (OSE) (20 mg/kg for 31 days beginning from 3 days before the first injection of DOX)	rat/H9C2 (15 mg/kg DOX within 2 weeks, 2.5 mg/kg for six times)	↓expression of DRP1	suppress mitochondrial fission and mitophagy	/	Qin et al. (2021)
				preserve cardiac function		
Natural modulators	Shenmai Injection (3/1/0.3 g/kg on days 1, 8, 15, 22, and 29)	mice/H9C2 (3 mg/kg DOX on days 9, 16, 23 and 30)	↑DRP1 ser 637 phosphorylation,	improve cardiac mitochondrial dynamic balance	/	Li et al. (2020b)
			↑L-OPA1 to S-OPA1	maintain mitochondrial homeostasis		
	Liensinine (LIEN) (60 mg/kg)	mice/ NMVMs (15 mg/kg for 6 days, single dose in total)	↓DRP1 ser 616 phosphorylation in Rab7/ERK/DRP1 manner	suppress mitochondrial fission	preserve its anti-cancer property of DOX in MDA-MB231 breast cancer cell line	Liang et al. (2020)
				alleviate mitochondrial fragmentation and apoptosis		
				preserve cardiac function		
	Ellagic acid (EA) (1/5/10/20 μM)	NRVMs (10 μM DOX for 18 h)	↓DRP1 ser 616 phosphorylation by inhibition of Bnip3	suppress cell death	not impair the efficacy of DOX in Hela or MCF-7	Dhingra et al. (2017)
	Luteolin (20 μM)	H9c2 and AC16 cells/zebrafish (1 μM Dox for 24 h)	↓DRP1 ser 616 phosphorylation	suppress mitochondrial fission	enhance anti-cancer effects with DOX in 4T1 and MDA-MB-231 and in triple-negative breast cancer of mice models	Shi et al. (2021)
				alleviate apoptosis		
				preserve cardiac function		
	Cyclosporine A (1 mg/kg/48 h)	Mice (a single intraperitoneal bolus for 10 mg/kg follow-up for 1.5 weeks, or 4 mg/kg/week for 5 weeks, follow-up for 16 weeks)	↑expression of MFN2 and Opa1	maintain mitochondrial fusion	/	Marechal et al. (2011)
			↓Fis1	preserve mitochondrial function		
	Resveratrol (RESV) (4 g RESV/kg of diet, equivalent to ~320 mg RESV/kg/day)	Mice (8 mg/kg/week for 8 weeks)	↑expression of MFN1/2	restore mitochondrial dysfunction	/	Dolinsky et al. (2013)
				preserve cardiac function		
	Honokiol (HKL) (10 μM)	NRVMs (2μM DOX for 24 h)	↑expression of MFN1 and Opa1	promote mitochondrial fusion	not impair the efficacy of DOX in mice implanted with PC3 cells	Pillai et al. (2017)
				restore mitochondrial dysfunction		
	Loulu flowers (LLF) (800 μg/mL in H9C2; pretreated with 100, 200 and 400 μg/mL in zebrafish)	H9C2/zebrafish (0.75 μM DOX for 24 h in H9C2 or zebrafish)	↑OPA1, MFN1	improve cardiac mitochondrial dynamic balance	/	Hu et al. (2022)
			↓MFF and Fis1	maintain mitochondrial homeostasis		

(Continued on following page)

TABLE 1 (*Continued*) An overview of current pharmacological and non-pharmacological interventions targeting mitochondrial dynamics proteins for cardiac damage caused by DOX.

Intervention	Agent	Model	Molecular action in mitochondrial dynamics	Effects on cardiac phenotype	Changes in anticancer effects	Reference
	F-A, F-B, F-C (10 μM)	H9C2 (2.5 μM DOX for 24 h)	↑expression of MFN1/2	maintain the stability of mitochondrial structure and function	/	Zhou et al. (2023)
	Paeonol (Pae) (75, 150, or 300 mg/kg each day after DOX)	rat/NRVMs (5 mg/kg Dox on days 1, 6 and 11, 3 times/ 2 weeks)	↑expression of MFN2 via the PKCε-Stat3-MFN2 pathway	promote mitochondrial fusion	not interfere with DOX's antitumor efficacy in B16 melanoma, SNU-368, Hepa 1–6 and 4 T1 cell	Ding et al. (2022b)
				restore mitochondrial dysfunction		
miRNAs and exosomes	miR-532-3p antagomir	NRVMs/mice (DOX 4 mg/kg/ week for 4 weeks)	↓DRP1 accumulation in mitochondria by targeting ARC	inhibit mitochondrial fission and cell death	not affect DOX-induced apoptosis in cancer cells including Hela, SGC-7901, SW-480 and HepG-2	Wang et al. (2015)
	miR-23a inhibitor	NRVMs (1, 3, or 5 μM DOX for 24 h)	↓DRP1 Ser616 phosphorylation mediated by miR-23a directly targeting PGC-1α/p-DRP1	inhibit mitochondrial fission	/	Du et al. (2019)
				preserve cardiac function		
	miR-140 antagomir	NRVMs/mice (1 μM DOX for 0-15 h)	↑expression of MFN1 through ablating the relationship between 3'-UTR of miR-140 and MFN1	attenuate mitochondrial fission and apoptosis	/	Li et al. (2014)
	TSC-Exos	mice/H9C2 (DOX 5 mg/kg/ week for 4 weeks)	↑expression of MFN2	recover mitochondrial fusion,	/	Duan et al. (2023)
				alleviate apoptosis		
Exercise	Endurance treadmill training (45 min, 5 days/week 10 min before DOX treatment)	Mice (8 mg/kg/week for 8 weeks, sacrificed on 48 h after the final exercise session)	↑expression of MFN1/2	restore mitochondrial dysfunction	/	Dolinsky et al. (2013)
				preserve cardiac function		
	Endurance treadmill training and voluntary free wheel activity (5 weeks before DOX and during DOX treatment)	Rat (DOX 2 mg/kg/week for 7 weeks)	↑expression of MFN1/2 and Opa1	improve cardiac mitochondrial dynamic balance	/	Marques-Aleixo et al. (2018)
			↓DRP1	regulate mitophagy, alleviate cell apoptosis		
	Endurance treadmill training (60 min/day for 4 weeks after the last DOX treatment)	Mice (5 mg/kg/week for 4 weeks)	↑DRP1	enhance the flux of auto/ mitophagy by enhancing mitochondrial fission-prone alterations	/	Lee et al. (2020)
			↓OPA1 and MFN2 along with enhancing the flux of auto/ mitophagy	preserve cardiac function		

LCZ696, acting as a novel angiotensin receptor neprilysin inhibitor and a standard treatment in patients with heart failure with reduced ejection fraction, can inhibit mitochondrial fission by reducing DRP1 phosphorylation at Ser616 and preventing cell apoptosis from DOX exposure. However, its cardioprotective effect can be reversed by DRP1 overexpression (Xia et al., 2017).

Metformin and melatonin, applied clinically in hypoglycemia and sleep disorder, exerted a protective effect on cardiac function during DOX treatment *in vivo* and vitro by improving mitochondrial dynamics balance through suppressing DRP1 phosphorylation at Ser616 and increasing the expression of MFN1/2 and OPA1, accompanied with improved mitochondrial biogenesis and mitophagy (Arinno et al., 2021).

Known as an antiviral classified as a neuraminidase1 (NEU1) inhibitor, oseltamivir (OSE), preserved cardiac function in models of DOX-induced cardiomyopathy, which was associated with the suppression of DRP1-dependent mitochondrial fission and mitophagy (Qin et al., 2021). Among the four varieties of NEUs (NEU1, NEU2, NEU3, and NEU4), NEU1 is the most abundantly expressed in the heart and is associated with a number of cardiovascular disorders (Glanz et al., 2019; Zhang et al., 2021). For example, NEU1 was shown to be strongly expressed in the hearts of patients with coronary artery disease, and it was also related to cardiac ischemia/ reperfusion injury, atherosclerosis formation, and plaque instability, as well as being a key cause of cardiac hypertrophy (Zhang et al., 2018a; Sieve et al., 2018; Heimerl et al., 2020; Chen et al., 2021). In DOX-induced cardiomyopathy in rat models, DRP1 expression was increased by the elevated NEU1, which subsequently boosted mitochondrial fission and PINK1/Parkin pathway-mediated mitophagy. This created a negative feedback loop that led to myocardial apoptosis and cell death (Qin et al., 2021). In summary, the above-mentioned study showed that NEU1 promoted DRP1-dependent mitochondrial fission and mitophagy, which was a critical initiator of DOX-induced cardiomyopathy, but NEU1 inhibition mediated by its inhibitors such as OSE demonstrated novel cardio-protective effects against DOX-induced cardiotoxicity.

6.3 Natural regulators

There have also been several studies on natural compounds as potent cardioprotective agents for alleviating DOX-induced cardiotoxicity.

For example, Shenmai Injection suppressed DOX-induced excessive mitochondrial fragmentation in cardiomyocytes by rebalancing mitochondrial dynamics. Mechanically, it reversed a decrease in DRP1 phosphorylation at Ser637 and an increase in DRP1 phosphorylation at Ser616 under treatment with DOX, and simultaneously increased the ratio of L-OPA1 to S-OPA1 via AMPK activation and PI3K/Akt/GSK-3β signaling pathway, which eventually alleviated mitochondria-dependent apoptosis (Li et al., 2020b). Liensinine (LIEN), an isoquinoline alkaloid derived from plants, is a recently discovered mitophagy inhibitor that can work in combination with DOX to treat breast cancer, and it was found that LIEN exhibited a beneficial effect in protecting against DOX-induced cardiomyopathy (Zhou et al., 2015). Liang found that LIEN suppressed DRP1 phosphorylation at the Ser616 site via Rab7 overexpression, thus reversing mitochondrial fragmentation and inhibiting mitochondrial fission–mediated cell death (Liang et al., 2020). Similar to LIEN, ellagic acid (EA), a natural polyphenol compound, can also target mitochondrial fission, attenuating DOX-induced DRP1 Ser616 phosphorylation mediated by the inhibition of Bnip3 (Dhingra et al., 2017). Notably, EA did not reduce DOX's effectiveness in killing Hela or MCF-7 cancer cells. Along these lines, another study observed that Luteolin (LUT), a naturally occurring flavone enriched in plants, ameliorated DOX-induced toxicity in H9c2 and AC16 cells by alleviating DRP1 expression and Ser616 phosphorylation induced by DOX in H9c2 and AC16 cells (Shi et al., 2021). Also, LUT improved the function of cardiac ventricles in zebrafish under DOX treatment. Furthermore, LUT inhibited proliferation and metastasis in mouse models of triple-negative breast cancer while improving the cytotoxicity (Shi et al., 2021).

Cyclosporine A improved DOX-induced cardiac dysfunction and mortality by normalizing the expression levels of MFN2 and Opa1, sustaining mitochondrial fusion, and preserving mitochondrial function (Marechal et al., 2011). Also, resveratrol (RESV), a naturally occurring polyphenol, was found to increase the expression of mitochondrial fusion proteins MFN1 and MFN2, restore mitochondrial dysfunction, and reduce oxidative stress, thereby protecting against DOX-associated cardiac injury (Dolinsky et al., 2013). It has been proven that SIRT3 defends against cardiotoxicity brought on by doxorubicin. Honokiol (HKL), an activator of SIRT3, was found to promote mitochondrial fusion by maintaining OPA and MFN1 levels, improving mitochondrial function and reducing mitochondrial DNA damage *in vivo* and *in vitro* (Pillai et al., 2017). Also, Loulu flowers (LLF), a member of the Compositae family, have been commonly used in the treatment of cardiovascular illnesses because of their detoxifying effects and capacity to eliminate heat (Hu et al., 2022). A study using H9c2 cells and zebrafish models demonstrated that LLF could alleviate cardiac injury via the blocking of NF-κB signaling and the re-balancing of mitochondrial dynamics by alleviation of the aberrant expression of mitochondrial dynamics-related proteins such as OPA1, MFN1, MFF, and Fis1 (Hu et al., 2022), indicating that LLF can alleviate DOX-induced cardiotoxicity. Wenna and co-workers found that, in order to maintain the stability of mitochondrial structure and function, the protective effect against DOX-induced cardiotoxicity in H9c2 cells of three flavonoids obtained by the separation and purification of sea buckthorn seed residue was partially achieved by increasing protein expression of mitochondrial mitofusins (MFN1, MFN2) (Zhou et al., 2023). Paeonol (Pae), a naturally occurring phenol antioxidant derived from the root bark of Paeonia suffruticosa, was approved as a novel mitochondrial fusion promoter in diabetic cardiomyopathy (Liu et al., 2021). A recent study demonstrated that Pae stimulated mitochondrial fusion and protected the heart from DOX-induced damage via the PKCε-Stat3-MFN2 pathway (Ding et al., 2022b). By targeting PKC and subsequently activating Stat3, which was directly bound to the MFN2 promoter and upregulated its expression at the transcriptional level, Pae enhanced MFN2-mediated mitochondrial fusion (Ding et al., 2022b). Furthermore, Pae did not obstruct Dox's anticancer activities on a variety of tumor cells.

6.4 MicroRNAs (miRNAs) and exosomes

Small non-coding RNAs, known as miRNAs, act as negative regulators of target genes by affecting the stability or translation of mRNA (Valencia-Sanchez et al., 2006), involving several physiological and pathological processes. According to previous studies, cardiac morphogenesis, contraction of the heart muscle, and electrical signal conductivity are all regulated by miRNAs (Thum et al., 2007). The manipulation of miRNAs can be used to develop therapeutic strategies. Given the significance of miRNAs in post-transcriptional regulation, miRNAs also significantly contribute to the cardiotoxicity caused by DOX.

MiR-532-3p was found to regulate mitochondrial fission and apoptosis by targeting ARC, an apoptosis repressor with caspase recruitment domain that acts as an abundantly expressed antiapoptotic protein and affects DRP1 accumulation in mitochondria (An et al., 2009; Wang et al., 2015). More importantly, MiR-532-3p did not affect apoptosis of cancer cells during DOX treatment. And as shown above, miR-23a induced DRP1 Ser616 phosphorylation by directly targeting PGC-1α/p-DRP1 to promote mitochondrial fission, mediating cardiomyocyte damage caused by DOX administration (Du et al., 2019). And MiR-23a inhibitor significantly reduced cardiac damage caused by DOX. Mitochondrial fusion protein can also be regulated by miRNAs. Accordingly, miR-140 can directly suppress the expression of MFN1 by targeting the 3′- UTR without affecting the levels of MFN2, OPA1 or DRP1, and anti-miR-140 can attenuate mitochondrial fission and apoptosis caused by DOX treatment (Li et al., 2014).

Exosomes have established their position as a therapeutic tool in recent years, with an increase in the types of exosomes generated by stem cells being employed in the treatment of heart failure (Roberts and Fisher, 2011; Sun et al., 2021). Exosomes generated from trophoblast stem cells (TSC-Exos) have been shown to guard against the cardiotoxicity caused by DOX (Duan et al., 2023), which has been confirmed both in H9c2 cells and in mice. The study showed that TSC-Exos play a cardio-protective role by recovering mitochondrial fusion through increasing MFN2 expression and alleviating myocardial cell loss.

6.5 Exercise

For cancer patients and survivors, exercise training has a cardioprotective effect against DOX-induced cardiotoxicity and has the potential to be a non-pharmacological intervention for the prevention and treatment of chemotherapy-induced cardiotoxicity. Many studies have consistently shown that exercise may lead to the preservation of left ventricular systolic function through a variety of mechanisms, including prevention of DOX accumulation and removal, increased cardiac antioxidant enzyme expression, mitochondrial function, and reduced pro-apoptotic signaling (Scott et al., 2011; Gaytan et al., 2023).

Aerobic training exercise prevents DOX-induced impairments in LV systolic and diastolic function and protects the heart against ROS by enhancing endogenous antioxidant protective machinery such as glutathione peroxidase 1, catalase, and manganese superoxide dismutase in cardiac tissue (Kavazis et al., 2010). Also, voluntary exercise training may provide resistance against the cardiac dysfunction and oxidative damage associated with DOX exposure and induce a significant increase in heat shock protein (HSP72) in the heart (Chicco et al., 2005). Due to the high affinity between DOX and cardiolipin in cardiomyocytes, DOX is more likely to accumulate in mitochondria than in cytoplasm, and studies have shown that DOX has a greater affinity for subsarcolemmal mitochondria compared to intermyofibrillar mitochondria, which difference occurs potentially as a result of greater concentrations of cardiolipin within this mitochondrial fraction (Kavazis et al., 2017). And exercise preconditioning greatly improves subsarcolemmal mitochondria homeostasis by acting on redox balance and iron handling in subsarcolemmal mitochondria upon acute DOX treatment (Montalvo et al., 2023). According to Morton, by boosting the expression of mitochondria-specific ATP-binding cassette (ABC) transporters and lowering the accumulation of mitochondrial DOX, 2 weeks of exercise preconditioning is sufficient to prevent cardiorespiratory failure (Morton et al., 2019). We will next highlight the relevant studies of exercise ameliorating DOX myocardial toxicity through the regulation of mitochondrial dynamics.

In mice given DOX, aerobic exercise training (endurance treadmill training before DOX treatment) enhanced the expression of MFN1/2, as well as the mitochondrial electron transport chain complexes, superoxide dismutase, and cardiac sarcoplasmic/ER calcium-ATPase 2a, and thus protected against DOX-associated cardiac injury (Dolinsky et al., 2013).

Recently, Marques conducted a study showing that no matter when exercise was performed prior to or during sub-chronic DOX treatment, both chronic exercise rat models (endurance treadmill training-TM and voluntary free wheel activity-FW) demonstrated cardio-protection. Mitochondrial dynamics and autophagy/mitophagy were regulated, resulting in decreased cell apoptosis and improved cardiac function (Marques-Aleixo et al., 2018). Specifically, in SD rat models of sub-chronic DOX treatment, administration of DOX caused a decrease in the expression of fusion proteins (MFN1, MFN2 and OPA1), and an increase in DRP1 expression. Augmentation in mPTP opening susceptibility and apoptotic signaling has also been observed, as well as activation of autophagy/mitophagy signaling. All of these effects can be prevented by TM and FW before DOX treatment (Marques-Aleixo et al., 2018).

As mentioned above, before receiving DOX treatment, endurance exercise (EXE) preconditioning can provide cardio-protection, but it is unknown if EXE postconditioning has the same effect. A study from Lee Y et al. has elucidated this subject (Lee et al., 2020). EXE mitigated cardiac tissue damage and prevented DOX-induced apoptosis. Additionally, with increased mitochondrial fission (DRP1) and decreased fusion markers (OPA1 and MFN2), EXE dramatically improved the flux of auto/mitophagy (Lee et al., 2020). Here comes the paradox. The study from Lee Y hinted that EXE interventions promoted mitochondrial autophagy by enhancing fission-prone changes in mitochondrial switching proteins, but another study conducted previously by Marques showed that EXE prevented DOX-induced fission changes and reduced mitochondrial autophagy, thereby providing cardio-protection (Marques-Aleixo et al., 2018). These disparate outcomes might be related to the experimental design. Lee Y began EXE intervention after DOX treatment lasting for 4 weeks, which represented a chronic response in which DOX exposure led to mitophagy delinquency where activation of mitophagy was required by enhancing mitochondrial fission-prone alterations. Marques made rats perform EXE for 5 weeks and then treated them with DOX for 7 weeks together with EXE. The rats were then sacrificed 7 days after the last administration of DOX, which represented an acute response (within 7 days) to DOX exposure, resulting in excessive mitochondrial fission and subsequent autophagy dysfunction.

To sum up, several pharmacological and non-pharmacological interventions such as pharmacological inhibitors or modulators targeting key proteins of mitochondrial dynamics, drug compounds, natural modulators, miRNAs and exosomes mentioned above, and even exercise, have proven that the re-balancing of mitochondrial dynamics by inhibiting mitochondrial fission or promoting mitochondrial fusion, whether specifically or not regulate the enzyme activity, expression level, oligomerization and intermolecular interaction of mitochondrial fission/fusion associated proteins, are effective strategies for DOX-induced cardiotoxicity. 1) Measures such as the development of pharmacological regulators targeting DRP1 and MFN2 like Mdivi-1 and M1 are being taken in order to develop novel therapeutic compounds for DOX-induced cardiotoxicity and even other cardiovascular diseases such as ischemia-reperfusion injury and diabetic cardiomyopathy. And whether Drpitor and Drpitor1a, as well as P110, pharmacological inhibitors by inhibiting DRP1's GTPase activity and blocking DRP1/Fis1 connections, play an important role in DOX-induced heart damage warrants further investigation. In addition, other regulatory proteins of mitochondrial fusion and fission like Fis1, OPA1, and MFN1, are also worthy of consideration as potential therapeutic targets. However, it is absolutely significant to note that there is still a need for determining the dosage and administration of these modulators. 2) As for drugs with the ability to regulate mitochondrial dynamics, previously used to treat other diseases like LCZ696, repurposing such drugs is an effective strategy to bring them into clinical practice more quickly. 3) Also, many natural compounds have been shown to exert cardioprotective effects through different molecular pathways, modulating abnormal mitochondrial dynamics in cardiomyocytes affected by DOX without weakening, in fact often strengthening, DOX's anticancer

capacity. However, it is worth noting that, due to the multi-target effect of drugs, the mechanism of action and side effects of each compound merit thorough study in the pre-clinical model before clinical studies should be carried out. 4) Furthermore, exosomes secreted by stem cells and miRNAs are increasingly being considered as a therapeutic tool for cardiovascular disease, as they can repair heart damage, and bring about cardiac regeneration through re-balancing impaired mitochondrial dynamics. In order to better understand the upstream and downstream mechanisms underlying protein changes, which facilitate the regulation of mitochondrial dynamic imbalance and mitigate DOX-induced myocardial injury, the effects of miRNA and exosomes on mitochondrial fission proteins and fusion proteins should be thoroughly studied. 5) With regard to exercise, based on the above-mentioned previous studies, whether employed as a therapeutic (postconditioning) or preconditioning approach, EXE is recognized as a vital regulator of mitochondrial turnover that can help maintain positive cellular alterations. Therefore, consistent physical exercise may be reasonably considered to be one of the most important non-drug interventions for DOX-induced cardiotoxicity. Further studies are merited to determine the most efficient, effective, and practical combination of EXE intensity and duration to help cancer patients avoid serious cardiac complications caused by DOX.

Last but not least, it is significant to emphasize that mitochondrial fission is a prerequisite for mitophagy, which is essential for mitochondrial quality control in different heart diseases by eliminating damaged mitochondria (Li et al., 2022). Although compared with mitochondrial fission, mitochondrial fusion has certain protective effects, such as inhibiting the release of cytochrome C and improving mitochondrial metabolism, it prevents the selective elimination of damaged mitochondria by mitophagy (Narendra et al., 2010), that is, the over-enhanced fusion of mitochondria may lead to the accumulation of damaged mitochondria and accelerate the progression of cardiomyopathy. However, in the current studies of cardiotoxicity caused by DOX, there are few studies on the usage of high doses or longer periods of mitochondrial dynamics regulators. Fortunately, the treatment time and pattern of exercise mentioned above provide some clues for the relationship between mitochondrial dynamics and mitophagy. According to Nan, mice treated with high dose show a greater degree of myocardial damage by I/R than control mice, and the short-term administration of Mdivi-1 has proved to be beneficial by limiting ischemic stress to a short period while long-term treatment with Mdivi-1 could be detrimental, which is likely because of excessive inhibition of mitochondrial fission which suppresses mitophagy to result in the accumulation of abnormal mitochondria (Nan et al., 2017). So, in the future, a large number of preclinical studies and clinical studies are needed to emphasize the effects of different dosages and duration of regulators so as to maintain the optimal balance between mitochondrial fission and fusion.

7 Conclusion

DOX-induced cardiotoxicity is a complex process involving an imbalance of mitochondrial dynamics, mitochondrial dysfunction, activation of apoptotic pathways in addition to DNA damage and oxidative stress. It has been clearly indicated that mitochondrial dynamics disorder is one of the leading causes of DOX-induced cardiotoxicity. Numerous studies have demonstrated that exposure to DOX causes the tendency of mitochondrial dynamics toward stronger mitochondrial fission and weakened mitochondrial fusion via upregulation of mitochondrial fission proteins such as DRP1 and downregulation of the mitochondrial fusion proteins MFN1, MFN2 and OPA1, resulting in mitochondrial fragmentation and a damaged mitochondrial network. Therefore, it is reasonable to consider the modulation of imbalanced mitochondrial dynamics in cardiomyocytes affected by DOX as a potential target.

And so far, several pharmacological inhibitors targeting key proteins of mitochondrial dynamics, drug compounds, natural modulators, miRNAs and exosomes mentioned above, and even exercise have proven that the re-balancing of mitochondrial dynamics is a potent approach to cardioprotection from DOX exposure by regulating the enzyme activity, expression level, oligomerization and intermolecular interaction of mitochondrial fission/fusion associated proteins.

In summary, rebalance of mitochondrial dynamics proteins is a potential therapeutic strategy for alleviation and avoidance of cardiotoxicity induced by DOX. Specially, inhibiting DRP1-mediated mitochondrial fission and enhancing MFN2-mediated mitochondrial fusion to promote cellular energy metabolic pattern shift may be a very promising therapeutic strategy, as it holds the promise of "killing two birds with one stone", that is reducing cardiac adverse reactions caused by Dox while improving its anticancer performance. But further research is merited in order to better understand the upstream and downstream molecular mechanics of these proteins, as well as the interactions of mitochondrial dynamics with autophagy and mitophagy in order to safeguard patients from the potentially fatal cardiotoxic effects of DOX.

Author contributions

RC contributed to the conception and design of the article; YH and XH provided supervision; MN revised the manuscript. All authors contributed to the article and approved the submitted version.

Funding

The research leading to these results has received funding from Department of Health of Jilin Province (2015Z012) and Jilin Provincial Department of Science and Technology (YDZJ202301ZYTS516). The financial support was received by YH.

Conflict of interest

The authors declare that the research was conducted in the absence of any commercial or financial relationships that could be construed as a potential conflict of interest.

Publisher's note

References

Accili, D., and Arden, K. C. (2004). FoxOs at the crossroads of cellular metabolism, differentiation, and transformation. *Cell* 117 (4), 421–426. doi:10.1016/s0092-8674(04)00452-0

An, J., Li, P., Li, J., Dietz, R., and Donath, S. (2009). ARC is a critical cardiomyocyte survival switch in doxorubicin cardiotoxicity. *J. Mol. Med. Berl.* 87 (4), 401–410. doi:10.1007/s00109-008-0434-z

Antonny, B., Burd, C., De Camilli, P., Chen, E., Daumke, O., Faelber, K., et al. (2016). Membrane fission by dynamin: What we know and what we need to know. *EMBO J.* 35 (21), 2270–2284. doi:10.15252/embj.201694613

Arinno, A., Maneechote, C., Khuanjing, T., Ongnok, B., Prathumsap, N., Chunchai, T., et al. (2021). Cardioprotective effects of melatonin and metformin against doxorubicin-induced cardiotoxicity in rats are through preserving mitochondrial function and dynamics. *Biochem. Pharmacol.* 192, 114743. doi:10.1016/j.bcp.2021.114743

Aung, L. H. H., Li, R., Prabhakar, B. S., and Li, P. (2017). Knockdown of Mtfp1 can minimize doxorubicin cardiotoxicity by inhibiting Dnm1l-mediated mitochondrial fission. *J. Cell Mol. Med.* 21 (12), 3394–3404. doi:10.1111/jcmm.13250

Bell, E. L., and Guarente, L. (2011). The SirT3 divining rod points to oxidative stress. *Mol. Cell* 42 (5), 561–568. doi:10.1016/j.molcel.2011.05.008

Bernardi, P., Rasola, A., Forte, M., and Lippe, G. (2015). The mitochondrial permeability transition pore: Channel formation by F-ATP synthase, integration in signal transduction, and role in pathophysiology. *Physiol. Rev.* 95 (4), 1111–1155. doi:10.1152/physrev.00001.2015

Bordt, E. A., Clerc, P., Roelofs, B. A., Saladino, A. J., Tretter, L., Adam-Vizi, V., et al. (2017). The putative Drp1 inhibitor mdivi-1 is a reversible mitochondrial complex I inhibitor that modulates reactive oxygen species. *Dev. Cell* 40 (6), 583–594. doi:10.1016/j.devcel.2017.02.020

Broeyer, F. J., Osanto, S., Suzuki, J., de Jongh, F., van Slooten, H., Tanis, B. C., et al. (2014). Evaluation of lecithinized human recombinant super oxide dismutase as cardioprotectant in anthracycline-treated breast cancer patients. *Br. J. Clin. Pharmacol.* 78 (5), 950–960. doi:10.1111/bcp.12429

Bures, J., Jirkovska, A., Sestak, V., Jansova, H., Karabanovich, G., Roh, J., et al. (2017). Investigation of novel dexrazoxane analogue JR-311 shows significant cardioprotective effects through topoisomerase IIbeta but not its iron chelating metabolite. *Toxicology* 392, 1–10. doi:10.1016/j.tox.2017.09.012

Campanella, M., Casswell, E., Chong, S., Farah, Z., Wieckowski, M. R., Abramov, A. Y., et al. (2008). Regulation of mitochondrial structure and function by the F1Fo-ATPase inhibitor protein, IF1. *Cell Metab.* 8 (1), 13–25. doi:10.1016/j.cmet.2008.06.001

Cao, Y. P., and Zheng, M. (2019). Mitochondrial dynamics and inter-mitochondrial communication in the heart. *Arch. Biochem. Biophys.* 663, 214–219. doi:10.1016/j.abb.2019.01.017

Carvalho, F. S., Burgeiro, A., Garcia, R., Moreno, A. J., Carvalho, R. A., and Oliveira, P. J. (2014). Doxorubicin-induced cardiotoxicity: From bioenergetic failure and cell death to cardiomyopathy. *Med. Res. Rev.* 34 (1), 106–135. doi:10.1002/med.21280

Cassidy-Stone, A., Chipuk, J. E., Ingerman, E., Song, C., Yoo, C., Kuwana, T., et al. (2008). Chemical inhibition of the mitochondrial division dynamin reveals its role in Bax/Bak-dependent mitochondrial outer membrane permeabilization. *Dev. Cell* 14 (2), 193–204. doi:10.1016/j.devcel.2007.11.019

Catanzaro, M. P., Weiner, A., Kaminaris, A., Li, C., Cai, F., Zhao, F., et al. (2019). Doxorubicin-induced cardiomyocyte death is mediated by unchecked mitochondrial fission and mitophagy. *FASEB J.* 33 (10), 11096–11108. doi:10.1096/fj.201802663R

Chan, D. C. (2020). Mitochondrial dynamics and its involvement in disease. *Annu. Rev. Pathol.* 15, 235–259. doi:10.1146/annurev-pathmechdis-012419-032711

Chang, C. R., and Blackstone, C. (2007). Cyclic AMP-dependent protein kinase phosphorylation of Drp1 regulates its GTPase activity and mitochondrial morphology. *J. Biol. Chem.* 282 (30), 21583–21587. doi:10.1074/jbc.C700083200

Chen, H., Detmer, S. A., Ewald, A. J., Griffin, E. E., Fraser, S. E., and Chan, D. C. (2003). Mitofusins Mfn1 and Mfn2 coordinately regulate mitochondrial fusion and are essential for embryonic development. *J. Cell Biol.* 160 (2), 189–200. doi:10.1083/jcb.200211046

Chen, Q. Q., Ma, G., Liu, J. F., Cai, Y. Y., Zhang, J. Y., Wei, T. T., et al. (2021). Neuraminidase 1 is a driver of experimental cardiac hypertrophy. *Eur. Heart J.* 42 (36), 3770–3782. doi:10.1093/eurheartj/ehab347

Chicco, A. J., Schneider, C. M., and Hayward, R. (2005). Voluntary exercise protects against acute doxorubicin cardiotoxicity in the isolated perfused rat heart. *Am. J. Physiol. Regul. Integr. Comp. Physiol.* 289 (2), R424-R431–R431. doi:10.1152/ajpregu.00636.2004

Cipolat, S., Martins de Brito, O., Dal Zilio, B., and Scorrano, L. (2004). OPA1 requires mitofusin 1 to promote mitochondrial fusion. *Proc. Natl. Acad. Sci. U. S. A.* 101 (45), 15927–15932. doi:10.1073/pnas.0407043101

Courtois, S., de Luxan-Delgado, B., Penin-Peyta, L., Royo-Garcia, A., Parejo-Alonso, B., Jagust, P., et al. (2021). Inhibition of mitochondrial dynamics preferentially targets pancreatic cancer cells with enhanced tumorigenic and invasive potential. *Cancers (Basel)* 13 (4), 698. doi:10.3390/cancers13040698

Cogliati, S., Frezza, C., Soriano, M. E., Varanita, T., Quintana-Cabrera, R., Corrado, M., et al. (2013). Mitochondrial cristae shape determines respiratory chain supercomplexes assembly and respiratory efficiency. *Cell* 155 (1), 160–171. doi:10.1016/j.cell.2013.08.032

Corremans, R., Adao, R., De Keulenaer, G. W., Leite-Moreira, A. F., and Bras-Silva, C. (2019). Update on pathophysiology and preventive strategies of anthracycline-induced cardiotoxicity. *Clin. Exp. Pharmacol. Physiol.* 46 (3), 204–215. doi:10.1111/1440-1681.13036

Cribbs, J. T., and Strack, S. (2007). Reversible phosphorylation of Drp1 by cyclic AMP-dependent protein kinase and calcineurin regulates mitochondrial fission and cell death. *EMBO Rep.* 8 (10), 939–944. doi:10.1038/sj.embor.7401062

Curigliano, G., Cardinale, D., Dent, S., Criscitiello, C., Aseyev, O., Lenihan, D., et al. (2016). Cardiotoxicity of anticancer treatments: Epidemiology, detection, and management. *CA Cancer J. Clin.* 66 (4), 309–325. doi:10.3322/caac.21341

Deng, S., Yan, T., Jendrny, C., Nemecek, A., Vincetic, M., Godtel-Armbrust, U., et al. (2014). Dexrazoxane may prevent doxorubicin-induced DNA damage via depleting both topoisomerase II isoforms. *BMC Cancer* 14, 842. doi:10.1186/1471-2407-14-842

Dhingra, A., Jayas, R., Afshar, P., Guberman, M., Maddaford, G., Gerstein, J., et al. (2017). Ellagic acid antagonizes Bnip3-mediated mitochondrial injury and necrotic cell death of cardiac myocytes. *Free Radic. Biol. Med.* 112, 411–422. doi:10.1016/j.freeradbiomed.2017.08.010

Ding, M., Shi, R., Cheng, S., Li, M., De, D., Liu, C., et al. (2022a). Mfn2-mediated mitochondrial fusion alleviates doxorubicin-induced cardiotoxicity with enhancing its anticancer activity through metabolic switch. *Redox Biol.* 52, 102311. doi:10.1016/j.redox.2022.102311

Ding, M., Shi, R., Fu, F., Li, M., De, D., Du, Y., et al. (2022b). Paeonol protects against doxorubicin-induced cardiotoxicity by promoting Mfn2-mediated mitochondrial fusion through activating the PKCε-Stat3 pathway. *J. Adv. Res.* 47, 151–162. doi:10.1016/j.jare.2022.07.002

Dolinsky, V. W., Rogan, K. J., Sung, M. M., Zordoky, B. N., Haykowsky, M. J., Young, M. E., et al. (2013). Both aerobic exercise and resveratrol supplementation attenuate doxorubicin-induced cardiac injury in mice. *Am. J. Physiol. Endocrinol. Metab.* 305 (2), E243–E253. doi:10.1152/ajpendo.00044.2013

Du, J., Hang, P., Pan, Y., Feng, B., Zheng, Y., Chen, T., et al. (2019). Inhibition of miR-23a attenuates doxorubicin-induced mitochondria-dependent cardiomyocyte apoptosis by targeting the PGC-1α/Drp1 pathway. *Toxicol. Appl. Pharmacol.* 369, 73–81. doi:10.1016/j.taap.2019.02.016

Duan, J., Liu, X., Shen, S., Tan, X., Wang, Y., Wang, L., et al. (2023). Trophoblast stem-cell-derived exosomes alleviate cardiotoxicity of doxorubicin via improving mfn2-mediated mitochondrial fusion. *Cardiovasc Toxicol.* 23, 23–31. doi:10.1007/s12012-022-09774-2

Felker, G. M., Thompson, R. E., Hare, J. M., Hruban, R. H., Clemetson, D. E., Howard, D. L., et al. (2000). Underlying causes and long-term survival in patients with initially unexplained cardiomyopathy. *N. Engl. J. Med.* 342 (15), 1077–1084. doi:10.1056/NEJM200004133421502

Ferreira, J. C. B., Campos, J. C., Qvit, N., Qi, X., Bozi, L. H. M., Bechara, L. R. G., et al. (2019). A selective inhibitor of mitofusin 1-βIIPKC association improves heart failure outcome in rats. *Nat. Commun.* 10 (1), 329. doi:10.1038/s41467-018-08276-6

Filichia, E., Hoffer, B., Qi, X., and Luo, Y. (2016). Inhibition of Drp1 mitochondrial translocation provides neural protection in dopaminergic system in a Parkinson's disease model induced by MPTP. *Sci. Rep.* 6, 32656. doi:10.1038/srep32656

Frezza, C., Cipolat, S., Martins de Brito, O., Micaroni, M., Beznoussenko, G. V., Rudka, T., et al. (2006). OPA1 controls apoptotic cristae remodeling independently from mitochondrial fusion. *Cell* 126 (1), 177–189. doi:10.1016/j.cell.2006.06.025

Frohlich, C., Grabiger, S., Schwefel, D., Faelber, K., Rosenbaum, E., Mears, J., et al. (2013). Structural insights into oligomerization and mitochondrial remodelling of dynamin 1-like protein. *EMBO J.* 32 (9), 1280–1292. doi:10.1038/emboj.2013.74

Gao, T., Zhang, X., Zhao, J., Zhou, F., Wang, Y., Zhao, Z., et al. (2020). SIK2 promotes reprogramming of glucose metabolism through PI3K/AKT/HIF-1α pathway and Drp1-mediated mitochondrial fission in ovarian cancer. *Cancer Lett.* 469, 89–101. doi:10.1016/j.canlet.2019.10.029

Gaytan, S. L., Lawan, A., Chang, J., Nurunnabi, M., Bajpeyi, S., Boyle, J. B., et al. (2023). The beneficial role of exercise in preventing doxorubicin-induced cardiotoxicity. *Front. Physiol.* 14, 1133423. doi:10.3389/fphys.2023.1133423

Gharanei, M., Hussain, A., Janneh, O., and Maddock, H. (2013). Attenuation of doxorubicin-induced cardiotoxicity by mdivi-1: A mitochondrial division/mitophagy inhibitor. *PLoS One* 8 (10), e77713. doi:10.1371/journal.pone.0077713

Giacomello, M., Pyakurel, A., Glytsou, C., and Scorrano, L. (2020). The cell biology of mitochondrial membrane dynamics. *Nat. Rev. Mol. Cell Biol.* 21 (4), 204–224. doi:10.1038/s41580-020-0210-7

Givvimani, S., Munjal, C., Tyagi, N., Sen, U., Metreveli, N., and Tyagi, S. C. (2012). Mitochondrial division/mitophagy inhibitor (Mdivi) ameliorates pressure overload induced heart failure. *PLoS One* 7 (3), e32388. doi:10.1371/journal.pone.0032388

Glanz, V. Y., Myasoedova, V. A., Grechko, A. V., and Orekhov, A. N. (2019). Sialidase activity in human pathologies. *Eur. J. Pharmacol.* 842, 345–350. doi:10.1016/j.ejphar.2018.11.014

Gomes, L. C., Di Benedetto, G., and Scorrano, L. (2011). During autophagy mitochondria elongate, are spared from degradation and sustain cell viability. *Nat. Cell Biol.* 13 (5), 589–598. doi:10.1038/ncb2220

Haileselassie, B., Mukherjee, R., Joshi, A. U., Napier, B. A., Massis, L. M., Ostberg, N. P., et al. (2019). Drp1/Fis1 interaction mediates mitochondrial dysfunction in septic cardiomyopathy. *J. Mol. Cell Cardiol.* 130, 160–169. doi:10.1016/j.yjmcc.2019.04.006

Hasinoff, B. B., Patel, D., and Wu, X. (2020). The role of topoisomerase IIβ in the mechanisms of action of the doxorubicin cardioprotective agent dexrazoxane. *Cardiovasc Toxicol.* 20 (3), 312–320. doi:10.1007/s12012-019-09554-5

Heimerl, M., Sieve, I., Ricke-Hoch, M., Erschow, S., Battmer, K., Scherr, M., et al. (2020). Neuraminidase-1 promotes heart failure after ischemia/reperfusion injury by affecting cardiomyocytes and invading monocytes/macrophages. *Basic Res. Cardiol.* 115 (6), 62. doi:10.1007/s00395-020-00821-z

Hom, J., Yu, T., Yoon, Y., Porter, G., and Sheu, S. S. (2010). Regulation of mitochondrial fission by intracellular Ca2+ in rat ventricular myocytes. *Biochim. Biophys. Acta* 1797 (6-7), 913–921. doi:10.1016/j.bbabio.2010.03.018

Hu, B., Zhen, D., Bai, M., Xuan, T., Wang, Y., Liu, M., et al. (2022). Ethanol extracts of Rhaponticum uniflorum (L) DC flowers attenuate doxorubicin-induced cardiotoxicity via alleviating apoptosis and regulating mitochondrial dynamics in H9c2 cells. *J. Ethnopharmacol.* 288, 114936. doi:10.1016/j.jep.2021.114936

Huang, J., Wu, R., Chen, L., Yang, Z., Yan, D., and Li, M. (2022). Understanding anthracycline cardiotoxicity from mitochondrial aspect. *Front. Pharmacol.* 13, 811406. doi:10.3389/fphar.2022.811406

Hull, T. D., Boddu, R., Guo, L., Tisher, C. C., Traylor, A. M., Patel, B., et al. (2016). Heme oxygenase-1 regulates mitochondrial quality control in the heart. *JCI Insight* 1 (2), e85817. doi:10.1172/jci.insight.85817

Inagaki, S., Suzuki, Y., Kawasaki, K., Kondo, R., Imaizumi, Y., and Yamamura, H. (2023). Mitofusin 1 and 2 differentially regulate mitochondrial function underlying Ca(2+) signaling and proliferation in rat aortic smooth muscle cells. *Biochem. Biophys. Res. Commun.* 645, 137–146. doi:10.1016/j.bbrc.2023.01.044

Inoue-Yamauchi, A., and Oda, H. (2012). Depletion of mitochondrial fission factor DRP1 causes increased apoptosis in human colon cancer cells. *Biochem. Biophys. Res. Commun.* 421 (1), 81–85. doi:10.1016/j.bbrc.2012.03.118

Jin, J. Y., Wei, X. X., Zhi, X. L., Wang, X. H., and Meng, D. (2021). Drp1-dependent mitochondrial fission in cardiovascular disease. *Acta Pharmacol. Sin.* 42 (5), 655–664. doi:10.1038/s41401-020-00518-y

Kalia, R., Wang, R. Y., Yusuf, A., Thomas, P. V., Agard, D. A., Shaw, J. M., et al. (2018). Structural basis of mitochondrial receptor binding and constriction by DRP1. *Nature* 558 (7710), 401–405. doi:10.1038/s41586-018-0211-2

Kalyanaraman, B. (2020). Teaching the basics of the mechanism of doxorubicin-induced cardiotoxicity: Have we been barking up the wrong tree? *Redox Biol.* 29, 101394. doi:10.1016/j.redox.2019.101394

Kamerkar, S. C., Kraus, F., Sharpe, A. J., Pucadyil, T. J., and Ryan, M. T. (2018). Dynamin-related protein 1 has membrane constricting and severing abilities sufficient for mitochondrial and peroxisomal fission. *Nat. Commun.* 9 (1), 5239. doi:10.1038/s41467-018-07543-w

Kavazis, A. N., Morton, A. B., Hall, S. E., and Smuder, A. J. (2017). Effects of doxorubicin on cardiac muscle subsarcolemmal and intermyofibrillar mitochondria. *Mitochondrion* 34, 9–19. doi:10.1016/j.mito.2016.10.008

Kavazis, A. N., Smuder, A. J., Min, K., Tumer, N., and Powers, S. K. (2010). Short-term exercise training protects against doxorubicin-induced cardiac mitochondrial damage independent of HSP72. *Am. J. Physiol. Heart Circ. Physiol.* 299 (5), H1515–H1524. doi:10.1152/ajpheart.00585.2010

Kleele, T., Rey, T., Winter, J., Zaganelli, S., Mahecic, D., Perreten Lambert, H., et al. (2021). Distinct fission signatures predict mitochondrial degradation or biogenesis. *Nature* 593 (7859), 435–439. doi:10.1038/s41586-021-03510-6

Kraus, F., and Ryan, M. T. (2017). The constriction and scission machineries involved in mitochondrial fission. *J. Cell Sci.* 130 (18), 2953–2960. doi:10.1242/jcs.199562

Kushnareva, Y. E., Gerencser, A. A., Bossy, B., Ju, W. K., White, A. D., Waggoner, J., et al. (2013). Loss of OPA1 disturbs cellular calcium homeostasis and sensitizes for excitotoxicity. *Cell Death Differ.* 20 (2), 353–365. doi:10.1038/cdd.2012.128

Landes, T., Emorine, L. J., Courilleau, D., Rojo, M., Belenguer, P., and Arnaune-Pelloquin, L. (2010). The BH3-only Bnip3 binds to the dynamin Opa1 to promote mitochondrial fragmentation and apoptosis by distinct mechanisms. *EMBO Rep.* 11 (6), 459–465. doi:10.1038/embor.2010.50

Lee, D. S., and Kim, J. E. (2018). PDI-mediated S-nitrosylation of DRP1 facilitates DRP1-S616 phosphorylation and mitochondrial fission in CA1 neurons. *Cell Death Dis.* 9 (9), 869. doi:10.1038/s41419-018-0910-5

Lee, Y. J., Jeong, S. Y., Karbowski, M., Smith, C. L., and Youle, R. J. (2004). Roles of the mammalian mitochondrial fission and fusion mediators Fis1, Drp1, and Opa1 in apoptosis. *Mol. Biol. Cell* 15 (11), 5001–5011. doi:10.1091/mbc.e04-04-0294

Lee, Y., Kwon, I., Jang, Y., Cosio-Lima, L., and Barrington, P. (2020). Endurance exercise attenuates doxorubicin-induced cardiotoxicity. *Med. Sci. Sports Exerc* 52 (1), 25–36. doi:10.1249/MSS.0000000000002094

Li, A., Gao, M., Jiang, W., Qin, Y., and Gong, G. (2020a). Mitochondrial dynamics in adult cardiomyocytes and heart diseases. *Front. Cell Dev. Biol.* 8, 584800. doi:10.3389/fcell.2020.584800

Li, J., Li, Y., Jiao, J., Wang, J., Li, Y., Qin, D., et al. (2014). Mitofusin 1 is negatively regulated by microRNA 140 in cardiomyocyte apoptosis. *Mol. Cell Biol.* 34 (10), 1788–1799. doi:10.1128/MCB.00774-13

Li, L., Li, J., Wang, Q., Zhao, X., Yang, D., Niu, L., et al. (2020b). Shenmai injection protects against doxorubicin-induced cardiotoxicity via maintaining mitochondrial homeostasis. *Front. Pharmacol.* 11, 815. doi:10.3389/fphar.2020.00815

Li, Y., Lin, R., Peng, X., Wang, X., Liu, X., Li, L., et al. (2022). The role of mitochondrial quality control in anthracycline-induced cardiotoxicity: From bench to bedside. *Oxid. Med. Cell Longev.* 2022, 3659278. doi:10.1155/2022/3659278

Liang, X., Wang, S., Wang, L., Ceylan, A. F., Ren, J., and Zhang, Y. (2020). Mitophagy inhibitor liensinine suppresses doxorubicin-induced cardiotoxicity through inhibition of Drp1-mediated maladaptive mitochondrial fission. *Pharmacol. Res.* 157, 104846. doi:10.1016/j.phrs.2020.104846

Liu, C., Han, Y., Gu, X., Li, M., Du, Y., Feng, N., et al. (2021). Paeonol promotes Opa1-mediated mitochondrial fusion via activating the CK2α-Stat3 pathway in diabetic cardiomyopathy. *Redox Biol.* 46, 102098. doi:10.1016/j.redox.2021.102098

Loson, O. C., Song, Z., Chen, H., and Chan, D. C. (2013). Fis1, mff, MiD49, and MiD51 mediate Drp1 recruitment in mitochondrial fission. *Mol. Biol. Cell* 24 (5), 659–667. doi:10.1091/mbc.E12-10-0721

Lunt, S. Y., and Vander Heiden, M. G. (2011). Aerobic glycolysis: Meeting the metabolic requirements of cell proliferation. *Annu. Rev. Cell Dev. Biol.* 27, 441–464. doi:10.1146/annurev-cellbio-092910-154237

Ma, Y., Wang, L., and Jia, R. (2020). The role of mitochondrial dynamics in human cancers. *Am. J. Cancer Res.* 10 (5), 1278–1293.

Macdonald, P. J., Stepanyants, N., Mehrotra, N., Mears, J. A., Qi, X., Sesaki, H., et al. (2014). A dimeric equilibrium intermediate nucleates Drp1 reassembly on mitochondrial membranes for fission. *Mol. Biol. Cell* 25 (12), 1905–1915. doi:10.1091/mbc.E14-02-0728

Maneechote, C., Khuanjing, T., Ongnok, B., Arinno, A., Prathumsap, N., Chunchai, T., et al. (2022). Promoting mitochondrial fusion in doxorubicin-induced cardiotoxicity: A novel therapeutic target for cardioprotection. *Clin. Sci. (Lond)* 136 (11), 841–860. doi:10.1042/cs20220074

Maneechote, C., Palee, S., Kerdphoo, S., Jaiwongkam, T., Chattipakorn, S. C., and Chattipakorn, N. (2019). Balancing mitochondrial dynamics via increasing mitochondrial fusion attenuates infarct size and left ventricular dysfunction in rats with cardiac ischemia/reperfusion injury. *Clin. Sci. (Lond)* 133 (3), 497–513. doi:10.1042/CS20190014

Marechal, X., Montaigne, D., Marciniak, C., Marchetti, P., Hassoun, S. M., Beauvillain, J. C., et al. (2011). Doxorubicin-induced cardiac dysfunction is attenuated by ciclosporin treatment in mice through improvements in mitochondrial bioenergetics. *Clin. Sci. (Lond)* 121 (9), 405–413. doi:10.1042/CS20110069

Marques-Aleixo, I., Santos-Alves, E., Torrella, J. R., Oliveira, P. J., Magalhaes, J., and Ascensao, A. (2018). Exercise and doxorubicin treatment modulate cardiac mitochondrial quality control signaling. *Cardiovasc Toxicol.* 18 (1), 43–55. doi:10.1007/s12012-017-9412-4

McClendon, A. K., and Osheroff, N. (2007). DNA topoisomerase II, genotoxicity, and cancer. *Mutat. Res.* 623 (1-2), 83–97. doi:10.1016/j.mrfmmm.2007.06.009

Mishra, P., and Chan, D. C. (2016). Metabolic regulation of mitochondrial dynamics. *J. Cell Biol.* 212 (4), 379–387. doi:10.1083/jcb.201511036

Mitry, M. A., and Edwards, J. G. (2016). Doxorubicin induced heart failure: Phenotype and molecular mechanisms. *Int. J. Cardiol. Heart Vasc.* 10, 17–24. doi:10.1016/j.ijcha.2015.11.004

Miyoshi, T., Nakamura, K., Amioka, N., Hatipoglu, O. F., Yonezawa, T., Saito, Y., et al. (2022). LCZ696 ameliorates doxorubicin-induced cardiomyocyte toxicity in rats. *Sci. Rep.* 12 (1), 4930. doi:10.1038/s41598-022-09094-z

Montalvo, R. N., Boeno, F. P., Dowllah, I. M., Moritz, C. E. J., Nguyen, B. L., Doerr, V., et al. (2023). Exercise and doxorubicin modify markers of iron overload and cardiolipin deficiency in cardiac mitochondria. *Int. J. Mol. Sci.* 24 (9), 7689. doi:10.3390/ijms24097689

Morton, A. B., Mor Huertas, A., Hinkley, J. M., Ichinoseki-Sekine, N., Christou, D. D., and Smuder, A. J. (2019). Mitochondrial accumulation of doxorubicin in cardiac and diaphragm muscle following exercise preconditioning. *Mitochondrion* 45, 52–62. doi:10.1016/j.mito.2018.02.005

Nan, J., Zhu, W., Rahman, M. S., Liu, M., Li, D., Su, S., et al. (2017). Molecular regulation of mitochondrial dynamics in cardiac disease. *Biochim. Biophys. Acta Mol. Cell Res.* 1864 (7), 1260–1273. doi:10.1016/j.bbamcr.2017.03.006

Narendra, D. P., Jin, S. M., Tanaka, A., Suen, D. F., Gautier, C. A., Shen, J., et al. (2010). PINK1 is selectively stabilized on impaired mitochondria to activate Parkin. *PLoS Biol.* 8 (1), e1000298. doi:10.1371/journal.pbio.1000298

Narezkina, A., and Nasim, K. (2019). Anthracycline cardiotoxicity. *Circ. Heart Fail* 12 (3), e005910. doi:10.1161/CIRCHEARTFAILURE.119.005910

Octavia, Y., Tocchetti, C. G., Gabrielson, K. L., Janssens, S., Crijns, H. J., and Moens, A. L. (2012). Doxorubicin-induced cardiomyopathy: From molecular mechanisms to therapeutic strategies. *J. Mol. Cell Cardiol.* 52 (6), 1213–1225. doi:10.1016/j.yjmcc.2012.03.006

Osataphan, N., Phrommintikul, A., Chattipakorn, S. C., and Chattipakorn, N. (2020). Effects of doxorubicin-induced cardiotoxicity on cardiac mitochondrial dynamics and mitochondrial function: Insights for future interventions. *J. Cell Mol. Med.* 24 (12), 6534–6557. doi:10.1111/jcmm.15305

Palmer, C. S., Osellame, L. D., Laine, D., Koutsopoulos, O. S., Frazier, A. E., and Ryan, M. T. (2011). MiD49 and MiD51, new components of the mitochondrial fission machinery. *EMBO Rep.* 12 (6), 565–573. doi:10.1038/embor.2011.54

Park, S. J., Bae, J. E., Jo, D. S., Kim, J. B., Park, N. Y., Fang, J., et al. (2021). Increased O-GlcNAcylation of Drp1 by amyloid-beta promotes mitochondrial fission and dysfunction in neuronal cells. *Mol. Brain* 14 (1), 6. doi:10.1186/s13041-020-00727-w

Peng, K., Yang, L., Wang, J., Ye, F., Dan, G., Zhao, Y., et al. (2017). The interaction of mitochondrial biogenesis and fission/fusion mediated by PGC-1α regulates rotenone-induced dopaminergic neurotoxicity. *Mol. Neurobiol.* 54 (5), 3783–3797. doi:10.1007/s12035-016-9944-9

Pillai, V. B., Kanwal, A., Fang, Y. H., Sharp, W. W., Samant, S., Arbiser, J., et al. (2017). Honokiol, an activator of Sirtuin-3 (SIRT3) preserves mitochondria and protects the heart from doxorubicin-induced cardiomyopathy in mice. *Oncotarget* 8 (21), 34082–34098. doi:10.18632/oncotarget.16133

Prudent, J., Zunino, R., Sugiura, A., Mattie, S., Shore, G. C., and McBride, H. M. (2015). MAPL SUMOylation of Drp1 stabilizes an ER/mitochondrial platform required for cell death. *Mol. Cell* 59 (6), 941–955. doi:10.1016/j.molcel.2015.08.001

Qin, Y., Lv, C., Zhang, X., Ruan, W., Xu, X., Chen, C., et al. (2021). Neuraminidase1 inhibitor protects against doxorubicin-induced cardiotoxicity via suppressing drp1-dependent mitophagy. *Front. Cell Dev. Biol.* 9, 802502. doi:10.3389/fcell.2021.802502

Quagliariello, V., De Laurentiis, M., Rea, D., Barbieri, A., Monti, M. G., Carbone, A., et al. (2021). The SGLT-2 inhibitor empagliflozin improves myocardial strain, reduces cardiac fibrosis and pro-inflammatory cytokines in non-diabetic mice treated with doxorubicin. *Cardiovasc Diabetol.* 20 (1), 150. doi:10.1186/s12933-021-01346-y

Rambold, A. S., Kostelecky, B., Elia, N., and Lippincott-Schwartz, J. (2011). Tubular network formation protects mitochondria from autophagosomal degradation during nutrient starvation. *Proc. Natl. Acad. Sci. U. S. A.* 108 (25), 10190–10195. doi:10.1073/pnas.1107402108

Rehman, J., Zhang, H. J., Toth, P. T., Zhang, Y., Marsboom, G., Hong, Z., et al. (2012). Inhibition of mitochondrial fission prevents cell cycle progression in lung cancer. *FASEB J.* 26 (5), 2175–2186. doi:10.1096/fj.11-196543

Renu, K., Abilash, G. A., Tirupathi pichiah, P, B., and Arunachalam, S. (2018). Molecular mechanism of doxorubicin-induced cardiomyopathy - an update. *Eur. J. Pharmacol.* 818, 241–253. doi:10.1016/j.ejphar.2017.10.043

Roberts, R. M., and Fisher, S. J. (2011). Trophoblast stem cells. *Biol. Reprod.* 84 (3), 412–421. doi:10.1095/biolreprod.110.088724

Rojo, M., Legros, F., Chateau, D., and Lombes, A. (2002). Membrane topology and mitochondrial targeting of mitofusins, ubiquitous mammalian homologs of the transmembrane GTPase Fzo. *J. Cell Sci.* 115 (Pt 8), 1663–1674. doi:10.1242/jcs.115.8.1663

Samant, S. A., Zhang, H. J., Hong, Z., Pillai, V. B., Sundaresan, N. R., Wolfgeher, D., et al. (2014). SIRT3 deacetylates and activates OPA1 to regulate mitochondrial dynamics during stress. *Mol. Cell Biol.* 34 (5), 807–819. doi:10.1128/MCB.01483-13

Sarraf, S. A., Raman, M., Guarani-Pereira, V., Sowa, M. E., Huttlin, E. L., Gygi, S. P., et al. (2013). Landscape of the PARKIN-dependent ubiquitylome in response to mitochondrial depolarization. *Nature* 496 (7445), 372–376. doi:10.1038/nature12043

Schirone, L., D'Ambrosio, L., Forte, M., Genovese, R., Schiavon, S., Spinosa, G., et al. (2022). Mitochondria and doxorubicin-induced cardiomyopathy: A complex interplay. *Cells* 11 (13), 2000. doi:10.3390/cells11132000

Scott, J. M., Khakoo, A., Mackey, J. R., Haykowsky, M. J., Douglas, P. S., and Jones, L. W. (2011). Modulation of anthracycline-induced cardiotoxicity by aerobic exercise in breast cancer: Current evidence and underlying mechanisms. *Circulation* 124 (5), 642–650. doi:10.1161/CIRCULATIONAHA.111.021774

Shan, M., Yu, X., Li, Y., Fu, C., and Zhang, C. (2021). Vitamin B6 alleviates lipopolysaccharide-induced myocardial injury by ferroptosis and apoptosis regulation. *Front. Pharmacol.* 12, 766820. doi:10.3389/fphar.2021.766820

Shi, Y., Li, F., Shen, M., Sun, C., Hao, W., Wu, C., et al. (2021). Luteolin prevents cardiac dysfunction and improves the chemotherapeutic efficacy of doxorubicin in breast cancer. *Front. Cardiovasc Med.* 8, 750186. doi:10.3389/fcvm.2021.750186

Sieve, I., Ricke-Hoch, M., Kasten, M., Battmer, K., Stapel, B., Falk, C. S., et al. (2018). A positive feedback loop between IL-1β, LPS and NEU1 may promote atherosclerosis by enhancing a pro-inflammatory state in monocytes and macrophages. *Vasc. Pharmacol.* 103-105, 16–28. doi:10.1016/j.vph.2018.01.005

Songbo, M., Lang, H., Xinyong, C., Bin, X., Ping, Z., and Liang, S. (2019). Oxidative stress injury in doxorubicin-induced cardiotoxicity. *Toxicol. Lett.* 307, 41–48. doi:10.1016/j.toxlet.2019.02.013

Sugiura, A., Nagashima, S., Tokuyama, T., Amo, T., Matsuki, Y., Ishido, S., et al. (2013). MITOL regulates endoplasmic reticulum-mitochondria contacts via Mitofusin2. *Mol. Cell* 51 (1), 20–34. doi:10.1016/j.molcel.2013.04.023

Sun, S. J., Wei, R., Li, F., Liao, S. Y., and Tse, H. F. (2021). Mesenchymal stromal cell-derived exosomes in cardiac regeneration and repair. *Stem Cell Rep.* 16 (7), 1662–1673. doi:10.1016/j.stemcr.2021.05.003

Swain, S. M., Whaley, F. S., and Ewer, M. S. (2003). Congestive heart failure in patients treated with doxorubicin: A retrospective analysis of three trials. *Cancer* 97 (11), 2869–2879. doi:10.1002/cncr.11407

Taguchi, N., Ishihara, N., Jofuku, A., Oka, T., and Mihara, K. (2007). Mitotic phosphorylation of dynamin-related GTPase Drp1 participates in mitochondrial fission. *J. Biol. Chem.* 282 (15), 11521–11529. doi:10.1074/jbc.M607279200

Tang, H., Tao, A., Song, J., Liu, Q., Wang, H., and Rui, T. (2017). Doxorubicin-induced cardiomyocyte apoptosis: Role of mitofusin 2. *Int. J. Biochem. Cell Biol.* 88, 55–59. doi:10.1016/j.biocel.2017.05.006

Tebbi, C. K., London, W. B., Friedman, D., Villaluna, D., De Alarcon, P. A., Constine, L. S., et al. (2007). Dexrazoxane-associated risk for acute myeloid leukemia/myelodysplastic syndrome and other secondary malignancies in pediatric Hodgkin's disease. *J. Clin. Oncol.* 25 (5), 493–500. doi:10.1200/JCO.2005.02.3879

Thum, T., Galuppo, P., Wolf, C., Fiedler, J., Kneitz, S., van Laake, L. W., et al. (2007). MicroRNAs in the human heart: A clue to fetal gene reprogramming in heart failure. *Circulation* 116 (3), 258–267. doi:10.1161/CIRCULATIONAHA.107.687947

Tilokani, L., Nagashima, S., Paupe, V., and Prudent, J. (2018). Mitochondrial dynamics: Overview of molecular mechanisms. *Essays Biochem.* 62 (3), 341–360. doi:10.1042/EBC20170104

Tondera, D., Czauderna, F., Paulick, K., Schwarzer, R., Kaufmann, J., and Santel, A. (2005). The mitochondrial protein MTP18 contributes to mitochondrial fission in mammalian cells. *J. Cell Sci.* 118 (Pt 14), 3049–3059. doi:10.1242/jcs.02415

Toyama, E. Q., Herzig, S., Courchet, J., Lewis, T. L., Jr., Loson, O. C., Hellberg, K., et al. (2016). Metabolism. AMP-activated protein kinase mediates mitochondrial fission in response to energy stress. *Science* 351 (6270), 275–281. doi:10.1126/science.aab4138

Tsushima, K., Bugger, H., Wende, A. R., Soto, J., Jenson, G. A., Tor, A. R., et al. (2018). Mitochondrial reactive oxygen species in lipotoxic hearts induce post-translational modifications of AKAP121, DRP1, and OPA1 that promote mitochondrial fission. *Circ. Res.* 122 (1), 58–73. doi:10.1161/CIRCRESAHA.117.311307

Valencia-Sanchez, M. A., Liu, J., Hannon, G. J., and Parker, R. (2006). Control of translation and mRNA degradation by miRNAs and siRNAs. *Genes. Dev.* 20 (5), 515–524. doi:10.1101/gad.1399806

Varga, Z. V., Ferdinandy, P., Liaudet, L., and Pacher, P. (2015). Drug-induced mitochondrial dysfunction and cardiotoxicity. *Am. J. Physiol. Heart Circ. Physiol.* 309 (9), H1453–H1467. doi:10.1152/ajpheart.00554.2015

Vejpongsa, P., and Yeh, E. T. (2014). Topoisomerase 2β: A promising molecular target for primary prevention of anthracycline-induced cardiotoxicity. *Clin. Pharmacol. Ther.* 95 (1), 45–52. doi:10.1038/clpt.2013.201

Wai, T., Garcia-Prieto, J., Baker, M. J., Merkwirth, C., Benit, P., Rustin, P., et al. (2015). Imbalanced OPA1 processing and mitochondrial fragmentation cause heart failure in mice. *Science* 350 (6265), aad0116. doi:10.1126/science.aad0116

Wallace, K. B., Sardao, V. A., and Oliveira, P. J. (2020). Mitochondrial determinants of doxorubicin-induced cardiomyopathy. *Circ. Res.* 126 (7), 926–941. doi:10.1161/CIRCRESAHA.119.314681

Wang, D., Wang, J., Bonamy, G. M., Meeusen, S., Brusch, R. G., Turk, C., et al. (2012). A small molecule promotes mitochondrial fusion in mammalian cells. *Angew. Chem. Int. Ed. Engl.* 51 (37), 9302–9305. doi:10.1002/anie.201204589

Wang, H., Song, P., Du, L., Tian, W., Yue, W., Liu, M., et al. (2011). Parkin ubiquitinates Drp1 for proteasome-dependent degradation: Implication of dysregulated mitochondrial dynamics in Parkinson disease. *J. Biol. Chem.* 286 (13), 11649–11658. doi:10.1074/jbc.M110.144238

Wang, J. X., Zhang, X. J., Feng, C., Sun, T., Wang, K., Wang, Y., et al. (2015). MicroRNA-532-3p regulates mitochondrial fission through targeting apoptosis repressor with caspase recruitment domain in doxorubicin cardiotoxicity. *Cell Death Dis.* 6 (3), e1677. doi:10.1038/cddis.2015.41

Wasiak, S., Zunino, R., and McBride, H. M. (2007). Bax/Bak promote sumoylation of DRP1 and its stable association with mitochondria during apoptotic cell death. *J. Cell Biol.* 177 (3), 439–450. doi:10.1083/jcb.200610042

Wu, D., Dasgupta, A., Chen, K. H., Neuber-Hess, M., Patel, J., Hurst, T. E., et al. (2020). Identification of novel dynamin-related protein 1 (Drp1) GTPase inhibitors: Therapeutic potential of Drpitor1 and Drpitor1a in cancer and cardiac ischemia-reperfusion injury. *FASEB J.* 34 (1), 1447–1464. doi:10.1096/fj.201901467R

Wu, L., Sowers, J. R., Zhang, Y., and Ren, J. (2022a). Targeting DNA damage response in cardiovascular diseases: From pathophysiology to therapeutic implications. *Cardiovasc Res.* 119, 691–709. doi:10.1093/cvr/cvac080

Wu, L., Wang, L., Du, Y., Zhang, Y., and Ren, J. (2022b). Mitochondrial quality control mechanisms as therapeutic targets in doxorubicin-induced cardiotoxicity. *Trends Pharmacol. Sci.* 44, 34–49. doi:10.1016/j.tips.2022.10.003

Xia, Y., Chen, Z., Chen, A., Fu, M., Dong, Z., Hu, K., et al. (2017). LCZ696 improves cardiac function via alleviating Drp1-mediated mitochondrial dysfunction in mice with doxorubicin-induced dilated cardiomyopathy. *J. Mol. Cell Cardiol.* 108, 138–148. doi:10.1016/j.yjmcc.2017.06.003

Xu, X., Persson, H. L., and Richardson, D. R. (2005). Molecular pharmacology of the interaction of anthracyclines with iron. *Mol. Pharmacol.* 68 (2), 261–271. doi:10.1124/mol.105.013383

Yamada, S., Sato, A., Ishihara, N., Akiyama, H., and Sakakibara, S. I. (2021). Drp1 SUMO/deSUMOylation by Senp5 isoforms influences ER tubulation and mitochondrial dynamics to regulate brain development. *iScience* 24 (12), 103484. doi:10.1016/j.isci.2021.103484

Yamada, T., Dawson, T. M., Yanagawa, T., Iijima, M., and Sesaki, H. (2019). SQSTM1/p62 promotes mitochondrial ubiquitination independently of PINK1 and PRKN/parkin in mitophagy. *Autophagy* 15 (11), 2012–2018. doi:10.1080/15548627.2019.1643185

Yeh, E. T., and Chang, H. M. (2016). Oncocardiology-past, present, and future: A review. *JAMA Cardiol.* 1 (9), 1066–1072. doi:10.1001/jamacardio.2016.2132

Yin, C. F., Chang, Y. W., Huang, H. C., and Juan, H. F. (2022). Targeting protein interaction networks in mitochondrial dynamics for cancer therapy. *Drug Discov. Today* 27 (4), 1077–1087. doi:10.1016/j.drudis.2021.11.006

Yin, J., Guo, J., Zhang, Q., Cui, L., Zhang, L., Zhang, T., et al. (2018). Doxorubicin-induced mitophagy and mitochondrial damage is associated with dysregulation of the PINK1/parkin pathway. *Toxicol Vitro* 51, 1–10. doi:10.1016/j.tiv.2018.05.001

Yu, C., Zhao, J., Yan, L., Qi, Y., Guo, X., Lou, Z., et al. (2020). Structural insights into G domain dimerization and pathogenic mutation of OPA1. *J. Cell Biol.* 219 (7), e201907098. doi:10.1083/jcb.201907098

Yu, R., Jin, S. B., Lendahl, U., Nister, M., and Zhao, J. (2019). Human Fis1 regulates mitochondrial dynamics through inhibition of the fusion machinery. *EMBO J.* 38 (8), e99748. doi:10.15252/embj.201899748

Yu, R., Liu, T., Jin, S. B., Ankarcrona, M., Lendahl, U., Nister, M., et al. (2021). MIEF1/2 orchestrate mitochondrial dynamics through direct engagement with both the fission and fusion machineries. *BMC Biol.* 19 (1), 229. doi:10.1186/s12915-021-01161-7

Yu, T., Robotham, J. L., and Yoon, Y. (2006). Increased production of reactive oxygen species in hyperglycemic conditions requires dynamic change of mitochondrial morphology. *Proc. Natl. Acad. Sci. U. S. A.* 103 (8), 2653–2658. doi:10.1073/pnas.0511154103

Zacharioudakis, E., and Gavathiotis, E. (2023). Mitochondrial dynamics proteins as emerging drug targets. *Trends Pharmacol. Sci.* 44 (2), 112–127. doi:10.1016/j.tips.2022.11.004

Zamorano, J. L., Lancellotti, P., Rodriguez Munoz, D., Aboyans, V., Asteggiano, R., Galderisi, M., et al. (2017). 2016 ESC Position Paper on cancer treatments and cardiovascular toxicity developed under the auspices of the ESC Committee for Practice Guidelines: The Task Force for cancer treatments and cardiovascular toxicity of the European Society of Cardiology (ESC). *Eur. J. Heart Fail* 19 (1), 9–42. doi:10.1002/ejhf.654

Zhang, J. Y., Chen, Q. Q., Li, J., Zhang, L., and Qi, L. W. (2021). Neuraminidase 1 and its inhibitors from Chinese herbal medicines: An emerging role for cardiovascular diseases. *Am. J. Chin. Med.* 49 (4), 843–862. doi:10.1142/S0192415X21500403

Zhang, L., Wei, T. T., Li, Y., Li, J., Fan, Y., Huang, F. Q., et al. (2018a). Functional metabolomics characterizes a key role for N-acetylneuraminic acid in coronary artery diseases. *Circulation* 137 (13), 1374–1390. doi:10.1161/CIRCULATIONAHA.117.031139

Zhang, S., Liu, X., Bawa-Khalfe, T., Lu, L. S., Lyu, Y. L., Liu, L. F., et al. (2012). Identification of the molecular basis of doxorubicin-induced cardiotoxicity. *Nat. Med.* 18 (11), 1639–1642. doi:10.1038/nm.2919

Zhang, Y., Li, H., Chang, H., Du, L., Hai, J., Geng, X., et al. (2018b). MTP18 overexpression contributes to tumor growth and metastasis and associates with poor survival in hepatocellular carcinoma. *Cell Death Dis.* 9 (10), 956. doi:10.1038/s41419-018-0987-x

Zhao, J., Zhang, J., Yu, M., Xie, Y., Huang, Y., Wolff, D. W., et al. (2013). Mitochondrial dynamics regulates migration and invasion of breast cancer cells. *Oncogene* 32 (40), 4814–4824. doi:10.1038/onc.2012.494

Zhou, J., Li, G., Zheng, Y., Shen, H. M., Hu, X., Ming, Q. L., et al. (2015). A novel autophagy/mitophagy inhibitor liensinine sensitizes breast cancer cells to chemotherapy through DNM1L-mediated mitochondrial fission. *Autophagy* 11 (8), 1259–1279. doi:10.1080/15548627.2015.1056970

Zhou, L., Li, R., Liu, C., Sun, T., Htet Aung, L. H., Chen, C., et al. (2017). Foxo3a inhibits mitochondrial fission and protects against doxorubicin-induced cardiotoxicity by suppressing MIEF2. *Free Radic. Biol. Med.* 104, 360–370. doi:10.1016/j.freeradbiomed.2017.01.037

Zhou, W., Ouyang, J., Hu, N., and Wang, H. (2023). Flavonoids from hippophae rhamnoides linn. Revert doxorubicin-induced cardiotoxicity through inhibition of mitochondrial dysfunction in H9c2 cardiomyoblasts *in vitro*. *Int. J. Mol. Sci.* 24 (4), 3174. doi:10.3390/ijms24043174

Ziviani, E., Tao, R. N., and Whitworth, A. J. (2010). Drosophila parkin requires PINK1 for mitochondrial translocation and ubiquitinates mitofusin. *Proc. Natl. Acad. Sci. U. S. A.* 107 (11), 5018–5023. doi:10.1073/pnas.0913485107

Zorov, D. B., Filburn, C. R., Klotz, L. O., Zweier, J. L., and Sollott, S. J. (2000). Reactive oxygen species (ROS)-induced ROS release: A new phenomenon accompanying induction of the mitochondrial permeability transition in cardiac myocytes. *J. Exp. Med.* 192 (7), 1001–1014. doi:10.1084/jem.192.7.1001

frontiers | Frontiers in Cell and Developmental Biology

TYPE Original Research
PUBLISHED 26 October 2023
DOI 10.3389/fcell.2023.1250643

OPEN ACCESS

EDITED BY
Emilia Bramanti,
National Research Council (CNR), Italy

REVIEWED BY
Wang Wang,
University of Washington, United States
Marta Marzullo,
Sapienza University of Rome, Italy

*CORRESPONDENCE
Erez Raz,
erez.raz@uni-muenster.de

RECEIVED 30 June 2023
ACCEPTED 16 October 2023
PUBLISHED 26 October 2023

CITATION
Tarbashevich K, Ermlich L, Wegner J, Pfeiffer J and Raz E (2023), The mitochondrial protein Sod2 is important for the migration, maintenance, and fitness of germ cells.
Front. Cell Dev. Biol. 11:1250643.
doi: 10.3389/fcell.2023.1250643

The mitochondrial protein Sod2 is important for the migration, maintenance, and fitness of germ cells

Katsiaryna Tarbashevich[1], Laura Ermlich[1], Julian Wegner[1], Jana Pfeiffer[1] and Erez Raz[1,2]*

[1]Institute of Cell Biology, Center for Molecular Biology of Inflammation (ZMBE), Muenster, Germany, [2]Max Planck Institute for Molecular Biomedicine, Münster, Germany

To maintain a range of cellular functions and to ensure cell survival, cells must control their levels of reactive oxygen species (ROS). The main source of these molecules is the mitochondrial respiration machinery, and the first line of defense against these toxic substances is the mitochondrial enzyme superoxide dismutase 2 (Sod2). Thus, investigating early expression patterns and functions of this protein is critical for understanding how an organism develops ways to protect itself against ROS and enhance tissue fitness. Here, we report on expression pattern and function of zebrafish Sod2, focusing on the role of the protein in migration and maintenance of primordial germ cells during early embryonic development. We provide evidence that Sod2 is involved in purifying selection of vertebrate germ cells, which can contribute to the fitness of the organism in the following generations.

KEYWORDS

SOD2, mitochondria, germ cells, zebrafish, cell competition, cell migration, PLLp, posterior lateral line primordium

Introduction

The control over the level of reactive oxygen species (ROS) in the cell is important for a range of physiological and pathological processes (reviewed in (Bowling et al., 2019; Lawlor et al., 2020; Sie et al., 2020; Shields et al., 2021)). A major source of these harmful ROS compounds is oxidative phosphorylation in the mitochondria, but mitochondria also have a way to handle them: ROS are neutralized by detoxifying enzymes such as superoxide dismutase 2 (SOD2), a mitochondrial enzyme that converts superoxide radicals into the less harmful compound hydrogen peroxide. Consequently, the function of SOD2 is critical for cell survival in *Drosophila* (Celotto et al., 2012) and for the immune response in zebrafish (Peterman et al., 2015). Mice that have a reduced SOD2 function are more likely to develop epilepsy (Liang and Patel, 2004), cardiomyopathy defects (Van Remmen et al., 2001), and oncological and aging-related phenotypes ((Justilien et al., 2007; Velarde et al., 2012; Weyemi et al., 2012); reviewed in (Lee et al., 2009)).

While SOD function has been shown to be important in different cell types, the role of the protein during the early development of vertebrate embryos is not well understood, in particular regarding its role in selecting for fitter germline cells that ensure the robustness of the organism across generations. So far, the process of "purifying selection" based on cell competition, namely, the selection for cells with optimal energy supply or metabolic status,

has been described for somatic cells during early mouse embryogenesis ((Döhla et al., 2022; Lima et al., 2021)). In the mouse, natural selection of male germ cells was reported to be based on differentiation efficiency but the impact of metabolic parameters on the process was not analyzed ((Nguyen and Laird, 2021; Nguyen et al., 2020)). Thus, not all aspects of competition among germ cells have been studied. To explore these issues, we employed the zebrafish model, benefiting from the extrauterine development of the embryo and the available genetic and reverse genetic tools. We examined the role of Sod2 in early embryogenesis with respect to cell maintenance as well as collective and single cell migration, focusing on its function in germ cells. We show that Sod2 is expressed in germ cells and is important for their development and provide evidence that Sod2 protein is involved in the selection for fitter germ cells, thereby contributing to the fitness of the organism across generations.

Materials and methods

Fish lines and husbandry

The following zebrafish (*Danio rerio*) lines were employed: wild-type of the AB background, *Tg(kop:EGFP-F'nos3'UTR)* (Blaser et al., 2005), *Tg(kop:mcherry-F-nos3'UTR)* (Tarbashevich et al., 2015), *Tg(gsc:GFP)* (Doitsidou et al., 2002), *Tg (cldnB:lynEGFP)*$^{+/+}$ (Haas and Gilmour, 2006), *mu13* (MZ*sod2*^{STOP31}) *Tg(kop:EGFP-F'nos3'UTR), mu14* (MZ*sod2*^{STOP19}) *Tg (cldnB:lynEGFP)*$^{+/+}$.

WT and manipulated embryos were collected, kept in 0.3× Danieau's solution [17.4 mM NaCl, 0.21 mM KCl, 0.12 mM $MgSO_4{\cdot}7H_2O$, 0.18 mM $Ca(NO_3)_2$, and 1.5 mM Hepes (pH 7.6)], and raised at 28°C. The general zebrafish maintenance was performed in compliance with the German, North-Rhine-Westphalia state law, following the regulations of the Landesamt für Natur, Umwelt und Verbraucherschutz Nordrhein-Westfalen and was supervised by the veterinarian office of the city of Muenster.

Microinjections into the zebrafish embryos

For all experiments except for the one presented in Figure 7, embryos were microinjected into the yolk with 2 nL of the injection mixture. The following capped sense mRNAs synthesized using the mMESSAGE mMACHINE (Thermo Fisher Scientific): GrpEL-EGFP (C131.GrpEL.EGFP.nos) (used as mitochondria marker for co-localization studies), Sod2-mCherry (C247.Sod2-mCherry-nos) (used to determine intracellular protein localization), Sod2 (C382.Sod2.nos, E046.Sod2ORF.sod2 3'UTR) (both used for rescue experiments), mCherry-H2B (B325.mCherry.H2B.globinUTR) (labels nuclei of all cells in the embryo, used for the correction for the gastrulation movement in the cell migration analysis), Mito-mCherry (C433.mCherryHA-Bcl2TM.nos3'UTR) (used for the fluorescence-based analysis of the mitochondria numbers in the PGCs).The mRNAs containing *nos* 3'UTR are cleared from somatic cells via miRNA430-mediated degradation and are, thus, predominantly expressed in germ cells (Kedde et al., 2007).

Translation-blocking morpholinos (MO, Gene tools) utilized for this work were: CntrMO (CCTCTTACCTCAGTTACAATTTATA), Sod2MO (CATGCTCTAGTCCGTCACACAGTGA). Both morpholinos were injected in 0.5 µM concentration.

For the experiment described in Figure 7, 8-cell-stage embryos were microinjected into one of the middle blastomeres with 1 nL injection mix containing Cas9 nuclease (0.5 µg/µL, Integrated DNA technologies (IDT), cat. Nr. 1081059), guide crRNA *egfp* (18 ng/µL, 5'-AAGGGCGAGGAGCTGTTCAC-3'), guide crRNA *sod2* (18 ng/µL, 5'-ACAAATCTGTCACCCAATGGCGG-3'), tracrRNA (33.5 ng/µL, cat. Nr. 1072534) according to the manufacturer's recommendations (IDT).

Transplantation experiments

For the posterior lateral line primordium (pLLP) transplantation experiments, wild-type and MZ*sod2*^{STOP31} embryos were injected with 500 pg of dextran conjugates (Invitrogen™, Dextran, Alexa Fluor™ 568; 10,000 MW, Anionic, Fixable, Catalogue number: D22912 or Alexa Fluor™ 680; 10,000 MW, Anionic, Fixable, Catalogue number: D34680) of distinct colors and used as donors. Uninjected wild-type embryos carrying a *cldnB:lynEGFP* transgene served as hosts.

Equal numbers of both types of donor embryos were grown to 4 h post fertilization (hpf), before removing the yolks. The cell caps were combined in a tube and carefully dissociated by tapping, until a homogeneous cell mixture was obtained. This cell mixture was transplanted into shield stage host embryos. At 31 hpf, dextran-labeled donor cells were distributed throughout the host embryos. Transplanted embryos were screened for cases in which both wild-type and MZ*sod2*^{STOP19} donor cells had integrated into the host pLLP. The primordium was then imaged with Z-steps of 20 µm.

For the PGC transplantations, wild-type (WT) (*Tg(kop:EGFP-F'nos3'UTR)*$^{+/+}$) or *sod2* knockout (KO) (MZ*sod2*^{STOP31} *Tg(kop:EGFP-F'nos3'UTR)*$^{+/+}$) germ cells from 4.7-5 hpf donor embryos expressing EGFP-F' transgene and dominant marker *Tg*(*cry:DsRed*) (red eyes) were transplanted into 4 hpf hosts (*Tg(kop:mcherry-F-nos3'UTR)*) expressing mCherry-F' transgene and dominant marker *Tg(cmlc:EGFP)* (green heart) or into "dark" MZ*sod2*^{STOP31} embryos. Embryos with mosaic germ cell clusters were selected at 24 hpf and raised to adulthood.

Immunohistochemistry

Whole-mount *in situ* hybridization using the DIG-labeled probe for the *sod2, egr2a*, *mab21l*, *en2a* and *foxa3d* was performed as previously described (Weidinger et al., 2002).

RNAscope was performed as described previously (Gross-Thebing et al., 2014) using the following probes: *sod2* (cat. Nr. 300031-C2/320269-C2), *vasa* (cat. Nr. 407271-C3), *cxcl12a* (cat. Nr. 406481), *noto* (cat. Nr. 4835511-C2), *gata1*(cat. Nr. 473371-C3), *neurog1* (cat. Nr. 505081-C2), *myoD* (cat. Nr. 402461-C2), *pax8* (cat. Nr. 494721-C2), *pcdh8* (cat. Nr. 494741-C3).

Fluorescence whole-mount immunostaining of the telomere repeats was performed using TelC-Cy3 (cat. Nr. TP-007) and TelC-Cy5 (cat. Nr. TP-009) according to the manufacturer's instructions (PNA Biotech).

Image acquisition and microscopy

For live imaging, embryos were dechorionated, and those older than 20 hpf were anesthetized using tricaine (concentration, A5040, Sigma-Aldrich) in 0.3× Danieau's solution, mounted in agarose-coated ramps covered with Danieau's solution and manually oriented. For experiments aimed at determining migration parameters, samples were incubated at 28°C on a heated stage (PeCon, TempController 2000-2).

Spinning disk confocal microscopy was performed using Carl Zeiss Axio Imager Z1 and M1 microscopes equipped with a Yokogawa CSUX1FW-06P-01 spinning disk units. Imaging was performed using a Hamamatsu ORCA-Flash4.0 LT C11440 camera and Visitron Systems acquisition software (VisiView). Imaging of RNAscope samples (×10 objective) was conducted by acquiring 400-µm *z*-stacks (80 Z planes, 5 µm apart). For the analysis of PGC speed, ×10 objective multi-stage time-lapses were acquired for 2 h with 2-min acquisition intervals. For the PGC blebbing analysis, ×63 objective high-magnification movies of individual cells were acquired with 5-s intervals for 5 min. For the neomycin treatment, dechorionated embryos were incubated in a 400 µM neomycin (Sigma, cat. Nr. N1142) solution in Danieau's buffer from 3 hpf until the end of the experiment. For the control treatments, the same amount (in µl) of DMSO (Sigma, cat. Nr. D8418) was used.

For the analysis of the pLLP migration, time-lapse movies were acquired at a rate of one frame every 30 min between 24 hpf 31 hpf. The samples were imaged using a1×0 objective to obtain150-µm Z-stacks of 10 µm optical slices.

High-magnification images for determining cell positioning and volume of the pLLP (40x) were performed by acquiring 2-µm optical slices. Analysis of the pLLP volumes was performed using the surface function of the Imaris software (Bitplane, version 9.5.1.).

Confocal laser scanning image acquisition was performed using LSM710 (Zeiss) upright microscope and ZEN software (Zeiss). If not stated otherwise, imaging was performed using a ×63 water-dipping objective with 2-µm optical slices.

Determination of the embryo size

Determination of zebrafish embryo size at the 5-somite stage was performed using the Fiji distribution function of ImageJ (NIH). First, the nuclei signal (Hoechst) of RNAscope image data, was projected along the *Z*-axis (400 µm in total), performing a maximum intensity projection. Rolling ball background-subtraction (radius = 50 pixels) was subsequently applied to the projected image. Next, a binary image was created by thresholding the image using the Otsu algorithm and adjusting the threshold such that the entire embryo was included. The "Fill holes" function was used to fill the area between the nuclei that were previously not segmented. The area of the obtained embryo segmentations was measured (for wild-type and MZ*sod*^{STOP31} embryos).

Analysis of cell migration

Analysis of the PGC migration speed was performed by tracking the germ cells using Imaris software (Bitplane, version 9.5.1.), with the correction of the gastrulation movement of the surrounding somatic cells. Analysis of PGC blebbing activity was performed manually (bleb count) using Fiji software. To determine the portion of blebs generated by PGCs at the back of a cell relative to the total number of blebs, the cells were divided into front and back halves and the total number of blebs, as well as the number of blebs at the back was counted for 5-min time-lapse movies.

For the analysis of the PGC cluster length, the value obtained for a cluster on one side of an embryo was normalized to the length of the yolk extension of the given embryo. Analysis was performed using Fiji software.

Analysis of the pLLP migration speed and distance were performed using Fiji software. The image orientation was adjusted, such that the lateral line was perfectly horizontal, with the primordium traveling to the right. The anterior point of the yolk extension was used as the point from which the distance to the tip of the traveling primordium was measured. The obtained values were normalized to the average wild-type pLLP speed/distance of travel for the given experiment.

qPCR

qPCR was performed as described in Cawthon (2009). Telomere primers: 5′ CGGTTTGTTTGGGTTTGGGTTTGGGTTTGGGTTTGGGTT-3′ and 5′- GGCTTGCCTTACCCTTACCCTTACCCTTACCCTTACCCT-3'. The house keeping gene *hmg (high mobility group)* was used as a reference RNA amplified with primers 5′-GTGGAAGACCCCGAAAACA-3′ and 5′- TTCCTCCTCTTCTTCCTCCTCG-3'. Additional normalization was performed to the values of the WT group.

Western blotting analysis

Western blotting analysis was performed on protein extracts from wild-type and MZ*sod2*^{STOP} embryos of 24hpf. The following primary antibodies were used: anti-Sod2 antibody (Proteintech, #24127-1-AP, in 1:3000 dilution) and a pan-Actin antibody (Thermofisher, #MA1-744, in 1:3000 dilution). For detection the following secondary antibodies were employed: goat-anti-mouse (Li-Cor, 926-68071, IRDye 680RD) and donkey-anti-rabbit (Li-Cor, 926-32213, IRDye 800RD) in 1: 5000 dilution.

ROS detection

For the detection of the level of the oxidative stress, 1hpf wild-type and MZ*sod2*^{STOP} embryos were manually dechorionated and incubated for 3 h in 10 µM CellRox (ThermoFisher, C10422) in Danieau's at 28°C followed by removal of the chemical and confocal imaging.

Statistical analysis

Statistical analysis (one-way ANOVA or Student's t-test) was performed using GraphPad Prism software (version 8). If not stated otherwise, all experiments were performed in three independent

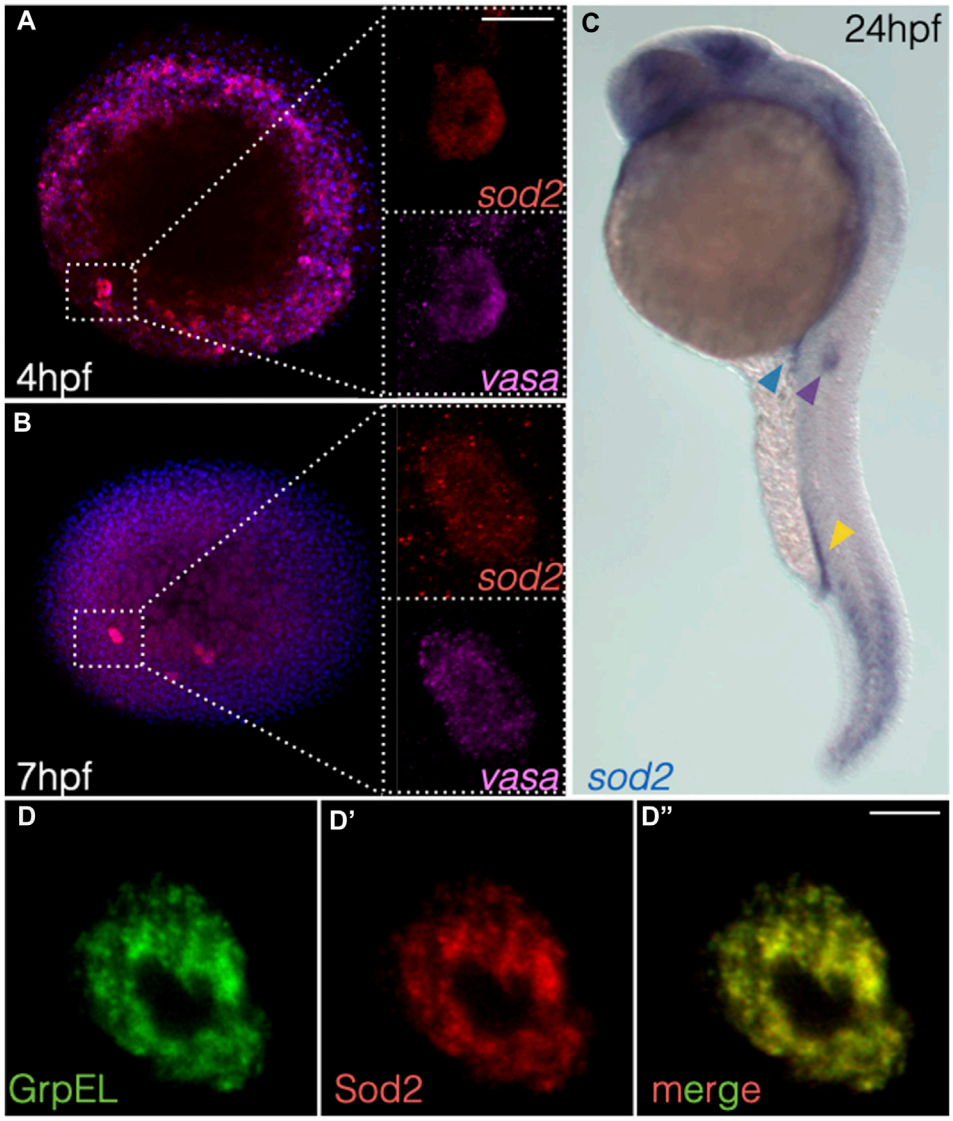

FIGURE 1
sod2 RNA expression pattern and localization of the protein during early embryogenesis. **(A, B)** RNAscope-based localization of *sod2* mRNA and the germ cell marker *vasa* mRNA at **(A)** 4 hpf and **(B)** 7 hpf. **(C)** Whole-mount *in situ* hybridization image probing for *sod2* mRNA in 24 hpf embryos. Blue arrowhead points at the PGC cluster, yellow arrowhead at hematopoietic precursor cells, and purple arrowhead at the migrating pLLP. **(D–D")** Representative confocal images of Sod2-mCherry protein in germ cells relative to the mitochondrial marker (GrpEL-EGFP). Scale bar 10 µm.

replicates. Where applicable, multiple comparisons were statistically analyzed using Dunn's multiple comparison test.

Results

sod2 mRNA is enriched in migratory cell populations

Upon screening for RNA molecules enriched in zebrafish primordial germ cells (deep sequencing data published in (Hartwig et al., 2014; Paksa et al., 2016)), we identified *superoxide dismutase type 2* (*sod2*) (ZFIN:ZDB-GENE-030131-7742). During early stages of embryogenesis (4 and 7 h post fertilization (hpf)), we found that *sod2* mRNA was expressed globally, but enriched in primordial germ cells (PGCs) (Figures 1A,B, Supplementary Figure S1A). At later stages of embryogenesis, *sod2* expression was detected in several structures such as the caudal somites as well as in specific regions within the developing brain (Figure 1C, Supplementary Figure S1A and Supplementary Figure S2). Intriguingly, in addition to being expressed in the PGCs (blue arrowhead in Figure 1C, Supplementary Figure S1, Supplementary Figure S2), *sod2* RNA was strongly expressed within two other populations of migratory cells: caudal hematopoietic trunk cells (CHT) (yellow arrowhead in Figure 1C, Supplementary Figure S1A) and cells of the posterior lateral line primordium (pLLP) (purple arrowhead in Figure 1C, Supplementary Figure S1A and Supplementary Figure S2). Consistent with its function, the Sod2-mCherry fusion protein localized to the mitochondria of cells of early embryos (e.g., in

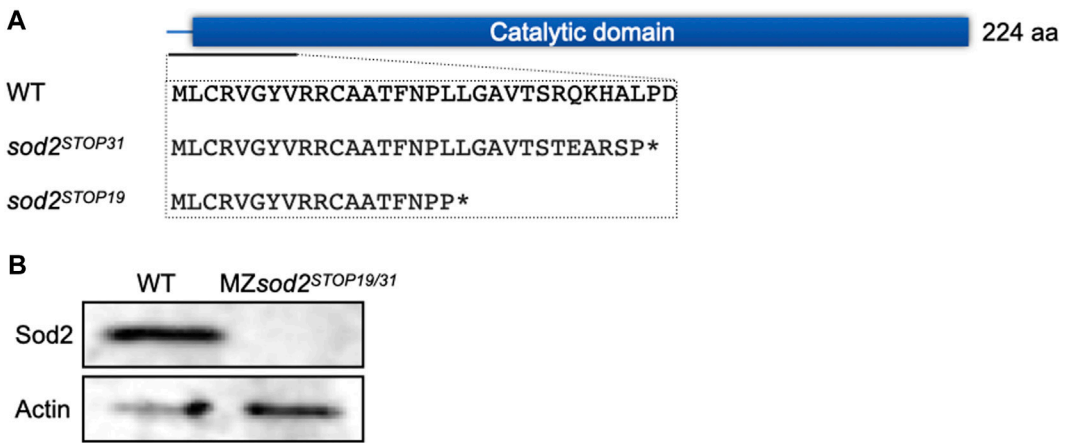

FIGURE 2
Generation of *sod2* maternal zygotic fish lines. **(A)** The schematic representation of the position of the two Cas9-induced mutations. The mutations resulted in stop codons at amino acid position 31 (*sod2*^{STOP31}) and 19 (*sod2*^{STOP19}) (marked by asterisks). **(B)** Western blotting analysis of the Sod2 protein expression in wild type and MZ*sod2* embryos.

germ cells expressing the mitochondrial protein GrpEL (Figure 1D-D")) (Srivastava et al., 2017).

Generation of sod2 maternal zygotic mutant fish lines

To study the function of Sod2 during early zebrafish embryogenesis, we generated two knockout (KO) alleles employing CRISPR/Cas9 technology. Both lines carry mutations at the beginning of the catalytic domain of the wild-type (WT) protein, resulting in frameshifts and stop codons shortly following the mutation sites (Figure 2A). Thus, we considered the two mutated alleles to result in full loss of function of Sod2 (see below).

Since *sod2* transcripts (and presumably the protein) are maternally provided to the embryo, we aimed at generating adult mutant fish that were homozygous for both knockout alleles. In this way, one can obtain embryos that do not contain maternally-provided material that are also incapable of expressing functional RNA from their own genome.

Interestingly, despite the central role that the protein plays in controlling ROS levels in the cell, under lab conditions the fish lacking the function of Sod2 were viable and developed into adults that proved to be fertile. This allowed us to generate and analyze embryos lacking both maternal and zygotically transcribed *sod2* RNAs (maternal-zygotic mutants (MZ), we designated as MZ*sod2*^{STOP19} and MZ*sod2*^{STOP31}). The schemes of crosses and genotypes analyzed in this manuscript are presented in Figure 3A. In such embryos, presumably as a result of nonsense-mediated RNA decay, no *sod2* RNA (whole-mount *in situ* hybridization, Supplementary Figure S1B) or protein (Western blotting analysis, Figure 2B) could be detected.

Nevertheless, a phenotype we did observe in MZ mutant embryos at early somitogenesis stages (11 hpf) was that of a mild reduction in body size (Supplementary Figure S3A). However, as judged by RNA expression, patterning events progressed normally in all germ layers, i.e., ectoderm, mesoderm and endoderm (Supplementary Figure S3B, C), and the embryos appeared morphologically normal at 5 days of development. Relevant for this report, the expression of *cxcl12a*, namely, the chemokine guiding the migration of both pLLP and PGCs, was expressed normally in the mutant embryos (Supplementary Figure S3C).

Sod2 function is dispensable for the collective migration of the pLLP cell cluster

The posterior lateral line primordium (pLLP) is a cluster of 100–150 cells that migrate collectively towards the tail of the zebrafish embryo (Haas and Gilmour, 2006). Interestingly, *sod2* mRNA was expressed within cells of the pLLP (Figure 1C, Supplementary Figure S1A), with elevated levels detected at the front of the cell cluster compared to the rear (Supplementary Figure S2). This expression pattern prompted us to examine the migration of the cell cluster in embryos lacking Sod2 function (MZ*sod2*^{STOP19}). As judged by the position of the pLLP at 24 hpf to 35 hpf (Supplementary Figure S4A), the cell clusters in mutant embryos migrated at the same speed as the non-manipulated wild-type clusters. Similarly, we did not observe an effect on the cluster size, suggesting a normal rate of cell division and death (S4B-B"). Last, in mosaic pLLP clusters in which only some of the cells lacked Sod2 function and the rest were wild-type, we found no role of the protein in dictating the position of the cells within the primordium (Supplementary Figure S4C–E).

Thus, based on the parameters investigated in Supplementary Figure S4, Sod2 function was not essential for proper migration of the pLLP, nor for cell behavior within the cluster.

Elevation of ROS affects PGC migration

To investigate the possible function of Sod2 in another cell population that expresses the protein, we turned to primordial germ cells (PGCs). In different organisms PGCs are specified

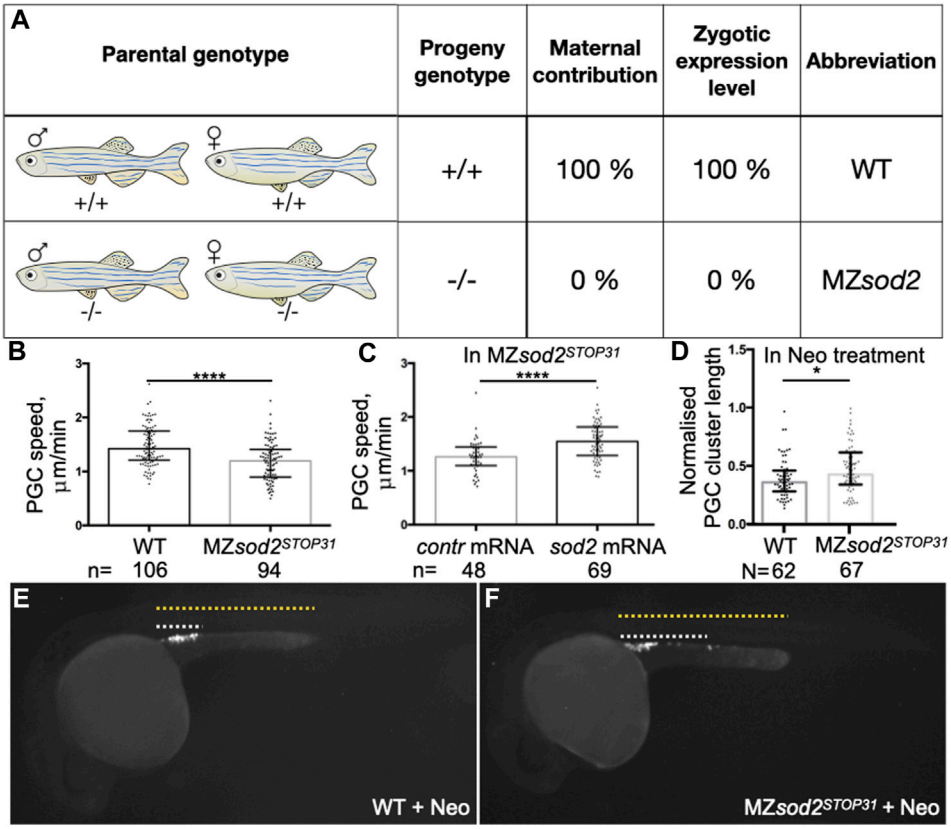

FIGURE 3
MZ*sod2* KO embryos exhibit reduction in the germ cell migration speed. **(A)** The scheme of crosses and genotypes analyzed in this manuscript. **(B, C)** PGC migration speed was determined by tracking cell migration for 70 min using Imaris software. **(D)** Normalized PGC cluster lengths at 24 hpf in WT and MZ*sod2* KO embryos treated with neomycin (enhanced ROS production condition). **(E, F)** Representative images of embryos analyzed for the PGC cluster length (quantification shown in **(D)**) ****$p < 0.0001$, *$p < 0.05$ was determined by Student's t-test. n - number of PGCs analyzed in 38 WT and 36 MZ*sod2* KO embryos **(B)**, 24 MZ*sod2* KO + control (contr) mRNA and 29 MZ*sod2* KO + *sod2* mRNA embryos **(C)**. N - number of PGC clusters (one cluster per embryo) analyzed.

during early embryonic development and migrate as single cells from their site of specification to the region where the gonad develops to give rise to gametes, sperm and egg ((Richardson and Lehmann, 2010; Aalto et al., 2021; Grimaldi and Raz, 2020)). We examined the migration speed of PGCs in seven to nine hpf embryos and observed a mild reduction in the speed of *sod2* mutant PGCs as compared with their wild-type counterparts (Figure 3B). In line with this finding, cells devoid of Sod2 function were less polar as manifested by an increase in the rate of bleb-type protrusion formation, particularly at the cell rear (Figures 4A–C, Supplementary Movie S1). Conversely, overexpression of Sod2 led to an increase in migration speed, suggesting that the Sod2 activity level constitutes a limiting factor for germ cell translocation (Figure 3C). Despite the defects in protrusion formation and the slower migration of PGCs in MZ*sod2*^{STOP31} embryos, normal size of PGC cluster formed at the region where the gonad develops (Supplementary Figure S5A).

In addition to the finding presented above, we detected higher ROS levels in cells deficient for Sod2 function (Supplementary Figure S5B). To examine whether Sod2 confers robustness to the migration process under conditions of increased oxidative stress in the PGCs, we subjected MZ*sod2*^{STOP31} and wild-type embryos to neomycin (Neo), which was shown to increase oxidative stress in cells ((Harris et al., 2003; Esterberg et al., 2016)). Increasing the oxidative stress in this way led to an increase in bleb formation and a reduction in cell polarity (Figures 4D–F, Movie S2) in wild-type embryos. We next checked whether the function of Sod2 could confer robustness to the arrival of germ cells at their target under these conditions. Indeed, increasing ROS level by subjecting embryos to Neomycin further enhances the oxidative stress in cells lacking SOD2 function (Supplementary Figure S5C). Interestingly, loss of Sod2 function coupled to neomycin treatment affected PGC cluster formation at the region where the gonad develops (Figures 3D–F).

Sod2 function is important for selection of fitter germ cells

To further examine the function of Sod2 in the germline, we monitored the mitochondria, the organelle within which the enzyme functions. Measuring the fluorescence intensity levels of a mitochondria-directed mCherry protein in 8 and 24 hpf embryos revealed a very strong reduction in the average fluorescence levels

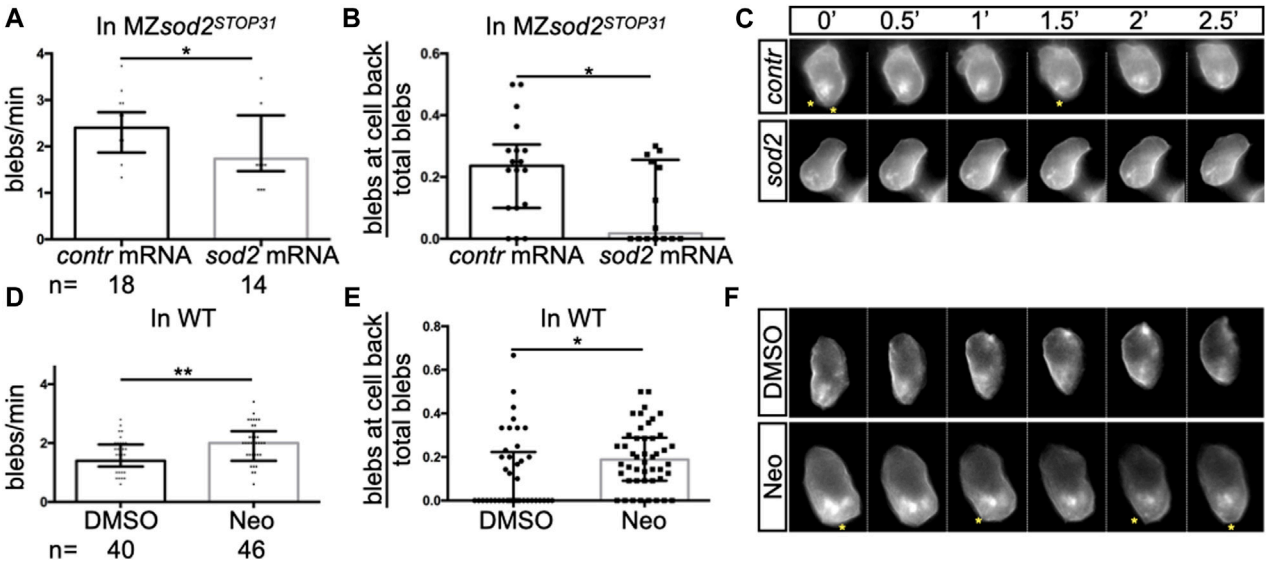

FIGURE 4
Defects in protrusion formation and germ cell polarity in *sod2* KO and neomycin-treated embryos. Analysis of **(A, D)** the number of blebs in PGCs per minute and **(B, E)** the proportion of blebs at the cell back. In graphs **A** and **B**, MZ*sod2*^{STOP31} embryos were injected with control RNA or with RNA directing Sod2 expression to the germ cells (see Methods); the same cells were analyzed in panels **A** and **(B)**. In graphs **D** and **E**, wild-type embryos were treated with DMSO or with neomycin; the same cells were analyzed in panels **D** and **(E)**. **(C, F)** Snapshots from the representative time-lapse movies (movies S1 and S2) analyzed in **(A,B,D, E)**. Yellow asterisks point at blebs at the rear of cells. n - the number of PGCs analyzed. One PGC per embryo was imaged and analyzed. $^{**}p < 0.01$, $^{*}p < 0.05$, were calculated by Student's t-test.

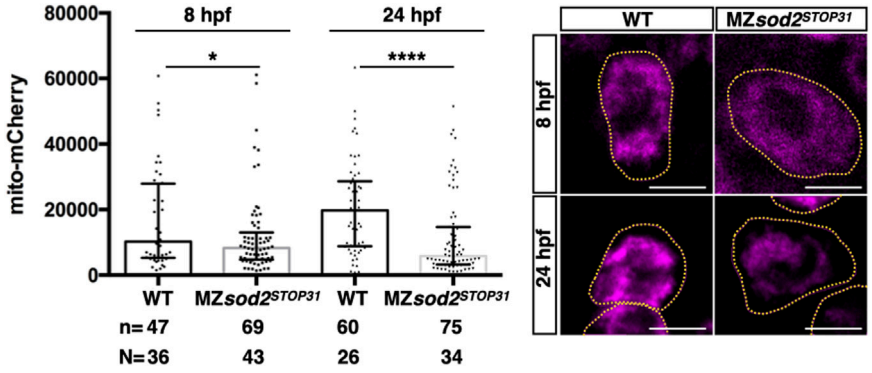

FIGURE 5
MZ*sod2* KO germ cells exhibit reduced mitochondria-derived fluorescence signal. Average intensity of the fluorescently-labeled mitochondria in WT and MZ*sod2* KO germ cells at 8 and 24 hpf. n - number of PGCs analyzed in N–number of embryos. $^{****}p < 0.0001$, $^{*}p < 0.05$ was determined by ANOVA test. Scale bar 10 µm.

particularly in MZ*sod2*^{STOP31} PGCs at 24 hpf as compared with their wild-type counterparts (Figure 5, Supplementary Figure S6).

It has previously been reported that, as quantified by the amount of mitochondrial DNA, the number of mitochondria decreases exponentially from the time of egg fertilization until late larval stages, when replication of these organelles reinitiates (Otten et al., 2016). In light of this, we hypothesized that the further decrease in mitochondria-derived fluorescence signal in MZ*sod2*^{STOP} germ cells could result in reduced fitness of these cells relative to wild-type cells during later stages of development (Figure 9).

To test this hypothesis, we transplanted germ cells from wild-type and MZ*sod2*^{STOP31} lines into either wild-type or MZ*sod2*^{STOP31} hosts, with the transplanted donor germ cells carrying a dominant marker (fluorescent eyes, Supplementary Figure S7). Chimeric embryos containing both host and donor germ cells were raised and mated with wild-type fish, and we scored for the embryos expressing the donor dominant marker (fluorescent eyes), which signifies the fitness of transplanted PGCs (Figure 6).

Following this experimental scheme, we detected F1 progeny derived from the transplanted germ cells in 7 of 13 (54%) adult fish when wild-type donor PGCs were transplanted into wild-type hosts. Similarly, 8 out of 16 (50%) adult fish had progeny expressing the donor domain marker when MZ*sod2*^{STOP31} PGCs were transplanted into MZ*sod2*^{STOP31} hosts. The result of the experiment changed when

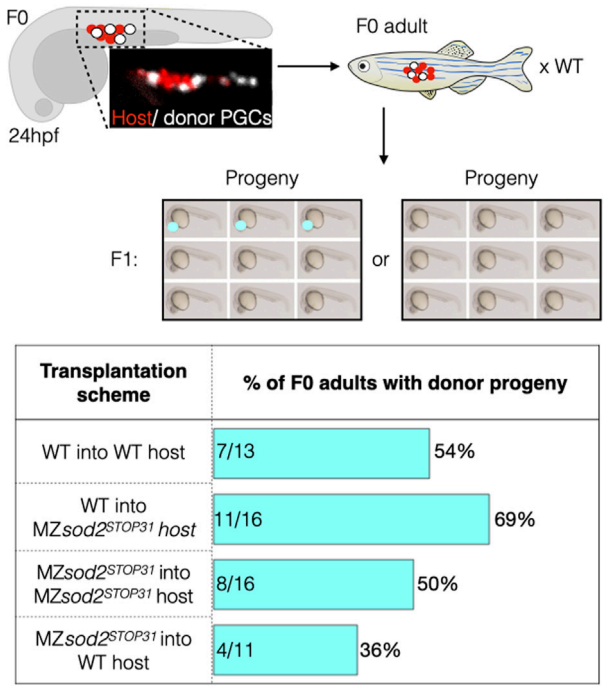

FIGURE 6
Analysis of zebrafish with mosaic gonads: PGC transplantation approach. Embryos with mosaic germ cell clusters (white cells are the transplanted donor PGCs, red cells are the host PGCs in the upper panels) were selected at 24 hpf and raised to adulthood and crossed to wild-type fish. If clutches contained embryos with the dominant marker of the donor line (red eyes), the outcrossed adult fish would be counted as "positive." Lower graph shows the number of such positive fish relative to the total number of adults tested is presented in percentage for each background. Numbers within the bars represent the number of F0 adults with donor progeny divided by the total number of F0 adults raised for this line.

germ cells were transplanted into heterologous backgrounds. In these cases, F1 progeny expressing donor dominant makers were observed in 11 of 16 (69%) animals in which wild-type germ cells transplanted into the MZ*sod2*^{STOP31} background. Conversely, the number of adult wild-type hosts giving rise to dominant-marker carrying progeny was only 4 of 11 fish (36%) in the case of MZ*sod2*^{STOP31} cells transplanted into wild-type hosts.

Due to the complexity and low throughput of the experiment presented above, only a relatively small number of chimeric animals could be generated. Thus, as an additional test for the hypothesis, we generated fish with chimeric gonads containing wild-type and MZ*sod2*^{STOP19} germ cells using a different approach (Figure 7A). To this end, we co-injected Cas9 protein and guide RNAs targeting *egfp* and *sod2* sequences into 1 blastomere of 8-cell-stage wild-type and MZ*sod2*^{STOP19} embryos. The injected embryos were homozygous for an EGFP transgene. The injected embryos were raised, and adult males were crossed with wild-type female fish, with the progeny analyzed for the percentage of embryos lacking a GFP signal. Thus, knocking out *sod2* according to this scheme resulted in adult fish with a chimeric germline, where progeny lacking the EGFP signal representing the proportion of *sod2* KO germ cells that contributed to the germline. Intriguingly, we found that the potency of cells lacking Sod2 to contribute to the germline and form gametes was very strongly reduced in wild-type animals as compared to their ability to do so when located within a gonad containing only Sod2 mutant cells (Figure 7B). We thus conclude that while Sod2 mutant cells can generate gametes, they are much less likely to do so when positioned within an environment containing wild-type cells. Thus, when located within an environment of wild-type cells, the Sod2-deficient germline cells are outcompeted and contribute less to the gametes (WT in Figure 7B). Importantly, the effect of germ cell competition was not observed in similarly generated control chimeric gonads of embryos injected only with guide RNA for the *egfp* sequence (no *sod2* knockout) (Figure 7C). Together, Sod2 deficient cells contribute less to the germline when located among wild-type germ cells. In contrast, the negative controls where Sod2 activity was not altered (anti *gfp* guides, or anti *sod2* guides in *sod2* mutant cells) the treated cells showed no difference in their contribution to the germline as compared with non-treated cells. Consistent with the importance of reduced ROS levels in germline cells for proper gametogenesis, MZ*sod2* homozygous mutant fish are less fertile (Supplementary Figure S8).

An interesting phenotype we observed, which may be relevant for the reduced potential of Sod2-depleted germ cells to generate gametes as compared to non-manipulated neighboring germ cells, is a reduction in the number of telomeric repeats in MZ*sod2* KO embryos. This analysis was performed using qPCR (Figure 8A), or fluorescence *in situ* hybridization using the telomere-specific probe (TelC-Cy3, Figures 8B–D, Supplementary Figure S9). A possible basis for the shortening of telomeres is DNA damage that telomere length reports on. The reduction in telomere length we observe in *sod2* mutants could affect the fitness of cells that carry the genetic information to future generations.

Discussion

The Sod2 protein has been shown to be involved in a range of physiological and pathological processes. For example, the *Drosophila sod2* mutant (*SOD2*^{Bewildered}) exhibits aberrant brain morphology, abnormal axonal targeting, and neurodegeneration (Celotto et al., 2012). We observed strong expression of *sod2* mRNA in the zebrafish brain as well, but, based on the molecular markers we examined and the apparent normal behavior of MZ*sod2* adult fish, the loss of Sod2 in zebrafish did not result in a pronounced phenotype in this tissue. Since the ROS level has been shown to affect lipid metabolism ((Quijano et al., 2016; Zhuang et al., 2021)), the main energy source of the early embryo, the reduction in body size of 12-hour-old MZ*sod2*^{STOP} mutant embryos could stem from defects in the availability of these molecules (reviewed in (Sant and Timme-Laragy, 2018; Quinlivan and Farber, 2017)).

The PGC migration phenotype we observed in MZ*sod2* mutants and the similar phenotype of neomycin-treated embryos could reflect defects in energy production as well, which in this case could stem from defects in the function of the mitochondria (Esterberg et al., 2016). We attribute the lack of migration defects in the pLLP to the more robust nature of collective cell migration in which mild locomotion aberrations in some cells can be compensated by other cells in the cluster ((Knutsdottir et al., 2017; Yamaguchi et al., 2022)).

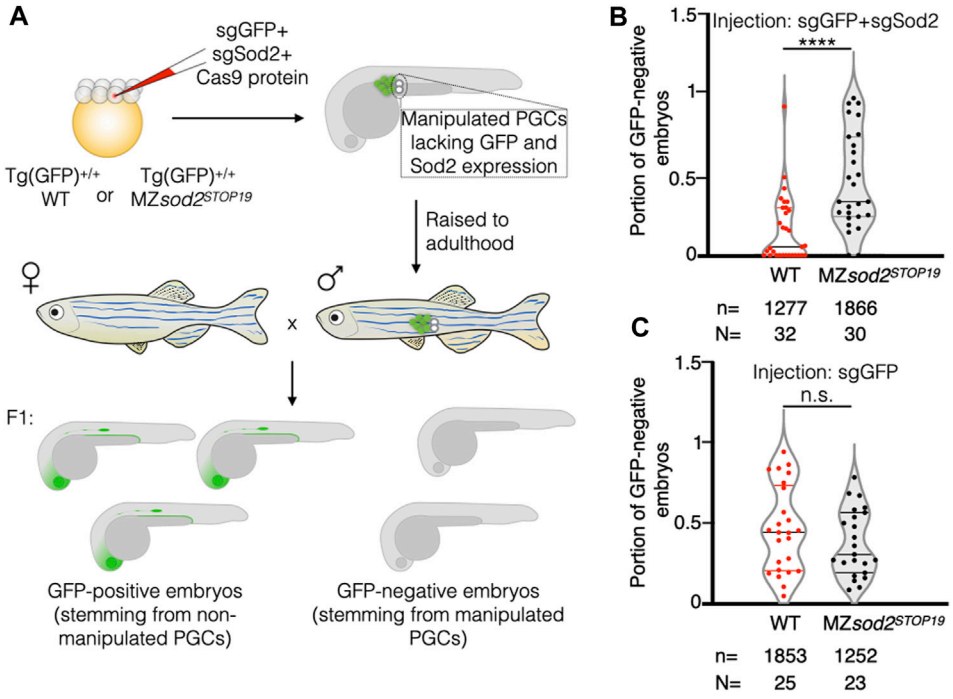

FIGURE 7
Generation and analysis of zebrafish with mosaic gonads: Cas9-based approach. **(A)** Embryos of WT or *sod2* KO backgrounds homozygous for *Tg(cldnB:lynEGFP)* (*Tg(GFP)* $^{+/+}$) were injected at the 8-cell stage into one of the middle blastomeres with Cas9 protein and two guide RNAs targeting *egfp* and *sod2* sequences (sgEGFP and sgSod2). This manipulation affected only a fraction of germ cells per embryo, allowing for a high-throughput generation of animals with mosaic gonads containing WT germ cells (expressing Sod2 and EGFP transgene) and KO germs cells (where both Sod2 and EGFP functions were eliminated). Such embryos were raised to adulthood. Adult males were outcrossed to WT females, and the percentage of GFP-negative embryos (lacking EGFP and Sod2 expression) within the clutch was calculated. Results are presented in graph **(B)**. The results of the negative control experiment with animals injected only with sgGFP (manipulating GFP expression only) are presented in graph **(C)**. n–number of embryos and N - number of adult fish analyzed. ****$p < 0.0001$, $^{n.s.}p > 0.05$ was determined by Student's t-test.

In contrast to the very mild or lack of phenotypes we observed in PGCs during early stages of embryonic development (first 1–2 days post fertilization), the phenotypes we detected at later stages were much more pronounced. A possible explanation could be that the PGC competition phenotype we observe reflects a cumulative effect of lack of Sod2 function over the 3-month period between the establishment of the germline and the generation of gametes.

A frequently documented type of cellular heterogeneity that is subjected to selection has been described in somatic cells in the form of mitochondrial heteroplasmy (e.g., mitochondrial function in human cells (Wei et al., 2019)). In this case, cells with an elevated proportion of defective mitochondria are eliminated by more robust neighboring cells in a process termed "purifying selection" (Lima et al., 2021). Heterogeneities in cellular functions have also been identified in other cell populations including stem cells ((Ellis et al., 2019; Lawlor et al., 2020; Lima et al., 2021), reviewed in (Muller-Sieburg et al., 2012; Krieger and Simons, 2015)). In germ cells, such heterogeneities can be especially consequential, as they are transmitted to the next-generation (Zhang et al., 2022).

Since during the embryonic stages studied here there was no *de novo* production of mitochondria, the number of the maternally provided organelles per cell declined with each cell division, reaching a very low number (estimated to be 100 per cell (Otten et al., 2016)). Indeed, the time of PGC migration we examined here corresponds to developmental stages with very low numbers of mitochondria per cell (Otten et al., 2016). The small number of mitochondria is an obvious parameter relevant for mitochondrial heteroplasmy in PGCs and for the so called mitochondrial "bottleneck" effect (Otten et al., 2016). In the case of germ cells, this time point can serve as the stage when purifying selection takes place, contributing to the transmission of healthier mitochondria to the progeny. Consistent with the Sod2 level being important for mitochondria function and DNA integrity, in *MZsod2*^{STOP} embryos the already low mitochondria number was further reduced (schematically presented in Figure 9), and telomeres were shorter. The low level of mitochondria observed in PGCs in *MZsod2*^{STOP} embryos and the aberrations in migration motivated us to study the possible evolutionary role of Sod2 in PGC maintenance and natural selection. Indeed, the results of the germline transplantation experiments (Figure 6) and those of the chimeric germline analysis (Figure 7) show that germ cells lacking Sod2 were less likely to generate gametes as compared with wild-type PGCs when positioned together within the developing gonad. Since such phenomenon has not been observed among cells of similar genotypes, these results fit the definition of cell competition ((de la Cova et al., 2004; Moreno and Basler, 2004)), which in this case involves germline cells. In the context of this work, such competition

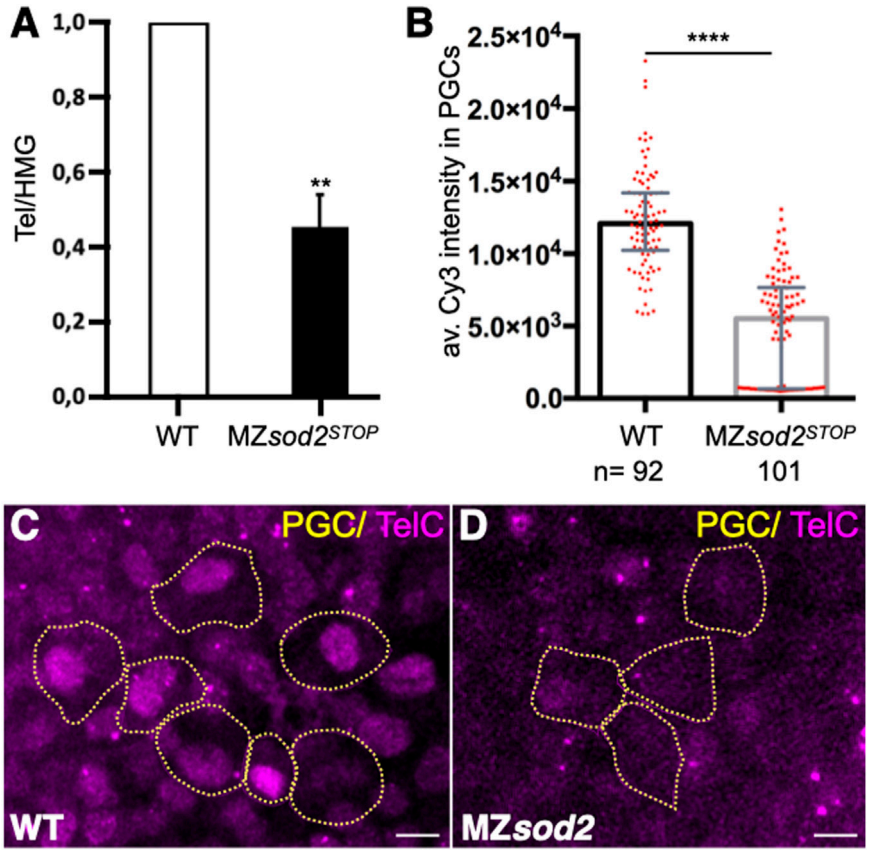

FIGURE 8
The number of telomeric repeats is reduced in *sod2* KO fish lines. **(A)** The relative length of telomeric repeats in wild type and MZ*sod2* mutants was determined by qPCR (graph). The qPCR values were normalized to the WT condition. **(B)** The relative number of telomeric repeats was determined by fluorescence *in situ* hybridization (FISH) using Cy3-conjugated TelC probes. The graph presents intensity measurements of the TelC signal in individual PGC nuclei. n–number of PGCs analyzed in 32 WT and 35 MZ*sod2* embryos **(C, D)** Representative confocal images of TelC-FISH staining. PGCs are identified by the expression of EGFP-F′ on their cell membranes (represented by yellow dotted lines). ****$p < 0.0001$was determined by Student's t-test. Scale bar 10 µm.

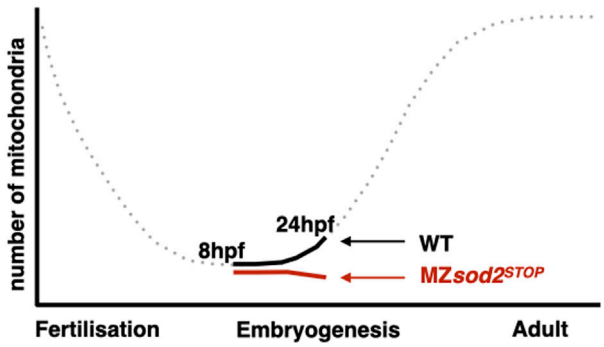

FIGURE 9
Schematic illustration of changes in mitochondria numbers during zebrafish development. Representation of mitochondria numbers per germ cell at 8 hpf and 24 hpf of zebrafish development in WT (black) and MZ*sod2* KO (red) animals. The dotted part of the graph is based on (33).

could select for germline cells with lower ROS-generated damage, thereby controlling the quality of gametes and, thereby, the fitness of somatic cells in the next-generation. Thus, it is likely that the full manifestation of the MZ*sod2*^{STOP} phenotype may only be appreciated on the evolutionary scale when followed over several generations.

Data availability statement

The raw data supporting the conclusions of this article will be made available by the authors, without undue reservation.

Ethics statement

The animal study was approved by Landesamt für Natur, Umwelt und Verbraucherschutz Nordrhein-Westfalen. The study was conducted in accordance with the local legislation and institutional requirements.

Author contributions

KT, LE, JW and JP performed the experiments and analyzed the data. KT and ER designed the study and wrote the manuscript. All authors contributed to the article and approved the submitted version.

Funding

This work was funded by the German Research Counsil (DFG), CRC1348 and CRU 326 program and by the Medical Faculty of the University of Muenster.

Acknowledgments

We thank E.-M. Messerschmidt, I. Sandbote and U. Jordan for technical assistance and C. Brennecka for comments on the manuscript.

Conflict of interest

The authors declare that the research was conducted in the absence of any commercial or financial relationships that could be construed as a potential conflict of interest.

Publisher's note

Supplementary material

The Supplementary Material for this article can be found online at: https://www.frontiersin.org/articles/10.3389/fcell.2023.1250643/full#supplementary-material

References

Aalto, A., Olguin-Olguin, A., and Raz, E. (2021). Zebrafish primordial germ cell migration. *Front. Cell Dev. Biol.* 9, 684460. doi:10.3389/fcell.2021.684460

Blaser, H., Eisenbeiss, S., Neumann, M., Reichman-Fried, M., Thisse, B., Thisse, C., et al. (2005). Transition from non-motile behaviour to directed migration during early PGC development in zebrafish. *J. Cell Sci.* 118 (17), 4027–4038. doi:10.1242/jcs.02522

Bowling, S., Lawlor, K., and Rodríguez, T. A. (2019). Cell competition: the winners and losers of fitness selection. *Development* 146 (13), dev167486. doi:10.1242/dev.167486

Cawthon, R. M. (2009). Telomere length measurement by a novel monochrome multiplex quantitative PCR method. *Nucleic Acids Res.* 37 (3), e21. doi:10.1093/nar/gkn1027

Celotto, A. M., Liu, Z., Vandemark, A. P., and Palladino, M. J. (2012). A novel Drosophila SOD2 mutant demonstrates a role for mitochondrial ROS in neurodevelopment and disease. *Brain Behav.* 2 (4), 424–434. doi:10.1002/brb3.73

de la Cova, C., Abril, M., Bellosta, P., Gallant, P., and Johnston, L. A. (2004). Drosophila myc regulates organ size by inducing cell competition. *Cell* 117 (1), 107–116. doi:10.1016/s0092-8674(04)00214-4

Döhla, J., Kuuluvainen, E., Gebert, N., Amaral, A., Englund, J. I., Gopalakrishnan, S., et al. (2022). Metabolic determination of cell fate through selective inheritance of mitochondria. *Nat. Cell Biol.* 24 (2), 148–154. doi:10.1038/s41556-021-00837-0

Doitsidou, M., Reichman-Fried, M., Stebler, J., Köprunner, M., Dörries, J., Meyer, D., et al. (2002). Guidance of primordial germ cell migration by the chemokine SDF-1. *Cell* 111 (5), 647–659. doi:10.1016/s0092-8674(02)01135-2

Ellis, S. J., Gomez, N. C., Levorse, J., Mertz, A. F., Ge, Y., and Fuchs, E. (2019). Distinct modes of cell competition shape mammalian tissue morphogenesis. *Nature* 569 (7757), 497–502. doi:10.1038/s41586-019-1199-y

Esterberg, R., Linbo, T., Pickett, S. B., Wu, P., Ou, H. C., Rubel, E. W., et al. (2016). Mitochondrial calcium uptake underlies ROS generation during aminoglycoside-induced hair cell death. *J. Clin. Invest.* 126 (9), 3556–3566. doi:10.1172/JCI84939

Grimaldi, C., and Raz, E. (2020). Germ cell migration—evolutionary issues and current understanding. *Semin. Cell Dev. Biol.* 100, 152–159. doi:10.1016/j.semcdb.2019.11.015

Gross-Thebing, T., Paksa, A., and Raz, E. (2014). Simultaneous high-resolution detection of multiple transcripts combined with localization of proteins in whole-mount embryos. *BMC Biol.* 12 (1), 55. doi:10.1186/s12915-014-0055-7

Haas, P., and Gilmour, D. (2006). Chemokine signaling mediates self-organizing tissue migration in the zebrafish lateral line. *Dev. Cell* 10 (5), 673–680. doi:10.1016/j.devcel.2006.02.019

Harris, J. A., Cheng, A. G., Cunningham, L. L., MacDonald, G., Raible, D. W., and Rubel, E. W. (2003). Neomycin-induced hair cell death and rapid regeneration in the lateral line of zebrafish (*Danio rerio*). *J. Assoc. Res. Otolaryngol. JARO* 4 (2), 219–234. doi:10.1007/s10162-002-3022-x

Hartwig, J., Tarbashevich, K., Seggewiß, J., Stehling, M., Bandemer, J., Grimaldi, C., et al. (2014). Temporal control over the initiation of cell motility by a regulator of G-protein signaling. *Proc. Natl. Acad. Sci.* 111 (31), 11389–11394. doi:10.1073/pnas.1400043111

Justilien, V., Pang, J. J., Renganathan, K., Zhan, X., Crabb, J. W., Kim, S. R., et al. (2007). SOD2 knockdown mouse model of early AMD. *Invest. Ophthalmol. Vis. Sci.* 48 (10), 4407–4420. doi:10.1167/iovs.07-0432

Kedde, M., Strasser, M. J., Boldajipour, B., Vrielink, JAFO, Slanchev, K., Le Sage, C., et al. (2007). RNA-binding protein Dnd1 inhibits MicroRNA access to target mRNA. *Cell* 131 (7), 1273–1286. doi:10.1016/j.cell.2007.11.034

Knutsdottir, H., Zmurchok, C., Bhaskar, D., Palsson, E., Dalle Nogare, D., Chitnis, A. B., et al. (2017). Polarization and migration in the zebrafish posterior lateral line system. *PLOS Comput. Biol.* 13 (4), 1005451. doi:10.1371/journal.pcbi.1005451

Krieger, T., and Simons, B. D. (2015). Dynamic stem cell heterogeneity. *Development* 142 (8), 1396–1406. doi:10.1242/dev.101063

Lawlor, K., Pérez-Montero, S., Lima, A., and Rodríguez, T. A. (2020). Transcriptional versus metabolic control of cell fitness during cell competition. *Semin. Cancer Biol.* 63, 36–43. doi:10.1016/j.semcancer.2019.05.010

Lee, Y. H., Lin, Q., Boelsterli, U. A., and Chung, M. C. M. (2009). The *Sod2* mutant mouse as a model for oxidative stress: a functional proteomics perspective. *Mass Spectrom. Rev.* 29, 179–196. doi:10.1002/mas.20226

Liang, L. P., and Patel, M. (2004). Mitochondrial oxidative stress and increased seizure susceptibility in Sod2−/+ mice. *Free Radic. Biol. Med.* 36 (5), 542–554. doi:10.1016/j.freeradbiomed.2003.11.029

Lima, A., Lubatti, G., Burgstaller, J., Hu, D., Green, A. P., Di Gregorio, A., et al. (2021). Cell competition acts as a purifying selection to eliminate cells with mitochondrial defects during early mouse development. *Nat. Metab.* 3 (8), 1091–1108. doi:10.1038/s42255-021-00422-7

Moreno, E., and Basler, K. (2004). dMyc transforms cells into super-competitors. *Cell* 117 (1), 117–129. doi:10.1016/s0092-8674(04)00262-4

Muller-Sieburg, C. E., Sieburg, H. B., Bernitz, J. M., and Cattarossi, G. (2012). Stem cell heterogeneity: implications for aging and regenerative medicine. *Blood* 119 (17), 3900–3907. doi:10.1182/blood-2011-12-376749

Nguyen, D. H., and Laird, D. J. (2021). Natural selection at the cellular level: insights from male germ cell differentiation. *Cell Death Differ.* 28 (7), 2296–2299. doi:10.1038/s41418-021-00812-0

Nguyen, D. H., Soygur, B., Peng, S. P., Malki, S., Hu, G., and Laird, D. J. (2020). Apoptosis in the fetal testis eliminates developmentally defective germ cell clones. *Nat. Cell Biol.* 22 (12), 1423–1435. doi:10.1038/s41556-020-00603-8

Otten, A. B. C., Theunissen, T. E. J., Derhaag, J. G., Lambrichs, E. H., Boesten, I. B. W., Winandy, M., et al. (2016). Differences in strength and timing of the mtDNA bottleneck

between zebrafish germline and non-germline cells. *Cell Rep.* 16 (3), 622–630. doi:10.1016/j.celrep.2016.06.023

Paksa, A., Bandemer, J., Hoeckendorf, B., Razin, N., Tarbashevich, K., Minina, S., et al. (2016). Repulsive cues combined with physical barriers and cell–cell adhesion determine progenitor cell positioning during organogenesis. *Nat. Commun.* 7 (1), 11288. doi:10.1038/ncomms11288

Peterman, E. M., Sullivan, C., Goody, M. F., Rodriguez-Nunez, I., Yoder, J. A., and Kim, C. H. (2015). Neutralization of mitochondrial superoxide by superoxide dismutase 2 promotes bacterial clearance and regulates phagocyte numbers in zebrafish. *Infect. Immun.* 83 (1), 430–440. doi:10.1128/IAI.02245-14

Quijano, C., Trujillo, M., Castro, L., and Trostchansky, A. (2016). Interplay between oxidant species and energy metabolism. *Redox Biol.* 8, 28–42. doi:10.1016/j.redox.2015.11.010

Quinlivan, V. H., and Farber, S. A. (2017). Lipid uptake, metabolism, and transport in the larval zebrafish. *Front. Endocrinol.* 8, 319. doi:10.3389/fendo.2017.00319

Richardson, B. E., and Lehmann, R. (2010). Mechanisms guiding primordial germ cell migration: strategies from different organisms. *Nat. Rev. Mol. Cell Biol.* 11 (1), 37–49. doi:10.1038/nrm2815

Sant, K. E., and Timme-Laragy, A. R. (2018). Zebrafish as a model for toxicological perturbation of yolk and nutrition in the early embryo. *Curr. Environ. Health Rep.* 5 (1), 125–133. doi:10.1007/s40572-018-0183-2

Shields, H. J., Traa, A., and Van Raamsdonk, J. M. (2021). Beneficial and detrimental effects of reactive oxygen species on lifespan: a comprehensive review of comparative and experimental studies. *Front. Cell Dev. Biol.* 9, 628157. doi:10.3389/fcell.2021.628157

Sies, H., and Jones, D. P. (2020). Reactive oxygen species (ROS) as pleiotropic physiological signalling agents. *Nat. Rev. Mol. Cell Biol.* 21 (7), 363–383. doi:10.1038/s41580-020-0230-3

Srivastava, S., Savanur, M. A., Sinha, D., Birje, A., Vigneshwaran, R., Saha, P. P., et al. (2017). Regulation of mitochondrial protein import by the nucleotide exchange factors GrpEL1 and GrpEL2 in human cells. *J. Biol. Chem.* 292 (44), 18075–18090. doi:10.1074/jbc.M117.788463

Tarbashevich, K., Reichman-Fried, M., Grimaldi, C., and Raz, E. (2015). Chemokine-dependent pH elevation at the cell front sustains polarity in directionally migrating zebrafish germ cells. *Curr. Biol.* 25 (8), 1096–1103. doi:10.1016/j.cub.2015.02.071

Van Remmen, H., Williams, M. D., Guo, Z., Estlack, L., Yang, H., Carlson, E. J., et al. (2001). Knockout mice heterozygous for Sod2 show alterations in cardiac mitochondrial function and apoptosis. *Am. J. Physiol. Heart Circ. Physiol.* 281 (3), H1422–H1432. doi:10.1152/ajpheart.2001.281.3.H1422

Velarde, M. C., Flynn, J. M., Day, N. U., Melov, S., and Campisi, J. (2012). Mitochondrial oxidative stress caused by Sod2 deficiency promotes cellular senescence and aging phenotypes in the skin. *Aging* 4 (1), 3–12. doi:10.18632/aging.100423

Wei, W., Tuna, S., Keogh, M. J., Smith, K. R., Aitman, T. J., Beales, P. L., et al. (2019). Germline selection shapes human mitochondrial DNA diversity. *Science* 364 (6442), 6520. doi:10.1126/science.aau6520

Weidinger, G., Wolke, U., Köprunner, M., Thisse, C., Thisse, B., and Raz, E. (2002). Regulation of zebrafish primordial germ cell migration by attraction towards an intermediate target. *Development* 129 (1), 25–36. doi:10.1242/dev.129.1.25

Weyemi, U., Parekh, P. R., Redon, C. E., and Bonner, W. M. (2012). SOD2 deficiency promotes aging phenotypes in mouse skin. *Aging* 4 (2), 116–118. doi:10.18632/aging.100433

Yamaguchi, N., Zhang, Z., Schneider, T., Wang, B., Panozzo, D., and Knaut, H. (2022). Rear traction forces drive adherent tissue migration *in vivo*. *Nat. Cell Biol.* 24 (2), 194–204. doi:10.1038/s41556-022-00844-9

Zhang, R., Tu, Y., Ye, D., Gu, Z., Chen, Z., and Sun, Y. (2022). A germline-specific regulator of mitochondrial fusion is required for maintenance and differentiation of germline stem and progenitor cells. *Adv. Sci.* 9 (36), 2203631. doi:10.1002/advs.202203631

Zhuang, A., Yang, C., Liu, Y., Tan, Y., Bond, S. T., Walker, S., et al. (2021). SOD2 in skeletal muscle: new insights from an inducible deletion model. *Redox Biol.* 47, 102135. doi:10.1016/j.redox.2021.102135

frontiers | Frontiers in Cell and Developmental Biology

TYPE Review
PUBLISHED 30 October 2023
DOI 10.3389/fcell.2023.1247339

OPEN ACCESS

EDITED BY
Francesca Forini,
National Research Council (CNR), Italy

REVIEWED BY
Mudasir Bashir Gugjoo,
Sher-e-Kashmir University of Agricultural Sciences and Technology of Kashmir, India
Luca Bonadies,
University of Padua, Italy

*CORRESPONDENCE
Dongmei Yue,
yuedm@sj-hospital.org

RECEIVED 25 June 2023
ACCEPTED 17 October 2023
PUBLISHED 30 October 2023

CITATION
Zhang S, Mulder C, Riddle S, Song R and Yue D (2023), Mesenchymal stromal/stem cells and bronchopulmonary dysplasia.
Front. Cell Dev. Biol. 11:1247339.
doi: 10.3389/fcell.2023.1247339

Mesenchymal stromal/stem cells and bronchopulmonary dysplasia

Shuqing Zhang[1], Cassidy Mulder[2], Suzette Riddle[3], Rui Song[4] and Dongmei Yue[5]*

[1]School of Pharmacy, China Medical University, Shenyang, China, [2]Liberty University College of Osteopathic Medicine, Lynchburg, VA, United States, [3]Cardiovascular Pulmonary Research Laboratories, Departments of Pediatrics and Medicine, University of Colorado Anschutz Medical Campus, Aurora, CO, United States, [4]Lawrence D. Longo, MD Center for Perinatal Biology, Department of Basic Sciences, Loma Linda University School of Medicine, Loma Linda, CA, United States, [5]Department of Pediatrics, Shengjing Hospital of China Medical University, Shenyang, Liaoning, China

Bronchopulmonary dysplasia (BPD) is a common complication in preterm infants, leading to chronic respiratory disease. There has been an improvement in perinatal care, but many infants still suffer from impaired branching morphogenesis, alveolarization, and pulmonary capillary formation, causing lung function impairments and BPD. There is an increased risk of respiratory infections, pulmonary hypertension, and neurodevelopmental delays in infants with BPD, all of which can lead to long-term morbidity and mortality. Unfortunately, treatment options for Bronchopulmonary dysplasia are limited. A growing body of evidence indicates that mesenchymal stromal/stem cells (MSCs) can treat various lung diseases in regenerative medicine. MSCs are multipotent cells that can differentiate into multiple cell types, including lung cells, and possess immunomodulatory, anti-inflammatory, antioxidative stress, and regenerative properties. MSCs are regulated by mitochondrial function, as well as oxidant stress responses. Maintaining mitochondrial homeostasis will likely be key for MSCs to stimulate proper lung development and regeneration in Bronchopulmonary dysplasia. In recent years, MSCs have demonstrated promising results in treating and preventing bronchopulmonary dysplasia. Studies have shown that MSC therapy can reduce inflammation, mitochondrial impairment, lung injury, and fibrosis. In light of this, MSCs have emerged as a potential therapeutic option for treating Bronchopulmonary dysplasia. The article explores the role of MSCs in lung development and disease, summarizes MSC therapy's effectiveness in treating Bronchopulmonary dysplasia, and delves into the mechanisms behind this treatment.

KEYWORDS

stem cells, bronchopulmonary dysplasia, development, extracellular vesicles, mitochondria

1 Introduction

Bronchopulmonary dysplasia (BPD) is a chronic lung disease of preterm infants characterized by impaired alveolar and vascular development, resulting in poor gas exchange and significant respiratory morbidity (Jobe, 2011; Gilfillan et al., 2021; Schmidt and Ramamoorthy, 2022). The primary drivers of BPD pathology are inflammation, oxidative stress, and parenchymal fibrosis (Higano et al., 2018; Benjamin et al., 2021; Holzfurtner et al., 2022; Kimble et al., 2022). BPD causes long-term issues like emphysema and pulmonary hypertension (Gough et al., 2014; Vom Hove et al., 2014).

MSCs have emerged as a promising candidate for BPD therapy due to their capacity for self-renewal, high proliferative potential, and ability to differentiate into cell types of mesodermal lineage (Thebaud et al., 2021). They also have immunomodulatory properties that allow allogeneic transplantation. Several clinical trials have evaluated MSC therapy in BPD patients. Intratracheal or intravenous MSC administration has decreased pro-inflammatory cytokines in tracheal aspirates, improved alveolarization, and reduced BPD severity (Alvarez-Fuente et al., 2018). While initially, it was thought that MSCs engrafted and differentiated directly into damaged lung tissue, recent evidence indicates paracrine signaling is the primary mechanism of action. Several recent studies have shown that MSCs communicate with other cells through paracrine signaling (Di Bernardo et al., 2014; Obendorf et al., 2020). MSC paracrine signaling of anti-apoptotic, anti-inflammatory, and pro-angiogenic bioactive substances to the microenvironment through extracellular vesicles (EVs) is thought to be the primary means of communication between MSCs and injured lung tissue (Lai et al., 2010; Aliotta et al., 2016; Reiter et al., 2017; Varkouhi et al., 2019; Varderidou-Minasian and Lorenowicz, 2020; Hao et al., 2022; Xiong et al., 2023). In particular, MSC-derived EVs like exosomes and endosomes have emerged as critical intercellular communicators that can reprogram damaged cells through the transfer of bioactive cargo (Jadli et al., 2020). MSC-EVs have been found to enhance cell proliferation, inhibit apoptosis, stimulate cell migration, modulate differentiation, promote angiogenesis, regulate immune responses, suppress inflammation, improve mitochondrial function, and attenuate oxidative stress. By orchestrating these diverse restorative effects in the damaged neonatal lung, MSC-EV therapies may alleviate structural and vascular defects associated with arrested alveolarization and dysregulated vascular development in BPD (Mansouri et al., 2019; Abele et al., 2022; Sharma et al., 2022).

The mitochondria are essential to the normal development and function of lung cells, including the regulation of metabolism, growth, differentiation, and injury responses (Zhang Y. et al., 2022). Bronchopulmonary dysplasia is associated with defects in mitochondrial structure, dynamics, DNA integrity, and oxidative metabolism (Xuefei et al., 2021). MSC therapy has been shown to alleviate mitochondrial dysfunction in BPD animal models, leading to improved alveolar and lung vascular growth (Islam et al., 2012; Dutra Silva et al., 2021). There is emerging evidence that mesenchymal stem cells (MSCs) can directly donate healthy mitochondria to damaged lung cells to restore mitochondrial function (Willis et al., 2018). In addition, MSCs could stimulate mitochondrial replication in injured lung cells through paracrine signaling molecules and extracellular vesicles (Phinney et al., 2015; Willis et al., 2018). Thus, MSCs may help resolve detrimental inflammation that can further impair mitochondrial and cellular function in lung cells injured by disease. By understanding how MSCs transfer mitochondria, promote mitochondrial biogenesis, and reduce mitochondrial inflammation, new therapeutic approaches may be developed to treat respiratory diseases and injuries caused by mitochondrial dysfunction.

This article explores the multifaceted role that MSCs play in lung development and disease. Additionally, we will provide an overview of current knowledge on the effectiveness of MSC therapy in treating BPD and shed light on the mechanisms driving this approach.

2 The role of mesenchymal stem cells in mammalian lung development

Mammalian lung development is precisely controlled by dynamic epithelial-mesenchymal interactions (Morrisey and Hogan, 2010). By controlling epithelial differentiation and function, MSCs play an essential role in lung morphogenesis and homeostasis (Driscoll et al., 2012). Through paracrine signaling, MSCs also secrete growth factors that influence lung development.

2.1 Lung MSC origins and characteristics

During embryogenesis, lung MSCs originate from the splanchnic mesoderm and undergo proliferation and differentiation into specialized mesenchymal cells (Cardoso and Lu, 2006). These lung MSCs exhibit clonogenicity, self-renewal, and multidifferentiation potential into mesodermal lineages (Jarvinen et al., 2008). Several studies have highlighted the intimate relationship between MSCs and their mitochondria. A healthy and efficient mitochondrial system is critical for optimizing MSCs (Forni et al., 2016). MSCs undergo rapid proliferation and differentiation during lung development, requiring mitochondrial energy. As differentiation proceeds, mitochondria undergo a metabolic shift toward OXPHOS, indicating their essential role in MSC maturation (Pattappa et al., 2011). For instance, during the differentiation of bone marrow mesenchymal stromal cells (BMSCs), mitochondrial length increased along with decreased DLP1 protein levels and increased OPA1 protein levels; this indicates a shift toward mitochondrial fusion, which maintains BMSC stemness (Feng et al., 2019). MSC differentiation can be hampered by dysfunctional mitochondria, characterized by decreased membrane potential, impaired OXPHOS, and increased ROS (Chen et al., 2008). Another fascinating aspect is MSCs' ability to transfer mitochondria. As a result of mitochondrial transfer from MSCs to damaged cells, the recipient cells are more likely to be repaired and recovered (Islam et al., 2012). The mechanism may be instrumental in repairing lung injuries and preserving lung health.

2.2 MSCs in lung branching morphogenesis

In the surrounding mesenchyme of the bronchi, mesenchymal progenitors contribute to the differentiation of smooth muscle and endothelial cells. Mitochondrial capacity and ATP production in the mesenchyme were disrupted, resulting in MSC absence and impaired airway branching (Zhang K. et al., 2022). Conducting airways are formed by dichotomous branching morphogenesis triggered by inductive signals from the distal lung mesenchyme, such as fibroblast growth factor 10 (FGF10) (Bellusci et al., 1997). MSCs provide key signals regulating this process. Deletion of β-catenin in lung MSCs disrupted airway branching (De Langhe et al., 2008). Also, Wnt signaling in MSCs regulated FGF10 expression and epithelial branching (Shu et al., 2005). Sonic hedgehog (SHH) signaling in MSCs similarly regulates airway patterning (Ikonomou et al., 2020). Intriguingly, disrupting mitochondrial dynamics in the mesenchyme impaired airway branching (Liu

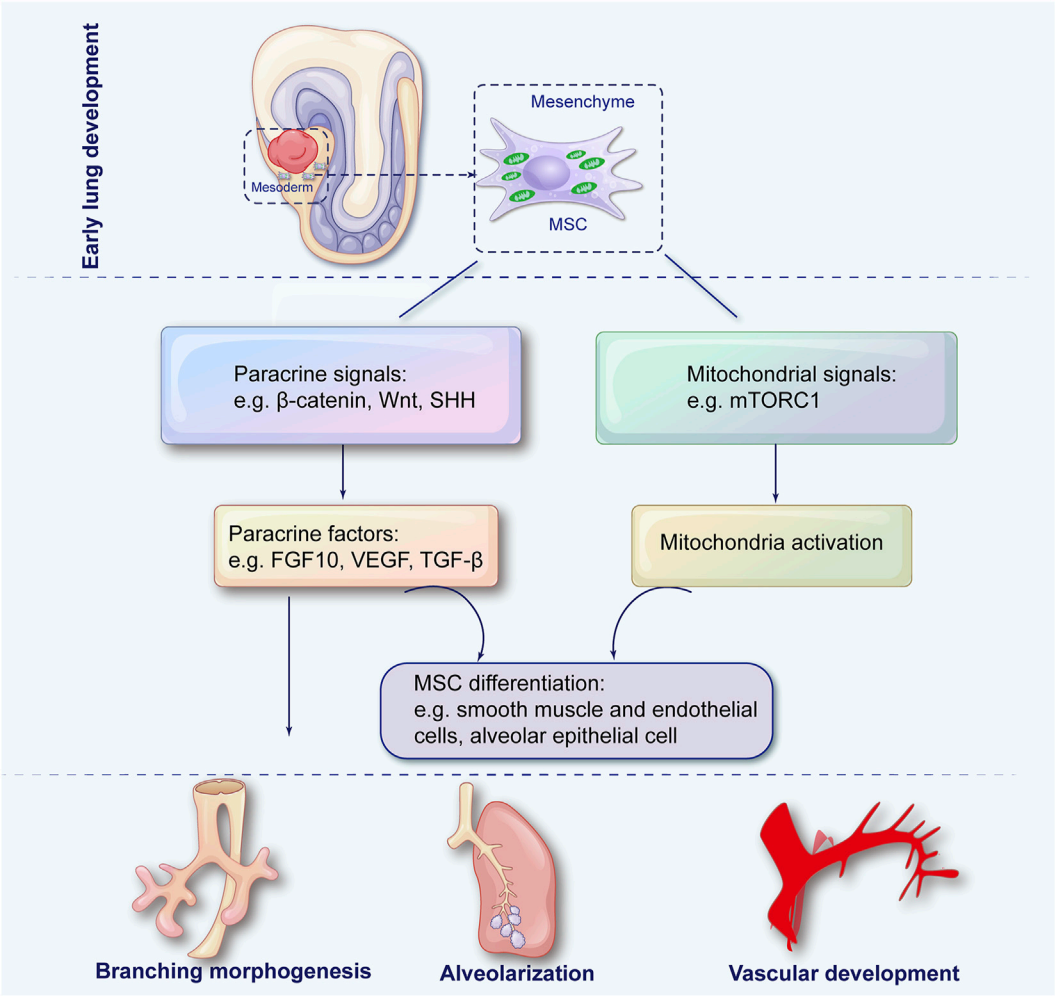

FIGURE 1
The role of mesenchymal stem cells in pulmonary development. During embryonic development, lung mesenchymal stem cells (MSCs) arise from the splanchnic mesoderm and subsequently differentiate into specialized mesenchymal lineages through paracrine signaling and mitochondrial regulation to coordinate key processes in lung morphogenesis, including airway branching, alveolarization, and vascular development.

et al., 2021). Crosstalk between mitochondrial networks and other cell signaling pathways that regulate MSC growth, migration, and paracrine signaling during branching morphogenesis is of particular interest.

2.3 MSCs in alveolar development and regeneration

Mesenchymal cells secrete VEGF, TGF-β, and FGFs, influencing alveolar differentiation, proliferation, and formation. The ablation of FGF10 from MSCs impaired alveolar formation (Volckaert et al., 2013). Paracrine signals such as SHH and VEGF regulate MSC differentiation of alveolar epithelial cells (Liu J. et al., 2022). Depleting lung MSCs post-pneumonectomy severely compromised compensatory alveolar regeneration (Zhen et al., 2008). A key role in alveolar formation is played by mesenchymal mitochondrial activity and distribution regulated by mTORC1 pathway. Therefore, MSCs are essential for alveolar development and regeneration after injury. Much is still to be learned about how modulating mitochondrial biogenesis, dynamics, and mitophagy in lung MSCs impacts alveolar epithelial cell growth, differentiation, and matrix production during alveolarization.

2.4 MSCs in vascular development

The mesenchyme layer and cells exhibit high VEGF, stimulating hemangioblasts to form blood pools (Greenberg et al., 2002). Deleting β-catenin in lung MSCs disrupted vascular patterning (De Langhe et al., 2008). Consequently, MSCs provide the trophic signals necessary for coordinated lung vascular development.

As a result, lung MSCs are crucial for airway branching, alveolarization, and vascular development throughout lung morphogenesis. Lung development is orchestrated by the intricate dance between mitochondria and MSCs (Figure 1). Despite our growing understanding over the years, much remains to be

explored. Future studies elucidating the molecular and cellular mechanisms underlying their interaction can pave the way for innovative therapeutic strategies in lung medicine.

3 Interaction between mesenchymal stem cells and bronchopulmonary dysplasia

Several prenatal risk factors for BPD have been identified, including maternal smoking, hypertension, placental insufficiency, and chorioamnionitis (Klinger et al., 2013; Mizikova and Thebaud, 2023). Placental abnormalities leading to imbalanced pro- and anti-angiogenic signaling may disrupt fetal lung vascular development, significantly impacting BPD susceptibility and severity (Hansen et al., 2010; Ozkan et al., 2012; Torchin et al., 2016; Sucre et al., 2021). Premature infants born during the canalicular and saccular stages of lung development are at highest risk for developing BPD (Jobe, 2011). Endogenous MSCs play a critical role in alveolarization through the tightly regulated processes of alveolar septation and vascularization (Morrisey and Hogan, 2010; Klein, 2021). The decrease or functional impairment in resident stem cells within the lung tissue of infants leads to simplified alveolar architecture and abnormal pulmonary vasculature contributing to BPD (Alphonse et al., 2012; Collins and Thebaud, 2014; Simones et al., 2018).

Extensive research has been conducted on how interference with MSCs and their signaling pathways can result in the onset of BPD. MSCs, similar to fibroblast cells, are found in the mesodermal tissue in adults and fetuses (Anker et al., 2003; Fang et al., 2019). Their presence has been noted in a variety of locations including bone marrow, adipose tissue, lung tissue, the placenta, and the stroma of the umbilical cord (Anker et al., 2003; Igura et al., 2004; Nguyen et al., 2022). BPD treatment methods such as hyperoxia and mechanical ventilation can negatively impact the functionality of the MSCs residing in the lung. Interestingly, these cells are copious in fetal lungs and can be a biomarker for predicting BPD onset when retrieved from tracheal aspirates of prematurely born infants. Growth factor expression involved in alveolar development and repair, such as VEGF and FGF10, is reduced in these MSCs (Mobius et al., 2019).

The precise mechanisms through which endogenous MSCs switch from protecting against BPD to contributing to BPD remain incompletely understood. The MSCs can repair damaged cells by promoting growth and differentiation. For instance, a subset of Dermo1+ endogenous MSCs has been recognized as having the capacity to function as stem cells in regenerating airway epithelial cells during the repair process following LPS-induced acute lung injury (Fang et al., 2019). Current data indicates that paracrine signaling and immune modulation are likely key players in mitigating hyperoxia-induced lung injury. EVs often facilitate paracrine signaling, carrying growth factors such as TGF-β. In a BPD model triggered by hyperoxia, an escalation in TGF-β expression was observed in the lungs, leading to structural changes; this included the multiplication of α-actin-positive myofibroblasts within the alveolar septal wall and the emergence of abnormal alveolar and vascular structures (Luan et al., 2015). Interestingly, when bone marrow stem cells were administered, a considerable decline in TGF-β levels was observed (Luan et al., 2015). These outcomes suggest that TGF-β could stimulate abnormal differentiation of alveolar mesenchymal progenitor cells into myofibroblasts, eventually playing a role in BPD progression. Furthermore, under intrauterine circumstances, human fetal lung MSCs were observed to generate considerable quantities of elastin and sulfated glycosaminoglycans, key constituents required for typical lung development. Examination of the secretome revealed that human fetal lung MSCs could be responsible for secreting molecules essential for angiogenic and inflammatory signaling, such as IL-8, VEGF, angiogenin and angiopoietin-1 (Mobius et al., 2019). Secretome analysis also revealed the existence of molecules that promote epithelial cell maturation and protection, such as keratinocyte growth factor/FGF7, FGF10 and the antioxidant known as stanniocalcin-1. In addition, inflammatory mediators such as monocyte chemotactic protein-1, stromal cell–derived factor-1, IL-6, and the tissue inhibitor of metalloproteinases 1 were also detected (Mobius et al., 2019). Exposing lung MSCs to hyperoxia recapitulated some harmful events associated with post-premature birth, such as cell apoptosis, decreased colony-forming capabilities, and alterations in MSCs' surface markers. It hindered the secretion of factors crucial for lung growth. These effects may play a part in the development of BPD (Mobius et al., 2019).

In the following section, we delve into the regulatory role of MSCs in the complex pathogenesis of BPD (Table 1), intending to identify potential targets for MSC-based BPD treatments.

3.1 Oxidative stress

While fetal lungs usually develop in a hypoxic intrauterine environment, BPD is a condition precipitated by premature exposure to hyperoxic conditions at birth, due either to oxygen treatment in efforts to oxygenate the infants sufficiently or simply by exposure to the relative hyperoxic conditions of the atmosphere. This condition subjects infants with extremely low birth weights to oxidative stress (Kimble et al., 2022). Cellular components such as the mitochondria: its DNA, the electron transport chain, and reactive oxygen generation machinery are particularly susceptible to oxidant damage. The function of mitochondria is pivotal in moderating the response to oxidative stress and affects the pluripotency and regenerative potential of MSCs (Paliwal et al., 2018). In a study exploring the correlation between mitochondrial function and the MSC function, electron transport chain complex-IV activity, basal and maximal oxygen consumption rates, spare respiratory capacity, and ATP-linked oxygen consumption rate were reduced. Proton leak was increased in MSCs from extremely low birth weight infants who either perished or developed moderate/severe BPD, compared to MSCs from infants who survived with none to mild BPD (Hazra et al., 2022).

PTEN-induced putative kinase 1 (PINK1) mediated mitophagy is one mechanism cells use to eliminate dysfunctional mitochondria. As a result, oxidative stress-induced mitochondrial dysfunction could lead to MSC depletion, thus obstructing lung development. Another finding described that MSCs from infants who died or developed moderate/severe BPD after O2 treatment showed lower PINK1 expression, implying decreased mitophagy (Hazra et al., 2022). The antioxidant stanniocalcin-1 was also reduced in fetal lung MSCs exposed to hyperoxia (Mobius et al., 2019).

TABLE 1 Effects of decreased and dysfunctional endogenous mesenchymal stem cells on BPD in preclinical experiments.

	Species	Pathophysiological factor	Signaling	Altered MSCs	Injured lung	References
In vitro	Human	oxidative stress/mitochondrial dysfunction	PINK1 stanniocalcin-1	↓ electron transport chain complex-IV activity, basal and maximal oxygen consumption rates, spare respiratory capacity, and ATP-linked OCR	disruption of lung development	Mobius et al. (2019); Hazra et al. (2022)
				↑ proton leak		
				↓ mitophagy ↓MSC number		
	Human	aberrant angiogenesis	SOX-2 and OCT-4	↓ MSC number ↓expression of VEGF, FGF-10, and angiogenin	↓ alveolar development and repair ↓lung vascularization	Mobius et al. (2019)
	Human	aberrant angiogenesis	SHH	↓ expression of proangiogenic genes FGF-9 and IL-6	↓ capillary density	White et al. (2007); Kwon et al. (2014)
	Human	Inflammation	FoxF1, Wnt5a, and Tbx3	↑ release of pro-inflammatory cytokines CXCL1, IL-6, and IL-8	↑ inflammation ↑ fibrosis	Bozyk et al. (2011)
				↓ CXCL1/GRO-α and HGF		
	Human	Inflammation	NFκB	↑ Pro-inflammatory cytokines TNF-α, IL-1β, IL-6, and IL-8	↑ inflammation	Reicherzer et al. (2018)
				↓MSCs number		
In vivo	Rat	aberrant angiogenesis	Semaphorins 3A and 3E	↓ expression of FGF10	↓ capillary density	Collins et al. (2018)
	Mouse	Inflammation	TGF-β	↑ MSCs apoptosis ↓MSCs number	↑ monocytes/macrophages and neutrophils	Ehrhardt et al. (2016)
					↑IL-1β, CXCL1, and MCP-1 ↑ impaired alveolar structure	

BPD, bronchopulmonary dysplasia; MSCs, mesenchymal stromal/stem cells; PINK1, PTEN-induced putative kinase 1; ATP, adenosine triphosphate; OCR, oxygen consumption rate; SOX-2, SRY-box2; OCT-4, Octamer-binding transcription factor 4; VEGF, vascular endothelial growth factor; FGF, fibroblast growth factor; SHH, sonic hedgehog; IL, interleukin; Tbx3, T-box transcription factor3; CXCL1, C-X-C motif chemokine ligand 1; GRO-α, growth-related oncogene-α; HGF, hepatocyte growth factor; NFκB, Nuclear factor kappa B, TNF-α, tumor necrosis factor-α; TGF-β, transforming growth factor-β; MCP-1, monocyte chemoattractant protein-1.

In conclusion, prenatal risk factors for BPD, such as hyperoxic conditions, lead to oxidative stress and MSC dysfunction, which can contribute to BPD's development and advancement.

3.2 Angiogenesis

Pulmonary microvascular dysplasia is a component of BPD pathogenesis; therefore, fostering pulmonary angiogenesis and enhancing vasculogenesis are crucial objectives to mitigate this dysplasia. Under hyperoxic conditions, it was found that MSCs in the tracheal aspirates of preterm infants' lungs exhibited reduced expression of growth factors crucial for alveolar development and repair, such as VEGF, FGF10, and angiogenin, through the decrease in SOX-2 and OCT-4 (Mobius et al., 2019). Moreover, the CD146+ MSCs in the lungs exposed to hyperoxia displayed decreased gene expression of notable proangiogenic genes, including FGF9 and IL-6, through SHH signaling (White et al., 2007; Kwon et al., 2014). In a rat model of BPD induced by hyperoxia, the resident lung CD146+ MSCs were found to inhibit rather than promote angiogenesis through the axon guidance signaling (Semaphorins 3A and 3E) (Collins et al., 2018). Consequently, BPD insults prompt alterations in angiogenic pathways, which result in an MSC phenotype with aberrant microvascular development, a key characteristic of BPD pathogenesis (Alvira, 2016).

An investigation involving hyperoxia-induced BPD in rodent models reported decreased endothelial progenitor cells within the bloodstream, lungs, and bone marrow (Balasubramaniam et al., 2007). Endothelial progenitor cells, also called endothelial colony-forming cells, are required for vasculogenesis in the developing lung and are associated with the support and maturation of endothelial progenitor cells. Crucial to the regional specialization of embryonic lung tissue, MSCs at the outer edge of branching epithelium are noted for producing FGF10, a vital element in the signaling interplay involving BMP, Wnt, and sonic hedgehog pathways that direct the differentiation of epithelial stem/progenitors during lung development (Morrisey and Hogan, 2010). *In vitro* studies have shown that MSCs substantially support the growth and differentiation of epithelial stem cells (McQualter et al., 2010). Further highlighting this critical microenvironmental association, recent *in vivo* research employing the naphthalene injury model showed that parabronchial mesenchymal cells discharge FGF10 to stimulate epithelial regeneration in the remaining progenitor cells

(McQualter et al., 2010). These findings support the theory that a reduction in MSCs or malfunctioning MSCs might cause the hindered growth of endothelial progenitor cells and affect their angiogenic supportive capacity, thereby contributing to the onset of BPD.

3.3 Inflammation

Inflammatory imbalance plays a significant role in the development of BPD. Various immune regulatory attributes have been credited to MSCs from different tissue origins, contributing to tissue regeneration, cell death prevention, tissue fibrosis inhibition, and the reduction of tissue damage (Li et al., 2019). MSCs isolated from the tracheal aspirates of preterm infants show a propensity towards inflammation, secreting increased levels of pro-inflammatory cytokines like CXCL-1, IL-6, and IL-8 and decreased anti-fibrotic factor levels of CXCL1/GRO-α and HGF, possibly through dysregulated FoxF1, Wnt5a, and Tbx3 signaling (Bozyk et al., 2011). Traditional pro-inflammatory cytokines such as TNF-α, IL-1β, IL-6, and IL-8 trigger comparable changes in MSCs derived from preterm infants with severe BPD. NFκB targeting was observed to reverse this pro-inflammatory tendency (Reicherzer et al., 2018). In the lungs of infants suffering from BPD, it was discovered that thicker alveolar walls were linked with a scarcity of PDGFR-α-positive cells in the malformed alveolar septa (Popova et al., 2014). A significant decrease in the volume of PDGFR-α-positive alveolar tips was observed in the lungs of neonatal mice exposed to excess oxygen in another study (Popova et al., 2014). Another study demonstrated enhanced apoptosis in PDGFR-α-positive mesenchymal cells through abrogation of TNF-α-mediated NFκB signaling and primarily influenced by TGF-β1 signaling (Ehrhardt et al., 2016). The authors concluded that this phenomenon explained much of the amplified lung damage during mechanical ventilation (Ehrhardt et al., 2016).

Alveolar macrophages, responsible for maintaining a balanced immune response in the lung, react to changing environmental conditions in various ways, often simplified into anti-inflammatory and pro-inflammatory effects. Hyperoxia, a prevalent condition in BPD supportive care, can damage alveolar macrophages. PGE2, a substance secreted by MSCs, plays a pivotal role in the bioenergetic shift in macrophages, increasing anti-inflammatory activation and decreasing pro-inflammatory activation through AMPK activity/SIRTUIN 1 signaling (Vasandan et al., 2016). Levels of prostaglandin E2 were found to be reduced in hyperoxia–exposed fetal lung MSCs (Mobius et al., 2019). Consequently, the decrease in anti-inflammatory MSCs or the impairment of their anti-inflammatory function contributes to the pathogenesis of BPD.

4 Stem cell-based BPD preclinical treatments

4.1 *In vivo* studies

Studies using animal models continue to refine the use of MSCs in therapeutic strategies. The potential of MSCs to restore normal lung function has sparked a desire to understand their interplay with damaged lung tissue. As discussed, MSCs act through paracrine signaling, with EVs playing an essential role in this mechanism (Figure 2). The EVs are between 30 and 1000 nm in size and are secreted by most cell types. After binding and internalization, they initiate signal transduction in target cells (Omar et al., 2022). Typically, they arise from multivesicular bodies whose plasma membranes are budding inward. The EVs contain cytokines, proteins, mRNA, microRNAs, DNA, lipids, metabolites and even mitochondria from the parent cells. Several mechanisms can enable EVs to transfer their molecular cargo when released, including fusing with target cell membranes or being endocytosed (Jadli et al., 2020). EVs can modulate recipient cells, affecting immunity, development, homeostasis, and disease pathogenesis. Preconditioning MSCs *in vitro* can enhance the regenerative capacity of secreted EVs. MSC-EVs can also be enhanced therapeutically by bioengineering or genetic modification (Figure 2). By optimizing EV production protocols and delivery strategies, MSC-EV therapy for BPD may be translated into clinical practice. A better understanding of MSC-EV cargo and underlying mechanisms of lung repair will facilitate the development of more potent acellular treatments. Several studies have found that MSC-EVs have protective effects on the lung by blocking inflammation, improving lung function, and reducing pulmonary hypertension (Mansouri et al., 2019; Abele et al., 2022; Sharma et al., 2022). A recent study discovered that MSCs release several growth factors linked to angiogenesis, predominantly VEGF, stored in EVs, particularly exosomes (Xi et al., 2022); this suggests a potential method for MSC-exosomes to increase VEGF-driven angiogenesis in BPD treatment (Xi et al., 2022). An experimental study evaluating a hyperoxia-induced BPD rat model compared the protective effects of intratracheally administered MSCs *versus* EVs to ascertain the differences between MSC and MSC-derived extracellular vesicle administration. The study found that both MSCs and MSC-EVs alleviated hyperoxia-induced damage, but MSC-EVs achieved superior outcomes regarding alveolarization and lung vascularization (Braun et al., 2018; Moreira et al., 2020). The benefits of using EVs over MSCs for treatment include easier intratracheal administration, the potential for modifications to enhance the benefits of extracellular vesicle treatment, and the option to freeze-dry (lyophilize) them to preserve their biological activity.

As highlighted earlier, decreased VEGF results in compromised angiogenesis, significantly contributing to BPD development. Extended hyperoxia interrupts normal lung development, a phenomenon linked with abnormal expression of Akt and VEGF (You et al., 2020). A study on a hyperoxia-induced rat model of BPD found that the expressions of phosphorylated Akt and VEGF-A significantly increased following treatment with small EVs derived from human umbilical cord mesenchymal stem cells. At the same time, PTEN and cleaved caspase-3 expression were found to negatively correlate with phosphorylated AKT in the lungs after treatment with these small EVs (You et al., 2020). PTEN functions as the primary regulator of Akt, and it has been documented that the signaling pathway involving PTEN and Akt governs cellular growth, programmed cell death (apoptosis), and the formation of new blood vessels (angiogenesis). Therefore, these findings suggest that small EVs, derived from human umbilical cord mesenchymal stem cells, boost pulmonary alveolarization and angiogenesis to counteract BPD through suppressing PTEN and activating Akt/VEGF pathway.

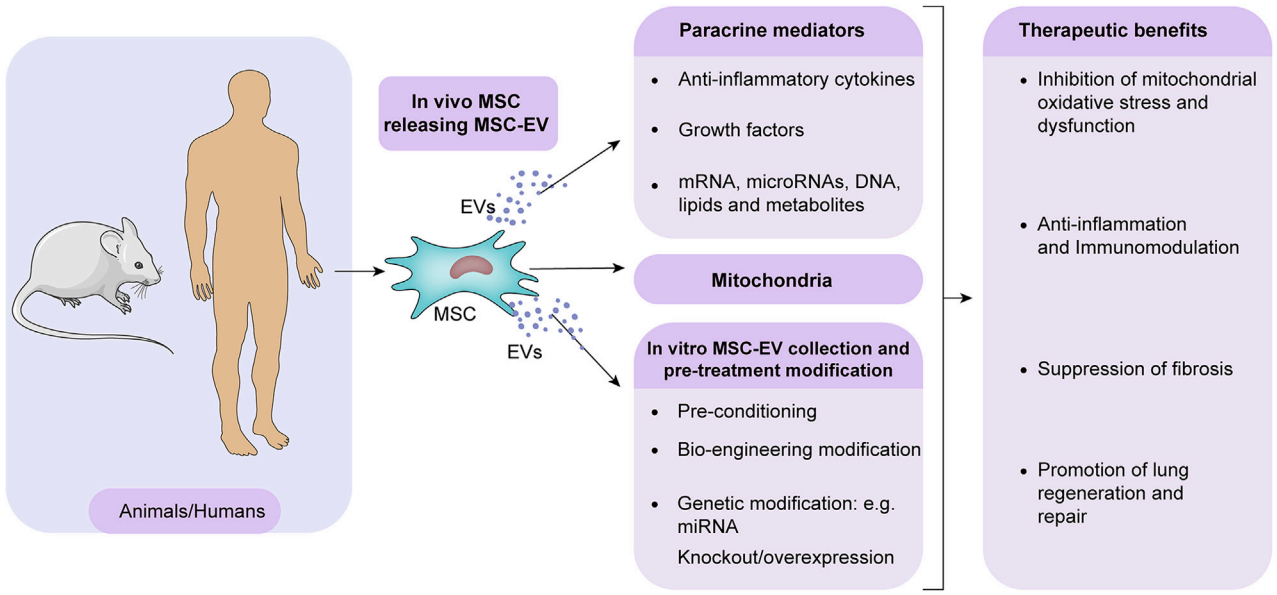

FIGURE 2
MSC-EVs mediate therapeutic effects in BPD. MSCs predominantly promote lung repair in BPD through paracrine. MSCs release EVs containing bioactive molecules and mitochondria that mitigate injury. In addition, EV isolation offers the potential for cell-free treatment. MSC-EVs are enhanced in their regenerative capacity by pre-conditioning, bioengineering, and genetic modification *in vitro*. Optimizing EV production and delivery to maximize lung localization may enable clinical translation for treating BPD.

Research into the paracrine signaling of MSCs via EVs has been paralleled by studies delving into microRNA. One study examined the effect of bone marrow-derived MSCs on microRNA (miR) in a trial involving newborn mice. MiRs, non-coding RNAs of 21–25 nucleotides in length, have roles in several biological processes, including cell proliferation, cell death, resistance to stress, and tumorigenesis. MiR-206 is known to be downregulated in both patients with BPD and newborn mice. Previous research has highlighted the role of miR-206 in BPD by demonstrating its impact on the expression of fibronectin 1. This glycoprotein, a vital component of the extracellular matrix (ECM), plays a crucial role in various biological processes such as cell adhesion and migration, embryonic development, wound repair, cancer metastasis, and immune responses (Zhang et al., 2013). Bone marrow-derived MSCs, when transfected with miR-206, showed functional regulation by enhancing the expression of surfactant protein C and reducing the levels of inflammatory cytokines such as fibronectin 1, TGF-β1, and IL-6. These changes led to a reduction in lung fluid accumulation (pulmonary edema) and an improvement in the formation of alveoli. This finding hints at the potential therapeutic benefits these MSCs might offer in treating BPD (Zhang et al., 2013).

Porzionato et al. (Porzionato et al., 2021) evaluated the protective effects of MSC-derived EVs administered intratracheally using a newborn rat model exposed to hyperoxia for 2 weeks and 4 weeks of recovery. The rats exposed to hyperoxia displayed decreased and expanded distal air spaces, along with sporadic areas of interstitial thickening. The study showed that the treatment with MSC-derived EVs prevented the accumulation of connective or fibrous tissue in the lung parenchyma and sustained the presence of CD163-positive macrophages in hyperoxia-exposed rats, compared to those maintained in normoxic conditions (Porzionato et al., 2021). The treatment did not decrease the total macrophage population but influenced the balance between pro-inflammatory and anti-inflammatory macrophages. Anti-inflammatory macrophages, identified by CD163, have been shown to facilitate alveolarization during normal lung development. The study disclosed that extracellular vesicle treatment averted a decline in the density of interstitial alveolar CD163+ macrophages in rats exposed to hyperoxia (Porzionato et al., 2021). Despite the theoretical benefit of preventing a decrease in CD163+ cells through extracellular vesicle treatment, ongoing damage might still cause these macrophages to stimulate excessive ECM deposition by activating resident fibroblasts via the release of pro-fibrotic factors (Porzionato et al., 2021); this implies additional mechanisms play a part in the anti-fibrotic effect of MSC-EVs, necessitating further research.

A recent study shows that MSC-derived extracellular vesicles can reshape the lung macrophage profile, reducing inflammation and immune reactions to counteract BPD caused by hyperoxia (Willis et al., 2018). The role of MSCs extends beyond paracrine processes (such as carriers of 150-nm exosomes). Alternatively, more giant vesicles (over 500 nm wide) or direct connections between cells might carry more intricate structures, such as mitochondria (Willis et al., 2018). Mitochondria's potential role in MSC action could pave the way for more refined, effective MSC therapies for BPD.

4.2 *In vitro* studies

The study of placental mesenchymal stem cells (PMSCs) has grown in recent years due to their application in various physiological and pathological conditions. Numerous benefits can be gained from PMSCs, including their multipotency and

immunomodulatory capabilities. In contrast to embryonic stem cells, PMSCs can be harvested from young donors in large quantities, overcoming ethical concerns associated with embryonic stem cells (Mathew et al., 2020; Zhang Y. et al., 2022). In an ex-vivo fetal lung culture model, PMSCs exert more effective stimulation on perinatal lung morphogenesis than BMSCs (Di Bernardo et al., 2014); this suggests PMSCs are excellent candidates for regenerative medicine, enabling their extensive use in various stem cell therapy studies. PMSCs have shown the capacity to preserve expanded umbilical cord blood $CD34^+$ cells during cryopreservation, enhancing the recovery, survival, and functionality of these cells upon revival; this is achieved through the reduction of oxidative stress. Interestingly, PMSCs have outperformed cord MSCs in providing cryoprotection to the umbilical cord blood cells (Kadekar et al., 2016). A recent study found that co-cultivation with PMSCs boosted ATP production in trophoblasts by regulating calcium channel expression and inducing mild oxidative stress (Seok et al., 2020). Moreover, exosomes derived from human placenta choriodecidual membrane-derived mesenchymal stem cells significantly mitigated LPS-induced lipid peroxidation and apoptosis in the lung (Seok et al., 2020). These studies suggest that PMSC may help treat the cellular metabolic alterations associated with BPD. However, further research is required to explore the regulatory role of PMSCs in oxidative stress and mitochondrial function in the context of BPD development and treatment. Mass augmenting mitochondrial function and electron transport chain complexes could contribute to the therapeutic efficacy of MSCs, a concept currently under evaluation in clinical trials.

Another provocative finding is that the conditioned medium from PMSCs has been found to contain both factors that stimulate and inhibit angiogenesis, aiding the enhancement of endothelial tube formation. It was observed that endothelial cells take in exosomes from PMSCs, which promotes the formation and migration of tubes and enhances the expression of genes linked to angiogenesis, leading to better angiogenesis *in vivo* (Komaki et al., 2017). Growing attention is being focused on the possible role of PMSCs in influencing angiogenesis in the progression and treatment of BPD. Notably, PMSCs display ease of propagation and superior immunoregulatory attributes, rendering them an appealing treatment option for diseases linked with inflammation in the future (Wu et al., 2017). Studies have shown that human PMSCs can counteract the polarization of pro-inflammatory macrophages and release pro-inflammatory cytokines triggered by LPS by modulating TLR4 expression and the NF-κB signaling pathway (Liu Y. et al., 2022). Therefore, in the landscape of BPD, immune cells may represent promising targets for therapeutic interventions employing PMSC-derived EVs.

5 Stem cell-based BPD clinical applications

Numerous preclinical studies have conducted comprehensive experimental studies, leading to a handful of clinical trials currently underway to examine the impact of MSC therapy (Table 2). A pioneering phase I clinical trial was conducted on nine preterm infants, with gestational ages ranging from 23 to 29 weeks, who needed mechanical ventilation within 5–14 days after birth (Ahn et al., 2017). These infants received an intratracheal delivery of either 10^7 or 2×10^7 MSCs derived from the umbilical cord. This group of infants did not experience any unfavorable events, thus affirming the safety of the MSC treatment administered intratracheally (Ahn et al., 2017). Following this, the same research team reported that the treated infants displayed no deficits in neurological, respiratory, or growth parameters even after 2 years (Ahn et al., 2017). A noteworthy aspect of this phase I clinical trial is its establishment of the safety of intratracheal MSC administration, opening doors for future clinical trials. A different clinical trial investigates the safety and effectiveness of allogeneic human umbilical cord-derived MSCs (hUC-MSCs) delivered intravenously. The dosage was incrementally increased to gather supportive data for the safety of intravenously delivered hUC-MSCs in treating patients with severe BPD. Importantly, this trial is the first to focus on the therapeutic effects of hUC-MSCs in children suffering from severe BPD rather than merely the preventative effects (Wu et al., 2020).

A case study recounted the treatment of an extremely premature baby suffering from severe BPD who received MSC therapy (1×10^7 cells/kg/dose) both intratracheally and intravenously on the 78th day after birth. Before the treatment, the baby had been dependent on mechanical ventilation, initially with volume-targeted conventional therapy and later with high-frequency oscillatory ventilation. Despite receiving four doses of surfactant and undergoing two cycles of steroid therapy, the infant showed no improvement (Yilmaz et al., 2021). Following the MSC treatment, no deterioration in blood gas or indications of sepsis were noted, and there were no reported adverse events. The treatment was initiated after detecting chronic changes in the infant's chest X-ray on the 78th day after birth. It yielded positive results of decreased emphysema and alveolar damage (Yilmaz et al., 2021). This encouraging case study indicates that MSC therapy may offer a promising therapeutic avenue for managing severe BPD in premature babies in the future.

6 Prospects and challenges

Mesenchymal stem cells (MSCs) have shown promising potential as a treatment for bronchopulmonary dysplasia (BPD), a chronic lung disease affecting premature infants. MSCs possess immunomodulatory and regenerative capacities that may mitigate lung injury and facilitate repair. However, several challenges must be addressed before MSC therapy can be widely adopted for BPD.

A significant hurdle is the inherent variability of MSCs depending on tissue source. MSCs derived from different donors and adult tissues exhibit differences in proliferative capacity, migratory abilities, cytokine secretion, and other functions relevant to BPD treatment. Standardizing and optimizing MSC-based therapies will require identifying the ideal MSC populations and culture methods tailored to BPD pathology. Factors influencing the localization, survival, and bioactivity of administered MSCs in the injured neonatal lung remain unclear.

Another concern is the potential influence of MSCs on cancer development. While MSCs appear less tumorigenic than other stem cells, their long-term safety requires further investigation, especially in vulnerable neonate populations. Animal studies have not detected tumor growth, but clinical evidence is still lacking.

It is imperative to note that MSCs are not intrinsically immune-privileged, and both autologous and allogeneic ways can stimulate

TABLE 2 Clinical trials targeting MSCs in BPD treatment.

Cell type	Clinical trials number	Phase	Study title	Status	Study model	Administration methods	Interventions
hMSCs	NCT03683953	I	The Treatment of Bronchopulmonary Dysplasia by Intratracheal Instillation of Mesenchymal Stem Cells	unknown	Parallel Assignment	intratracheal administration	25 million cells/kg
							Normal saline without hUCB-MSCs
hMSCs	NCT02443961	I	Mesenchymal Stem Cell Therapy for Bronchopulmonary Dysplasia in Preterm Babies	completed	Single Group	N/A	3 doses of 5 million MSC
hUC-MSCs	NCT04062136	I	Umbilical Cord Mesenchymal Stem Cells Transplantation in the Treatment of Bronchopulmonary Dysplasia	unknown	Single Group	intravenous infusion	1 million cells per body kg
hUC-MSCs	NCT03558334	I	Human Mesenchymal Stem Cells For Bronchopulmonary Dysplasia	unknown	Parallel Assignment	intravenous infusion	Dose A- 1 million cells per body kg; Dose B- 5 million cells per body kg
							No intravenous infusion of hUC-MSCs
hUC-MSCs	NCT03601416	II	Human Mesenchymal Stem Cells For Moderate and Severe Bronchopulmonary Dysplasia	unknown	Parallel Assignment	intravenous infusion	Dose A- 1 million cells per body kg; Dose B- 5 million cells per body kg
							No intravenous infusion of hUC-MSCs
hUC-MSCs	NCT03631420	I	Mesenchymal Stem Cells for Prevention of Bronchopulmonary	recruiting	Single Group	N/A	Cohort 1: 3 million cells/kg; Cohort 2 : 10 million cells/kg; Cohort 3 : 30 million cells/kg
hUC-MSCs	NCT03873506	I	Follow-Up Study of Mesenchymal Stem Cells for Bronchopulmonary Dysplasia	unknown	Single Group	intravenous infusion	Dose A- 1 million cells per body kg; Dose B- 5 million cells per body kg
hUC-MSCs	NCT03645525	I/II	Intratracheal Umbilical Cord-derived Mesenchymal Stem Cell for the Treatment of Bronchopulmonary Dysplasia (BPD)	recruiting	Parallel Assignment	Single intratracheal administration	2 × 107/kg per body kg
							Saline without hUC-MSCs
hUC-MSCs	NCT02381366	I/II	Safety and Efficacy of PNEUMOSTEM® in Premature Infants at High Risk for Bronchopulmonary Dysplasia (BPD) - a US Study	completed	Single Group	N/A	Dose A: 10 million cells per kg; Dose B: 20 million cells per kg
hUC-MSCs	NCT03774537	I/II	Human Mesenchymal Stem Cells For Infants At High Risk For Bronchopulmonary Dysplasia	unknown	Parallel Assignment	intravenous infusion	Dose A- 1 million cells per kg; Dose B- 5 million cells per kg
							No intravenous infusion of hUC-MSCs
hUC-MSCs	NCT01207869	I	Intratracheal Umbilical Cord-derived Mesenchymal Stem Cells for Severe Bronchopulmonary Dysplasia	unknown	Parallel Assignment	Single intratracheal administration	3 × 106 cells per kg
							Normal saline without hUCB-MSCs
hCT-MSCs	NCT04255147	I	Cellular Therapy for Extreme Preterm Infants at Risk of Developing Bronchopulmonary Dysplasia	recruiting	Single Group	intravenous infusion	1 million cells/body kg; 3 million cells/body kg; 10 million cells/body kg
hUCB-MSCs	NCT01297205	I	Safety and Efficacy Evaluation of PNEUMOSTEM® Treatment in Premature Infants With Bronchopulmonary Dysplasia	completed	Single Group	Single intratracheal administration	Dose A- 10 million cells per kg; Dose B- 20 million cells per kg
hUCB-MSCs	NCT01632475	I	Follow-Up Study of Safety and Efficacy of Pneumostem® in Premature Infants With Bronchopulmonary Dysplasia	active, not recruiting	Single Group	Single intratracheal administration	Low Dose Group: 1.0 × 107 cells/kg; High Dose Group: 2.0 × 107 cells/kg

(Continued on following page)

TABLE 2 (*Continued*) Clinical trials targeting MSCs in BPD treatment.

Cell type	Clinical trials number	Phase	Study title	Status	Study model	Administration methods	Interventions
hUCB-MSCs	NCT04003857	II	Follow-up Study of Safety and Efficacy in Subjects Who Completed PNEUMOSTEM® Phase II (MP-CR-012) Clinical Trial	recruiting	Parallel Assignment	Single intratracheal administration	1.0 × 107 cells/kg
							Saline without hUC-MSCs
hUCB-MSCs	NCT01828957	II	Efficacy and Safety Evaluation of Pneumostem® Versus a Control Group for Treatment of BPD in Premature Infants	completed	Parallel Assignment	Single intratracheal administration	1.0 × 107 cells/kg
							Normal saline without hUCB-MSCs
hUCB-MSCs	NCT01897987	II	Follow-up Safety and Efficacy Evaluation on Subjects Who Completed PNEUMOSTEM® Phase-II Clinical Trial	completed	Parallel Assignment	Single intratracheal administration	1.0 × 107 cells/kg
							Normal saline without hUCB-MSCs
hUCB-MSCs	NCT03392467	II	PNEUMOSTEM for the Prevention and Treatment of Severe BPD in Premature Infants	recruiting	Parallel Assignment	N/A	hUCB-MSCs
							Normal saline without hUCB-MSCs
hUCB-MSCs	NCT02023788	I	Long-term Safety and Efficacy Follow-up Study of PNEUMOSTEM® in Patients Who Completed PNEUMOSTEM® Phase-I Study	completed	Single Group	Single intratracheal administration	Low Dose Group: 1.0 × 107 cells/kg; High Dose Group: 2.0 × 107 cells/kg

hUC-MSCs, human umbilical cord mesenchymal stem cells; hCT-MSCs, human cord tissue mesenchymal stem cells; hUCB-MSCs, human umbilical cord blood-derived mesenchymal stem cells.

anti-MSC immune responses, which can negatively impact their survival and efficacy. It is crucial to understand these complex dynamics to improve MSC-based therapies.

Additionally, guidelines are needed for identifying patients most likely to benefit from MSC treatment and the optimal administration timeline. Recent trials in ventilated preterm infants suggest efficacy, but more extensive studies are necessary to evaluate long-term outcomes and standardize cell production. Variations in manufacturing processes can alter MSC potency.

Future research should clarify mechanisms underlying MSC-mediated lung repair in BPD, such as paracrine signaling via EVs mitochondria through more giant vesicles (over 500 nm wide) or direct connections between cells. Strategies to enhance MSC engraftment and survival post-transplantation warrant exploration. As MSC therapy for BPD advances, international consensus on cell preparation, characterization, and delivery protocols will enable meaningful comparisons across clinical trials. A precision medicine approach adapting MSC therapy to each patient's disease phenotype may prove optimal.

7 Conclusion

Bronchopulmonary dysplasia (BPD) is a chronic pulmonary disease that affects preterm infants, and its prevalence is increasing due to improved survival rates among this at-risk group. This condition arises from various factors, including maternal health, prenatal environment, and modern treatments for preterm babies, such as mechanical ventilation. Recent experimental studies have increased our understanding of the underlying pathogenetic mechanisms of BPD and revealed potential therapeutic targets. As BPD primarily manifests as a functional decline and reduction in lung stem cell populations, the prospect of replenishing and regenerating these cells could be crucial to its treatment. Recent clinical trials have validated the safety and effectiveness of MSC transplantation, with outcomes including a reduction in inflammation, mitochondrial oxidative stress, lung damage, and fibrosis. MSC-based therapy holds significant promise for promoting lung repair and regeneration in BPD. Realizing the full potential of MSCs will require systematic preclinical studies to elucidate mechanisms, optimize treatment protocols, and assess long-term safety. Well-designed clinical trials are needed to evaluate different MSC sources, combination therapies, and cell-free approaches. If critical challenges are addressed, MSCs could become an effective treatment for this debilitating developmental lung disease.

Author contributions

DY conceptualization; SZ and CM writing–original draft preparation; SR, RS, and DY writing–review and editing. All authors contributed to the article and approved the submitted version.

Funding

This work was supported by funding from Science and Technology Plan Project of Liaoning Province (No. 2020JH2/10300128) and Natural Science Foundation of Liaoning Province (No. 201602873).

Conflict of interest

The authors declare that the research was conducted in the absence of any commercial or financial relationships that could be construed as a potential conflict of interest.

Publisher's note

References

Abele, A. N., Taglauer, E. S., Almeda, M., Wilson, N., Abikoye, A., Seedorf, G. J., et al. (2022). Antenatal mesenchymal stromal cell extracellular vesicle treatment preserves lung development in a model of bronchopulmonary dysplasia due to chorioamnionitis. *Am. J. Physiol. Lung Cell Mol. Physiol.* 322, L179–L190. doi:10.1152/ajplung.00329.2021

Ahn, S. Y., Chang, Y. S., Kim, J. H., Sung, S. I., and Park, W. S. (2017). Two-year follow-up outcomes of premature infants enrolled in the phase I trial of mesenchymal stem cells transplantation for bronchopulmonary dysplasia. *J. Pediatr.* 185, 49–54. doi:10.1016/j.jpeds.2017.02.061

Aliotta, J. M., Pereira, M., Wen, S., Dooner, M. S., Del Tatto, M., Papa, E., et al. (2016). Exosomes induce and reverse monocrotaline-induced pulmonary hypertension in mice. *Cardiovasc Res.* 110, 319–330. doi:10.1093/cvr/cvw054

Alphonse, R. S., Rajabali, S., and Thebaud, B. (2012). Lung injury in preterm neonates: the role and therapeutic potential of stem cells. *Antioxid. Redox Signal* 17, 1013–1040. doi:10.1089/ars.2011.4267

Alvarez-Fuente, M., Arruza, L., Lopez-Ortego, P., Moreno, L., Ramirez-Orellana, M., Labrandero, C., et al. (2018). Off-label mesenchymal stromal cell treatment in two infants with severe bronchopulmonary dysplasia: clinical course and biomarkers profile. *Cytotherapy* 20, 1337–1344. doi:10.1016/j.jcyt.2018.09.003

Alvira, C. M. (2016). Aberrant pulmonary vascular growth and remodeling in bronchopulmonary dysplasia. *Front. Med. (Lausanne)* 3, 21. doi:10.3389/fmed.2016.00021

Anker, P. S., Noort, W. A., Scherjon, S. A., Kleijburg-Van Der Keur, C., Kruisselbrink, A. B., Van Bezooijen, R. L., et al. (2003). Mesenchymal stem cells in human second-trimester bone marrow, liver, lung, and spleen exhibit a similar immunophenotype but a heterogeneous multilineage differentiation potential. *Haematologica* 88, 845–852.

Balasubramaniam, V., Mervis, C. F., Maxey, A. M., Markham, N. E., and Abman, S. H. (2007). Hyperoxia reduces bone marrow, circulating, and lung endothelial progenitor cells in the developing lung: implications for the pathogenesis of bronchopulmonary dysplasia. *Am. J. Physiol. Lung Cell Mol. Physiol.* 292, L1073–L1084. doi:10.1152/ajplung.00347.2006

Bellusci, S., Grindley, J., Emoto, H., Itoh, N., and Hogan, B. L. (1997). Fibroblast growth factor 10 (FGF10) and branching morphogenesis in the embryonic mouse lung. *Development* 124, 4867–4878. doi:10.1242/dev.124.23.4867

Benjamin, J. T., Plosa, E. J., Sucre, J. M., Van Der Meer, R., Dave, S., Gutor, S., et al. (2021). Neutrophilic inflammation during lung development disrupts elastin assembly and predisposes adult mice to COPD. *J. Clin. Invest.* 131, e139481. doi:10.1172/JCI139481

Bozyk, P. D., Popova, A. P., Bentley, J. K., Goldsmith, A. M., Linn, M. J., Weiss, D. J., et al. (2011). Mesenchymal stromal cells from neonatal tracheal aspirates demonstrate a pattern of lung-specific gene expression. *Stem Cells Dev.* 20, 1995–2007. doi:10.1089/scd.2010.0494

Braun, R. K., Chetty, C., Balasubramaniam, V., Centanni, R., Haraldsdottir, K., Hematti, P., et al. (2018). Intraperitoneal injection of MSC-derived exosomes prevent experimental bronchopulmonary dysplasia. *Biochem. Biophys. Res. Commun.* 503, 2653–2658. doi:10.1016/j.bbrc.2018.08.019

Cardoso, W. V., and Lu, J. (2006). Regulation of early lung morphogenesis: questions, facts and controversies. *Development* 133, 1611–1624. doi:10.1242/dev.02310

Chen, C. T., Shih, Y. R., Kuo, T. K., Lee, O. K., and Wei, Y. H. (2008). Coordinated changes of mitochondrial biogenesis and antioxidant enzymes during osteogenic differentiation of human mesenchymal stem cells. *Stem Cells* 26, 960–968. doi:10.1634/stemcells.2007-0509

Collins, J. J., and Thebaud, B. (2014). Lung mesenchymal stromal cells in development and disease: to serve and protect? *Antioxid. Redox Signal* 21, 1849–1862. doi:10.1089/ars.2013.5781

Collins, J. J. P., Lithopoulos, M. A., Dos Santos, C. C., Issa, N., Mobius, M. A., Ito, C., et al. (2018). Impaired angiogenic supportive capacity and altered gene expression profile of resident CD146(+) mesenchymal stromal cells isolated from hyperoxia-injured neonatal rat lungs. *Stem Cells Dev.* 27, 1109–1124. doi:10.1089/scd.2017.0145

De Langhe, S. P., Carraro, G., Tefft, D., Li, C., Xu, X., Chai, Y., et al. (2008). Formation and differentiation of multiple mesenchymal lineages during lung development is regulated by beta-catenin signaling. *PLoS One* 3, e1516. doi:10.1371/journal.pone.0001516

Di Bernardo, J., Maiden, M. M., Jiang, G., Hershenson, M. B., and Kunisaki, S. M. (2014). Paracrine regulation of fetal lung morphogenesis using human placenta-derived mesenchymal stromal cells. *J. Surg. Res.* 190, 255–263. doi:10.1016/j.jss.2014.04.013

Driscoll, B., Kikuchi, A., Lau, A. N., Lee, J., Reddy, R., Jesudason, E., et al. (2012). Isolation and characterization of distal lung progenitor cells. *Methods Mol. Biol.* 879, 109–122. doi:10.1007/978-1-61779-815-3_7

Dutra Silva, J., Su, Y., Calfee, C. S., Delucchi, K. L., Weiss, D., Mcauley, D. F., et al. (2021). Mesenchymal stromal cell extracellular vesicles rescue mitochondrial dysfunction and improve barrier integrity in clinically relevant models of ARDS. *Eur. Respir. J.* 58, 2002978. doi:10.1183/13993003.02978-2020

Ehrhardt, H., Pritzke, T., Oak, P., Kossert, M., Biebach, L., Forster, K., et al. (2016). Absence of TNF-alpha enhances inflammatory response in the newborn lung undergoing mechanical ventilation. *Am. J. Physiol. Lung Cell Mol. Physiol.* 310, L909–L918. doi:10.1152/ajplung.00367.2015

Fang, S., Zhang, S., Dai, H., Hu, X., Li, C., and Xing, Y. (2019). The role of pulmonary mesenchymal cells in airway epithelium regeneration during injury repair. *Stem Cell Res. Ther.* 10, 366. doi:10.1186/s13287-019-1452-1

Feng, X., Zhang, W., Yin, W., and Kang, Y. J. (2019). Feature Article: the involvement of mitochondrial fission in maintenance of the stemness of bone marrow mesenchymal stem cells. *Exp. Biol. Med. (Maywood)* 244, 64–72. doi:10.1177/1535370218821063

Forni, M. F., Peloggia, J., Trudeau, K., Shirihai, O., and Kowaltowski, A. J. (2016). Murine mesenchymal stem cell commitment to differentiation is regulated by mitochondrial dynamics. *Stem Cells* 34, 743–755. doi:10.1002/stem.2248

Gilfillan, M., Bhandari, A., and Bhandari, V. (2021). Diagnosis and management of bronchopulmonary dysplasia. *BMJ* 375, n1974. doi:10.1136/bmj.n1974

Gough, A., Linden, M., Spence, D., Patterson, C. C., Halliday, H. L., and Mcgarvey, L. P. (2014). Impaired lung function and health status in adult survivors of bronchopulmonary dysplasia. *Eur. Respir. J.* 43, 808–816. doi:10.1183/09031936.00039513

Greenberg, J. M., Thompson, F. Y., Brooks, S. K., Shannon, J. M., Mccormick-Shannon, K., Cameron, J. E., et al. (2002). Mesenchymal expression of vascular endothelial growth factors D and A defines vascular patterning in developing lung. *Dev. Dyn.* 224, 144–153. doi:10.1002/dvdy.10095

Hansen, A. R., Barnes, C. M., Folkman, J., and Mcelrath, T. F. (2010). Maternal preeclampsia predicts the development of bronchopulmonary dysplasia. *J. Pediatr.* 156, 532–536. doi:10.1016/j.jpeds.2009.10.018

Hao, C., You, J., Qiu, H., Zhou, O., Liu, J., Zou, W., et al. (2022). Hypoxic preconditioning improves the survival and pro-angiogenic capacity of transplanted human umbilical cord mesenchymal stem cells via HIF-1α signaling in a rat model of bronchopulmonary dysplasia. *Biochem. Biophys. Res. Commun.* 605, 111–118. doi:10.1016/j.bbrc.2022.03.044

Hazra, S., Li, R., Vamesu, B. M., Jilling, T., Ballinger, S. W., Ambalavanan, N., et al. (2022). Mesenchymal stem cell bioenergetics and apoptosis are associated with risk for bronchopulmonary dysplasia in extremely low birth weight infants. *Sci. Rep.* 12, 17484. doi:10.1038/s41598-022-22478-5

Higano, N. S., Spielberg, D. R., Fleck, R. J., Schapiro, A. H., Walkup, L. L., Hahn, A. D., et al. (2018). Neonatal pulmonary magnetic resonance imaging of bronchopulmonary dysplasia predicts short-term clinical outcomes. *Am. J. Respir. Crit. Care Med.* 198, 1302–1311. doi:10.1164/rccm.201711-2287OC

Holzfurtner, L., Shahzad, T., Dong, Y., Rekers, L., Selting, A., Staude, B., et al. (2022). When inflammation meets lung development-an update on the pathogenesis of bronchopulmonary dysplasia. *Mol. Cell Pediatr.* 9, 7. doi:10.1186/s40348-022-00137-z

Igura, K., Zhang, X., Takahashi, K., Mitsuru, A., Yamaguchi, S., and Takashi, T. A. (2004). Isolation and characterization of mesenchymal progenitor cells from chorionic villi of human placenta. *Cytotherapy* 6, 543–553. doi:10.1080/14653240410005366-1

Ikonomou, L., Herriges, M. J., Lewandowski, S. L., Marsland, R., 3rd, Villacorta-Martin, C., Caballero, I. S., et al. (2020). The *in vivo* genetic program of murine primordial lung epithelial progenitors. *Nat. Commun.* 11, 635. doi:10.1038/s41467-020-14348-3

Islam, M. N., Das, S. R., Emin, M. T., Wei, M., Sun, L., Westphalen, K., et al. (2012). Mitochondrial transfer from bone-marrow-derived stromal cells to pulmonary alveoli protects against acute lung injury. *Nat. Med.* 18, 759–765. doi:10.1038/nm.2736

Jadli, A. S., Ballasy, N., Edalat, P., and Patel, V. B. (2020). Inside(sight) of tiny communicator: exosome biogenesis, secretion, and uptake. *Mol. Cell Biochem.* 467, 77–94. doi:10.1007/s11010-020-03703-z

Jarvinen, L., Badri, L., Wettlaufer, S., Ohtsuka, T., Standiford, T. J., Toews, G. B., et al. (2008). Lung resident mesenchymal stem cells isolated from human lung allografts inhibit T cell proliferation via a soluble mediator. *J. Immunol.* 181, 4389–4396. doi:10.4049/jimmunol.181.6.4389

Jobe, A. H. (2011). The new bronchopulmonary dysplasia. *Curr. Opin. Pediatr.* 23, 167–172. doi:10.1097/MOP.0b013e3283423e6b

Kadekar, D., Rangole, S., Kale, V., and Limaye, L. (2016). Conditioned medium from placental mesenchymal stem cells reduces oxidative stress during the cryopreservation of *ex vivo* expanded umbilical cord blood cells. *PLoS One* 11, e0165466. doi:10.1371/journal.pone.0165466

Kimble, A., Robbins, M. E., and Perez, M. (2022). Pathogenesis of bronchopulmonary dysplasia: role of oxidative stress from 'omics' studies, *Antioxidants (Basel)* 11, 2380. doi:10.3390/antiox11122380

Klein, D. (2021). Lung multipotent stem cells of mesenchymal nature: cellular basis, clinical relevance, and implications for stem cell therapy. *Antioxid. Redox Signal* 35, 204–216. doi:10.1089/ars.2020.8190

Klinger, G., Sokolover, N., Boyko, V., Sirota, L., Lerner-Geva, L., Reichman, B., et al. (2013). Perinatal risk factors for bronchopulmonary dysplasia in a national cohort of very-low-birthweight infants. *Am. J. Obstet. Gynecol.* 208, 115.e1–115.e9. doi:10.1016/j.ajog.2012.11.026

Komaki, M., Numata, Y., Morioka, C., Honda, I., Tooi, M., Yokoyama, N., et al. (2017). Exosomes of human placenta-derived mesenchymal stem cells stimulate angiogenesis. *Stem Cell Res. Ther.* 8, 219. doi:10.1186/s13287-017-0660-9

Kwon, H. M., Hur, S. M., Park, K. Y., Kim, C. K., Kim, Y. M., Kim, H. S., et al. (2014). Multiple paracrine factors secreted by mesenchymal stem cells contribute to angiogenesis. *Vasc. Pharmacol.* 63, 19–28. doi:10.1016/j.vph.2014.06.004

Lai, R. C., Arslan, F., Lee, M. M., Sze, N. S., Choo, A., Chen, T. S., et al. (2010). Exosome secreted by MSC reduces myocardial ischemia/reperfusion injury. *Stem Cell Res.* 4, 214–222. doi:10.1016/j.scr.2009.12.003

Li, H., Shen, S., Fu, H., Wang, Z., Li, X., Sui, X., et al. (2019). Immunomodulatory functions of mesenchymal stem cells in tissue engineering. *Stem Cells Int.* 2019, 9671206. doi:10.1155/2019/9671206

Liu, D., Gao, Y., Liu, J., Huang, Y., Yin, J., Feng, Y., et al. (2021). Intercellular mitochondrial transfer as a means of tissue revitalization. *Signal Transduct. Target Ther.* 6, 65. doi:10.1038/s41392-020-00440-z

Liu, J., Xiao, Q., Xiao, J., Niu, C., Li, Y., Zhang, X., et al. (2022a). Wnt/β-catenin signalling: function, biological mechanisms, and therapeutic opportunities. *Signal Transduct. Target Ther.* 7, 3. doi:10.1038/s41392-021-00762-6

Liu, Y., Zhang, X., Hu, Y., Kang, M., Wu, Y., Wang, Y., et al. (2022b). Human placental mesenchymal stem cells regulate inflammation via the NF-κB signaling pathway. *Exp. Ther. Med.* 24, 654. doi:10.3892/etm.2022.11591

Luan, Y., Ding, W., Ju, Z. Y., Zhang, Z. H., Zhang, X., and Kong, F. (2015). Bone marrow-derived mesenchymal stem cells protect against lung injury in a mouse model of bronchopulmonary dysplasia. *Mol. Med. Rep.* 11, 1945–1950. doi:10.3892/mmr.2014.2959

Mansouri, N., Willis, G. R., Fernandez-Gonzalez, A., Reis, M., Nassiri, S., Mitsialis, S. A., et al. (2019). Mesenchymal stromal cell exosomes prevent and revert experimental pulmonary fibrosis through modulation of monocyte phenotypes. *JCI Insight* 4, e128060. doi:10.1172/jci.insight.128060

Mathew, S. A., Naik, C., Cahill, P. A., and Bhonde, R. R. (2020). Placental mesenchymal stromal cells as an alternative tool for therapeutic angiogenesis. *Cell Mol. Life Sci.* 77, 253–265. doi:10.1007/s00018-019-03268-1

Mcqualter, J. L., Yuen, K., Williams, B., and Bertoncello, I. (2010). Evidence of an epithelial stem/progenitor cell hierarchy in the adult mouse lung. *Proc. Natl. Acad. Sci. U. S. A.* 107, 1414–1419. doi:10.1073/pnas.0909207107

Mizikova, I., and Thebaud, B. (2023). Perinatal origins of bronchopulmonary dysplasia-deciphering normal and impaired lung development cell by cell. *Mol. Cell Pediatr.* 10, 4. doi:10.1186/s40348-023-00158-2

Mobius, M. A., Freund, D., Vadivel, A., Koss, S., Mcconaghy, S., Ohls, R. K., et al. (2019). Oxygen disrupts human fetal lung mesenchymal cells. Implications for bronchopulmonary dysplasia. *Am. J. Respir. Cell Mol. Biol.* 60, 592–600. doi:10.1165/rcmb.2018-0358OC

Moreira, A., Winter, C., Joy, J., Winter, L., Jones, M., Noronha, M., et al. (2020). Intranasal delivery of human umbilical cord Wharton's jelly mesenchymal stromal cells restores lung alveolarization and vascularization in experimental bronchopulmonary dysplasia. *Stem Cells Transl. Med.* 9, 221–234. doi:10.1002/sctm.18-0273

Morrisey, E. E., and Hogan, B. L. (2010). Preparing for the first breath: genetic and cellular mechanisms in lung development. *Dev. Cell* 18, 8–23. doi:10.1016/j.devcel.2009.12.010

Nguyen, L. T., Tran, N. T., Than, U. T. T., Nguyen, M. Q., Tran, A. M., Do, P. T. X., et al. (2022). Optimization of human umbilical cord blood-derived mesenchymal stem cell isolation and culture methods in serum- and xeno-free conditions. *Stem Cell Res. Ther.* 13, 15. doi:10.1186/s13287-021-02694-y

Obendorf, J., Fabian, C., Thome, U. H., and Laube, M. (2020). Paracrine stimulation of perinatal lung functional and structural maturation by mesenchymal stem cells. *Stem Cell Res. Ther.* 11, 525. doi:10.1186/s13287-020-02028-4

Omar, S. A., Abdul-Hafez, A., Ibrahim, S., Pillai, N., Abdulmageed, M., Thiruvenkataramani, R. P., et al. (2022). Stem-cell therapy for bronchopulmonary dysplasia (BPD) in newborns. *Cells* 11, 1275. doi:10.3390/cells11081275

Ozkan, H., Cetinkaya, M., and Koksal, N. (2012). Increased incidence of bronchopulmonary dysplasia in preterm infants exposed to preeclampsia. *J. Matern. Fetal Neonatal Med.* 25, 2681–2685. doi:10.3109/14767058.2012.708371

Paliwal, S., Chaudhuri, R., Agrawal, A., and Mohanty, S. (2018). Regenerative abilities of mesenchymal stem cells through mitochondrial transfer. *J. Biomed. Sci.* 25, 31. doi:10.1186/s12929-018-0429-1

Pattappa, G., Heywood, H. K., De Bruijn, J. D., and Lee, D. A. (2011). The metabolism of human mesenchymal stem cells during proliferation and differentiation. *J. Cell Physiol.* 226, 2562–2570. doi:10.1002/jcp.22605

Phinney, D. G., Di Giuseppe, M., Njah, J., Sala, E., Shiva, S., St Croix, C. M., et al. (2015). Mesenchymal stem cells use extracellular vesicles to outsource mitophagy and shuttle microRNAs. *Nat. Commun.* 6, 8472. doi:10.1038/ncomms9472

Popova, A. P., Bentley, J. K., Cui, T. X., Richardson, M. N., Linn, M. J., Lei, J., et al. (2014). Reduced platelet-derived growth factor receptor expression is a primary feature of human bronchopulmonary dysplasia. *Am. J. Physiol. Lung Cell Mol. Physiol.* 307, L231–L239. doi:10.1152/ajplung.00342.2013

Porzionato, A., Zaramella, P., Dedja, A., Guidolin, D., Bonadies, L., Macchi, V., et al. (2021). Intratracheal administration of mesenchymal stem cell-derived extracellular vesicles reduces lung injuries in a chronic rat model of bronchopulmonary dysplasia. *Am. J. Physiol. Lung Cell Mol. Physiol.* 320, L688–L704. doi:10.1152/ajplung.00148.2020

Reicherzer, T., Haffner, S., Shahzad, T., Gronbach, J., Mysliwietz, J., Hubener, C., et al. (2018). Activation of the NF-κB pathway alters the phenotype of MSCs in the tracheal aspirates of preterm infants with severe BPD. *Am. J. Physiol. Lung Cell Mol. Physiol.* 315, L87–L101. doi:10.1152/ajplung.00505.2017

Reiter, J., Drummond, S., Sammour, I., Huang, J., Florea, V., Dornas, P., et al. (2017). Stromal derived factor-1 mediates the lung regenerative effects of mesenchymal stem cells in a rodent model of bronchopulmonary dysplasia. *Respir. Res.* 18, 137. doi:10.1186/s12931-017-0620-z

Schmidt, A. R., and Ramamoorthy, C. (2022). Bronchopulmonary dysplasia. *Paediatr. Anaesth.* 32, 174–180. doi:10.1111/pan.14365

Seok, J., Jun, S., Lee, J. O., and Kim, G. J. (2020). Mitochondrial dynamics in placenta-derived mesenchymal stem cells regulate the invasion activity of trophoblast. *Int. J. Mol. Sci.* 21, 8599. doi:10.3390/ijms21228599

Sharma, M., Bellio, M. A., Benny, M., Kulandavelu, S., Chen, P., Janjindamai, C., et al. (2022). Mesenchymal stem cell-derived extracellular vesicles prevent experimental bronchopulmonary dysplasia complicated by pulmonary hypertension. *Stem Cells Transl. Med.* 11, 828–840. doi:10.1093/stcltm/szac041

Shu, W., Guttentag, S., Wang, Z., Andl, T., Ballard, P., Lu, M. M., et al. (2005). Wnt/beta-catenin signaling acts upstream of N-myc, BMP4, and FGF signaling to regulate proximal-distal patterning in the lung. *Dev. Biol.* 283, 226–239. doi:10.1016/j.ydbio.2005.04.014

Simones, A. A., Beisang, D. J., Panoskaltsis-Mortari, A., and Roberts, K. D. (2018). Mesenchymal stem cells in the pathogenesis and treatment of bronchopulmonary dysplasia: a clinical review. *Pediatr. Res.* 83, 308–317. doi:10.1038/pr.2017.237

Sucre, J., Haist, L., Bolton, C. E., and Hilgendorff, A. (2021). Early changes and indicators characterizing lung aging in neonatal chronic lung disease. *Front. Med. (Lausanne)* 8, 665152. doi:10.3389/fmed.2021.665152

Thebaud, B., Lalu, M., Renesme, L., Van Katwyk, S., Presseau, J., Thavorn, K., et al. (2021). Benefits and obstacles to cell therapy in neonates: the INCuBAToR (innovative neonatal cellular therapy for bronchopulmonary dysplasia: accelerating translation of research). *Stem Cells Transl. Med.* 10, 968–975. doi:10.1002/sctm.20-0508

Torchin, H., Ancel, P. Y., Goffinet, F., Hascoet, J. M., Truffert, P., Tran, D., et al. (2016). Placental complications and bronchopulmonary dysplasia: EPIPAGE-2 cohort study. *Pediatrics* 137, e20152163. doi:10.1542/peds.2015-2163

Varderidou-Minasian, S., and Lorenowicz, M. J. (2020). Mesenchymal stromal/stem cell-derived extracellular vesicles in tissue repair: challenges and opportunities. *Theranostics* 10, 5979–5997. doi:10.7150/thno.40122

Varkouhi, A. K., Jerkic, M., Ormesher, L., Gagnon, S., Goyal, S., Rabani, R., et al. (2019). Extracellular vesicles from interferon-gamma-primed human umbilical cord mesenchymal stromal cells reduce Escherichia coli-induced acute lung injury in rats. *Anesthesiology* 130, 778–790. doi:10.1097/ALN.0000000000002655

Vasandan, A. B., Jahnavi, S., Shashank, C., Prasad, P., Kumar, A., and Prasanna, S. J. (2016). Human Mesenchymal stem cells program macrophage plasticity by altering their metabolic status via a PGE(2)-dependent mechanism. *Sci. Rep.* 6, 38308. doi:10.1038/srep38308

Volckaert, T., Campbell, A., Dill, E., Li, C., Minoo, P., and De Langhe, S. (2013). Localized Fgf10 expression is not required for lung branching morphogenesis but prevents differentiation of epithelial progenitors. *Development* 140, 3731–3742. doi:10.1242/dev.096560

Vom Hove, M., Prenzel, F., Uhlig, H. H., and Robel-Tillig, E. (2014). Pulmonary outcome in former preterm, very low birth weight children with bronchopulmonary dysplasia: a case-control follow-up at school age. *J. Pediatr.* 164, 40–45. doi:10.1016/j.jpeds.2013.07.045

White, A. C., Lavine, K. J., and Ornitz, D. M. (2007). FGF9 and SHH regulate mesenchymal Vegfa expression and development of the pulmonary capillary network. *Development* 134, 3743–3752. doi:10.1242/dev.004879

Willis, G. R., Fernandez-Gonzalez, A., Anastas, J., Vitali, S. H., Liu, X., Ericsson, M., et al. (2018). Mesenchymal stromal cell exosomes ameliorate experimental bronchopulmonary dysplasia and restore lung function through macrophage immunomodulation. *Am. J. Respir. Crit. Care Med.* 197, 104–116. doi:10.1164/rccm.201705-0925OC

Wu, Q., Fang, T., Lang, H., Chen, M., Shi, P., Pang, X., et al. (2017). Comparison of the proliferation, migration and angiogenic properties of human amniotic epithelial and mesenchymal stem cells and their effects on endothelial cells. *Int. J. Mol. Med.* 39, 918–926. doi:10.3892/ijmm.2017.2897

Wu, X., Xia, Y., Zhou, O., Song, Y., Zhang, X., Tian, D., et al. (2020). Allogeneic human umbilical cord-derived mesenchymal stem cells for severe bronchopulmonary dysplasia in children: study protocol for a randomized controlled trial (MSC-BPD trial). *Trials* 21, 125. doi:10.1186/s13063-019-3935-x

Xi, Y., Ju, R., and Wang, Y. (2022). Mesenchymal stem cell-derived extracellular vesicles for the treatment of bronchopulmonary dysplasia. *Front. Pediatr.* 10, 852034. doi:10.3389/fped.2022.852034

Xiong, J., Ai, Q., Bao, L., Gan, Y., Dai, X., Han, M., et al. (2023). Dose-dependent effects of human umbilical cord-derived mesenchymal stem cell treatment in hyperoxia-induced lung injury of neonatal rats. *Front. Pediatr.* 11, 1111829. doi:10.3389/fped.2023.1111829

Xuefei, Y., Xinyi, Z., Qing, C., Dan, Z., Ziyun, L., Hejuan, Z., et al. (2021). Effects of hyperoxia on mitochondrial homeostasis: are mitochondria the hub for bronchopulmonary dysplasia? *Front. Cell Dev. Biol.* 9, 642717. doi:10.3389/fcell.2021.642717

Yilmaz, A., Aslan, M. T., Ince, Z., and Vural, M. (2021). Mesenchymal stem cell therapy in a preterm infant with bronchopulmonary dysplasia. *Indian J. Pediatr.* 88, 1262. doi:10.1007/s12098-021-03946-8

You, J., Zhou, O., Liu, J., Zou, W., Zhang, L., Tian, D., et al. (2020). Human umbilical cord mesenchymal stem cell-derived small extracellular vesicles alleviate lung injury in rat model of bronchopulmonary dysplasia by affecting cell survival and angiogenesis. *Stem Cells Dev.* 29, 1520–1532. doi:10.1089/scd.2020.0156

Zhang, K., Yao, E., Chuang, E., Chen, B., Chuang, E. Y., and Chuang, P. T. (2022a). mTORC1 signaling facilitates differential stem cell differentiation to shape the developing murine lung and is associated with mitochondrial capacity. *Nat. Commun.* 13, 7252. doi:10.1038/s41467-022-34763-y

Zhang, X., Xu, J., Wang, J., Gortner, L., Zhang, S., Wei, X., et al. (2013). Reduction of microRNA-206 contributes to the development of bronchopulmonary dysplasia through up-regulation of fibronectin 1. *PLoS One* 8, e74750. doi:10.1371/journal.pone.0074750

Zhang, Y., Zhong, Y., Zou, L., and Liu, X. (2022b). Significance of placental mesenchymal stem cell in placenta development and implications for preeclampsia. *Front. Pharmacol.* 13, 896531. doi:10.3389/fphar.2022.896531

Zhen, G., Liu, H., Gu, N., Zhang, H., Xu, Y., and Zhang, Z. (2008). Mesenchymal stem cells transplantation protects against rat pulmonary emphysema. *Front. Biosci.* 13, 3415–3422. doi:10.2741/2936

frontiers | Frontiers in Cell and Developmental Biology

TYPE Review
PUBLISHED 06 November 2023
DOI 10.3389/fcell.2023.1290046

OPEN ACCESS

EDITED BY
Azhar Ali,
National University of Singapore, Singapore

REVIEWED BY
Andreas Brodehl,
Heart and Diabetes Center North Rhine-Westphalia, Germany
Dorota Katarzyna Dymkowska,
Polish Academy of Sciences, Poland

*CORRESPONDENCE
Magali Noval Rivas,
magali.novalrivas@csmc.edu

RECEIVED 06 September 2023
ACCEPTED 16 October 2023
PUBLISHED 06 November 2023

CITATION
Atici AE, Crother TR and Noval Rivas M (2023), Mitochondrial quality control in health and cardiovascular diseases. *Front. Cell Dev. Biol.* 11:1290046. doi: 10.3389/fcell.2023.1290046

Mitochondrial quality control in health and cardiovascular diseases

Asli E. Atici[1,2], Timothy R. Crother[1,2] and Magali Noval Rivas[1,2]*

[1]Department of Pediatrics, Division of Infectious Diseases and Immunology, Guerin Children's at Cedars-Sinai Medical Center, Los Angeles, CA, United States, [2]Infectious and Immunologic Diseases Research Center (IIDRC), Department of Biomedical Sciences, Cedars-Sinai Medical Center, Los Angeles, CA, United States

Cardiovascular diseases (CVDs) are one of the primary causes of mortality worldwide. An optimal mitochondrial function is central to supplying tissues with high energy demand, such as the cardiovascular system. In addition to producing ATP as a power source, mitochondria are also heavily involved in adaptation to environmental stress and fine-tuning tissue functions. Mitochondrial quality control (MQC) through fission, fusion, mitophagy, and biogenesis ensures the clearance of dysfunctional mitochondria and preserves mitochondrial homeostasis in cardiovascular tissues. Furthermore, mitochondria generate reactive oxygen species (ROS), which trigger the production of pro-inflammatory cytokines and regulate cell survival. Mitochondrial dysfunction has been implicated in multiple CVDs, including ischemia-reperfusion (I/R), atherosclerosis, heart failure, cardiac hypertrophy, hypertension, diabetic and genetic cardiomyopathies, and Kawasaki Disease (KD). Thus, MQC is pivotal in promoting cardiovascular health. Here, we outline the mechanisms of MQC and discuss the current literature on mitochondrial adaptation in CVDs.

KEYWORDS

mitochondria, cardiovascular disease, mitochondrial dynamics, mitophagy, mitobiogenesis, ROS

1 Introduction

Mitochondria are central signaling hubs for eukaryotic cells involved in metabolism, inflammation, calcium regulation, and cell death (Figure 1) (Galluzzi et al., 2012; Lopez-Crisosto et al., 2017; Mehta et al., 2017; Galluzzi et al., 2018). Mitochondria are double membrane organelles consisting of an outer (OMM) and an inner mitochondrial membrane (IMM), both delimiting an intermembrane space (Figure 1). The IMM folds inwards, forming crests (cristae), which increase the surface area available for mitochondrial reactions (Protasoni and Zeviani, 2021) (Figure 1). Through the breakdown of carbohydrates and fatty acids and the production of adenosine triphosphate (ATP) via oxidative phosphorylation (OXPHOS), mitochondria are the primary source of energy for eukaryotic cells (Madeira, 2018). This process is mediated by products from the tricarboxylic acid cycle (TCA cycle) entering the mitochondrial electron transport chain (ETC), a group of proteins located in the IMM (Figure 1) (Martínez-Reyes and Chandel, 2020). Eleven ETC subunits are encoded in mitochondria's circular DNA (mtDNA) and are crucial to correctly assembling these complexes (Vercellino and Sazanov, 2022). The remaining ETC subunits are encoded by the nuclear DNA and imported into the mitochondria (Yan et al., 2019) (Figure 1). Mitochondria are also involved in ROS production and communicate with other organelles, such as the endoplasmic reticulum (ER), via channels and pores, allowing

metabolites and protein transport (Figure 1). Mitochondria are a highly dynamic network of organelles, strictly regulated by mitochondrial quality control mechanisms (MQC) (Ni et al., 2015). Due to cardiac tissues' elevated energy requirement, maintenance of cardiovascular homeostasis is heavily dependent on mitochondrial quality. Indeed, cardiomyocytes utilize the ATP that mitochondria produce from carbohydrates and fatty acid-driven oxidative phosphorylation. Therefore, mitochondrial dysfunction affects cardiomyocytes' function and contractility. Calcium levels are also central to cardiac activity. Calcium storage and regulation by mitochondria and the ER modulate cardiac function and impact electrical conduction (Lai and Qiu, 2020). Damaged or dysfunctional mitochondria are constantly eliminated via a mitochondria-specific degradation machinery, known as mitophagy (Sica et al., 2015; Harper et al., 2018). When mitophagy is dysregulated, damaged mitochondria accumulate inside cardiomyocytes, vascular smooth muscle cells (VSMCs), and endothelial cells, which can trigger inflammatory responses. Severe mitochondrial dysfunction and lack of clearance of damaged mitochondria can also initiate cell death and lead to tissue damage or loss (Hu et al., 2015; Amgalan et al., 2017; Gisterå and Hansson, 2017). Therefore, perturbations in mitochondrial quality promote the pathogenesis of CVDs, including ischemia/reperfusion, hypertension, atherosclerosis, heart failure, diabetic and genetic cardiomyopathies, and Kawasaki Disease (KD) (Bravo-San Pedro et al., 2017; Suomalainen and Battersby, 2018). Herein, we discuss several pathways related to mitochondrial metabolism and dynamics, how aged and dysfunctional mitochondria are eliminated, how new mitochondria are produced, and the importance of MQC to several CVDs.

2 Mitochondrial metabolism and function

2.1 Tricarboxylic acid (TCA) cycle

The Tricarboxylic acid (TCA) cycle (citric acid cycle or Krebs cycle) comprises a series of reactions occurring in the mitochondrial matrix, involving numerous substrates crucial to cellular metabolism (Figure 1). Metabolites of the TCA cycle regulate cellular function. They are necessary for the biosynthesis of lipids, nucleotides, and proteins (McDonnell et al., 2016), as well as chromatin modifications, DNA methylation, and post-translational protein modifications (Wellen et al., 2009; Moussaieff et al., 2015). The TCA cycle is initiated by a reaction that produces six-carbon citrate from two-carbon acetyl-CoA. Acetyl-CoA is generated from the oxidation of amino acids, glucose, fatty acids, or pyruvate (Figure 2). Acetyl-CoA combines with a four-carbon oxaloacetate molecule to yield citrate, which initiates the TCA cycle (Figure 2). Then, the oxidative decarboxylation of citrate isomer, isocitrate, forms α-ketoglutarate, a five-carbon molecule. Conversion of α-ketoglutarate to succinyl-CoA, a four-carbon molecule, yields two carbon dioxide (CO_2) and two nicotinamide adenine dinucleotide (NADH or NAD^+) molecules. Succinyl-CoA is then converted into

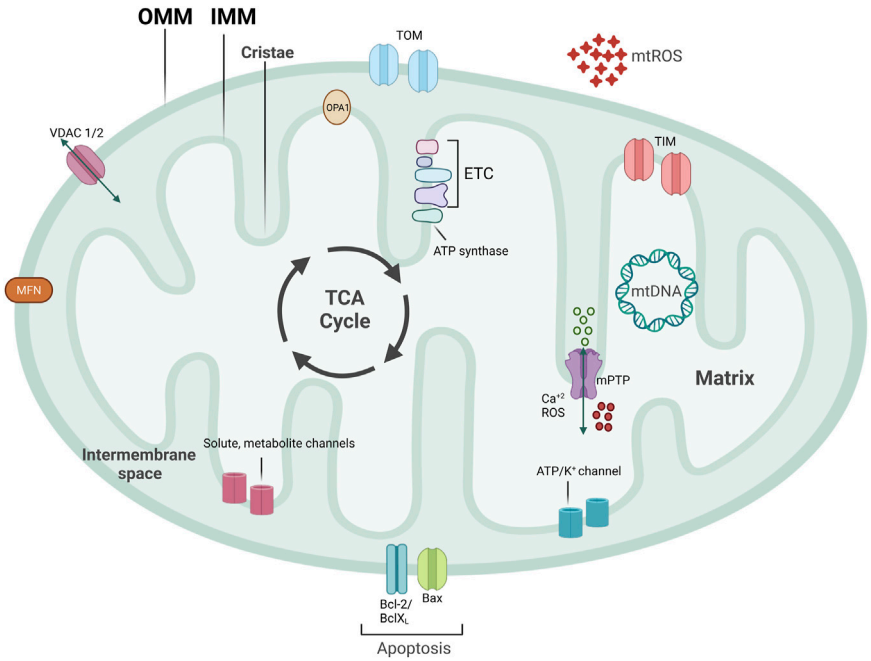

FIGURE 1
Mitochondrial structure. Mitochondria are double-membraned organelles with cristae formation. Mitochondria functioning is central for bioenergetic activities, producing ATP, an important source of ROS production. Mitochondria have several channels and pores to allow for metabolite and protein import, pivotal for inter-organelle communication. Part of ETC subunits are encoded in mitochondria's circular DNA, named mtDNA. TCA cycle that produces important electron carriers for ETC, as well as ATP, and resides on the IMM. mtROS, mitochondrial reactive oxygen species; ETC, electron transport chain; mtDNA, mitochondrial DNA; IMM, inner mitochondrial membrane; OMM, outer mitochondrial membrane; mPTP, mitochondrial permeability transition pore; VDAC, voltage-dependent anion channel.

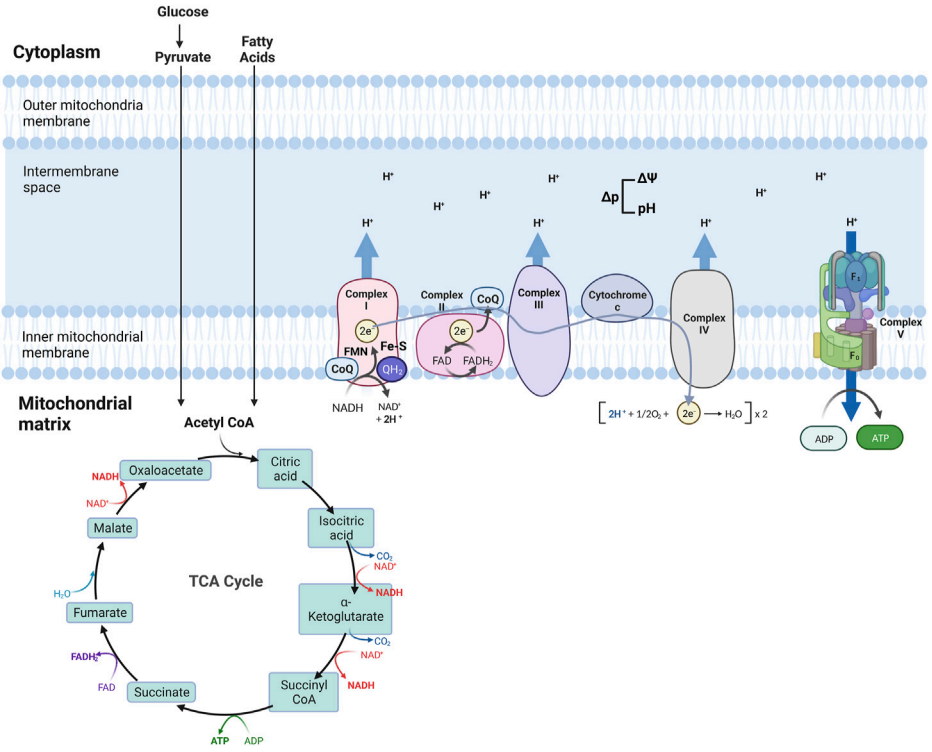

FIGURE 2
Schematic of mitochondria electron transport chain (ETC) and Oxidative phosphorylation (OXPHOS). ETC comprises four complexes that reside in the inner mitochondrial membrane that leads to the production of ATP. The TCA cycle is the source of NADH and $FADH_2$, which are required for electron transport between the complexes, finalized by the production of ATP at the last step.

succinate-producing GTP, which can later be converted into ATP (Shi and Tu, 2015; Martínez-Reyes et al., 2016). Oxidation of succinate to four-carbon fumarate transfers two hydrogens to flavin adenine dinucleotide (FAD), forming $FADH_2$ (hydroquinone form). Lastly, fumarate is converted to malate and oxaloacetate, forming acetyl-CoA to proceed with the cycle (Martínez-Reyes and Chandel, 2020) (Figure 2). As detailed in the next section, byproducts NADH and $FADH_2$ from the TCA cycle are essential electron donors for mitochondrial OXPHOS (Figure 2).

2.2 Oxidative phosphorylation (OXPHOS)

Four transmembrane complexes form the ETC. These complexes use cytochrome c and ubiquinone to transfer electrons through the IMM, where the ETC is located (Figure 2). ETC complexes form hetero-, or homodimers called super-complexes to optimize their functioning (Iwata et al., 1998; Guo et al., 2017). Together with ATP synthase, these complexes form the OXPHOS system in the mitochondrial inner membrane (Figure 2).

The ETC is fueled by electrons supplied via by-products from the TCA cycle that are transferred to oxygen (O_2), a process that also results in the formation of a proton gradient in the mitochondrial intermembrane space and the production of ATP (Martínez-Reyes et al., 2016). More specifically, byproducts of the TCA cycle, NADH and $FADH_2$, are electron sources for Complex I (NADH: ubiquinone oxidoreductase) or Complex II (succinate dehydrogenase), respectively (Figure 2). Transfer of electrons from NADH to Complex I is achieved by ubiquinone (CoQ) and requires co-factors flavin-mononucleotide (FMN) and iron-sulfur (FeS) clusters, where CoQ is reduced to ubiquinol (QH_2). Transfer of electrons to Complex I promotes the pumping of four protons into the mitochondria intermembrane space by Complex I. Electrons from $FADH_2$ are conveyed to CoQ, with the co-factor FeS, and ultimately transferred to Complex II. Electrons entering the ETC are transferred to Complex III (coenzyme Q: cytochrome c reductase) via the oxidation of QH_2 and the activity of the 2Fe-2S cluster. Electrons are then transferred to Cytochrome c, which releases two more protons into the mitochondrial intermembrane space. Cytochrome c is a mobile electron carrier that cargoes electrons from Complex III to Complex IV (cytochrome c oxidase). Complex IV comprises three subunits: I, II, and III. Subunit II interacts with reduced cytochrome c, transferring electrons to subunit I. This transfer also causes O_2 to bind to Complex IV, which is reduced to water. Complex IV pumps protons from the mitochondrial matrix; some of them go into the intermembrane space and contribute to the proton gradient, while the remaining protons are used to form water molecules. The use of O_2 for this process is known as the mitochondrial respiration (Fernie et al., 2004; Guo et al., 2018; Zhao et al., 2019; Vercellino and Sazanov, 2022).

As a result of the electron transport process, ten protons are pumped from the mitochondrial matrix into the intermembrane space where a proton gradient is built, which is the basis for the

mitochondrial membrane potential (ΔΨ) (Figure 2) (Zorova et al., 2018). As the last step of oxidative phosphorylation, ATP synthase uses the proton motive force (Δp), the combination of ΔΨ and proton concentration, to produce ATP. More specifically, Δp couples electron transport from the other complexes to the activity of ATP synthase. ATP synthase consists of an extra-membranous (F_1) and a transmembrane (F_0) domain, which functions with a rotational mechanism to produce ATP. At the last step of OXPHOS, protons pumped to the intermembrane space return to the mitochondrial matrix through F_0, dispersing the proton gradient. This allows for the rotation of ATP synthase, which induces the addition of phosphate to ADP to form ATP (Figure 2) (Reid et al., 1966; Capaldi and Aggeler, 2002; Harrington et al., 2023).

2.3 Mitochondrial reactive oxygen species (ROS) production, detoxification, and mtDNA damage

The process of electron transfer between the ETC complexes could be more efficient. Protons may leak and migrate into the mitochondrial matrix, which results in incomplete coupling of O_2 with no ATP production (Cheng et al., 2017). Electrons may also leak and exit the ETC before being converted into water from Complex I and III, resulting in reduced O_2 and increased production of reactive oxygen species (ROS) (Cheng et al., 2017). Mitochondria are a significant source of ROS, which can damage mitochondria and result in cell death when produced at high concentrations or act as a signaling molecule when made at low concentrations (Murphy et al., 2016). ROS comprises superoxide anion ($O_2^{\bullet -}$), hydroxyl radical ($^{\bullet}OH$), and hydrogen peroxide (H_2O_2). Reduction of O_2 by one electron causes the formation of $O_2^{\bullet -}$ and can be dismutated to H_2O_2 (Murphy, 2009; Cadenas, 2018). Complex II has also been shown to be involved in ROS production as it performs a reverse transfer of electrons from succinate to ubiquinone and back to Complex I, a ROS production site (Liu et al., 2002; Yankovskaya et al., 2003). Various other mitochondrial enzymes also contribute to mitochondrial ROS production. Oxidation of lipids by acyl-CoA dehydrogenase or glycerol-α-phosphate dehydrogenase yields mitochondrial ROS in the tissues (St-Pierre et al., 2002; Lambertucci et al., 2008). In addition, the TCA cycle enzymes pyruvate and α-ketoglutarate dehydrogenase also increase mitochondrial ROS production (Starkov et al., 2004).

Voltage-dependent anion channels (VDACs) are OMM proteins that form aqueous pores to exchange metabolites (Colombini et al., 1996). There are three VDAC isoforms (VDAC1, 2, and 3), which are very similar in sequence and are expressed in cardiac tissue cells but have diverse functions (Zinghirino et al., 2021). VDAC1 and 2 play a role in mitochondrial bioenergetics and mitochondrial apoptotic pathways (Ravi et al., 2021). Nuclear-encoded proteins are responsible for modulating the redox state, and VDACs can sense the imbalance in the redox state in the mitochondria (Storz et al., 2005). It has been suggested that VDAC3 is a sensor of mtROS and VDAC1 is involved in ROS-induced apoptotic pathways (Brahimi-Horn et al., 2015; Reina et al., 2016). VDAC1 also partakes in the translocation of $O_2^{\bullet -}$ to the cytosol from the mitochondria (Han et al., 2003). Furthermore, VDAC3 has also been shown as a target of ROS produced by Complex III of the ETC in mitochondria isolated from rat hearts (Bleier et al., 2015). In support of this, mice lacking VDAC3 have elevated mtROS production after being fed a high-salt diet (Zou et al., 2018). Similarly, a recent study showed that the absence of VDAC3 in human cells results in elevated ROS production and an increase in the ROS scavenging system to cope with oxidative stress, hinting at the protective effects of VDAC3 during oxidative damage. Additionally, the same study showed that VDAC3 deletion suppresses mitochondrial biogenesis (Reina et al., 2022).

$O_2^{\bullet -}$ can react with nitric oxide (NO) that produces reactive nitrogen species (RNS). NO is critical during inflammation and acts as a pro-inflammatory mediator by promoting neutrophil accumulation, downregulation of adhesion molecules, and upregulation of apoptosis at high concentrations (Albina et al., 1991; Lu et al., 1996; Shin et al., 1996). NO also boosts vasodilatation in the cardiovascular system and activates macrophages (Coleman, 2001).

Numerous enzymes manage ROS detoxification and convert these byproducts into less reactive forms (Dubois-Deruy et al., 2020). $O_2^{\bullet -}$ is very reactive and exhibits a short half-life, as it is constantly converted to H_2O_2 by mitochondrial manganese superoxide dismutase (MnSOD). H_2O_2 is less reactive and can diffuse out of the mitochondria as a cytosolic messenger (Giorgio et al., 2007; Candas and Li, 2014). Catalases detoxify H_2O_2 (Sepasi Tehrani and Moosavi-Movahedi, 2018). These Fe-heme-containing enzymes catalyze hydrogen peroxide into water and oxygen, mainly in the cytoplasmic peroxisomes (Kirkman and Gaetani, 2007). Glutathione peroxidases (GPx) and peroxiredoxins (Prx) are also involved in the breakdown of hydrogen peroxide. Glutathione is a co-factor and an electron donor for GPx. Prx is mainly located in the mitochondria, and like GPx, it converts H_2O_2 to water (Forman et al., 2009; Murphy, 2009; Forkink et al., 2010; Hossain et al., 2015).

ROS production can affect mtDNA integrity and lead to mtDNA damage. ROS production site is close to mtDNA in the IMM (Sampath, 2014). Importantly, mtDNA replication occurs in an asymmetric route, where heavy strands are left single-stranded, causing spontaneous deamination on the exposed nucleotides (Tanaka and Ozawa, 1994; Reyes et al., 1998). ROS-induced mtDNA damage causes missense mutations, deletions, or base substitutions, jeopardizing mtDNA integrity and mitochondrial functioning (Richter et al., 1988; Yakes and Van Houten, 1997). Numerous mtDNA repair pathways are used by the mitochondria, which take advantage of genomic DNA repair mechanisms (Kazak et al., 2012; Stein and Sia, 2017). The base excision repair (BER) pathway is the primary mechanism for mtDNA repair. Overall, BER eliminates oxidized, deaminated, or methylated bases, single-strand breaks, and alkylation damage (Sykora et al., 2012; Krokan and Bjørås, 2013). BER is a multi-step process that involves 1) recognition and removal of the target bases, 2) removal of abasic site, 3) end processing/gap filling, and finally, 4) DNA ligation (Jacobs and Schär, 2012). DNA glycosylases recognize and remove damaged DNA, and mitochondrial glycosylases include Uracil DNA glycosylase (UNG), 8-Oxoguanine DNA glycosylase (OGG1), and Nei-like DNA glycosylase 1 (NEIL1) (Hu et al., 2005). When damaged mtDNA accumulates, this interferes with the

OXPHOS functioning (Ma et al., 2020). Consequently, mitophagy pathways are activated to clear defective mitochondria.

2.4 mtDNA mutations

Mutations of mtDNA itself or nuclear genes that encode for mitochondrial proteins can lead to perturbations in mitochondrial functioning and cause mitochondrial diseases (Russell et al., 2020). These mutations can include point mutations and rearrangements in mtDNA. Point mutations can alter genes that encode proteins, transfer RNA (tRNA) or ribosomal RNA (rRNA) and are inherited maternally (Pereira et al., 2021). Rearrangements of mtDNA are usually deletions or duplications and can either be inherited maternally or occur *de novo* (Chinnery and Hudson, 2013). Mutations that arise on nuclear genes that encode mitochondrial proteins can be inherited as X-linked, autosomal dominant, or autosomal recessive. These mutations usually affect ETC-related nuclear genes, mitochondrial import machinery, mitochondrial translational factors, or CoQ_{10} biosynthesis (Coenen et al., 2004; MacKenzie and Payne, 2007; Potgieter et al., 2013). Various nuclear-encoded proteins are responsible for maintaining mtDNA, which controls the synthesis of mitochondria deoxyribonucleoside triphosphates (dNTPs) and mtDNA replication. Any mutations in these genes may lead to the depletion of dNTPs or deficiency in mtDNA replication, inducing a decrease in the overall levels of mtDNA (El-Hattab and Scaglia, 2013). These mutations result in disturbances in ETC assembly and functioning, ultimately leading to a deficiency in organ ATP production, especially in high-energy-demanding cardiac tissues (Chinnery, 1993). Furthermore, as the OXPHOS system is defective due to mutations of mtDNA or nuclear DNA, NADH accumulates, blocking the TCA cycle and favoring the production of lactate from pyruvate, resulting in elevated levels of lactate that interferes with proper cardiac tissue functioning (El-Hattab and Scaglia, 2013). Cells can have identical mtDNA (homoplasmy), as well as a combination of different types (heteroplasmy) (Pereira et al., 2021). Mutations that alter all copies of mtDNA are homoplasmic, whereas mutations that affect certain copies of mtDNA and cause co-existence of normal and mutant mtDNA are called heteroplasmic mutations (Ballana et al., 2008; Stefano et al., 2017). Mitochondria are randomly distributed to the daughter cells during cell division, causing heteroplasmic mtDNA mutations to be inherited by chance. Therefore, mutant mtDNAs can accumulate at different rates in different tissues. Hence, as the mutated mtDNA content increases, energy production decreases, enabling CVDs susceptibility (Saneto and Sedensky, 2013; Gonçalves, 2019).

3 Mitochondrial quality control (MQC)

MQC mechanisms are essential to maintain cellular mitochondrial homeostasis. MQC consists of a spectrum of various coordinated pathways. The primary function of MQC mechanisms is to ensure mitochondrial quality and maintain mitochondrial functions by limiting oxidative damage to mitochondria (Picca et al., 2018). ROS scavenging is a crucial first response to oxidative damage, and under physiological conditions, ROS production and detoxification are efficiently maintained (Lennicke and Cochemé, 2021). However, organelle damage can occur if ROS scavenging is insufficient to prevent a proper defense (Richter et al., 1995). ROS generation can also damage mtDNA due to the mitochondria's inadequate DNA repair system (Druzhyna et al., 2008). At this point, a secondary line of defense is necessary for the mitochondria to continue normal functioning. These MQC mechanisms can be divided into two categories: molecular or organelle-level quality control mechanisms (Ng et al., 2021). Molecular level quality control includes the activation of mitochondrial chaperones, precisely heat shock protein 60 (HSP60), HSP70, and HSP90 (Bahr et al., 2022). These chaperones ensure proper folding of newly synthesized proteins and refolding of damaged ones before they are imported into the mitochondria (Becker and Craig, 1994). When misfolded or damaged proteins accumulate, they must be degraded via the ubiquitin-proteasome system (UPS). However, if the mitochondrial damage cannot be repaired via chaperones or UPS, organelle-level quality control mechanisms come into play, as summarized below (Kwon and Ciechanover, 2017; Jin et al., 2018) (Figure 3).

3.1 Mitochondrial biogenesis (mitobiogenesis)

The transcription and replication of the nuclear and mitochondrial genome are essential to mitochondrial biogenesis (mitobiogenesis), the process of self-replication of mitochondria. mtDNA encodes for 11 polypeptides of the ETC, as well as 22 tRNA and 2 rRNA (Fernández-Silva et al., 2003). Nonetheless, most of the mitochondrial proteins are encoded in the nuclear genome and transported into the mitochondria. For this reason, replication of mitochondria relies on mtDNA and nuclear DNA transcription to promote protein and lipid synthesis. Lipids, such as phosphatidylethanolamine (PE) or cardiolipin, are necessary for mitochondrial functioning and are made in the mitochondria but require ER-derived lipids (Tatsuta et al., 2014). Therefore, importing essential proteins and lipids from the nucleus or ER is critical for mitobiogenesis.

The master regulator of mitobiogenesis is the transcriptional coregulator peroxisome proliferator-activated receptor γ (PPARγ) coactivator 1α (PGC1α), which was first identified in brown adipose tissue as a coactivator of PPARγ (Puigserver et al., 1998). Numerous transcription factors are induced by PGC1α during external stimuli, such as exercise, cold, or fasting (Wu et al., 1999; Zong et al., 2002; Nisoli et al., 2005). Nuclear respiratory factors 1 and 2 (NRF1, 2) are two of such transcription factors, increasing the expression of mitochondrial transcription factor A (TFAM), which in turn translocates to mitochondria and induces mtDNA transcription (Virbasius and Scarpulla, 1994). Mitochondria resident micro-RNAs (miRs) also fine-tune mitobiogenesis by targeting TFAM or other mitobiogenesis factors, as well as relaying signals from the nucleus to the mitochondria to replenish the mitochondrial pool when necessary (Das et al., 2012; Das et al., 2014; Roman et al., 2020; Dogan et al., 2022). During mitobiogenesis, nuclear-encoded genes necessary for mitochondrial function are transcribed in the nucleus and translated into the cytosol with a mitochondrial localization

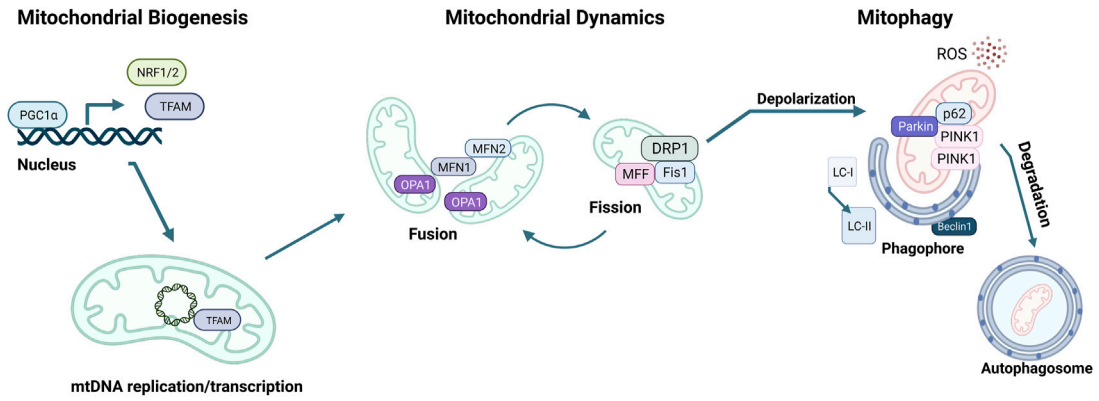

FIGURE 3
Mitochondrial quality control (MQC) mechanisms. The master regulator of mitochondrial biogenesis is PGC-1α, which induces NRF1, NRF2, and TFAM expression in the nucleus. Mitochondria life cycle includes fusion, which forms elongated mitochondrial networks, and fission, which creates fragmented mitochondria. MFN1, MFN2, and OPA1 are responsible for the membrane fusion of mitochondria, whereas DRP1, FIS1, and MFF mediate fission. Mitochondria accumulate oxidative damage during their expected lifespan or in the case of CVDs. Fission enables the fragmentation of damaged mitochondria to be separated and degraded. The elimination of damaged mitochondria is achieved via mitophagy, initiated by the accumulation of PINK1 kinase in the mitochondrial membrane, followed by the recruitment of Parkin, which targets the mitochondria to the autophagosome. p62 targets the mitochondria to the autophagosome and is eliminated during active autophagy. Assembly of the autophagosome requires Beclin1 and attachment of LC3-I onto phosphatidylethanolamine to form LC3-II.

signal. These proteins are transported to the mitochondria and are folded by mitochondrial chaperones (Wiedemann et al., 2004). Similarly, lipids are synthesized in the ER and transferred to the mitochondria during mitobiogenesis. This process involves the mitochondria-associated membranes (MAMs), which are mitochondria-ER contact sites (Gaigg et al., 1995).

Numerous external stimuli regulate PGC1α activity. Cold exposure and exercise induce PGC1α expression through β-adrenergic stimulation and cAMP response element-binding protein (cAMP/CREB) signaling (Wu et al., 1999; Baar et al., 2002). Moreover, AMPK activation in response to exercise also boosts PGC1α expression (Little et al., 2010). Posttranslational modifications are essential for the PGC1α activity (Miller et al., 2019). It has been shown that AMPK phosphorylates PGC1α on T177 and S538 in skeletal muscle (Jäger et al., 2007). Another crucial posttranslational modification on PGC1α is done by the NAD^+-dependent deacetylase Sirtuin 1 (SIRT1). Deacetylation and activation of PGC1α by SIRT1 are essential, as NAD^+ levels are highly dependent on AMPK activity. Therefore, in addition to its role in mitobiogenesis, PGC1α conjugates cellular energy metabolism, redox state, and mitochondrial activity (Gerhart-Hines et al., 2007; Coste et al., 2008; Cantó et al., 2009).

3.2 Mitochondrial fission-fusion

The mitochondrial network is highly dynamic, constantly remodeling through fission and fusion to decrease stress and replace damaged components (Parra et al., 2011; Chan, 2020). Fusion of two mitochondria is driven by dynamin-related GTPases mitofusin1 and 2 (MFN1, MFN2) on the OMM surface and optic atrophy protein 1 (OPA1) and cardiolipin on the IMM (Chen et al., 2003; Olichon et al., 2007; Paradies et al., 2019) (Figure 3). MFN1 also participates in ER-associated degradation (ERAD) through the degradation of damaged mitochondria via polyubiquitination by the E3 ubiquitin ligase Parkin (Picca et al., 2018). Mitochondrial fusion allows for the fusion of two mitochondria that are in close proximity to share mtDNA, metabolites, and enzymes. Fusion of the OMM requires homo- and heterodimerization of MFN1 and MFN2 (Figure 3) (Ishihara et al., 2004; Chen and Chan, 2009; Hall et al., 2014). OPA1 plays a role in the fusion of the IMM while preserving the cristae structure (Malka et al., 2005; Song et al., 2007). This fusion process sustains the mitochondrial membrane and its permeability to enhance protection from oxidative damage.

Damaged mitochondria can also undergo fission, where one mitochondrion divides into two mitochondria (Chen and Chan, 2009; Ong and Hausenloy, 2010; Elgass et al., 2013). Fission is orchestrated by GTPase dynamin-related protein 1 (DRP1), mitochondrial fission one protein (FIS1), and mitochondrial fission factor (MFF). FIS1 inhibits mitochondrial fusion and acts as a receptor for the binding of DRP1 to the OMM. Once recruited, DRP1 triggers cleavage of mitochondria via interacting with FIS1 and MFF (Palmer et al., 2011; Onoue et al., 2013; Otera et al., 2013; Atkins et al., 2016). Splitting off damaged mitochondria through fission preserves the healthy pool of mitochondria, optimal OXPHOS functioning, and efficient allocation of mitochondrial materials (Quiles and Gustafsson Å, 2022).

A balance between mitochondrial fission and fusion is critical for maintaining optimal mitochondria functioning at homeostasis or during pathological conditions, especially in CVDs. Clearance of damaged mitochondria is central to the control of mitochondrial quality. It is achieved through mitophagy, a process linked to fission since fragmented mitochondria are degraded via the autophagolysosomes (Zaffagnini and Martens, 2016). Mitochondrial fission occurs on the MAMs, where DRP1 also localizes and promotes nucleation of mitochondrial fission. ER

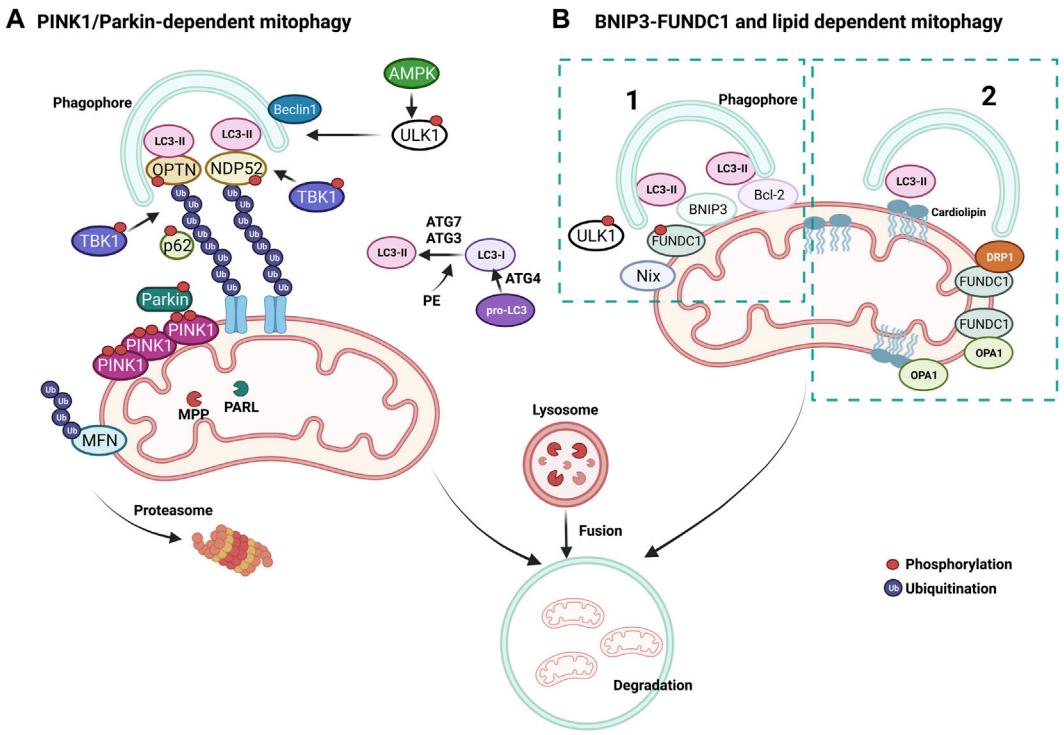

FIGURE 4
Mechanisms of mitophagy. **(A)** PINK1/Parkin-dependent mitophagy. PINK1 accumulates on damaged mitochondria and recruits Parkin to promote the ubiquitination of OMM proteins. Poly-ubiquitin chains provide an eat me signal to initiate autophagy. TBK1 phosphorylates OPTN and NDP52 to induce clearance of damaged mitochondria. **(B)** Parkin-independent mitophagy pathways, (1) BNIP3/FUNDC1 mediated and (2) lipid-mediated mitophagy. Mitophagy receptors BNIP3 and FUNDC1 favor mitochondrial fission via DRP1 interaction and OPA1 release.

tubules can also wrap around the mitochondria and cause constriction of mitochondrial membranes during fission (Friedman et al., 2011; Yang and Yang, 2013).

3.3 Mitochondrial clearance via autophagy/mitophagy

A pivotal mechanism of MQC is a mitochondria-specific autophagy process named mitophagy (Figure 4). Clearance of mitochondria by mitophagy is indispensable during cellular differentiation, as well as for tissues that require high energy, such as the cardiovascular system (McWilliams et al., 2018). Mitophagy is needed to overcome stress in pathological conditions, and evidence from multiple studies suggests that a deficit in mitophagy mechanisms contributes to the progression of CVDs (Tong et al., 2019; Tan et al., 2021). Briefly, the elimination of mitochondria by mitophagy requires the autophagy receptors to load mitochondrion to the autophagosome through light chain-3 (LC3) (Figures 3, 4). Mitochondria are then engulfed by the autophagosome, which merges with a lysosome to degrade its contents through the lysosomal enzymatic activity (Rüb et al., 2017). Mitophagy can be ubiquitin-dependent or receptor-dependent. Ubiquitin-dependent mitophagy mainly includes PINK1/Parkin-dependent pathways (Figure 4A). Receptor-dependent mitophagy includes Bcl-2 and adenovirus E1B19kDa-interacting protein 3 (BNIP3), FUNDC1, and lipid-dependent mitophagy pathways (Figure 4B).

3.3.1 PINK1/Parkin-dependent mitophagy

During basal conditions, serine/threonine kinase PTEN-induced kinase 1 (PINK1) is constantly imported into the mitochondria as it bears a mitochondrial target signal (Lazarou et al., 2012). Once imported, PINK1 is cleaved by matrix processing peptidases, mitochondrial processing peptidase (MPP), and presenilins-associated rhomboid-like protein (PARL) to eliminate the mitochondrial target signal and its hydrophobic transmembrane helix within the transmembrane domain. After processing, PINK1 is released into the cytoplasm, where the UPS constantly degrades it. When mitochondrial damage occurs, PINK1 cannot be transported back to the IMM and accumulates on the OMM, unable to be cleaved by PARL, forming homodimers. Phosphorylation of PINK1 on S228 and S402 is required for its activation and engages Parkin to the OMM, inducing mitophagy (Lazarou et al., 2012; Okatsu et al., 2013; Yamano and Youle, 2013). Interaction of Parkin with PINK1 causes conformational changes that allow for its opening and phosphorylation on S65 by PINK1, simultaneously activating its E3 ubiquitin ligase activity (Ordureau et al., 2014; Pickrell and Youle, 2015) (Figure 4A). As a mechanism that further augments mitophagy, Parkin-mediated ubiquitination of OMM proteins serves as substrates for PINK1, which consequently recruits more Parkin (Nguyen et al., 2016). MFN2 can also be phosphorylated by PINK1 on the OMM and ubiquitinated by Parkin to prevent the fusion of damaged mitochondria with healthy ones (Chen et al., 2013) (Figure 4A). Mitochondria undergoing mitophagy are isolated through the interaction of

autophagy-related gene (ATG) and LC3 proteins with a phagophore formation. First, the carboxyl-terminal region of pro-LC3 is processed by ATG4, a cysteine protease (Figure 4A). This results in glycine residues being exposed and the formation of LC3-I. Then, phosphatidylethanolamine (PE) binds to LC3-I via ATG7 and ATG3, forming LC-II as the first ubiquitin-like reaction. Following this reaction, together with ATG10, ATG7 deposits ATG12 to ATG5, which assembles the ATG12-5 complex. This complex later binds to ATG16, which endorses the recruitment of ATG8 with PE on the autophagosomes. Damaged mitochondria are identified through their LC3-interacting region (LIR), which ultimately leads to their engulfment by the autophagosome (Tanida et al., 2004; Nakatogawa, 2013; Dooley et al., 2014). Adaptor proteins sequestosome 1 (p62/SQSTM1), nuclear dot protein 52kDa (NDP52), optineurin (OPTN), and Tax-binding protein-1 (TAX1BP1) are crucial during the tethering of damaged mitochondria to the autophagosomal membranes via recognition of ubiquitinated proteins (Villa et al., 2018). The OMM proteins are eliminated when mitochondrial adaptor proteins contact LC3, which binds to the autophagosomal membranes. OPTN and NDP52 are found on the OMM of damaged mitochondria (Figure 4A). TANK-binding kinase 1 (TBK1) is responsible for the phosphorylation of OPTN and p62 at S177 and S403, respectively. These phosphorylations induce their tethering with ubiquitinated sites and LC3 (Figure 4A). Consecutively, OPTN and NDP52 induce autophagy via recruiting autophagy-related unc-51-like autophagy-activating kinase 1 (ULK1), which is phosphorylated and activated by AMP-activated protein kinase (AMPK) on S555 (Egan et al., 2011). Next, ULK1 recruits the Beclin-1 complex, which promotes the nucleation of phagophores, making autophagosome formation more efficient around the damaged mitochondria (Russell et al., 2013). This final step fully isolates targeted mitochondria inside the autophagosomes and triggers their fusion with lysosomes to form autolysosomes, leading to the degradation of the targeted mitochondria (Narendra et al., 2010; Weil et al., 2018; Yamano et al., 2020). Activation of mitophagy is not strictly dependent on AMPK activation, whereas ULK1 deficiency impairs PINK1/Parkin-dependent mitophagy (Vargas et al., 2019).

3.3.2 BNIP3 and FUNDC1-dependent mitophagy

Bcl-2, BNIP3, and BNIP3-like (Nix) are all part of the Bcl-2 family of proteins and are constitutively expressed on the OMM (Ma et al., 2020) (Figure 4B). They have a prominent role in apoptosis but are also essential mitophagy receptors. These receptors are bound to the OMM and mainly interact with LC3 via the LIR motif to facilitate mitophagy, independent of the ubiquitin (Gustafsson Å and Dorn, 2019). It has been shown that BNIP3 and Nix are involved in the elimination of mitochondria in adult heart tissues (Lampert et al., 2019) and that hypoxic conditions can upregulate BNIP3 (Gálvez et al., 2006). Another mitophagy receptor, the FUN14 domain containing 1 (FUNDC1), mediates mitophagy (Figure 4B). This receptor is also relevant to hypoxia and ischemia, as hypoxic stimuli are linked with FUNDC1 dephosphorylation on its LIR via Phosphoglycerate mutase family Member 5 (PGAM5) to promote its binding with LC3 (Ren et al., 2020; Xiao et al., 2020). ULK1 is also known to phosphorylate FUNDC1 on its LIR motif to favor interaction with LC3 during mitophagy (Chen et al., 2014; Wu et al., 2014). Intriguingly, FUNDC1 has also been shown to interact with OPA1 and DRP1 to regulate mitochondrial dynamics during mitochondrial stress (Chen M. et al., 2016).

3.3.3 Lipid-dependent mitophagy

Lipids, such as ceramide or cardiolipin, which can prompt mitophagy with their LIR motif, are present in the OMM. Ceramide is a sphingolipid synthesized by ceramide synthase (CeS). During ER stress, ceramides are translocated from the ER and accumulate on the OMM, triggering mitophagy (Chu et al., 2013). Accumulated ceramides on the OMM can bind LC3 through its ceramide-binding domain and promote the binding of Beclin1. Ceramide-mediated mitophagy also relies on DRP1, which initiates the recognition of ceramide in the OMM by the autophagolysosomes (Sentelle et al., 2012; Antón et al., 2016) (Figure 4B). Importantly, ceramides can build a channel with active BCL2-associated X protein (BAX) that allows the release of cytochrome c to initiate apoptosis. Another important lipid in mitophagy, cardiolipin, is a phospholipid synthesized by cardiolipin synthase (CRD1) in the mitochondria. Cardiolipin (CL) is present on mitochondrial membranes and cristae structures and is primarily found in the IMM (Daum, 1985). CL binds to OPA1 in physiological conditions to regulate OPA1 assembly during mitochondrial fusion and interacts with LC3 during mitochondrial stress (Liu et al., 2003). During mitochondrial damage, CL is transported from the IMM to the OMM (Chu et al., 2013). This movement allows CL to be exposed to the cytosol, bind to LC3, and serve as a recruitment site for adaptor proteins during mitophagy (Chu et al., 2013). Exposed CL preferentially associates with Beclin1 on the OMM during mitophagy and is crucial for phagophore formation (Huang et al., 2012). Notably, pro-IL-1α directly binds to CL in lipopolysaccharide (LPS)-treated macrophages through an LC3 binding domain while blocking mitophagy and activating NLRP3 inflammasome, further supporting the importance of CL in mitochondrial homeostasis (Dagvadorj et al., 2021).

3.4 Mitochondrial communication with other organelles

Mitochondrial networks cannot function separately from other subcellular compartments and rely heavily on inter-organelle communication. Mitochondria continuously coordinate with the nucleus, the ER, and other vesicular organelles (Lin et al., 2020). Importantly, inter-organelle communication of mitochondria and cytosolic organelles is crucial in the development and pathogenesis of several diseases. Most of the mitochondrial proteins are encoded in the nucleus and must be translocated into the mitochondria via transmembrane complexes (Pfanner et al., 2019). As mitochondria are self-monitoring organelles, any perturbations trigger retrograde signaling from mitochondria to the nucleus or other organelles to cope with the stress and reestablish proper mitochondrial functioning (Chowdhury et al., 2020; Vizioli et al., 2020; Booth et al., 2021).

3.4.1 Mitochondrial unfolded protein response (UPR^{mt})

When mitochondrial protein import is dysfunctional, a signal from the mitochondria, called $UPR^{mt,}$ is initiated and relayed to the

nucleus. This signal activates the required transcription factors to cope with stress and induces a repair mechanism to normalize the mitochondrial protein import (Shpilka and Haynes, 2018). UPR^{mt} aims to optimize metabolism by blocking oxidative phosphorylation and the TCA cycle, decreasing the mitochondrial load and ultimately alleviating mitochondrial stress. Simultaneously, the expression of genes responsible for glycolysis and amino acid metabolism is augmented to provide alternative energy resources (Anzell et al., 2018). Aside from switching the reliance on specific energy resources, UPR^{mt} also promotes the expression of mitochondrial chaperones, anti-oxidative proteins, and proteases to cope with the accumulation of dysfunctional proteins (Zhu L. et al., 2021). This decreases the mitochondrial burden while enabling the proper processing of damaged mitochondrial proteins (Quirós et al., 2016). Impairment of OXPHOS machinery, mtDNA damage, disruption of mitochondrial protein synthesis, accumulation of misfolded or unfolded proteins in the mitochondria, or the buildup of ROS causes mitochondrial dysfunction. These events trigger UPR^{mt} (Qureshi et al., 2017). It has been shown that during mammalian UPR^{mt}, transcription factors C/EBP homologous protein (CHOP), activating transcription factor 4 (ATF4), and ATF5 are activated, which are also involved in the unfolded protein response of the ER to alleviate ER stress caused by the accumulation of unfolded or misfolded proteins (Shpilka and Haynes, 2018; Yildirim et al., 2022). Activation of the kinases general control non-derepressible-2 kinase (GCN2), protein kinase RNA (PKR), PKR-like endoplasmic reticulum kinase (PERK), and heme-regulated inhibitor kinase (HRI) controls the phosphorylation of eukaryotic translation initiation factor 2 subunit 1 (eIF2**α**), which is the major player during organelle stress (Teske et al., 2013). Activated eIF2**α** inhibits global protein translation to reduce organelle stress, enhancing the expression of specific transcription factors like CHOP, ATF4, and ATF5. These transcription factors promote the expression of chaperones and proteases to cope with the UPR^{mt}. Notably, the expression of ROS detoxifying enzymes, mitobiogenesis machinery, and mitochondrial import proteins are also enhanced to favor mitochondrial remodeling during stress (Qureshi et al., 2017).

3.4.2 Calcium (Ca^{2+}) signaling

Mitochondrial stress, which stems from the loss of mitochondrial membrane potential, releases calcium (Ca^{2+}) from the mitochondria to the cytoplasm through voltage-dependent L-type Ca^{2+} channels. This increase in cytosolic Ca^{2+} triggers more Ca^{2+} to be released from the sarcoplasmic reticulum through the ryanodine receptor 2 (RYR2). Consequently, Ca^{2+} is cleared away from the cytoplasm via sarcoplasmic or ER resident ATPase (SERCA) family proteins, as well as solute carrier family 8 member A1 (SLC8A1) (Kho et al., 2012). During basal conditions, Ca^{2+} enters the mitochondria via the calcium uniporter protein (MCU) (Baughman et al., 2011). In addition, Ca^{2+} release occurs through the Ca^{2+} antiporter SLC8B1. Transient increases in Ca^{2+} levels can aid OXPHOS machinery. However, during mitochondrial membrane potential loss, free cytosolic Ca^{2+} activates calcineurin. In turn, the nuclear factor-κB (NF-κB) and nuclear factor of activated T cells (NFATC) are activated and translocated to the nucleus. This translocation stimulates the expression of genes responsible for Ca^{2+} storage or transport (Liu et al., 2017). Increased Ca^{2+} levels can activate various kinases like calcium/calmodulin-dependent protein kinase IV (CAMKIV), Ca^{2+}-dependent protein kinase C, c-Jun N-terminal kinases (JNK), and p38 MAPK. These kinases fine-tune the mitochondrial adaptation to Ca^{2+} level fluctuations and metabolism, as well as cell proliferation and glucose metabolism (Giorgi et al., 2018).

3.4.3 Intrinsic apoptosis pathway

During severe unresolved stress, like calcium overload, excessive ROS, or mtDNA damage, intrinsic apoptosis is initiated as mitochondrial homeostasis is jeopardized (Brumatti et al., 2010). Programmed cell death is orchestrated by pro-apoptotic proteins of the B cell lymphoma (BCL) 2 family. When apoptosis is triggered, BCL-associated X (BAX) and Bcl2 homologous antagonist/killer (BAK) are incorporated into the OMM and oligomerize, resulting in a pore formation on the mitochondria. This pore increases membrane permeability and promotes the release of pro-apoptotic factors (Lomonosova and Chinnadurai, 2008). Under physiological conditions, BAX is inactive and shuttles between the cytosol and the OMM, whereas BAK resides on the OMM and interacts with VDAC2 (Cheng et al., 2003; Schellenberg et al., 2013). Under apoptotic stimuli, BAX is no longer shuttled to the cytosol and together with BAK, gets activated via the pro-apoptotic Bcl2 homology-3 (BH3) domain-containing factors, BCL2 binding component 3 (also known as p53-upregulated modulator of apoptosis, PUMA), BCL2-interacting mediator of cell death (BIM), phorbol-12-myristate-13-acetate-induced protein 1 (NOXA) and BH3-interacting domain death agonist (BID) (Kuwana et al., 2005). Multiple pro-survival proteins counteract with the pro-apoptotic factors to reduce the permeabilization of the OMM, such as BCL2, BCL2 like 1 (BCL2L1 also known as BCL-XL), myeloid cell leukemia 1 (MCL1), BCL2 like 2 (BCL2L2, also known as BCL-W), and BCL2 related protein A1 (BCL2A1) (Moldoveanu et al., 2014). These factors reside on the OMM or ER and inhibit the binding of pro-apoptotic proteins (Czabotar et al., 2014). If the permeabilization of OMM is maintained, cytochrome c is released to initiate caspase-independent cell death. Notably, the release of cytochrome c causes apoptosome formation, a multi-protein structure composed of apoptotic protease-activating factor-1 (APAF-1), deoxyATP (dATP), and pro-caspase-9, where pro-caspase-9 gets activated (Chen et al., 2011). Consequently, caspases 3 and 7 are also cleaved and activated to promote cell death (Li et al., 1997; McArthur et al., 2018).

3.5 Mitochondria and inflammation

Mitochondrial apoptosis can produce type I interferon when caspases are inhibited (Rongvaux et al., 2014; White et al., 2014). In this context, mtDNA is released to the cytosol as a damage-associated molecular pattern (DAMP) during BAX/BAK-mediated pore formation and apoptosis (Cosentino et al., 2022). The presence of any DNA in the cytoplasm (e.g., pathogenic, nuclear, or mitochondrial) triggers a signal to activate 2′3′-cyclic GMP-AMP (cGAMP) synthase (cGAS), which detects cytosolic DNA. This detection allows cGAS dimerization and production of second messenger cGAMP to relay the message to and activate the stimulator of interferon genes (STING) (Diner et al., 2013; Sun et al., 2013). ER resident STING then shuttles to

TABLE 1 Mitochondrial phenotype in CVDs. Overview of mitochondrial impairment during multiple CVDs.

Ischemia/ Reperfusion	Hypertension	Atherosclerosis	Cardiac hypertrophy/ heart failure	Diabetic cardiomyopathy	Genetic cardiomyopathies	Kawasaki disease
• Mitochondrial fragmentation	• Decreased endothelial NO levels	• Increased mitochondrial permeability	• Decreased mitochondrial mass	• Increased FA in cardiomyocytes	• mtDNA mutations in genes encoding for subunits of assembly factors Complex I, II or IV	• Increased NLRP3 inflammasome activation and IL1-β production
• Loss of mitochondrial membrane potential	• Elevated oxidative stress and mtROS	• Elevated mtROS	• Low ATP production	• Elevated mtROS production	• Impaired NADH-linked respiration	• Impaired clearance of damaged mitochondria *in vivo*
• Low ATP production	• ETC dysfunction	• NLRP3 inflammasome formation and impaired mitophagy	• Mitochondrial fragmentation	• Increased IMM potential and oxidative damage	• Downregulation in expression of genes related to ATP synthesis	• Decreased expression of autophagy-mitophagy related genes
• Increased mitochondrial membrane permeability	• Enhanced mitophagy during Ang-II induced model as protective mechanism	• Accumulation of damaged mitochondria	• Reduced ETC Complex I and IV activity	• Impaired mitochondrial dynamics and mitophagy	• Downregulation in mitochondrial mass and ETC super-complex formation	• Increased platelet subpopulations with different mitochondrial membrane potentials
• Ca^{2+} flux into mitochondria	• Reduced mitochondrial size		• Impaired mtDNA replication	• ETC dysfunction	• Dysregulated Ca^{2+} signaling	
• Increased mtROS						
• Impaired mitophagy						

mtROS, mitochondrial reactive oxygen species; ETC, electron transport chain; mtDNA, mitochondrial DNA; FA, fatty acid; IMM, inner mitochondrial membrane.

Golgi, activates TBK1, and gets phosphorylated by TBK1 (Zhang C. et al., 2019). Interferon regulatory factor 3 (IRF3) phosphorylation by active TBK1 promotes its dimerization and transport to the nucleus, which activates interferons and other cytokines (Tanaka and Chen, 2012). Oxidized mtDNA can exit the mitochondria through mPTP and VDAC, where oxidation promotes its fragmentation (Xian et al., 2022). In the cytosol, mtDNA fragments interact with NLRP3 to induce inflammasome activation and STING phosphorylation on S365, a pre-requisite for IRF3 activation (Chen Q. et al., 2016). Similarly, when released to the cytosol during programmed cell death, oxidized mtDNA binds to the NLRP3 inflammasome and activates it (Shimada et al., 2012). It has been recently shown that glycolytic enzyme Hexokinase 2 dissociation from VDAC on the OMM is essential for NLRP3 inflammasome activation. This dissociation results in Ca^{2+} uptake by mitochondria released from the ER and pore formation by VDAC oligomerization, allowing protein and mtDNA to exit from the mitochondria (Baik et al., 2023). Consequently, NLRP3 assembly is promoted and crucial during inflammatory responses.

Pathogenic or mitochondrial dsRNA in the cytoplasm is detected by the retinoic acid-inducible gene I (RIG-I) as well as melanoma differentiation-associated protein 5 (MDA5), which enables activation and aggregation of mitochondrial antiviral signaling protein (MAVS) on the OMM (Reikine et al., 2014). Accumulation of MAVS promotes IRF3 activation and stimulates the expression of antiviral response genes in the nucleus (Hou et al., 2011). Furthermore, bacterial infection can also activate an innate immune response that involves mitochondria. LPS or glycans on the bacterial wall can induce immune responses via ubiquitylation. This allows for the formation of pro-inflammatory ubiquitin linkages with the mitochondria and causes OMM permeabilization, enabling the formation of endolysosomes (Hamacher-Brady et al., 2014).

4 Mitochondrial dysfunction and CVDs

Mitochondrial dysfunction has been involved in the development of several CVDs (Killackey et al., 2020). CVDs are often associated with defective ETC machinery, excessive ROS production, impaired energetics, and MQC, as well as abnormal Ca^{2+} homeostasis (Forte et al., 2021). Notably, the dysregulation of proteins responsible for mitochondrial dynamics, mitophagy, or mitobiogenesis is closely linked to the advancement of CVDs (Chehaitly et al., 2022). Hence, understanding the contribution of mitochondrial health and normal functions to CVDs is crucial to develop novel and more efficient therapeutic approaches for these conditions. Here, we discuss various CVDs and the implications of mitochondrial dysfunction in this context (Table 1).

4.1 Ischemia/reperfusion (I/R) injury

Blood flow restoration of ischemic tissues or areas results in functional and structural tissue alterations, known as

ischemia-reperfusion (I/R) injury. I/R injury usually stems from occlusion of coronary vessels, leading to tissue hypoxia and a deficiency in ATP levels (Peoples et al., 2019).

Mitochondria respond to cardiac tissue I/R injury, and a cascade of mitochondrial fragmentation and cell death, associated with elevated oxidative stress and loss of mitochondrial membrane potential is initiated upon reperfusion (Murphy and Steenbergen, 2008). Oxygen deprivation immediately results in mitochondrial dysfunction since heart tissues rely heavily on OXPHOS for their energy demand. *In vitro*, hypoxia/reoxygenation of cardiomyocytes revealed that these cells exhibit less mitochondrial fusion, lower ATP production, and higher membrane permeability (Liu and Hajnóczky, 2011). Furthermore, overexpression of mitochondrial fusion protein MFN2 or DRP1-dependent blockade of mitochondrial fission increased cell survival (Jahani-Asl et al., 2007). Mice overexpressing OPA1 display less severe I/R injury with better mitochondrial cristae remodeling (Varanita et al., 2015). Similarly, reduced OPA1 levels indicating a decrease in mitochondrial fusion during I/R injury in mice were rescued by melatonin treatment, which promotes AMPK signaling and diminishes caspase-9-dependent apoptosis (Zhang Y. et al., 2019). Supporting these findings, melatonin treatment also increased the expression of SIRT3 and the activity of the ROS-metabolizing enzyme SOD2 in cardiomyocytes during I/R by blocking the mitochondrial fission (Bai et al., 2021). Reduced infarct size is also observed in rats when mitochondrial fusion is promoted pharmacologically (Maneechote et al., 2019). Supporting these notions, cardiac-specific MFN1 knock-out mice are protected against excessive ROS production as these mice have a delayed mitochondrial permeability transition pore (mPTP) opening, resulting in increased cell survival (Papanicolaou et al., 2012). I/R injury also causes an increase in oxidative stress and promotes Ca^{2+} flux into the mitochondria, allowing a dysfunctional electrochemical gradient of IMM and impairing the ETC activity (Halestrap, 1999). Excess Ca^{2+} inside the mitochondria and elevated ROS levels cause the opening of the mPTP and render permeability of the IMM, resulting in depolarization, membrane potential loss, and cell death (Kwong and Molkentin, 2015). Similarly, overflow of Ca^{2+} into mitochondria due to mitochondrial calcium uniporter (MCU) activation is fundamental to I/R injury. Overexpression of Histidine triad nucleotide-binding 2 (HINT2) blocks MCU activity and alleviates Ca^{+2} burden and fragmentation of mitochondria in mice during I/R injury (Li et al., 2021).

Clearance of defective mitochondria by mitophagy is beneficial during I/R injury. Evidence indicates defective mitophagy, dysfunctional mitochondria, and myocardial impairment after I/R injury in DRP1 knock-out mice (Ikeda et al., 2015). Similarly, Parkin knock-out mice have exacerbated infarct size and dysfunctional mitochondria with impaired mitophagy, suggesting that by clearing defective mitochondria, mitophagy is beneficial during I/R injury (Kubli et al., 2013). Also, autophagy proteins such as Beclin 1, BNIP3, and FUNDC1 are implicated in the I/R injury (Georgakopoulos et al., 2017). FUNDC1 protects the heart by promoting mitophagy to eliminate damaged or non-functional mitochondria (Zhang et al., 2017). Furthermore, in a hypoxia model, the overexpression of necroptosis modulator receptor-interacting protein 3 (RIPK3) blocks the AMPK pathway and inhibits Parkin-dependent mitophagy in cardiomyocytes, leading to cardiomyocyte necroptosis and exacerbated cardiac damage (Zhu P. et al., 2021).

Data from FUNDC1 knock-out mice showed that this mitophagy factor regulates MQC, is essential for platelet activation, and ultimately decreases heart I/R injury (Zhang et al., 2016). In addition, an anti-diabetes drug, empagliflozin, has been reported to promote AMPK1/ULK1/FUNDC1-dependent mitophagy and attenuated mitochondrial dysfunction in both *in vitro* and *in vivo* I/R injury models (Cai et al., 2022). Upregulation of mitophagy and mitobiogenesis is observed in human cardiac tissues after cardiopulmonary bypass surgery, indicating that a balance between these two arms of MQC is crucial during surgery-induced I/R injury (Andres et al., 2017). These findings provide insight into how mechanisms of MQC regulate tissue homeostasis during I/R injury. However, therapeutic strategies to fine-tune mitochondrial dynamics during I/R injury need further investigation.

4.2 Hypertension

Hypertension, characterized by increased blood pressure and a decline in vascular function, is associated with inflammation, endothelial impairment, and mitochondrial dysfunction (Barki-Harrington et al., 2004; Lahera et al., 2017). During hypertension, oxidative damage in mitochondria is triggered by the activation of Angiotensin (Ang) II, which decreases endothelial NO levels and exacerbates vascular oxidative stress. ROS production increases during hypertension due to Ang II-mediated protein kinase-C activity and excess production of $O_2\bullet^-$ and H_2O_2 (Doughan et al., 2008). Excessive ROS production may lead to mtDNA mutations and ETC machinery dysfunction, both contributing to hypertension progression (Griendling et al., 2021).

MQC also plays a pivotal role in the development of angiogenic function. It has been shown that the knock-down of MFN1, a protein involved in mitochondrial fusion, results in a less angiogenic response of endothelial cells to vascular endothelial growth factor (VEGF), induces endothelial NO synthase (eNOS) and decreases mitochondrial membrane potential (Lugus et al., 2011). Moreover, inhibition of mitochondrial fission by blocking DRP1 activity results in a blockade of apoptosis in an Ang II hypertensive rat model. In this context, SIRT1 is degraded by Ang II, resulting in p53 acetylation, which promotes DRP1 expression and cell apoptosis (Qi et al., 2018). Furthermore, genetic deletion of SIRT3 in mice leads to hypertension by inducing endothelial dysfunction, vascular inflammation, and hypertrophy. In contrast, global SIRT3 overexpression blocks Ang II-induced hypertension (Dikalova et al., 2020). Elevated FUNDC1-mediated mitophagy during hypoxic pulmonary hypertension induces hypoxia-inducible factor 1α (HIF1**α**) and pulmonary artery smooth muscle cell proliferation, leading to pulmonary vascular remodeling (Liu et al., 2022).

Mitophagy acts as a protective mechanism during hypertension and enhanced ATG-5-mediated mitophagy during Ang II-induced hypertension results in reduced levels of ROS and inflammation (Pan et al., 2012). Mitochondrial mass and structure are also affected

during hypertension. Reduced mitochondrial size and osmotic swelling disrupt the mitochondrial OXPHOS efficiency (Ritz and Berrut, 2005). Cristae structure and ETC stability of mitochondria are jeopardized during hypertension, as it has been shown that there is a loss of CL, a crucial phospholipid for the membrane structure (Cogliati et al., 2013).

4.3 Atherosclerosis

Atherosclerosis is a progressive cardiovascular disease resulting in the formation of plaques containing inflammatory cells, the narrowing of arteries, and decreased blood flow, increasing the risks of cardiovascular complications, such as myocardial infarction and stroke. Plaque formation occurs via low-density lipoprotein (LDL) uptake in the arterial wall, leading to immune cell infiltration, inflammation, calcification, and vascular smooth muscle (VSMC) migration into the plaque (Gimbrone and García-Cardeña, 2016). Accumulation of oxidized LDL in the arterial wall can interfere with the proper functioning of mitochondrial respiration dynamics, cause the opening of mPTP and increase mitochondrial permeabilization, and promote ROS production (Khwaja et al., 2021). This eventually results in endothelial cell apoptosis and accelerates atherosclerosis. In addition, excess ROS production and mitochondrial dysfunction during atherosclerosis have been shown to activate NLRP3 inflammasome formation and boosts mitophagy (Jin Y. et al., 2022). Of note, loss of OGG1 induces oxidative mtDNA damage and subsequent NLRP3 inflammasome activation, exacerbating atherosclerosis in mice (Tumurkhuu et al., 2016). Importantly, depletion of an abundant cholesterol biosynthetic intermediate in coronary lesions, desmosterol, results in mtROS accumulation and NLRP3 inflammasome activation in macrophages, favoring atherosclerotic plaque formation (Zhang X. et al., 2021).

VSMCs can be activated by the platelet-derived growth factor (PDGF) during atherosclerotic plaque formation. MFN2 is less expressed in the atherosclerotic plaques, which favors mitochondrial fission. Inhibition of mitochondrial fission decreases VSMCs proliferation (Salabei and Hill, 2013). Similarly, inhibition of DRP1, a mitochondrial fission regulator, decreased endothelial impairment and atherosclerosis progression in apolipoprotein E (ApoE) knock-out mice, as well as VSMCs calcification (Rogers et al., 2017; Wang et al., 2017). Accumulation of p62 and LC3-II has been reported in cells from atherosclerotic plaques, which indicates impaired autophagy/mitophagy (Sergin et al., 2016). Decreased LC3-II levels are detected in patients with unstable atherosclerotic plaques, leading to reduced autophagy/mitophagy and defective clearance of damaged mitochondria and cell death in the arterial wall (Swaminathan et al., 2014). Supporting these findings, deleting the ATG-5 gene in mice, which is involved in autophagy, results in increased production of IL-1β, impaired cholesterol clearance, and increased atherosclerotic plaque formation (Razani et al., 2012). SIRT1 inhibition accelerates mouse atherosclerosis progression through the increased acetylation of ATG5 (Yang et al., 2017). Similarly, VSMC-specific deletion of ATG7 in *ApoE*$^{-/-}$ mice leads to impaired autophagic flux, accumulation of fragmented mitochondria, and inefficient OXPHOS activity with unstable atherosclerotic plaque formation susceptible to rupture (Nahapetyan et al., 2019). Furthermore, the importance of ER-mitochondria signaling in atherosclerosis progression has been shown through the modulation of the ER-resident kinase PERK. Lipid-activated PERK can activate Lon protease-1, resulting in mitochondrial PINK1 degradation and blockade of mitophagy. Inhibition of mitophagy increases ROS production due to the accumulation of damaged mitochondria and boosts inflammasome activation in macrophages, contributing further to atherosclerotic plaque formation (Onat et al., 2019). In addition, in the absence of a secreted protein known to participate in atherosclerosis, apolipoprotein A-I binding protein (AIBP), PINK1 is cleaved, and mitophagy is blocked, which also promotes atherosclerosis progression and plaque formation (Duan et al., 2022).

4.4 Cardiac hypertrophy and heart failure

Cardiac hypertrophy, a condition that results in the thickening of heart muscles, is an acute response to enhanced hemodynamic overload and mechanical stress on cardiac tissues. When prolonged, cardiac hypertrophy becomes pathological and can result in heart failure (Levy et al., 1990). Cardiac hypertrophy is associated with increased sarcomere production, thickening of the ventricular wall and induces changes in cardiac tissue gene expression, metabolism, and contractility (Schiattarella and Hill, 2015; Nakamura and Sadoshima, 2018). After hypertrophy, cardiomyocytes need more energy and increase mitochondrial mass at an early stage. However, this is followed by a decrease in mitochondrial mass and an impairment of cardiac contractility as the disease progresses (Zak et al., 1980; Goffart et al., 2004). Ultimately, the decline in mitochondrial mass reduces the production of ATP and diastolic dysfunction, causing heart failure (Flarsheim et al., 1996). BNIP3 expression increases in stressed cardiomyocytes, favoring mitochondrial fragmentation (Chaanine et al., 2016). Blocking mitochondrial fission through the deletion of DRP1 in mice leads to hypertrophy caused by norepinephrine signaling. On the other hand, inhibition of mitochondrial fusion by blocking MFN2 stimulates the hypertrophic response (Pennanen et al., 2014). Mitochondrial fusion is affected during cardiac hypertrophy, as reduced expression of MFN2 and OPA1 has been reported in cardiomyocytes in the context of heart failure (Chen et al., 2009). Furthermore, the activity of Complex I and IV from the mitochondrial ETC is also reduced during heart failure (Arbustini et al., 1998). mtDNA replication is also impaired in heart failure, causing a decrease in mtDNA-encoded proteins and mitochondrial biogenesis (Sheeran and Pepe, 2017). Interestingly, the deletion of OMA1, an inner mitochondrial membrane protease that determines cristae structure for optimal ETC functioning, alleviates myocardial damage by preventing cardiomyocyte death (Acin-Perez et al., 2018). The expression of dual-specificity tyrosine-regulated kinase 1B (DYRK1B) is increased in failing hearts of humans and mice and overexpression of this kinase impairs ejection fraction as well as cardiac fibrosis in mice by downregulating the mitobiogenesis regulator PGC1α (Zhuang et al., 2022). An important inflammatory response during pathological conditions is pyroptosis, a form of inflammatory cell

death (Shi et al., 2015). During this process, NLRP3 inflammasome is induced, activating caspase-1, which cleaves gasdermin D (GSDMD) to permeabilize the cells, resulting in IL-1β and IL-18 secretion from the rupturing cells (Kayagaki et al., 2015; Shi et al., 2015). In mouse and human hypertrophic myocardia, it has been shown that there is an amplification of GSDMD that activates the mitochondrial STING axis, causing mitochondrial dysfunction and contributing to cardiomyocyte pyroptosis (Han et al., 2022). Notably, choline supplementation in rats alleviated cardiac hypertrophy by promoting UPR^{mt} through activating the SIRT3-AMPK axis as an adaptive response to cardiac dysfunction (Xu et al., 2019). Mitochondrial ROS scavenging is crucial to protect the cardiac tissues from oxidative damage (Xin et al., 2021). Recently, the deletion of mitochondrial peroxiredoxin 3 (Prdx3) in mice has been shown to cause cardiac hypertrophy and heart failure. In addition, the same study showed that Prdx3 interacts with PINK1 and blocks its proteolytic cleavage during mitophagy, playing a protective role during hypertrophy-induced mitochondrial dysfunction (Sonn et al., 2022). Of note, Parkin levels decline in hypertrophic cardiomyocytes, as well as mouse hearts, and overexpression of Parkin in mice blocked Ang-II-induced hypertrophy and improved heart function via boosting mitophagy, highlighting the importance of clearance of damaged mitochondria during cardiac hypertrophy (Sun et al., 2022).

4.5 Diabetic cardiomyopathy

Diabetic cardiomyopathy is a pathological process leading to changes in myocardial structure and function observed in patients with diabetes mellitus in the absence of other cardiac risk factors, such as coronary artery diseases or hypertension (Jia et al., 2018). Elevated levels of fatty acids in cardiomyocytes from diabetic patients can interfere with mitochondrial metabolism. In a healthy heart, ATP is produced by fatty acid oxidation and, to some extent, from carbohydrates (Duncan, 2011). Mitochondria and peroxisomes are responsible for the β-oxidation of fatty acids (FAO), a process that depends on oxygen availability. This process is not optimal when cardiac tissue needs high levels of ATP. In the context of diabetes, increased levels of fatty acids and ATP produced from the oxidation of FAO result in a loss of flexibility as to mitochondrial fuel sources (Duncan, 2011). Consequently, heart contraction efficiency starts to decline, causing a lack of blood flow and cardiomyopathy (Liesa and Shirihai, 2013). Nuclear receptor family PPARs are heavily involved in the pathogenesis of diabetic cardiomyopathy. Elevated levels of fatty acids inside cardiomyocytes interfere with FAO and lead to increased PPAR-γ expression and decreased PPAR-α expression (Wang L. et al., 2021). In line with this, an increase in fatty acids boosts ROS production by increasing IMM potential, resulting in oxidative damage and mitochondrial dysfunction (Schilling, 2015). Prolonged ROS levels increase and induce cardiomyocyte apoptosis, which is compensated by fibroblast recruitment. This changes the cellular composition of cardiac tissue, which can lead to heart failure (Flarsheim et al., 1996; Dabkowski et al., 2010).

Type 2 diabetic cardiomyopathy results in perturbations in the mitochondrial Ca^{2+} signaling (Dillmann, 2019). In a murine model of diabetic cardiomyopathy, mice fed with a high-fat and high-sucrose diet showed cardiac hypertrophy, dysfunction, and insulin resistance (Dia et al., 2020). This phenotype was associated with decreased interactions between IP3R and VDAC1, causing a decline in Ca^{2+} flux into the mitochondria (Dia et al., 2020). In a rat model of type 2 diabetes, the expression of secreted frizzled-related protein 2 (SFRP2), a protein involved in Wnt signaling and angiogenesis, is downregulated in rat cardiomyocytes and cardiac tissues. This was associated with a reduction in mitochondrial membrane potential and increased oxidative stress via the regulation of mitobiogenesis through the AMPK/PGC1α axis (Ma et al., 2021). While exercise in mice increased the expression of the mitochondrial deacetylase SIRT3 during diabetes-induced cardiac impairment and preserved cardiac functions by promoting the AMPK/SIRT3 pathway (Jin L. et al., 2022), SIRT3 deficiency exacerbates diabetic cardiomyopathy by activating NLRP3 and promoting the accumulation of mtROS (Song et al., 2021). The anti-diabetic drug empagliflozin has also been shown to inhibit cardiac dysfunction during diabetic cardiomyopathy by increasing the expression of *Nrf2* in type 2 diabetic mice. Additionally, in mice treated with empagliflozin, the expression of mitochondrial fission proteins was decreased with an upregulation of the fusion machinery, contributing to the recovery of cardiac tissues during this pathogenic condition (Wang J. et al., 2022). Notably, a decline in NAD^+ to NADH ratio in diabetic mice is linked to the downregulation of SOD2, deficit in mitochondrial bioenergetics, and a concomitant increase in oxidative damage. Increasing NAD^+ levels via nicotinamide phosphoribosyltransferase (NAMPT), the enzyme producing the intermediate for NAD^+, relieved cardiac dysfunction in diabetic mice, showing the possible therapeutic potential of NAD^+ supplementation in this disease (Chiao et al., 2021).

Mitochondrial dynamics are also impaired in type 2 diabetic cardiomyopathy. The decline in MFN1,2, OPA1, and DRP1 function has been implicated in the development of diabetic cardiomyopathy (Williams and Caino, 2018). A decrease in MFN2 expression, followed by impaired mitochondrial fusion, mitochondrial fragmentation, and related OXPHOS dysfunction, has been reported in diabetic cardiomyopathy (Montaigne et al., 2014). Perturbations in mitochondrial dynamics activate mitophagy and autophagy, the mechanisms of MQC. Previous data suggest that autophagy is blocked in type 1 diabetes, as shown by decreased levels of LC3, ATG5, and 12 in cardiomyocytes (Xu et al., 2013). Lower levels of PINK1 and Parkin are also reported in the same study, hinting at the suppression of mitophagy in the hearts of type 1 diabetic mice (Xu et al., 2013). In mouse models of type 1 diabetes, autophagy and mitophagy are augmented in cardiac tissues (Tao and Xu, 2020; Zhang M. et al., 2021). Furthermore, feeding mice with a high saturated fatty acid diet induces autophagy and cardiomyopathy (Russo et al., 2012). In addition, mice fed a high-fat diet developing diabetic cardiomyopathy show an initial peak of cardiac autophagy, which declines later. However, in this study, mitophagy activation was sustained for 2 months, leading to Parkin deficiency and impaired mitophagy, worsening the disease and suggesting a protective effect of mitophagy during the early stages of diabetic cardiomyopathy (Tong et al., 2019). Interestingly, the expression of TOM70, a mitochondrial outer membrane protein, is decreased in the heart tissues of diabetic mice (Wang et al., 2020). Overexpressing TOM70 rescues mitochondrial dysfunction,

oxidative damage, and apoptosis in cardiac tissues, indicating that TOM70 could be a therapeutic target in treating diabetic cardiomyopathy (Wang et al., 2020).

4.6 Genetic cardiomyopathies

Genetic cardiomyopathies arise from chromosomal abnormalities interfering with the normal function of the heart (McKenna et al., 2017). Hypertrophic cardiomyopathy is the most prevailing, affecting 1 in 500 people (Tuohy et al., 2020). It is usually caused by autosomal dominant mutations of genes that code for sarcomere proteins and mutations of mitochondria-related genes (Teekakirikul et al., 2019). Arrhythmogenic right ventricular cardiomyopathy is a familial heart disease that manifests by mutations of desmosomal proteins, which are intermediate muscle tissue filaments (Krahn et al., 2022). Consequently, ventricular wall thinning and ballooning occur in affected patients (Shah et al., 2023). Another congenital cardiomyopathy is left ventricular non-compaction, which is initiated during the embryonic stage and perturbs the normal development of the heart muscle (Singh and Patel, 2023). In addition, restrictive cardiomyopathy is characterized by the restriction of the left ventricle, causing a significant increase in ventricular pressure and myocardial stiffness (Rapezzi et al., 2022). Finally, dilated cardiomyopathy is manifested with enlarged ventricles, causes systolic dysfunction, and is inherited in an autosomally dominant manner (De Paris et al., 2019).

Genetic cardiomyopathies are mitochondrial diseases related to either disruption in ETC complex subunits or factors involved in their assembly, mitochondria encoded tRNAs, rRNAs, and proteins responsible for mtDNA maintenance and CoQ_{10} synthesis (Yamada and Nomura, 2021). These cardiomyopathies are often associated with mutations in mtDNA encoded Complex I subunit genes NADH-ubiquinone oxidoreductase chain 1 and 5 (MT-ND1 and 5) and nuclear-encoded Complex I subunit genes such as NADH: ubiquinone oxidoreductase core subunits S2 (NDUFS2), V2 (NDUFV2) or A2 (NDUFA2). Similarly, mutations in nuclear factors involved in Complex I assembly such as acyl-CoA dehydrogenase family member 9 (ACAD9) and NADH: ubiquinone oxidoreductase complex assembly factor 1 (NDUFAF1), are also associated with the development of genetic cardiomyopathies (Fassone and Rahman, 2012; Brecht et al., 2015; Dubucs et al., 2023). All subunits of Complex II are nuclear-encoded, and mutations of subunits A, D (SDHA and SDHD), as well as Complex II assembly factor 4, have been reported in patients with hypertrophic, dilated, and non-compaction cardiomyopathies (Jain-Ghai et al., 2013; Alston et al., 2015; Wang X. et al., 2022). Likewise, mutations in mtDNA encoded cytochrome b gene (MTCYB) have also been identified in patients with hypertrophic and dilated cardiomyopathy (Hagen et al., 2013; Carossa et al., 2014). Supporting these findings, mutations in Complex IV subunit genes COX6B1, MTCO2, and MTCO3 have been associated with dilated and hypertrophic cardiomyopathies (Abdulhag et al., 2015; Yang et al., 2022). Moreover, a possibly pathogenic m.9856T>C (Ile217Thr) mutation in MTCO3 has been identified in a left ventricular non-compaction cardiomyopathy patient, together with a significant decrease in mtDNA copy number in the patient group compared with controls (Liu et al., 2013). Interestingly, hypertrophic cardiomyopathy has been associated with m.2336T>C homoplasmic mutation of mitochondrial 16S rRNA gene (MTRNR2), and restrictive cardiomyopathy has been linked to m.1555A>G mutation of the mitochondrial 12S rRNA gene (MTRNR1) (Liu et al., 2014; Li et al., 2019). Furthermore, c.467T>G and c.950C>G mutations in mitochondrial ribosomal proteins L44 and L3 (MRPL44 and 3) have also been reported in hypertrophic cardiomyopathy, respectively (Galmiche et al., 2011; Distelmaier et al., 2015). Mutation in genes involved in CoQ_{10} biosynthesis, specifically COQ2, 4, and 9, have been reported in patients with hypertrophic cardiomyopathy (Doimo et al., 2014; Desbats et al., 2015; Mantle et al., 2023).

Mitochondrial dysfunction in hypertrophic cardiomyopathy has recently been associated with impaired NADH-linked respiration, as well as fatty acid oxidation in septal myectomy tissues from patients, due to mitochondrial fragmentation, which was rescued by NAD^+ supplementation (Nollet et al., 2023). Interestingly, cardiac-specific deletion of cytochrome c assembly factor *Cox10* resulted in mitochondrial cardiomyopathy in mice, leading to OXPHOS defects. Furthermore, the activation of mitochondrial peptidase OMA1 appears protective during mitochondrial cardiomyopathy (Ahola et al., 2022). A multi-omics study investigating healthy controls and patients with hypertrophic cardiomyopathy indicates a global downregulation in the expression of mitochondrial genes involved in ATP synthesis, coupled with mitochondrial damage manifested by low cristae density and less oxidative phosphorylation (Ranjbarvaziri et al., 2021).

During dilated cardiomyopathy, mitochondria numbers first increase to compensate for the energy deficit and then decrease over time, which results in less ATP production, deficiencies in cardiac contractility, and more ROS production (Goffart et al., 2004; Ramaccini et al., 2020). It has been reported that cardiomyocytes lacking the circadian rhythm activation factor basic helix-loop-helix ARNT like 1 (BMAL1) gene exhibit a dilated cardiomyopathy-like phenotype with reduced expression of mitochondrial BCL2 interacting protein 3 (BNIP3) protein, resulting in defective mitophagy and cardiomyocyte function (Li et al., 2020). Additionally, in a doxorubicin-induced mice model of dilated cardiomyopathy, increased expression of full-length SIRT3 prevented cardiac dysfunction by blocking superoxide generation (Tomczyk et al., 2022).

Mitochondrial dysfunction also contributes heavily to arrhythmogenic cardiomyopathy, as there are deficits in intracellular Ca^{2+} dynamics and ion channel functioning (Kim et al., 2019). Connexin 43 (Cx43), found on IMM of subsarcolemmal cardiomyocytes for regulation of ATP synthesis and respiration, is shown to decrease in arrhythmogenic cardiomyopathy patients, resulting in dysfunctional cardiomyocyte excitability (Noorman et al., 2013).

Pathogenic variants of desmin, a crucial component of the intermediate filaments of cardiac or skeletal muscle cells, can cause desminopathy, characterized by cardiomyopathy and skeletal myopathy (van Spaendonck-Zwarts et al., 2011). Dilated, arrhythmogenic, and restricted cardiomyopathy is often linked to desminopathy (Taylor et al., 2007; Otten et al., 2010; Lorenzon et al., 2013). A recent study identified a p.(S57L) mutation in desmin, which was associated with a striking downregulation of

mitochondrial proteins and bioenergetics, coupled with a decrease in ETC Complex I + III + IV super-complex formation (Kubánek et al., 2020). In addition, VDAC1 has been shown to aggregate on muscle fibers together with apoptotic proteins, both in patients with desminopathy and in the rat model of this disease (Li et al., 2016).

4.7 Kawasaki disease (KD)

KD is an acute febrile systemic vasculitis of unknown etiology, affecting infants and young children, and is the leading cause of acquired heart disease in developed countries (Kawasaki et al., 1974; Newburger et al., 2016; McCrindle et al., 2017). Coronary arteritis and coronary artery aneurysms (CAAs) occur in approximately 25% of untreated children, which is reduced to 3%–5% with high-dose intravenous immunoglobulin (IVIG) treatment (Burns et al., 1998; Tremoulet et al., 2008). Transcriptome analysis of whole blood from KD patients as well as cardiovascular tissues collected from *Lactobacillus casei* cell wall extract (LCWE)-injected mice, an experimental mouse model mimicking KD vasculitis, showed increased expression of genes associated with IL-1β and the NLRP3 inflammasome pathway (Hoang et al., 2014; Lee et al., 2015; Wakita et al., 2016; Porritt et al., 2021). Supporting NLRP3 activation, high levels of serum concentration of the pro-inflammatory cytokines IL-1β and IL-18 have been reported in the plasma of children with KD during the acute phase of the disease (Alphonse et al., 2016). Blocking the IL-1 pathway in two different experimental mouse models of KD, the LCWE- and the *Candida albicans* water-soluble fraction (CAWS), either pharmacologically or using knock-out mice, significantly decreases vasculitis severity (Lee et al., 2012; Lee et al., 2015; Anzai et al., 2020; Porritt et al., 2020). Several case studies have also demonstrated the efficacy of Anakinra, an IL-1 receptor antagonist, in treating IVIG-resistant KD patients (Cohen et al., 2012; Shafferman et al., 2014; Guillaume et al., 2018; Blonz et al., 2020; Koné-Paut et al., 2021).

Mitochondrial dysfunction and impaired autophagy and mitophagy can trigger NLRP3 inflammasome activation (Zhang N. P. et al., 2019). Impaired clearance of damaged mitochondria has been reported in the LCWE-induced murine model of KD vasculitis, shown by a decreased autophagic flux and blockade of autophagy by mTOR pathway activity, contributing to NLRP3 inflammasome activation and ROS accumulation (Marek-Iannucci et al., 2021). The expression of *LC3B*, *BECN1,* and *ATG16L1* mRNA is reduced in whole blood of KD patients compared with febrile and healthy controls, while IVIG treatment increases the expression of these autophagy-related genes (Huang et al., 2020). However, low expression of *ATG16L1* mRNA persists in patients developing coronary artery lesions, further indicating that the autophagy/mitophagy pathway is disrupted during KD and could be a possible therapeutic target (Huang et al., 2020). Statins, specifically atorvastatin, have been used to treat KD patients developing giant coronary aneurysms to improve endothelial cell homeostasis (Niedra et al., 2014). Studies have shown that statins also block NLRP3 inflammasome activation by promoting autophagy/mitophagy (Andres et al., 2014; Peng et al., 2018; Tremoulet et al., 2019). In addition, alleviating ER stress in mice by deletion or pharmacological inhibition of ER resident endoribonuclease IRE1 also reduces LCWE-induced KD vasculitis as well as caspase-1 activity and IL-1β production, highlighting the importance of ER stress pathways in KD progression (Marek-Iannucci et al., 2022). Serum levels of β-hydroxy-γ-trimethylammonium butyrate (carnitine), an amine that transfers long-chain fatty acids across the IMM for β-oxidation, is found to be higher in IVIG non-responsive KD patients, hinting towards altered mitochondrial fatty acid metabolism and mitochondrial fuel dependency (Muto et al., 2022).

Increased platelet count is commonly reported in KD patients in the second to third week of disease onset (Levin et al., 1985; Arora et al., 2020), as well as in the LCWE-induced mouse model of KD (Kocatürk et al., 2023). Two separate platelet sub-populations co-exist in the peripheral blood of KD patients (Pietraforte et al., 2014). The first one is characterized by mitochondrial membrane potential loss, whereas the second one exhibits mitochondrial membrane potential hyperpolarization. These platelet sub-populations may potentially influence inflammasome responses, the redox state, and calcium balance in the development of the KD vasculitis (Pietraforte et al., 2014). Therefore, further studies are warranted to investigate the potential role of mitophagy and autophagy on the development of KD cardiovascular lesions.

5 Therapeutic strategies targeting mitochondria in CVDs

Modulating mitochondrial function and reducing mitochondrial oxidative stress could be a therapeutic target to prevent and/or ameliorate CVDs. Mitochondria-targeted antioxidant MitoQ, is a synthetic ROS-scavenger that mimics the activity of mitochondrial CoQ_{10} (Murphy and Smith, 2007). MitoQ treatment is available orally, and safe (Rossman et al., 2018; Oliver and Reddy, 2019), and its uptake by the mitochondria is dependent on membrane potential (James et al., 2007). MitoQ alleviates doxorubicin-induced cardiomyopathy in rats (Chandran et al., 2009) and promotes vascular endothelial function in older patients by reducing age-related ROS accumulation (Rossman et al., 2018). Similarly, another mitochondria-targeted ROS scavenger mimetic, mitoTEMPO, decreases mPTP opening to prevent mitochondrial apoptosis (Liang et al., 2010), and reduces diabetic cardiomyopathy in mice (Ni et al., 2016).

Mitochondria generate ATP through OXPHOS, and byproducts of the TCA cycle, such as NAD^+ in its reduced form, NADH, contribute as a primary source of electrons to this process (Figure 2). NAD^+ is a cofactor involved in cellular metabolism and mitochondrial fitness, and reduced NAD^+ levels are associated with dysfunctional mitochondria (Srivastava, 2016). Therefore, targeting and boosting NAD^+ could improve mitochondrial function in CVDs. Dietary supplementation with NAD^+ precursor nicotinamide mononucleotide (NMN) can restore mitochondrial function in murine models of heart failure (HF) (Wang Y. J. et al., 2021), dilated cardiomyopathy (Martin et al., 2017) and I/R injury (Yamamoto et al., 2014). NMN has also been shown to promote autophagy and to decrease hypertension-mediated stroke in rats (Forte et al., 2020). Oral supplementation of mice with nicotinamide riboside (NR), another NAD^+ intermediate, also boosts NAD^+ and attenuates heart failure and dilated cardiomyopathy (Diguet et al., 2018). Chronic

supplementation with NR is well tolerated and effectively boosts NAD^+ levels in healthy middle-aged and older adults (Martens et al., 2018).

Another important regulator of autophagy/mitophagy, SIRT1, an NAD-dependent deacetylase, is non-specifically activated by resveratrol, a natural polyphenol produced in plants (Baur and Sinclair, 2006), as well as synthetic sirtuin-activating compounds such as SRT1720 (Bonkowski and Sinclair, 2016). These molecules have been shown to limit disease severity in multiple rodent CVD models, including Ang-II-induced atherosclerosis (Chen et al., 2015), cardiac hypertrophy (Chan et al., 2008), and diabetic cardiomyopathy (Sulaiman et al., 2010). Boosting NAD^+ levels activates sirtuins and improves mitochondrial function (Kane and Sinclair, 2018).

The AMPK pathway is another crucial regulator of mitochondrial biogenesis and mitophagy. As mentioned above, AMPK activates PGC1α to promote mitochondrial biogenesis (Kukidome et al., 2006; Jäger et al., 2007). Metformin activates AMPK and promotes survival during heart failure in mice (Gundewar et al., 2009). Resveratrol activates mitochondrial biogenesis via AMPK and downstream PGC1α and TFAM (Lagouge et al., 2006). Notably, resveratrol improves cardiac function in mice and rats with hypertension (Rimbaud et al., 2011; Magyar et al., 2012). Caloric restriction and exercise can also induce the AMPK pathway, promote mitophagy, and prevent inflammatory response (Laker et al., 2017; Chen et al., 2020). Furthermore, inhibition of mTOR with rapamycin induces mitophagy in mice cardiomyocytes and increases lifespan (Wei et al., 2015; Yang et al., 2019). Promising developments in approaches/drugs improving mitochondrial homeostasis in cardiac tissues are crucial for discovering novel therapeutic agents, and future studies are needed to explore better targets in the context of CVDs.

6 Conclusion

Proper mitochondrial functioning is essential for tissue homeostasis, particularly in cardiac tissues with high demand for energy, such as the heart. Therefore, MQC mechanisms are central to maintaining cardiac homeostasis via the clearance of damaged mitochondria. Adapting the mitochondrial network to stress allows the heart to preserve its function during disease. The pathology of CVDs is highly connected to mitochondrial structure, membrane potential, dynamics, and clearance. Maintaining the health of the mitochondrial network via MQC is necessary for the outcome of CVDs. Therefore, mitochondria-targeting agents are critical therapeutic options to prevent or alleviate mitochondrial dysfunction during cardiac pathology. Current studies have shown that cardiac tissue protection can be achieved through mitophagy, ROS detoxification mechanisms, replenishing mitochondria pool, and inter-organelle communication. Targeting these MQC pathways is pivotal in discovering new treatments for CVDs in the future.

Author contributions

AA: Conceptualization, Data curation, Formal analysis, Investigation, Methodology, Writing–original draft, Writing–review and editing. TC: Conceptualization, Formal analysis, Investigation, Methodology, Supervision, Writing–review and editing. MN: Conceptualization, Formal analysis, Funding acquisition, Investigation, Methodology, Resources, Supervision, Writing–review and editing.

Funding

The authors declare financial support was received for the research, authorship, and/or publication of this article. This work was supported by the National Institutes of Health (grant number: R01 HL159297).

Conflict of interest

The authors declare that the research was conducted in the absence of any commercial or financial relationships that could be construed as a potential conflict of interest.

Publisher's note

References

Abdulhag, U. N., Soiferman, D., Schueler-Furman, O., Miller, C., Shaag, A., Elpeleg, O., et al. (2015). Mitochondrial complex IV deficiency, caused by mutated COX6B1, is associated with encephalomyopathy, hydrocephalus and cardiomyopathy. *Eur. J. Hum. Genet.* 23 (2), 159–164. doi:10.1038/ejhg.2014.85

Acin-Perez, R., Lechuga-Vieco, A. V., Del Mar Muñoz, M., Nieto-Arellano, R., Torroja, C., Sánchez-Cabo, F., et al. (2018). Ablation of the stress protease OMA1 protects against heart failure in mice. *Sci. Transl. Med.* 10 (434), eaan4935. doi:10.1126/scitranslmed.aan4935

Ahola, S., Rivera Mejías, P., Hermans, S., Chandragiri, S., Giavalisco, P., Nolte, H., et al. (2022). OMA1-mediated integrated stress response protects against ferroptosis in mitochondrial cardiomyopathy. *Cell. Metab.* 34 (11), 1875–1891.e7. doi:10.1016/j.cmet.2022.08.017

Albina, J. E., Abate, J. A., and Henry, W. L., Jr. (1991). Nitric oxide production is required for murine resident peritoneal macrophages to suppress mitogen-stimulated T cell proliferation. Role of IFN-gamma in the induction of the nitric oxide-synthesizing pathway. *J. Immunol.* 147 (1), 144–148. doi:10.4049/jimmunol.147.1.144

Alphonse, M. P., Duong, T. T., Shumitzu, C., Hoang, T. L., McCrindle, B. W., Franco, A., et al. (2016). Inositol-triphosphate 3-kinase C mediates inflammasome activation and treatment response in Kawasaki disease. *J. Immunol.* 197 (9), 3481–3489. doi:10.4049/jimmunol.1600388

Alston, C. L., Ceccatelli Berti, C., Blakely, E. L., Oláhová, M., He, L., McMahon, C. J., et al. (2015). A recessive homozygous p.Asp92Gly SDHD mutation causes prenatal cardiomyopathy and a severe mitochondrial complex II deficiency. *Hum. Genet.* 134 (8), 869–879. doi:10.1007/s00439-015-1568-z

Amgalan, D., Chen, Y., and Kitsis, R. N. (2017). Death receptor signaling in the heart: Cell survival, apoptosis, and necroptosis. *Circulation* 136 (8), 743–746. doi:10.1161/circulationaha.117.029566

Andres, A. M., Hernandez, G., Lee, P., Huang, C., Ratliff, E. P., Sin, J., et al. (2014). Mitophagy is required for acute cardioprotection by simvastatin. *Antioxid. Redox Signal* 21 (14), 1960–1973. doi:10.1089/ars.2013.5416

Andres, A. M., Tucker, K. C., Thomas, A., Taylor, D. J., Sengstock, D., Jahania, S. M., et al. (2017). Mitophagy and mitochondrial biogenesis in atrial tissue of patients undergoing heart surgery with cardiopulmonary bypass. *JCI Insight* 2 (4), e89303. doi:10.1172/jci.insight.89303

Antón, Z., Landajuela, A., Hervás, J. H., Montes, L. R., Hernández-Tiedra, S., Velasco, G., et al. (2016). Human Atg8-cardiolipin interactions in mitophagy: Specific properties of LC3B, GABARAPL2 and GABARAP. *Autophagy* 12 (12), 2386–2403. doi:10.1080/15548627.2016.1240856

Anzai, F., Watanabe, S., Kimura, H., Kamata, R., Karasawa, T., Komada, T., et al. (2020). Crucial role of NLRP3 inflammasome in a murine model of Kawasaki disease. *J. Mol. Cell. Cardiol.* 138, 185–196. doi:10.1016/j.yjmcc.2019.11.158

Anzell, A. R., Maizy, R., Przyklenk, K., and Sanderson, T. H. (2018). Mitochondrial quality control and disease: Insights into ischemia-reperfusion injury. *Mol. Neurobiol.* 55 (3), 2547–2564. doi:10.1007/s12035-017-0503-9

Arbustini, E., Diegoli, M., Fasani, R., Grasso, M., Morbini, P., Banchieri, N., et al. (1998). Mitochondrial DNA mutations and mitochondrial abnormalities in dilated cardiomyopathy. *Am. J. Pathol.* 153 (5), 1501–1510. doi:10.1016/s0002-9440(10)65738-0

Arora, K., Guleria, S., Jindal, A. K., Rawat, A., and Singh, S. (2020). Platelets in Kawasaki disease: Is this only a numbers game or something beyond? *Genes. Dis.* 7 (1), 62–66. doi:10.1016/j.gendis.2019.09.003

Atkins, K., Dasgupta, A., Chen, K. H., Mewburn, J., and Archer, S. L. (2016). The role of Drp1 adaptor proteins MiD49 and MiD51 in mitochondrial fission: Implications for human disease. *Clin. Sci. (Lond)* 130 (21), 1861–1874. doi:10.1042/cs20160030

Baar, K., Wende, A. R., Jones, T. E., Marison, M., Nolte, L. A., Chen, M., et al. (2002). Adaptations of skeletal muscle to exercise: Rapid increase in the transcriptional coactivator PGC-1. *Faseb J.* 16 (14), 1879–1886. doi:10.1096/fj.02-0367com

Bahr, T., Katuri, J., Liang, T., and Bai, Y. (2022). Mitochondrial chaperones in human health and disease. *Free Radic. Biol. Med.* 179, 363–374. doi:10.1016/j.freeradbiomed.2021.11.015

Bai, Y., Yang, Y., Gao, Y., Lin, D., Wang, Z., and Ma, J. (2021). Melatonin postconditioning ameliorates anoxia/reoxygenation injury by regulating mitophagy and mitochondrial dynamics in a SIRT3-dependent manner. *Eur. J. Pharmacol.* 904, 174157. doi:10.1016/j.ejphar.2021.174157

Baik, S. H., Ramanujan, V. K., Becker, C., Fett, S., Underhill, D. M., and Wolf, A. J. (2023). Hexokinase dissociation from mitochondria promotes oligomerization of VDAC that facilitates NLRP3 inflammasome assembly and activation. *Sci. Immunol.* 8 (84), eade7652. doi:10.1126/sciimmunol.ade7652

Ballana, E., Govea, N., de Cid, R., Garcia, C., Arribas, C., Rosell, J., et al. (2008). Detection of unrecognized low-level mtDNA heteroplasmy may explain the variable phenotypic expressivity of apparently homoplasmic mtDNA mutations. *Hum. Mutat.* 29 (2), 248–257. doi:10.1002/humu.20639

Barki-Harrington, L., Perrino, C., and Rockman, H. A. (2004). Network integration of the adrenergic system in cardiac hypertrophy. *Cardiovasc Res.* 63 (3), 391–402. doi:10.1016/j.cardiores.2004.03.011

Baughman, J. M., Perocchi, F., Girgis, H. S., Plovanich, M., Belcher-Timme, C. A., Sancak, Y., et al. (2011). Integrative genomics identifies MCU as an essential component of the mitochondrial calcium uniporter. *Nature* 476 (7360), 341–345. doi:10.1038/nature10234

Baur, J. A., and Sinclair, D. A. (2006). Therapeutic potential of resveratrol: The *in vivo* evidence. *Nat. Rev. Drug Discov.* 5 (6), 493–506. doi:10.1038/nrd2060

Becker, J., and Craig, E. A. (1994). Heat-shock proteins as molecular chaperones. *Eur. J. Biochem.* 219 (1-2), 11–23. doi:10.1007/978-3-642-79502-2_2

Bleier, L., Wittig, I., Heide, H., Steger, M., Brandt, U., and Dröse, S. (2015). Generator-specific targets of mitochondrial reactive oxygen species. *Free Radic. Biol. Med.* 78, 1–10. doi:10.1016/j.freeradbiomed.2014.10.511

Blonz, G., Lacroix, S., Benbrik, N., Warin-Fresse, K., Masseau, A., Trewick, D., et al. (2020). Severe late-onset Kawasaki disease successfully treated with anakinra. *J. Clin. Rheumatol.* 26 (2), e42–e43. doi:10.1097/rhu.0000000000000814

Bonkowski, M. S., and Sinclair, D. A. (2016). Slowing ageing by design: The rise of NAD(+) and sirtuin-activating compounds. *Nat. Rev. Mol. Cell. Biol.* 17 (11), 679–690. doi:10.1038/nrm.2016.93

Booth, D. M., Várnai, P., Joseph, S. K., and Hajnóczky, G. (2021). Oxidative bursts of single mitochondria mediate retrograde signaling toward the ER. *Mol. Cell.* 81 (18), 3866–3876.e2. doi:10.1016/j.molcel.2021.07.014

Brahimi-Horn, M. C., Giuliano, S., Saland, E., Lacas-Gervais, S., Sheiko, T., Pelletier, J., et al. (2015). Knockout of Vdac1 activates hypoxia-inducible factor through reactive oxygen species generation and induces tumor growth by promoting metabolic reprogramming and inflammation. *Cancer Metab.* 3, 8. doi:10.1186/s40170-015-0133-5

Bravo-San Pedro, J. M., Kroemer, G., and Galluzzi, L. (2017). Autophagy and mitophagy in cardiovascular disease. *Circ. Res.* 120 (11), 1812–1824. doi:10.1161/circresaha.117.311082

Brecht, M., Richardson, M., Taranath, A., Grist, S., Thorburn, D., and Bratkovic, D. (2015). Leigh syndrome caused by the MT-ND5 m.13513G>A mutation: A case presenting with WPW-like conduction defect, cardiomyopathy, hypertension and hyponatraemia. *JIMD Rep.* 19, 95–100. doi:10.1007/8904_2014_375

Brumatti, G., Salmanidis, M., and Ekert, P. G. (2010). Crossing paths: Interactions between the cell death machinery and growth factor survival signals. *Cell. Mol. Life Sci.* 67 (10), 1619–1630. doi:10.1007/s00018-010-0288-8

Burns, J. C., Capparelli, E. V., Brown, J. A., Newburger, J. W., and Glode, M. P. (1998). Intravenous gamma-globulin treatment and retreatment in Kawasaki disease. US/Canadian Kawasaki syndrome study group. *Pediatr. Infect. Dis. J.* 17 (12), 1144–1148. doi:10.1097/00006454-199812000-00009

Cadenas, S. (2018). Mitochondrial uncoupling, ROS generation and cardioprotection. *Biochim. Biophys. Acta Bioenerg.* 1859 (9), 940–950. doi:10.1016/j.bbabio.2018.05.019

Cai, C., Guo, Z., Chang, X., Li, Z., Wu, F., He, J., et al. (2022). Empagliflozin attenuates cardiac microvascular ischemia/reperfusion through activating the AMPKα1/ULK1/FUNDC1/mitophagy pathway. *Redox Biol.* 52, 102288. doi:10.1016/j.redox.2022.102288

Candas, D., and Li, J. J. (2014). MnSOD in oxidative stress response-potential regulation via mitochondrial protein influx. *Antioxid. Redox Signal* 20 (10), 1599–1617. doi:10.1089/ars.2013.5305

Cantó, C., Gerhart-Hines, Z., Feige, J. N., Lagouge, M., Noriega, L., Milne, J. C., et al. (2009). AMPK regulates energy expenditure by modulating NAD+ metabolism and SIRT1 activity. *Nature* 458 (7241), 1056–1060. doi:10.1038/nature07813

Capaldi, R. A., and Aggeler, R. (2002). Mechanism of the F(1)F(0)-type ATP synthase, a biological rotary motor. *Trends Biochem. Sci.* 27 (3), 154–160. doi:10.1016/s0968-0004(01)02051-5

Carossa, V., Ghelli, A., Tropeano, C. V., Valentino, M. L., Iommarini, L., Maresca, A., et al. (2014). A novel in-frame 18-bp microdeletion in MT-CYB causes a multisystem disorder with prominent exercise intolerance. *Hum. Mutat.* 35 (8), 954–958. doi:10.1002/humu.22596

Chaanine, A. H., Kohlbrenner, E., Gamb, S. I., Guenzel, A. J., Klaus, K., Fayyaz, A. U., et al. (2016). FOXO3a regulates BNIP3 and modulates mitochondrial calcium, dynamics, and function in cardiac stress. *Am. J. Physiol. Heart Circ. Physiol.* 311 (6), H1540-H1559–h1559. doi:10.1152/ajpheart.00549.2016

Chan, A. Y., Dolinsky, V. W., Soltys, C. L., Viollet, B., Baksh, S., Light, P. E., et al. (2008). Resveratrol inhibits cardiac hypertrophy via AMP-activated protein kinase and Akt. *J. Biol. Chem.* 283 (35), 24194–24201. doi:10.1074/jbc.M802869200

Chan, D. C. (2020). Mitochondrial dynamics and its involvement in disease. *Annu. Rev. Pathol.* 15, 235–259. doi:10.1146/annurev-pathmechdis-012419-032711

Chandran, K., Aggarwal, D., Migrino, R. Q., Joseph, J., McAllister, D., Konorev, E. A., et al. (2009). Doxorubicin inactivates myocardial cytochrome c oxidase in rats: Cardioprotection by mito-Q. *Biophys. J.* 96 (4), 1388–1398. doi:10.1016/j.bpj.2008.10.042

Chehaitly, A., Guihot, A. L., Proux, C., Grimaud, L., Aurrière, J., Legouriellec, B., et al. (2022). Altered mitochondrial opa1-related fusion in mouse promotes endothelial cell dysfunction and atherosclerosis. *Antioxidants (Basel)* 11 (6), 1078. doi:10.3390/antiox11061078

Chen, G., Han, Z., Feng, D., Chen, Y., Chen, L., Wu, H., et al. (2014). A regulatory signaling loop comprising the PGAM5 phosphatase and CK2 controls receptor-mediated mitophagy. *Mol. Cell.* 54 (3), 362–377. doi:10.1016/j.molcel.2014.02.034

Chen, G., Kroemer, G., and Kepp, O. (2020). Mitophagy: An emerging role in aging and age-associated diseases. *Front. Cell. Dev. Biol.* 8, 200. doi:10.3389/fcell.2020.00200

Chen, H., and Chan, D. C. (2009). Mitochondrial dynamics--fusion, fission, movement, and mitophagy--in neurodegenerative diseases. *Hum. Mol. Genet.* 18 (R2), R169–R176. doi:10.1093/hmg/ddp326

Chen, H., Detmer, S. A., Ewald, A. J., Griffin, E. E., Fraser, S. E., and Chan, D. C. (2003). Mitofusins Mfn1 and Mfn2 coordinately regulate mitochondrial fusion and are essential for embryonic development. *J. Cell. Biol.* 160 (2), 189–200. doi:10.1083/jcb.200211046

Chen, L., Gong, Q., Stice, J. P., and Knowlton, A. A. (2009). Mitochondrial OPA1, apoptosis, and heart failure. *Cardiovasc Res.* 84 (1), 91–99. doi:10.1093/cvr/cvp181

Chen, M., Chen, Z., Wang, Y., Tan, Z., Zhu, C., Li, Y., et al. (2016a). Mitophagy receptor FUNDC1 regulates mitochondrial dynamics and mitophagy. *Autophagy* 12 (4), 689–702. doi:10.1080/15548627.2016.1151580

Chen, Q., Sun, L., and Chen, Z. J. (2016b). Regulation and function of the cGAS-STING pathway of cytosolic DNA sensing. *Nat. Immunol.* 17 (10), 1142–1149. doi:10.1038/ni.3558

Chen, Y. B., Aon, M. A., Hsu, Y. T., Soane, L., Teng, X., McCaffery, J. M., et al. (2011). Bcl-xL regulates mitochondrial energetics by stabilizing the inner membrane potential. *J. Cell. Biol.* 195 (2), 263–276. doi:10.1083/jcb.201108059

Chen, Y., Dorn, G. W., and 2nd, (2013). PINK1-phosphorylated mitofusin 2 is a Parkin receptor for culling damaged mitochondria. *Science* 340 (6131), 471–475. doi:10.1126/science.1231031

Chen, Y. X., Zhang, M., Cai, Y., Zhao, Q., and Dai, W. (2015). The Sirt1 activator SRT1720 attenuates angiotensin II-induced atherosclerosis in apoE$^{-/-}$ mice through inhibiting vascular inflammatory response. *Biochem. Biophys. Res. Commun.* 465 (4), 732–738. doi:10.1016/j.bbrc.2015.08.066

Cheng, E. H., Sheiko, T. V., Fisher, J. K., Craigen, W. J., and Korsmeyer, S. J. (2003). VDAC2 inhibits BAK activation and mitochondrial apoptosis. *Science* 301 (5632), 513–517. doi:10.1126/science.1083995

Cheng, J., Nanayakkara, G., Shao, Y., Cueto, R., Wang, L., Yang, W. Y., et al. (2017). Mitochondrial proton leak plays a critical role in pathogenesis of cardiovascular diseases. *Adv. Exp. Med. Biol.* 982, 359–370. doi:10.1007/978-3-319-55330-6_20

Chiao, Y. A., Chakraborty, A. D., Light, C. M., Tian, R., Sadoshima, J., Shi, X., et al. (2021). NAD(+) redox imbalance in the heart exacerbates diabetic cardiomyopathy. *Circ. Heart Fail* 14 (8), e008170. doi:10.1161/circheartfailure.120.008170

Chinnery, P. F. (1993). "Primary mitochondrial disorders overview," in *GeneReviews(®)*, eds M. P. Adam, G. M. Mirzaa, R. A. Pagon, S. E. Wallace, L. J. H. Bean, K. W. Gripp, et al. (Seattle (WA): University of Washington, Seattle

Chinnery, P. F., and Hudson, G. (2013). Mitochondrial genetics. *Br. Med. Bull.* 106 (1), 135–159. doi:10.1093/bmb/ldt017

Chowdhury, A. R., Zielonka, J., Kalyanaraman, B., Hartley, R. C., Murphy, M. P., and Avadhani, N. G. (2020). Mitochondria-targeted paraquat and metformin mediate ROS production to induce multiple pathways of retrograde signaling: A dose-dependent phenomenon. *Redox Biol.* 36, 101606. doi:10.1016/j.redox.2020.101606

Chu, C. T., Ji, J., Dagda, R. K., Jiang, J. F., Tyurina, Y. Y., Kapralov, A. A., et al. (2013). Cardiolipin externalization to the outer mitochondrial membrane acts as an elimination signal for mitophagy in neuronal cells. *Nat. Cell. Biol.* 15 (10), 1197–1205. doi:10.1038/ncb2837

Coenen, M. J., Antonicka, H., Ugalde, C., Sasarman, F., Rossi, R., Heister, J. G., et al. (2004). Mutant mitochondrial elongation factor G1 and combined oxidative phosphorylation deficiency. *N. Engl. J. Med.* 351 (20), 2080–2086. doi:10.1056/NEJMoa041878

Cogliati, S., Frezza, C., Soriano, M. E., Varanita, T., Quintana-Cabrera, R., Corrado, M., et al. (2013). Mitochondrial cristae shape determines respiratory chain supercomplexes assembly and respiratory efficiency. *Cell.* 155 (1), 160–171. doi:10.1016/j.cell.2013.08.032

Cohen, S., Tacke, C. E., Straver, B., Meijer, N., Kuipers, I. M., and Kuijpers, T. W. (2012). A child with severe relapsing Kawasaki disease rescued by IL-1 receptor blockade and extracorporeal membrane oxygenation. *Ann. Rheum. Dis.* 71 (12), 2059–2061. doi:10.1136/annrheumdis-2012-201658

Coleman, J. W. (2001). Nitric oxide in immunity and inflammation. *Int. Immunopharmacol.* 1 (8), 1397–1406. doi:10.1016/s1567-5769(01)00086-8

Colombini, M., Blachly-Dyson, E., and Forte, M. (1996). VDAC, a channel in the outer mitochondrial membrane. *Ion. Channels* 4, 169–202. doi:10.1007/978-1-4899-1775-1_5

Cosentino, K., Hertlein, V., Jenner, A., Dellmann, T., Gojkovic, M., Peña-Blanco, A., et al. (2022). The interplay between BAX and BAK tunes apoptotic pore growth to control mitochondrial-DNA-mediated inflammation. *Mol. Cell.* 82 (5), 933–949.e9. doi:10.1016/j.molcel.2022.01.008

Coste, A., Louet, J. F., Lagouge, M., Lerin, C., Antal, M. C., Meziane, H., et al. (2008). The genetic ablation of SRC-3 protects against obesity and improves insulin sensitivity by reducing the acetylation of PGC-1{alpha}. *Proc. Natl. Acad. Sci. U. S. A.* 105 (44), 17187–17192. doi:10.1073/pnas.0808207105

Czabotar, P. E., Lessene, G., Strasser, A., and Adams, J. M. (2014). Control of apoptosis by the BCL-2 protein family: Implications for physiology and therapy. *Nat. Rev. Mol. Cell. Biol.* 15 (1), 49–63. doi:10.1038/nrm3722

Dabkowski, E. R., Baseler, W. A., Williamson, C. L., Powell, M., Razunguzwa, T. T., Frisbee, J. C., et al. (2010). Mitochondrial dysfunction in the type 2 diabetic heart is associated with alterations in spatially distinct mitochondrial proteomes. *Am. J. Physiol. Heart Circ. Physiol.* 299 (2), H529–H540. doi:10.1152/ajpheart.00267.2010

Dagvadorj, J., Mikulska-Ruminska, K., Tumurkhuu, G., Ratsimandresey, R. A., Carriere, J., Andres, A. M., et al. (2021). Recruitment of pro-IL-1α to mitochondrial cardiolipin, via shared LC3 binding domain, inhibits mitophagy and drives maximal NLRP3 activation. *Proc. Natl. Acad. Sci. U. S. A.* 118 (1), e2015632118. doi:10.1073/pnas.2015632118

Das, S., Bedja, D., Campbell, N., Dunkerly, B., Chenna, V., Maitra, A., et al. (2014). miR-181c regulates the mitochondrial genome, bioenergetics, and propensity for heart failure *in vivo*. *PLoS One* 9 (5), e96820. doi:10.1371/journal.pone.0096820

Das, S., Ferlito, M., Kent, O. A., Fox-Talbot, K., Wang, R., Liu, D., et al. (2012). Nuclear miRNA regulates the mitochondrial genome in the heart. *Circ. Res.* 110 (12), 1596–1603. doi:10.1161/circresaha.112.267732

Daum, G. (1985). Lipids of mitochondria. *Biochim. Biophys. Acta* 822 (1), 1–42. doi:10.1016/0304-4157(85)90002-4

De Paris, V., Biondi, F., Stolfo, D., Merlo, M., and Sinagra, G. (2019). "Pathophysiology," in *Dilated cardiomyopathy: From genetics to clinical management*. Editors G. Sinagra, M. Merlo, and B. Pinamonti (Cham (CH): Springer).

Desbats, M. A., Lunardi, G., Doimo, M., Trevisson, E., and Salviati, L. (2015). Genetic bases and clinical manifestations of coenzyme Q10 (CoQ 10) deficiency. *J. Inherit. Metab. Dis.* 38 (1), 145–156. doi:10.1007/s10545-014-9749-9

Dia, M., Gomez, L., Thibault, H., Tessier, N., Leon, C., Chouabe, C., et al. (2020). Reduced reticulum-mitochondria Ca(2+) transfer is an early and reversible trigger of mitochondrial dysfunctions in diabetic cardiomyopathy. *Basic Res. Cardiol.* 115 (6), 74. doi:10.1007/s00395-020-00835-7

Diguet, N., Trammell, S. A. J., Tannous, C., Deloux, R., Piquereau, J., Mougenot, N., et al. (2018). Nicotinamide riboside preserves cardiac function in a mouse model of dilated cardiomyopathy. *Circulation* 137 (21), 2256–2273. doi:10.1161/circulationaha.116.026099

Dikalova, A. E., Pandey, A., Xiao, L., Arslanbaeva, L., Sidorova, T., Lopez, M. G., et al. (2020). Mitochondrial deacetylase Sirt3 reduces vascular dysfunction and hypertension while Sirt3 depletion in essential hypertension is linked to vascular inflammation and oxidative stress. *Circ. Res.* 126 (4), 439–452. doi:10.1161/circresaha.119.315767

Dillmann, W. H. (2019). Diabetic cardiomyopathy. *Circ. Res.* 124 (8), 1160–1162. doi:10.1161/circresaha.118.314665

Diner, E. J., Burdette, D. L., Wilson, S. C., Monroe, K. M., Kellenberger, C. A., Hyodo, M., et al. (2013). The innate immune DNA sensor cGAS produces a noncanonical cyclic dinucleotide that activates human STING. *Cell. Rep.* 3 (5), 1355–1361. doi:10.1016/j.celrep.2013.05.009

Distelmaier, F., Haack, T. B., Catarino, C. B., Gallenmüller, C., Rodenburg, R. J., Strom, T. M., et al. (2015). MRPL44 mutations cause a slowly progressive multisystem disease with childhood-onset hypertrophic cardiomyopathy. *Neurogenetics* 16 (4), 319–323. doi:10.1007/s10048-015-0444-2

Dogan, A. E., Hamid, S. M., Yildirim, A. D., Yildirim, Z., Sen, G., Riera, C. E., et al. (2022). PACT establishes a posttranscriptional brake on mitochondrial biogenesis by promoting the maturation of miR-181c. *J. Biol. Chem.* 298(7), 102050. doi:10.1016/j.jbc.2022.102050

Doimo, M., Desbats, M. A., Cerqua, C., Cassina, M., Trevisson, E., and Salviati, L. (2014). Genetics of coenzyme q10 deficiency. *Mol. Syndromol.* 5(3-4), 156–162. doi:10.1159/000362826

Dooley, H. C., Razi, M., Polson, H. E., Girardin, S. E., Wilson, M. I., and Tooze, S. A. (2014). WIPI2 links LC3 conjugation with PI3P, autophagosome formation, and pathogen clearance by recruiting Atg12-5-16L1. *Mol. Cell.* 55 (2), 238–252. doi:10.1016/j.molcel.2014.05.021

Doughan, A. K., Harrison, D. G., and Dikalov, S. I. (2008). Molecular mechanisms of angiotensin II-mediated mitochondrial dysfunction: Linking mitochondrial oxidative damage and vascular endothelial dysfunction. *Circ. Res.* 102 (4), 488–496. doi:10.1161/circresaha.107.162800

Druzhyna, N. M., Wilson, G. L., and LeDoux, S. P. (2008). Mitochondrial DNA repair in aging and disease. *Mech. Ageing Dev.* 129 (7-8), 383–390. doi:10.1016/j.mad.2008.03.002

Duan, M., Chen, H., Yin, L., Zhu, X., Novák, P., Lv, Y., et al. (2022). Mitochondrial apolipoprotein A-I binding protein alleviates atherosclerosis by regulating mitophagy and macrophage polarization. *Cell. Commun. Signal* 20 (1), 60. doi:10.1186/s12964-022-00858-8

Dubois-Deruy, E., Peugnet, V., Turkieh, A., and Pinet, F. (2020). Oxidative stress in cardiovascular diseases. *Antioxidants (Basel)* 9 (9), 864. doi:10.3390/antiox9090864

Dubucs, C., Aziza, J., Sartor, A., Heitz, F., Sevely, A., Sternberg, D., et al. (2023). Severe antenatal hypertrophic cardiomyopathy secondary to ACAD9-related mitochondrial complex I deficiency. *Mol. Syndromol.* 14 (2), 101–108. doi:10.1159/000526022

Duncan, J. G. (2011). Mitochondrial dysfunction in diabetic cardiomyopathy. *Biochim. Biophys. Acta* 1813 (7), 1351–1359. doi:10.1016/j.bbamcr.2011.01.014

Egan, D. F., Shackelford, D. B., Mihaylova, M. M., Gelino, S., Kohnz, R. A., Mair, W., et al. (2011). Phosphorylation of ULK1 (hATG1) by AMP-activated protein kinase connects energy sensing to mitophagy. *Science* 331 (6016), 456–461. doi:10.1126/science.1196371

El-Hattab, A. W., and Scaglia, F. (2013). Mitochondrial DNA depletion syndromes: Review and updates of genetic basis, manifestations, and therapeutic options. *Neurotherapeutics* 10 (2), 186–198. doi:10.1007/s13311-013-0177-6

Elgass, K., Pakay, J., Ryan, M. T., and Palmer, C. S. (2013). Recent advances into the understanding of mitochondrial fission. *Biochim. Biophys. Acta* 1833 (1), 150–161. doi:10.1016/j.bbamcr.2012.05.002

Fassone, E., and Rahman, S. (2012). Complex I deficiency: Clinical features, biochemistry and molecular genetics. *J. Med. Genet.* 49 (9), 578–590. doi:10.1136/jmedgenet-2012-101159

Fernández-Silva, P., Enriquez, J. A., and Montoya, J. (2003). Replication and transcription of mammalian mitochondrial DNA. *Exp. Physiol.* 88 (1), 41–56. doi:10.1113/eph8802514

Fernie, A. R., Carrari, F., and Sweetlove, L. J. (2004). Respiratory metabolism: Glycolysis, the TCA cycle and mitochondrial electron transport. *Curr. Opin. Plant Biol.* 7 (3), 254–261. doi:10.1016/j.pbi.2004.03.007

Flarsheim, C. E., Grupp, I. L., and Matlib, M. A. (1996). Mitochondrial dysfunction accompanies diastolic dysfunction in diabetic rat heart. *Am. J. Physiol.* 271 (2), H192–H202. doi:10.1152/ajpheart.1996.271.1.H192

Forkink, M., Smeitink, J. A., Brock, R., Willems, P. H., and Koopman, W. J. (2010). Detection and manipulation of mitochondrial reactive oxygen species in mammalian cells. *Biochim. Biophys. Acta* 1797 (6-7), 1034–1044. doi:10.1016/j.bbabio.2010.01.022

Forman, H. J., Zhang, H., and Rinna, A. (2009). Glutathione: Overview of its protective roles, measurement, and biosynthesis. *Mol. Asp. Med.* 30 (1-2), 1–12. doi:10.1016/j.mam.2008.08.006

Forte, M., Bianchi, F., Cotugno, M., Marchitti, S., De Falco, E., Raffa, S., et al. (2020). Pharmacological restoration of autophagy reduces hypertension-related stroke occurrence. *Autophagy* 16 (8), 1468–1481. doi:10.1080/15548627.2019.1687215

Forte, M., Schirone, L., Ameri, P., Basso, C., Catalucci, D., Modica, J., et al. (2021). The role of mitochondrial dynamics in cardiovascular diseases. *Br. J. Pharmacol.* 178 (10), 2060–2076. doi:10.1111/bph.15068

Friedman, J. R., Lackner, L. L., West, M., DiBenedetto, J. R., Nunnari, J., and Voeltz, G. K. (2011). ER tubules mark sites of mitochondrial division. *Science* 334 (6054), 358–362. doi:10.1126/science.1207385

Gaigg, B., Simbeni, R., Hrastnik, C., Paltauf, F., and Daum, G. (1995). Characterization of a microsomal subfraction associated with mitochondria of the yeast, *Saccharomyces cerevisiae*. Involvement in synthesis and import of phospholipids into mitochondria. *Biochim. Biophys. Acta* 1234 (2), 214–220. doi:10.1016/0005-2736(94)00287-y

Galluzzi, L., Kepp, O., Trojel-Hansen, C., and Kroemer, G. (2012). Mitochondrial control of cellular life, stress, and death. *Circ. Res.* 111 (9), 1198–1207. doi:10.1161/circresaha.112.268946

Galluzzi, L., Vitale, I., Aaronson, S. A., Abrams, J. M., Adam, D., Agostinis, P., et al. (2018). Molecular mechanisms of cell death: Recommendations of the nomenclature committee on cell death 2018. *Cell. Death Differ.* 25 (3), 486–541. doi:10.1038/s41418-017-0012-4

Galmiche, L., Serre, V., Beinat, M., Assouline, Z., Lebre, A. S., Chretien, D., et al. (2011). Exome sequencing identifies MRPL3 mutation in mitochondrial cardiomyopathy. *Hum. Mutat.* 32 (11), 1225–1231. doi:10.1002/humu.21562

Gálvez, A. S., Brunskill, E. W., Marreez, Y., Benner, B. J., Regula, K. M., Kirschenbaum, L. A., et al. (2006). Distinct pathways regulate proapoptotic Nix and BNip3 in cardiac stress. *J. Biol. Chem.* 281 (3), 1442–1448. doi:10.1074/jbc.M509056200

Georgakopoulos, N. D., Wells, G., and Campanella, M. (2017). The pharmacological regulation of cellular mitophagy. *Nat. Chem. Biol.* 13 (2), 136–146. doi:10.1038/nchembio.2287

Gerhart-Hines, Z., Rodgers, J. T., Bare, O., Lerin, C., Kim, S. H., Mostoslavsky, R., et al. (2007). Metabolic control of muscle mitochondrial function and fatty acid oxidation through SIRT1/PGC-1alpha. *Embo J.* 26 (7), 1913–1923. doi:10.1038/sj.emboj.7601633

Gimbrone, M. A., Jr., and García-Cardeña, G. (2016). Endothelial cell dysfunction and the pathobiology of atherosclerosis. *Circ. Res.* 118 (4), 620–636. doi:10.1161/circresaha.115.306301

Giorgi, C., Marchi, S., and Pinton, P. (2018). The machineries, regulation and cellular functions of mitochondrial calcium. *Nat. Rev. Mol. Cell. Biol.* 19 (11), 713–730. doi:10.1038/s41580-018-0052-8

Giorgio, M., Trinei, M., Migliaccio, E., and Pelicci, P. G. (2007). Hydrogen peroxide: A metabolic by-product or a common mediator of ageing signals? *Nat. Rev. Mol. Cell. Biol.* 8 (9), 722–728. doi:10.1038/nrm2240

Gisterå, A., and Hansson, G. K. (2017). The immunology of atherosclerosis. *Nat. Rev. Nephrol.* 13 (6), 368–380. doi:10.1038/nrneph.2017.51

Goffart, S., von Kleist-Retzow, J. C., and Wiesner, R. J. (2004). Regulation of mitochondrial proliferation in the heart: Power-plant failure contributes to cardiac failure in hypertrophy. *Cardiovasc Res.* 64 (2), 198–207. doi:10.1016/j.cardiores.2004.06.030

Gonçalves, V. F. (2019). Mitochondrial genetics. *Adv. Exp. Med. Biol.* 1158, 247–255. doi:10.1007/978-981-13-8367-0_13

Griendling, K. K., Camargo, L. L., Rios, F. J., Alves-Lopes, R., Montezano, A. C., and Touyz, R. M. (2021). Oxidative stress and hypertension. *Circ. Res.* 128 (7), 993–1020. doi:10.1161/circresaha.121.318063

Guillaume, M. P., Reumaux, H., and Dubos, F. (2018). Usefulness and safety of anakinra in refractory Kawasaki disease complicated by coronary artery aneurysm. *Cardiol. Young* 28 (5), 739–742. doi:10.1017/s1047951117002864

Gundewar, S., Calvert, J. W., Jha, S., Toedt-Pingel, I., Ji, S. Y., Nunez, D., et al. (2009). Activation of AMP-activated protein kinase by metformin improves left ventricular function and survival in heart failure. *Circ. Res.* 104 (3), 403–411. doi:10.1161/circresaha.108.190918

Guo, R., Gu, J., Zong, S., Wu, M., and Yang, M. (2018). Structure and mechanism of mitochondrial electron transport chain. *Biomed. J.* 41 (1), 9–20. doi:10.1016/j.bj.2017.12.001

Guo, R., Zong, S., Wu, M., Gu, J., and Yang, M. (2017). Architecture of human mitochondrial respiratory megacomplex I(2)III(2)IV(2). *Cell.* 170 (6), 1247–1257. doi:10.1016/j.cell.2017.07.050

Gustafsson Å, B., and Dorn, G. W., 2nd (2019). Evolving and expanding the roles of mitophagy as a homeostatic and pathogenic process. *Physiol. Rev.* 99 (1), 853–892. doi:10.1152/physrev.00005.2018

Hagen, C. M., Aidt, F. H., Havndrup, O., Hedley, P. L., Jespersgaard, C., Jensen, M., et al. (2013). MT-CYB mutations in hypertrophic cardiomyopathy. *Mol. Genet. Genomic Med.* 1 (1), 54–65. doi:10.1002/mgg3.5

Halestrap, A. P. (1999). The mitochondrial permeability transition: Its molecular mechanism and role in reperfusion injury. *Biochem. Soc. Symp.* 66, 181–203. doi:10.1042/bss0660181

Hall, A. R., Burke, N., Dongworth, R. K., and Hausenloy, D. J. (2014). Mitochondrial fusion and fission proteins: Novel therapeutic targets for combating cardiovascular disease. *Br. J. Pharmacol.* 171 (8), 1890–1906. doi:10.1111/bph.12516

Hamacher-Brady, A., Choe, S. C., Krijnse-Locker, J., and Brady, N. R. (2014). Intramitochondrial recruitment of endolysosomes mediates Smac degradation and constitutes a novel intrinsic apoptosis antagonizing function of XIAP E3 ligase. *Cell. Death Differ.* 21 (12), 1862–1876. doi:10.1038/cdd.2014.101

Han, D., Antunes, F., Canali, R., Rettori, D., and Cadenas, E. (2003). Voltage-dependent anion channels control the release of the superoxide anion from mitochondria to cytosol. *J. Biol. Chem.* 278 (8), 5557–5563. doi:10.1074/jbc.M210269200

Han, J., Dai, S., Zhong, L., Shi, X., Fan, X., Zhong, X., et al. (2022). GSDMD (gasdermin D) mediates pathological cardiac hypertrophy and generates a feed-forward amplification cascade via mitochondria-STING (stimulator of interferon genes) Axis. *Hypertension* 79 (11), 2505–2518. doi:10.1161/hypertensionaha.122.20004

Harper, J. W., Ordureau, A., and Heo, J. M. (2018). Building and decoding ubiquitin chains for mitophagy. *Nat. Rev. Mol. Cell. Biol.* 19 (2), 93–108. doi:10.1038/nrm.2017.129

Harrington, J. S., Ryter, S. W., Plataki, M., Price, D. R., and Choi, A. M. K. (2023). Mitochondria in health, disease, and aging. *Physiol. Rev.* 103, 2349–2422. doi:10.1152/physrev.00058.2021

Hoang, L. T., Shimizu, C., Ling, L., Naim, A. N., Khor, C. C., Tremoulet, A. H., et al. (2014). Global gene expression profiling identifies new therapeutic targets in acute Kawasaki disease. *Genome Med.* 6 (11), 541. doi:10.1186/s13073-014-0102-6

Hossain, M. A., Bhattacharjee, S., Armin, S. M., Qian, P., Xin, W., Li, H. Y., et al. (2015). Hydrogen peroxide priming modulates abiotic oxidative stress tolerance: Insights from ROS detoxification and scavenging. *Front. Plant Sci.* 6, 420. doi:10.3389/fpls.2015.00420

Hou, F., Sun, L., Zheng, H., Skaug, B., Jiang, Q. X., and Chen, Z. J. (2011). MAVS forms functional prion-like aggregates to activate and propagate antiviral innate immune response. *Cell.* 146 (3), 448–461. doi:10.1016/j.cell.2011.06.041

Hu, J., de Souza-Pinto, N. C., Haraguchi, K., Hogue, B. A., Jaruga, P., Greenberg, M. M., et al. (2005). Repair of formamidopyrimidines in DNA involves different glycosylases: Role of the OGG1, NTH1, and NEIL1 enzymes. *J. Biol. Chem.* 280 (49), 40544–40551. doi:10.1074/jbc.M508772200

Hu, Y. F., Chen, Y. J., Lin, Y. J., and Chen, S. A. (2015). Inflammation and the pathogenesis of atrial fibrillation. *Nat. Rev. Cardiol.* 12 (4), 230–243. doi:10.1038/nrcardio.2015.2

Huang, F. C., Huang, Y. H., Kuo, H. C., and Li, S. C. (2020). Identifying downregulation of autophagy markers in Kawasaki disease. *Child. (Basel)* 7 (10), E166. doi:10.3390/children7100166

Huang, W., Choi, W., Hu, W., Mi, N., Guo, Q., Ma, M., et al. (2012). Crystal structure and biochemical analyses reveal Beclin 1 as a novel membrane binding protein. *Cell. Res.* 22 (3), 473–489. doi:10.1038/cr.2012.24

Ikeda, Y., Shirakabe, A., Maejima, Y., Zhai, P., Sciarretta, S., Toli, J., et al. (2015). Endogenous Drp1 mediates mitochondrial autophagy and protects the heart against energy stress. *Circ. Res.* 116 (2), 264–278. doi:10.1161/circresaha.116.303356

Ishihara, N., Eura, Y., and Mihara, K. (2004). Mitofusin 1 and 2 play distinct roles in mitochondrial fusion reactions via GTPase activity. *J. Cell. Sci.* 117 (26), 6535–6546. doi:10.1242/jcs.01565

Iwata, S., Lee, J. W., Okada, K., Lee, J. K., Iwata, M., Rasmussen, B., et al. (1998). Complete structure of the 11-subunit bovine mitochondrial cytochrome bc1 complex. *Science* 281 (5373), 64–71. doi:10.1126/science.281.5373.64

Jacobs, A. L., and Schär, P. (2012). DNA glycosylases: In DNA repair and beyond. *Chromosoma* 121 (1), 1–20. doi:10.1007/s00412-011-0347-4

Jäger, S., Handschin, C., St-Pierre, J., and Spiegelman, B. M. (2007). AMP-activated protein kinase (AMPK) action in skeletal muscle via direct phosphorylation of PGC-1alpha. *Proc. Natl. Acad. Sci. U. S. A.* 104 (29), 12017–12022. doi:10.1073/pnas.0705070104

Jahani-Asl, A., Cheung, E. C., Neuspiel, M., MacLaurin, J. G., Fortin, A., Park, D. S., et al. (2007). Mitofusin 2 protects cerebellar granule neurons against injury-induced cell death. *J. Biol. Chem.* 282 (33), 23788–23798. doi:10.1074/jbc.M703812200

Jain-Ghai, S., Cameron, J. M., Al Maawali, A., Blaser, S., MacKay, N., Robinson, B., et al. (2013). Complex II deficiency--a case report and review of the literature. *Am. J. Med. Genet. A* 161a (2), 285–294. doi:10.1002/ajmg.a.35714

James, A. M., Sharpley, M. S., Manas, A. R., Frerman, F. E., Hirst, J., Smith, R. A., et al. (2007). Interaction of the mitochondria-targeted antioxidant MitoQ with phospholipid bilayers and ubiquinone oxidoreductases. *J. Biol. Chem.* 282 (20), 14708–14718. doi:10.1074/jbc.M611463200

Jia, G., Hill, M. A., and Sowers, J. R. (2018). Diabetic cardiomyopathy: An update of mechanisms contributing to this clinical entity. *Circ. Res.* 122 (4), 624–638. doi:10.1161/circresaha.117.311586

Jin, L., Geng, L., Ying, L., Shu, L., Ye, K., Yang, R., et al. (2022a). FGF21-Sirtuin 3 Axis confers the protective effects of exercise against diabetic cardiomyopathy by governing mitochondrial integrity. *Circulation* 146 (20), 1537–1557. doi:10.1161/circulationaha.122.059631

Jin, Q., Li, R., Hu, N., Xin, T., Zhu, P., Hu, S., et al. (2018). DUSP1 alleviates cardiac ischemia/reperfusion injury by suppressing the Mff-required mitochondrial fission and Bnip3-related mitophagy via the JNK pathways. *Redox Biol.* 14, 576–587. doi:10.1016/j.redox.2017.11.004

Jin, Y., Liu, Y., Xu, L., Xu, J., Xiong, Y., Peng, Y., et al. (2022b). Novel role for caspase 1 inhibitor VX765 in suppressing NLRP3 inflammasome assembly and atherosclerosis via promoting mitophagy and efferocytosis. *Cell. Death Dis.* 13 (5), 512. doi:10.1038/s41419-022-04966-8

Kane, A. E., and Sinclair, D. A. (2018). Sirtuins and NAD(+) in the development and treatment of metabolic and cardiovascular diseases. *Circ. Res.* 123 (7), 868–885. doi:10.1161/circresaha.118.312498

Kawasaki, T., Kosaki, F., Okawa, S., Shigematsu, I., and Yanagawa, H. (1974). A new infantile acute febrile mucocutaneous lymph node syndrome (MLNS) prevailing in Japan. *Pediatrics* 54 (3), 271–276. doi:10.1542/peds.54.3.271

Kayagaki, N., Stowe, I. B., Lee, B. L., O'Rourke, K., Anderson, K., Warming, S., et al. (2015). Caspase-11 cleaves gasdermin D for non-canonical inflammasome signalling. *Nature* 526 (7575), 666–671. doi:10.1038/nature15541

Kazak, L., Reyes, A., and Holt, I. J. (2012). Minimizing the damage: Repair pathways keep mitochondrial DNA intact. *Nat. Rev. Mol. Cell. Biol.* 13 (10), 659–671. doi:10.1038/nrm3439

Kho, C., Lee, A., and Hajjar, R. J. (2012). Altered sarcoplasmic reticulum calcium cycling--targets for heart failure therapy. *Nat. Rev. Cardiol.* 9 (12), 717–733. doi:10.1038/nrcardio.2012.145

Khwaja, B., Thankam, F. G., and Agrawal, D. K. (2021). Mitochondrial DAMPs and altered mitochondrial dynamics in OxLDL burden in atherosclerosis. *Mol. Cell. Biochem.* 476 (4), 1915–1928. doi:10.1007/s11010-021-04061-0

Killackey, S. A., Philpott, D. J., and Girardin, S. E. (2020). Mitophagy pathways in health and disease. *J. Cell. Biol.* 219 (11), e202004029. doi:10.1083/jcb.202004029

Kim, J. C., Pérez-Hernández, M., Alvarado, F. J., Maurya, S. R., Montnach, J., Yin, Y., et al. (2019). Disruption of Ca(2+)(i) homeostasis and connexin 43 hemichannel function in the right ventricle precedes overt arrhythmogenic cardiomyopathy in plakophilin-2-deficient mice. *Circulation* 140 (12), 1015–1030. doi:10.1161/circulationaha.119.039710

Kirkman, H. N., and Gaetani, G. F. (2007). Mammalian catalase: A venerable enzyme with new mysteries. *Trends Biochem. Sci.* 32 (1), 44–50. doi:10.1016/j.tibs.2006.11.003

Kocatürk, B., Lee, Y., Nosaka, N., Abe, M., Martinon, D., Lane, M. E., et al. (2023). Platelets exacerbate cardiovascular inflammation in a murine model of Kawasaki disease vasculitis. *JCI Insight* 8 (14), e169855. doi:10.1172/jci.insight.169855

Koné-Paut, I., Tellier, S., Belot, A., Brochard, K., Guitton, C., Marie, I., et al. (2021). Phase II open label study of anakinra in intravenous immunoglobulin-resistant Kawasaki disease. *Arthritis Rheumatol.* 73 (1), 151–161. doi:10.1002/art.41481

Krahn, A. D., Wilde, A. A. M., Calkins, H., La Gerche, A., Cadrin-Tourigny, J., Roberts, J. D., et al. (2022). Arrhythmogenic right ventricular cardiomyopathy. *JACC Clin. Electrophysiol.* 8 (4), 533–553. doi:10.1016/j.jacep.2021.12.002

Krokan, H. E., and Bjørås, M. (2013). Base excision repair. *Cold Spring Harb. Perspect. Biol.* 5 (4), a012583. doi:10.1101/cshperspect.a012583

Kubánek, M., Schimerová, T., Piherová, L., Brodehl, A., Krebsová, A., Ratnavadivel, S., et al. (2020). Desminopathy: Novel desmin variants, a new cardiac phenotype, and further evidence for secondary mitochondrial dysfunction. *J. Clin. Med.* 9 (4), 937. doi:10.3390/jcm9040937

Kubli, D. A., Zhang, X., Lee, Y., Hanna, R. A., Quinsay, M. N., Nguyen, C. K., et al. (2013). Parkin protein deficiency exacerbates cardiac injury and reduces survival following myocardial infarction. *J. Biol. Chem.* 288 (2), 915–926. doi:10.1074/jbc.M112.411363

Kukidome, D., Nishikawa, T., Sonoda, K., Imoto, K., Fujisawa, K., Yano, M., et al. (2006). Activation of AMP-activated protein kinase reduces hyperglycemia-induced mitochondrial reactive oxygen species production and promotes mitochondrial biogenesis in human umbilical vein endothelial cells. *Diabetes* 55 (1), 120–127. doi:10.2337/diabetes.55.01.06.db05-0943

Kuwana, T., Bouchier-Hayes, L., Chipuk, J. E., Bonzon, C., Sullivan, B. A., Green, D. R., et al. (2005). BH3 domains of BH3-only proteins differentially regulate Bax-mediated mitochondrial membrane permeabilization both directly and indirectly. *Mol. Cell.* 17 (4), 525–535. doi:10.1016/j.molcel.2005.02.003

Kwon, Y. T., and Ciechanover, A. (2017). The ubiquitin code in the ubiquitin-proteasome system and autophagy. *Trends Biochem. Sci.* 42 (11), 873–886. doi:10.1016/j.tibs.2017.09.002

Kwong, J. Q., and Molkentin, J. D. (2015). Physiological and pathological roles of the mitochondrial permeability transition pore in the heart. *Cell. Metab.* 21 (2), 206–214. doi:10.1016/j.cmet.2014.12.001

Lagouge, M., Argmann, C., Gerhart-Hines, Z., Meziane, H., Lerin, C., Daussin, F., et al. (2006). Resveratrol improves mitochondrial function and protects against metabolic disease by activating SIRT1 and PGC-1alpha. *Cell.* 127 (6), 1109–1122. doi:10.1016/j.cell.2006.11.013

Lahera, V., de Las Heras, N., López-Farré, A., Manucha, W., and Ferder, L. (2017). Role of mitochondrial dysfunction in hypertension and obesity. *Curr. Hypertens. Rep.* 19 (2), 11. doi:10.1007/s11906-017-0710-9

Lai, L., and Qiu, H. (2020). The physiological and pathological roles of mitochondrial calcium uptake in heart. *Int. J. Mol. Sci.* 21 (20), 7689. doi:10.3390/ijms21207689

Laker, R. C., Drake, J. C., Wilson, R. J., Lira, V. A., Lewellen, B. M., Ryall, K. A., et al. (2017). Ampk phosphorylation of Ulk1 is required for targeting of mitochondria to lysosomes in exercise-induced mitophagy. *Nat. Commun.* 8 (1), 548. doi:10.1038/s41467-017-00520-9

Lambertucci, R. H., Hirabara, S. M., Silveira Ldos, R., Levada-Pires, A. C., Curi, R., and Pithon-Curi, T. C. (2008). Palmitate increases superoxide production through mitochondrial electron transport chain and NADPH oxidase activity in skeletal muscle cells. *J. Cell. Physiol.* 216 (3), 796–804. doi:10.1002/jcp.21463

Lampert, M. A., Orogo, A. M., Najor, R. H., Hammerling, B. C., Leon, L. J., Wang, B. J., et al. (2019). BNIP3L/NIX and FUNDC1-mediated mitophagy is required for mitochondrial network remodeling during cardiac progenitor cell differentiation. *Autophagy* 15 (7), 1182–1198. doi:10.1080/15548627.2019.1580095

Lazarou, M., Jin, S. M., Kane, L. A., and Youle, R. J. (2012). Role of PINK1 binding to the TOM complex and alternate intracellular membranes in recruitment and activation of the E3 ligase Parkin. *Dev. Cell.* 22 (2), 320–333. doi:10.1016/j.devcel.2011.12.014

Lee, Y., Schulte, D. J., Shimada, K., Chen, S., Crother, T. R., Chiba, N., et al. (2012). Interleukin-1β is crucial for the induction of coronary artery inflammation in a mouse model of Kawasaki disease. *Circulation* 125 (12), 1542–1550. doi:10.1161/circulationaha.111.072769

Lee, Y., Wakita, D., Dagvadorj, J., Shimada, K., Chen, S., Huang, G., et al. (2015). IL-1 signaling is critically required in stromal cells in Kawasaki disease vasculitis mouse model: Role of both IL-1α and IL-1β. *Arterioscler. Thromb. Vasc. Biol.* 35 (12), 2605–2616. doi:10.1161/atvbaha.115.306475

Lennicke, C., and Cochemé, H. M. (2021). Redox metabolism: ROS as specific molecular regulators of cell signaling and function. *Mol. Cell.* 81 (18), 3691–3707. doi:10.1016/j.molcel.2021.08.018

Levin, M., Holland, P. C., Nokes, T. J., Novelli, V., Mola, M., Levinsky, R. J., et al. (1985). Platelet immune complex interaction in pathogenesis of Kawasaki disease and childhood polyarteritis. *Br. Med. J. Clin. Res. Ed.* 290 (6480), 1456–1460. doi:10.1136/bmj.290.6480.1456

Levy, D., Garrison, R. J., Savage, D. D., Kannel, W. B., and Castelli, W. P. (1990). Prognostic implications of echocardiographically determined left ventricular mass in the Framingham Heart Study. *N. Engl. J. Med.* 322 (22), 1561–1566. doi:10.1056/nejm199005313222203

Li, D., Sun, Y., Zhuang, Q., Song, Y., Wu, B., Jia, Z., et al. (2019). Mitochondrial dysfunction caused by m.2336T>C mutation with hypertrophic cardiomyopathy in cybrid cell lines. *Mitochondrion* 46, 313–320. doi:10.1016/j.mito.2018.08.005

Li, E., Li, X., Huang, J., Xu, C., Liang, Q., Ren, K., et al. (2020). BMAL1 regulates mitochondrial fission and mitophagy through mitochondrial protein BNIP3 and is critical in the development of dilated cardiomyopathy. *Protein Cell.* 11 (9), 661–679. doi:10.1007/s13238-020-00713-x

Li, H., Zheng, L., Mo, Y., Gong, Q., Jiang, A., and Zhao, J. (2016). Voltage-dependent anion channel 1(VDAC1) participates the apoptosis of the mitochondrial dysfunction in desminopathy. *PLoS One* 11 (12), e0167908. doi:10.1371/journal.pone.0167908

Li, P., Nijhawan, D., Budihardjo, I., Srinivasula, S. M., Ahmad, M., Alnemri, E. S., et al. (1997). Cytochrome c and dATP-dependent formation of Apaf-1/caspase-9 complex initiates an apoptotic protease cascade. *Cell.* 91 (4), 479–489. doi:10.1016/s0092-8674(00)80434-1

Li, S., Chen, J., Liu, M., Chen, Y., Wu, Y., Li, Q., et al. (2021). Protective effect of HINT2 on mitochondrial function via repressing MCU complex activation attenuates cardiac microvascular ischemia-reperfusion injury. *Basic Res. Cardiol.* 116 (1), 65. doi:10.1007/s00395-021-00905-4

Liang, H. L., Sedlic, F., Bosnjak, Z., and Nilakantan, V. (2010). SOD1 and MitoTEMPO partially prevent mitochondrial permeability transition pore opening, necrosis, and mitochondrial apoptosis after ATP depletion recovery. *Free Radic. Biol. Med.* 49 (10), 1550–1560. doi:10.1016/j.freeradbiomed.2010.08.018

Liesa, M., and Shirihai, O. S. (2013). Mitochondrial dynamics in the regulation of nutrient utilization and energy expenditure. *Cell. Metab.* 17 (4), 491–506. doi:10.1016/j.cmet.2013.03.002

Lin, T. K., Lin, K. J., Lin, K. L., Liou, C. W., Chen, S. D., Chuang, Y. C., et al. (2020). When friendship turns sour: Effective communication between mitochondria and intracellular organelles in Parkinson's disease. *Front. Cell. Dev. Biol.* 8, 607392. doi:10.3389/fcell.2020.607392

Little, J. P., Safdar, A., Cermak, N., Tarnopolsky, M. A., and Gibala, M. J. (2010). Acute endurance exercise increases the nuclear abundance of PGC-1alpha in trained human skeletal muscle. *Am. J. Physiol. Regul. Integr. Comp. Physiol.* 298 (4), R912–R917. doi:10.1152/ajpregu.00409.2009

Liu, J., Dai, Q., Chen, J., Durrant, D., Freeman, A., Liu, T., et al. (2003). Phospholipid scramblase 3 controls mitochondrial structure, function, and apoptotic response. *Mol. Cancer Res.* 1 (12), 892–902.

Liu, R., Xu, C., Zhang, W., Cao, Y., Ye, J., Li, B., et al. (2022). FUNDC1-mediated mitophagy and HIF1α activation drives pulmonary hypertension during hypoxia. *Cell. Death Dis.* 13 (7), 634. doi:10.1038/s41419-022-05091-2

Liu, S., Bai, Y., Huang, J., Zhao, H., Zhang, X., Hu, S., et al. (2013). Do mitochondria contribute to left ventricular non-compaction cardiomyopathy? New findings from myocardium of patients with left ventricular non-compaction cardiomyopathy. *Mol. Genet. Metab.* 109 (1), 100–106. doi:10.1016/j.ymgme.2013.02.004

Liu, T., Zhang, L., Joo, D., and Sun, S. C. (2017). NF-κB signaling in inflammation. *Signal Transduct. Target Ther.* 2, 17023-. doi:10.1038/sigtrans.2017.23

Liu, X., and Hajnóczky, G. (2011). Altered fusion dynamics underlie unique morphological changes in mitochondria during hypoxia-reoxygenation stress. *Cell. Death Differ.* 18 (10), 1561–1572. doi:10.1038/cdd.2011.13

Liu, Y., Fiskum, G., and Schubert, D. (2002). Generation of reactive oxygen species by the mitochondrial electron transport chain. *J. Neurochem.* 80 (5), 780–787. doi:10.1046/j.0022-3042.2002.00744.x

Liu, Z., Song, Y., Li, D., He, X., Li, S., Wu, B., et al. (2014). The novel mitochondrial 16S rRNA 2336T>C mutation is associated with hypertrophic cardiomyopathy. *J. Med. Genet.* 51 (3), 176–184. doi:10.1136/jmedgenet-2013-101818

Lomonosova, E., and Chinnadurai, G. (2008). BH3-only proteins in apoptosis and beyond: An overview. *Oncogene* 27(1), S2–S19. doi:10.1038/onc.2009.39

Lopez-Crisosto, C., Pennanen, C., Vasquez-Trincado, C., Morales, P. E., Bravo-Sagua, R., Quest, A. F. G., et al. (2017). Sarcoplasmic reticulum-mitochondria communication in cardiovascular pathophysiology. *Nat. Rev. Cardiol.* 14 (6), 342–360. doi:10.1038/nrcardio.2017.23

Lorenzon, A., Beffagna, G., Bauce, B., De Bortoli, M., Li Mura, I. E., Calore, M., et al. (2013). Desmin mutations and arrhythmogenic right ventricular cardiomyopathy. *Am. J. Cardiol.* 111 (3), 400–405. doi:10.1016/j.amjcard.2012.10.017

Lu, L., Bonham, C. A., Chambers, F. G., Watkins, S. C., Hoffman, R. A., Simmons, R. L., et al. (1996). Induction of nitric oxide synthase in mouse dendritic cells by IFN-gamma, endotoxin, and interaction with allogeneic T cells: Nitric oxide production is associated with dendritic cell apoptosis. *J. Immunol.* 157 (8), 3577–3586. doi:10.4049/jimmunol.157.8.3577

Lugus, J. J., Ngoh, G. A., Bachschmid, M. M., and Walsh, K. (2011). Mitofusins are required for angiogenic function and modulate different signaling pathways in cultured endothelial cells. *J. Mol. Cell. Cardiol.* 51 (6), 885–893. doi:10.1016/j.yjmcc.2011.07.023

Ma, K., Chen, G., Li, W., Kepp, O., Zhu, Y., and Chen, Q. (2020). Mitophagy, mitochondrial homeostasis, and cell fate. *Front. Cell. Dev. Biol.* 8, 467. doi:10.3389/fcell.2020.00467

Ma, T., Huang, X., Zheng, H., Huang, G., Li, W., Liu, X., et al. (2021). SFRP2 improves mitochondrial dynamics and mitochondrial biogenesis, oxidative stress, and apoptosis in diabetic cardiomyopathy. *Oxid. Med. Cell. Longev.* 2021, 9265016. doi:10.1155/2021/9265016

MacKenzie, J. A., and Payne, R. M. (2007). Mitochondrial protein import and human health and disease. *Biochim. Biophys. Acta* 1772 (5), 509–523. doi:10.1016/j.bbadis.2006.12.002

Madeira, V. M. C. (2018). Overview of mitochondrial bioenergetics. *Methods Mol. Biol.* 1782, 1–6. doi:10.1007/978-1-4939-7831-1_1

Magyar, K., Halmosi, R., Palfi, A., Feher, G., Czopf, L., Fulop, A., et al. (2012). Cardioprotection by resveratrol: A human clinical trial in patients with stable coronary artery disease. *Clin. Hemorheol. Microcirc.* 50 (3), 179–187. doi:10.3233/ch-2011-1424

Malka, F., Guillery, O., Cifuentes-Diaz, C., Guillou, E., Belenguer, P., Lombès, A., et al. (2005). Separate fusion of outer and inner mitochondrial membranes. *EMBO Rep.* 6 (9), 853–859. doi:10.1038/sj.embor.7400488

Maneechote, C., Palee, S., Kerdphoo, S., Jaiwongkam, T., Chattipakorn, S. C., and Chattipakorn, N. (2019). Balancing mitochondrial dynamics via increasing mitochondrial fusion attenuates infarct size and left ventricular dysfunction in rats with cardiac ischemia/reperfusion injury. *Clin. Sci. (Lond)* 133 (3), 497–513. doi:10.1042/cs20190014

Mantle, D., Millichap, L., Castro-Marrero, J., and Hargreaves, I. P. (2023). Primary coenzyme Q10 deficiency: An update. *Antioxidants (Basel)* 12 (8), 1652. doi:10.3390/antiox12081652

Marek-Iannucci, S., Ozdemir, A. B., Moreira, D., Gomez, A. C., Lane, M., Porritt, R. A., et al. (2021). Autophagy-mitophagy induction attenuates cardiovascular inflammation in a murine model of Kawasaki disease vasculitis. *JCI Insight* 6 (18), e151981. doi:10.1172/jci.insight.151981

Marek-Iannucci, S., Yildirim, A. D., Hamid, S. M., Ozdemir, A. B., Gomez, A. C., Kocatürk, B., et al. (2022). Targeting IRE1 endoribonuclease activity alleviates cardiovascular lesions in a murine model of Kawasaki disease vasculitis. *JCI Insight* 7 (6), e157203. doi:10.1172/jci.insight.157203

Martens, C. R., Denman, B. A., Mazzo, M. R., Armstrong, M. L., Reisdorph, N., McQueen, M. B., et al. (2018). Chronic nicotinamide riboside supplementation is well-tolerated and elevates NAD(+) in healthy middle-aged and older adults. *Nat. Commun.* 9 (1), 1286. doi:10.1038/s41467-018-03421-7

Martin, A. S., Abraham, D. M., Hershberger, K. A., Bhatt, D. P., Mao, L., Cui, H., et al. (2017). Nicotinamide mononucleotide requires SIRT3 to improve cardiac function and bioenergetics in a Friedreich's ataxia cardiomyopathy model. *JCI Insight* 2 (14), e93885. doi:10.1172/jci.insight.93885

Martínez-Reyes, I., and Chandel, N. S. (2020). Mitochondrial TCA cycle metabolites control physiology and disease. *Nat. Commun.* 11 (1), 102. doi:10.1038/s41467-019-13668-3

Martínez-Reyes, I., Diebold, L. P., Kong, H., Schieber, M., Huang, H., Hensley, C. T., et al. (2016). TCA cycle and mitochondrial membrane potential are necessary for diverse biological functions. *Mol. Cell.* 61 (2), 199–209. doi:10.1016/j.molcel.2015.12.002

McArthur, K., Whitehead, L. W., Heddleston, J. M., Li, L., Padman, B. S., Oorschot, V., et al. (2018). BAK/BAX macropores facilitate mitochondrial herniation and mtDNA efflux during apoptosis. *Science* 359 (6378), eaao6047. doi:10.1126/science.aao6047

McCrindle, B. W., Rowley, A. H., Newburger, J. W., Burns, J. C., Bolger, A. F., Gewitz, M., et al. (2017). Diagnosis, treatment, and long-term management of Kawasaki disease: A scientific statement for health professionals from the American heart association. *Circulation* 135 (17), e927–e999. doi:10.1161/cir.0000000000000484

McDonnell, E., Crown, S. B., Fox, D. B., Kitir, B., Ilkayeva, O. R., Olsen, C. A., et al. (2016). Lipids reprogram metabolism to become a major carbon source for histone acetylation. *Cell. Rep.* 17 (6), 1463–1472. doi:10.1016/j.celrep.2016.10.012

McKenna, W. J., Maron, B. J., and Thiene, G. (2017). Classification, epidemiology, and global burden of cardiomyopathies. *Circ. Res.* 121 (7), 722–730. doi:10.1161/circresaha.117.309711

McWilliams, T. G., Prescott, A. R., Montava-Garriga, L., Ball, G., Singh, F., Barini, E., et al. (2018). Basal mitophagy occurs independently of PINK1 in mouse tissues of high metabolic demand. *Cell. Metab.* 27 (2), 439–449. doi:10.1016/j.cmet.2017.12.008

Mehta, M. M., Weinberg, S. E., and Chandel, N. S. (2017). Mitochondrial control of immunity: Beyond ATP. *Nat. Rev. Immunol.* 17 (10), 608–620. doi:10.1038/nri.2017.66

Miller, K. N., Clark, J. P., and Anderson, R. M. (2019). Mitochondrial regulator PGC-1a-Modulating the modulator. *Curr. Opin. Endocr. Metab. Res.* 5, 37–44. doi:10.1016/j.coemr.2019.02.002

Moldoveanu, T., Follis, A. V., Kriwacki, R. W., and Green, D. R. (2014). Many players in BCL-2 family affairs. *Trends Biochem. Sci.* 39 (3), 101–111. doi:10.1016/j.tibs.2013.12.006

Montaigne, D., Marechal, X., Coisne, A., Debry, N., Modine, T., Fayad, G., et al. (2014). Myocardial contractile dysfunction is associated with impaired mitochondrial function and dynamics in type 2 diabetic but not in obese patients. *Circulation* 130 (7), 554–564. doi:10.1161/circulationaha.113.008476

Moussaieff, A., Rouleau, M., Kitsberg, D., Cohen, M., Levy, G., Barasch, D., et al. (2015). Glycolysis-mediated changes in acetyl-CoA and histone acetylation control the early differentiation of embryonic stem cells. *Cell. Metab.* 21 (3), 392–402. doi:10.1016/j.cmet.2015.02.002

Murphy, E., Ardehali, H., Balaban, R. S., DiLisa, F., Dorn, G. W., 2nd, Kitsis, R. N., et al. (2016). Mitochondrial function, Biology, and role in disease: A scientific statement from the American heart association. *Circ. Res.* 118 (12), 1960–1991. doi:10.1161/res.0000000000000104

Murphy, E., and Steenbergen, C. (2008). Mechanisms underlying acute protection from cardiac ischemia-reperfusion injury. *Physiol. Rev.* 88 (2), 581–609. doi:10.1152/physrev.00024.2007

Murphy, M. P. (2009). How mitochondria produce reactive oxygen species. *Biochem. J.* 417 (1), 1–13. doi:10.1042/bj20081386

Murphy, M. P., and Smith, R. A. (2007). Targeting antioxidants to mitochondria by conjugation to lipophilic cations. *Annu. Rev. Pharmacol. Toxicol.* 47, 629–656. doi:10.1146/annurev.pharmtox.47.120505.105110

Muto, T., Nakamura, N., Masuda, Y., Numoto, S., Kodama, S., Miyamoto, R., et al. (2022). Serum free carnitine levels in children with Kawasaki disease. *Pediatr. Int.* 64 (1), e14849. doi:10.1111/ped.14849

Nahapetyan, H., Moulis, M., Grousset, E., Faccini, J., Grazide, M. H., Mucher, E., et al. (2019). Altered mitochondrial quality control in Atg7-deficient VSMCs promotes enhanced apoptosis and is linked to unstable atherosclerotic plaque phenotype. *Cell. Death Dis.* 10 (2), 119. doi:10.1038/s41419-019-1400-0

Nakamura, M., and Sadoshima, J. (2018). Mechanisms of physiological and pathological cardiac hypertrophy. *Nat. Rev. Cardiol.* 15 (7), 387–407. doi:10.1038/s41569-018-0007-y

Nakatogawa, H. (2013). Two ubiquitin-like conjugation systems that mediate membrane formation during autophagy. *Essays Biochem.* 55, 39–50. doi:10.1042/bse0550039

Narendra, D., Kane, L. A., Hauser, D. N., Fearnley, I. M., and Youle, R. J. (2010). p62/SQSTM1 is required for Parkin-induced mitochondrial clustering but not mitophagy; VDAC1 is dispensable for both. *Autophagy* 6 (8), 1090–1106. doi:10.4161/auto.6.8.13426

Newburger, J. W., Takahashi, M., and Burns, J. C. (2016). Kawasaki disease. *J. Am. Coll. Cardiol.* 67 (14), 1738–1749. doi:10.1016/j.jacc.2015.12.073

Ng, M. Y. W., Wai, T., and Simonsen, A. (2021). Quality control of the mitochondrion. *Dev. Cell.* 56 (7), 881–905. doi:10.1016/j.devcel.2021.02.009

Nguyen, T. N., Padman, B. S., and Lazarou, M. (2016). Deciphering the molecular signals of PINK1/parkin mitophagy. *Trends Cell. Biol.* 26 (10), 733–744. doi:10.1016/j.tcb.2016.05.008

Ni, H. M., Williams, J. A., and Ding, W. X. (2015). Mitochondrial dynamics and mitochondrial quality control. *Redox Biol.* 4, 6–13. doi:10.1016/j.redox.2014.11.006

Ni, R., Cao, T., Xiong, S., Ma, J., Fan, G. C., Lacefield, J. C., et al. (2016). Therapeutic inhibition of mitochondrial reactive oxygen species with mito-TEMPO reduces diabetic cardiomyopathy. *Free Radic. Biol. Med.* 90, 12–23. doi:10.1016/j.freeradbiomed.2015.11.013

Niedra, E., Chahal, N., Manlhiot, C., Yeung, R. S., and McCrindle, B. W. (2014). Atorvastatin safety in Kawasaki disease patients with coronary artery aneurysms. *Pediatr. Cardiol.* 35 (1), 89–92. doi:10.1007/s00246-013-0746-9

Nisoli, E., Tonello, C., Cardile, A., Cozzi, V., Bracale, R., Tedesco, L., et al. (2005). Calorie restriction promotes mitochondrial biogenesis by inducing the expression of eNOS. *Science* 310 (5746), 314–317. doi:10.1126/science.1117728

Nollet, E. E., Duursma, I., Rozenbaum, A., Eggelbusch, M., Wüst, R. C. I., Schoonvelde, S. A. C., et al. (2023). Mitochondrial dysfunction in human hypertrophic cardiomyopathy is linked to cardiomyocyte architecture disruption and corrected by improving NADH-driven mitochondrial respiration. *Eur. Heart J.* 44 (13), 1170–1185. doi:10.1093/eurheartj/ehad028

Noorman, M., Hakim, S., Kessler, E., Groeneweg, J. A., Cox, M. G., Asimaki, A., et al. (2013). Remodeling of the cardiac sodium channel, connexin43, and plakoglobin at the intercalated disk in patients with arrhythmogenic cardiomyopathy. *Heart rhythm.* 10 (3), 412–419. doi:10.1016/j.hrthm.2012.11.018

Okatsu, K., Uno, M., Koyano, F., Go, E., Kimura, M., Oka, T., et al. (2013). A dimeric PINK1-containing complex on depolarized mitochondria stimulates Parkin recruitment. *J. Biol. Chem.* 288 (51), 36372–36384. doi:10.1074/jbc.M113.509653

Olichon, A., Elachouri, G., Baricault, L., Delettre, C., Belenguer, P., and Lenaers, G. (2007). OPA1 alternate splicing uncouples an evolutionary conserved function in mitochondrial fusion from a vertebrate restricted function in apoptosis. *Cell. Death Differ.* 14 (4), 682–692. doi:10.1038/sj.cdd.4402048

Oliver, D. M. A., and Reddy, P. H. (2019). Small molecules as therapeutic drugs for Alzheimer's disease. *Mol. Cell. Neurosci.* 96, 47–62. doi:10.1016/j.mcn.2019.03.001

Onat, U. I., Yildirim, A. D., Tufanli, Ö., Çimen, I., Kocatürk, B., Veli, Z., et al. (2019). Intercepting the lipid-induced integrated stress response reduces atherosclerosis. *J. Am. Coll. Cardiol.* 73 (10), 1149–1169. doi:10.1016/j.jacc.2018.12.055

Ong, S. B., and Hausenloy, D. J. (2010). Mitochondrial morphology and cardiovascular disease. *Cardiovasc Res.* 88 (1), 16–29. doi:10.1093/cvr/cvq237

Onoue, K., Jofuku, A., Ban-Ishihara, R., Ishihara, T., Maeda, M., Koshiba, T., et al. (2013). Fis1 acts as a mitochondrial recruitment factor for TBC1D15 that is involved in regulation of mitochondrial morphology. *J. Cell. Sci.* 126 (1), 176–185. doi:10.1242/jcs.111211

Ordureau, A., Sarraf, S. A., Duda, D. M., Heo, J. M., Jedrychowski, M. P., Sviderskiy, V. O., et al. (2014). Quantitative proteomics reveal a feedforward mechanism for mitochondrial PARKIN translocation and ubiquitin chain synthesis. *Mol. Cell.* 56 (3), 360–375. doi:10.1016/j.molcel.2014.09.007

Otera, H., Ishihara, N., and Mihara, K. (2013). New insights into the function and regulation of mitochondrial fission. *Biochim. Biophys. Acta* 1833 (5), 1256–1268. doi:10.1016/j.bbamcr.2013.02.002

Otten, E., Asimaki, A., Maass, A., van Langen, I. M., van der Wal, A., de Jonge, N., et al. (2010). Desmin mutations as a cause of right ventricular heart failure affect the intercalated disks. *Heart rhythm.* 7 (8), 1058–1064. doi:10.1016/j.hrthm.2010.04.023

Palmer, C. S., Osellame, L. D., Laine, D., Koutsopoulos, O. S., Frazier, A. E., and Ryan, M. T. (2011). MiD49 and MiD51, new components of the mitochondrial fission machinery. *EMBO Rep.* 12 (6), 565–573. doi:10.1038/embor.2011.54

Pan, L., Li, Y., Jia, L., Qin, Y., Qi, G., Cheng, J., et al. (2012). Cathepsin S deficiency results in abnormal accumulation of autophagosomes in macrophages and enhances Ang II-induced cardiac inflammation. *PLoS One* 7 (4), e35315. doi:10.1371/journal.pone.0035315

Papanicolaou, K. N., Ngoh, G. A., Dabkowski, E. R., O'Connell, K. A., Ribeiro, R. F., Jr., Stanley, W. C., et al. (2012). Cardiomyocyte deletion of mitofusin-1 leads to mitochondrial fragmentation and improves tolerance to ROS-induced mitochondrial dysfunction and cell death. *Am. J. Physiol. Heart Circ. Physiol.* 302 (1), H167–H179. doi:10.1152/ajpheart.00833.2011

Paradies, G., Paradies, V., Ruggiero, F. M., and Petrosillo, G. (2019). Role of cardiolipin in mitochondrial function and dynamics in health and disease: Molecular and pharmacological aspects. *Cells* 8 (7), 728. doi:10.3390/cells8070728

Parra, V., Verdejo, H., del Campo, A., Pennanen, C., Kuzmicic, J., Iglewski, M., et al. (2011). The complex interplay between mitochondrial dynamics and cardiac metabolism. *J. Bioenerg. Biomembr.* 43 (1), 47–51. doi:10.1007/s10863-011-9332-0

Peng, S., Xu, L. W., Che, X. Y., Xiao, Q. Q., Pu, J., Shao, Q., et al. (2018). Atorvastatin inhibits inflammatory response, attenuates lipid deposition, and improves the stability of vulnerable atherosclerotic plaques by modulating autophagy. *Front. Pharmacol.* 9, 438. doi:10.3389/fphar.2018.00438

Pennanen, C., Parra, V., López-Crisosto, C., Morales, P. E., Del Campo, A., Gutierrez, T., et al. (2014). Mitochondrial fission is required for cardiomyocyte hypertrophy mediated by a Ca2+-calcineurin signaling pathway. *J. Cell. Sci.* 127 (12), 2659–2671. doi:10.1242/jcs.139394

Peoples, J. N., Saraf, A., Ghazal, N., Pham, T. T., and Kwong, J. Q. (2019). Mitochondrial dysfunction and oxidative stress in heart disease. *Exp. Mol. Med.* 51 (12), 1–13. doi:10.1038/s12276-019-0355-7

Pereira, C. V., Gitschlag, B. L., and Patel, M. R. (2021). Cellular mechanisms of mtDNA heteroplasmy dynamics. *Crit. Rev. Biochem. Mol. Biol.* 56 (5), 510–525. doi:10.1080/10409238.2021.1934812

Pfanner, N., Warscheid, B., and Wiedemann, N. (2019). Mitochondrial proteins: From biogenesis to functional networks. *Nat. Rev. Mol. Cell. Biol.* 20 (5), 267–284. doi:10.1038/s41580-018-0092-0

Picca, A., Mankowski, R. T., Burman, J. L., Donisi, L., Kim, J. S., Marzetti, E., et al. (2018). Mitochondrial quality control mechanisms as molecular targets in cardiac ageing. *Nat. Rev. Cardiol.* 15 (9), 543–554. doi:10.1038/s41569-018-0059-z

Pickrell, A. M., and Youle, R. J. (2015). The roles of PINK1, parkin, and mitochondrial fidelity in Parkinson's disease. *Neuron* 85 (2), 257–273. doi:10.1016/j.neuron.2014.12.007

Pietraforte, D., Gambardella, L., Marchesi, A., Tarissi de Jacobis, I., Villani, A., Del Principe, D., et al. (2014). Platelets in Kawasaki patients: Two different populations with different mitochondrial functions. *Int. J. Cardiol.* 172 (2), 526–528. doi:10.1016/j.ijcard.2014.01.022

Porritt, R. A., Markman, J. L., Maruyama, D., Kocaturk, B., Chen, S., Lehman, T. J. A., et al. (2020). Interleukin-1 beta-mediated sex differences in Kawasaki disease vasculitis development and response to treatment. *Arterioscler. Thromb. Vasc. Biol.* 40 (3), 802–818. doi:10.1161/ATVBAHA.119.313863

Porritt, R. A., Zemmour, D., Abe, M., Lee, Y., Narayanan, M., Carvalho, T. T., et al. (2021). NLRP3 inflammasome mediates immune-stromal interactions in vasculitis. *Circ. Res.* 129 (9), e183–e200. doi:10.1161/circresaha.121.319153

Potgieter, M., Pretorius, E., and Pepper, M. S. (2013). Primary and secondary coenzyme Q10 deficiency: The role of therapeutic supplementation. *Nutr. Rev.* 71 (3), 180–188. doi:10.1111/nure.12011

Protasoni, M., and Zeviani, M. (2021). Mitochondrial structure and bioenergetics in normal and disease conditions. *Int. J. Mol. Sci.* 22 (2), 586. doi:10.3390/ijms22020586

Puigserver, P., Wu, Z., Park, C. W., Graves, R., Wright, M., and Spiegelman, B. M. (1998). A cold-inducible coactivator of nuclear receptors linked to adaptive thermogenesis. *Cell.* 92 (6), 829–839. doi:10.1016/s0092-8674(00)81410-5

Qi, J., Wang, F., Yang, P., Wang, X., Xu, R., Chen, J., et al. (2018). Mitochondrial fission is required for angiotensin II-induced cardiomyocyte apoptosis mediated by a sirt1-p53 signaling pathway. *Front. Pharmacol.* 9, 176. doi:10.3389/fphar.2018.00176

Quiles, J. M., and Gustafsson Å, B. (2022). The role of mitochondrial fission in cardiovascular health and disease. *Nat. Rev. Cardiol.* 19 (11), 723–736. doi:10.1038/s41569-022-00703-y

Quirós, P. M., Mottis, A., and Auwerx, J. (2016). Mitonuclear communication in homeostasis and stress. *Nat. Rev. Mol. Cell. Biol.* 17 (4), 213–226. doi:10.1038/nrm.2016.23

Qureshi, M. A., Haynes, C. M., and Pellegrino, M. W. (2017). The mitochondrial unfolded protein response: Signaling from the powerhouse. *J. Biol. Chem.* 292 (33), 13500–13506. doi:10.1074/jbc.R117.791061

Ramaccini, D., Montoya-Uribe, V., Aan, F. J., Modesti, L., Potes, Y., Wieckowski, M. R., et al. (2020). Mitochondrial function and dysfunction in dilated cardiomyopathy. *Front. Cell. Dev. Biol.* 8, 624216. doi:10.3389/fcell.2020.624216

Ranjbarvaziri, S., Kooiker, K. B., Ellenberger, M., Fajardo, G., Zhao, M., Vander Roest, A. S., et al. (2021). Altered cardiac energetics and mitochondrial dysfunction in hypertrophic cardiomyopathy. *Circulation* 144 (21), 1714–1731. doi:10.1161/circulationaha.121.053575

Rapezzi, C., Aimo, A., Barison, A., Emdin, M., Porcari, A., Linhart, A., et al. (2022). Restrictive cardiomyopathy: Definition and diagnosis. *Eur. Heart J.* 43 (45), 4679–4693. doi:10.1093/eurheartj/ehac543

Ravi, B., Kanwar, P., Sanyal, S. K., Bheri, M., and Pandey, G. K. (2021). VDACs: An outlook on biochemical regulation and function in animal and plant systems. *Front. Physiol.* 12, 683920. doi:10.3389/fphys.2021.683920

Razani, B., Feng, C., Coleman, T., Emanuel, R., Wen, H., Hwang, S., et al. (2012). Autophagy links inflammasomes to atherosclerotic progression. *Cell. Metab.* 15 (4), 534–544. doi:10.1016/j.cmet.2012.02.011

Reid, R. A., Moyle, J., and Mitchell, P. (1966). Synthesis of adenosine triphosphate by a protonmotive force in rat liver mitochondria. *Nature* 212 (5059), 257–258. doi:10.1038/212257a0

Reikine, S., Nguyen, J. B., and Modis, Y. (2014). Pattern recognition and signaling mechanisms of RIG-I and MDA5. *Front. Immunol.* 5, 342. doi:10.3389/fimmu.2014.00342

Reina, S., Checchetto, V., Saletti, R., Gupta, A., Chaturvedi, D., Guardiani, C., et al. (2016). VDAC3 as a sensor of oxidative state of the intermembrane space of mitochondria: The putative role of cysteine residue modifications. *Oncotarget* 7 (3), 2249–2268. doi:10.18632/oncotarget.6850

Reina, S., Nibali, S. C., Tomasello, M. F., Magrì, A., Messina, A., and De Pinto, V. (2022). Voltage Dependent Anion Channel 3 (VDAC3) protects mitochondria from oxidative stress. *Redox Biol.* 51, 102264. doi:10.1016/j.redox.2022.102264

Ren, J., Sun, M., Zhou, H., Ajoolabady, A., Zhou, Y., Tao, J., et al. (2020). FUNDC1 interacts with FBXL2 to govern mitochondrial integrity and cardiac function through an IP3R3-dependent manner in obesity. *Sci. Adv.* 6 (38), eabc8561. doi:10.1126/sciadv.abc8561

Reyes, A., Gissi, C., Pesole, G., and Saccone, C. (1998). Asymmetrical directional mutation pressure in the mitochondrial genome of mammals. *Mol. Biol. Evol.* 15 (8), 957–966. doi:10.1093/oxfordjournals.molbev.a026011

Richter, C., Gogvadze, V., Laffranchi, R., Schlapbach, R., Schweizer, M., Suter, M., et al. (1995). Oxidants in mitochondria: From physiology to diseases. *Biochim. Biophys. Acta* 1271 (1), 67–74. doi:10.1016/0925-4439(95)00012-s

Richter, C., Park, J. W., and Ames, B. N. (1988). Normal oxidative damage to mitochondrial and nuclear DNA is extensive. *Proc. Natl. Acad. Sci. U. S. A.* 85 (17), 6465–6467. doi:10.1073/pnas.85.17.6465

Rimbaud, S., Ruiz, M., Piquereau, J., Mateo, P., Fortin, D., Veksler, V., et al. (2011). Resveratrol improves survival, hemodynamics and energetics in a rat model of hypertension leading to heart failure. *PLoS One* 6 (10), e26391. doi:10.1371/journal.pone.0026391

Ritz, P., and Berrut, G. (2005). Mitochondrial function, energy expenditure, aging and insulin resistance. *Diabetes Metab.* 31(2), 5s67–5S73. doi:10.1016/s1262-3636(05)73654-5

Rogers, M. A., Maldonado, N., Hutcheson, J. D., Goettsch, C., Goto, S., Yamada, I., et al. (2017). Dynamin-related protein 1 inhibition attenuates cardiovascular calcification in the presence of oxidative stress. *Circ. Res.* 121 (3), 220–233. doi:10.1161/circresaha.116.310293

Roman, B., Kaur, P., Ashok, D., Kohr, M., Biswas, R., O'Rourke, B., et al. (2020). Nuclear-mitochondrial communication involving miR-181c plays an important role in cardiac dysfunction during obesity. *J. Mol. Cell. Cardiol.* 144, 87–96. doi:10.1016/j.yjmcc.2020.05.009

Rongvaux, A., Jackson, R., Harman, C. C., Li, T., West, A. P., de Zoete, M. R., et al. (2014). Apoptotic caspases prevent the induction of type I interferons by mitochondrial DNA. *Cell.* 159 (7), 1563–1577. doi:10.1016/j.cell.2014.11.037

Rossman, M. J., Santos-Parker, J. R., Steward, C. A. C., Bispham, N. Z., Cuevas, L. M., Rosenberg, H. L., et al. (2018). Chronic supplementation with a mitochondrial antioxidant (MitoQ) improves vascular function in healthy older adults. *Hypertension* 71 (6), 1056–1063. doi:10.1161/hypertensionaha.117.10787

Rüb, C., Wilkening, A., and Voos, W. (2017). Mitochondrial quality control by the Pink1/Parkin system. *Cell. Tissue Res.* 367 (1), 111–123. doi:10.1007/s00441-016-2485-8

Russell, O. M., Gorman, G. S., Lightowlers, R. N., and Turnbull, D. M. (2020). Mitochondrial diseases: Hope for the future. *Cell.* 181 (1), 168–188. doi:10.1016/j.cell.2020.02.051

Russell, R. C., Tian, Y., Yuan, H., Park, H. W., Chang, Y. Y., Kim, J., et al. (2013). ULK1 induces autophagy by phosphorylating Beclin-1 and activating VPS34 lipid kinase. *Nat. Cell. Biol.* 15 (7), 741–750. doi:10.1038/ncb2757

Russo, S. B., Baicu, C. F., Van Laer, A., Geng, T., Kasiganesan, H., Zile, M. R., et al. (2012). Ceramide synthase 5 mediates lipid-induced autophagy and hypertrophy in cardiomyocytes. *J. Clin. Investig.* 122 (11), 3919–3930. doi:10.1172/jci63888

Salabei, J. K., and Hill, B. G. (2013). Mitochondrial fission induced by platelet-derived growth factor regulates vascular smooth muscle cell bioenergetics and cell proliferation. *Redox Biol.* 1 (1), 542–551. doi:10.1016/j.redox.2013.10.011

Sampath, H. (2014). Oxidative DNA damage in disease--insights gained from base excision repair glycosylase-deficient mouse models. *Environ. Mol. Mutagen* 55 (9), 689–703. doi:10.1002/em.21886

Saneto, R. P., and Sedensky, M. M. (2013). Mitochondrial disease in childhood: mtDNA encoded. *Neurotherapeutics* 10 (2), 199–211. doi:10.1007/s13311-012-0167-0

Schellenberg, B., Wang, P., Keeble, J. A., Rodriguez-Enriquez, R., Walker, S., Owens, T. W., et al. (2013). Bax exists in a dynamic equilibrium between the cytosol and mitochondria to control apoptotic priming. *Mol. Cell.* 49 (5), 959–971. doi:10.1016/j.molcel.2012.12.022

Schiattarella, G. G., and Hill, J. A. (2015). Inhibition of hypertrophy is a good therapeutic strategy in ventricular pressure overload. *Circulation* 131 (16), 1435–1447. doi:10.1161/circulationaha.115.013894

Schilling, J. D. (2015). The mitochondria in diabetic heart failure: From pathogenesis to therapeutic promise. *Antioxid. Redox Signal* 22 (17), 1515–1526. doi:10.1089/ars.2015.6294

Sentelle, R. D., Senkal, C. E., Jiang, W., Ponnusamy, S., Gencer, S., Selvam, S. P., et al. (2012). Ceramide targets autophagosomes to mitochondria and induces lethal mitophagy. *Nat. Chem. Biol.* 8 (10), 831–838. doi:10.1038/nchembio.1059

Sepasi Tehrani, H., and Moosavi-Movahedi, A. A. (2018). Catalase and its mysteries. *Prog. Biophys. Mol. Biol.* 140, 5–12. doi:10.1016/j.pbiomolbio.2018.03.001

Sergin, I., Bhattacharya, S., Emanuel, R., Esen, E., Stokes, C. J., Evans, T. D., et al. (2016). Inclusion bodies enriched for p62 and polyubiquitinated proteins in macrophages protect against atherosclerosis. *Sci. Signal* 9 (409), ra2. doi:10.1126/scisignal.aad5614

Shafferman, A., Birmingham, J. D., and Cron, R. Q. (2014). High dose anakinra for treatment of severe neonatal Kawasaki disease: A case report. *Pediatr. Rheumatol. Online J.* 12, 26. doi:10.1186/1546-0096-12-26

Shah, S. N., Umapathi, K. K., and Oliver, T. I. (2023). "Arrhythmogenic right ventricular cardiomyopathy," in *StatPearls* (Treasure Island (FL): StatPearls Publishing).

Sheeran, F. L., and Pepe, S. (2017). Mitochondrial bioenergetics and dysfunction in failing heart. *Adv. Exp. Med. Biol.* 982, 65–80. doi:10.1007/978-3-319-55330-6_4

Shi, J., Zhao, Y., Wang, K., Shi, X., Wang, Y., Huang, H., et al. (2015). Cleavage of GSDMD by inflammatory caspases determines pyroptotic cell death. *Nature* 526 (7575), 660–665. doi:10.1038/nature15514

Shi, L., and Tu, B. P. (2015). Acetyl-CoA and the regulation of metabolism: Mechanisms and consequences. *Curr. Opin. Cell. Biol.* 33, 125–131. doi:10.1016/j.ceb.2015.02.003

Shimada, K., Crother, T. R., Karlin, J., Dagvadorj, J., Chiba, N., Chen, S., et al. (2012). Oxidized mitochondrial DNA activates the NLRP3 inflammasome during apoptosis. *Immunity* 36 (3), 401–414. doi:10.1016/j.immuni.2012.01.009

Shin, W. S., Hong, Y. H., Peng, H. B., De Caterina, R., Libby, P., and Liao, J. K. (1996). Nitric oxide attenuates vascular smooth muscle cell activation by interferon-gamma. The role of constitutive NF-kappa B activity. *J. Biol. Chem.* 271 (19), 11317–11324. doi:10.1074/jbc.271.19.11317

Shpilka, T., and Haynes, C. M. (2018). The mitochondrial UPR: Mechanisms, physiological functions and implications in ageing. *Nat. Rev. Mol. Cell. Biol.* 19 (2), 109–120. doi:10.1038/nrm.2017.110

Sica, V., Galluzzi, L., Bravo-San Pedro, J. M., Izzo, V., Maiuri, M. C., and Kroemer, G. (2015). Organelle-specific initiation of autophagy. *Mol. Cell.* 59 (4), 522–539. doi:10.1016/j.molcel.2015.07.021

Singh, D. P., and Patel, H. (2023). "Left ventricular noncompaction cardiomyopathy," in *StatPearls* (Treasure Island (FL): StatPearls Publishing).

Song, S., Ding, Y., Dai, G. L., Zhang, Y., Xu, M. T., Shen, J. R., et al. (2021). Sirtuin 3 deficiency exacerbates diabetic cardiomyopathy via necroptosis enhancement and NLRP3 activation. *Acta Pharmacol. Sin.* 42 (2), 230–241. doi:10.1038/s41401-020-0490-7

Song, Z., Chen, H., Fiket, M., Alexander, C., and Chan, D. C. (2007). OPA1 processing controls mitochondrial fusion and is regulated by mRNA splicing, membrane potential, and Yme1L. *J. Cell. Biol.* 178 (5), 749–755. doi:10.1083/jcb.200704110

Sonn, S. K., Song, E. J., Seo, S., Kim, Y. Y., Um, J. H., Yeo, F. J., et al. (2022). Peroxiredoxin 3 deficiency induces cardiac hypertrophy and dysfunction by impaired mitochondrial quality control. *Redox Biol.* 51, 102275. doi:10.1016/j.redox.2022.102275

Srivastava, S. (2016). Emerging therapeutic roles for NAD(+) metabolism in mitochondrial and age-related disorders. *Clin. Transl. Med.* 5 (1), 25. doi:10.1186/s40169-016-0104-7

St-Pierre, J., Buckingham, J. A., Roebuck, S. J., and Brand, M. D. (2002). Topology of superoxide production from different sites in the mitochondrial electron transport chain. *J. Biol. Chem.* 277 (47), 44784–44790. doi:10.1074/jbc.M207217200

Starkov, A. A., Fiskum, G., Chinopoulos, C., Lorenzo, B. J., Browne, S. E., Patel, M. S., et al. (2004). Mitochondrial alpha-ketoglutarate dehydrogenase complex generates reactive oxygen species. *J. Neurosci.* 24 (36), 7779–7788. doi:10.1523/jneurosci.1899-04.2004

Stefano, G. B., Bjenning, C., Wang, F., Wang, N., and Kream, R. M. (2017). Mitochondrial heteroplasmy. *Adv. Exp. Med. Biol.* 982, 577–594. doi:10.1007/978-3-319-55330-6_30

Stein, A., and Sia, E. A. (2017). Mitochondrial DNA repair and damage tolerance. *Front. Biosci. (Landmark Ed.* 22 (5), 920–943. doi:10.2741/4525

Storz, P., Döppler, H., and Toker, A. (2005). Protein kinase D mediates mitochondrion-to-nucleus signaling and detoxification from mitochondrial reactive oxygen species. *Mol. Cell. Biol.* 25 (19), 8520–8530. doi:10.1128/mcb.25.19.8520-8530.2005

Sulaiman, M., Matta, M. J., Sunderesan, N. R., Gupta, M. P., Periasamy, M., and Gupta, M. (2010). Resveratrol, an activator of SIRT1, upregulates sarcoplasmic calcium ATPase and improves cardiac function in diabetic cardiomyopathy. *Am. J. Physiol. Heart Circ. Physiol.* 298 (3), H833–H843. doi:10.1152/ajpheart.00418.2009

Sun, L., Wu, J., Du, F., Chen, X., and Chen, Z. J. (2013). Cyclic GMP-AMP synthase is a cytosolic DNA sensor that activates the type I interferon pathway. *Science* 339 (6121), 786–791. doi:10.1126/science.1232458

Sun, T., Han, Y., Li, J. L., Jiao, X. Y., Zuo, L., Wang, J., et al. (2022). FOXO3a-dependent PARKIN negatively regulates cardiac hypertrophy by restoring mitophagy. *Cell. Biosci.* 12 (1), 204. doi:10.1186/s13578-022-00935-y

Suomalainen, A., and Battersby, B. J. (2018). Mitochondrial diseases: The contribution of organelle stress responses to pathology. *Nat. Rev. Mol. Cell. Biol.* 19 (2), 77–92. doi:10.1038/nrm.2017.66

Swaminathan, B., Goikuria, H., Vega, R., Rodríguez-Antigüedad, A., López Medina, A., Freijo Mdel, M., et al. (2014). Autophagic marker MAP1LC3B expression levels are associated with carotid atherosclerosis symptomatology. *PLoS One* 9 (12), e115176. doi:10.1371/journal.pone.0115176

Sykora, P., Wilson, D. M., 3rd, and Bohr, V. A. (2012). Repair of persistent strand breaks in the mitochondrial genome. *Mech. Ageing Dev.* 133 (4), 169–175. doi:10.1016/j.mad.2011.11.003

Tan, Y., Li, M., Wu, G., Lou, J., Feng, M., Xu, J., et al. (2021). Short-term but not long-term high fat diet feeding protects against pressure overload-induced heart failure through activation of mitophagy. *Life Sci.* 272, 119242. doi:10.1016/j.lfs.2021.119242

Tanaka, M., and Ozawa, T. (1994). Strand asymmetry in human mitochondrial DNA mutations. *Genomics* 22 (2), 327–335. doi:10.1006/geno.1994.1391

Tanaka, Y., and Chen, Z. J. (2012). STING specifies IRF3 phosphorylation by TBK1 in the cytosolic DNA signaling pathway. *Sci. Signal* 5 (214), ra20. doi:10.1126/scisignal.2002521

Tanida, I., Ueno, T., and Kominami, E. (2004). LC3 conjugation system in mammalian autophagy. *Int. J. Biochem. Cell. Biol.* 36 (12), 2503–2518. doi:10.1016/j.biocel.2004.05.009

Tao, T., and Xu, H. (2020). Autophagy and obesity and diabetes. *Adv. Exp. Med. Biol.* 1207, 445–461. doi:10.1007/978-981-15-4272-5_32

Tatsuta, T., Scharwey, M., and Langer, T. (2014). Mitochondrial lipid trafficking. *Trends Cell. Biol.* 24 (1), 44–52. doi:10.1016/j.tcb.2013.07.011

Taylor, M. R., Slavov, D., Ku, L., Di Lenarda, A., Sinagra, G., Carniel, E., et al. (2007). Prevalence of desmin mutations in dilated cardiomyopathy. *Circulation* 115 (10), 1244–1251. doi:10.1161/circulationaha.106.646778

Teekakirikul, P., Zhu, W., Huang, H. C., and Fung, E. (2019). Hypertrophic cardiomyopathy: An overview of genetics and management. *Biomolecules* 9 (12), 878. doi:10.3390/biom9120878

Teske, B. F., Fusakio, M. E., Zhou, D., Shan, J., McClintick, J. N., Kilberg, M. S., et al. (2013). CHOP induces activating transcription factor 5 (ATF5) to trigger apoptosis in response to perturbations in protein homeostasis. *Mol. Biol. Cell.* 24 (15), 2477–2490. doi:10.1091/mbc.E13-01-0067

Tomczyk, M. M., Cheung, K. G., Xiang, B., Tamanna, N., Fonseca Teixeira, A. L., Agarwal, P., et al. (2022). Mitochondrial sirtuin-3 (SIRT3) prevents doxorubicin-induced dilated cardiomyopathy by modulating protein acetylation and oxidative stress. *Circ. Heart Fail* 15 (5), e008547. doi:10.1161/circheartfailure.121.008547

Tong, M., Saito, T., Zhai, P., Oka, S. I., Mizushima, W., Nakamura, M., et al. (2019). Mitophagy is essential for maintaining cardiac function during high fat diet-induced diabetic cardiomyopathy. *Circ. Res.* 124 (9), 1360–1371. doi:10.1161/circresaha.118.314607

Tremoulet, A. H., Best, B. M., Song, S., Wang, S., Corinaldesi, E., Eichenfield, J. R., et al. (2008). Resistance to intravenous immunoglobulin in children with Kawasaki disease. *J. Pediatr.* 153 (1), 117–121. doi:10.1016/j.jpeds.2007.12.021

Tremoulet, A. H., Jain, S., Jone, P. N., Best, B. M., Duxbury, E. H., Franco, A., et al. (2019). Phase I/IIa trial of atorvastatin in patients with acute Kawasaki disease with coronary artery aneurysm. *J. Pediatr.* 215, 107–117. doi:10.1016/j.jpeds.2019.07.064

Tumurkhuu, G., Shimada, K., Dagvadorj, J., Crother, T. R., Zhang, W., Luthringer, D., et al. (2016). Ogg1-Dependent DNA repair regulates NLRP3 inflammasome and prevents atherosclerosis. *Circ. Res.* 119 (6), e76–e90. doi:10.1161/circresaha.116.308362

Tuohy, C. V., Kaul, S., Song, H. K., Nazer, B., and Heitner, S. B. (2020). Hypertrophic cardiomyopathy: The future of treatment. *Eur. J. Heart Fail* 22 (2), 228–240. doi:10.1002/ejhf.1715

University of Washington (2023). *Seattle. GeneReviews is a registered trademark of the University of Washington*. Seattle. All rights reserved.

van Spaendonck-Zwarts, K. Y., van Hessem, L., Jongbloed, J. D., de Walle, H. E., Capetanaki, Y., van der Kooi, A. J., et al. (2011). Desmin-related myopathy. *Clin. Genet.* 80 (4), 354–366. doi:10.1111/j.1399-0004.2010.01512.x

Varanita, T., Soriano, M. E., Romanello, V., Zaglia, T., Quintana-Cabrera, R., Semenzato, M., et al. (2015). The OPA1-dependent mitochondrial cristae remodeling pathway controls atrophic, apoptotic, and ischemic tissue damage. *Cell. Metab.* 21 (6), 834–844. doi:10.1016/j.cmet.2015.05.007

Vargas, J. N. S., Wang, C., Bunker, E., Hao, L., Maric, D., Schiavo, G., et al. (2019). Spatiotemporal control of ULK1 activation by NDP52 and TBK1 during selective autophagy. *Mol. Cell.* 74 (2), 347–362. doi:10.1016/j.molcel.2019.02.010

Vercellino, I., and Sazanov, L. A. (2022). The assembly, regulation and function of the mitochondrial respiratory chain. *Nat. Rev. Mol. Cell. Biol.* 23 (2), 141–161. doi:10.1038/s41580-021-00415-0

Villa, E., Marchetti, S., and Ricci, J. E. (2018). No parkin zone: Mitophagy without parkin. *Trends Cell. Biol.* 28 (11), 882–895. doi:10.1016/j.tcb.2018.07.004

Virbasius, J. V., and Scarpulla, R. C. (1994). Activation of the human mitochondrial transcription factor A gene by nuclear respiratory factors: A potential regulatory link between nuclear and mitochondrial gene expression in organelle biogenesis. *Proc. Natl. Acad. Sci. U. S. A.* 91 (4), 1309–1313. doi:10.1073/pnas.91.4.1309

Vizioli, M. G., Liu, T., Miller, K. N., Robertson, N. A., Gilroy, K., Lagnado, A. B., et al. (2020). Mitochondria-to-nucleus retrograde signaling drives formation of cytoplasmic chromatin and inflammation in senescence. *Genes. Dev.* 34 (5-6), 428–445. doi:10.1101/gad.331272.119

Wakita, D., Kurashima, Y., Crother, T. R., Noval Rivas, M., Lee, Y., Chen, S., et al. (2016). Role of interleukin-1 signaling in a mouse model of Kawasaki disease-associated abdominal aortic aneurysm. *Arterioscler. Thromb. Vasc. Biol.* 36 (5), 886–897. doi:10.1161/atvbaha.115.307072

Wang, J., Huang, X., Liu, H., Chen, Y., Li, P., Liu, L., et al. (2022a). Empagliflozin ameliorates diabetic cardiomyopathy via attenuating oxidative stress and improving mitochondrial function. *Oxid. Med. Cell. Longev.* 2022, 1122494. doi:10.1155/2022/1122494

Wang, L., Cai, Y., Jian, L., Cheung, C. W., Zhang, L., and Xia, Z. (2021a). Impact of peroxisome proliferator-activated receptor-α on diabetic cardiomyopathy. *Cardiovasc Diabetol.* 20 (1), 2. doi:10.1186/s12933-020-01188-0

Wang, P., Wang, D., Yang, Y., Hou, J., Wan, J., Ran, F., et al. (2020). Tom70 protects against diabetic cardiomyopathy through its antioxidant and antiapoptotic properties. *Hypertens. Res.* 43 (10), 1047–1056. doi:10.1038/s41440-020-0518-x

Wang, Q., Zhang, M., Torres, G., Wu, S., Ouyang, C., Xie, Z., et al. (2017). Metformin suppresses diabetes-accelerated atherosclerosis via the inhibition of drp1-mediated mitochondrial fission. *Diabetes* 66 (1), 193–205. doi:10.2337/db16-0915

Wang, X., Zhang, X., Cao, K., Zeng, M., Fu, X., Zheng, A., et al. (2022b). Cardiac disruption of SDHAF4-mediated mitochondrial complex II assembly promotes dilated cardiomyopathy. *Nat. Commun.* 13 (1), 3947. doi:10.1038/s41467-022-31548-1

Wang, Y. J., Paneni, F., Stein, S., and Matter, C. M. (2021b). Modulating sirtuin Biology and nicotinamide adenine diphosphate metabolism in cardiovascular disease-from bench to bedside. *Front. Physiol.* 12, 755060. doi:10.3389/fphys.2021.755060

Wei, Y., Zhang, Y. J., Cai, Y., and Xu, M. H. (2015). The role of mitochondria in mTOR-regulated longevity. *Biol. Rev. Camb Philos. Soc.* 90 (1), 167–181. doi:10.1111/brv.12103

Weil, R., Laplantine, E., Curic, S., and Génin, P. (2018). Role of optineurin in the mitochondrial dysfunction: Potential implications in neurodegenerative diseases and cancer. *Front. Immunol.* 9, 1243. doi:10.3389/fimmu.2018.01243

Wellen, K. E., Hatzivassiliou, G., Sachdeva, U. M., Bui, T. V., Cross, J. R., and Thompson, C. B. (2009). ATP-citrate lyase links cellular metabolism to histone acetylation. *Science* 324 (5930), 1076–1080. doi:10.1126/science.1164097

White, M. J., McArthur, K., Metcalf, D., Lane, R. M., Cambier, J. C., Herold, M. J., et al. (2014). Apoptotic caspases suppress mtDNA-induced STING-mediated type I IFN production. *Cell.* 159 (7), 1549–1562. doi:10.1016/j.cell.2014.11.036

Wiedemann, N., Frazier, A. E., and Pfanner, N. (2004). The protein import machinery of mitochondria. *J. Biol. Chem.* 279 (15), 14473–14476. doi:10.1074/jbc.R400003200

Williams, M., and Caino, M. C. (2018). Mitochondrial dynamics in type 2 diabetes and cancer. *Front. Endocrinol. (Lausanne)* 9, 211. doi:10.3389/fendo.2018.00211

Wu, W., Tian, W., Hu, Z., Chen, G., Huang, L., Li, W., et al. (2014). ULK1 translocates to mitochondria and phosphorylates FUNDC1 to regulate mitophagy. *EMBO Rep.* 15 (5), 566–575. doi:10.1002/embr.201438501

Wu, Z., Puigserver, P., Andersson, U., Zhang, C., Adelmant, G., Mootha, V., et al. (1999). Mechanisms controlling mitochondrial biogenesis and respiration through the thermogenic coactivator PGC-1. *Cell.* 98 (1), 115–124. doi:10.1016/s0092-8674(00)80611-x

Xian, H., Watari, K., Sanchez-Lopez, E., Offenberger, J., Onyuru, J., Sampath, H., et al. (2022). Oxidized DNA fragments exit mitochondria via mPTP- and VDAC-dependent channels to activate NLRP3 inflammasome and interferon signaling. *Immunity* 55 (8), 1370–1385.e8. doi:10.1016/j.immuni.2022.06.007

Xiao, Y., Chen, W., Zhong, Z., Ding, L., Bai, H., Chen, H., et al. (2020). Electroacupuncture preconditioning attenuates myocardial ischemia-reperfusion injury by inhibiting mitophagy mediated by the mTORC1-ULK1-FUNDC1 pathway. *Biomed. Pharmacother.* 127, 110148. doi:10.1016/j.biopha.2020.110148

Xin, Y., Zhang, X., Li, J., Gao, H., Li, J., Li, J., et al. (2021). New insights into the role of mitochondria quality control in ischemic heart disease. *Front. Cardiovasc Med.* 8, 774619. doi:10.3389/fcvm.2021.774619

Xu, M., Xue, R. Q., Lu, Y., Yong, S. Y., Wu, Q., Cui, Y. L., et al. (2019). Choline ameliorates cardiac hypertrophy by regulating metabolic remodelling and UPRmt through SIRT3-AMPK pathway. *Cardiovasc Res.* 115 (3), 530–545. doi:10.1093/cvr/cvy217

Xu, X., Kobayashi, S., Chen, K., Timm, D., Volden, P., Huang, Y., et al. (2013). Diminished autophagy limits cardiac injury in mouse models of type 1 diabetes. *J. Biol. Chem.* 288 (25), 18077–18092. doi:10.1074/jbc.M113.474650

Yakes, F. M., and Van Houten, B. (1997). Mitochondrial DNA damage is more extensive and persists longer than nuclear DNA damage in human cells following oxidative stress. *Proc. Natl. Acad. Sci. U. S. A.* 94 (2), 514–519. doi:10.1073/pnas.94.2.514

Yamada, T., and Nomura, S. (2021). Recent findings related to cardiomyopathy and genetics. *Int. J. Mol. Sci.* 22 (22), 12522. doi:10.3390/ijms222212522

Yamamoto, T., Byun, J., Zhai, P., Ikeda, Y., Oka, S., and Sadoshima, J. (2014). Nicotinamide mononucleotide, an intermediate of NAD+ synthesis, protects the heart from ischemia and reperfusion. *PLoS One* 9 (6), e98972. doi:10.1371/journal.pone.0098972

Yamano, K., Kikuchi, R., Kojima, W., Hayashida, R., Koyano, F., Kawawaki, J., et al. (2020). Critical role of mitochondrial ubiquitination and the OPTN-ATG9A axis in mitophagy. *J. Cell. Biol.* 219 (9), e201912144. doi:10.1083/jcb.201912144

Yamano, K., and Youle, R. J. (2013). PINK1 is degraded through the N-end rule pathway. *Autophagy* 9 (11), 1758–1769. doi:10.4161/auto.24633

Yan, C., Duanmu, X., Zeng, L., Liu, B., and Song, Z. (2019). Mitochondrial DNA: Distribution, mutations, and elimination. *Cells* 8 (4), 379. doi:10.3390/cells8040379

Yang, J., Chen, S., Duan, F., Wang, X., Zhang, X., Lian, B., et al. (2022). Mitochondrial cardiomyopathy: Molecular epidemiology, diagnosis, models, and therapeutic management. *Cells* 11 (21), 3511. doi:10.3390/cells11213511

Yang, J. Y., and Yang, W. Y. (2013). Bit-by-bit autophagic removal of parkin-labelled mitochondria. *Nat. Commun.* 4, 2428. doi:10.1038/ncomms3428

Yang, M., Linn, B. S., Zhang, Y., and Ren, J. (2019). Mitophagy and mitochondrial integrity in cardiac ischemia-reperfusion injury. *Biochim. Biophys. Acta Mol. Basis Dis.* 1865 (9), 2293–2302. doi:10.1016/j.bbadis.2019.05.007

Yang, X., Wei, J., He, Y., Jing, T., Li, Y., Xiao, Y., et al. (2017). SIRT1 inhibition promotes atherosclerosis through impaired autophagy. *Oncotarget* 8 (31), 51447–51461. doi:10.18632/oncotarget.17691

Yankovskaya, V., Horsefield, R., Törnroth, S., Luna-Chavez, C., Miyoshi, H., Léger, C., et al. (2003). Architecture of succinate dehydrogenase and reactive oxygen species generation. *Science* 299 (5607), 700–704. doi:10.1126/science.1079605

Yildirim, A. D., Citir, M., Dogan, A. E., Veli, Z., Yildirim, Z., Tufanli, O., et al. (2022). ER stress-induced sphingosine-1-phosphate lyase phosphorylation potentiates the mitochondrial unfolded protein response. *J. Lipid Res.* 63 (10), 100279. doi:10.1016/j.jlr.2022.100279

Zaffagnini, G., and Martens, S. (2016). Mechanisms of selective autophagy. *J. Mol. Biol.* 428 (9), 1714–1724. doi:10.1016/j.jmb.2016.02.004

Zak, R., Rabinowitz, M., Rajamanickam, C., Merten, S., and Kwiatkowska-Patzer, B. (1980). Mitochondrial proliferation in cardiac hypertrophy. *Basic Res. Cardiol.* 75 (1), 171–178. doi:10.1007/bf02001410

Zhang, C., Shang, G., Gui, X., Zhang, X., Bai, X. C., and Chen, Z. J. (2019a). Structural basis of STING binding with and phosphorylation by TBK1. *Nature* 567 (7748), 394–398. doi:10.1038/s41586-019-1000-2

Zhang, M., Sui, W., Xing, Y., Cheng, J., Cheng, C., Xue, F., et al. (2021a). Angiotensin IV attenuates diabetic cardiomyopathy via suppressing FoxO1-induced excessive autophagy, apoptosis and fibrosis. *Theranostics* 11 (18), 8624–8639. doi:10.7150/thno.48561

Zhang, N. P., Liu, X. J., Xie, L., Shen, X. Z., and Wu, J. (2019b). Impaired mitophagy triggers NLRP3 inflammasome activation during the progression from nonalcoholic fatty liver to nonalcoholic steatohepatitis. *Lab. Investig.* 99 (6), 749–763. doi:10.1038/s41374-018-0177-6

Zhang, W., Ren, H., Xu, C., Zhu, C., Wu, H., Liu, D., et al. (2016). Hypoxic mitophagy regulates mitochondrial quality and platelet activation and determines severity of I/R heart injury. *Elife* 5, e21407. doi:10.7554/eLife.21407

Zhang, W., Siraj, S., Zhang, R., and Chen, Q. (2017). Mitophagy receptor FUNDC1 regulates mitochondrial homeostasis and protects the heart from I/R injury. *Autophagy* 13 (6), 1080–1081. doi:10.1080/15548627.2017.1300224

Zhang, X., McDonald, J. G., Aryal, B., Canfrán-Duque, A., Goldberg, E. L., Araldi, E., et al. (2021b). Desmosterol suppresses macrophage inflammasome activation and protects against vascular inflammation and atherosclerosis. *Proc. Natl. Acad. Sci. U. S. A.* 118 (47), e2107682118. doi:10.1073/pnas.2107682118

Zhang, Y., Wang, Y., Xu, J., Tian, F., Hu, S., Chen, Y., et al. (2019c). Melatonin attenuates myocardial ischemia-reperfusion injury via improving mitochondrial fusion/mitophagy and activating the AMPK-OPA1 signaling pathways. *J. Pineal Res.* 66 (2), e12542. doi:10.1111/jpi.12542

Zhao, R. Z., Jiang, S., Zhang, L., and Yu, Z. B. (2019). Mitochondrial electron transport chain, ROS generation and uncoupling (Review). *Int. J. Mol. Med.* 44 (1), 3–15. doi:10.3892/ijmm.2019.4188

Zhu, L., Zhou, Q., He, L., and Chen, L. (2021a). Mitochondrial unfolded protein response: An emerging pathway in human diseases. *Free Radic. Biol. Med.* 163, 125–134. doi:10.1016/j.freeradbiomed.2020.12.013

Zhu, P., Wan, K., Yin, M., Hu, P., Que, Y., Zhou, X., et al. (2021b). RIPK3 induces cardiomyocyte necroptosis via inhibition of AMPK-parkin-mitophagy in cardiac remodelling after myocardial infarction. *Oxid. Med. Cell. Longev.* 2021, 6635955. doi:10.1155/2021/6635955

Zhuang, L., Jia, K., Chen, C., Li, Z., Zhao, J., Hu, J., et al. (2022). DYRK1B-STAT3 drives cardiac hypertrophy and heart failure by impairing mitochondrial bioenergetics. *Circulation* 145 (11), 829–846. doi:10.1161/circulationaha.121.055727

Zinghirino, F., Pappalardo, X. G., Messina, A., Nicosia, G., De Pinto, V., and Guarino, F. (2021). VDAC genes expression and regulation in mammals. *Front. Physiol.* 12, 708695. doi:10.3389/fphys.2021.708695

Zong, H., Ren, J. M., Young, L. H., Pypaert, M., Mu, J., Birnbaum, M. J., et al. (2002). AMP kinase is required for mitochondrial biogenesis in skeletal muscle in response to chronic energy deprivation. *Proc. Natl. Acad. Sci. U. S. A.* 99 (25), 15983–15987. doi:10.1073/pnas.252625599

Zorova, L. D., Popkov, V. A., Plotnikov, E. Y., Silachev, D. N., Pevzner, I. B., Jankauskas, S. S., et al. (2018). Mitochondrial membrane potential. *Anal. Biochem.* 552, 50–59. doi:10.1016/j.ab.2017.07.009

Zou, L., Linck, V., Zhai, Y. J., Galarza-Paez, L., Li, L., Yue, Q., et al. (2018). Knockout of mitochondrial voltage-dependent anion channel type 3 increases reactive oxygen species (ROS) levels and alters renal sodium transport. *J. Biol. Chem.* 293 (5), 1666–1675. doi:10.1074/jbc.M117.798645

frontiers | Frontiers in Cell and Developmental Biology

TYPE Original Research
PUBLISHED 07 November 2023
DOI 10.3389/fcell.2023.1264076

OPEN ACCESS

EDITED BY
Milena Rizzo,
National Research Council (CNR), Italy

REVIEWED BY
Francisco O. Silva,
University of Texas Southwestern Medical Center, United States
Zhaohua Cai,
Shanghai Jiao Tong University, China

*CORRESPONDENCE
Tomohiro Numata,
numata@med.akita-u.ac.jp
Hideaki Tagashira,
htagashira@med.akita-u.ac.jp

RECEIVED 20 July 2023
ACCEPTED 06 October 2023
PUBLISHED 07 November 2023

CITATION
Tagashira H, Abe F, Sato-Numata K, Aizawa K, Hirasawa K, Kure Y, Iwata D and Numata T (2023), Cardioprotective effects of Moku-boi-to and its impact on AngII-induced cardiomyocyte hypertrophy. *Front. Cell Dev. Biol.* 11:1264076. doi: 10.3389/fcell.2023.1264076

Cardioprotective effects of Moku-boi-to and its impact on AngII-induced cardiomyocyte hypertrophy

Hideaki Tagashira[1]*, Fumiha Abe[1], Kaori Sato-Numata[1], Karen Aizawa[2], Kei Hirasawa[2], Yoshinobu Kure[2], Daiki Iwata[2] and Tomohiro Numata[1]*

[1]Department of Integrative Physiology, Graduate School of Medicine, Akita University, Akita, Japan, [2]School of Medicine, Akita University, Akita, Japan

Cardiomyocyte hypertrophy, induced by elevated levels of angiotensin II (AngII), plays a crucial role in cardiovascular diseases. Current therapeutic approaches aim to regress cardiac hypertrophy but have limited efficacy. Widely used Japanese Kampo medicines are highly safe and potential therapeutic agents. This study aims to explore the impact and mechanisms by which Moku-boi-to (MBT), a Japanese Kampo medicine, exerts its potential cardioprotective benefits against AngII-induced cardiomyocyte hypertrophy, bridging the knowledge gap and contributing to the development of novel therapeutic strategies. By evaluating the effects of six Japanese Kampo medicines with known cardiovascular efficiency on AngII-induced cardiomyocyte hypertrophy and cell death, we identified MBT as a promising candidate. MBT exhibited preventive effects against AngII-induced cardiomyocyte hypertrophy, cell death and demonstrated improvements in intracellular Ca^{2+} signaling regulation, ROS production, and mitochondrial function. Unexpectedly, experiments combining MBT with the AT_1 receptor antagonist losartan suggested that MBT may target the AT_1 receptor. In an isoproterenol-induced heart failure mouse model, MBT treatment demonstrated significant effects on cardiac function and hypertrophy. These findings highlight the cardioprotective potential of MBT through AT_1 receptor-mediated mechanisms, offering valuable insights into its efficacy in alleviating AngII-induced dysfunction in cardiomyocytes. The study suggests that MBT holds promise as a safe and effective prophylactic agent for cardiac hypertrophy, providing a deeper understanding of its mechanisms for cardioprotection against AngII-induced dysfunction.

KEYWORDS

Kampo medicine, cardiomyocyte hypertrophy, mitochondria, angiotensin-receptor blocker, mitochondria fission/fusion dynamics, ROS, Ca^{2+} homeostasis, cell volume regulation

Introduction

Heart Failure (HF) occurs when the heart cannot pump enough blood to meet the body's needs, causing various symptoms such as shortness of breath, fatigue, and swelling of the legs and ankles. It is a rapidly growing public health problem, affecting at least 20–40 million people worldwide (Ziaeian and Fonarow, 2016; Savarese and Lund, 2017). Drug therapy is a

cornerstone of HF treatment to address this problem. Various drugs targeting G protein-coupled receptors and ion channels are available to prevent the deterioration of ventricular systolic function and reduce mortality in patients (Rahm et al., 2018; Thai et al., 2023). On the other hand, medications used for conditions other than HF, such as antihypertensives and antidiabetic drugs, are prescribed only to people with pre-existing conditions because they can make HF worse (Page et al., 2016). Therefore, there is an urgent need to develop more effective therapeutic agents to improve the quality of life of patients and reduce the burden of medical costs associated with HF.

Excessive activation of a bioactive substance, angiotensin II (AngII), has been suggested to be involved in the onset and progression of HF. AngII induces physiological changes such as vasoconstriction, fibrosis, and cell death, associated with impaired mitochondrial function (Benigni et al., 2010). Recent studies have shown that continuous intracellular Ca^{2+} signaling is the cause of cardiac hypertrophy and HF (Bers, 2006). Furthermore, intracellular Ca^{2+} homeostasis regulation has been shown that a good balance between mitochondrial fission and fusion is critical for maintaining mitochondrial morphology and function in the heart and that disruption of this balance leads to the development of heart disease (Brown et al., 2017; Zhou and Tian, 2018; Yang et al., 2021). Therefore, excessive stimulation of AngII to cardiomyocytes that exacerbates HF can lead to abnormally elevated intracellular Ca^{2+} concentration $[(Ca^{2+})_i]$ levels, leading to cell death associated with mitochondrial dysfunction and cell volume regulation failure (Hunyady and Catt, 2006; Okada et al., 2019).

Moku-boi-to (MBT), a Japanese herbal medicine, is composed of four crude drugs: Sekkou; *Gypsum Fibrosum*, Keishi; bark of *Cinnamomumi* cassia Blume, Boui; *Sinomeni Caulis et Wilson*, and Ninjin; roots of *Panax ginseng C.A. Mayer*. MBT has an antiarrhythmic effect on the myocardium, and sinomenine, a crude drug component contained in MBT, exerts a myocardial protective effect by reducing Ca^{2+} influx into cells (Satoh, 2005; Satoh, 2017). It is empirically known to be effective mainly for renal edema and HF and has been used clinically in Japan for centuries (Yaku et al., 2022).

In this study, we used an AngII-induced cardiomyocyte hypertrophy model to evaluate the effects of MBT on AngII-induced mitochondrial dysfunction and cell death. Furthermore, we investigated the regulatory mechanisms of calcium homeostasis and elucidated the impact of MBT on this process.

Materials and methods

Materials

The following Japanese Kampo medicines were used in this study: Sho-seiryu-to (TJ-19), Boi-ogi-to (TJ-20), Mao-to (TJ-27), Moku-boi-to (MBT) (TJ-36), Yokukan-san (TJ-54), and Mashinin-gan (TJ-126). These Japanese Kampo medicines were obtained from TSUMURA & CO. (Tokyo, Japan). Each reagent was dissolved in dimethyl sulfoxide (DMSO) at a concentration of 250 mg/mL and diluted to the desired final concentration as aliquots.

Isoproterenol hydrochloride (ISO) was purchased from Sigma-Aldrich (MO, United States). Losartan potassium and carboxymethyl cellulose sodium salt (CMC) was purchased from Fujifilm Wako (Osaka, Japan). Angiotensin II (AngII) was purchased from Peptide Institute Inc. (Osaka, Japan). Immunostaining reagents, including rhodamine-conjugated phalloidin were obtained from Abcam (ab235138, Abcam, Cambridge, United Kingdom), and MitoTracker Red CMXRos were obtained from Invitrogen (CA, United States). The reactive oxygen species (ROS) indicator, H_2DCFDA, was obtained from Invitrogen, and the Ca^{2+} indicator, Fluo-4, was obtained from Dojindo (Kumamoto, Japan).

Animals

All animal-related procedures were conducted in strict accordance with the Guide for Care and Use of Laboratory Animals and received prior approval from the Animal Ethics Committee of Akita University (Akita, Japan). The ethics review number for these protocols were a-1-0412 and b-1-0408. For neonatal rat ventricular myocytes (NRVMs), to obtain neonatal rat ventricular myocytes (NRVMs) for the experiment, Wistar rats aged 1–3 days after birth were used. For the mice experiments, 10–12 weeks old male C57BL/6J mice, bred to the local environment, were employed. These mice were housed in polypropylene cages under controlled environmental conditions, which incubated a temperature of 25°C ± 1°C, humidity regulation, and a 12-h light/dark cycle.

ISO injection and drug administration

ISO group mice were treated with daily intraperitoneal injections of ISO (30 mg/kg body weight, once a day) (Sigma-Aldrich), following the established protocol detailed in previous studies (Park et al., 2018; Cheng et al., 2020). MBT was dissolved in 0.5% CMC (Fujifilm Wako). Vehicle and MBT (500 mg/body weight, once a day, p.o.) was administered orally for 14 days (once daily) in a volume of 1 mL/100 g of a body weight of mice, starting from the onset of ISO injection.

Echocardiography and measurement of cardiac hypertrophy

Noninvasive echocardiographic measurements were conducted on anesthetized mice using a mixture of ketamine (50 mg/kg body weight, i.p.) (Daiichi Sankyo Pharmaceutical Co., Ltd., Tokyo, Japan) and xylazine (5 mg/kg body weight, i.p.) (Bayer Yakuhin, Ltd., Osaka, Japan). A VisualSonics Vevo 770 system, equipped with a 30-MHz linear transducer, was used (FUJIFILM VisualSonics Inc., Toronto, Canada). To visualize the heart, two-dimensional parasternal short-axis views were obtained, and an M-mode echocardiogram of the midventricle was recorded, focusing on the papillary muscles. Echocardiographic measurements included diastolic and systolic LV wall thickness, LV end-diastolic diameter (LVEDD), and LV end-systolic diameter (LVESD). All

measurements adhered to the guidelines the American Society of Echocardiography set forth and were taken from leading edge to leading edge. The percentage of LV fractional shortening (FS%) was computed using the formula [(LVEDD—LVESD)/LVEDD] × 100. Two-dimensional (2D)-guided M-mode measurements were used to determine both FS% and the percentage of LV Ejection Fraction (EF %). Following the completion of echocardiography and before sacrifice, mice were euthanized through cervical spine fracture-dislocation for cardiac hypertrophy assessment. Subsequently, the thoracic cavity was opened, and the hearts were promptly excised and weighed.

Mouse tissue collection, histochemical staining

For mouse tissue collection, fixation, and sectioning, the mice were initially weighed and then subjected to deep anesthesia through a mixture of ketamine (100 mg/kg body weight, i.p.) (Daiichi Sankyo Pharmaceutical Co., Ltd.) and xylazine (10 mg/kg body weight, i.p.) (Bayer Yakuhin, Ltd.). Subsequently, their hearts were removed, any blood was carefully wiped away, and the heart weights were measured. The hearts were then fixed in 4% paraformaldehyde phosphate buffer solution (Nacalai Tesque, Kyoto, Japan) at 4°C overnight and subsequently embedded in paraffin. Tissue sections with a thickness of 3 μm were obtained from various locations. For histochemical staining, the tissue sections were deparaffinized and subjected to H&E (HE: hematoxylin and eosin) and Masson's trichrome (MT) staining following standard protocols. The slides were observed and imaged using a BZ-X800 Keyence inverted microscope (Osaka, Japan). Heart sections from a minimum of 5 mice per group were analyzed. To account for individual variations, the heart weight presented in Figure 7G was calculated by dividing the heart weight by the body weight and expressed as heart weight (HW)/body weight (BW) (mg/g).

Cell culture

NRVMs were isolated from the hearts of 1-3-day-old Wistar rats. The rat pups were sacrificed by decapitation. NRVMs were isolated using the Pierce cardiomyocyte isolation kit (Thermo Fisher Scientific, MA, United States) following the provided protocol. Briefly, the heart tissue was minced using scissors and subjected to enzymatic treatment. The tissue was then filtered through a 100 μm filter to remove large tissue fragments. The enzyme in the medium was removed by washing it with Hank's Balanced Salt Solution (HBSS) buffer (Thermo Fisher Scientific). The cell suspension was subsequently resuspended in Dulbecco's Modified Eagle Medium (DMEM) (Thermo Fisher Scientific) and gently agitated by pipetting. The NRVMs were seeded onto uncoated 100 mm culture dishes and placed in a CO_2 incubator at 37°C for 90 min; this incubation period allowed non-cardiomyocytes that did not attach to the bottom of the culture dish to be removed. After the incubation, the NRVMs adhering to the culture dish were recovered. The number of NRVMs was determined based on the specific requirements of each experiment. The cells were cultured for 3–4 days before the experiments were conducted. In accordance with the manufacturer's manual and consistent with previous findings (Ali et al., 2019), our cell population exhibited high cardiomyocyte purity, with over 95% of cells testing positive for cardiac troponin T (cTnT) (cTnT-positive cells: 95.8% ± 2.6%, n = 5), while endothelial cells {platelet endothelial cell adhesion molecule-1 [PECAM-1 (CD31)]-positive cells} were minimally present (PECAM-1-positive cells: 3.8% ± 2.3%, n = 5). We used cTnT antibody (1:500) (sc-20025, Santa Cruz, CA, United States) and PECAM-1 antibody (1:500) (sc-376764, Santa Cruz) for immunostaining, and confirmation was obtained through fluorescence microscopy (BZ-X800, Keyence).

Morphological analysis and immunocytochemistry of NRVMs

Morphological analysis of NRVM hypertrophy and immunocytochemistry were conducted following previously described methods (Tagashira et al., 2023). NRVM cells subjected to each experimental condition were fixed with 4% formaldehyde. The fixed cells were then blocked by incubation with 1% bovine serum albumin (BSA) in phosphate-buffered saline (PBS). For cell size measurements, the fixed cells were incubated with rhodamine-phalloidin reagent (Abcam) in PBS containing 1% BSA for 1 h at room temperature. Mitochondrial staining was performed as previously described (Tagashira et al., 2023). For mitochondrial membrane potential and size measurements, the cells were stained with 0.1 μM MitoTracker Red CMXRos (M7512, Invitrogen) in serum-free DMEM for 30 min. For immunocytochemistry, the cells were incubated with anti-dynamin related protein 1 (DRP1) antibody (sc-101270, Santa Cruz) (1:200) in PBS containing 1% BSA at 4°C for overnight to assess DRP1 morphology.

Random cell images were captured using a fluorescence microscope (BZ-X800, Keyence, Osaka, Japan) with a BZ-X filter for cell size measurements. Cross sectional area (CSA) was quantified using the ImageJ program (Schneider et al., 2012). All cells from randomly selected fields were analyzed, and a minimum of 100 myocytes were measured for each experimental condition. Immunofluorescence images for DRP1, mitochondrial membrane potential, and mitochondrial morphology measurements were acquired randomly using a confocal laser scanning microscope (LSM980, Carl Zeiss Microscopy, Jena, Germany) at the appropriate excitation/emission wavelengths. Fluorescence intensity and mitochondrial length were measured using the ImageJ program. For mitochondrial length analysis, at least 60 mitochondria were calculated for each experimental condition, including all mitochondria within the cells (Jong et al., 2019). The Calmpfit software (Clampex 11.2, Molecular Devices, CA, United States) was utilized to determine the average value obtained through Gaussian fitting of the distribution map, with the length of mitochondria plotted along the horizontal axis. The 50% inhibition concentration (IC_{50}) of MBT was calculated in GraphPad Prism 9 (GraphPad software, CA, United States), using the sigmoidal dose-response equation "log [inhibitor] vs. response–variable slope," defined as:

$$Y = \text{Bottom} + \left(\text{Top} - \text{Bootom}\right) \Big/ \left(1 + 10^{\left(\text{LogIC50}-X\right)*\text{Hill slope}}\right)$$

Where "Top" represents the maximal response, "Bottom" represents the maximally inhibited response, and "Hill slope" represents the steepness of the curve.

Measurement of cell viability and cytotoxicity

Cell viability was assessed using a colorimetric MTT assay kit (Cell counting kit-8; Dojindo). NRVMs were cultured at 4.0×10^5 cells/mL in 96-well plates and maintained in DMEM. Measurements were conducted 72 h after treatment with 100 nM AngII using absorbance at 450 nm wavelengths on a Multiskan JX plate reader (model 353, Thermo Fisher Scientific). The cell viability depicted in Figures 2E, 5C is presented as a relative value (%) of the absorbance obtained in each experiment, normalized to the average value of the control condition. To assess cardiomyocyte cytotoxicity, we employed a colorimetric lactate dehydrogenase (LDH) activity assay kit (Cytotoxicity LDH Assay Kit-WST, Dojindo) following the manufacturer's protocol. NRVMs were plated at a 4.0×10^5 cells/mL density in 96-well plates and cultured in DMEM. Measurements were conducted 72 h after exposure to 100 nM AngII. The release of LDH activity was quantified using an Infinite M200 microplate reader (Tecan Group Ltd., Männedorf, Switzerland) by measuring the absorbance of the formazan dye at an optical wavelength of 490 nm. Cytotoxicity data, as presented in Figures 2F, 5D, were calculated in accordance with the manufacturer's instructions.

Measurement of intracellular Ca^{2+}, ROS, and ATP content

$[Ca^{2+}]_i$ measurements using Fluo-4 AM (F312, Dojindo) and ROS measurements using H_2DCFDA (C400, Invitrogen) were conducted following the manufacturer's protocol. NRVMs were cultured in 96-well plates at 4.0×10^5 cells/mL and maintained in DMEM. $[Ca^{2+}]_i$ and ROS measurements were performed 48 h after treatment with 100 nM AngII. For $[Ca^{2+}]_i$ measurements, cells were incubated with 5 μM Fluo-4 AM in Hank's Balanced Salt Solution (HBSS) (Thermo Fisher Scientific) containing 1 mM $CaCl_2$ for 30 min at 37°C in a CO_2 incubator. After washing with HBSS, $[Ca^{2+}]_i$ levels at excitation/emission wavelength = 485/538 nm were quantified using a fluorescence microplate reader (Fluoroskan Ascent, Thermo Fisher Scientific). For ROS measurements, cells were treated with 5 μM H_2DCFDA in HBSS for 30 min at 37°C in a CO_2 incubator. Subsequently, the cells were washed with HBSS, and ROS levels at excitation/emission wavelength = 485/538 nm were measured using a fluorescence microplate reader (Fluoroskan Ascent, Thermo Fisher Scientific). ATP measurement was performed using an ATP assay kit (Fujifilm Wako), following the manufacturer's protocol as previously described (Tagashira et al., 2023). Luminescence was recorded using a Lumitester C-110 (Kikkoman Biochemifa, Tokyo, Japan). The ATP content presented in Figure 2G is expressed as a relative value (%) of the absorbance obtained in each experiment, normalized to the average value of the control condition.

RNA isolation and real time-PCR

RNA isolation followed a previously described protocol (Numata et al., 2021). Total RNA was extracted from NRVMs using the NucleoSpin® RNA Plus kit (Takara-Bio, Otsu, Japan) according to the manufacturer's instructions. The concentration and purity of the extracted RNA were assessed using a Nanodrop-ND1000 spectrophotometer (Thermo Fisher Scientific). Reverse transcription of the total RNA samples was performed using the Prime-Script™ II 1st Strand cDNA Synthesis Kit (Takara-Bio) with Prime-Script RTase for 60 min at 42°C, following the manufacturer's protocol. Quantitative real-time PCR was carried out using the SYBR Green Real time PCR Master Mix -Plus (Toyobo Co., Ltd., Osaka, Japan) on a LightCycler® 480 real-time PCR system (Roche Diagnostics Ltd., Rotkreuz, Switzerland), following the manufacturer's instructions. Gene-specific primer sequences were synthesized by FASMAC (Kanagawa, Japan). The rat primer sequences used were as follows: Atrial natriuretic peptide (ANP) (NM_012612.2, 105 bp) forward and reverse primers: 5′-AAATCC CGTATACAGTGCGG-3′, and 5′-GGAGGCATGACCTCATCT TC-3′, respectively (Böckmann et al., 2019); Brain natriuretic peptide (BNP) (NM_031545.1, 364 bp) forward and reverse primers: 5′-CCATCGCAGCTGCCTGGCCCATCACTTCTG-3′, and 5′-GACTGCGCCGATCCGGTC-3′, respectively (Birnbaum et al., 2019); β-myosin heavy chain (β-MHC) (NM_017240.2, 238 bp) forward and reverse primers: 5′-TGCAGTTAAAGGTGAAGG C-3′, and 5′-CAGGGCTTCACAGGCAT-3′, respectively (Liu et al., 2018); Regulator of calcineurin 1 (RCAN1) (NM_153724.2, 206 bp) forward and reverse primers: 5′-GCCCGTTGAAAAAGCAGAAT-3′, and 5′-GACAGGGGGTTGCTGAAGTT-3′, respectively (Friedrich et al., 2014); $AT_{1A}R$ (NM_030985.4, 306 bp) forward and reverse primers: 5′-CGTCATCCATGACTGTAAAATTTC-3′, and 5′-GGGCATTACATTGCCAGTGTG-3′, respectively (Miyata et al., 1999); $AT_{1B}R$ (NM_031009.2, 345 bp) forward and reverse primers: 5′-CATTATCCGTGACTGTGAAATTG-3′, and 5′-GCT GCTTAGCCCAAATGGTCC-3′, respectively (Miyata et al., 1999); AT_2R (NM_012494.4, 1126 bp) forward and reverse primers: 5′-TTGCTGCCACCAGCAGAAAC-3′, and 5′-GTGTGGGCCTCC AAACCATTGCTA-3′, respectively (Xu et al., 2002); Sodium-calcium exchanger 1 (NCX1) (NM_019268.4, 334 bp) forward and reverse primers: 5′-GGATGTGGTTGAAAATGACCCAGT-3′, and 5′-TATGCCATCTTCCGAGACTTCTGA-3′, respectively (Nagano et al., 2004); Ryanodine receptor 1 (RyR1), (NM_ 001419537.1, 101 bp) forward and reverse primers: 5′-CAAGCG GAAGGTTCTGGACA-3′, and 5′-TGTGGGCTGTGATCTCCA GAG-3′, respectively (Ferretti et al., 2015); RyR2 (NM_032078.3, 130 bp) forward and reverse primers: 5′-CATCGGTGATGAAAT TGAAGA-3′, and 5′-AGCATCAATGATCAAACCTTG-3′, respectively (Jurkovicova et al., 2007); type 2 inositol 1,4,5-trisphosphate receptor (IP_3R2) (NM_031046.4, 362 bp) forward and reverse primers: 5′-GCTCTTGTCCCTGACATTG-3′, and 5′-CCCATGTCTCCATTCTCATAGC-3′, respectively (Jurkovicova et al., 2007); DRP1 (NM_053655.3, 148 bp) forward and reverse primers: 5′-AGAATATTCAAGACAGCGTCCCAAAG-3′, and 5′-CGCTGTGCCATGTCCTCGGATTC-3′, respectively (da Silva et al., 2014); Translocase of the outer mitochondrial membrane 20 (Tom20) (NM_152935.2, 198 bp) forward and reverse primers: 5′-TGGGCTTTCCAAGTTACCTGATT-3′, and 5′-ACTGGTGGT GGAAGAGTCTGTTGTA-3′, respectively (Tian et al., 2022); Voltage-dependent anion channel 1 (VDAC1) (NM_031353.2, 242 bp) forward and reverse primers: 5′-CAACACGGAGAC CACCAAAG-3′, and 5′-CACAGCCCAGGTTGATATGC-3′,

respectively (Li et al., 2023); Mitofusin 1 (Mfn1) (NM_138976.2, 140 bp) forward and reverse primers: 5′-CTCGGAATCAACGCTGATGAAC-3′, and 5′-TGCGCACATCCTCCATATATTCT-3′, respectively (Leduc-Gaudet et al., 2018); Mfn2 (NM_130894.4, 412 bp) forward and reverse primers: 5′-CTCAGGAGCAGCGGGTTTATTGTCT-3′, and 5′-TGTCGAGGGACCAGCATGTCTATCT-3′, respectively (Gao et al., 2012); Opa1 (NM_133585.3, 189 bp) forward and reverse primers: 5′-AAGAACCTGGAATCTCGAGGAGTCG-3′, and 5′-CCAGAACAGGACCACGTCGTTGC-3′, respectively (da Silva et al., 2014); Mitochondrial fission 1 protein (Fis1) NM_001401051.1, 130 bp) forward and reverse primers: 5′-ACAATGACGACATCCGTAGAGG-3′, and 5′-GCCTTTTCATATTCCTTGAGCCG-3′, respectively (Leduc-Gaudet et al., 2018); Mitochondrial fission process protein 1 (Mtfp1) (NM_001006960.1, 102 bp) forward and reverse primers: 5′-AGATGAAGGCCCTGAGGAGT-3′, and 5′-CCAGTGTTCGTTCCCACTCA-3′, respectively (designed by authors using Primer-BLAST); β-actin (NM_031144.3, 77 bp) forward and reverse primers: 5′-ACTATCGGCAATGAGCGGTTC-3′, and 5′-ATGCCACAGGATTCCATACCC-3′, respectively (Bao et al., 2017); Glyceraldehyde-3-phosphate dehydrogenase (GAPDH) (NM_017008.4, 140 bp) forward and reverse primers: 5′-GCAAGTTCAACGGCACAG-3′, and 5′-GCCAGTAGACTCCACGACAT-3′, respectively (Liu et al., 2018). PCR was conducted using KOD-Plus-Ver.2 (Toyobo) with the following conditions: initial denaturation at 94°C for 2 min, followed by 35 cycles of denaturation at 98°C for 10 s, annealing at 55°C for 30 s, and a final extension at 68°C for 60 s. The real-time PCR reactions were performed in triplicate for each sample, and the cycling conditions were as follows: initial denaturation at 95°C for 30 min, followed by 40 cycles of denaturation at 95°C for 5 s, annealing at 55°C for 10 s, and extension at 72°C for 90 s. Melting curve analysis was performed to verify the specificity of the amplification. The relative expression levels of the target genes were normalized to the expression of the housekeeping gene *GAPDH*. To ensure the reliability of the normalization process, we also evaluated the expression of another housekeeping gene, *β-actin*. This analysis was conducted meticulously and confirmed no significant differences compared to the expression levels of *GAPDH*. The data were analyzed using the ΔΔCt method to calculate the mRNA level. Additionally, a representative gel image of the real-time PCR products was captured using gel electrophoresis to confirm the specificity of the amplification. The PCR products were separated on a 2% agarose gel and visualized using GelRed™ (Fujifilm Wako) staining.

Western blot analysis

Western blot analysis followed established procedures, as previously described (Numata et al., 2021). Briefly, NRVMs were lysed in radio-immunoprecipitation assay (RIPA) buffer (Nacalai Tesque) and centrifuged at 15,000 g for 15 min. Whole-cell lysates were fractionated by SDS-PAGE (sodium dodecyl sulfate-polyacrylamide gel electrophoresis) on either 10% polyacrylamide gels. Following electrophoresis, proteins were transferred onto a polyvinylidene fluoride (PVDF) membrane. The PVDF membrane was then incubated with primary antibodies, specifically anti-DRP1 antibody (1:500) (sc-101270, Santa Cruz) and anti-β-actin antibody (1:2000) (A1978, Sigma-Aldrich) as internal standard. After the primary antibody incubation, the blots were incubated with the secondary antibody of mouse IgG (1:2000) (NA9310, Amersham, Little Chalfont, United Kingdom). Immunoreactivities were visualized using a chemiluminescence reagent (ImmunoStar Zeta, Fujifilm Wako). The chemiluminescence emitted by the membrane was detected using the LumiVision Pro 400EX system (Aisin Seiki Co., Ltd., Aichi, Japan). Quantitative analysis of the Western blot results was performed using the ImageJ program.

Statistical analysis

Statistical analysis and preparation of figures were performed using GraphPad prism software (version 9, GraphPad software). Results were expressed as mean ± standard error of the mean (SEM). To assess the difference between two means, the Student's t-test was employed after conducting an F-test to verify the equality of variances within the population of assessments. A p-value of $p < 0.05$ was considered statistically significant to determine the presence of a significant difference. Experimental procedures were repeated at least three times independently to ensure reproducibility of results. Data are represented visually using bar or line graphs, mean values are shown, and error bars represent SEM. We followed Chou's paper as a reference in calculating the combination index (CI) (Chou, 2010).

Results

Effect of MBT on AngII-induced cardiomyocyte hypertrophy and death in cultured NRVMs

Angiotensin II (AngII) is a well-established inducer of cardiomyocyte hypertrophy (Sadoshima and Izumo, 1993). Previous studies have commonly used a concentration of 100 nM AngII to induce hypertrophy and cell death in cardiomyocytes (Huang et al., 2014; Li et al., 2014; Chhor et al., 2023). Therefore, we employed primary neonatal rat ventricular cardiomyocytes (NRVMs) and induced cardiomyocyte hypertrophy by treating them with 100 nM AngII in this study.

As shown in Figure 1, we observed cardiomyocyte hypertrophy at 0, 12, 24, and 48 h after 100 nM AngII administration. The CSA increased to 140.09% ± 6.90%, 168.43% ± 8.85%, and 209.46% ± 11.51% (n = 102–112), respectively. These findings are consistent with previous reports on cell hypertrophy induced by AngII (Feng et al., 2019). Notably, the most significant cardiomyocyte hypertrophy was observed 48 h after AngII administration, and cytotoxicity became apparent at 72 h. Based on these observations, we decided to conduct further experiments at the 48 h.

Building upon the positive outcomes observed in previous cases and reports regarding the efficacy of Japanese Kampo medicines in cardiac amyloidosis, myocarditis, and HF [TJ-20 (Gautam et al., 2014), TJ-27 (Shijie et al., 2010), TJ-36 (Miho et al., 2019), TJ-126 (Imamura et al., 2022)], our study focused on investigating their direct effects on ventricular myocytes. This investigation aimed to assess the impact of these medicines. In addition, to explore

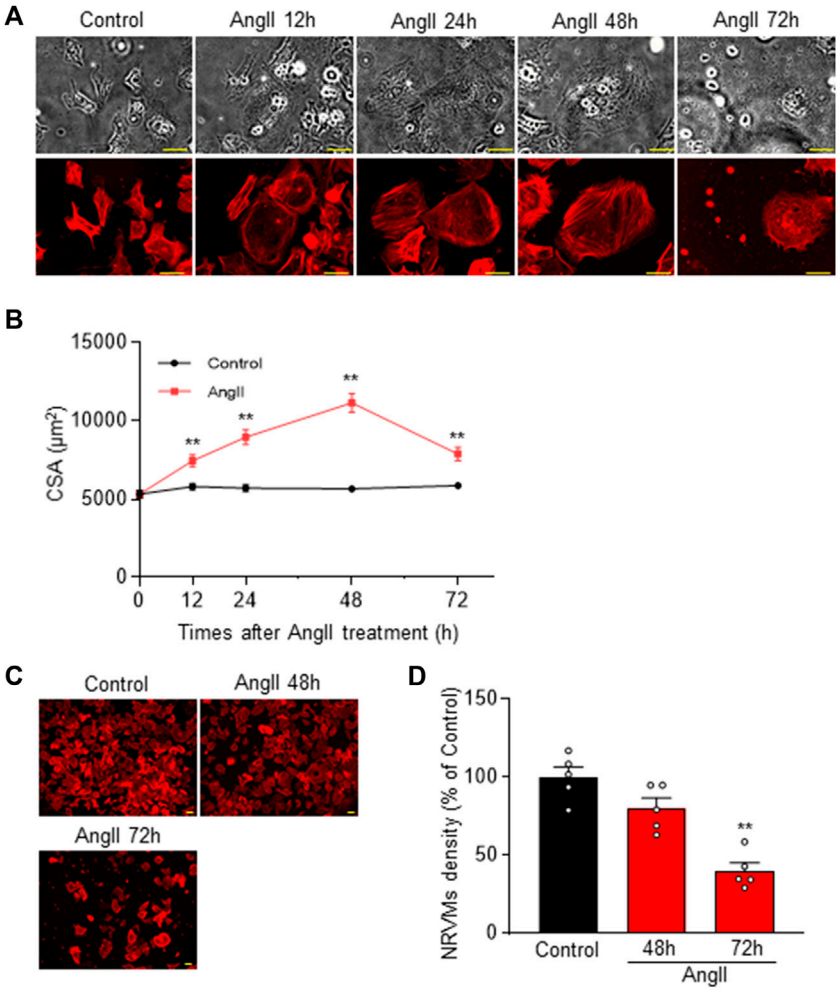

FIGURE 1
Cardiomyocyte hypertrophy in Neonatal Rat Ventricular Myocytes (NRVM) induced by 48 h after AngII challenge. **(A)** Time course of AngII-induced cardiomyocyte hypertrophy in NRVM. Representative cells are shown in transmitted light images (upper row) and rhodamine-conjugated phalloidin-stained fluorescence images (lower row). Hypertrophy of NRVM cells occurs up to 72 h (h) after administration of 100 nM AngII. Scale bar = 50 μm. **(B)** Quantification of CSA from the rhodamine-conjugated phalloidin stained images in **(A)**, demonstrating the temporal progression of CSA across multiple samples (n = 102–112). **(C)** Rhodamine-conjugated phalloidin staining shows cell density at 48 and 72 h post AngII administration. Scale bar = 50 μm. **(D)** Statistical analysis of cell density based on multiple observations as depicted in **(C)** (n = 5). Each column represents the mean ± SEM. **, p < 0.01 versus control cells.

unexplored aspects, we included TJ-19 (Amagaya et al., 2001) and TJ-54 (Yoshida et al., 2022) demonstrating an exacerbating effect on electrocardiograms and conducted a comprehensive analysis involving six specific herbal medicines.

Previous reports of cell-based Kampo medicines screening tests have shown efficacy at concentration ranging from 250 to 500 μg/mL (Liao et al., 2013; Teklemichael et al., 2020). In line with these reports, we examined the effect of these herbal medicines on AngII-induced cardiomyocyte hypertrophy at a concentration of 500 μg/mL.

Six herbal medicines treatment in control NRVMs had no effect on CSA. However, administration of MBT (Hypertrophic cells + MBT) partially but significantly inhibited cell hypertrophy at 48 h after AngII administration (Figures 2A, B), whereas none of the other five Japanese Kampo medicines (Sho-seiryu-to, Boi-ogi-to, Mao-to, Yokukan-san, and Mashinin-gan) showed any significant effect. Subsequently, we investigated the dose dependence of MBT on AngII-induced hypertrophy. MBT dose-dependently inhibited hypertrophy induced by AngII, with an IC_{50} of 214.7 μg/mL and Hill slope of 0.7 (Figure 2C). Based on these results, we treated the cells with MBT at a 500 μg/mL concentration to further investigate the factors associated with the anti-hypertrophic effect, specifically at 48 h following AngII treatment.

To further elucidate the effect of MBT on cardiac hypertrophy, we conducted qRT-PCR experiments to measure the expression of *ANP*, *BNP*, *β-MHC*, and *RCAN1* mRNA levels, all of which serve as markers of cardiac hypertrophy (Figure 2D). In response to AngII treatment, the expression of these markers increased significantly, but their levels were suppressed by MBT treatment. Additionally, MBT ameliorated AngII-induced cellular cytotoxicity (Figures 2E, F). Importantly, treatment with MBT alone did not result in any significant changes compared to control cells, demonstrating that MBT at a concentration of 500 μg/mL does not induce cardiomyocyte toxicity (Figures 2E, F).

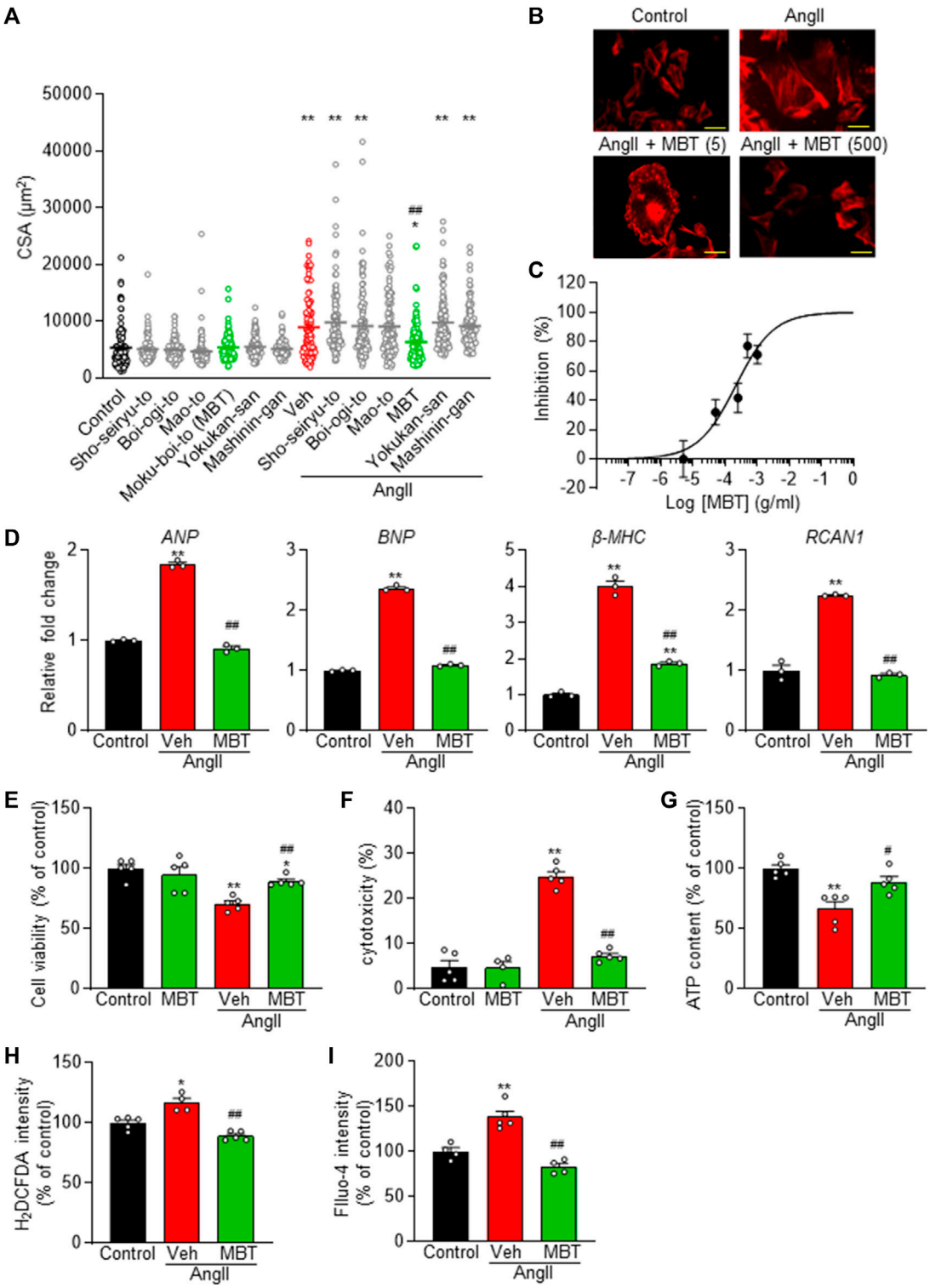

FIGURE 2
Dose-dependent prevention of AngII-induced cardiomyocyte hypertrophy and preservation of cell viability in NRVM by Japanese Kampo Moku-Boi-To. **(A)** Evaluation of the antihypertrophic effect of six types of Japanese Kampo medicines on AngII-induced myocardial hypertrophy. Each group comprises more than 100 cells (n = 101–118). **(B)** Dose-dependent inhibition of 100 nM AngII-induced hypertrophy by MBT. Representative image of cells stained with rhodamine-conjugated phalloidin at each concentration. Scale bar = 50 μm. **(C)** Statistical analysis of dose-dependent inhibition curve of MBT against 100 nM AngII-induced hypertrophy, based on multiple observations as depicted in **(B)**. Each group comprises more than 100 cells (n = 100–111). **(D–I)** Evaluation of the effects of AngII and MBT. NRVMs were treated with control, 100 nM AngII treatment (Veh: vehicle), or AngII +500 μg/mL MBT. **(D)** Quantitative real-time PCR analysis of hypertrophic gene markers, including *ANP*, *BNP*, *β-MHC*, and *RCAN1*. **(E)** Cell viability (n = 5). **(F)** Cytotoxicity (n = 4–5). **(G)** Intracellular ATP content (n = 4–5). **(H)** Intracellular ROS generation (H_2DCFDA intensity) (n = 4–5). **(I)** Intracellular Ca^{2+} concentration (Fluo-4 intensity) (n = 4–5). Each column represents the mean ± SEM. *, $p < 0.05$; **, $p < 0.01$ indicate a significant difference compared to control cells. #, $p < 0.05$, ##, $p < 0.01$ indicate a significant difference compared to AngII + vehicle (Veh) treated cells.

Cardiomyocyte hypertrophy is known to be associated with abnormalities in elevated intracellular levels of ATP, ROS, and $[Ca^{2+}]_i$ (Brown et al., 2017; Quiles and Gustafsson Å, 2022). To investigate the protective effect of MBT, we investigated intracellular signals when NRVM was treated with AngII for 48 h. The results depicted in Figures 2G–I reveal that the AngII-treated group exhibited a notable reduction in ATP content and increase in intracellular ROS and Ca^{2+} concentrations. These results are consistent with previous reports (Wang et al., 2012; Tagashira et al., 2014; Zhao et al., 2020) regarding the effects of AngII on ATP, ROS, and $[Ca^{2+}]_i$ levels. However, in the MBT-treated group, the AngII-induced depletion of ATP and elevation in ROS and $[Ca^{2+}]_i$ were effectively mitigated, indicating the protective effect of MBT against these abnormalities.

Collectively, these results provide strong evidence that MBT effectively mitigates AngII-induced cardiomyocyte hypertrophy and cell death.

Effects of MBT on mitochondrial morphology and function in AngII-treated NRVMs

Figures 3A, B demonstrates increased mitochondrial accumulation of DRP1, a protein essential for mitochondrial fragmentation, in the AngII-treated group (AngII). Additionally, a decrease in the fluorescence intensity of MitoTracker Red CMXRos, a marker that enters mitochondria in a voltage-dependent manner, was observed (Figures 3A, C, AngII, Veh). Mitochondrial fragmentation was enhanced, leading to a significant decrease in mitochondrial length compared to control NRVMs, although the expression level of DRP1 was not affected (Figures 3A, D, E, G–J). These findings indicate that AngII treatment induces abnormalities in mitochondrial morphology and function at 48 h, contributing to cardiomyocyte hypertrophy and death. In contrast, MBT treatment prevented the increased accumulation of DRP1 in mitochondria induced by AngII, restored the fluorescence intensity of MitoTracker Red CMXRos, and attenuated mitochondrial fragmentation (Figures 3A–C, F, G). Collectively, these results demonstrate that MBT directly acts on cardiomyocytes to ameliorate mitochondrial morphological and functional abnormalities.

Effects of MBT on AngII receptors pathway in NRVMs

Ang II receptor antagonists have been implicated in mitochondria protection and the modulation of Ca^{2+} signaling through the AT receptors (ATRs) pathway (Javadov and Escobales, 2015). Thus, we aimed to elucidate the expression patterns of the specific AngII receptor subtypes, AT_1 and AT_2, in NRVMs. Our analysis revealed a prominent expression of $AT_{1A}R$ in NRVMs, while $AT_{1B}R$ and AT_2R expression levels were minimal (Figures 4A, B). Although no significant changes were observed in AngII-treated NRVMs compared to control NRVMs, a notable declining trend in $AT_{1A}R$ mRNA levels were evident (Figures 4A, B). On the other hand, $AT_{1A}R$ mRNA expression was upregulated in the MBT-treated group (Figures 4A, B).

In the context of hypertrophic myocardium induced by AngII, intracellular Ca^{2+} levels are known to be elevated (Wang et al., 2012), and we observed an improvement in Ca^{2+} homeostasis in the MBT treatment group (Figure 2I). To further explore these findings, we conducted a qRT-PCR experiment to assess the expression of critical genes associated with Ca^{2+} homeostasis, specifically IP_3R2, *RyR1*, *RyR2*, and *NCX1* (Figure 4C). After 48 h of AngII treatment, a noticeable decrease in *NCX1* expression and concomitant increase in *RyR1* mRNA levels were observed. These changes indicated disturbances in Ca^{2+} homeostasis resulting from altered expression of these channels. Remarkably, MBT treatment mitigated the increase in RyR1 expression (Figure 4C), suggesting a potential role in restoring Ca^{2+} homeostasis.

Furthermore, considering the observed improvements in ATP and ROS levels in hypertrophic myocardium following MBT treatment (Figures 2G, H), we examined the mRNA expression levels of mitochondrial proteins associated with membrane permeability and chloride channels, including *Tom20* and *VDAC1* (Chacinska et al., 2009; Camara et al., 2017). However, the expression of these mitochondrial-related genes remained unchanged upon stimulation with AngII or administration of MBT treatment (Figure 4D). Subsequently, we explored the mRNA expression of genes related to mitochondrial fusion (*Mfn1/2* and *Opa1*) and mitochondrial fragmentation (*Fis1* and *Mtfp1*) (Donnarumma et al., 2022; Wu et al., 2023) (Figure 4E). Notably, *Opa1*, a mitochondrial fusion protein, exhibited a significant reduction in response to AngII treatment, indicative of mitochondrial fragmentation. In contrast, MBT treatment effectively attenuated this decrease in *Opa1* expression induced by AngII. On the other hand, the mRNA expression levels of *Mfn1/2*, *Fis1*, and *Mtfp1* did not change with AngII stimulation or MBT treatment. These results collectively suggest that MBT administration may play a role in ameliorating Ca^{2+} signaling abnormalities and mitochondrial fragmentation induced by AngII.

Combination effects of MBT and losartan on AngII-induced cardiomyocyte hypertrophy and death in cultured NRVMs.

Based on the results of AT_1Rs expression in NRVMs, we explored the possibility that AT_1R-mediated AngII affects cardiomyocyte hypertrophy. To examine the additional effect of MBT on AngII-induced cardiac hypertrophy, we used the AT_1R inhibitor losartan.

AngII-induced cardiomyocyte hypertrophy was suppressed by losartan, with an IC_{50} of 80.0 nM and Hill slope of 0.6 (Figure 5A). Notably, the concentration-dependent inhibition curve of losartan in the presence of 500 μg/mL MBT showed a substantial effect at losartan concentrations equal to or greater than 1 μM (Figure 5B). Moreover, losartan effectively counteracted the decrease in cell viability, and the increase in cytotoxicity, ROS production, and the increase in $[Ca^{2+}]_i$ induced by AngII (Figures 5C–F). Intriguingly, when comparing the combination treatment of losartan and MBT with the individual therapies, no significant difference were observed in their inhibitory effects on these AngII-induced responses (Figures 5C–F).

Additionally, we investigated the mRNA levels of ATRs. Our findings indicate that both losartan and MBT treatments, whether administered individually or in combination, increased $AT_{1A}R$ expression (Figure 5G). These results suggest that similar to

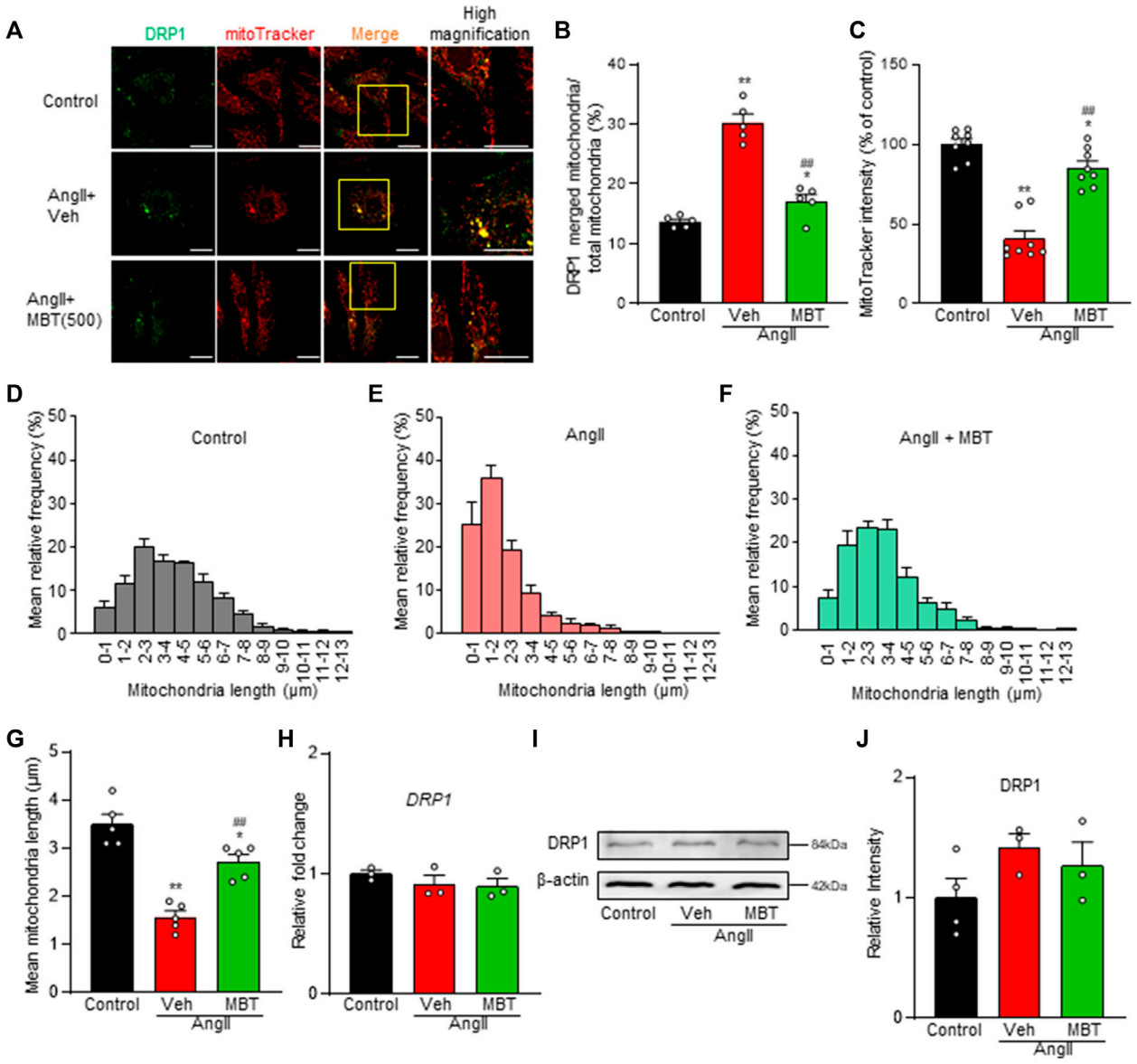

FIGURE 3
Mitochondrial Improvement by MBT in AngII-Treated NRVMs. Mitochondrial assessment of NRVMs under different conditions: control, 100 nM AngII treatment [vehicle (Veh)], and AngII +500 μg/mL MBT. **(A)** Immunofluorescence imaging showing DRP1 (green) and mitochondria (red). Scale bar = 20 μm. **(B)** Ratio of DRP1-bound mitochondria to total mitochondria (n = 5). **(C)** Quantification of mitochondrial membrane potential using MitoTracker Red CMXRos intensity (n = 8–9). **(D–F)** Distribution of mitochondrial length (n = 5). **(G)** Bar graph representing the average mitochondrial length obtained by Gaussian fitting of data from **(D–F)** (n = 5). **(H)** Quantitative real-time PCR analysis of DRP1 (n = 3). **(I)** Representative images of Western blot analysis of DRP1 and β-actin expression are shown. **(J)** Densitometric quantification of DRP1/β-actin immunoreactive bands (n = 3–4). Each column represents the mean ± SEM. *, $p < 0.05$ and **, $p < 0.01$ indicate significant differences compared to the control. ##, $p < 0.01$ indicates a significant difference compared to AngII + vehicle (Veh) treated cells.

losartan, MBT may function by blocking $AT_{1A}R$, leading to its upregulation. Subsequently, we explored the impact of losartan and MBT, either alone or in combination, on mitochondrial morphology and function during AngII-induced cardiomyocyte hypertrophy. We assessed mitochondrial damage by evaluating DRP1 accumulation, function, and morphology. Interestingly, no significant differences were observed in the reduction of DRP1 aggregation upon AngII stimulation when comparing the losartan or MBT monotherapy group to the combination treatment group (Figures 6A, B).

Additionally, we measured a decrease in the fluorescence intensity of MitoTracker Red CMXRos, and both losartan and MBT monotherapy effectively ameliorated this decrease (Figures 6A, C). However, the combination of losartan and MBT did not provide any additional effect. Furthermore, we observed that AngII-induced mitochondrial fragmentation was ameliorated by losartan or MBT alone, but co-administration of losartan and MBT exerted no further effects (Figures 6A, D–H). Notably, there was no change in DRP1 expression among the different treatment groups (Figures 6J–L).

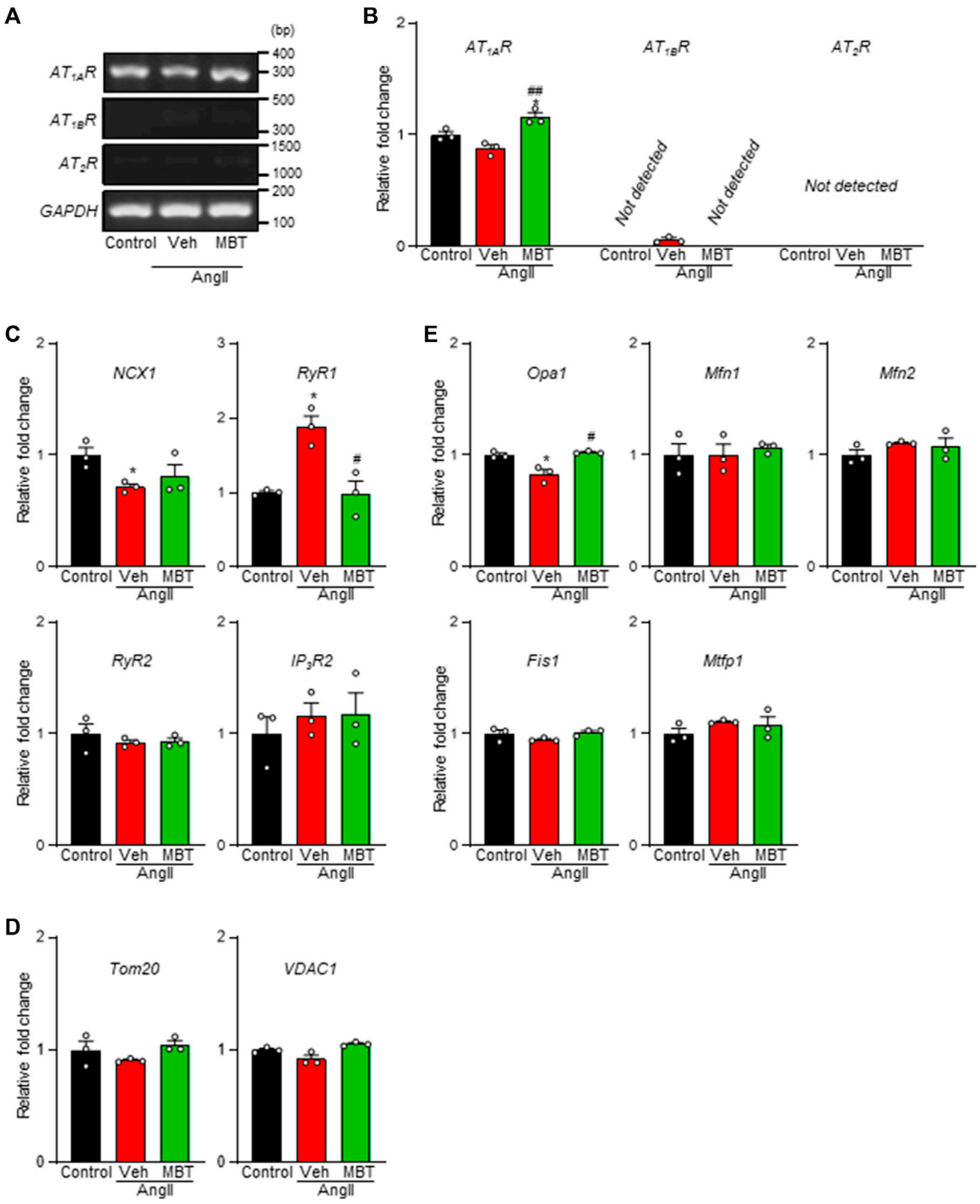

FIGURE 4
Expression of ATRs, Ca^{2+} homeostasis-related genes, and mitochondria-related genes in NRVMs. Evaluation of mRNA expression changes in ATRs, Ca^{2+} homeostasis-related genes, and mitochondrial fusion/fission factors in NRVMs under different conditions: control, 100 nM AngII treatment [vehicle (Veh)], and AngII +500 μg/mL MBT. **(A)** mRNA expression of ATRs. PCR products obtained from NRVMs treated under different conditions show the expression of $AT_{1A}R$, $AT_{1B}R$, AT_2R, and a constitutively transcribed control *GAPDH*. Nucleotide sequences of the PCR products obtained using ATRs-specific primers are identical to the corresponding sequences of $AT_{1A}R$ (306 bp), $AT_{1B}R$ (345 bp), AT_2R (1126 bp), and *GAPDH* (140 bp), respectively. **(B)** Quantitative real-time PCR analysis of $AT_{1A}R$, $AT_{1B}R$, and AT_2R mRNA levels (n = 3). **(C)** Quantitative real-time PCR analysis of Ca^{2+} homeostasis-related genes *NCX1*, *RyR1*, *RyR2*, and IP_3R2 (n = 3). **(D)** Quantitative real-time PCR analysis of mitochondrial transport-related factors *Tom20* and *VDAC1* (n = 3). **(E)** Quantitative real-time PCR analysis of mitochondrial fusion factors *Mfn1/2* and *Opa1* and mitochondrial fragmentation factors *Fis1* and *Mtfp1* (n = 3). Data are presented as fold changes compared to control NRVM values. Each column represents mean ± SEM. *, $p < 0.05$ indicates a significant difference compared to control. #, $p < 0.05$ and ##, $p < 0.01$ indicate significant differences compared to AngII + vehicle (Veh) treated cells.

10.3389/fcell.2023.1264076

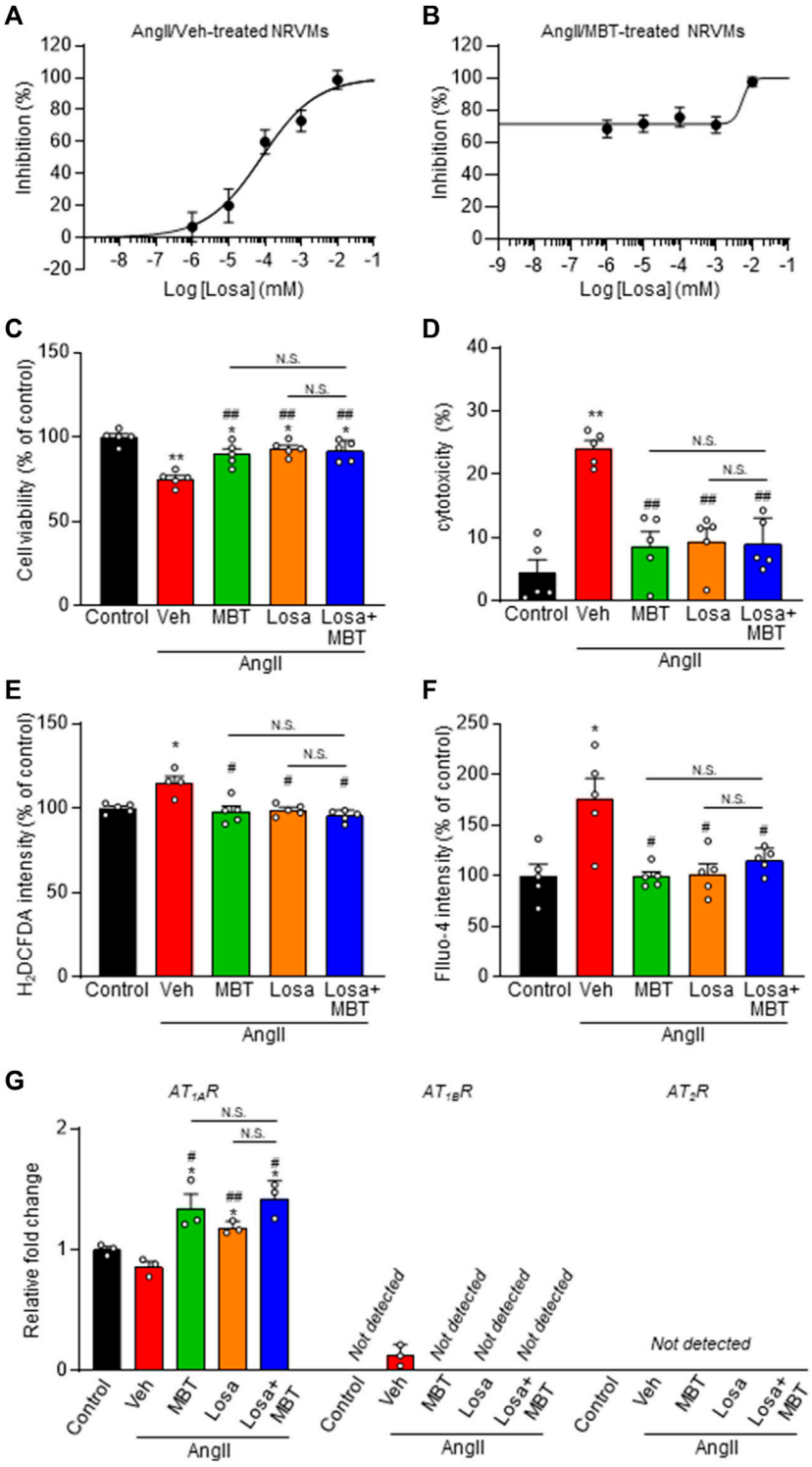

FIGURE 5
Effect of losartan and MBT on NRVMs. **(A,B)** Evaluation of NRVM CSA based on rhodamine-conjugated phalloidin staining in response to 100 nM AngII-induced hypertrophy. **(A)** Dose-dependent inhibition curve of losartan (Losa) (n = 101–111). **(B)** Dose-dependent inhibition curve of losartan co-treated with AngII and 500 μg/mL MBT (n = 104–115). Each group consists of more than 100 cells. **(C–F)** Evaluation of the effects of control, vehicle (Veh), 500 μg/mL MBT, 1 μM Losa, or co-treatment of 1 μM losartan and 500 μg/mL MBT on 100 nM AngII-induced cardiomyocyte hypertrophy, including cell viability (n = 5) **(C)**, cytotoxicity (n = 5) **(D)**, ROS production (H_2DCFDA intensity) (n = 4–5) **(E)**, and intracellular Ca^{2+} concentration (Fluo-4 intensity) (n = 5) **(F)**. **(G)** Quantitative real-time PCR analysis of ATRs (n = 3). Each column represents mean ± SEM. *, $p < 0.05$; **, $p < 0.01$ indicate significant differences compared to control cells. #, $p < 0.05$; ##, $p < 0.01$ indicate significant differences compared to AngII + vehicle (Veh) treated cells. N.S. indicates no significant difference.

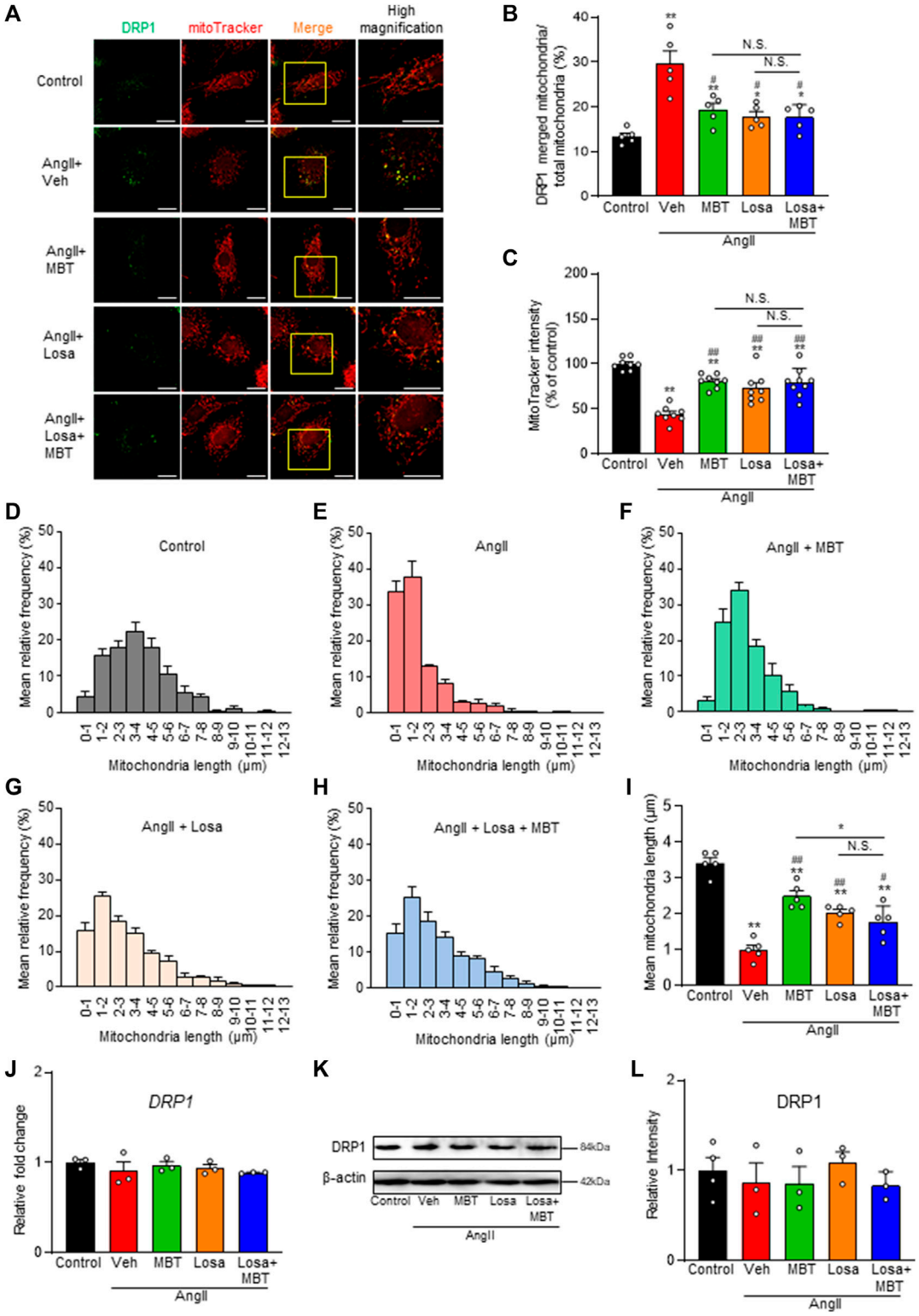

FIGURE 6
Effect of losartan and MBT co-administration on mitochondrial morphology and dysfunction in AngII-induced myocardial hypertrophy. Evaluation of mitochondrial changes induced by 100 nM AngII, control, vehicle (Veh), 500 μg/mL MBT, 1 μM losartan (Losa), or co-treatment of 1 μM losartan and 500 μg/mL MBT (Losa + MBT). **(A)** Immunofluorescence image showing DRP1 in green and mitochondria in red. Scale bar = 20 μm. **(B)** Ratio of DRP1-bound mitochondria/total mitochondria (n = 5). **(C)** Quantification of mitochondrial membrane potential using MitoTracker Red CMXRos intensity (n = 8–9). **(D–H)** Distribution of mitochondrial length measured from images in A (n = 5). **(I)** Bar graph representing the average mitochondrial length obtained by Gaussian fitting from individual panels **(D–H)** (n = 5). **(J)** Quantitative real-time PCR analysis of DRP1 (n = 3). **(K)** Representative images of Western blot analysis showing DRP1 and β-actin expression. **(L)** Densitometric quantification of DRP1/β-actin immunoreactive bands (n = 3–4). Each column represents the mean ± SEM. *, $p < 0.05$ and **, $p < 0.01$, indicating a significant difference compared to control cells. #, $p < 0.05$ and ##, $p < 0.01$ denote a significant difference compared to AngII + vehicle (Veh) treated cells. N.S. indicates no significant difference.

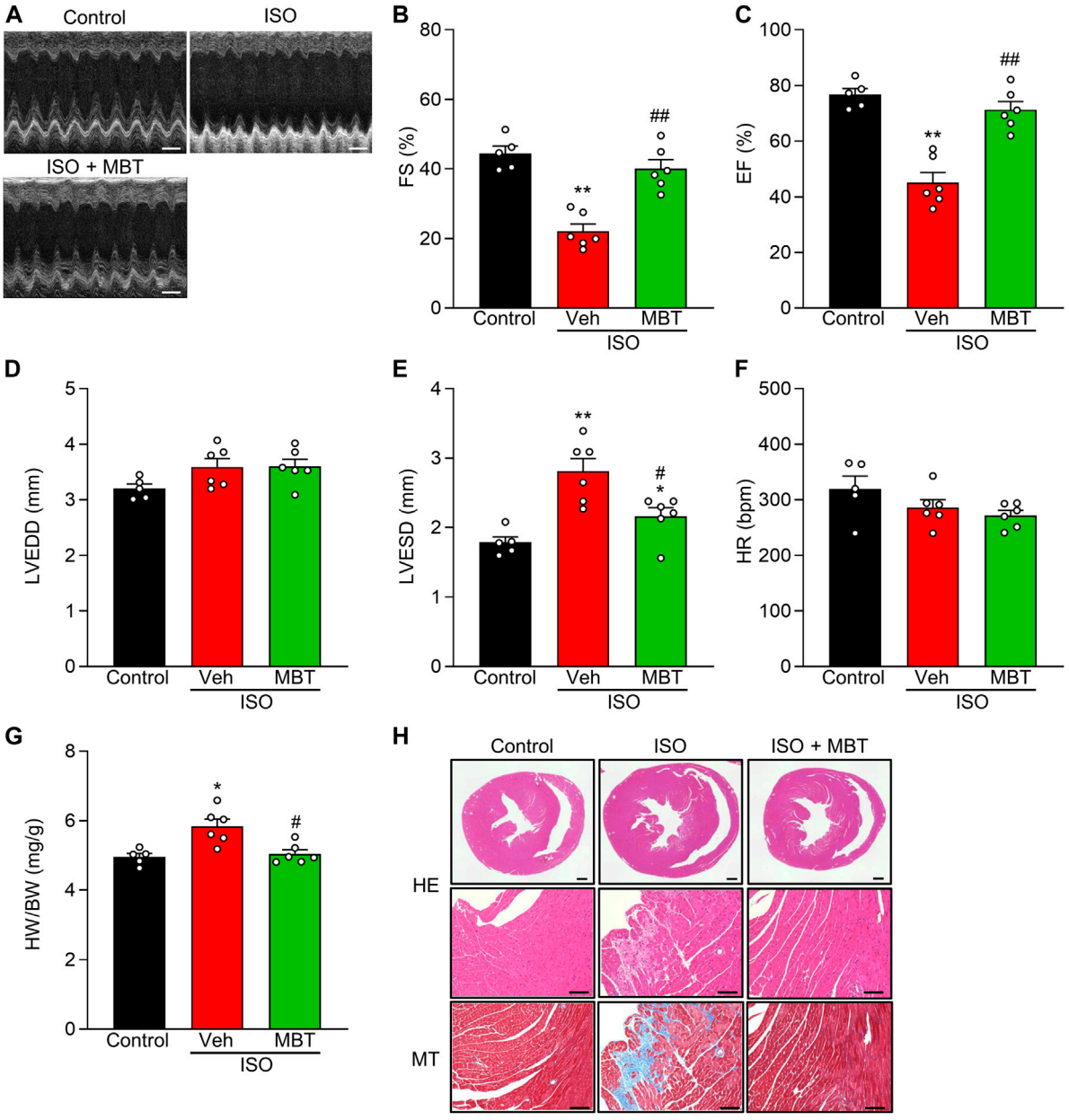

FIGURE 7
Effect of MBT on ISO-induced cardiac hypertrophy and dysfunctions *in vivo*. **(A)** Representative M-mode echocardiograms of mice with or without ISO and/or MBT treatments. Scale bar = 200 ms. **(B)** Changes in percentage of left ventricular (LV) fractional shortening (FS%) (n = 5–6). **(C)** Changes in percentage of LV ejection fraction (EF%) (n = 5–6). **(D)** Changes of left ventricular LV end-diastolic diameter (LVEDD) (n = 5–6). **(E)** Changes of LV end-systolic diameter (LVESD) (n = 5–6). **(F)** Changes in Heart rate (HR) (n = 5–6). **(G)** ISO-induced cardiac hypertrophy as indicated by the heart weight/body weight (HW/BW) ratio (n = 5–6). **(H)** Profiles of heart tissues in mice treated with or without ISO and/or MBT (HE staining and Masson staining) (n = 5–6). Scale bar = 500 μm (whole heart) and 100 μm (High magnification), respectively. Each column represents the mean ± SEM. *, $p < 0.05$ and **, $p < 0.01$, indicating a significant difference compared to control mice. #, $p < 0.05$ and ##, $p < 0.01$ denote a significant difference compared to ISO + vehicle (Veh) treated mice.

Effect of MBT on isoproterenol-induced cardiac hypertrophy and dysfunctions in mice

To assess the protective effect of MBT against ISO-induced cardiac hypertrophy and dysfunction model, we conducted echocardiography in mice (Figure 7A). MBT was administered at a concentration of 500 mg/kg based on previous *in vivo* studies (Wang et al., 1998) and our NRVM findings in this study.

ISO treatment (30 mg/kg body weight, once a day, i.p.) significantly reduced LV FS% and EF% while concurrently increasing LVESD and HW/BW compared to control mice (Figures 7B–E, G). These findings were consistent with previous reports (Park et al., 2018; Cheng et al., 2020). Notably, the administration of MBT (500 mg/kg body weight, p.o.) ameliorated ISO-induced cardiac hypertrophy and cardiac dysfunction (Figures 7B–E, G). HR measurements were performed to ensure that anesthesia depth did not interfere with

the results. No significant changes were observed in any of the experimental groups (Figure 7F). Histological examination of heart tissue from the model group revealed prominent tissue fibrosis and collagen deposition. At the same time, MBT administration prevented the occurrence of these injuries (Figure 7H). In conclusion, our results suggest that MBT effectively improves ISO-induced cardiac hypertrophy and cardiac dysfunction in *in vivo* model mice.

Discussion

The effects of Japanese Kampo medicines on the heart, particularly cardiac mitochondrial function and Ca^{2+} signaling, remain poorly understood despite their widespread use for various diseases. In this study, we conducted a screening analysis and demonstrated, for the first time, that MBT directly acts on cardiomyocytes to prevent AngII-induced hypertrophy and cell death. Furthermore, we found that MBT protects against AngII-induced disruption of intracellular Ca^{2+} homeostasis and mitochondrial dysfunction. In addition, MBT improves ISO-induced cardiac hypertrophy and cardiac dysfunction *in vivo*. Although the exact mechanism of action is not fully elucidated, our findings suggest that these effects may be mediated, at least in part, by angiotensin type I receptor (AT_1R) blocking.

Previous studies have highlighted the association between cardiomyocyte hypertrophy and impaired mitochondrial metabolism (Rosca et al., 2013). For instance, inhibition of mitochondrial fission has been reported to protect the heart against I/R injury *in vivo* (Ong et al., 2010). Additionally, treatment of neonatal rat ventricular myocytes (NRVMs) with AngII induces mitochondrial fission and apoptosis, which can be prevented by the knockdown of DRP1 (Qi et al., 2018). Furthermore, mitochondrial fission has been implicated in endothelin-1-induced hypertrophy and cell death, as well as leptin-induced hypertrophy (Jong et al., 2019; Tagashira et al., 2023). These studies collectively emphasize the importance of mitochondrial quality control in cardiomyocyte hypertrophy and death induced by various stimuli.

Mitochondrial fragmentation leads to increased reactive oxygen species (ROS) production, promotes mitophagy, and decreases ATP production (Tagashira et al., 2013; Tagashira et al., 2014; Yang et al., 2021; Quiles and Gustafsson Å, 2022). ATP depletion and elevated ROS production contribute significantly to the pathogenesis of HF (Doenst et al., 2013; Peoples et al., 2019). Consistent with these findings, our study revealed that AngII treatment induced mitochondrial fragmentation, while MBT treatment ameliorated this effect and suppressed the subsequent increase in ROS production and decrease ATP production (Figures 2G, H).

DRP1, an essential protein involved in mitochondrial fragmentation (Smirnova et al., 2001), accumulates in cardiac mitochondria, implying mitochondrial dysfunction (Aung et al., 2021). Mechanisms such as phosphorylation, mediated by norepinephrine-induced intracellular Ca^{2+} increase and calcineurin activation, have been reported (Pennanen et al., 2014; Aung et al., 2021). Mitochondrial fission 1 protein (Fis1) is another molecule that cooperates with DRP1 to contribute to mitochondrial fragmentation (Zerihun et al., 2023). Meanwhile, mitochondrial fission process protein 1 (Mtfp1) is a key player in mitochondrial fragmentation in cardiac muscle and play an essential role in maintaining heart structure and function (Tondera et al., 2005; Aung et al., 2017). In our study, we observed accumulation of DRP1 in mitochondria of AngII-treated NRVMs, which was ameliorated by MBT treatment, although the expression levels of *DRP1*, *Fis1*, and *Mtfp1* were not affected (Figures 3H–J, 4E).

Interestingly, *Opa1* mRNA exhibited a significant reduction in response to AngII, while MBT treatment attenuated this decrease in *Opa1* mRNA expression (Figure 4E). A previous study using H9c2 cells reported a similar reduction in *Opa1* mRNA with AngII treatment, while *DRP1* and *Fis1* mRNA levels remained unchanged (Gul et al., 2023), which aligns with the findings of our study. These results suggest that the regulation of *Opa1* expression may also play a partial role in the cardioprotective mechanism of MBT. Additionally, MBT inhibited the AngII-induced increase in $[Ca^{2+}]_i$ (Figure 2I), which might contribute to the inhibition of DRP1 accumulation by MBT.

Interestingly, MBT treatment alone resulted in nearly complete improvement in mitochondrial length distribution, suggesting its superiority in terms of mitochondrial quality control (Figures 3C, F, G). This indicates that the effects of MBT may extend beyond AT_1R blocking. Furthermore, while MBT partially suppressed mitochondrial quality control and myocardial hypertrophy, it suppressed AngII-induced intracellular Ca^{2+} overload (Figures 2I, 5F). This improvement in Ca^{2+} homeostasis may be related to the regulation of RyR1 expression (Figure 4C). These results indicate that MBT may act on Ca^{2+}-independent mitochondrial quality control mechanisms crucial for HF development. Detailed investigations are required to determine the precise mechanism by which MBT prevents AngII-induced mitochondrial dysfunction.

Among the six commonly used Japanese Kampo medicines that indicated cardiac effects in human and rodents investigated in this study, MBT was the only one that demonstrated inhibition of cardiac hypertrophy induced by AngII (Figure 2). Unexpectedly, neither inhibitory nor exacerbating effects on AngII-induced cardiomyocyte hypertrophy were detected with treatment of Sho-seiryu-to (TJ-19), Boi-ogi-to (TJ-20), Mao-to (TJ-27), and Yokukan-san (TJ-54), suggesting that the effect of treatment on humans and rodents is not a direct effect on cardiomyocytes or they lack anti-hypertrophic effects. On the other hand, mashinin-gan (TJ-126) had no adverse effects on NRVMs, consistent with previous report (Imamura et al., 2022), indicating that its safe use in patients with cardiac amyloidosis. MBT exhibited significant suppressive effects against AngII-induced hypertrophy, consistent with previous clinical research (Miho et al., 2019). Furthermore, we demonstrated that MBT mitigates cardiac dysfunction and cardiac hypertrophy accompanied by fibrosis in ISO-induced cardiac hypertrophy model mice (Figure 7). This finding aligns with a previous report, which indicated that MBT had a survival benefit in HF model mice (Wang et al., 1998).

Comprising four herbal medicines, MBT has traditionally been employed to alleviate dyspnea, wheezing, and cardiac edema accompanying HF. Although rare, hypersensitivity and gastrointestinal diseases have been reported as side effects. Overall, MBT is considered a safe therapeutic drug. In Japan, it has been utilized for the treatment of HF, and several case reports have highlighted its efficacy (Ezaki et al., 2019; Miho et al., 2019). For example, combination therapy with MBT and standard medical treatment was found to be effective in inoperable

patients with severe aortic regurgitation (Miho et al., 2019). Furthermore, a randomized controlled trial demonstrated that MBT significantly improved HF symptoms in hospitalized patients with acute decompensated HF compared to standard care (Ezaki et al., 2019). Despite its clinical use, the direct effect of MBT on cardiomyocytes and its cardioprotective mechanism has yet to be fully elucidated. This study demonstrated that MBT protects against AngII-induced disruption of intracellular Ca^{2+} homeostasis and mitochondrial dysfunction (Figures 2, 3).

Losartan, a selective AT_1R antagonist without affinity for AT_2R (Schorb et al., 1993), has shown similar effects to angiotensin-converting enzyme inhibitors in animal experiments (Milavetz et al., 1996). Furthermore, losartan has been reported to have beneficial effects on cardiomyocyte contractility, Ca^{2+} regulation, post-infarction remodeling, and gene expression in rat models of chronic HF (Loennechen et al., 2002). Hence, the inhibition of AT_1R is valuable for HF treatment.

In our study, we delved into the competitive inhibition of AT_1R by investigating the combined effects of losartan and MBT in effectively treating cardiomyocyte hypertrophy and cell death. Specifically, we performed a detailed examination of the inhibitory effects of losartan in response to AngII stimulation in NRVM and investigated the potential synergy between losartan and MBT. Remarkably, the concentration-dependent inhibition curve of losartan in the presence of 500 μg/mL MBT showed substantial effects at losartan concentrations of 1 μM and higher (Figure 5B). The inhibition observed with 1 μM losartan in Figure 5B was 71.6%. Based on the data in Figures 2C, 5A, the concentrations of MBT and losartan required for 71.6% inhibition were determined to be 760.3 μg/mL and 409 nM, respectively. As a result, the combination index (CI) calculated for the combination of 1 μM losartan and 500 μg/mL MBT in Figure 5B was 3.1, suggesting the possibility of competitive inhibition between MBT and losartan on $AT_{1A}R$. Notably, the deviation from the dose dependence of losartan alone observed at the 1 μM concentration in Figure 5B may be due to anomalous mole fraction effects resulting from the simultaneous binding of multiple substances to one binding site. It is worth mentioning that the phenomenon has been observed with the same multiple-occupancy theory in a related study (Lester and Dougherty, 1998).

Furthermore, in experiments aimed at confirming the effects of MBT on AngII stimulation, changes in cell viability, cytotoxicity, ROS production, ATP production, ATRs expression, and changes in mitochondrial function and morphology were thoroughly investigated (Figures 5, 6). The comprehensive findings showing that losartan and MBT exhibit similar behavior support the concept that MBT and losartan may target the same site and raise the possibility that $AT_{1A}R$ is potentially a target of MBT. These findings support the hypothesis that MBT may act on AT_1R, although the precise nature of this interaction, whether direct or indirect, remains unclear.

Although it did not reach statistical significance, we observed a trend toward decreased $AT_{1A}R$ expression in response to AngII. This decrease may be due to the increased ATR-mediated signal induced by AngII, leading to the downregulation of $AT_{1A}R$ to attenuate the signal strength. Interestingly, $AT_{1A}R$ expression increased in response to AngII + MBT, AngII + losartan, and AngII + losartan + MBT treatments. This increase in $AT_{1A}R$ expression is thought to be a compensatory mechanism to counteract the attenuation of $AT_{1A}R$-mediated signals. This observation of such a compensatory mechanism is consistent with the previous finding that losartan can upregulate AT_1R in ischemia/reperfusion (I/R) rat hearts (Xu et al., 2002). These results suggest that similar to losartan, MBT may inhibit $AT_{1A}R$, leading to its upregulation. These findings support the hypothesis that MBT exerts its effects by blocking $AT_{1A}R$. However, in the case of $AT_{1B}R$ or AT_2R expression, it remained consistently low, and the underlying mechanism of this phenomenon remains unknown.

In conclusion, our study demonstrates that MBT acts directly on cardiomyocytes, protecting against AngII-induced cardiomyocyte injury and ISO-induced cardiac dysfunction through the regulation of intracellular Ca^{2+} signaling and mitochondrial quality control. These effects may be mediated, at least in part, by the blocking of AT_1R. The findings from this study support the potential use of MBT as an adjunctive therapy for HF. Further research is needed to fully elucidate the underlying mechanisms and explore the clinical implications of MBT treatment in HF management.

Data availability statement

The raw data supporting the conclusion of this article will be made available by the authors, without undue reservation.

Ethics statement

The study was conducted in accordance with the local legislation and institutional requirements.

Author contributions

HT: Formal Analysis, Funding acquisition, Investigation, Methodology, Visualization, Writing–original draft. FA: Investigation, Writing–review and editing. KS-N: Investigation, Methodology, Validation, Writing–review and editing. KA: Investigation, Writing–review and editing. KH: Investigation, Writing–review and editing. YK: Investigation, Writing–review and editing. DI: Investigation, Writing–review and editing. TN: Conceptualization, Data curation, Funding acquisition, Investigation, Methodology, Project administration, Resources, Software, Supervision, Validation, Visualization, Writing–original draft, Writing–review and editing.

Funding

The author(s) declare financial support was received for the research, authorship, and/or publication of this article. This work was supported in part by grants-in-aid for Scientific Research

from the Ministry of Education, Science, Sports and Culture of Japan (KAKENHI 22K06659, 22K06659DK to HT, and 21K06792 to TN), Funding for Advanced Research by the Dean of the Graduate School of Medicine, Akita University (to HT), Akita Prefecture Technology Innovation Creation and Utilization Promotion Project (to HT), and Nishinomiya Basic Research Fund (to HT).

Acknowledgments

We express our gratitude to Ms. Ayako Sakai for her valuable contribution in terms of active preparation and technical support provided for this research.

Conflict of interest

The authors declare that the research was conducted in the absence of any commercial or financial relationships that could be construed as a potential conflict of interest.

Publisher's note

References

Ali, I. I., Al-Salam, S., Howarth, F. C., and Shmygol, A. (2019). Oxytocin induces intracellular Ca^{2+} release in cardiac fibroblasts from neonatal rats. *Cell Calcium* 84, 102099. doi:10.1016/j.ceca.2019.102099

Amagaya, S., Iizuka, A., Makino, B., Kubo, M., Komatsu, Y., Cheng, F. C., et al. (2001). General pharmacological properties of Sho-seiryu-to (TJ-19) extracts. *Phytomedicine* 8 (5), 338–347. doi:10.1078/0944-7113-00061

Aung, L. H. H., Jumbo, J. C. C., Wang, Y., and Li, P. (2021). Therapeutic potential and recent advances on targeting mitochondrial dynamics in cardiac hypertrophy: a concise review. *Mol. Ther. Nucleic Acids* 25, 416–443. doi:10.1016/j.omtn.2021.06.006

Aung, L. H. H., Li, R., Prabhakar, B. S., and Li, P. (2017). Knockdown of Mtfp1 can minimize doxorubicin cardiotoxicity by inhibiting Dnm1l-mediated mitochondrial fission. *J. Cell Mol. Med.* 21 (12), 3394–3404. doi:10.1111/jcmm.13250

Bao, Q., Zhao, M., Chen, L., Wang, Y., Wu, S., Wu, W., et al. (2017). MicroRNA-297 promotes cardiomyocyte hypertrophy via targeting sigma-1 receptor. *Life Sci.* 175, 1–10. doi:10.1016/j.lfs.2017.03.006

Benigni, A., Cassis, P., and Remuzzi, G. (2010). Angiotensin II revisited: new roles in inflammation, immunology and aging. *EMBO Mol. Med.* 2 (7), 247–257. doi:10.1002/emmm.201000080

Bers, D. M. (2006). Altered cardiac myocyte Ca regulation in heart failure. *Physiol. (Bethesda)* 21, 380–387. doi:10.1152/physiol.00019.2006

Birnbaum, Y., Tran, D., Chen, H., Nylander, S., Sampaio, L. C., and Ye, Y. (2019). Ticagrelor improves remodeling, reduces apoptosis, inflammation and fibrosis and increases the number of progenitor stem cells after myocardial infarction in a rat model of ischemia reperfusion. *Cell Physiol. Biochem.* 53 (6), 961–981. doi:10.33594/000000189

Böckmann, I., Lischka, J., Richter, B., Deppe, J., Rahn, A., Fischer, D. C., et al. (2019). FGF23-mediated activation of local RAAS promotes cardiac hypertrophy and fibrosis. *Int. J. Mol. Sci.* 20 (18), 4634. doi:10.3390/ijms20184634

Brown, D. A., Perry, J. B., Allen, M. E., Sabbah, H. N., Stauffer, B. L., Shaikh, S. R., et al. (2017). Expert consensus document: mitochondrial function as a therapeutic target in heart failure. *Nat. Rev. Cardiol.* 14 (4), 238–250. doi:10.1038/nrcardio.2016.203

Camara, A. K. S., Zhou, Y., Wen, P. C., Tajkhorshid, E., and Kwok, W. M. (2017). Mitochondrial VDAC1: a key gatekeeper as potential therapeutic target. *Front. Physiol.* 8, 460. doi:10.3389/fphys.2017.00460

Chacinska, A., Koehler, C. M., Milenkovic, D., Lithgow, T., and Pfanner, N. (2009). Importing mitochondrial proteins: machineries and mechanisms. *Cell* 138 (4), 628–644. doi:10.1016/j.cell.2009.08.005

Cheng, H., Wu, X., Ni, G., Wang, S., Peng, W., Zhang, H., et al. (2020). Citri Reticulatae Pericarpium protects against isoproterenol-induced chronic heart failure via activation of PPARγ. *Ann. Transl. Med.* 8 (21), 1396. doi:10.21037/atm-20-2200

Chhor, M., Chen, H., Jerotić, D., Tešić, M., Nikolić, V. N., Pavlović, M., et al. (2023). FK506-Binding Protein like (FKBPL) has an important role in heart failure with preserved ejection fraction pathogenesis with potential diagnostic utility. *Biomolecules* 13 (2), 395. doi:10.3390/biom13020395

Chou, T. C. (2010). Drug combination studies and their synergy quantification using the Chou-Talalay method. *Cancer Res.* 70 (2), 440–446. doi:10.1158/0008-5472.Can-09-1947

Da Silva, V. K., De Freitas, B. S., Da Silva Dornelles, A., Nery, L. R., Falavigna, L., Ferreira, R. D., et al. (2014). Cannabidiol normalizes caspase 3, synaptophysin, and mitochondrial fission protein DNM1L expression levels in rats with brain iron overload: implications for neuroprotection. *Mol. Neurobiol.* 49 (1), 222–233. doi:10.1007/s12035-013-8514-7

Doenst, T., Nguyen, T. D., and Abel, E. D. (2013). Cardiac metabolism in heart failure: implications beyond ATP production. *Circ. Res.* 113 (6), 709–724. doi:10.1161/circresaha.113.300376

Donnarumma, E., Kohlhaas, M., Vimont, E., Kornobis, E., Chaze, T., Gianetto, Q. G., et al. (2022). Mitochondrial Fission Process 1 controls inner membrane integrity and protects against heart failure. *Nat. Commun.* 13 (1), 6634. doi:10.1038/s41467-022-34316-3

Ezaki, H., Ayaori, M., Sato, H., Maeno, Y., Taniwaki, M., Miyake, T., et al. (2019). Effects of Mokuboito, a Japanese Kampo medicine, on symptoms in patients hospitalized for acute decompensated heart failure - a prospective randomized pilot study. *J. Cardiol.* 74 (5), 412–417. doi:10.1016/j.jjcc.2019.05.003

Feng, H., Wu, J., Chen, P., Wang, J., Deng, Y., Zhu, G., et al. (2019). MicroRNA-375-3p inhibitor suppresses angiotensin II-induced cardiomyocyte hypertrophy by promoting lactate dehydrogenase B expression. *J. Cell Physiol.* 234 (8), 14198–14209. doi:10.1002/jcp.28116

Ferretti, R., Marques, M. J., Khurana, T. S., and Santo Neto, H. (2015). Expression of calcium-buffering proteins in rat intrinsic laryngeal muscles. *Physiol. Rep.* 3 (6), e12409. doi:10.14814/phy2.12409

Friedrich, F. W., Reischmann, S., Schwalm, A., Unger, A., Ramanujam, D., Münch, J., et al. (2014). FHL2 expression and variants in hypertrophic cardiomyopathy. *Basic Res. Cardiol.* 109 (6), 451. doi:10.1007/s00395-014-0451-8

Gao, Q., Wang, X. M., Ye, H. W., Yu, Y., Kang, P. F., Wang, H. J., et al. (2012). Changes in the expression of cardiac mitofusin-2 in different stages of diabetes in rats. *Mol. Med. Rep.* 6 (4), 811–814. doi:10.3892/mmr.2012.1002

Gautam, M., Izawa, A., Saigusa, T., Yamasaki, S., Motoki, H., Tomita, T., et al. (2014). The traditional Japanese medicine (Kampo) boiogito has a dual benefit in cardiorenal syndrome: a pilot observational study. *Shinshu Med. J.* 62 (2), 89–97.

Gul, R., Dar, M. A., Nawaz, S., and Alfadda, A. A. (2023). Protective effects of nanoceria against mitochondrial dysfunction and angiotensin II-induced hypertrophy in H9c2 cardiomyoblasts. *Antioxidants (Basel)* 12 (4), 877. doi:10.3390/antiox12040877

Huang, C. Y., Kuo, W. W., Yeh, Y. L., Ho, T. J., Lin, J. Y., Lin, D. Y., et al. (2014). ANG II promotes IGF-IIR expression and cardiomyocyte apoptosis by inhibiting HSF1 via JNK activation and SIRT1 degradation. *Cell Death Differ.* 21 (8), 1262–1274. doi:10.1038/cdd.2014.46

Hunyady, L., and Catt, K. J. (2006). Pleiotropic AT1 receptor signaling pathways mediating physiological and pathogenic actions of angiotensin II. *Mol. Endocrinol.* 20 (5), 953–970. doi:10.1210/me.2004-0536

Imamura, T., Hori, M., Tanaka, S., and Kinugawa, K. (2022). Successful management of refractory constipation using Kampo medicine Mashiningan in a patient with wild-type ATTR cardiac amyloidosis. *J. Cardiol. Cases* 25 (1), 34–36. doi:10.1016/j.jccase.2021.06.004

Javadov, S., and Escobales, N. (2015). The role of SIRT3 in mediating cardioprotective effects of RAS inhibition on cardiac ischemia-reperfusion. *J. Pharm. Pharm. Sci.* 18 (3), 547–550. doi:10.18433/j3nw2k

Jong, C. J., Yeung, J., Tseung, E., and Karmazyn, M. (2019). Leptin-induced cardiomyocyte hypertrophy is associated with enhanced mitochondrial fission. *Mol. Cell Biochem.* 454 (1-2), 33–44. doi:10.1007/s11010-018-3450-5

Jurkovicova, D., Kopacek, J., Stefanik, P., Kubovcakova, L., Zahradnikova, A., Jr., Zahradnikova, A., et al. (2007). Hypoxia modulates gene expression of IP3 receptors in rodent cerebellum. *Pflugers Arch.* 454 (3), 415–425. doi:10.1007/s00424-007-0214-6

Leduc-Gaudet, J. P., Reynaud, O., Chabot, F., Mercier, J., Andrich, D. E., St-Pierre, D. H., et al. (2018). The impact of a short-term high-fat diet on mitochondrial respiration,

reactive oxygen species production, and dynamics in oxidative and glycolytic skeletal muscles of young rats. *Physiol. Rep.* 6 (4), e13548. doi:10.14814/phy2.13548

Lester, H. A., and Dougherty, D. A. (1998). New views of multi-ion channels. *J. Gen. Physiol.* 111 (2), 181–183. doi:10.1085/jgp.111.2.181

Li, J., Qi, M., Li, C., Shi, D., Zhang, D., Xie, D., et al. (2014). Tom70 serves as a molecular switch to determine pathological cardiac hypertrophy. *Cell Res.* 24 (8), 977–993. doi:10.1038/cr.2014.94

Li, L., Huang, T., Yang, J., Yang, P., Lan, H., Liang, J., et al. (2023). PINK1/Parkin pathway-mediated mitophagy by AS-IV to explore the molecular mechanism of muscle cell damage. *Biomed. Pharmacother.* 161, 114533. doi:10.1016/j.biopha.2023.114533

Liao, J., Zhao, L., Yoshioka, M., Hinode, D., and Grenier, D. (2013). Effects of Japanese traditional herbal medicines (Kampo) on growth and virulence properties of porphyromonas gingivalis and viability of oral epithelial cells. *Pharm. Biol.* 51 (12), 1538–1544. doi:10.3109/13880209.2013.801995

Liu, Y., Shen, H. J., Wang, X. Q., Liu, H. Q., Zheng, L. Y., and Luo, J. D. (2018). EndophilinA2 protects against angiotensin II-induced cardiac hypertrophy by inhibiting angiotensin II type 1 receptor trafficking in neonatal rat cardiomyocytes. *J. Cell Biochem.* 119 (10), 8290–8303. doi:10.1002/jcb.26862

Loennechen, J. P., Wisløff, U., Falck, G., and Ellingsen, O. (2002). Effects of cariporide and losartan on hypertrophy, calcium transients, contractility, and gene expression in congestive heart failure. *Circulation* 105 (11), 1380–1386. doi:10.1161/hc1102.105258

Milavetz, J. J., Raya, T. E., Johnson, C. S., Morkin, E., and Goldman, S. (1996). Survival after myocardial infarction in rats: captopril versus losartan. *J. Am. Coll. Cardiol.* 27 (3), 714–719. doi:10.1016/0735-1097(95)00506-4

Miho, E., Iwai-Takano, M., Saitoh, H., and Watanabe, T. (2019). Acute and chronic effects of mokuboito in a patient with heart failure due to severe aortic regurgitation. *Fukushima J. Med. Sci.* 65 (2), 61–67. doi:10.5387/fms.2019-05

Miyata, N., Park, F., Li, X. F., and Cowley, A. W., Jr. (1999). Distribution of angiotensin AT1 and AT2 receptor subtypes in the rat kidney. *Am. J. Physiol.* 277 (3), F437–F446. doi:10.1152/ajprenal.1999.277.3.F437

Nagano, T., Kawasaki, Y., Baba, A., Takemura, M., and Matsuda, T. (2004). Up-regulation of Na^+-Ca^{2+} exchange activity by interferon-gamma in cultured rat microglia. *J. Neurochem.* 90 (4), 784–791. doi:10.1111/j.1471-4159.2004.02511.x

Numata, T., Sato-Numata, K., Hermosura, M. C., Mori, Y., and Okada, Y. (2021). TRPM7 is an essential regulator for volume-sensitive outwardly rectifying anion channel. *Commun. Biol.* 4 (1), 599. doi:10.1038/s42003-021-02127-9

Okada, Y., Numata, T., Sato-Numata, K., Sabirov, R. Z., Liu, H., Mori, S. I., et al. (2019). Roles of volume-regulatory anion channels, VSOR and Maxi-Cl, in apoptosis, cisplatin resistance, necrosis, ischemic cell death, stroke and myocardial infarction. *Curr. Top. Membr.* 83, 205–283. doi:10.1016/bs.ctm.2019.03.001

Ong, S. B., Subrayan, S., Lim, S. Y., Yellon, D. M., Davidson, S. M., and Hausenloy, D. J. (2010). Inhibiting mitochondrial fission protects the heart against ischemia/reperfusion injury. *Circulation* 121 (18), 2012–2022. doi:10.1161/circulationaha.109.906610

Page, R. L., 2nd, O'bryant, C. L., Cheng, D., Dow, T. J., Ky, B., Stein, C. M., et al. (2016). Drugs that may cause or exacerbate heart failure: a scientific statement from the american heart association. *Circulation* 134 (6), e32–e69. doi:10.1161/cir.0000000000000426

Park, S. W., Persaud, S. D., Ogokeh, S., Meyers, T. A., Townsend, D., and Wei, L. N. (2018). CRABP1 protects the heart from isoproterenol-induced acute and chronic remodeling. *J. Endocrinol.* 236 (3), 151–165. doi:10.1530/joe-17-0613

Pennanen, C., Parra, V., López-Crisosto, C., Morales, P. E., Del Campo, A., Gutierrez, T., et al. (2014). Mitochondrial fission is required for cardiomyocyte hypertrophy mediated by a Ca^{2+}-calcineurin signaling pathway. *J. Cell Sci.* 127 (12), 2659–2671. doi:10.1242/jcs.139394

Peoples, J. N., Saraf, A., Ghazal, N., Pham, T. T., and Kwong, J. Q. (2019). Mitochondrial dysfunction and oxidative stress in heart disease. *Exp. Mol. Med.* 51 (12), 1–13. doi:10.1038/s12276-019-0355-7

Qi, J., Wang, F., Yang, P., Wang, X., Xu, R., Chen, J., et al. (2018). Mitochondrial fission is required for angiotensin II-induced cardiomyocyte apoptosis mediated by a Sirt1-p53 signaling pathway. *Front. Pharmacol.* 9, 176. doi:10.3389/fphar.2018.00176

Quiles, J. M., and Gustafsson Å, B. (2022). The role of mitochondrial fission in cardiovascular health and disease. *Nat. Rev. Cardiol.* 19 (11), 723–736. doi:10.1038/s41569-022-00703-y

Rahm, A. K., Lugenbiel, P., Schweizer, P. A., Katus, H. A., and Thomas, D. (2018). Role of ion channels in heart failure and channelopathies. *Biophys. Rev.* 10 (4), 1097–1106. doi:10.1007/s12551-018-0442-3

Rosca, M. G., Tandler, B., and Hoppel, C. L. (2013). Mitochondria in cardiac hypertrophy and heart failure. *J. Mol. Cell Cardiol.* 55, 31–41. doi:10.1016/j.yjmcc.2012.09.002

Sadoshima, J., and Izumo, S. (1993). Molecular characterization of angiotensin II--induced hypertrophy of cardiac myocytes and hyperplasia of cardiac fibroblasts. Critical role of the AT1 receptor subtype. *Circ. Res.* 73 (3), 413–423. doi:10.1161/01.res.73.3.413

Satoh, H. (2005). Electropharmacological actions of the constituents of Sinomeni Caulis et Rhizome and Mokuboi-to in Guinea pig heart. *Am. J. Chin. Med.* 33 (6), 967–979. doi:10.1142/s0192415x05003569

Satoh, H. (2017). Electrophysiology and cardiovascular pharmacology of Mokuboito (Formula Aristolochiae): cardiotonic and cardioprotective actions for chronic heart failure. *Cardiol. Res. Cardiovasc Med.* 2, 117. doi:10.29011/2575-7083.000017

Savarese, G., and Lund, L. H. (2017). Global public health burden of heart failure. *Card. Fail Rev.* 3 (1), 7–11. doi:10.15420/cfr.2016:25:2

Schneider, C. A., Rasband, W. S., and Eliceiri, K. W. (2012). NIH Image to ImageJ: 25 years of image analysis. *Nat. Methods* 9 (7), 671–675. doi:10.1038/nmeth.2089

Schorb, W., Booz, G. W., Dostal, D. E., Conrad, K. M., Chang, K. C., and Baker, K. M. (1993). Angiotensin II is mitogenic in neonatal rat cardiac fibroblasts. *Circ. Res.* 72 (6), 1245–1254. doi:10.1161/01.res.72.6.1245

Shijie, Z., Moriya, J., Yamakawa, J., Chen, R., Takahashi, T., Sumino, H., et al. (2010). Mao-to prolongs the survival of and reduces TNF-alpha expression in mice with viral myocarditis. *Evid. Based Complement. Altern. Med.* 7 (3), 341–349. doi:10.1093/ecam/nen010

Smirnova, E., Griparic, L., Shurland, D. L., and Van Der Bliek, A. M. (2001). Dynamin-related protein Drp1 is required for mitochondrial division in mammalian cells. *Mol. Biol. Cell* 12 (8), 2245–2256. doi:10.1091/mbc.12.8.2245

Tagashira, H., Bhuiyan, M. S., Shinoda, Y., Kawahata, I., Numata, T., and Fukunaga, K. (2023). Sigma-1 receptor is involved in modification of ER-mitochondria proximity and Ca^{2+}homeostasis in cardiomyocytes. *J. Pharmacol. Sci.* 151 (2), 128–133. doi:10.1016/j.jphs.2022.12.005

Tagashira, H., Bhuiyan, M. S., Shioda, N., and Fukunaga, K. (2014). Fluvoxamine rescues mitochondrial Ca^{2+} transport and ATP production through σ(1)-receptor in hypertrophic cardiomyocytes. *Life Sci.* 95 (2), 89–100. doi:10.1016/j.lfs.2013.12.019

Tagashira, H., Zhang, C., Lu, Y. M., Hasegawa, H., Kanai, H., Han, F., et al. (2013). Stimulation of σ1-receptor restores abnormal mitochondrial Ca^{2+} mobilization and ATP production following cardiac hypertrophy. *Biochim. Biophys. Acta* 1830 (4), 3082–3094. doi:10.1016/j.bbagen.2012.12.029

Teklemichael, A. A., Mizukami, S., Toume, K., Mosaddeque, F., Kamel, M. G., Kaneko, O., et al. (2020). Anti-malarial activity of traditional Kampo medicine Coptis rhizome extract and its major active compounds. *Malar. J.* 19 (1), 204. doi:10.1186/s12936-020-03273-x

Thai, B. S., Chia, L. Y., Nguyen, A. T. N., Qin, C., Ritchie, R. H., Hutchinson, D. S., et al. (2023). Targeting G protein-coupled receptors for heart failure treatment. *Br. J. Pharmacol.* doi:10.1111/bph.16099

Tian, L., Li, N., Li, K., Tan, Y., Han, J., Lin, B., et al. (2022). Ambient ozone exposure induces ROS related-mitophagy and pyroptosis via NLRP3 inflammasome activation in rat lung cells. *Ecotoxicol. Environ. Saf.* 240, 113663. doi:10.1016/j.ecoenv.2022.113663

Tondera, D., Czauderna, F., Paulick, K., Schwarzer, R., Kaufmann, J., and Santel, A. (2005). The mitochondrial protein MTP18 contributes to mitochondrial fission in mammalian cells. *J. Cell Sci.* 118 (14), 3049–3059. doi:10.1242/jcs.02415

Wang, S., Han, H. M., Pan, Z. W., Hang, P. Z., Sun, L. H., Jiang, Y. N., et al. (2012). Choline inhibits angiotensin II-induced cardiac hypertrophy by intracellular calcium signal and p38 MAPK pathway. *Naunyn Schmiedeb. Arch. Pharmacol.* 385 (8), 823–831. doi:10.1007/s00210-012-0740-4

Wang, W. Z., Matsumori, A., Matoba, Y., Matsui, S., Sato, Y., Hirozane, T., et al. (1998). Protective effects of Mu-Fang-Ji-Tang against myocardial injury in a murine model of congestive heart failure induced by viral myocarditis. *Life Sci.* 62 (13), 1139–1146. doi:10.1016/s0024-3205(98)00039-3

Wu, L., Wang, L., Du, Y., Zhang, Y., and Ren, J. (2023). Mitochondrial quality control mechanisms as therapeutic targets in doxorubicin-induced cardiotoxicity. *Trends Pharmacol. Sci.* 44 (1), 34–49. doi:10.1016/j.tips.2022.10.003

Xu, Y., Kumar, D., Dyck, J. R., Ford, W. R., Clanachan, A. S., Lopaschuk, G. D., et al. (2002). AT_1 and AT_2 receptor expression and blockade after acute ischemia-reperfusion in isolated working rat hearts. *Am. J. Physiol. Heart Circ. Physiol.* 282 (4), H1206–H1215. doi:10.1152/ajpheart.00839.2000

Yaku, H., Kaneda, K., Kitamura, J., Kato, T., and Kimura, T. (2022). Kampo medicine for the holistic approach to older adults with heart failure. *J. Cardiol.* 80 (4), 306–312. doi:10.1016/j.jjcc.2021.12.011

Yang, D., Liu, H. Q., Liu, F. Y., Guo, Z., An, P., Wang, M. Y., et al. (2021). Mitochondria in pathological cardiac hypertrophy research and therapy. *Front. Cardiovasc Med.* 8, 822969. doi:10.3389/fcvm.2021.822969

Yoshida, C., Yamamoto, H., Inoue, T., Itoh, M., Shimane, A., Kawai, H., et al. (2022). Torsade de pointes in an older patient with Takotsubo cardiomyopathy caused by licorice-induced pseudoaldosteronism: a case report. *Clin. Case Rep.* 10 (7), e6104. doi:10.1002/ccr3.6104

Zerihun, M., Sukumaran, S., and Qvit, N. (2023). The Drp1-mediated mitochondrial fission protein interactome as an emerging core player in mitochondrial dynamics and cardiovascular disease therapy. *Int. J. Mol. Sci.* 24 (6), 5785. doi:10.3390/ijms24065785

Zhao, G. J., Zhao, C. L., Ouyang, S., Deng, K. Q., Zhu, L., Montezano, A. C., et al. (2020). Ca^{2+}-dependent NOX5 (NADPH oxidase 5) exaggerates cardiac hypertrophy through reactive oxygen species p roduction. *Hypertension* 76 (3), 827–838. doi:10.1161/hypertensionaha.120.15558

Zhou, B., and Tian, R. (2018). Mitochondrial dysfunction in pathophysiology of heart failure. *J. Clin. Invest.* 128 (9), 3716–3726. doi:10.1172/jci120849

Ziaeian, B., and Fonarow, G. C. (2016). Epidemiology and aetiology of heart failure. *Nat. Rev. Cardiol.* 13 (6), 368–378. doi:10.1038/nrcardio.2016.25

frontiers | Frontiers in Cell and Developmental Biology

TYPE Original Research
PUBLISHED 12 January 2024
DOI 10.3389/fcell.2023.1324158

OPEN ACCESS

EDITED BY
Milena Rizzo,
National Research Council (CNR), Italy

REVIEWED BY
Tanmoy Saha,
Brigham and Women's Hospital and Harvard Medical School, United States
Veronica Andrea Burzio,
Andres Bello University, Chile

*CORRESPONDENCE
Eduardo Silva-Pavez,
eduardo.silva@uss.cl
Yessia Hidalgo,
yhidalgo@uandes.cl

†These authors have contributed equally to this work and share first authorship

‡These authors have contributed equally to this work and share last authorship

RECEIVED 19 October 2023
ACCEPTED 27 December 2023
PUBLISHED 12 January 2024

CITATION
Cereceda L, Cardenas JC, Khoury M, Silva-Pavez E and Hidalgo Y (2024), Impact of platelet-derived mitochondria transfer in the metabolic profiling and progression of metastatic MDA-MB-231 human triple-negative breast cancer cells.
Front. Cell Dev. Biol. 11:1324158.
doi: 10.3389/fcell.2023.1324158

Impact of platelet-derived mitochondria transfer in the metabolic profiling and progression of metastatic MDA-MB-231 human triple-negative breast cancer cells

Lucas Cereceda[1,2†], J. Cesar Cardenas[3,4,5,6], Maroun Khoury[1,2,7], Eduardo Silva-Pavez[8*†‡] and Yessia Hidalgo[1,2*‡]

[1]IMPACT, Center of Interventional Medicine for Precision and Advanced Cellular Therapy, Santiago, Chile, [2]Laboratory of Nano-Regenerative Medicine, Faculty of Medicine, Universidad de los Andes, Santiago, Chile, [3]Center for Integrative Biology, Faculty of Sciences, Universidad Mayor, Santiago, Chile, [4]Geroscience Center for Brain Health and Metabolism, Santiago, Chile, [5]Buck Institute for Research on Aging, Novato, CA, United States, [6]Department of Chemistry and Biochemistry, University of California, Santa Barbara, Santa Barbara, CA, United States, [7]Cells for Cells and Consorcio Regenero, Chilean Consortium for Regenerative Medicine, Santiago, Chile, [8]Facultad de Odontología y Ciencias de la Rehabilitación, Universidad San Sebastián, Bellavista, Santiago, Chile

Introduction: An active role of platelets in the progression of triple-negative breast cancer (TNBC) cells has been described. Even the role of platelet-derived extracellular vesicles on the migration of MDA-MB-231 cells has been reported. Interestingly, upon activation, platelets release functional mitochondria into the extracellular environment. However, the impact of these platelet-derived mitochondria on the metabolic properties of MDA-MB-231 cells remains unclear.

Methods: MDA-MB-231 and MDA-MB-231-Rho-0 cells were co-cultured with platelets, which were isolated from donor blood. Mitochondrial transfer was assessed through confocal microscopy and flow cytometry, while metabolic analyses were conducted using a Seahorse XF HS Mini Analyzer. The mitochondrial DNA (mtDNA) copy number was determined via quantitative PCR (qPCR) following platelet co-culture. Finally, cell proliferation and colony formation assay were performed using crystal violet staining.

Results and Discussion: We have shown that platelet-derived mitochondria are internalized by MDA-MB-231 cells in co-culture with platelets, increasing ATP production, oxygen (O_2) consumption rate (OCR), cell proliferation, and metabolic adaptability. Additionally, we observed that MDA-MB-231 cells depleted from mtDNA restore cell proliferation in uridine/pyruvate-free cell culture medium and mitochondrial O_2 consumption after co-culture with platelets, indicating a reconstitution of mtDNA facilitated by platelet-derived mitochondria. In conclusion, our study provides new insights into the role of platelet-derived mitochondria in the metabolic adaptability and progression of metastatic MDA-MB-231 TNBC cells.

KEYWORDS

platelets, platelet-derived mitochondria, cancer, mitochondria transfer, metabolic adaptability

Introduction

Breast cancer is the most prevalent type among women, leading to an estimated 685,000 deaths in 2020. This number is projected to rise to 7 million by 2040 (Vismara et al., 2022b). Among the various subtypes of breast cancer, triple-negative breast cancer (TNBC) is particularly aggressive and is known for its potential to metastasize (Grasset et al., 2022). TNBC is characterized by the absence of estrogen, progesterone, and human epidermal growth factor receptor 2 (HER2) receptors (Garrido-Castro et al., 2019). This lack of receptors contributes to TNBC's reduced susceptibility to hormonal and anti-HER2 therapies, posing significant treatment challenges (Garrido-Castro et al., 2019).

Platelets, which are small (2–4 μm) anucleate cellular fragments released by megakaryocytes present in bone marrow, play a significant role in the progression and aggressiveness of cancer (Vismara et al., 2021; Yu et al., 2021; Chen et al., 2023). When activated, they release platelet-derived extracellular vesicles (PEVs), which participate in both physiological and pathological contexts, including cancer (Dovizio et al., 2020; Żmigrodzka et al., 2020). Indeed, PEVs are essential to the complex interactions between platelets and cancer cells, especially breast cancer cells (Vismara et al., 2021). These cancer cells can stimulate platelet activation, subsequently triggering the release of PEVs into the extracellular environment (Gomes et al., 2017; Zarà et al., 2018).

Interestingly, platelets serve as the major reservoir for mitochondria within the circulatory system. Upon activation, platelets release respiratory-competent mitochondria enclosed within vesicles and as free organelles (Boudreau et al., 2014). These organelles, which are essential for ATP production through aerobic respiration and the regulation of cellular metabolism, also play a role in metastasis (Scheid et al., 2021). Despite their significance, the implications of mitochondrial release from activated platelets into TNBC cells, specifically MDA-MB-231 cells, remain unclear.

In this study, we discovered that platelet-derived mitochondria can be internalized by MDA-MB-231 cells in co-culture, increasing ATP production, oxygen (O_2) consumption rate (OCR), cell proliferation, and metabolic adaptability. Interestingly, we observed that MDA-MB-231 cells depleted of mitochondrial DNA (mtDNA) can restore cell proliferation in uridine/pyruvate-free cell culture medium and regain mitochondrial O_2 consumption after co-culturing with platelets. This suggests that platelet-derived mitochondria facilitate the replenishment of mtDNA. This discovery provides new insights into the impact of mitochondria derived by platelets on the metabolic adaptability and progression of MDA-MB-231 human metastatic TNBC cells.

Materials and methods

Cell culture

MDA-MB-231 cells were cultured using DMEM-HG (Sartorius, Cat. #01-055-1A) supplemented with Penicillin/Streptomycin (P/S) (Corning, Cat. #30-002-CI) 1X, 4 mM glutamine (Corning, Cat. #25-005-CI) and 10% fetal bovine serum (FBS) (Gibco™, Cat. #10437-028). MDA-MB-231-Rho-0 (Rho-0) cells were generated as previously described (Rabas et al., 2021) and maintained in DMEM-HG supplemented with 50 μg/mL uridine (Sigma Aldrich, Cat. #U3003), 1 mM pyruvate (Sartorius, Cat. #03-042-1B), P/S-1X, 4 mM glutamine, and 10% FBS. Breast cancer cells were cultured at 37°C with 5% CO_2 in a humidified incubator.

Co-culture of platelets with MDA-MB-231 cells

For co-culture experiments, MDA-MB-231 and Rho-0 were seeded in cell culture medium with 10% FBS at approximately 8×10^3 cells/cm^2 the day before platelets were added. The next day, platelets were added at a final concentration of 1.5×10^5 platelets/μL. In the case of MDA-MB-231, the culture medium was replaced by fresh culture medium without FBS before adding platelets. In the case of Rho-0 cells, the cell culture medium was replaced with the same fresh culture medium before the addition of platelets. Control MDA-MB-231 cells were cultured with the same buffer that contained platelets. MDA-MB-231 cells and platelets were incubated for 24 h. After co-culture, MDA-MB-231 cells were washed twice with PBS-1X to remove platelets. Washed MDA-MB-231 cells were split using TrypLE™ Express (Gibco™) and manually counted with trypan blue. MDA-MB-231 cells were resuspended in cell culture medium with 10% FBS in all the cases and used for subsequent experiments.

Platelet isolation

Blood was recollected from the cubital vein of healthy donors using a 21-gauge needle (BD Vacutainer®, Cat. #367287) and blood recollection tubes with acid-citrate-dextrose solution A (ACD-A) as anticoagulant (BD Vacutainer®, Cat. #364606). The tourniquet was applied only to detect the vein and recollect the first 2.5 mL of blood, which were discarded. Blood was centrifuged at 150 g for 20 min to obtain platelet-rich plasma (PRP). PRP was gently taken to a new tube and was added 1 μM prostaglandin E1 (PGE1) (Focus Biomolecules, Cat. #10-4455). PRP was centrifuged at 150 g for 10 min to remove red blood cells and leukocytes. The supernatant was transferred to a new tube. Platelets were pelleted by centrifugation at 1,500 g for 15 min. All centrifugation steps were done at room temperature (RT) without acceleration and break in a swinging-bucket centrifuge. Platelet pellet was washed twice with platelet wash buffer (PWB) (10 mM sodium citrate, 150 mM NaCl, 1 mM EDTA, 1% (w/v) glucose, pH 7.4) and gently resuspended in tyrode's buffer (TB) (134 mM NaCl, 12 mM $NaHCO_3$, 2.9 mM KCl, 0.34 mM Na_2HPO_4, 1 mM $MgCl_2$, 10 mM HEPES, 5 mM glucose, pH 7.4) without calcium. Platelets were left at 37°C and counted by flow cytometry using CountBright™ Plus Absolute Counting Beads (Cat. #C36995). Before adding platelets to MDA-MB-231 cells, platelet-poor plasma (PPP) was added to platelet preparation to achieve a final concentration of at least 0.05%–0.1% (v/v) in the well.

Platelet activation

Platelets post isolation or after co-culture were fixed with PFA 2% for 15 min at RT. Fixed platelets were resuspended in PBS-1X plus 2% FBS and stained for 15 min at 4°C with CD42a-FITC (BD Pharmigen™, Cat. #558818) (1:200) and CD62p-APC (BD

Pharmigen™, Cat. #550888) (1:200). Platelets were washed with PBS-1X plus 2% FBS and acquired using a BD FACSCanto™ II flow cytometer.

Mitochondrial transfer assessment

Mitochondrial transfer was assessed by flow cytometry and confocal microscopy. For flow cytometry assessment, MDA-MB-231 cells were previously stained with 5 μM CellTrace™ Violet (CTV) (Cat. #C34557) according to the manufacturer's instructions. For confocal microscopy assessment, MDA-MB-231 cells were previously stained with 150 nM MitoTracker™ Deep Red (MTDR) (Cat. #M22426) for 25 min at 37°C, washed and seeded over coverslips. In both cases, platelets, at a concentration of 5×10^8 platelets/mL, were stained with 100 nM MitoTracker™ Green (MTG) (Cat. #M7514) for 25 min at 37°C, washed with TB plus 1% BSA and 0.5 μM PGE1 and added to MDA-MB-231 cells. The co-culture system was done as described previously. After 24 h incubation, cells were analyzed using a BD FACSCanto™ II flow cytometer or a Leica SP8 AT CIAN (Leica Microsystems) confocal microscopy. MTG does not depend on the mitochondrial membrane potential (ΔΨm), unlike MTDR which does rely on this potential (Agnello et al., 2008; Cottet-Rousselle et al., 2011; Xiao et al., 2016).

Seahorse XF HS mini analyzer

Multiparameter metabolic analysis of MDA-MB-231 cells was performed in an extracellular flux analyzer (Agilent, United States of America). MDA-MB-231 cells were seeded on XF HS Mini 8-well plates and kept overnight at 37°C in 5% CO_2 with DMEM-HG. After 48 h, the cell culture medium was replaced with Agilent Seahorse XF DMEM medium pH 7.4 (with 5 mM HEPES) with 10 mM glucose 1 h before the assay. Mitochondrial function (Mito stress test) was evaluated using 2 μM oligomycin (Oligo), 200 nM FCCP, 1 μM rotenone (Rot), and 1 μM antimycin-A (AA).

ATP levels analysis

ATP analysis was done using the kit CellTiter Glo® Luminescent Cell Viability (Promega, Cat. #G7571). After platelet co-culture, 1×10^4 MDA-MB-231 cells or 5×10^3 sorted MDA-MB-231 cells were added to a 96-well white microplate. Cells were allowed to rest at RT for 30 min. Then, 100 μL of the kit reagent was added, and the plate was incubated for 2 min at 140rpm in an orbital shaker. ATP analysis was done by measuring luminescence in a Biotek® FLx800 luminometer. In the case of platelet-rescued Rho-1, Rho-2, and Rho-3 cells, 5×10^3 cells were seeded in 96 well-white microplates and incubated for 48 h. In parallel, a mirror plate was seeded for protein quantification and normalization. After 48 h, the culture medium was removed, and new medium with 5 μM Oligo (Tocris, Cat. #4110) was added. Cells were incubated for 20 h. After incubation, ATP analysis was conducted as described previously. For protein quantification and normalization, cells were lysed with RIPA-1X (ThermoFisher™, Cat. #899000) with protease inhibitor (Sigma Aldrich, Cat. #5056489001), and protein quantification was done using the Pierce™ BCA Protein Assay kit (ThermoFisher™, Cat. #23225). Data was expressed as ATP luminescence normalized by the number of cells or μg of the total protein.

Mitochondrial DNA (mtDNA) copy number

The total DNA of MDA-MB-231 cells was manually isolated according to (Laird et al., 1991) with some modifications. Briefly, cells were lysed with lysis buffer (100 mM TRIS-HCl pH 8.5, 5 mM EDTA, 0.2% SDS, 200 mM NaCl, 50 μg/mL proteinase K) at 37°C for several hours. Next, one volume of isopropanol was added to the lysate, and the sample was centrifuged at 16000 g for 20 min at 4°C. The supernatant was discarded, and DNA was resuspended in TE buffer (10 mM TRIS-HCl, 0.1 mM EDTA, pH 8). Relative mitochondrial DNA (mtDNA) levels were determined using quantitative PCR (qPCR) by simultaneous amplification of mtDNA and nuclear DNA (ncDNA). The forward and reverse primers for mtDNA, complementary to mitochondrial encoded NADH dehydrogenase 1 (MT-ND1), were 5′-CATGGCCAACCT CCTACTCCTC-3′ and 5′-TGGGGCCTTTGCGTAGTTGT-3′. The forward and reverse primers for ncDNA, complementary to ribosomal protein lateral stalk subunit P0 (RPLP0), were 5′-CAA CGGGTACAAACGAGTCCTG-3′ and 5′-AAGCAGTAAGGT AGAAGGCCACA-3′. The specificity of primers was confirmed by *in silico* analysis using the UCSC genome browser. Each PCR reaction was run in duplicate and contained 6.25 μL 2X Brilliant SYBR® Green qPCR Master Mix (Cat. #600828–51), 0.19 μL Reference Dye ROX (Cat. #600530–53), 0.375 μL primer forward (final concentration 300 nM), 0.375 μL primer reverse (final concentration 300 nM) and variable volume of UltraPure™ Distilled H_2O (Invitrogen™, Cat. #10977–015) and DNA. The combined volume of H_2O and DNA was 5.3 μL, and 10 ng of DNA was used. PCR was done in a Stratagene Mx3000P (Agilent) by using the following protocol: 95°C (10:00 min) + [95°C (0:30 s) + 61°C (0:30 s)] × 40 cycles +95°C (01:00 min). Results were calculated using the $2^{*}2^{\Delta Ct}$ method (Rooney et al., 2015). Products of qPCR were loaded into a 2% agarose gel, and electrophoresis was performed. Gel was visualized using UV light to confirm the expected amplicon.

Colony formation assay

A colony formation assay was performed on sorted MDA-MB-231 and Rho-0 cells after platelet co-culture. Sorted MDA-MB-231, 1×10^3 cells were seeded in a 6-well plate with glucose-free DMEM-1X (Sigma-Aldrich®, Cat. #D5030) supplemented with 10 mM galactose, 4 mM glutamine, and 10% FBS, and grew for 12–13 days. Colonies were visualized by staining with 0.5% crystal violet for 45 min. In the case of Rho-0 cells, 5×10^3 cells after platelet co-culture were seeded in a 6-well plate with medium supplemented with uridine and pyruvate. Cancer cells were maintained for 48 h in cell culture medium with uridine and pyruvate. Then, cell culture medium was replaced with uridine/pyruvate-free DMEM-HG. Cells were cultured for 20 days without uridine/pyruvate, and colony isolation was performed. Colonies were visualized by staining with 0.5% crystal violet for 45 min.

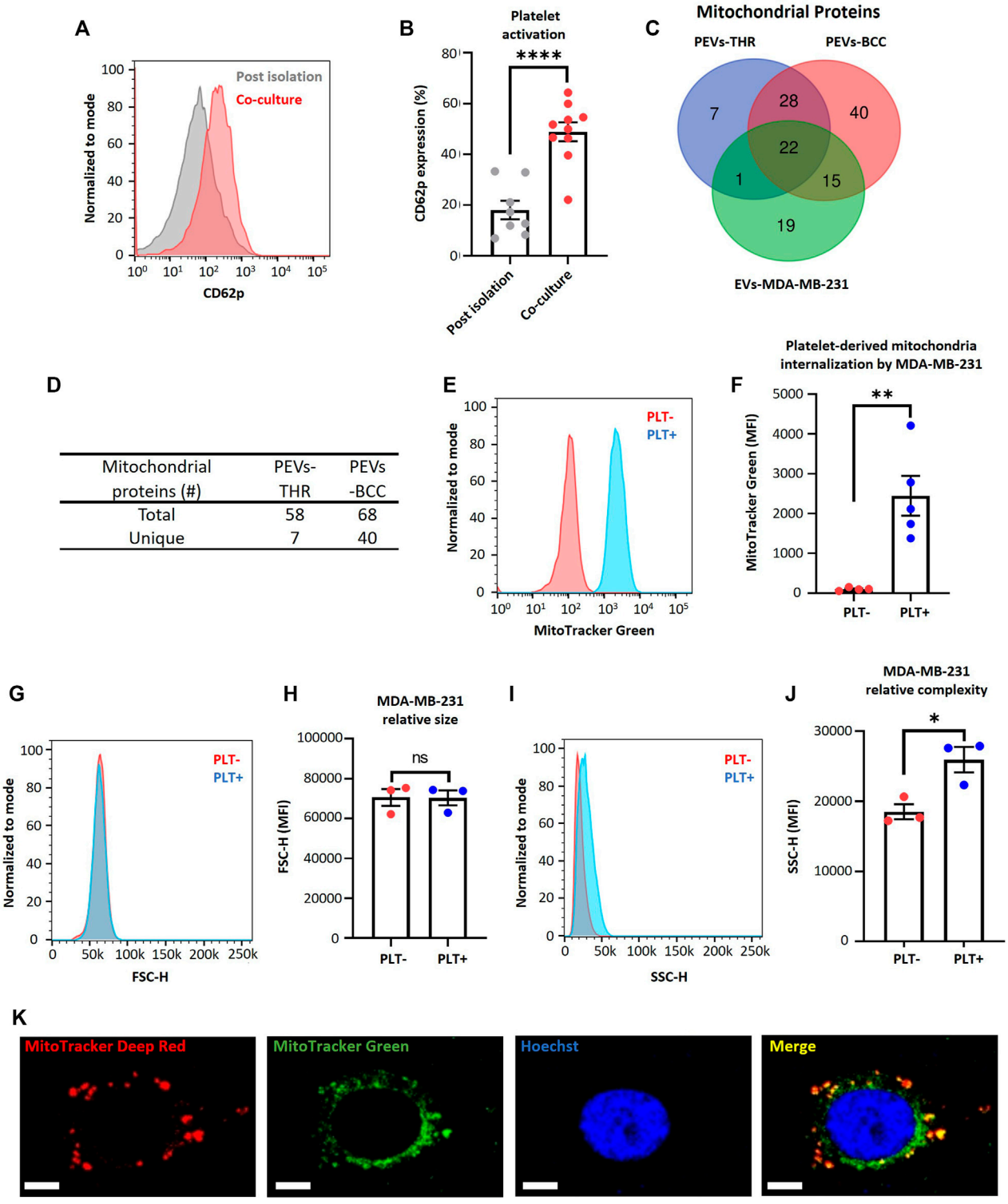

FIGURE 1
MDA-MB-231 cells acquire platelet-derived mitochondria. **(A)** Flow cytometry histograms of CD62p expression in platelets after isolation or after 24 h co-culture with MDA-MB-231 cells. **(B)** Frequency of platelet activation after isolation or after 24 h co-culture with MDA-MB-231 cells. **(C)** Venn diagram of mitochondrial proteins from three samples: PEVs-THR, PEVs-BCC, and EVs-MDA-MB-231. **(D)** Amount of total and unique mitochondrial proteins for PEVs-THR and PEVs-BCC. Common mitochondrial proteins between PEVs-BCC and EVs-MDA-MB-231 were discarded to avoid possible contamination with proteins from EVs released by MDA-MB-231 cells. **(E)** Flow cytometry histograms of MitoTracker™ Green (MTG) signal on MDA-MB-231 cells after 24 h co-culture. MDA-MB-231 cells were cultured with buffer or platelets previously stained with MTG. **(F)** MTG MFI on MDA-MB-231 cells cultured with buffer or MTG platelets. **(G)** Flow cytometry histograms of FSC-H for MDA-MB-231 cells cultured with buffer or platelets for 24 h. **(H)** FSC-H MFI for MDA-MB-231 cells cultured with buffer or platelets for 24 h. **(I)** Flow cytometry histograms of SSC-H for MDA-MB-231 cells cultured with buffer or platelets for 24 h. **(J)** SSC-H MFI for MDA-MB-231 cells cultured with buffer or platelets 24 h. **(K)** Confocal microscopy images of
(*Continued*)

FIGURE 1 (Continued)
platelet-derived mitochondria internalization by MDA-MB-231 cells. These cells were previously stained with MitoTracker™ Deep Red (MTDR) and co-cultured with MTG platelets for 24 h. Scale bar = 10 μm. A t-student statistical test was performed. *$p < 0.05$; **$p < 0.01$; ****$p < 0.0001$; ns = not significant.

Isolated Rho-0 colonies were recovered by platelet co-culture and maintained in uridine/pyruvate-free DMEM-HG.

Proteomic analysis

Protein data sets related to PEVs-THR, PEVs-BCC, and EVs-MDA were generated by (Vismara et al., 2022a). Mitochondrial proteins in each sample were obtained by comparing every sample with the mitochondrial proteins in the Human MitoCarta 3.0 (Rath et al., 2021). Each sample's list of identified mitochondrial proteins was compared with the others to identify common and unique ones. Afterward, GO-annotation analysis was performed using STRING V11.5 (Szklarczyk et al., 2019) gene ontology tools. Biological processes with strength >1 and false discovery rate (FDR) < 0.5 were selected.

Mitochondrial membrane potential (ΔΨm)

The co-culture system was done as described previously, and MDA-MB-231 cells were stained with CTV. Mitochondrial membrane potential was analyzed in MDA-MB-231 cells after platelet co-culture using tetramethyl rhodamine, ethyl ester, and perchlorate (TMRE) (Invitrogen™, Cat. #T669), a dye that is dependent on mitochondrial membrane potential. MDA-MB-231 cells were washed with PBS-1X plus 2% FBS, resuspended in PBS-1X plus 2% FBS, and stained with Ghost Dye™ Violet 510 (Tonbo™, Cat. #13-0870-T100) (1:1,000) for 20 min at 4°C. After that, cells were washed with PBS-1X plus 2% FBS, resuspended in PBS-1X, and stained with 100 nM TMRE for 30 min at 37°C. MDA-MB-231 cells were washed with PBS-1X plus 2% FBS and analyzed using a BD FACSCanto™ II flow cytometer.

Cell proliferation assay

After co-culture, 2.5×10^3 MDA-MB-231 cells in DMEM-HG with 10% FBS were seeded in duplicate in a 96-well flat bottom microplate. At 24, 48, and 72 h, cell proliferation was assessed by 0.5% crystal violet staining for 45 min. Crystal violet was washed, and the plates were allowed to dry out. Next, 200 μL methanol was added to the plate, and absorbance was recorded at 570 nm using an Infinite® 200 NanoQuant plate reader (Tecan™).

Cell sorting

As described previously, platelets were stained with MTG and co-cultured with MDA-MB-231 cells. After co-culture, MDA-MB-231 cells that acquired platelet-derived mitochondria were identified as MTG-positive cells. The MTG-positive cells were separated based on MTG fluorescence intensity using a BD FACSAria™ Fusion Cell Sorter. Two subpopulations were recovered: those with high MTG intensity, named MITO-High, and those with low MTG intensity, named MITO-Low. As a control, MDA-MB-231 cells cultured without platelets were subject to the same cell sorting process.

Data analysis

Flow cytometry data was acquired using the FACS Diva program and analyzed using the FlowJo V10 software. The strategies used to analyze the flow cytometry data associated with each experiment are presented in Supplementary Figure S1. Confocal microscopy images were acquired and analyzed using LAS X software. The area fraction of colonies was measured using ImageJ software. Statistical analysis was performed using GraphPad Prism 8 version 8.0.2 (GraphPad Software, San Diego, CA, United States of America). For statistical analysis, the t-student statistical test was performed. Results are presented as mean ± SEM. Significance level of statistical tests: *$p < 0.05$; **$p < 0.01$; ***$p < 0.001$ and ns: not significant.

Results

Mitochondrial transfer from platelets to MDA-MB-231 breast cancer cells

The platelet activation by MDA-MB-231 cells has been previously described (Vismara et al., 2022a). Interestingly, the activation of platelets by MDA-MB-231 cells leads to the release of platelet-derived vesicles into the extracellular environment (Zarà et al., 2017). These platelet-derived microparticles play a fundamental role in the complex interaction between the hemostatic system and cancer progression (Vismara et al., 2021). We consistently observed a significant increase in the platelet activation marker (CD62p) on the plasma membrane of platelets, using cytometry flow upon co-culturing with MDA-MB-231 cells compared to the post-isolation platelets (Figures 1A, B).

In addition, retrospective analysis of previously published data (Vismara et al., 2022a), as verified through liquid chromatography-tandem mass spectrometry, identified that the protein constituents of two subpopulations of platelet-derived extracellular vesicles (PEVs) in response to thrombin exposure (PEVs-THR) and during co-culture with MDA-MB-231 cells (PEVs-BCC) were associated with mitochondrial function (Vismara et al., 2022a) (Figures 1C, D). Interestingly, PEVs-BCC exhibited a higher total amount of mitochondrial proteins than PEVs-THR and an increased amount of unique mitochondrial proteins exclusively associated with this condition (Figures 1C, D). These results suggest that platelets likely release mitochondria when activated by MDA-MB-231 cells.

10.3389/fcell.2023.1324158

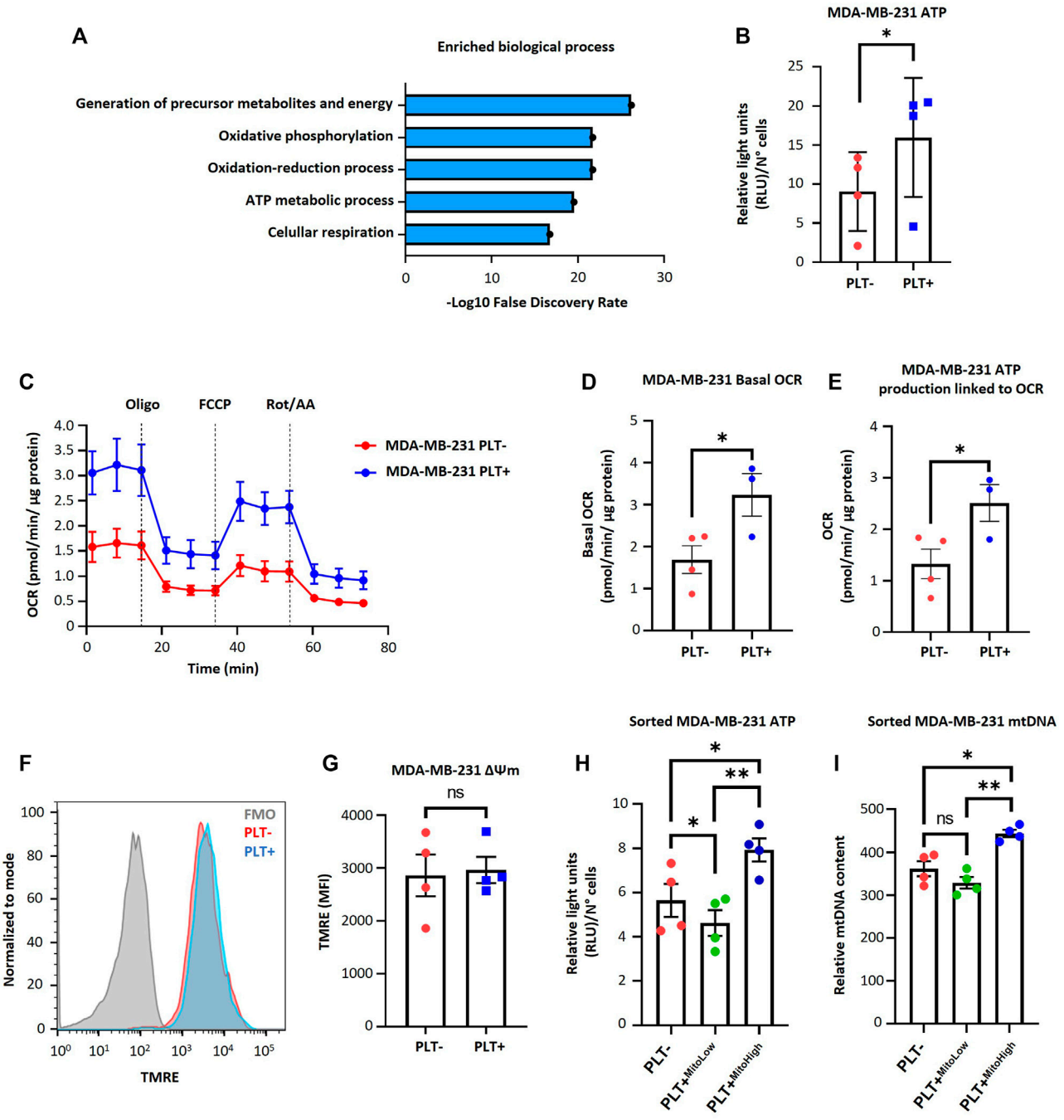

FIGURE 2
Effect of platelet-derived mitochondria on the bioenergetic properties of MDA-MB-231 cells. **(A)** Gene ontology results of enriched biological process identified for mitochondrial proteins related to PEVs-BCC. GO-annotation analysis was performed using STRING V11.5 gene ontology tools. Biological processes with strength >1 and false discovery rate (FDR) < 0.05 were selected. **(B)** Analysis of ATP content of MDA-MB-231 cells cultured with buffer or platelets for 24 h. Results were expressed as relative light units (RLU) normalized by a total number of cells. **(C)** Seahorse assay results of OCR for MDA-MB-231 cells cultured with buffer or platelets. MDA-MB-231 cells were co-cultured with platelets for 24 h. After that, cells were washed, reseeded, and cultured for 48 h before performing the seahorse assay. Results were normalized to µg of a total protein of each well. **(D)** Basal OCR of MDA-MB-231 cells cultured with buffer or platelets. **(E)** ATP-linked OCR of MDA-MB-231 cells cultured with buffer or platelets. **(F)** Flow cytometry histograms of TMRE signal in MDA-MB-231 cells after 24 h co-culture. MDA-MB-231 cells were cultured with buffer or platelets, and mitochondrial membrane potential (ΔΨm) was analyzed using TMRE dye. **(G)** TMRE MFI in MDA-MB-231 cells cultured with buffer or platelets. **(H)** Analysis of ATP content of sorted MDA-MB-231 cells cultured with buffer or platelets for 24 h. MDA-MB-231 cells were cultured with platelets previously stained with MTG. MDA-MB-231 cells positive for MTG signal were separated according to MTG intensity, retrieving two populations. Those with low MTG intensity are named MITO-Low, and those with high MTG intensity are named MITO-High. Results are expressed as RLU normalized by the total number of cells. **(I)** Analysis of relative mitochondrial DNA (mtDNA) levels of sorted MDA-MB-231 cells. Relative mtDNA levels were determined using quantitative PCR (qPCR) by amplifying mtDNA and nuclear DNA (ncDNA). A t-student statistical test was performed. *$p < 0.05$; **$p < 0.01$; ns = not significant.

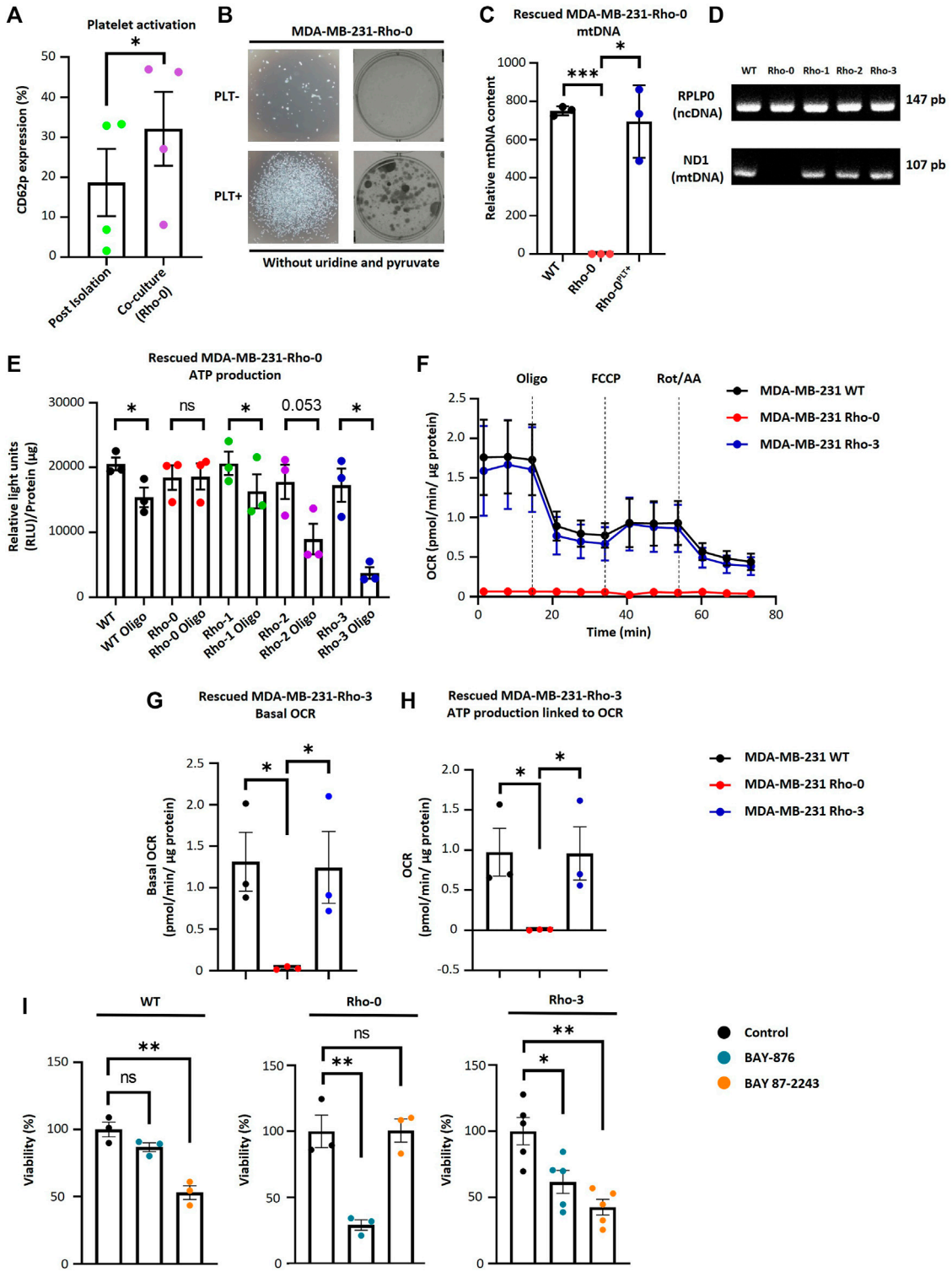

FIGURE 3
MDA-MB-231-Rho-0 cells restore impaired mitochondrial function by acquiring platelet-derived mitochondria. **(A)** Frequency of platelet activation after isolation or after 24 h co-culture with Rho-0 cells. **(B)** Microscopic (left panel) and macroscopic (right panel) images of colonies formed by platelet-rescued Rho-0 cells in pyruvate/uridine-free cell culture medium. Rho-0 cells were cultured with buffer or platelets for 24 h. After that, cells were washed, reseeded, and cultured for 48 h in medium with pyruvate/uridine. Next, cells were maintained in pyruvate/uridine-free medium to evidence mitochondrial function recovery and colony isolation was performed. Colonies were visualized by 0.5% crystal violet staining. **(C)** Analysis of relative mtDNA levels of platelet-rescued Rho-0 cells by three different donors (Rho-1, Rho-2, and Rho-3). Relative mtDNA levels were determined using quantitative PCR (qPCR) by simultaneous amplification of mtDNA and ncDNA. **(D)** Gel agarose electrophoresis for amplified products of mitochondrial encoded NADH dehydrogenase 1 (MT-ND1) gene and ribosomal protein lateral stalk subunit P0 (RPLP0) gene. Products of qPCR were loaded into a 2% agarose gel, and electrophoresis was performed. Gel was visualized using UV light to confirm the expected amplicon for each primer pair. **(E)** ATP
(*Continued*)

FIGURE 3 (Continued)
production analysis of platelet-rescued Rho-1, Rho-2, and Rho-3 cells. ATP production was modulated with 5 μM oligomycin (Oligo) for 20 h. Results were expressed as RLU normalized to μg of total protein. **(F)** Seahorse assay results of OCR for platelet-rescued Rho-3 cells. Results were normalized to μg of the protein of each well. **(G)** Basal OCR of platelet-rescued Rho-3 cells. **(H)** ATP production linked to OCR of platelet-rescued Rho-3 cells. **(I)** Cell viability assay of MDA-MB-231 WT, Rho-0, and platelet-rescued Rho-3. Cells were treated with BAY-876 or BAY 87–2243 for 72 h as control cells were treated with vehicle (DMSO). Cell viability was determined by 0.5% crystal violet stained. Results were normalized to control. A t-student statistical test was performed. *$p < 0.05$; **$p < 0.01$; ****$p < 0.0001$; ns = not significant.

To verify that MDA-MB-231 cells can acquire platelet-derived mitochondria, we stained mitochondria platelets with MitoTracker™ Green (MTG) dye, and then these platelets were co-cultured with MDA-MB-231 cells. Notably, the platelet-derived mitochondria internalization in MDA-MB-231 cells was confirmed using flow cytometry (Figures 1E, F). Additionally, we managed to rule out leakage of MTG from platelets to MDA-MB-231 cells (Supplementary Figure S2). These findings are consistent with previous studies associating platelet activation and release of platelet-derived mitochondria (Boudreau et al., 2014). To confirm that stained platelets did not adhere to the cell surface of MDA-MB-231 cells, which could increase their size, we analyzed the size of MDA-MB-231 cells after co-culture with platelets. As shown in (Figures 1G, H), there was no relative change in the size of MDA-MB-231 cells. Nonetheless, it is essential to note that the internal complexity within the MDA-MB-231 cells was considerably increased upon co-culture with platelets (Figures 1I, J). This observation suggests the possible internalization of platelet-derived vesicles and platelet-derived mitochondria within MDA-MB-231 cells (Zoellner et al., 2019).

Furthermore, we employed confocal microscopy to assess the internalization of platelet-derived mitochondria by MDA-MB-231 cells (Figure 1K). We used MTG dye to stain the mitochondria of platelets and MitoTracker™ Deep Red (MTDR) to stain the mitochondria of MDA-MB-231 cells, followed by co-culture. Surprisingly, we observed co-localization of platelet-derived mitochondria (green) with mitochondria of MDA-MB-231 cells (red) (Figure 1K). In summary, these findings evidence the transfer of mitochondria *in vitro* from activated platelets to metastatic MDA-MB-231 cells.

Effect of platelet-derived mitochondria on the mitochondrial function in MDA-MB-231 cells

To understand the metabolic impact of the internalization of platelet-derived mitochondria by MDA-MB-231 cells, we examined the 68 mitochondrial proteins previously identified in the PEVs-BCC condition using gene ontology (GO)-annotation analysis (Figure 2A). Our results indicated that the most significantly enriched processes are inherently associated with mitochondria-associated respiration and energy metabolism (Figure 2A). Next, we evaluated ATP levels in MDA-MB-231 cells after co-culture with platelets. As shown in (Figure 2B), a significant increase in ATP levels was observed in MDA-MB-231 cells after co-culture with platelets. These findings suggest increased energy production within MDA-MB-231 cells after co-culture with platelets. To further investigate the functional impact of mitochondrial transfer, we used a Seahorse XF HS Mini Analyzer to assess mitochondrial bioenergetics of MDA-MB-231 cells during co-culture with platelets. As shown in (Figures 2C–E), there is a significant increase in basal OCR and ATP-linked OCR, indicating a functional effect of the transfer of mitochondria from activated platelets to MDA-MB-231 cells. Next, we evaluated mitochondrial membrane potential (ΔΨm) in MDA-MB-231 cells after co-culture with platelets. As shown in (Figures 2F, G), no significant differences were observed between MDA-MB-231 cells cultured in the presence or absence of platelets.

Additionally, we labeled platelet mitochondria using MTG dye before co-culturing them with MDA-MB-231 cells. Subsequently, we identified MDA-MB-231 cells that internalized platelet-derived mitochondria as MTG-positive cells. These cells were categorized based on MTG fluorescence intensity using cell sorting, resulting in two distinct subpopulations. One subpopulation exhibited high fluorescence intensity of MTG, which we designated MITO-High, while the other subpopulation had low intensity and was designated MITO-Low. In addition, we subjected MDA-MB-231 WT cells cultured without platelets to the same cell sorting procedure for comparison. As shown in (Figure 2H), MITO-High cells had significantly higher ATP content than MITO-Low cells and the MDA-MB-231 cells cultured without platelets. We repeated the abovementioned procedure to confirm whether the increase in ATP production was associated with increased mitochondria within MDA-MB-231 cells. Notably, MITO-High cells possessed more copies of mitochondrial DNA (mtDNA) than MITO-Low and MDA-MB-231 cells cultured without platelets (Figure 2I), suggesting a likely more significant number of mitochondria within MITO-High cells.

Mitochondrial DNA-deficient MDA-MB-231 cells restore impaired mitochondrial function through acquisition of platelet-derived mitochondria

To study the functional significance of mitochondrial transfer from activated platelets to MDA-MB-231 cells, we generated MDA-MB-231 cells depleted of mtDNA (Rho-0), as described in Rabas et al. (2021). Rho-0 relies on uridine and pyruvate for their growth due to the absence of a functional respiratory chain (King and Atrardi, 1989; Kukat et al., 2008). The absence of these two metabolic requirements was a selectable marker for reintroducing exogenous mitochondria into Rho-0 cells by co-culture with platelets. We performed co-culture experiments between Rho-0 cells and platelets. As shown in (Figure 3A), we observed a significant increase in platelet activation when co-cultured with Rho-0 cells compared to the post-isolation platelets.

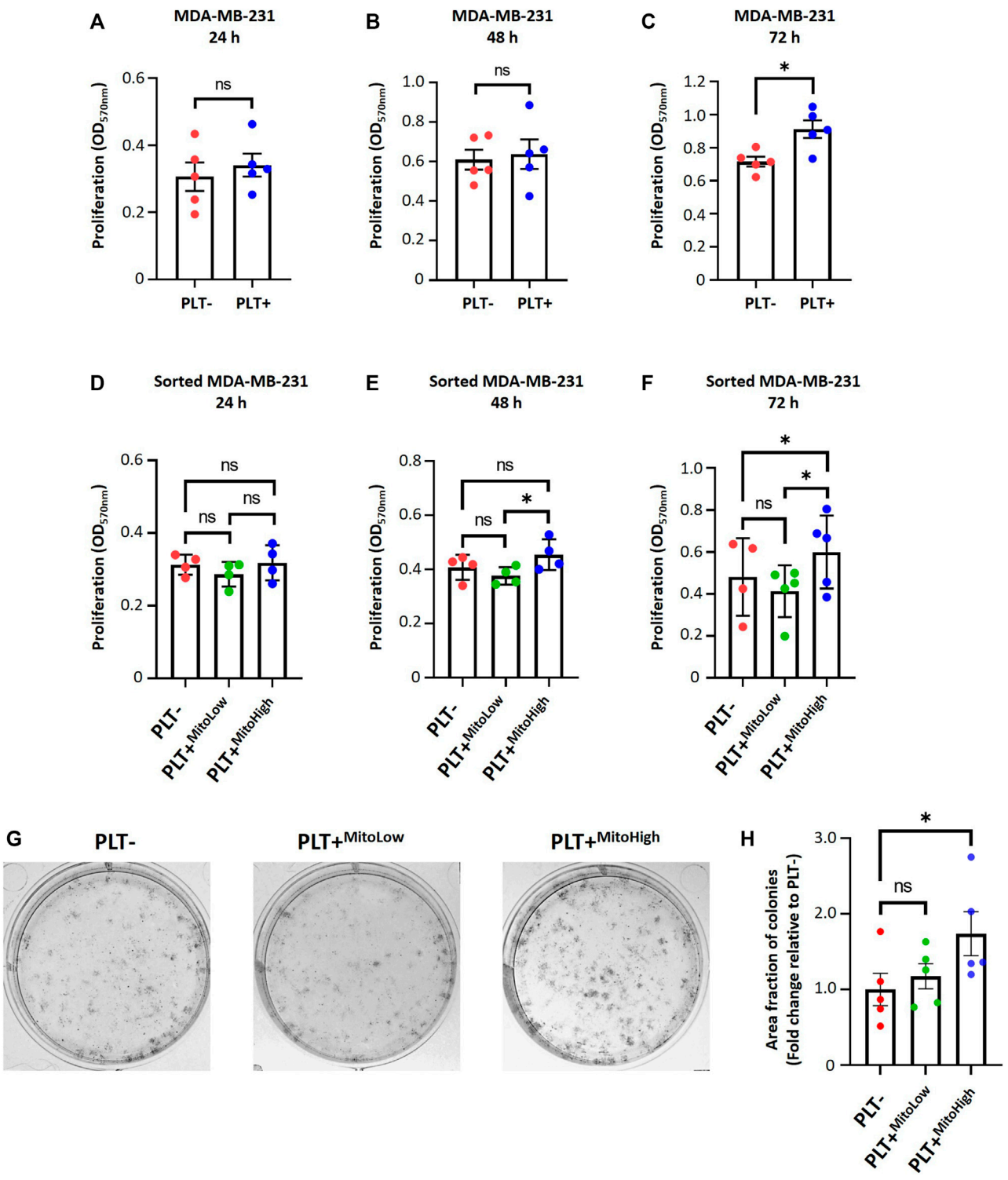

FIGURE 4
Platelet-derived mitochondria promote proliferation and increase clonogenic potential by augmenting the metabolic adaptability of MDA-MB-231 cells. Proliferation analysis of MDA-MB-231 cells cultured with buffer or platelets for 24 h. MDA-MB-231 cells were co-cultured with platelets. After that, cells were washed, reseeded, and proliferation was evaluated at 24 **(A)**, 48 **(B)**, and 72 h **(C)** by 0.5% crystal violet staining. Cell proliferation assay of sorted MDA-MB-231 cells cultured with buffer or platelets for 24 h. MDA-MB-231 cells were cultured with platelets previously stained with MTG. MDA-MB-231 cells positive for MTG signal were separated according to MTG intensity, retrieving two populations. Those with low MTG intensity are named MITO-Low, and those with high MTG intensity are named MITO-High. Sorted cells were seeded, and proliferation was evaluated at 24 **(D)**, 48 **(E)**, and 72 h **(F)** by 0.5% crystal violet staining. **(G)** Macroscopic images of colonies formed by sorted MDA-MB-231 cells in a glucose-free culture medium with 10 mM galactose and 4 mM glutamine. Sorted cells were cultured in a glucose-free cell culture medium to evidence metabolic adaptability, and colony visualization was performed by 0.5% crystal violet staining. **(H)** Quantification of the area covered by colonies formed in a glucose-free culture medium with 10 mM galactose and 4 mM glutamine. Results were expressed as fold change relative to PLT- (without platelets). A t-student statistical test was performed. *$p < 0.05$; ns = not significant.

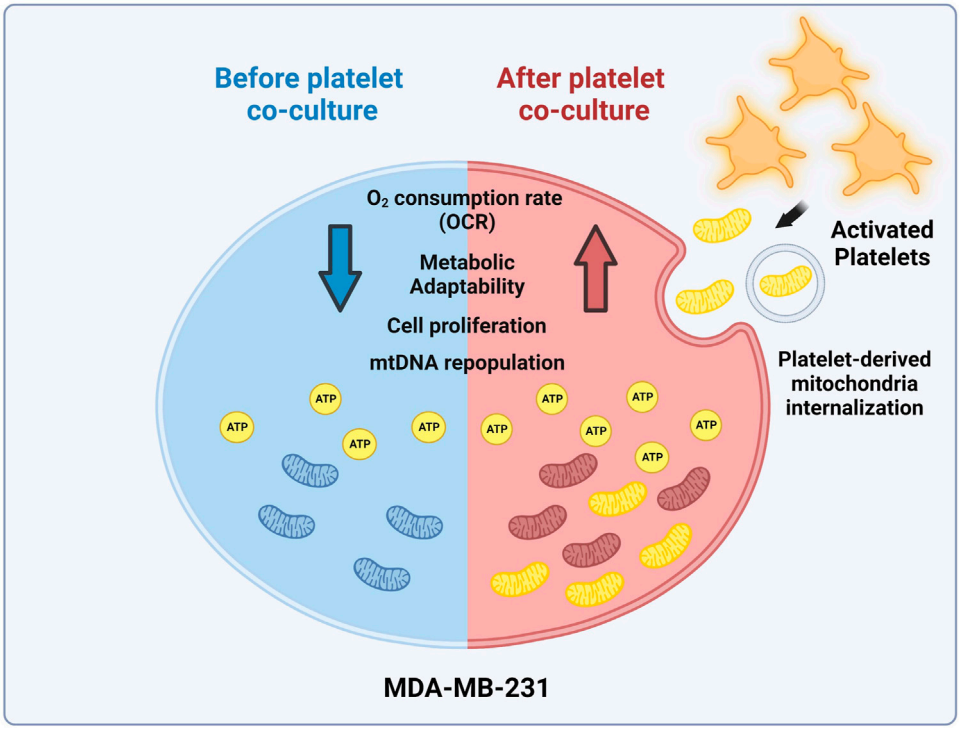

FIGURE 5
Model of mitochondrial transfer from platelets to MDA-MB-231 cells. Activation of platelets by MDA-MB-231 human triple-negative breast cancer (TNBC) cells triggers the release of platelet-derived mitochondria. These cells then internalize these mitochondria, leading to the reconstitution of mitochondrial DNA (mtDNA), increasing ATP production, oxygen (O_2) consumption rate (OCR), and cell proliferation. Interestingly, MDA-MB-231 cells with high levels of platelet-derived mitochondria exhibit superior metabolic adaptability. This highlights the significant influence of platelet-derived mitochondria on the progression of MDA-MB-231 TNBC cells (Created with BioRender.com).

Furthermore, we performed a colony formation assay to confirm whether Rho-0 cells can acquire mitochondria derived from activated platelets. We cultured Rho-0 cells with and without platelets in uridine/pyruvate-free cell culture medium (Figure 3B). Surprisingly, Rho-0 cells cultured with platelets could form colonies in uridine/pyruvate-free cell culture medium. This raised the question of whether these cells successfully repopulated with platelet-derived mitochondria, thus allowing the growth of Rho-0 cells (Figures 3C, D). Indeed, Rho-0 cells cultured with platelets were found to repopulate with platelet-derived mtDNA from the three healthy donors (i.e., platelet-rescued Rho-1, Rho-2, and Rho-3 cells).

To investigate the functional consequences of transferring platelet-derived mitochondria from three donors to Rho-0 cells, specifically on ATP production and OCR. We used oligomycin, a well-known ATP synthase inhibitor, in platelet-rescued Rho-0, Rho-1, Rho-2, and Rho-3 cells. Interestingly, all cell lines showed decreased ATP production after oligomycin (Oligo) treatment, except for Rho-0 cells (Figure 3E). Additionally, we used a Seahorse XF HS Mini Analyzer to assess the mitochondrial bioenergetics of platelet-rescued Rho-3 cells compared to MDA-MB-231 WT and Rho-0 cells. Surprisingly, as shown in (Figures 3F–H), there is a significant increase in basal OCR and ATP-linked OCR, indicating a functional effect of mitochondria transfer from activated platelets in Rho-3 cells compared to Rho-0 cells. Interestingly, in platelet-rescued Rho-3 cells, no differences in basal OCR and ATP-linked OCR were observed with MDA-MB-231 WT cells.

We evaluated the cell viability in MDA-MB-231 WT, Rho-0, and Rho-3 cells following treatment with GLUT-1 inhibitor (BAY-876) and the inhibitor of mitochondrial complex I (BAY 87–2243) (Figure 3I). Notably, using BAY-876 resulted in a significant decrease in the viability of Rho-0 cells, suggesting that these cells rely on glucose metabolism for survival. In contrast, the viability of Rho-0 cells remained stable after treatment with BAY 87–2243, while both MDA-MB-231 WT and platelet-rescued Rho-3 cells showed a marked reduction in cell viability. This decrease in cell viability could be attributed to their oxidative profile, likely resulting from the internalization of platelet-derived mitochondria.

Platelet-derived mitochondria promote proliferation and increase clonogenic potential by augmenting the metabolic adaptability of MDA-MB-231 cells

To study the functional significance of internalization of platelet-derived mitochondria on cell proliferation and metabolic adaptation of MDA-MB-231 cells. First, we examined the proliferation of MDA-MB-231 cells in co-culture with platelets. Cell proliferation was evaluated using

crystal violet staining at different times following the co-culture (Figures 4A–C). As shown in (Figure 4C), MDA-MB-231 cells cultured with platelets exhibited a significant increase in cell proliferation at 72 h compared to MDA-MB-231 cells not co-cultured with platelets. In the same way as Figure 2H, we assessed the cell proliferation of the MITO-High and the MITO-Low cell subpopulations and MDA-MB-231 cells cultured without platelets (Figures 4D–F). As shown in (Figures 4E, F), the MITO-High subpopulation significantly increased cell proliferation compared to the MITO-Low cells and MDA-MB-231 cells not co-cultured with platelets.

In addition, we performed a clonogenic assay using the MITO-High and MITO-Low subpopulations to assess the metabolic adaptability of MDA-MB-231 cells cultured with platelets. For this assay, we used a culture medium without glucose but supplemented with 10 mM galactose and 4 mM glutamine to induce a metabolic shift towards a more oxidative phenotype (Urra et al., 2018). As shown in (Figures 4G, H), we observed that the populations that covered the most area of the plate were MITO-High cells compared to MITO-Low and MDA-MB-231 cultured without platelets. This result confirms an adaptation towards a more oxidative metabolism, possibly due to the more significant number of mitochondria in MITO-high cells. Altogether, our data demonstrate that platelet-derived mitochondria increase cell proliferation and metabolic adaptability of MDA-MB-231 TNBC cells (Figure 5).

Conclusion

We have demonstrated that platelet-derived mitochondria can be internalized by MDA-MB-231 cells in co-culture, leading to increased ATP production, oxygen (O_2) consumption rate (OCR), cell proliferation, and metabolic adaptability. Interestingly, we observed that MDA-MB-231 cells depleted from mitochondrial DNA (mtDNA) recover cell proliferation in uridine/pyruvate-free cell culture medium and mitochondrial oxygen (O_2) consumption after co-culture with platelets, indicating a replenishment of mtDNA facilitated by platelet-derived mitochondria. Altogether, this finding provides new insight into the role of mitochondria derived by platelets in the metabolic adaptability and progression of metastatic MDA-MB-231 human triple-negative breast cancer (TNBC) cells.

Discussion

Interactions between cancer cells and platelets are well-known phenomena. Upon entering the circulatory system, tumor cells activate and aggregate platelets to evade the immune system and shield themselves from the shear forces of blood flow. This process is crucial for the survival of cancer cells in the circulatory system (Bambace and Holmes, 2011). Recently, it has been described that cancer cells enhance their tumor potential by acquiring exogenous mitochondria (Watson et al., 2023). However, the role of mitochondria-derived from platelets in influencing the metabolic and functional properties of MDA-MB-231 triple-negative breast cancer (TNBC) cells remains unclear.

Initially, we verified through flow cytometry that platelets become activated when co-cultured with MDA-MB-231 cells. However, the specific mechanism of platelet activation employed by MDA-MB-231 cells remained unidentified in our study. It is worth noting that a variety of mechanisms, including the use of pro-coagulant proteins, molecules such as ADP, and the release of inflammatory cytokines and microparticles, have been described for the activation of platelets by tumor cells (Razak et al., 2018). Additionally, previous research has shown that breast cancer cells, specifically MDA-MB-231 cells, can induce platelet activation. This process has been linked to the production of thrombin from plasma and is facilitated by the release of ADP from dense granules (Zarà et al., 2018).

Upon confirming platelet activation, our next objective was to determine if MDA-MB-231 cells internalized mitochondria derived from platelets. It has been reported that activated platelets release mitochondria into the extracellular environment (Boudreau et al., 2014). Using flow cytometry, we demonstrated that MDA-MB-231 cells acquire mitochondria from platelets in an *in vitro* co-culture system. Additionally, confocal microscopy revealed co-localization of platelet-derived mitochondria with endogenous mitochondria in MDA-MB-231 cells. Although we did not establish a connection between platelet-derived mitochondria and the mitochondria of cancer cells, our findings suggest that MDA-MB-231 cells acquire mitochondria from platelets when co-cultured *in vitro*. These results align with recent findings describing the internalization of platelet-derived mitochondria in osteosarcoma (Zhang et al., 2023) and mesenchymal stem cells (MSC) (Levoux et al., 2021).

Our study also utilized MitoTracker™ Deep Red (MTDR), a dye dependent on the mitochondrial membrane potential. In contrast, MitoTracker™ Green (MTG) does not rely on the mitochondrial membrane potential (Agnello et al., 2008; Cottet-Rousselle et al., 2011; Xiao et al., 2016). This dependency raises the possibility that the MTDR dye might not have been effectively retained by throughout the experiment. This could explain why MDA-MB-231 cells exhibit a higher MTG staining than MTDR (Figure 1K). This concern is particularly relevant considering that MDA-MB-231 cells were initially stained with MTDR, co-cultured with MTG-stained platelets, and then analyzed on the third day.

In addition, the more intense staining with MTG could be attributed to the MDA-MB-231 cells exposed to high quantities of platelet-derived mitochondria (Figure 1K). As a result, some of these mitochondria might co-localize with the endogenous mitochondrial network, potentially due to mitochondrial fusion, as observed in the confocal microscopy images (Figure 1K). To verify a connection between the mitochondria of platelets and cancer cells, we could study the morphology of the mitochondrial network in MDA-MB-231 cells cultured individually or with platelets using transmission electron microscopy (TEM). Furthermore, an analysis of protein or gene expression related to mitochondrial dynamics, such as mitofusins, could be analyzed.

Our study shows that incorporating mitochondria from platelets by MDA-MB-231 increases the OCR. However, we did not observe the OCR surpassing the basal rate in all these trials (Figure 2C; Figure 3F). This observation led us to conclude that it is likely that MDA-MB-231 cells consume oxygen at their maximum capacity or that there is a possibility of adjusting the amount of FCCP. We found that 200 nM FCCP is the better concentration for this study

and is the concentration used in the seahorse assays (Supplementary Figure S3).

To elucidate the functional impact of acquiring platelet-derived mitochondria by MDA-MB-231 cells, we co-cultured these cancer cells with platelets previously stained with MTG. Using cell sorting, we then separated the cancer cells based on the intensity of the MTG signal, yielding two populations: those with low MTG intensity (MITO-Low) and those with high MTG intensity (MITO-High). As a control, MDA-MB-231 cells cultured alone were subjected to the same cell sorting process. The sorted cancer cells' relative mitochondrial DNA (mtDNA) content was analyzed by qPCR to authenticate the validity of our experimental approach, which showed differential acquisition of platelet-derived mitochondria by the MDA-MB-231 cells.

On the one hand, we expected that the MITO-Low population had more mitochondria than the PLT-condition. Figure 2I shows that the MITO-High population has greater mtDNA content than the MITO-Low population and PLT-condition. However, no significant differences exist between the MITO-Low and PLT-conditions. This could be explained by the nature of our experimental strategy, in which we used the MTG dye to sort the cells that acquired platelet-derived mitochondria. We thought that there was a possibility that the MITO-Low population acquired cell structures that were MTG positive but were not complete mitochondrion (i.e., structurally damaged mitochondria). If we used platelets with GFP-labeled mitochondria, our experimental strategy could be more accurate, with the expected result of the MITO-Low population with more mitochondria than the PLT-condition. In addition, it has been described that MSC acquires mitochondria from platelets via endocytosis (Levoux et al., 2021). Moreover, cancer cells display notable heterogeneity in gene expression, both *in vitro* and *in vivo,* and alterations in endocytic pathways are frequently seen in cancer cells (Mellman and Yarden, 2013; Kinker et al., 2020). Such variability could lead to a subset of cancer cells possessing enhanced endocytic capabilities, resulting in greater internalization of mitochondria (Patel et al., 2017; Jayashankar and Edinger, 2020).

Our observations underscored that the MITO-High subpopulation of sorted MDA-MB-231 cells had higher ATP content and exhibited more cell proliferation than the MITO-Low subpopulation and the bulk of MDA-MB-231 cells. Conversely, we observed that the ATP content in the MITO-Low subpopulation was lower than in the bulk of MDA-MB-231 cells. Interestingly, the MITO-High subpopulation also had higher mtDNA levels, followed by the PLT-condition and then the MITO-Low subpopulation. The observed effects could be attributed to the amount and quality of platelet-derived mitochondria internalized by the MDA-MB-231 cells. We are exploring the "Mitohormesis" effect, which might yield different outcomes based on various signals like reactive oxygen species (ROS), mitochondrial metabolites, proteotoxic signals, and the mitochondria-cytosol stress response (Kenny et al., 2020). The mitochondria have been recognized as a pivotal organelle within cancer cells (Wallace, 2012). This is further supported by findings that cancer cells devoid of functional mitochondria require more time to form tumors than those with functional mitochondria (Tan et al., 2015). In addition, through the tricarboxylic acid cycle (TCA), mitochondria generate molecules that serve as the building blocks for synthesizing essential macromolecules, aiding in the proliferation of cancer cells (Vasan et al., 2020). Consequently, it is conceivable that the MITO-High subpopulation possesses a superior capacity for metabolite and ATP production, which might facilitate a more active state of cell proliferation. This supposition aligns with recent studies, where it was noted that glioblastoma cells with newly acquired exogenous mitochondria displayed increased cell proliferation (Watson et al., 2023).

On the other hand, elevated platelet counts during diagnosis often signal poorer outcomes, particularly in breast cancer (Giannakeas et al., 2021; Tao et al., 2021). This leads us to hypothesize that platelets play a pivotal role in the pathophysiology of hematogenous metastasis. This hypothesis is corroborated by the widespread expression of the clot-initiating protein, tissue factor (TF), across various solid tumors, a factor typically associated with advanced stages of the disease (Gomes et al., 2017). Given these insights, it is plausible that therapeutic strategies aimed at reducing platelet count or inhibiting their activation could slow cancer progression and improve patient outcomes. This perspective opens avenues for exploring pharmacological strategies that target platelets, which may significantly influence the course of cancer. Within this context, drugs that modulate platelet activation could be potential tools for mitigating TNBC progression.

Data availability statement

The original contributions presented in the study are included in the article/Supplementary Materials, further inquiries can be directed to the corresponding authors.

Ethics statement

The studies involving humans were approved by the Scientific Ethics Committee of Universidad de los Andes, Santiago, Chile. The studies were conducted in accordance with the local legislation and institutional requirements. The participants provided their written informed consent to participate in this study. Ethical approval was not required for the studies on animals in accordance with the local legislation and institutional requirements because only commercially available established cell lines were used.

Author contributions

LC: Conceptualization, Data curation, Formal Analysis, Investigation, Methodology, Writing–original draft, Writing–review and editing. JC: Conceptualization, Funding acquisition, Investigation, Resources, Writing–review and editing. MK: Conceptualization, Funding acquisition, Investigation, Resources, Writing–review and editing. ES-P: Conceptualization, Data curation, Formal Analysis, Funding acquisition, Investigation, Methodology, Project administration, Resources, Supervision, Writing–original draft, Writing–review and editing. YH: Conceptualization, Data

curation, Formal Analysis, Funding acquisition, Investigation, Methodology, Project administration, Resources, Supervision, Writing–original draft, Writing–review and editing.

Funding

The author(s) declare financial support was received for the research, authorship, and/or publication of this article. This research was funded by ANID/FONDECYT Postdoctoral Grant #3220604 (ES-P), ANID/FONDECYT Initiation Grant #11221017 (YH), ANID/FONDECYT Regular Grant #1200255 (JC), and ANID/FONDAP#15150012 (JC). ANID/FONDECYT Regular Grant #1211749 (MK), and ANID/Basal funding for Scientific and Technological Center of Excellence, IMPACT, #FB210024 (YH and MK).

Acknowledgments

We thank the Agencia Nacional de Investigación y Desarrollo (ANID) of the Government of Chile for its financial support.

Conflict of interest

MK is the chief scientific officer of Cells for Cells and Regenero, the Chilean Consortium for Regenerative Medicine.

The remaining authors declare that the research was conducted without commercial or financial relationships that could be construed as a potential conflict of interest.

The author(s) declared that they were an editorial board member of Frontiers, at the time of submission. This had no impact on the peer review process and the final decision.

Publisher's note

Supplementary material

The Supplementary Material for this article can be found online at: https://www.frontiersin.org/articles/10.3389/fcell.2023.1324158/full#supplementary-material

SUPPLEMENTARY FIGURE S1
Gating strategies for analyzing flow cytometry data. **(A)** Flow cytometry analysis was used to evaluate the internalization of mitochondria by MDA-MB-231 cells. MDA-MB-231 cells were selected using the SSC-A v/s FSC-A plot. Double events were excluded via the FSC-H v/s FSC-A plot. MDA-MB-231 cells positive for CellTrace™ Violet (CTV) were gated using the FSC-A v/s CTV plot. The internalization of mitochondria was analyzed using flow cytometry histograms and median fluorescence intensity (MFI) for MitoTracker™ Green (MTG). **(B)** Flow cytometry analysis evaluated mitochondrial membrane potential and morphological changes in MDA-MB-231 cells. MDA-MB-231 cells were selected using the SSC-A v/s FSC-A plot. Double events were discarded via the FSC-H v/s FSC-A plot. MDA-MB-231 cells positive for CTV were gated using the FSC-A v/s CTV. Relative cell size and complexity were analyzed using flow cytometry histograms MFI for FSC-H and SSC-H, respectively. Then, live MDA-MB-231 cells were identified using the FSC-A compared to the live/dead plot from flow cytometry histograms. The mitochondrial membrane potential was analyzed using median fluorescence intensity (MFI) for TMRE. **(C)** Flow cytometry analysis was utilized to assess platelet activation. Platelets were selected using the SSC-A v/s FSC-A plot. Double events were not discarded due to the impact of platelet activation on their morphological properties. Platelets positive for CD42a were selected using the FSC-A v/s CD42a plot. Platelet activation was analyzed by measuring CD62p expression using the FSC-A v/s CD62p plot, flow cytometry histograms, and MFI for CD62p.

SUPPLEMENTARY FIGURE S2
Evaluation of MitoTracker™ Green leakage from platelets to MDA-MB-231 cells. Transwell™ (TW) experiments (TW+) were performed to evaluate the potential leakage of MitoTracker™ Green (MTG) from platelets (PLT) to MDA-MB-231 cells. MTG-stained platelets were placed in the upper compartment, and MDA-MB-231 cells were placed in the lower compartment of the Transwell™ inserts (TW+) (pore size of 0.4 µm) for 24 h. In addition, we used PLT stained with MTG in co-culture with MDA-MB-231 cells (TW-) as a control for 24 h. The potential leakage of MTG from PLT to MDA-MB-231 cells was analyzed using flow cytometer. The histograms and median fluorescence intensity (MFI) of MTG signal in MDA-MB-231 cells are shown. A t-student statistical test was performed $*p < 0.05$.

SUPPLEMENTARY FIGURE S3
Determination of optimal FCCP concentration for the Agilent Seahorse XF Cell Mito Stress Test. Seahorse experiments were performed to determine the optimal concentration of FCCP for seahorse trials. MDA-MB-231 cells were seeded on XF HS Mini 8-well plates with DMEM-HG. After 48 h, the cell culture medium was replaced with Agilent Seahorse XF DMEM medium pH 7.4 containing 10 mM glucose. Mitochondrial function was evaluated using 2 µM oligomycin (Oligo), a range of FCCP concentrations [100 nM (FCCP 1), 150 nM (FCCP 2), 200 nM (FCCP 3), 300 nM (FCCP 4), and 400 nM (FCCP 5)], 1 µM rotenone (Rot), and 1 µM antimycin-A (AA).

References

Agnello, M., Morici, G., and Rinaldi, A. M. (2008). A method for measuring mitochondrial mass and activity. *Cytotechnology* 56, 145–149. doi:10.1007/s10616-008-9143-2

Bambace, N. M., and Holmes, C. E. (2011). The platelet contribution to cancer progression. *J. Thromb. Haemost.* 9, 237–249. doi:10.1111/j.1538-7836.2010.04131.x

Boudreau, L. H., Duchez, A. C., Cloutier, N., Soulet, D., Martin, N., Bollinger, J., et al. (2014). Platelets release mitochondria serving as substrate for bactericidal group IIA-secreted phospholipase A2 to promote inflammation. *Blood* 124, 2173–2183. doi:10.1182/blood-2014-05-573543

Chen, L., Zhu, C., Pan, F., Chen, Y., Xiong, L., Li, Y., et al. (2023). Platelets in the tumor microenvironment and their biological effects on cancer hallmarks. *Front. Oncol.* 13, 1121401–1121412. doi:10.3389/fonc.2023.1121401

Cottet-Rousselle, C., Ronot, X., Leverve, X., and Mayol, J. F. (2011). Cytometric assessment of mitochondria using fluorescent probes. *Cytom. Part A* 79 A, 405–425. doi:10.1002/cyto.a.21061

Dovizio, M., Ballerini, P., Fullone, R., Tacconelli, S., Contursi, A., and Patrignani, P. (2020). Multifaceted functions of platelets in cancer: from tumorigenesis to liquid biopsy tool and drug delivery system. *Int. J. Mol. Sci.* 21, 9585–9631. doi:10.3390/ijms21249585

Garrido-Castro, A. C., Lin, N. U., and Polyak, K. (2019). Insights into molecular classifications of triple-negative breast cancer: improving patient selection for treatment. *Cancer Discov.* 9, 176–198. doi:10.1158/2159-8290.CD-18-1177

Giannakeas, V., Kotsopoulos, J., Cheung, M. C., Rosella, L., Brooks, J. D., Lipscombe, L., et al. (2021). Analysis of platelet count and new cancer diagnosis over a 10-year period. *JAMA Netw. Open* 5, e21–e13. doi:10.1001/jamanetworkopen.2021.41633

Gomes, F. G., Sandim, V., Almeida, V. H., Rondon, A. M. R., Succar, B. B., Hottz, E. D., et al. (2017). Breast-cancer extracellular vesicles induce platelet activation and aggregation by tissue factor-independent and -dependent mechanisms. *Thromb. Res.* 159, 24–32. doi:10.1016/j.thromres.2017.09.019

Grasset, E. M., Dunworth, M., Sharma, G., Loth, M., Tandurella, J., Cimino-Mathews, A., et al. (2022).Triple-negative breast cancer metastasis involves complex epithelial-

mesenchymal transition dynamics and requires vimentin, *Sci. Transl. Med.*, 14, 7571. doi:10.1126/scitranslmed.abn7571

Jayashankar, V., and Edinger, A. L. (2020). Macropinocytosis confers resistance to therapies targeting cancer anabolism. *Nat. Commun.* 11, 1121–1215. doi:10.1038/s41467-020-14928-3

Kenny, T. C., Gomez, M., and Germain, D. (2020). Mitohormesis, UPRmt, and the complexity of mitochondrial DNA landscapes in cancer. *Cancer Res.* 79, 6057–6066. doi:10.1158/0008-5472.CAN-19-1395

King, M. P., and Atrardi, G. (1989). Human cells lacking mtDNA: repopulation with exogenous mitochondria by complementation. *Sci. (80-.)* 820, 6–9. doi:10.1126/science.2814477

Kinker, G. S., Greenwald, A. C., Tal, R., Orlova, Z., Cuoco, M. S., McFarland, J. M., et al. (2020). Pan-cancer single-cell RNA-seq identifies recurring programs of cellular heterogeneity. *Nat. Genet.* 52, 1208–1218. doi:10.1038/s41588-020-00726-6

Kukat, A., Kukat, C., Brocher, J., Schäfer, I., Krohne, G., Trounce, I. A., et al. (2008). Generation of rho0 cells utilizing a mitochondrially targeted restriction endonuclease and comparative analyses. *Nucleic Acids Res.* 36, e44. doi:10.1093/nar/gkn124

Laird, P. W., Zijderveld, A., Linders, K., Rudnicki, M. A., Jaenisch, R., and Berns, A. (1991). Simplified mammalian DNA isolation procedure. *Nucleic Acids Res.* 19, 4293. doi:10.1093/nar/19.15.4293

Levoux, J., Prola, A., Lafuste, P., Gervais, M., Chevallier, N., Koumaiha, Z., et al. (2021). Platelets facilitate the wound-healing capability of mesenchymal stem cells by mitochondrial transfer and metabolic reprogramming. *Cell. Metab.* 33, 283–299.e9. doi:10.1016/j.cmet.2020.12.006

Mellman, I., and Yarden, Y. (2013). Endocytosis and cancer. *Cold Spring Harb. Perspect. Biol.* 5, a016949. doi:10.1101/cshperspect.a016949

Patel, D., Rorbach, J., Downes, K., Szukszto, M. J., Pekalski, M. L., and Minczuk, M. (2017). Macropinocytic entry of isolated mitochondria in epidermal growth factor-activated human osteosarcoma cells. *Sci. Rep.* 7, 12886–12913. doi:10.1038/s41598-017-13227-0

Rabas, N., Palmer, S., Mitchell, L., Ismail, S., Gohlke, A., Riley, J. S., et al. (2021). Pink1 drives production of mtDNA-containing extracellular vesicles to promote invasiveness. *J. Cell. Biol.* 220, e202006049. doi:10.1083/JCB.202006049

Rath, S., Sharma, R., Gupta, R., Ast, T., Chan, C., Durham, T. J., et al. (2021). MitoCarta3.0: an updated mitochondrial proteome now with sub-organelle localization and pathway annotations. *Nucleic Acids Res.* 49, D1541–D1547. doi:10.1093/nar/gkaa1011

Razak, N. B. A., Jones, G., Bhandari, M., Berndt, M. C., and Metharom, P. (2018). Cancer-associated thrombosis: an overview of mechanisms, risk factors, and treatment. *Cancers (Basel)* 10, 1–21. doi:10.3390/cancers10100380

Rooney, J. P., Ryde, I. T., Sanders, L. H., Howlett, E. V., Colton, M. D., Germ, K. E., et al. (2015). PCR based determination of mitochondrial DNA copy number in multiple species. *Methods Mol. Biol.* 1241, 23–38. doi:10.1007/978-1-4939-1875-1_3

Scheid, A. D., Beadnell, T. C., and Welch, D. R. (2021). Roles of mitochondria in the hallmarks of metastasis. *Br. J. Cancer* 124, 124–135. doi:10.1038/s41416-020-01125-8

Szklarczyk, D., Gable, A. L., Lyon, D., Junge, A., Wyder, S., Huerta-Cepas, J., et al. (2019). STRING v11: protein-protein association networks with increased coverage, supporting functional discovery in genome-wide experimental datasets. *Nucleic Acids Res.* 47, D607–D613. doi:10.1093/nar/gky1131

Tan, A. S., Baty, J. W., Dong, L. F., Bezawork-Geleta, A., Endaya, B., Goodwin, J., et al. (2015). Mitochondrial genome acquisition restores respiratory function and tumorigenic potential of cancer cells without mitochondrial DNA. *Cell. Metab.* 21, 81–94. doi:10.1016/j.cmet.2014.12.003

Tao, D. L., Tassi Yunga, S., Williams, C. D., and McCarty, O. J. T. (2021). Aspirin and antiplatelet treatments in cancer. *Blood* 137, 3201–3211. doi:10.1182/blood.2019003977

Urra, F. A., Muñoz, F., Córdova-Delgado, M., Ramírez, M. P., Peña-Ahumada, B., Rios, M., et al. (2018). FR58P1a; a new uncoupler of OXPHOS that inhibits migration in triple-negative breast cancer cells via Sirt1/AMPK/β1-integrin pathway. *Sci. Rep.* 8, 13190–13216. doi:10.1038/s41598-018-31367-9

Vasan, K., Werner, M., and Chandel, N. S. (2020). Mitochondrial metabolism as a target for cancer Therapy. *Cell. Metab.* 32, 341–352. doi:10.1016/j.cmet.2020.06.019

Vismara, M., Manfredi, M., Zarà, M., Trivigno, S. M. G., Galgano, L., Barbieri, S. S., et al. (2022a). Proteomic and functional profiling of platelet-derived extracellular vesicles released under physiological or tumor-associated conditions. *Cell. Death Discov.* 8, 467–468. doi:10.1038/s41420-022-01263-3

Vismara, M., Negri, S., Scolari, F., Brunetti, V., Maria, S., Trivigno, G., et al. (2022b). *Platelet-derived extracellular vesicles stimulate migration through partial remodelling of the Ca 2 + handling machinery in MDA-MB-231 breast cancer cells 2.*

Vismara, M., Zarà, M., Negri, S., Canino, J., Canobbio, I., Barbieri, S. S., et al. (2021). Platelet-derived extracellular vesicles regulate cell cycle progression and cell migration in breast cancer cells. *Biochim. Biophys. Acta - Mol. Cell. Res.* 1868, 118886. doi:10.1016/j.bbamcr.2020.118886

Wallace, D. C. (2012). Mitochondria and cancer. *Nat. Rev. Cancer* 12, 685–698. doi:10.1038/nrc3365

Watson, D. C., Bayik, D., Storevik, S., Moreino, S. S., Sprowls, S. A., Han, J., et al. (2023). GAP43-dependent mitochondria transfer from astrocytes enhances glioblastoma tumorigenicity. *Nat. Cancer* 4, 648–664. doi:10.1038/s43018-023-00556-5

Xiao, B., Deng, X., Zhou, W., and Tan, E. K. (2016). Flow cytometry-based assessment of mitophagy using mitotracker. *Front. Cell. Neurosci.* 10, 76–84. doi:10.3389/fncel.2016.00076

Yu, L., Guo, Y., Chang, Z., Zhang, D., Zhang, S., Pei, H., et al. (2021). Bidirectional interaction between cancer cells and platelets provides potential strategies for cancer therapies. *Front. Oncol.* 11, 764119–764218. doi:10.3389/fonc.2021.764119

Zarà, M., Canobbio, I., Visconte, C., Canino, J., Torti, M., and Guidetti, G. F. (2018). Molecular mechanisms of platelet activation and aggregation induced by breast cancer cells. *Cell. Signal* 48, 45–53. doi:10.1016/j.cellsig.2018.04.008

Zarà, M., Guidetti, G., Boselli, D., Villa, C., Canobbio, I., Seppi, C., et al. (2017). Release of prometastatic platelet-derived microparticles induced by breast cancer cells: a novel positive feedback mechanism for metastasis. *TH Open* 01, e155–e163. doi:10.1055/s-0037-1613674

Zhang, W., Zhou, H., Li, H., Mou, H., Yinwang, E., Xue, Y., et al. (2023). Cancer cells reprogram to metastatic state through the acquisition of platelet mitochondria. *Cell. Rep.* 42, 113147. doi:10.1016/j.celrep.2023.113147

Żmigrodzka, M., Witkowska-Piłaszewicz, O., and Winnicka, A. (2020). Platelets extracellular vesicles as regulators of cancer progression—an updated perspective. *Int. J. Mol. Sci.* 21, 5195–5218. doi:10.3390/ijms21155195

Zoellner, H., Chami, B., Kelly, E., and Moore, M. A. S. (2019). Increased cell size, structural complexity and migration of cancer cells acquiring fibroblast organelles by cell-projection pumping. *PLoS One* 14, 0222–e113. doi:10.1371/journal.pone.0224800

frontiers | Frontiers in Cell and Developmental Biology

TYPE Original Research
PUBLISHED 23 February 2024
DOI 10.3389/fcell.2024.1331351

OPEN ACCESS

EDITED BY
Elena Levantini,
National Research Council (CNR), Italy

REVIEWED BY
Filippo M. Santorelli,
Stella Maris Foundation (IRCCS), Italy
Francesco Pallotti,
University of Insubria, Italy

*CORRESPONDENCE
L. Vilarinho,
laura.vilarinho@insa.min-saude.pt

†These authors have contributed equally to this work

RECEIVED 31 October 2023
ACCEPTED 30 January 2024
PUBLISHED 23 February 2024

CITATION
Nogueira C, Pereira C, Silva L, Laranjeira M, Lopes A, Neiva R, Rodrigues E, Campos T, Martins E, Bandeira A, Coelho M, Magalhães M, Damásio J, Gaspar A, Janeiro P, Gomes AL, Ferreira AC, Jacinto S, Vieira JP, Diogo L, Santos H, Mendonça C and Vilarinho L (2024), The genetic landscape of mitochondrial diseases in the next-generation sequencing era: a Portuguese cohort study.
Front. Cell Dev. Biol. 12:1331351.
doi: 10.3389/fcell.2024.1331351

The genetic landscape of mitochondrial diseases in the next-generation sequencing era: a Portuguese cohort study

C. Nogueira[1,2†], C. Pereira[2†], L. Silva[1,2], Mateus Laranjeira[1], A. Lopes[2], R. Neiva[2], E. Rodrigues[3], T. Campos[3], E. Martins[4], A. Bandeira[4], M. Coelho[4], M. Magalhães[5], J. Damásio[5], A. Gaspar[6], P Janeiro[6], A. Levy Gomes[7], A. C. Ferreira[8], S. Jacinto[8], J. P. Vieira[8], L. Diogo[9], H. Santos[10], C. Mendonça[11] and L. Vilarinho[1,2*]

[1]Research & Development Unit, Human Genetics Department, National Institute of Health Doutor Ricardo Jorge, Lisbon, Portugal, [2]Newborn Screening, Metabolism & Genetics Unit, Human Genetics Department, National Institute of Health Doutor Ricardo Jorge, Lisbon, Portugal, [3]Inherited Metabolic Diseases Reference Centre, São João Hospital University Centre, Porto, Portugal, [4]Inherited Metabolic Diseases Reference Centre, Santo António Hospital University Centre, Porto, Portugal, [5]Neurology Department, Santo António Hospital University Centre, Porto, Portugal, [6]Inherited Metabolic Diseases Reference Centre, Lisboa Norte Hospital University Centre, Lisboa, Portugal, [7]Neurology Department, Lisboa Norte Hospital University Centre, Lisboa, Portugal, [8]Inherited Metabolic Diseases Reference Centre, Lisboa Central Hospital Centre, Lisboa, Portugal, [9]Inherited Metabolic Diseases Reference Centre, Coimbra Hospital and University Centre, Coimbra, Portugal, [10]Inherited Metabolic Diseases Reference Centre, Vila Nova de Gaia Hospital Centre, Vila Nova de Gaia, Portugal, [11]Pediatric Department, Faro Hospital and University Centre, Faro, Portugal

Introduction: Rare disorders that are genetically and clinically heterogeneous, such as mitochondrial diseases (MDs), have a challenging diagnosis. Nuclear genes codify most proteins involved in mitochondrial biogenesis, despite all mitochondria having their own DNA. The development of next-generation sequencing (NGS) technologies has revolutionized the understanding of many genes involved in the pathogenesis of MDs. In this new genetic era, using the NGS approach, we aimed to identify the genetic etiology for a suspected MD in a cohort of 450 Portuguese patients.

Methods: We examined 450 patients using a combined NGS strategy, starting with the analysis of a targeted mitochondrial panel of 213 nuclear genes, and then proceeding to analyze the whole mitochondrial DNA.

Results and Discussion: In this study, we identified disease-related variants in 134 (30%) analyzed patients, 88 with nuclear DNA (nDNA) and 46 with mitochondrial DNA (mtDNA) variants, most of them being pediatric patients (66%), of which 77% were identified in nDNA and 23% in mtDNA. The molecular analysis of this cohort revealed 72 already described pathogenic and 20 novel, probably pathogenic, variants, as well as 62 variants of unknown significance. For this cohort of patients with suspected MDs, the use of a customized gene panel provided a molecular diagnosis in a timely and cost-effective manner. Patients who cannot be diagnosed after this initial approach will be further selected for whole-exome sequencing.

Conclusion: As a national laboratory for the study and research of MDs, we demonstrated the power of NGS to achieve a molecular etiology, expanding the mutational spectrum and proposing accurate genetic counseling in this group of heterogeneous diseases without therapeutic options.

KEYWORDS

mitochondrial diseases, next-generation sequencing, mitochondrial DNA, nuclear DNA, nuclear genes, respiratory chain, oxidative phosphorylation

1 Introduction

Through the oxidative phosphorylation (OXPHOS) process, mitochondria play a crucial role in producing over 90% of the cell's energy in the form of adenosine triphosphate (ATP), earning them the nickname "powerhouses of the cell." Distinguished by their unique features, mitochondria possess their own genetic material, referred to as mitochondrial DNA (mtDNA), which is formed by a double-stranded circular molecule of 16,569 base pairs. This genome is formed by 37 genes responsible for encoding 13 polypeptides vital for facilitating protein synthesis within the organelle, 22 tRNAs, and 2 rRNAs. However, the majority of the remaining 1,500 mitochondrial proteins are encoded by nuclear genes, which are initially translated in the cytoplasm before being subsequently imported into the mitochondrion (Friedman and Nunnari, 2014; Mishra and Chari, 2014; Kotrys and Szczesny, 2019).

Mitochondrial diseases (MDs) have become a prevalent cause of inherited metabolic diseases, impacting approximately 1 in 5,000 individuals (Gorman et al., 2015) and revealing a high genetic heterogeneity as they can result from pathogenic variants in either the nuclear DNA (nDNA) or mtDNA. Consequently, a MD can manifest through various inheritance patterns, from an autosomal dominant or recessive pattern to X-linked, *de novo* or maternal inheritance (Rahman and Rahman, 2018). Morbimortality rates among the affected individuals vary significantly due to this heterogeneous nature, which tends to be higher in cases with a rapidly progressive pattern and a pediatric onset (Gorman et al., 2016).

High-energy-demand tissues such as the brain, muscles, peripheral nerves, eyes, and heart tend to be the most affected tissues when an impairment of mitochondrial function is present. Clinically, this tends to result in multisystem involvement, although certain patients can only exhibit involvement in a single system, usually the neurological system (DiMauro et al., 2013; Maresca et al., 2020).

In the pre-molecular era, the diagnosis of a MD traditionally depended on invasive techniques, such as tissue biopsies for histochemical and biochemical analysis. With the description of the first disease-causing mutation in the mtDNA in 1988, the molecular era of mitochondrial medicine began (Holt et al., 1988; Wallace et al., 1988; Zeviani et al., 1988).

In this molecular era, next-generation sequencing (NGS) technology can generate an enormous amount of sequence data in a short time at an affordable cost, making this approach ideal for the analysis of large patient cohorts (Stenton and Prokisch, 2020), allowing the identification of pathogenic mutations affecting both the mitochondrial and nuclear genomes (Riley et al., 2020), and shortening the diagnostic odyssey (Schon et al., 2020). Thus, NGS strategies not only allow the identification of known pathogenic variants but also enable the identification of suspected pathogenic variants in the candidate genes, novel variants in the mitochondrial disease-related genes, several variants of unknown significance (VUS), and even variants in disease genes not yet associated with MD but presenting similar phenotypes (Schlieben and Prokisch, 2020). To date, the causes of mitochondriopathies have been recognized to originate from pathogenic variants in more than 400 genes in both the mitochondrial and nuclear DNA (Frazier et al., 2019; Falk, 2020; Rahman, 2020; Stenton and Prokisch, 2020).

Providing these patients and their families with a definitive genetic diagnosis offers significant advantages, whether by facilitating genetic counseling, enabling personalized information about the treatment and prognosis, or providing access to reproductive options, including prenatal diagnosis (French et al., 2019; Poulton et al., 2019).

The primary aim of this study was to determine the genetic basis of the patients clinically and/or biochemically suspected of MDs in the NGS era and how this diagnostic tool has remarkably reduced the cost and increased the availability to reach a definitive diagnosis in a short time. This work, covering more than 304 patients, complemented the previous study of 146 patients already published (Nogueira et al., 2019) and allowed the evaluation of the phenotypic characteristics and genetic landscape of 450 MD patients in Portugal.

2 Patients and methods

2.1 Patients

We examined 450 patients, comprising 219 males and 231 females, with 262 in the pediatric group and 188 in the adult group, across seven Portuguese hospitals. These individuals, lacking a molecular diagnosis, were referred to our laboratory when the clinical, biochemical, and/or neuroimaging findings suggested a MD, following the criteria established by the Mitochondrial Medicine Society (Parikh et al., 2015). Notably, 146 out of the 450 patients had previously undergone a comprehensive investigation in our national laboratory. This involved traditional Sanger sequencing of the most prevalent mtDNA mutations and a group of genes linked to specific biochemical defects and/or clinical presentations. Most of the patients underwent metabolic evaluation, which included the analysis of the redox state, amino acids, organic acids, and acylcarnitines. Mitochondrial respiratory chain (MRC), multiple deletions, and/or mtDNA depletion were also investigated in 115/450 (26%) patients suspicious of mtDNA maintenance defects.

Approval for this study was granted by the Ethics Committee of the National Institute of Health Doutor Ricardo Jorge and the Local Ethics Committee of the participating hospitals. In accordance with the Declaration of Helsinki, informed consent for genetic studies was obtained from all examined patients or, when applicable, from their relatives.

2.2 Methods

2.2.1 DNA/RNA isolation

Bio Robot EZ1 (QIAGEN, Hilden, Germany) was used to extract genomic DNA from peripheral blood samples following the standard procedures.

In accordance with the manufacturer's recommendations, total RNA was extracted using the PAXgene Blood RNA Kit (PreAnalytiX, QIAGEN, Germantown, MD, United States), and the quantification of both DNA and RNA was performed using a NanoDrop 2000 C spectrophotometer (Thermo Fisher Scientific, Waltham, MA, United States).

2.2.2 Next-generation sequencing

2.2.2.1 Targeted nuclear panel

For DNA studies, we employed a NGS-guided strategy performed on a MiSeq Illumina platform. Using a SureSelect XT HS Kit (Agilent Technologies, Santa Clara, CA, United States), a set of targeted nuclear gene panels designed with SureDesign software (Agilent Technologies) was captured. This panel covered 213 nuclear genes, 188 of which were known to be associated with MDs, while 25 of these consisted of candidate genes based on their involvement in various pathways or the capability of their clinical presentations to mimic MDs (Supplementary Data Sheet S1).

Using commercially available programs, such as SureCall (Agilent Technologies, Santa Clara, CA, United States) and wANNOVAR (wannovar.wglab.org/), variant calling and annotation were carried out, respectively. As described in previous studies by our group (Nogueira et al., 2019), we filtered the variants considering the following criteria: i) the type of mutation, ii) *in silico* predictions from tools such as SIFT, MutationTaster, PolyPhen-2, and CADD (Kumar et al., 2009; Schwarz et al., 2010; Adzhubei et al., 2013; Kircher et al., 2014), iii) their presence in various databases (gnomAD, ExAC, 1000 Genomes, ClinVar, dbSNP, OMIM, and HGMD Professional), and iv) the population frequency. Variants in the Exome Variant Server databases (http://evs.gs.washington.edu) and 1000 Genomes Project (http://www.1000genomes.org) were filtered out if their minor allele frequency (MAF) was greater than 1%.

2.2.2.2 Whole human mitochondrial genome

The whole human mtDNA was enriched through a single amplicon using a long-range PCR approach (Zhang et al., 2012), and libraries were prepared using Illumina's manufacturer's instructions. FASTQ files were aligned using the tool SeqMan NGen (DNAStar) to the mtDNA reference sequence, and commercially available programs SeqMan Pro and SeqMan NGen (DNAStar) were employed to perform the variant calling and respective annotation. Variants were filtered, considering the following criteria: i) population frequency, ii) type of mutation, iii) presence in databases (MITOMAP, MitImpact2, and HmtVar) and their *in silico* predictions, and iv) heteroplasmy exceeding 5%, as detailed in our previous study (Nogueira et al., 2019).

2.2.3 Confirmatory Sanger sequencing analysis

Sanger sequencing was performed to confirm all the identified variants with the potential to be disease-causing. For this, the BigDye Terminator Cycle Sequencing Version 3.1 protocol (Applied Biosystems, Foster City, CA, United States) was used according to the standard procedures, and the sequencing results were analyzed using an ABI 3130XL DNA analyzer. Co-segregation studies were conducted in cases where DNA from additional family members was accessible to further assess the association of the identified variants with the observed phenotype.

2.2.4 RNA studies

SuperScript III First-Strand Synthesis SuperMix for RT-PCR (Invitrogen, Thermo Fisher, Waltham, Massachusetts, United States) was used to synthesize cDNA, following the manufacturer's guidelines. *NARS2* and *DARS2* cDNA were amplified using specific forward/reverse primers (Supplementary Table S1) and the following PCR program: initial denaturation at 95°C for 10 min; denaturation at 95°C for 30 s, annealing for 45 s; extension at 72°C for 60 s (35 cycles); and final extension at 72°C for 10 min.

3 Results

3.1 Demographics and clinical and genetic characteristics

This multicenter study enrolled patients from seven Portuguese hospitals distributed all over the country, with the majority from hospitals in the north and south. The age of onset was highly variable, ranging from 4 days to 78 years old. More than 40% of the patients presented neurologic symptoms, followed by muscular, ophthalmological, cardiac, and hearing symptoms (Figure 1).

The pediatric group represents most of the patients in this cohort, at 58% (262/450), while the adult-onset group accounted for 42% of the patients (188/450), with 29 deceased patients (6%), 23 and 6 in each group, respectively. In the post-mortem studies, a molecular diagnosis was achieved in 62% of them.

In this study, we identified a possible molecular cause in 134/450 (30%) of the studied patients, with 66% of them being identified in the nuclear genome and 34% in the mitochondrial genome.

In these positive cases, 89 patients presented pathogenic or likely pathogenic variants, more commonly in nDNA. Furthermore, we identified 45/134 patients with VUS according to the American College of Medical Genetics and Genomics guidelines (ACMG), some of which were previously published by our group (Nogueira et al., 2019).

Reflecting changes in diagnostic procedures over the last decades, among these 134 MD patients with a positive molecular result, only 39 had also undergone a muscle biopsy. Histological analysis revealed morphological abnormalities in the majority of the adults. Nineteen out of these 39 patients were also confirmed to have OXPHOS enzyme deficiencies, such as isolated defects in complex I (n = 2), complex II + III (n = 2), complex IV (n = 2), multiple MRC defects (n = 7), multiple mtDNA deletions (n = 3), and mtDNA depletion (n = 3).

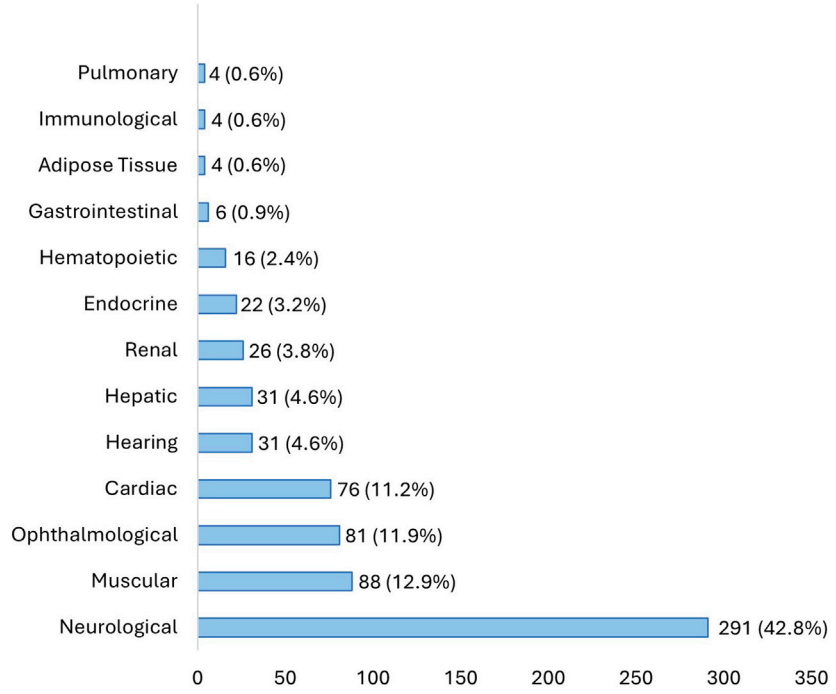

FIGURE 1
Affected systems at disease onset in our cohort.

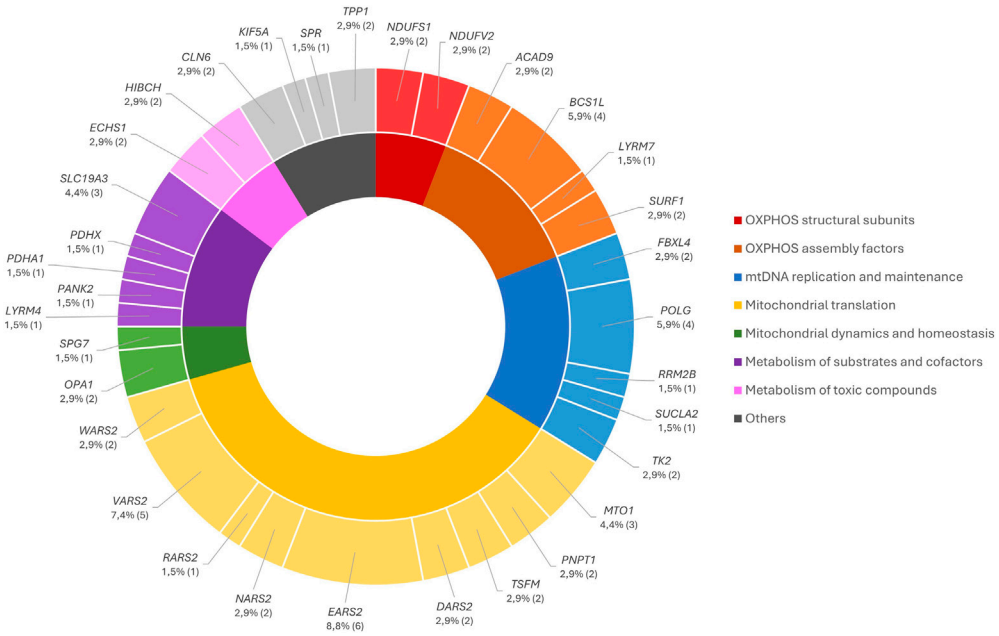

FIGURE 2
Distribution of the nDNA pathogenic/probably pathogenic variants by the affected genes according to their functional groups.

3.2 Nuclear genome

3.2.1 Pathogenic and likely pathogenic variants

Out of the 450 patients, 51 (11%) with pathogenic or likely pathogenic variants in nDNA presented 58 published and 14 novel likely pathogenic variants (Supplementary Table S2). These variants are distributed by genes involved in i) OXPHOS nuclear-encoded genes, ii) OXPHOS assembly genes, iii) mtDNA maintenance genes, iv) mtDNA transcription and translation genes, v) mitochondrial dynamics and homeostasis, vi) metabolism of substrates and cofactors, vii) metabolism of toxic compounds, and viii) other genes that mimic MDs and are known to cause monogenic disorders.

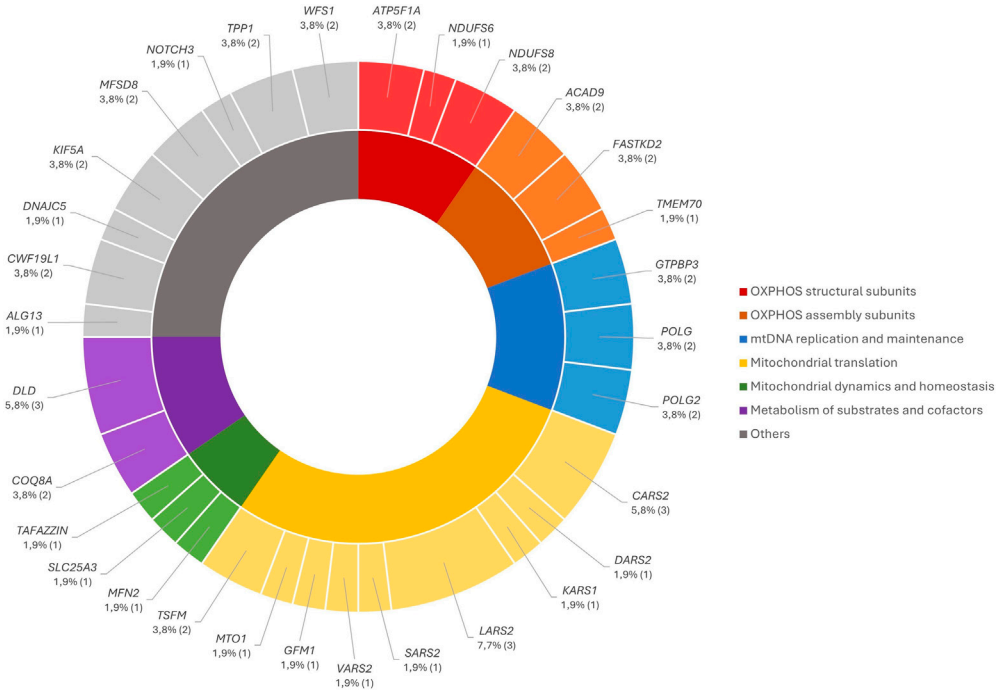

FIGURE 3
Distribution of the nDNA VUS by the affected genes according to their functional groups.

Affected genes with nDNA pathogenic and probably pathogenic variants in our cohort are described in Figure 2, according to the groups previously defined. The number of variants identified in each gene ranges from approximately 1% to 5%; however, *EARS2* and *VARS2* presented the largest number of variants, accounting for 9% and 7%, respectively.

The identified variants were comprised of i) already known causative mutations, ii) novel predicted pathogenic variants, and iii) variants that were previously validated (Nogueira et al., 2019).

Novel variants were classified as likely pathogenic when several of the following criteria were found: i) they occurred in genes where a reported pathogenic variant had already been identified, ii) the patient's phenotypes overlapped with clinical presentations previously documented for the corresponding gene, iii) the variant exhibited an overall MAF of less than 0.01% in the gnomAD database, iv) referred *in silico* predictors labeled the variant as damaging, such as CADD stringent scores (≥20) or extremely stringent scores (≥25), and v) confirmation was obtained by Sanger sequencing on the proband's DNA and, when available, in the DNA of family members.

3.2.2 Variants of unknown significance

We identified 52 VUS, classified according to the ACMG guidelines (Richards et al., 2015), in 37/450 (8%) additional patients (Supplementary Table S3). Thirty of these VUS have been published in the literature by our group (Nogueira et al., 2019), and the remaining 22 are novel.

The identified VUS were distributed according to their functional groups, with the affected genes represented in Figure 3.

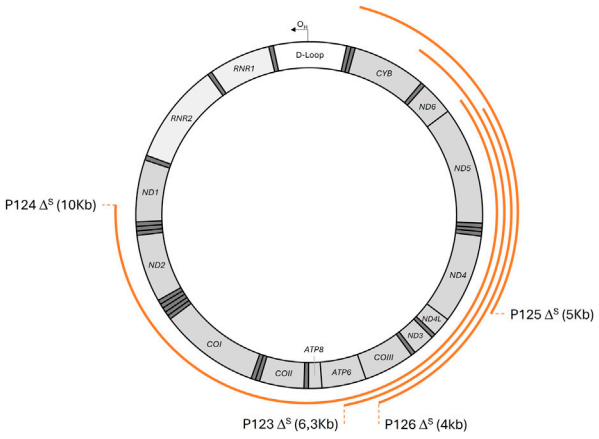

FIGURE 4
Localization and size of mtDNA large-scale deletions identified in this study.

3.3 Mitochondrial genome

3.3.1 Pathogenic and likely pathogenic variants

Sequencing of the whole human mitochondrial genome allowed the identification of: i) 11 additional pathogenic variants already described, ii) five likely pathogenic variants, three previously published (m.3251A>G/*MT-TL1*, m.3946G>A/*MT-ND1*, and m.6547T>C/*MT-CO1*) and two novel (m.4311G>A/*MT-TI* and m.12213G>A/*MT-TS2*), as well as iii) four single large-scale mtDNA deletions. Six of the most frequent variants of the mtDNA associated

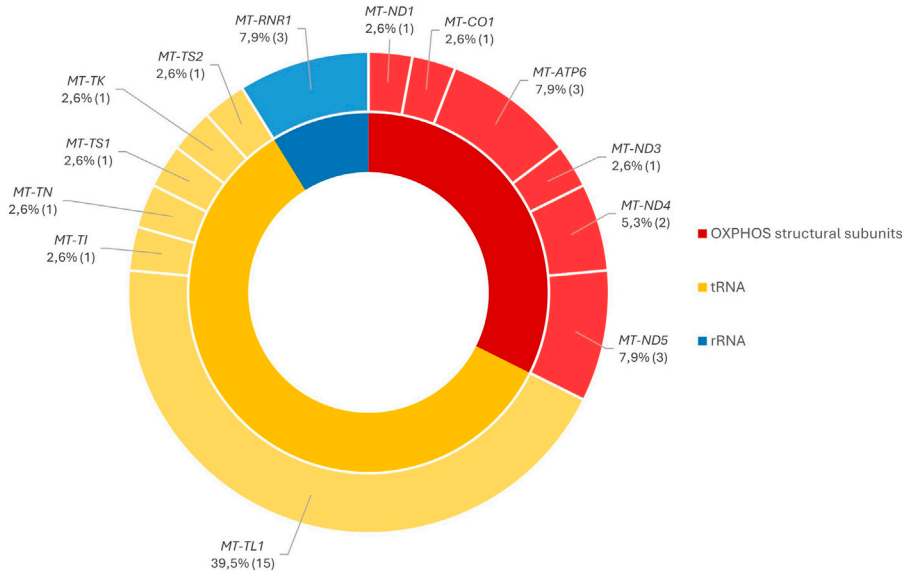

FIGURE 5
Distribution of the pathogenic/likely pathogenic variants through the mtDNA genes according to their functional groups.

with MDs were identified in more than one patient: m.1555A>G in *MT-RNR1*, m.3243A>G and m.3271T>C in *MT-TL1*, m.8993T>G in *MT-ATP6*, m.11778A>G in *MT-ND4*, and m.13513A>G in the *MT-ND5* gene. The deafness-causing variant m.1555A>G was identified in three patients. Mitochondrial encephalopathy, lactic acidosis, and stroke-like episodes (MELAS) variants m.3243A>G and m.3271T>C were found in 11 and three patients, respectively. Leber hereditary optic neuropathy (LHON)-associated variant m.11778A>G was found in two cases, and m.8993T>G and m.13513A>G, usually associated with LS (Leigh syndrome), were present in two and three patients, respectively. The variants m.5703G>A/*MT-TN*, m.7471insC/*MT-TS1*, m.8344A>G/*MT-TK*, m.9176T>G/*MT-ATP6*, and m.10197G>A/*MT-ND3* were identified only in one patient in the studied cohort. Additionally, we were able to detect four distinct single large-scale mtDNA deletions ranging from 4 to 10 kilobases in P123 to P126.

The total variants and deletions were found in 38/450 patients (9%) (Supplementary Table S4) and were distributed in the mtDNA genes encoding the structural subunits of OXPHOS, tRNAs, and rRNAs. We highlight that the deletions, because of their large scales, encompass several genes, as shown in Figure 4.

Genes encoding tRNAs represent the larger group with identified variants since the *MT-TL1* gene holds the largest number of molecular characterizations in mtDNA, particularly due to the presence of m.3243A>G in 11 patients. The variants identified in the genes encoding OXPHOS subunits were, in general, equally distributed in most of them. In the case of *MT-ATP6*, *MT-ND5*, and *MT-RNR1* gene encoding the 12S rRNA, we observed a slightly higher percentage since variants in these *loci* were identified in more than one patient (Figure 5).

Most variants were detected in various degrees of heteroplasmy (ranging from 5% to 95%), except for m.1555A>G, m.9176T>G, m.10197T>G, and m.11778A>G, which were identified in homoplasmy (Supplementary Table S4). DNA extracted from muscle was only available for nine patients, harboring the following variants: m.3243A>G (P92), m.3251A>G (P103), m.3271T>C (P104), m.4311A>G (P108), m.5703G>A (P109), m.6547T>C (P110), m.10197G>A (P116), m.12213G>A (P119), and m.13513A>G (P120). A sample from buccal mucosa was studied for P93, in whom the m.3243A>G variant was also detected in this tissue. The segregation study was possible in the mothers of patients P104, P106, and P108, in whom the variants were identified in heteroplasmy, and in the mothers of patients P92, P107, P115, P119, and P120, in whom the variants were not detected.

3.3.2 Variants of unknown significance in the mitochondrial genome

Complete sequencing of the mtDNA also revealed eight VUS (Supplementary Table S5) in eight different individuals [8/450 patients (2%)], distributed randomly in the structural genes of OXPHOS and in the genes encoding the MT-TG and MT-RNR2 (Figure 6).

All the variants were found in the heteroplasmic state, except m.9331T>C in *MT-CO3*, which was detected in homoplasmy in patient P131 and his mother. Another segregation study was possible in patient P130, the variant m.8975T>C was in heteroplasmy in the DNA from the patient's blood and muscle and absent in his mother. In patient P134, the muscle and buccal mucosa samples were also available, but the m.13115T>C variant was not detected in those tissues.

3.4 Mortality rate

The mortality rate in our cohort was 6% (29/450), and a molecular diagnosis was achieved in 62% of the deceased patients in this cohort. A total of 27 variants were identified: 19 pathogenic variants already described in the literature, four

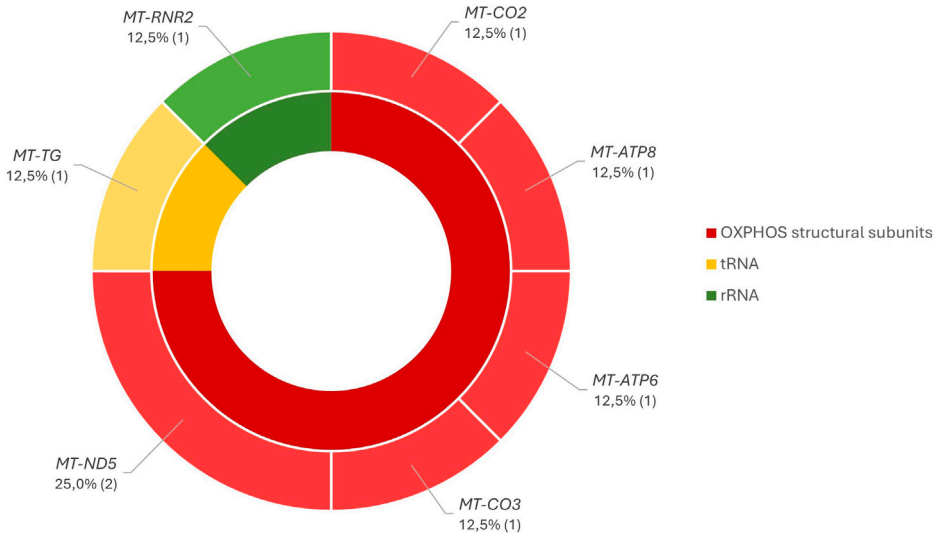

FIGURE 6
Distribution of VUS through the mtDNA genes according to their groups.

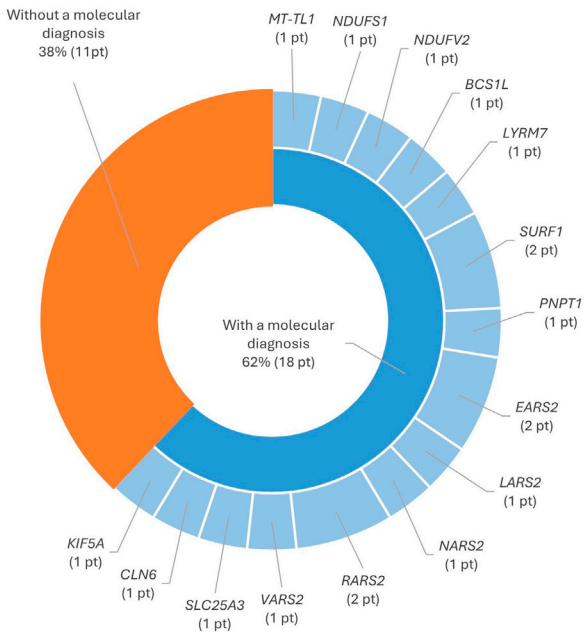

FIGURE 7
Molecular results of deceased patients.

likely pathogenic variants, and four VUS. Most of the patients that passed away were children and presented variants in the nuclear genes involved in mitochondrial translation, as shown in Figure 7.

4 Discussion

Until 2016, traditional Sanger sequencing was performed to detect the most common mtDNA variants and a group of nuclear genes associated with a clinical presentation and/or a specific biochemical defect. Afterward, we applied a combined NGS approach based on a customized targeted mitochondrial panel of 213 nuclear genes, followed by the entire mitochondrial genome analysis. Initially, we applied this strategy to a cohort of 146 patients suspected of MDs without a molecular diagnosis, as detailed in our previous publication (Nogueira et al., 2019). Later, we expanded this approach to include an additional 304 patients, resulting in a comprehensive study covering a total of 450 patients. This expanded study allowed us to achieve a possible genetic diagnosis in 134/450 patients (30%), 88 in nDNA and 46 in mtDNA, identifying a total of 154 variants: 126 (82%) in the nuclear genome and 28 (18%) in the mitochondrial genome. Furthermore, 20 of these variants are novel, 72 are described, and the remaining 62 are VUS. In our study, mtDNA variants account for more adult-onset MDs, while nDNA variants more frequently result in infancy-onset MDs, which was also demonstrated in the literature in some reviews of MDs (Pronicka et al., 2016; Subathra et al., 2016).

Based on these results, we propose the diagnostic algorithm for MDs referred to in Figure 8.

We used blood as the primary tissue of choice for the sequence-targeted mitochondrial nuclear gene panel and the whole mitochondrial genome. However, to infer the potential pathogenicity of a VUS, detected either in nDNA or mtDNA, muscle tissue was required to perform the biochemical study of MRC, multiple deletions, and/or mtDNA depletions because it contains a large number of mitochondria. Muscle tissue was also required to detect the degree of heteroplasmy when a low level of mutated mtDNA was identified in the blood as mutation levels can change over time and increase in post-mitotic tissues (Lawless et al., 2020). Despite being a mitochondria-rich tissue, the invasive nature of muscle biopsies positions this analysis as a final step of our investigations. Furthermore, segregation studies should always be carried out for both confirmed pathogenic variants and VUS.

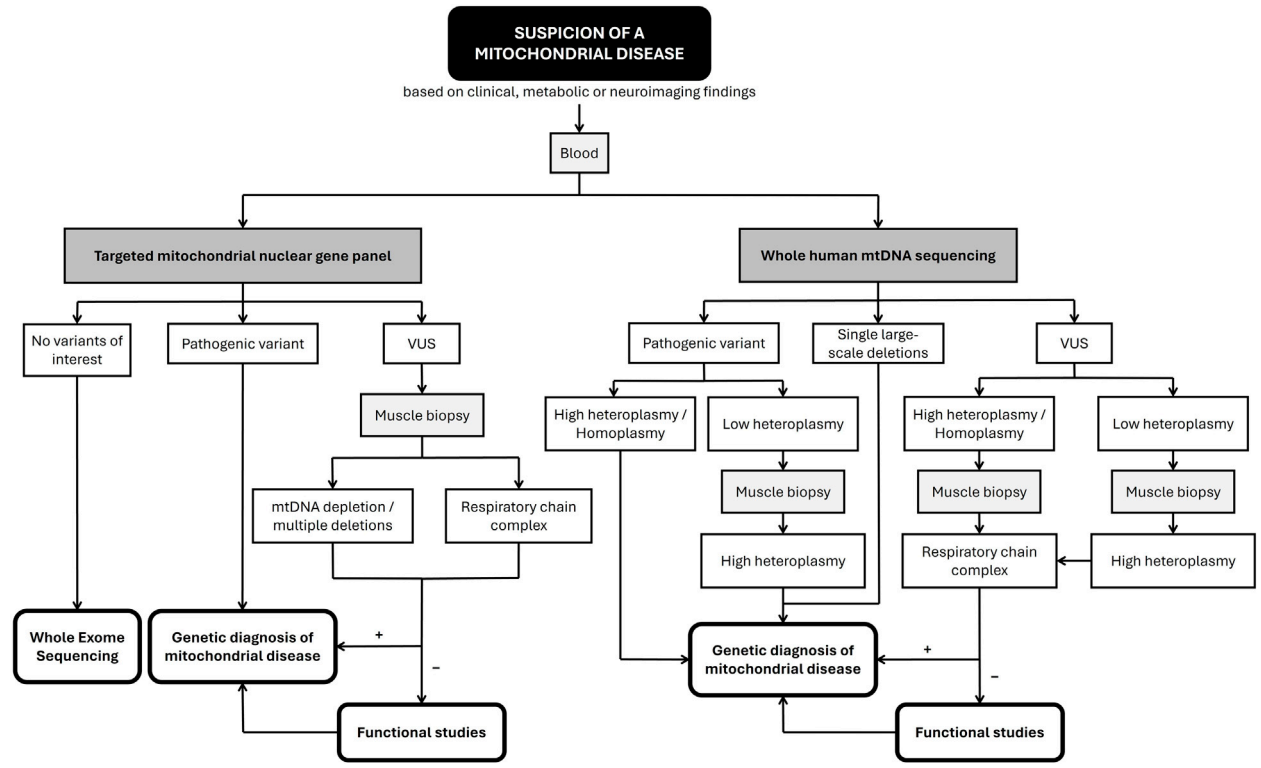

FIGURE 8
Diagnostic algorithm for a suspicion of mitochondrial disease.

4.1 Nuclear genome

4.1.1 Pathogenic and likely pathogenic variants

In 51/450 patients (11%), 12 novel likely pathogenic variants and 55 pathogenic variants, already reported in the literature, were identified in the nDNA, which were already reported in the literature (Supplementary Table S2). These variants were distributed according to the groups of genes defined in Figure 2, with most of the pathogenic variants described in the group of OXPHOS nuclear/assembly-encoded genes and the novel variants likely pathogenic in the group of mtDNA transcription and translation genes. However, we highlighted the nuclear gene *EARS2* as it had the largest number of described and novel variants identified in the pediatric group of this cohort (8%).

The likely pathogenic variants were identified in the following genes: *BCS1L* (P5), *FBXL4* (P11), *POLG* (P14 and P15), *RRM2B* (P16), *MTO1* (P19), *TSFM* (P22 and P23), *EARS2* (P28), *NARS2* (P29), *RARS2* (P30 and P31), *VARS2* (P32 and P34), and *SLC19A3* (P45). Among this group, we highlight P29, who was a female newborn with intrauterine growth restriction and preterm birth. After birth, she developed severe mitochondrial dysfunction, presenting lactic acidosis, severe generalized hyperaminoaciduria, congenital heart disease, neonatal diabetes, and omphalocele. Her clinical condition had a progressively fatal outcome. The primary analysis of P29 identified a described pathogenic variant in *NARS2*, c.500A>G (p.His167Arg), in heterozygosity. This gene is responsible for encoding the enzyme asparaginyl-tRNA synthetase, which is imported into the mitochondria in order to catalyze the binding of asparagine to the respective tRNA molecule (Simon et al., 2015). Biallelic pathogenic variants in this gene are one of the causes of OXPHOS complex dysfunction and result in neurodegenerative disorders, such as spastic paraplegia, Leigh syndrome, and Alpers syndrome (Štěrbová et al., 2021). As it is an autosomal recessive disease and only one causal allele had been identified, we continued the study of *NARS2* cDNA, which revealed a large heterozygous deletion covering exons 7, 8, and 9 [c.690-?_959+?del (p.Ala231_Ile320del)], confirming the definitive diagnosis of this patient.

The following pairs of patients, P9 and P10, P12 and P13, P22 and P23, P25 and P26, and P30 and P31, are siblings harboring pathogenic and/or likely pathogenic variants in the *SURF1*, *FBXL4*, *TSFM*, *EARS2*, and *RARS2* genes, respectively. The clinical phenotypes of the siblings with pathogenic variants are similar to those described in the literature (Tiranti et al., 1998; Steenweg et al., 2012).

Most of the characterized patients with pathogenic and likely pathogenic variants in the nuclear genome were children (76%), which is in agreement with the literature (Chinnery et al., 2014). The remaining 23% of patients were adults and presented variants in the following genes: *POLG*, *RRM2B*, *OPA1*, *KIF5A*, *SPR*, *NDUFV2*, *TK2*, *PNPT1*, *VARS2*, *WARS2*, *PDHX*, and *SPG7*, the first five with autosomal dominant patterns and the remaining in autosomal recessive patterns. Moreover, multiple mtDNA deletions were confirmed in two of the patients with variants in the *POLG* and *TK2* genes, consistent with what is described in the literature.

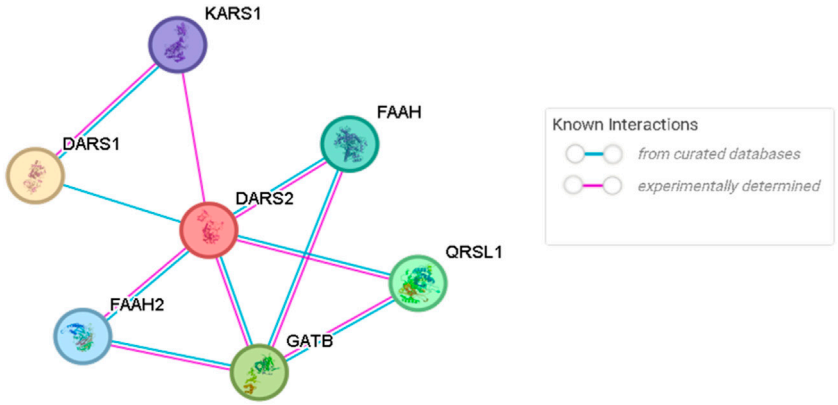

FIGURE 9
Physical network of genetic interactions associated with the *DARS2* gene. Adapted from the STRING platform (https://string-db.org/).

4.1.2 Variants of unknown significance

Furthermore, we identified 54 VUS (Supplementary Table S3), according to the ACMG, in 37/450 patients (8%), which were distributed according to their functional groups defined in Figure 3.

In the group of OXPHOS subunits and their respective assembly factors 10 VUS were identified, seven of which were already described by our group in previous studies (Nogueira et al., 2019), and three were novel; one was identified in *NDUFS1* and the others in *ATP5F1A*.

In the mtDNA replication and maintenance group, a total of six VUS were detected, with three of them identified for the first time in this study in the *GTPBP3* and *POLG2* genes.

The group of mitochondrial DNA transcription and translation genes group accounts for 15 VUS, nine of which were novel, localized in the *CARS2*, *KARS1*, *LARS2*, *VARS2*, *TSFM*, and *GFM1* genes. In this group, we highlight P65, a 2-year-old male child with hyperlactacidemia, hyperalaninemia, ataxia, non-progressive hypotonia, and a normal MRI. His primary molecular analysis identified a described heterozygous variant in the *DARS2*, c.90C>A (p.Tyr30*), but the cDNA study did not allow the identification of the second causal allele in this gene. Thus, as it is described in the literature (Papadimitriou et al., 2019), there are additional genes (*KARS1*, *DARS1*, *FAAH*, *FAAH2*, *GATB*, and *QRSL1*) that interact with *DARS2*, as shown by the STRING platform (https://string-db.org/) (Figure 9).

Among these, *KARS1* (OMIM *601421) stands out, in which the variant c.1609C>T (p.Arg537Trp) was identified in heterozygosity. In addition to these two proteins having some sequence similarity, their interaction has already been previously described in the literature and may reinforce this hypothesis (Robinson et al., 2000).

Co-segregation studies were also performed, with his father being the carrier of the *KARS1* variant and his mother being the carrier of the *DARS2* variant, confirming the digenic inheritance in this patient. In the group of dynamics and homeostasis, three VUS were identified; one of them was novel in the *MFN2* gene and present in two siblings (P73 and P74) with a similar clinical picture of neurodegenerative disease. In the metabolism of substrates and cofactors group, five VUS were identified, three of them novel, in *COQ8A* and *DLD* genes. Finally, in the group of genes that mimic MDs, a total of 13 VUS were identified, with six of them being novel in *ALG13*, *CWF19L1*, *DNAJC5*, *KIF5A*, and *NOTCH3* genes.

The identified VUS require additional analysis through animal and/or functional studies to establish their pathogenicity. Although it is beyond the scope of this work, these studies may involve various approaches, including the search for biomarkers, rescue experiments, animal models, micro-organism models, CRISPR/Cas9 technology, induced pluripotent stem cells (iPSC), and other relevant methodologies. To definitively validate the impact of these variants on protein function, these studies are essential for conclusive diagnosis within this cohort of patients.

4.2 Mitochondrial genome

The sequencing of mtDNA revealed a total of 24 variants (16 pathogenic/likely pathogenic and 8 VUS) and four single large-scale mtDNA deletions, which eventually led to a molecular diagnosis in 46/450 (10%) patients. The percentage of variants identified in the mitochondrial genome was conditioned by the fact that some of the patients with a well-defined syndrome were ruled out since the first approach of their study was orientated and positive for the most frequent variants in mtDNA or multiple deletions in the muscle biopsy. Nevertheless, we still identified some of these frequent variants in the patients of this cohort since the approach has been to sequence the complete mtDNA by NGS in all suspected MD patients. Another factor for the relatively low percentage of identified variants in mtDNA was the age of the patients in this cohort, in which most of the patients were pediatric, 262 (58%), for whom the presence of a causal variant in the nuclear genes associated with MDs is more probable.

4.2.1 Pathogenic/likely pathogenic variants

The associated phenotypes with the eleven previously reported pathogenic variants in mtDNA found in this research were, generally, in agreement with the already described presentations. However, we identified the deafness-associated m.1555A>G/*MT-TRNR1* variant in patient P89, who presented parkinsonism without hearing loss, and in patients P90 and P91, who had neurological symptoms in addition to deafness. The association of the m.1555A>G variant with distinct

presentations is already known, and recently, it has been hypothesized that this variant may be associated with multi-organ disorder, with penetrance correlated with the level of heteroplasmy in different tissues (Sobenin et al., 2013; Valiente-Pallejà et al., 2018; Finsterer, 2020). Another variant that is usually associated with deafness, the m.7471insC in *MT-TS1*, was identified in patient P111, who presented with progressive external ophthalmoplegia, head drop syndrome, and tetraparesis. This variant was formerly reported in patients with neurological presentations (Jaksch et al., 1998; Cardaioli et al., 2006; Valente et al., 2009).

It is common for an mtDNA variant to cause a broad spectrum of clinical symptoms at variable heteroplasmy levels, and this was observed for the MELAS m.3243A>G in *MT-TL1*, which was identified in patients with variable but known presentations (Vilarinho et al., 1997; Vilarinho et al., 1999). We confirmed that the level of heteroplasmy in the blood is not representative of the penetrance of this mutation, and, although it was not always possible in this study, the load of m.3243A>G should be estimated in other tissues (Chin et al., 2014; Shen and Du, 2021). This evaluation would be particularly relevant for patients P92 and P95, who must have a higher rate of mutation in the heart and kidney tissues, respectively.

It is also relevant to mention that in patient P109, in addition to the *MT-TN* variant m.5703G>A, multiple mtDNA deletions were identified in the muscular biopsy. The m.5703G>A variant has been reported with a similar presentation, but multiple mtDNA deletions were not reported (Zereg et al., 2020). We speculate that the presence of this variant may have enhanced the level of multiple mtDNA deletions in this patient and/or that these rearrangements were a consequence of aging despite her age of 57 years (Sevini et al., 2014).

We also highlight our group report about the m.9176T>G in P115, in which the low citrulline level prompted the investigation of mtDNA and revealed this *de novo* pathogenic variant in a nearly homoplasmic state (Baldo et al., 2023).

The likely pathogenic variants m.3251A>G/*MT-TL1* in patient P103, m.3946G>A/*MT-ND1* in patient P107, and m.6547T>C/*MT-CO1* in patient P110 have previously been described but have not been classified with a confirmed pathogenic status. The m.3251A>G variant has already been associated with myopathy, and, in our patient, the biochemical study of the complexes of MRC revealed severe multiple deficiencies, which are usually present in causal mutations in mitochondrial tRNA genes (Sweeney et al., 1993; Houshmand et al., 1996). Additionally, the percentage of heteroplasmy in the muscle biopsy was higher (95%) than the rate detected in the blood (70%). The m.3946G>A variant appeared *de novo* in LS patient P107. There is a previous report with the same presentation, and the variant was detected in a high level of heteroplasmy in his blood sample. These findings, the *in silico* predictions, the frequency of 0.002% in the MITOMAP database, and the conservation of this *locus* are in favor of a pathogenic status (Ogawa et al., 2017). The m.6547T>C variant identified in P110, first described by Yoneda in 1990 and later reported by our group (Pereira et al., 2019), was recently reclassified by the new version of APOGEE (APG2) as likely pathogenic.

The m.4311G>A/*MT-TI* variant in patient P108 and m.12213G>A/*MT-TS2* in patient P119 are newly reported in our study as being associated with diseases. The m.4311G>A variant exhibited high heteroplasmy in the blood and muscle samples of this patient and was present in only 15% of the molecules in the blood sample of the asymptomatic mother. The MitoTip tool classified this variant as likely pathogenic; it is absent from the population database of MITOMAP, and it is in a conserved position in the mtDNA. The m.12213G>A/*MT-TS2* variant was detected with a 25% heteroplasmy rate in the blood sample and 98% in the muscle biopsy of patient P119 and was absent in her asymptomatic mother. The MitoTip tool classified the variant as possibly pathogenic; it is absent from the MITOMAP database, and it is a highly conserved *locus* in mtDNA. Additionally, the MRC study revealed multiple deficiencies of the MRC complexes.

We detected four single large-scale mtDNA deletions in the blood samples of four pediatric patients. These deletions are generally not detected in the blood, except for Pearson syndrome (PS)/ Kearn–Sayre syndrome (KSS). It is worth noting that these four patients (P123–P126) did not exhibit the classical presentation of PS, and their mitochondrial genome were screened due to a suspected MD with no indication of a particular syndrome. These cases bring new insights for the clinical presentation of PS and add an advantage for the utility of NGS analysis of mtDNA in blood samples of children with a suspected MD (Wild et al., 2020; Yoshimi et al., 2022).

4.2.2 Variants of unknown significance

In accordance with the recommendations of the ACMG/AMP (Association of Molecular Pathology) and guidelines for mitochondrial DNA variant interpretation, we classified eight of the variants found in the mtDNA as VUS (McCormick et al., 2020).

The frequency of all these VUS is below 0.002% in the MITOMAP database, and these variants have been detected in heteroplasmy, apart from m.9331T>C in *MT-CO3*. This variant found in patient P131, although in homoplasmy, was also identified in his mother, who presented cardiac symptoms and myalgia like her son. Three of the VUS, m.2862C>T/*MT-RNR2*, m.10011A>G/*MT-TG*, and m.13115T>C/*MT-ND5*, are newly reported to be associated with diseases in this study. The remaining variants have already been described, and we emphasize that the m.8382C>T/*MT-ATP8* and m.8975T>C/*MT-ATP6* variants were investigated by functional studies (Rucheton et al., 2020). We also highlight that the m.8975T>C variant in *MT-ATP6* appeared *de novo* in patient P130 with no family history of MDs. The m.12425delA variant, located in *MT-ND5*, a hotspot gene for mtDNA pathogenic variants, predicted a severe truncation of the mature ND5 protein and was reported in a young girl with an isolated complex-I deficiency associated with an unusual MD presentation (Alston et al., 2010). Multiple lines of computational evidence support a deleterious effect for most of the VUS, except for the m.2862C>T in *MT-RNR2* variants since there are currently no readily accessible informatics tools for the prediction of rRNA variant effects.

As mentioned above, there is some evidence suggesting that these variants may play a causative role in the clinical presentation of these patients with VUS. However, further studies must be performed involving segregation investigation, the rating of heteroplasmy of the variants in other tissues, the determination of the activity of the complexes of MRC, and functional studies.

4.3 Mortality rate

The mortality rate in our cohort (6%) was below the range of 14%–46% described in several other studies looking into MD

mortality (Debray et al., 2007; Eom et al., 2017; Papadopoulos et al., 2020; Wong et al., 2023). Of the 62% deceased patients with a molecular diagnosis, the majority were children and presented mutations in the nuclear genes involved in mitochondrial translation. Defects in nucleus-encoded mitochondrial aminoacyl-tRNA synthetases, key components of the mitochondrial translation apparatus, result in severe combined MRC deficiencies and often lead to a fatal outcome in infancy (Gomez and Ibba, 2020).

5 Conclusion

The successful completion of the Human Genome Project in 2003, coupled with significant advancements in NGS technologies, marked unparalleled advances in the field of human genomics research, which has reshaped clinical medicine and biomedical exploration.

This research provided a comprehensive overview of the genetic makeup and clinical features of a group of Portuguese individuals suspected of having MDs. The NGS data provided by our study emphasize the effectiveness of employing this combined NGS approach for achieving genetic diagnoses in numerous cases involving both children and adults. Many of these cases have proven challenging to resolve through conventional Sanger sequencing-based screening of specific nuclear genes and the most common mtDNA mutations, which is why the use of custom-designed panels is so useful when seeking to obtain a molecular diagnosis in a timely and cost-effective manner. Additionally, concerning *post-mortem* diagnoses, we emphasize the significance of NGS data, which can facilitate subsequent prenatal diagnosis.

Comparing this study with our previous study (Nogueira et al., 2019), for this extended cohort of studied patients, there was a significant contribution of this manuscript to achieve more molecular diagnosis, increasing the possible genetic diagnosis from 25% to 30%. Nevertheless, to address the remaining 316 patients (70%) without a definitive genetic diagnosis, performing whole-exome sequencing analysis could increase the molecular characterization for this set of patients, as the analysis of targeted gene panels often leads to the omission of newly discovered genetic causes.

Nonetheless, as a national laboratory for the study and research of MDs, the results of our center contributed to the expansion of the mutational spectrum of pathogenic variants and are expected to provide appropriate family counseling, including prenatal and preimplantation screening. Given the genetic heterogeneity of these disorders and the absence of effective therapeutic options to date, these results carry substantial implications for enhancing our understanding and management of MDs.

Data availability statement

The original contributions presented in the study are included in the article/Supplementary Material; further inquiries can be directed to the corresponding author.

Ethics statement

The studies involving humans were approved by Ethics Committee of the National Institute of Health Doctor Ricardo Jorge. The studies were conducted in accordance with the local legislation and institutional requirements. Written informed consent for participation in this study was provided by the participants' legal guardians/next of kin.

Author contributions

CN: conceptualization, data curation, formal analysis, investigation, methodology, supervision, validation, visualization, writing–original draft, writing–review and editing, and software. CP: conceptualization, formal analysis, investigation, methodology, validation, visualization, writing–original draft, and writing–review and editing. LS: data curation, formal analysis, methodology, writing–review and editing, conceptualization, funding acquisition, investigation, project administration, resources, software, supervision, validation, visualization, and writing–original draft. ML: data curation, formal analysis, methodology, and writing–review and editing. AL: data curation, formal analysis, methodology, and writing–review and editing. RN: data curation, formal analysis, methodology, and writing–review and editing. ER: validation, visualization, and writing–review and editing. TC: validation, visualization, writing–review and editing. EM: validation, visualization, writing–review and editing. AB: validation, visualization, writing–review and editing. MC: validation, visualization, writing–review and editing. MM: validation, visualization, writing–review and editing. JD: validation, visualization, writing–review and editing. AG: validation, visualization, writing–review and editing. PJ: validation, visualization, writing–review and editing. AG: validation, visualization, writing–review and editing. AF: validation, visualization, writing–review and editing. SJ: validation, visualization, writing–review and editing. JV: validation, visualization, writing–review and editing. LD: validation, visualization, writing–review and editing. HS: validation, visualization, writing–review and editing. CM: validation, visualization, writing–review and editing. LV: conceptualization, data curation, formal analysis, funding acquisition, investigation, methodology, project administration, resources, software, supervision, validation, visualization, writing–original draft, and writing–review and editing.

Funding

The author(s) declare that financial support was received for the research, authorship, and/or publication of this article. This work was supported by FCT (PTDC/DTP-PIC/2220/2014) and NORTE 2020 (NORTE-01-0246-FEDER-000014). The content is solely the responsibility of the authors and does not necessarily represent the official views of the National Institute of Health.

Acknowledgments

The authors thank all the patients and their family members who participated in this study and contributed to advance their understanding of MDs. They are also grateful to the clinicians Gabriela Soares, Teresa Cardoso, and Paulo Chaves for the selection of some patients and Marisa Encarnação for technical support in the NGS sequencer.

Conflict of interest

The authors declare that the research was conducted in the absence of any commercial or financial relationships that could be construed as a potential conflict of interest.

Publisher's note

All claims expressed in this article are solely those of the authors and do not necessarily represent those of their affiliated organizations, or those of the publisher, the editors, and the reviewers. Any product that may be evaluated in this article, or claim that may be made by its manufacturer, is not guaranteed or endorsed by the publisher.

Supplementary material

The Supplementary Material for this article can be found online at: https://www.frontiersin.org/articles/10.3389/fcell.2024.1331351/full#supplementary-material

References

Adzhubei, I., Jordan, D. M., and Sunyaev, S. R. (2013). Predicting functional effect of human missense mutations using PolyPhen-2. *Curr. Protoc. Hum. Genet.* 7, 7.20. doi:10.1002/0471142905.hg0720s76

Alston, C. L., Morak, M., Reid, C., Hargreaves, I. P., Pope, S. A., Land, J. M., et al. (2010). A novel mitochondrial MTND5 frameshift mutation causing isolated complex I deficiency, renal failure and myopathy. *Disord.* 20 (2), 131–135. doi:10.1016/j.nmd.2009.10.010

Baldo, M. S., Nogueira, C., Pereira, C., Janeiro, P., Ferreira, S., Lourenço, C. M., et al. (2023). Leigh syndrome spectrum: a Portuguese population cohort in an evolutionary genetic era. *Genes* 14 (8), 1536. doi:10.3390/genes14081536

Cardaioli, E., Da Pozzo, P., Cerase, A., Sicurelli, F., Malandrini, A., De Stefano, N., et al. (2006). Rapidly progressive neurodegeneration in a case with the 7472insC mutation and the A7472C polymorphism in the mtDNA tRNA ser(UCN) gene. *Neuromuscul. Disord.* 16 (1), 26–31. doi:10.1016/j.nmd.2005.11.001

Chin, J., Marotta, R., Chiotis, M., Allan, E. H., and Collins, S. J. (2014). Detection rates and phenotypic spectrum of m.3243A>G in the MT-TL1 gene: a molecular diagnostic laboratory perspective. *Mitochondrion* 17, 34–41. doi:10.1016/j.mito.2014.05.005

Chinnery, P. F. (2014). Mitochondrial disorders overview in *GeneReviews®* (Seattle: University of Washington).

Debray, F. G., Lambert, M., Chevalier, I., Robitaille, Y., Decarie, J. C., Shoubridge, E. A., et al. (2007). Long-term outcome and clinical spectrum of 73 pediatric patients with mitochondrial diseases. *Pediatrics* 119 (4), 722–733. doi:10.1542/peds.2006-1866

DiMauro, S., Schon, E. A., Carelli, V., and Hirano, M. (2013). The clinical maze of mitochondrial neurology. *Nat. Rev. Neurol.* 9 (8), 429–444. doi:10.1038/nrneurol.2013.126

Eom, S., Lee, H. N., Lee, S., Kang, H. C., Lee, J. S., Kim, H. D., et al. (2017). Cause of death in children with mitochondrial diseases. *Pediatr. Neurol.* 66, 82–88. doi:10.1016/j.pediatrneurol.2016.10.006

Falk, M. J. (2020). *Mitochondrial disease gene compendium - from genes to clinical manifestations*. Cambridge, MA: Academic Press.

Finsterer, J. (2020). Variant m.1555A>G in MT-RNR1 causes hearing loss and multiorgan mitochondrial disorder. *Medicine* 99 (6), e18488. doi:10.1097/MD.0000000000018488

Frazier, A. E., Thorburn, D. R., and Compton, A. G. (2019). Mitochondrial energy generation disorders: genes, mechanisms, and clues to pathology. *J. Biol. Chem.* 294, 5386–5395. doi:10.1074/jbc.R117.809194

French, C. E., Delon, I., Dolling, H., Sanchis-Juan, A., Shamardina, O., Mégy, K., et al. (2019). Whole genome sequencing reveals that genetic conditions are frequent in intensively ill children. *J. Intensive Care Med.* 45 (5), 627–636. doi:10.1007/s00134-019-05552-x

Friedman, J. R., and Nunnari, J. (2014). Mitochondrial form and function. *Nature* 505 (7483), 335–343. doi:10.1038/nature12985

Gomez, M. A. R., and Ibba, M. (2020). Aminoacyl-tRNA synthetases. *RNA* 26 (8), 910–936. doi:10.1261/rna.071720.119

Gorman, G. S., Chinnery, P. F., DiMauro, S., Hirano, M., Koga, Y., McFarland, R., et al. (2016). Mitochondrial diseases. *Nat. Rev. Dis. Prim.* 2, 16080. doi:10.1038/nrdp.2016.80

Gorman, G. S., Schaefer, A. M., Ng, Y., Gomez, N., Blakely, E. L., Alston, C. L., et al. (2015). Prevalence of nuclear and mitochondrial DNA mutations related to adult mitochondrial disease. *Ann. Neurol.* 77 (5), 753–759. doi:10.1002/ana.24362

Holt, I. J., Harding, A. E., and Morgan-Hughes, J. A. (1988). Deletions of muscle mitochondrial DNA in patients with mitochondrial myopathies. *Nature* 331 (6158), 717–719. doi:10.1038/331717a0

Houshmand, M., Larsson, N. G., Oldfors, A., Tulinius, M., and Holme, E. (1996). Fatal mitochondrial myopathy, lactic acidosis, and complex I deficiency associated with a heteroplasmic A--> G mutation at position 3251 in the mitochondrial tRNALeu(UUR) gne. *Hum. Genet.* 97 (3), 269–273. doi:10.1007/BF02185750

Jaksch, M., Klopstock, T., Kurlemann, G., Dörner, M., Hofmann, S., Kleinle, S., et al. (1998). Progressive myoclonus epilepsy and mitochondrial myopathy associated with mutations in the tRNA(Ser(UCN)) gene. *Ann. Neurol.* 44 (4), 635–640. doi:10.1002/ana.410440409

Kircher, M., Witten, D. M., Jain, P., O'Roak, B. J., Cooper, G. M., and Shendure, J. (2014). A general framework for estimating the relative pathogenicity of human genetic variants. *Nat. Genet.* 46 (3), 310–315. doi:10.1038/ng.2892

Kotrys, A. V., and Szczesny, R. J. (2019). Mitochondrial gene expression and beyond-novel aspects of cellular physiology. *Cells* 9 (1), 17. doi:10.3390/cells9010017

Kumar, P., Henikoff, S., and Ng, P. C. (2009). Predicting the effects of coding non-synonymous variants on protein function using the SIFT algorithm. *Nat. Protoc.* 4 (7), 1073–1081. doi:10.1038/nprot.2009.86

Lawless, C., Greaves, L., Reeve, A. K., Turnbull, D. M., and Vincent, A. E. (2020). The rise and rise of mitochondrial DNA mutations. *Open. Biol.* 10 (5), 200061. doi:10.1098/rsob.200061

Maresca, A., Del Dotto, V., Romagnoli, M., La Morgia, C., Di Vito, L., Capristo, M., et al. (2020). Expanding and validating the biomarkers for mitochondrial diseases. *J. Mol. Med.* 98 (10), 1467–1478. doi:10.1007/s00109-020-01967-y

McCormick, E. M., Lott, M. T., Dulik, M. C., Shen, L., Attimonelli, M., Vitale, O., et al. (2020). Specifications of the ACMG/AMP standards and guidelines for mitochondrial DNA variant interpretation. *Hum. Mutat.* 41 (12), 2028–2057. doi:10.1002/humu.24107

Mishra, P., and Chan, D. C. (2014). Mitochondrial dynamics and inheritance during cell division, development and disease. *Nat. Rev. Mol. Cell Biol.* 15 (10), 634–646. doi:10.1038/nrm3877

Nogueira, C., Silva, L., Pereira, C., Vieira, L., Leão Teles, E., Rodrigues, E., et al. (2019). Targeted next generation sequencing identifies novel pathogenic variants and provides molecular diagnoses in a cohort of pediatric and adult patients with unexplained mitochondrial dysfunction. *Mitochondrion* 47, 309–317. doi:10.1016/j.mito.2019.02.006

Ogawa, E., Shimura, M., Fushimi, T., Tajika, M., Ichimoto, K., Matsunaga, A., et al. (2017). Clinical validity of biochemical and molecular analysis in diagnosing Leigh syndrome: a study of 106 Japanese patients. *J. Inherit. Metab. Dis.* 40 (5), 685–693. doi:10.1007/s10545-017-0042-6

Papadimitriou, S., Gazzo, A., Versbraegen, N., Nachtegael, C., Aerts, J., Moreau, Y., et al. (2019). Predicting disease-causing variant combinations. *Proc. Natl. Acad. Sci. U. S. A.* 116 (24), 11878–11887. doi:10.1073/pnas.1815601116

Papadopoulos, C., Wahbi, K., Behin, A., Bougouin, W., Stojkovic, T., Leonard-Louis, S., et al. (2020). Incidence and predictors of total mortality in 267 adults presenting with mitochondrial diseases. *J. Inherit. Metab. Dis.* 43 (3), 459–466. doi:10.1002/jimd.12185

Parikh, S., Goldstein, A., Koenig, M. K., Scaglia, F., Enns, G. M., Saneto, R., et al. (2015). Diagnosis and management of mitochondrial disease: a consensus statement from the Mitochondrial Medicine Society. *Diagnosis Manag. mitochondrial Dis. a consensus statement Mitochondrial Med. Soc. Genet. Med* 17 (9), 689–701. doi:10.1038/gim.2014.177

Pereira, C., Souza, C. F., Vedolin, L., Vairo, F., Lorea, C., Sobreira, C., et al. (2019). Leigh syndrome due to mtDNA pathogenic variants. *Screen.* 7 (1), e20180003. doi:10.1590/2326-4594-jiems-2018-0003

Poulton, J., Steffann, J., Burgstaller, J., and McFarland, R. (2019). 243rd ENMC international workshop: developing guidelines for management of reproductive options for families with maternally inherited mtDNA disease, Amsterdam, The Netherlands, 22-24 March 2019. *Neuromuscul. Disord.* 29 (9), 725–733. doi:10.1016/j.nmd.2019.08.004

Pronicka, E., Piekutowska-Abramczuk, D., Ciara, E., Trubicka, J., Rokicki, D., Karkucińska-Więckowska, A., et al. (2016). New perspective in diagnostics of mitochondrial disorders: two years' experience with whole-exome sequencing at a National Paediatric Centre. *J. Transl. Med.* 14 (1), 174. doi:10.1186/s12967-016-0930-9

Rahman, J., and Rahman, S. (2018). Mitochondrial medicine in the omics era. *Lancet* 391 (10139), 2560–2574. doi:10.1016/S0140-6736(18)30727-X

Rahman, S. (2020). Mitochondrial disease in children. *J. Intern. Med.* 287, 609–633. doi:10.1111/joim.13054

Richards, S., Aziz, N., Bale, S., Bick, D., Das, S., Gastier-Foster, J., et al. (2015). Standards and guidelines for the interpretation of sequence variants: a joint consensus recommendation of the American College of medical genetics and genomics and the association for molecular pathology. *Genet. Med.* 17 (5), 405–424. doi:10.1038/gim.2015.30

Riley, L. G., Cowley, M. J., Gayevskiy, V., Minoche, A. E., Puttick, C., Thorburn, D. R., et al. (2020). The diagnostic utility of genome sequencing in a pediatric cohort with suspected mitochondrial disease. *Genet. Med.* 22 (7), 1254–1261. doi:10.1038/s41436-020-0793-6

Robinson, J. C., Kerjan, P., and Mirande, M. (2000). Macromolecular assemblage of aminoacyl-tRNA synthetases: quantitative analysis of protein-protein interactions and mechanism of complex assembly. *J. Mol.Biol.* 304 (5), 983–994. doi:10.1006/jmbi.2000.4242

Rucheton, B., Jardel, C., Filaut, S., Amador, M. D. M., Maisonobe, T., Serre, I., et al. (2020). Homoplasmic deleterious MT-ATP6/8 mutations in adult patients. *Mitochondrion* 55, 64–77. doi:10.1016/j.mito.2020.08.004

Schlieben, L. D., and Prokisch, H. (2020). The dimensions of primary mitochondrial disorders. *Cell Dev. Biol.* 8, 600079. doi:10.3389/fcell.2020.600079

Schon, K. R., Ratnaike, T., van den Ameele, J., Horvath, R., and Chinnery, P. F. (2020). Mitochondrial diseases: a diagnostic revolution. *Trends Genet.* 36 (9), 702–717. doi:10.1016/j.tig.2020.06.009

Schwarz, J. M., Rödelsperger, C., Schuelke, M., and Seelow, D. (2010). MutationTaster evaluates disease-causing potential of sequence alterations. *Nat. Methods* 7 (8), 575–576. doi:10.1038/nmeth0810-575

Sevini, F., Giuliani, C., Vianello, D., Giampieri, E., Santoro, A., Biondi, F., et al. (2014). mtDNA mutations in human aging and longevity: controversies and new perspectives opened by high-throughput technologies. *Exp. Gerontol.* 56, 234–244. doi:10.1016/j.exger.2014.03.022

Shen, X., and Du, A. (2021). The non-syndromic clinical spectrums of mtDNA 3243A>G mutation. *Neurosciences* 26 (2), 128–133. doi:10.17712/nsj.2021.2.20200145

Simon, M., Richard, E. M., Wang, X., Shahzad, M., Huang, V. H., Qaiser, T. A., et al. (2015). Mutations of human NARS2, encoding the mitochondrial asparaginyl-tRNA synthetase, cause nonsyndromic deafness and Leigh syndrome. *PLoS Genet.* 11 (3), e1005097. doi:10.1371/journal.pgen.1005097

Sobenin, I. A., Sazonova, M. A., Postnov, A. Y., Bobryshev, Y. V., and Orekhov, A. N. (2013). Changes of mitochondria in atherosclerosis: possible determinant in the pathogenesis of the disease. *Atherosclerosis* 227 (2), 283–288. doi:10.1016/j.atherosclerosis.2013.01.006

Steenweg, M. E., Ghezzi, D., Haack, T., Abbink, T. E., Martinelli, D., van Berkel, C. G., et al. (2012). Leukoencephalopathy with thalamus and brainstem involvement and high lactate 'LTBL' caused by EARS2 mutations. *Brain* 135 (5), 1387–1394. doi:10.1093/brain/aws070

Stenton, S. L., and Prokisch, H. (2020). Genetics of mitochondrial diseases: identifying mutations to help diagnosis. *eBio Med.* 56, 102784. doi:10.1016/j.ebiom.2020.102784

Štěrbová, K., Vlčková, M., Hansíková, H., Sebroňová, V., Sedláčková, L., Pavlíček, P., et al. (2021). Novel variants in the NARS2 gene as a cause of infantile-onset severe epilepsy leading to fatal refractory status epilepticus: case study and literature review. *Neurogenetics* 22 (4), 359–364. doi:10.1007/s10048-021-00659-0

Subathra, M., Ramesh, A., Selvakumari, M., Karthikeyen, N. P., and Srisailapathy, C. R. (2016). Genetic epidemiology of mitochondrial pathogenic variants causing nonsyndromic hearing loss in a large cohort of south indian hearing impaired individuals. *Ann. Hum. Genet.* 80 (5), 257–273. doi:10.1111/ahg.12161

Sweeney, M. G., Bundey, S., Brockington, M., Poulton, K. R., Winer, J. B., and Harding, A. E. (1993). Mitochondrial myopathy associated with sudden death in young adults and a novel mutation in the mitochondrial DNA leucine transfer RNA(UUR) gene. *Q. J. Med.* 86 (11), 709–713. doi:10.1093/oxfordjournals.qjmed.a068750

Tiranti, V., Hoertnagel, K., Carrozzo, R., Galimberti, C., Munaro, M., Granatiero, M., et al. (1998). Mutations of SURF-1 in Leigh disease associated with cytochrome c oxidase deficiency. *Am. J. Hum. Genet.* 63 (6), 1609–1621. doi:10.1086/302150

Valente, L., Piga, D., Lamantea, E., Carrara, F., Uziel, G., Cudia, P., et al. (2009). Identification of novel mutations in five patients with mitochondrial encephalomyopathy. *Biochim. Biophys. Acta - Bioenerg.* 1787 (5), 491–501. doi:10.1016/j.bbabio.2008.10.001

Valiente-Pallejà, A., Torrell, H., Muntané, G., Cortés, M. J., Martínez-Leal, R., Abasolo, N., et al. (2018). Genetic and clinical evidence of mitochondrial dysfunction in autism spectrum disorder and intellectual disability. *Hum. Mol. Genet.* 27 (5), 891–900. doi:10.1093/hmg/ddy009

Vilarinho, L., Santorelli, F. M., Coelho, I., Rodrigues, L., Maia, M., Barata, I., et al. (1999). The mitochondrial DNA A3243G mutation in Portugal: clinical and molecular studies in 5 families. *J. Neurol. Sci.* 163 (2), 168–174. doi:10.1016/s0022-510x(99)00030-1

Vilarinho, L., Santorelli, F. M., Rosas, M. J., Tavares, C., Melo-Pires, M., and DiMauro, S. (1997). The mitochondrial A3243G mutation presenting as severe cardiomyopathy. *J. Med. Genet.* 34 (7), 607–609. doi:10.1136/jmg.34.7.607

Wallace, D. C., Singh, G., Lott, M. T., Hodge, J. A., Schurr, T. G., Lezza, A. M., et al. (1988). Mitochondrial DNA mutation associated with Leber's hereditary optic neuropathy. *Science* 242, 1427–1430. doi:10.1126/science.3201231

Wild, K. T., Goldstein, A. C., Muraresku, C., and Ganetzky, R. D. (2020). Broadening the phenotypic spectrum of Pearson syndrome: five new cases and a review of the literature. *Am. J. Med. Genet. A* 182 (2), 365–373. doi:10.1002/ajmg.a.61433

Wong, T. S., Belaramani, K. M., Chan, C. K., Chan, W. K., Chan, W. L., Chang, S. K., et al. (2023). Mitochondrial diseases in Hong Kong: prevalence, clinical characteristics and genetic landscape. *Rare Dis.* 18 (1), 43. doi:10.1186/s13023-023-02632-6

Yoshimi, A., Ishikawa, K., Niemeyer, C., and Grünert, S. C. (2022). Pearson syndrome: a multisystem mitochondrial disease with bone marrow failure. *Rare Dis.* 17 (1), 379. doi:10.1186/s13023-022-02538-9

Zereg, E., Chaussenot, A., Morel, G., Bannwarth, S., Sacconi, S., Soriani, M. H., et al. (2020). Single-fiber studies for assigning pathogenicity of eight mitochondrial DNA variants associated with mitochondrial diseases. *Hum. Mutat.* 41 (8), 1394–1406. doi:10.1002/humu.24037

Zeviani, M., Moraes, C. T., DiMauro, S., Nakase, H., Bonilla, E., Schon, E. A., et al. (1988). Deletions of mitochondrial DNA in Kearns-Sayre syndrome. *Neurology* 38, 1339–1346. doi:10.1212/wnl.38.9.1339

Zhang, W., Cui, H., and Wong, L. J. (2012). Comprehensive one-step molecular analyses of mitochondrial genome by massively parallel sequencing. *Clin. Chem.* 58 (9), 1322–1331. doi:10.1373/clinchem.2011.181438

frontiers | Frontiers in Cell and Developmental Biology

TYPE Review
PUBLISHED 12 April 2024
DOI 10.3389/fcell.2024.1381417

OPEN ACCESS

EDITED BY
Filippo M. Santorelli,
Stella Maris Foundation (IRCCS), Italy

REVIEWED BY
François Singh,
University of Iceland, Iceland
Daniela Ramaccini,
University of Ferrara, Italy
Ioanna Daskalaki,
École polytechnique fédérale de Lausanne (EPFL), Switzerland

*CORRESPONDENCE
Yang Li,
liyang_2015@jlu.edu.cn
Luyan Shen,
shenly@jlu.edu.cn

RECEIVED 03 February 2024
ACCEPTED 29 March 2024
PUBLISHED 12 April 2024

CITATION
Lin F, Sun L, Zhang Y, Gao W, Chen Z, Liu Y, Tian K, Han X, Liu R, Li Y and Shen L (2024), Mitochondrial stress response and myogenic differentiation.
Front. Cell Dev. Biol. 12:1381417.
doi: 10.3389/fcell.2024.1381417

Mitochondrial stress response and myogenic differentiation

Fu Lin[1], Liankun Sun[1], Yu Zhang[2], Weinan Gao[1], Zihan Chen[1,3], Yanan Liu[1], Kai Tian[1,4], Xuyu Han[1,4], Ruize Liu[1,4], Yang Li[5]* and Luyan Shen[1]*

[1]Key Laboratory of Pathobiology, Department of Pathophysiology, Ministry of Education, College of Basic Medical Sciences, Jilin University, Changchun, China, [2]Experimental Teaching Center of Basic Medicine, College of Basic Medical Sciences, Jilin University, Changchun, China, [3]Clinical Medical College of Jilin University, The First Hospital of Jilin University, Changchun, China, [4]China Japan Union Hospital of Jilin University, Changchun, China, [5]Department of Physiology, College of Basic Medical Sciences, Jilin University, Changchun, China

Regeneration and repair are prerequisites for maintaining effective function of skeletal muscle under high energy demands, and myogenic differentiation is one of the key steps in the regeneration and repair process. A striking feature of the process of myogenic differentiation is the alteration of mitochondria in number and function. Mitochondrial dysfunction can activate a number of transcriptional, translational and post-translational programmes and pathways to maintain cellular homeostasis under different types and degrees of stress, either through its own signaling or through constant signaling interactions with the nucleus and cytoplasm, a process known as the mitochondrial stress responses (MSRs). It is now believed that mitochondrial dysfunction is closely associated with a variety of muscle diseases caused by reduced levels of myogenic differentiation, suggesting the possibility that MSRs are involved in messaging during myogenic differentiation. Also, MSRs may be involved in myogenesis by promoting bioenergetic remodeling and assisting myoblast survival during myogenic differentiation. In this review, we will take MSRs as an entry point to explore its concrete regulatory mechanisms during myogenic differentiation, with a perspective to provide a theoretical basis for the treatment and repair of related muscle diseases.

KEYWORDS

myogenic differentiation, ISR, UPRmt, mitochondrial biogenesis, mitochondrial fusion and fission, mitophagy, apoptosis

1 Introduction

Skeletal muscle accounts for 30%–40% of healthy body weight and plays key roles in human voluntary movement, postural maintenance, respiration, and thermogenesis, the maintenance of which relies heavily on the regeneration and repair of skeletal muscle (Dumont et al., 2015; He et al., 2021). Skeletal muscle regeneration and repair is a complex process mediated by muscle satellite cells (MuSCs). MuSCs, located between the muscle membrane and the basal lamina of myofibers, are normally quiescent until they are activated by growth signals or injury stimuli. Upon activation, these cells will migrate and proliferate extensively to form mononuclear precursor cells, i.e., myoblasts. Subsequently, once the population of myoblasts has expanded, they exit the cell cycle and activate a differentiation programme to form multinucleated myotubes, which eventually fuse with existing myofibers to facilitate myofiber replenishment and repair.

One of these key steps, the differentiation from myoblasts to myotubes, has been termed myogenic differentiation (Walsh and Perlman, 1997; Morgan and Partridge, 2003; Remels et al., 2010; Relaix and Zammit, 2012). This step is coordinated by a number of specific genes, such as myogenic regulatory factors (MRFs), including myogenic factor 5 (Myf5), myogenic regulatory factor 4 (MRF4), myoblast determination protein 1 (MyoD) and myogenin (MyoG), which direct progenitor cells to establish a myogenic lineage and activate the myogenic differentiation programme. MRFs also regulate the level of myosin heavy chain (MyHC), which determines the contractile properties of myofibers (Zammit, 2017). Reduced myogenic differentiation capacity has been reported to be associated with the progression of several muscle diseases, such as sarcopenia (Sun et al., 2022), skeletal muscle atrophy (Rahman and Quadrilatero, 2023) and Duchenne muscular dystrophy (Meyer et al., 2021).

Mitochondria are closely associated with myogenic differentiation due to the high energy requirements of skeletal muscle and the fact that mitochondria are the principal energy-supplying organelles in the cell (Wagatsuma and Sakuma, 2013). A striking feature of the process of myogenic differentiation is the change in the number, morphology and functional properties of mitochondria. Mitochondria in myoblasts are in an immature state, with low numbers, underdeveloped cristae and low levels of β-oxidation and overall respiration; whereas, when stimulated by differentiation factors, myoblasts must switch to a more oxidative phenotype to support a differentiation programme accompanied by metabolic reprogramming. As a result, mitochondria within differentiated myotubes appear more mature, with high numbers, enhanced levels of oxidative phosphorylation and increased ATP production (Vertel and Fischman, 1977; Barbieri et al., 2011; Rahman and Quadrilatero, 2021). To further elucidate the relationship between mitochondria and myogenic differentiation, several studies have used rotenone (complex I inhibitor), trifluoroacetone (complex II inhibitor) (Chabi et al., 2021), carbonylcyanide p-trifluoromethoxy-phenylhydrazone (FCCP) (mitochondrial uncoupler) (Wang et al., 2014), mitochondrial division inhibitor-1 (Mdivi-1) (dynamin-related protein 1 (Drp1) inhibitor) (Kim et al., 2013), ethidium bromide (EB) (mitochondrial DNA transcriptional inhibitor), rifampicin (mitochondrial RNA synthesis inhibitor) (Brunk and Yaffe, 1976), chloramphenicol (mitochondrial protein synthesis inhibitor) (Seyer et al., 2011), and UCF101 (High-Temperature Requirement Protein A2(HtrA2) inhibitor) (Sun et al., 2022) and others were used in differentiation model experiments, and it was found that affecting mitochondrial function from multiple aspects can have a negative impact on myogenic differentiation, indicating that mitochondrial diversity function controls the fate of myoblast differentiation.

When mitochondrial dysfunction occurs, mitochondria can continuously crosstalk with the nucleus and cytoplasm through signaling pathways originating from their own activation, activating a number of transcriptional, translational and post-translational programmes and pathways to execute multiple mitochondrial stress responses (MSRs). Short-term, mild stress can aid cellular homeostasis, whereas prolonged and severe stress can trigger apoptosis by causing an unresolved intracellular imbalance. Thus, the effect of MSRs is closely related to the duration and magnitude of the stress effects. (O'Malley et al., 2020; Picard and Shirihai, 2022). Furthermore, influenced by factors that initiate differentiation, skeletal muscle differentiation and formation itself is accompanied by significant levels of cellular stress changes such as caspase activation, increased reactive oxygen species (ROS), and upregulation of transcription of oxidative stress-related genes. (Jahnke et al., 2009; Baechler et al., 2019; Li et al., 2021; Gugliuzza and Crist, 2022), which confers the possibility that MSRs are involved in the transfer of information during myogenic differentiation. It is clear that MSRs play an important role in myogenic differentiation under both physiological and pathological conditions. Therefore, in this review, we describe multiple response pathways activated by mitochondrial stress, including integrated stress response (ISR), mitochondrial unfolded protein response (UPRmt), mitochondrial biogenesis, mitochondrial fusion and fission, mitophagy, apoptosis, as well as some of their known or potential effects on myogenic differentiation. With the aim of providing new perspectives and ideas to address related issues of muscle health and disease by exploring the link between MSRs and myogenic differentiation.

2 Selective transcriptional/translational effects of mitochondrial-nuclear interaction regulation on myogenic differentiation

2.1 ISR

In response to different stressful stimuli, eukaryotic cells activate a broader adaptive pathway known as the ISR. In mammals, four eukaryotic translation initiation factor 2alpha (eIF2α) kinases have now been identified, namely, general control non-derepressible 2 (GCN2), double-stranded RNA-dependent protein kinase (PKR), PKR-like ER kinase (PERK) and heme-regulated eIF2alpha kinase (HRI) (Donnelly et al., 2013). Stress activation of the four eIF2α kinases mentioned above phosphorylates the α-subunit of eIF2α at serine 51, and this phosphorylation blocks the formation of the ternary complex consisting of eIF2, GTP, and Met-tRNAi, which is a key step in 5′cap-dependent translation initiation, and thus can inhibit the overall translational initiation activity, leading to reduced protein synthesis (English et al., 2022). Next, ISR activation allows preferential expression of specific genes containing upstream open reading frames, such as the transcription factors activating transcription factor 4 (ATF4), C/EBP homologous protein (CHOP) and activating transcription factor 5 (ATF5), to ensure the subsequent generation of factors that aid in cellular recovery or, in some cases, initiate apoptosis (Eckl et al., 2021; Licari et al., 2021).

Of interest, a recent study by Guo X et al. (Guo et al., 2020) found that mitochondria can transmit stress signals into the cytoplasm via the OMA1-DAP3 binding cell death enhancer-1 (DELE1)-HRI pathway, which subsequently triggers ISR (Figure 1). Upon stress onset, DELE1 is cleaved by the inner mitochondrial membrane protease OMA1 and subsequently translocates to the cytoplasm to interact with HRI, which phosphorylates eIF2α, inhibits cytoplasmic protein translation,

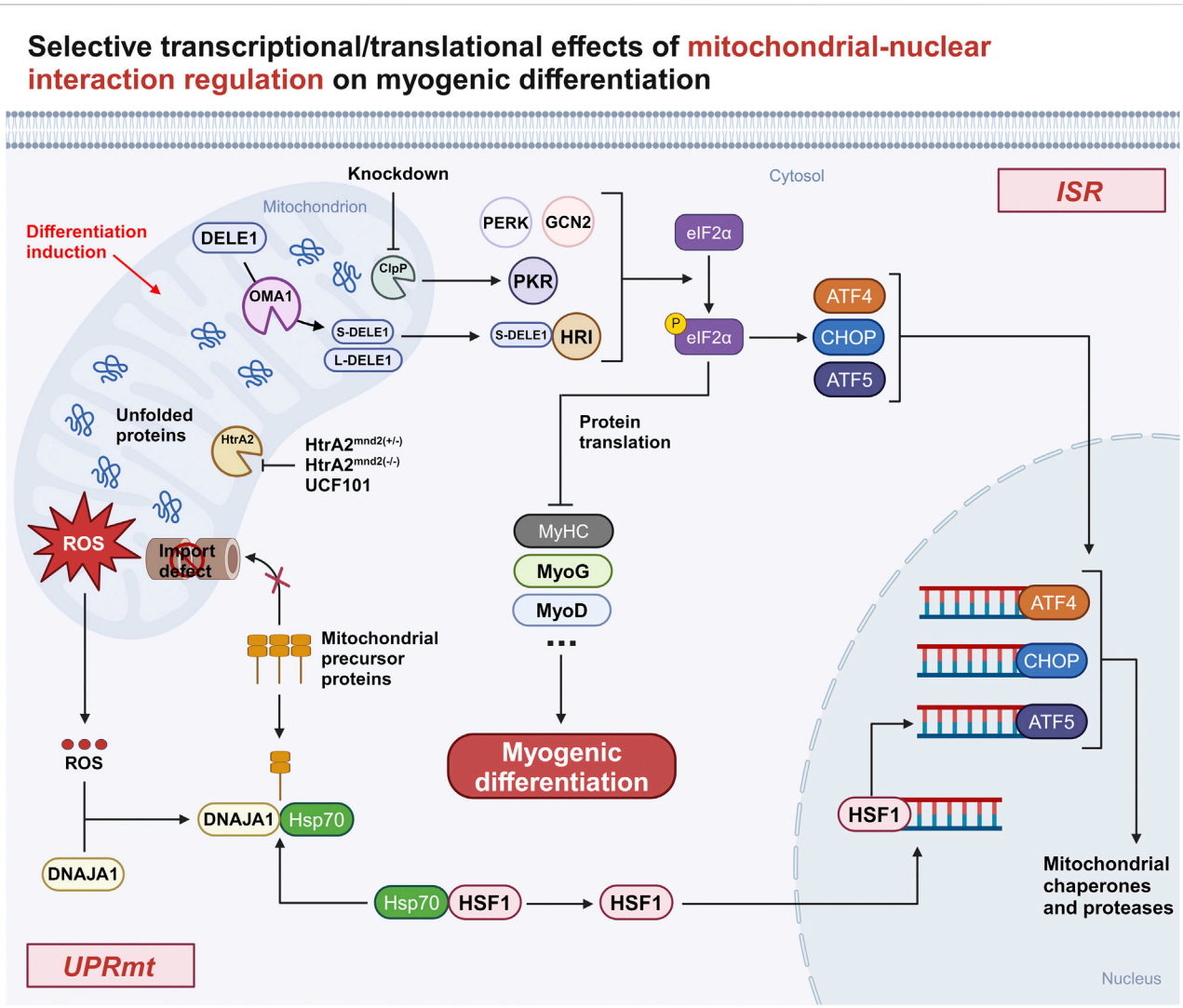

FIGURE 1
Selective transcriptional/translational effects of mitochondrial-nuclear interaction regulation on myogenic differentiation. Both knockdown ClpP and using UCF101 to inhibit HtrA2 or HtrA2 inactivation in Mnd2 mouse models show that activated mitochondrial-nuclear retrograde signaling inhibits myogenic differentiation by affecting the translation of myogenic genes. Abbreviation: ISR, integrated stress response; DELE1, DAP3 binding cell death enhancer-1; GCN2, general control non-derepressible 2; PKR, Double-stranded RNA-dependent protein kinase; PERK, PKR-like ER kinase; HRI, heme-regulated eIF2α kinase; elf2α, eukaryotic translation initiation factor 2alpha; p-elf2α, phosphorylation of elf2α; ATF4, activating transcription factor 4; CHOP, C/EBP homologous protein; ATF5, activating transcription factor 5; UPRmt, mitochondrial unfolded protein response; DNAJA1, DnaJ homolog subfamily A member 1; HSP70, heat shock 70 protein; HSF1, heat shock factor 1; HtrA2, High-Temperature Requirement Protein A2; ClpP, caseinolytic protease P; MyHC, myosin heavy chain; MyoG, myogenin; MyoD, myoblast determination protein 1.

activates the transcription factors ATF4, CHOP, and ATF5, and initiates the expression of stress-related genes.

2.1.1 ISR and myogenic differentiation

ATF4 is considered to be a key regulator of the ISR, and it is also involved in the regulation of myogenic differentiation. During myogenic differentiation, the transcription factor c-Myc is thought to promote myoblast proliferation and hinder myoblast differentiation by regulating the expression of its target genes, miRNAs and lincRNAs (Luo et al., 2019). Recently Memme JM et al. (Memme et al., 2023) found that ATF4 can affect myotube formation via c-Myc and MyoD and also control mitochondrial biogenesis via the PPAR-gamma coactivator-1alpha (PGC-1α). In addition, Sestrin2 (SESN2) is thought to be a downstream gene of ATF4 and is involved in mitochondrial stress-induced ISR (Garaeva et al., 2016). Piochi LF et al. (Piochi et al., 2021) proposed a theoretically possible role for SESN2 during myogenic differentiation: after the onset of differentiation, an increase in SESN2 expression, which induces the activation of AMP-activated protein kinase (AMPK) and the upregulation of nuclear factor erythroid 2-related factor 2 (NRF2) transcriptional levels, could enhance the efficiency of differentiation through three pathways:a) promotion of mitophagy b) generation of antioxidant responses c) increase in mitochondrial biogenesis. Meanwhile, another article (Brearley et al., 2019) noted that mRNA transcript levels of ISR-related genes, including SESN2 and ATF5, showed a similar trend with MyoG, reaching a maximum after about 48 h of induced differentiation and then starting to decline. It is suggested that

SESN2 and ATF5 may coordinate MyoG to play some roles in the differentiation of the mouse myoblast cell line C2C12, but experiments are still needed to further verify this.

CHOP is an important transcription factor regulating the ISR, and Alter J et al. (Alter and Bengal, 2011) demonstrated that CHOP can inhibit MyoD transcription to delay myoblast differentiation. Normally, CHOP expression is downregulated early in the differentiation of C2C12 cells. Upon knockdown of CHOP, the fusion index and differentiation rate of C2C12 cells were significantly increased. In contrast, overexpression of CHOP significantly delayed C2C12 cell differentiation, and the resulting result was caused by CHOP inhibition of MyoD. This suggests that downregulation of CHOP expression is required for the activation of the myogenic differentiation programme in C2C12 myoblasts.

Although no direct evidence for the involvement of ATF5 in myogenic differentiation was found, the differentiation effects of ATF5 for tissues such as bone, liver, brain and adipose were well characterised (Sears and Angelastro, 2017). This suggests that ATF5 has more potential roles in developmental and normal physiological processes, and may provide new research directions for exploring the regulatory mechanisms of myoblast proliferation and differentiation.

The effect of the OMA1-mediated DELE1-HRI axis on myogenic differentiation has not been reported in detail. Whether the OMA1-mediated DELE1-HRI axis is then a necessary pathway for the activation of the ISR-associated transcription factors ATF4, CHOP, and ATF5 involved in myogenic differentiation is worth exploring subsequently. Although, a direct effect of this signaling axis on myogenic differentiation was not seen, it was described in a study of mitochondrial myopathy. CHCHD10, a nuclear gene-encoded mitochondrial protein, is mainly situated in the mitochondrial intermembrane space (IMS) and, in conjunction with its homologue CHCHD2, has a vital function in preserving mitochondrial inner membrane integrity and electron transport chain (ETC) function (Jiang et al., 2022). Mutations in the CHCHD10 G58R gene can lead to mitochondrial myopathy. According to this study (Shammas et al., 2022), OMA1 is activated in response to misfolding of the CHCHD10 G58R protein. This activation triggers the ISR through the OMA1-DELE1-HRI signaling pathway, ultimately providing a protective effect that prolongs the survival of newborn infants with CHCHD10 G58R gene mutations. Given the correlation between mitochondrial myopathy and myogenic differentiation, this suggests that the OMA1-mediated DELE1-HRI axis may have an effect on myogenic differentiation.

2.2 UPRmt

UPRmt was discovered by Hoogenraad's laboratory as early as 1996 (Martinus et al., 1996). As an adaptive intracellular stress mechanism, it primarily responds to stress signals by promoting the transcription of genes for nuclear DNA-encoded mitochondrial chaperone proteins and proteases in order to maintain mitochondrial proteostasis. Among them, mitochondrial chaperone proteins, which enable newly synthesised proteins to fold correctly and help misfolded proteins to restore their normal conformation, mainly include heat shock protein 70 (HSP70), heat shock protein 60 (HSP60), heat shock protein 10 (HSP10), and others. Whereas proteases are capable of degrading damaged proteins, the main ones include caseinolytic protease P (ClpP), YME1 Like 1 ATPase (YME1L1) and Lon protease 1 (LonP1) (Zhu et al., 2021).

How does UPRmt transmit information about mitochondrial misfolding stress (MMS) to the nucleus to exert its effects? A recent study by Sutandy FXR et al. (Sutandy et al., 2023) gave the explanation that MMS can lead to the accumulation of mitochondrial protein precursors in the cytosol (c-mtProt), while at the same time, MMS can contribute to the release of mitochondrial reactive oxygen species (mtROS) into the cytosol and oxidation of the HSP40 family protein DnaJ homolog subfamily A member 1 (DNAJA1). Subsequently, binding of HSP70 to oxidised DNAJA1 resulted in enhanced recruitment of HSP70 to c-mtProt. This process leads to a reduction in the binding of HSP70 to the conventional chaperone heat shock factor 1 (HSF1), and the released HSF1 translocates to the nucleus to activate ATF5 transcription, thereby triggering the anti-stress mechanism (Figure 1).

2.2.1 UPRmt and myogenic differentiation

ClpP is an important protease within the mitochondrial matrix involved in the initiation of UPRmt. ClpP expression is higher in skeletal muscle compared to other tissues (Bross et al., 1995). In C2C12 cells after ClpP knockdown (KD), Drp1 was upregulated, leading to altered mitochondrial morphology, while the ETC subunit protein expression level was reduced, attenuating the activity of the ETC complex and thus affecting mitochondrial respiration, suggesting that ClpP is essential for maintaining mitochondrial function in myoblasts (Deepa et al., 2016). In addition, treatment of ClpP KD C2C12 cells using doxycycline (UPRmt inducer) showed no upregulation of the UPRmt-associated protein Hsp60 in both the dosed and undosed groups, suggesting that ClpP is one of the major pathways for mitochondrial stress-induced activation of UPRmt. Moreover, in the experimental group of ClpP KD C2C12 cells, enhanced expression levels of PKR and phosphorylation of eIf2α (p-eIf2α) were also found, whereas the expression of myogenic differentiation-associated proteins, such as MyHC and MyoG, was not upregulated, suggesting that myogenic differentiation is significantly impaired when protein translation is inhibited (Deepa et al., 2016). The aforementioned findings indicate that ClpP has an impact on myogenic differentiation via UPRmt and also plays a role in regulating myogenic differentiation through ISR. This highlights the strong correlation between UPRmt and ISR.

HtrA2 is a protease located in the mitochondrial IMS that is involved in UPRmt to maintain mitochondrial homeostasis (Riar et al., 2017). Previously published results from our team (Sun et al., 2022) showed that inhibition of HtrA2 enzyme activity using UCF101 resulted in blocked differentiation of C2C12 myoblasts. Considering that the loss of HtrA2 enzyme activity-induced proteostasis imbalance and mitochondrial IMS stress are the main triggers of UPRmt, we hypothesised that UPRmt could be associated with impaired differentiation due to HtrA2 enzyme activity inhibition. To this end, C2C12 cells in the differentiated state were treated with UCF101, and Western blotting results

TABLE 1 Heat shock proteins (HSPs) are involved in myogenic differentiation.

Protein	Subcellular localization	Expression changes during myogenic differentiation	Participating processe/ function	PMID
Hsp25	Cytoplasm	↓	Involved in myofiber assembly	31098840
Hsp40	Cytoplasm, Nucleus	↓	Control of myoblast cycle exit	31098840
Hsp60	Translocation from perinuclear to cytoplasm	↓	Inhibition of myotubes apoptosis	31098840, 28274921
Hsp70	Cytoplasm, Nucleus	↑	Driving myoblast fusion	32605905, 30275345
Hsp90	Cytoplasm	—	Supporting myoblast survival	31098840, 21739150

showed upregulation of the expression of the UPRmt-related protein CHOP, the HSP family of molecular chaperones, and the LonP1 protein. This suggests that loss of HtrA2 enzyme activity activates UPRmt to inhibit the translation of myogenic differentiation-related proteins, resulting in blocked myogenic differentiation.

The effect of the mtROS/c-mtProt-driven DNAJA1-HSF1 axis on myoblast differentiation has not been reported in detail. However, relevant signaling molecules targeting this axis have been described. A study (Kim et al., 2018) indicated that mtROS rapidly increases during differentiation and that mtROS can activate the phosphatidylinositol three kinase (PI3K)/AKT/mammalian target of rapamycin (mTOR) signaling pathway by inducing tensin homolog deleted on chromosome 10 (PTEN) oxidation. After activation, mTORC1 promotes phosphorylation at uncoordinated-51 like kinase 1 (ULK1) S317 and upregulates the expression of Atg protein, leading to autophagy and participating in the myogenic differentiation process. In addition, several studies have shown that heat shock proteins (HSPs) are involved in myogenic differentiation (Table 1). While muscle repair is significantly diminished in aged mice undergoing severe injury, aged mice overexpressing HSP70 reversed this outcome, which may be related to the promotion of myoblast fusion by HSP70 (McArdle et al., 2006; Thakur et al., 2020). HSPs are transcriptionally regulated by two members of the heat shock transcription factor family, HSF1 and heat shock factor 2 (HSF2), with HSF1 functioning primarily by responding to a variety of stressful environments, while HSF2 functions under non-stressful conditions such as differentiation and development (Santopolo et al., 2021). It has been shown (McArdle et al., 2006) that during myogenic differentiation, HSF1 levels increase significantly in the late stages, whereas HSF2 levels increase rapidly in the early stages and then return to normal levels. It is suggested that the early development and recombination of skeletal muscle cells is regulated by HSF2, and the ability of cells to respond to acute stress depends mainly on HSF1 and the UPRmt regulated by it.

In conclusion, both ISR and UPRmt are mitochondria-nuclear interactive regulatory responses, which can activate the same signaling molecules to exercise different signaling pathways (Roca-Portoles and Tait, 2021). Some literature indicates that in mammals, ISR is a prerequisite for the induction of UPRmt, as the expression of the three basic leucine zip (bZIP) transcription factors ATF4, CHOP, and ATF5 involved in UPRmt requires the activation of ISR (Rainbolt et al., 2013; Melber and Haynes, 2018; Anderson and Haynes, 2020). A typical example is arsenite-induced MSRs (Rainbolt et al., 2013), in which arsenite first activates the ISR and the transient phosphorylation of eIF2α leads to a reduction in Tim17A synthesis, which reduces the import efficiency of mitochondrial proteins and induces the expression of UPRmt-related genes. It has also been noted in the literature (Khan et al., 2017) that UPRmt is part of ISRmt. This interactive regulation at the level of front and back, whole and part, reflects the close connection between the two. Even though both are “saviours” of the cell against stress, myogenic differentiation is affected during differentiation, whether they are over-activated or inhibited (Figure 1). This is because the general translational decline caused by overactivation affects the expression of differentiation-related proteins, and overrepression weakens the ability of cells to withstand stress during differentiation. It is thus clear that the interactive effects between such signaling pathways induced by the stress response are extremely complex, and the mechanisms of their regulation on myogenic differentiation still need to be further explored.

3 The role of mitochondrial dynamics in remodeling the mitochondrial network during myogenic differentiation

3.1 Mitochondrial biogenesis

Mitochondrial biogenesis is the process of generating new mitochondria from existing mitochondria and is regulated by both the mitochondrial and nuclear genomes (Scarpulla, 2008). The peroxisome proliferator-activated receptor-gamma coactivator-1 (PGC-1) family includes three members, PGC-1α, PGC-1β and PGC related coactivator, of which PGC-1α is considered to be a master regulator of mitochondrial biogenesis, binding to and enhancing the activity of transcription factors such as NRF1/2, ERR alpha, *etc.*, causing NRF1/2 to activate the expression of TFAM, TFB1M, TFB2M and a number of mitochondrial matrix proteins to drive the replication and transcription of mtDNA and its translation into proteins and ultimately assembly into new mitochondria (Scarpulla, 2008; Fernandez-Marcos and Auwerx, 2011).

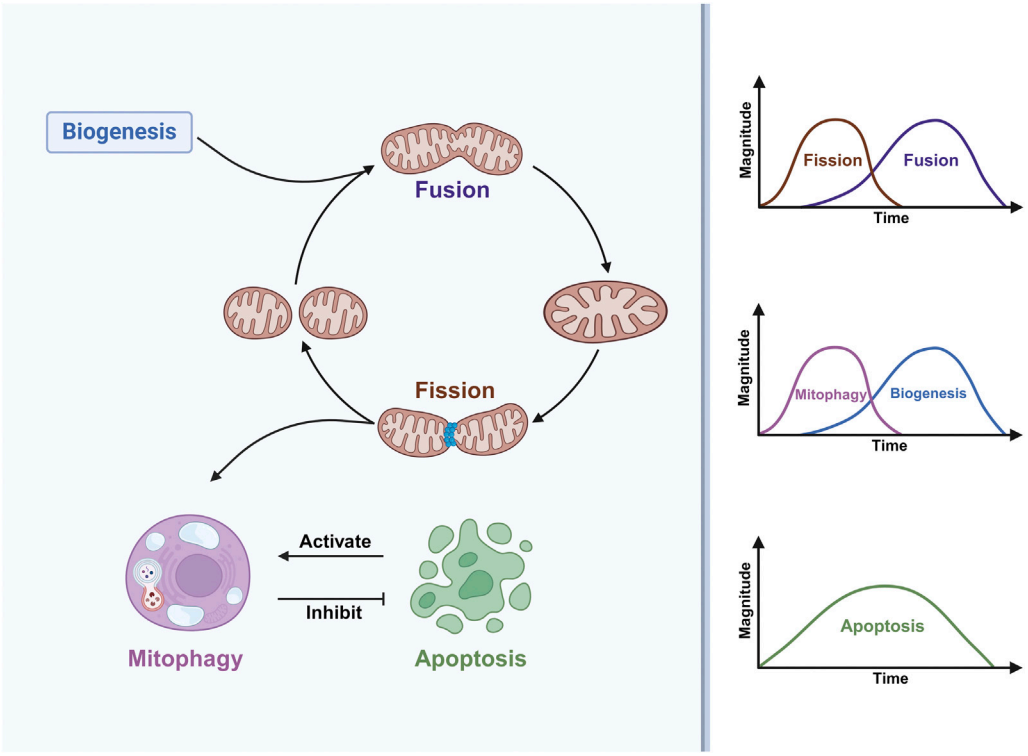

FIGURE 2
Mitochondrial dynamics are involved in myogenic differentiation. Mitochondrial fission is a prerequisite for the occurrence of mitophagy, which inhibits apoptosis, and apoptosis in turn activates mitophagy. During myogenic differentiation, mitochondrial fission and mitophagy occur early, mitochondrial fusion and mitochondrial biogenesis occur in the middle and late stages, while apoptosis persists throughout differentiation, with a high level of apoptosis in the middle of differentiation.

3.1.1 Mitochondrial biogenesis and myogenic differentiation

The process of myogenic differentiation is accompanied by increased levels of mitochondrial biogenesis, resulting in an increase in the number and activity of mitochondria, enabling myoblasts to adapt to stressful conditions and increase cell viability (Fortini et al., 2016; Piochi et al., 2021). As a transcriptional co-activator, the role of PGC-1α in myogenic differentiation has been elucidated. PGC-1α serves a dual role in both triggering mitochondrial biogenesis to increase mitochondrial mass and buffering the expression of genes involved in mitophagy mediated by ROS/FOXO1 (Baldelli et al., 2014). This not only indicates that PGC-1α is an important integrating molecule for mitochondrial biogenesis and mitophagy, but also suggests that there is a close collaboration between mitochondrial biogenesis and mitophagy during myogenic differentiation. A study (Sin et al., 2016) showed that downregulating PGC-1α in C2C12 myoblasts increases ROS generation, causes mitochondrial damage, and leads to poor differentiation. In contrast, in vivo studies in mice, upregulation of PGC-1α expression alters MRFs and exhibits a positive protective effect on skeletal muscle regeneration by promoting myogenic differentiation (Washington et al., 2022). In addition, some important transcription factors, such as NRF1/2 and TFAM, have been found to show a trend of transcriptional upregulation during differentiation (Kraft et al., 2006; Remels et al., 2010), and NRF1 has been shown to mediate PGC-1β-induced mitochondrial biogenesis and activation of cellular respiration in conjunction with ERR alpha (Shao et al., 2010). So far, a number of studies have shown that activation of mitochondrial biogenesis-related signaling pathways can promote myogenic differentiation (Li et al., 2007; Barbieri et al., 2016; Lee and Choi, 2018; Niu et al., 2021; You et al., 2023). Thus, mitochondrial biogenesis plays an important role in myogenic differentiation.

3.2 Mitochondrial fusion and fission

Dynamic changes in mitochondria provide a wide range of benefits to mitochondria, including efficient transport, increased homogeneity of the mitochondrial population, and efficient oxidative phosphorylation. These benefits are achieved through mitochondrial fusion and fission, which control mitochondrial number, morphology, equitable inheritance of mitochondria, material exchange and maintenance of a high quality mitochondrial genome, as well as degradation of isolated bioenergetically inefficient mitochondria by mitophagy (Chan, 2020). Relevant molecules that mediate mitochondrial fusion and fission include mitofusin-1 (MFN1), mitofusin-2 (MFN2), optic atrophy 1 (OPA1), Drp1 and mitochondrial fission 1 (Fis1), signaling molecules that endow mitochondria with the ability to sense and respond to a variety of environmental conditions (Humphries et al., 2020).

3.2.1 Mitochondrial fusion and fission and myogenic differentiation

There is a link between mitochondrial dynamics and myogenic differentiation (Figure 2). In the early stages of muscle differentiation, mitochondrial fission is activated while fusion is inhibited, resulting in a loose mitochondrial network; in the later stages, the opposite occurs, resulting in a tight mitochondrial network (Huang et al., 2020). This fully reflects the adaptive response of mitochondrial fusion and fission activity to environmental changes during myogenic differentiation. It was recently shown (Luo et al., 2021) that the expression of MFN2 proteins involved in mitochondrial fusion is upregulated during myogenic differentiation, and that myoblasts isolated from MFN2-null mice exhibit abnormal mitochondrial respiration with elevated ROS. However, interestingly, these alterations do not negatively affect the proliferation and differentiation of myoblasts, which may be due to a potential compensatory function of MFN1 that prevents these alterations from affecting muscle development and regeneration (Luo et al., 2021). In conjunction with some existing work a) inhibition of dihydroorotate dehydrogenase (DHODH) activity increases MFN2 expression and promotes mitochondrial fusion via the pyrimidine *de novo* synthesis pathway (Miret-Casals et al., 2018) b) knockdown of MFN2 limits the synthesis and consumption of aspartate, a raw material for the pyrimidines *de novo* synthesis (Yao et al., 2019) c) DHODH is localised in the inner mitochondrial membrane and is linked to the respiratory chain via the coenzyme Q pool and is involved in oxidative phosphorylation (Boukalova et al., 2020) d) DHODH in skeletal muscle mitochondria can produce H_2O_2 directly or indirectly (Hey-Mogensen et al., 2014). This suggests that there may be a feedback mechanism for MFN2 knockout to affect DHODH activity through the pyrimidine *de novo* synthesis pathway. If so, can it be argued that the abnormal mitochondrial respiration and elevated ROS exhibited in MFN2-null cells may be caused by DHODH affecting the mitochondrial respiratory chain? Further work is needed to verify this. This further suggests the potential involvement of DHODH in myogenic differentiation through the regulation of MFN2-mediated mitochondrial fusion. In addition to MFN2, another key molecule of mitochondrial fusion, OPA1, has also been reported to have an effect on myogenic differentiation, and cells under oxidative stress induced by the application of tert-butylhydroperoxide (t-BHP) or FCCP treatments to C2C12 cells can inhibit myogenic differentiation by cleaving OPA1 to reduce MyHC expression (Wang et al., 2014).

The effect of mitochondrial fission activity on myogenic differentiation has been described. One study (Kim et al., 2013) noted that inhibition of Drp1 activity using Mdivi-1 impairs myogenic differentiation. Interestingly, another study (De Palma et al., 2010) pointed out that nitric oxide inhibition of Drp1-mediated mitochondrial fission is an essential step in the process of early myogenic differentiation, which seems to contradict the previous findings. Further studies are needed to fully explain this discrepancy. In addition, a study on muscle regeneration after frostbite (Wagatsuma et al., 2011) found that Fis1 expression was upregulated early in muscle regeneration, along with its concomitant upregulation of the myogenic differentiation-associated proteins MyoD and MyoG. This suggests that mitochondrial fission may not only regulate myogenic differentiation by affecting mitochondrial dynamics and morphological alterations, but also that mitochondrial fission-associated proteins may be involved as signaling molecules in regulating the expression of factors associated with myogenic differentiation. These findings re-emphasise that tight regulation of the activity of mitochondrial fusion and fission proteins and, more importantly, the maintenance of a dynamic balance between mitochondrial morphology and function are essential for the initiation and progression of myogenic differentiation.

3.3 Mitophagy

The concept of mitophagy was first formalised by Lemasters JJ in 2005 (Lemasters, 2005). When stress damage is severe, mitochondria signal that they can remove damaged mitochondria by mitophagy on their own, thus preventing further damage to the mitochondrial network caused by stress. Mitophagy is a degradation process that begins with the engulfment of mitochondria into a double-membrane structure known as an autophagosome, and finally completes the degradation after fusion with lysosomes (Picca et al., 2021). In general, mitophagy can be divided into the sequestosome-like receptor (SLR)-dependent mitophagy pathways mediated by PINK1 and the E3 ubiquitin ligase PRKN, and SLR-independent mitophagy pathways mediated by autophagy receptors, specific classes of lipids, and partial E3 ubiquitin ligases (Sun et al., 2021; Ganley and Simonsen, 2022).

3.3.1 Mitophagy and myogenic differentiation

McMillan EM et al. (McMillan and Quadrilatero, 2014) demonstrated for the first time that myogenic differentiation requires the involvement of autophagy, which prevents apoptosis generated during myogenic differentiation. Afterwards, some workers directed their research specifically to mitophagy to explore the link between mitophagy and myogenic differentiation. Sin J et al. (Sin et al., 2016) proposed that the shift in energy metabolism from glycolysis to oxidative phosphorylation during the differentiation of myoblasts to myotubes requires the involvement of mitophagy. Notably, Brown HMG et al. found that mitophagy is a transient phenomenon that is specifically upregulated only in the early stages of differentiation (Figure 2), whereas the overall cellular autophagic flux persists throughout the differentiation phase (Brown et al., 2021). Mitochondrial network remodeling is an important feature of myogenesis (Rahman and Quadrilatero, 2021). One study (Li et al., 2022) claimed that tetrandrine can inhibit myogenic differentiation by blocking autophagic flux leading to impaired mitochondrial network remodeling, which shows that autophagy-mediated mitochondrial network remodeling can also have an effect on myogenic differentiation. The impact of mitophagy on the entire myogenic differentiation event is profound, specifically regulating multiple aspects of mitochondrial network remodeling, oxidative stress, ER-associated stress, mitochondria-mediated apoptotic signaling that occur during differentiation (Baechler et al., 2019; Jiang et al., 2021).

(1) Impact of SLR-dependent mitophagy pathways on myogenic differentiation

PINK1, an important participant in mitophagy (Lazarou et al., 2015), has been shown to affect myoblast differentiation, and interfering with PINK1 using siRNAs in C2C12 cells leads to a decrease in the transcriptional level of MyoG (Baldelli et al., 2014). Similarly, PRKN, another important player in mitophagy, has now been shown to be recruited into mitochondria during early differentiation of C2C12 (Esteca et al., 2020), which supports the conclusion that mitophagy is involved in early myogenic differentiation as suggested by Sin J et al. (Sin et al., 2016). Importantly, PRKN deficiency results in myoblasts remaining in a proliferative state, delayed differentiation and even a reduction in myofiber area (Peker et al., 2018; Esteca et al., 2020); in contrast, overexpression of PRKN has been shown to increase muscle mass and strength in aged mice (Leduc-Gaudet et al., 2019). This suggests that PRKN is involved in the regulation of skeletal muscle growth and development. Moreover, Huang S et al. (Huang et al., 2020) found that LonP1 regulates mitochondrial network remodeling through the PINK1/PRKN-mediated mitophagy pathway to promote myogenic differentiation. This suggests that the regulatory role of Lonp1 on myogenic differentiation is not only limited to its role in UPRmt, but its role in mitophagy is also involved. It indicates that Lonp1 may be an integrated molecule of different MSRs during myogenic differentiation.

(2) Impact of SLR-independent mitophagy pathways on myogenic differentiation

Baechler BL et al. (Baechler et al., 2019) used CRISPR-Cas9 technology to construct a Bcl-2/adenovirus E1B 19 kDa interacting protein 3 (BNIP3)$^{-/-}$ C2C12 cell model, and the experimental results showed that knockout of BNIP3 impaired myogenic differentiation, which was associated with mitophagy defects. And supplementation of Insulin-like growth factor 1 could attenuate the impaired myogenic differentiation caused by defective mitophagy (Guan et al., 2022). Meanwhile, knockout of BNIP3 also caused increased caspase-3 and caspase-9 activities and DNA fragmentation, which could lead to apoptosis of myoblasts. Another mitophagy receptor, FUN14 domain containing 1 (FUNDC1), has not been found to have a direct correlation with myogenic differentiation but has been shown to be closely related to skeletal muscle mitochondrial function, and FUNDC1 deficiency leads to defects in mitophagy mediated by microtubule-associated protein light chain 3 (LC3), causing impaired skeletal muscle mitochondrial function (Fu et al., 2018). Of interest, FUNDC1 not only mediates mitophagy in skeletal muscle cells involved in the differentiation process, but also plays a role in the differentiation process of human cardiac progenitor cells (Lampert et al., 2019).

3.4 Apoptosis

Apoptosis is a conserved physiological mechanism responsible for eliminating dysfunctional, damaged or unwanted cells in order to precisely control cell numbers. The signaling pathway that initiates endogenous apoptosis is triggered by mitochondria, and key to the regulation and execution of this event is the B-cell lymphoma/leukaemia-2 (Bcl-2) family of proteins (Rosa et al., 2022). When confronted with stress stimuli such as DNA damage, cellular hypoxia, and cellular growth factor deficiency, cells can activate BH3-only proteins, which subsequently inhibit the Bcl-2 family of anti-apoptotic proteins, activate free Bax and Bak to form oligomers at the outer mitochondrial membrane, resulting in the outer mitochondrial membrane permeabilization (MOMP), and release cytochrome c (Cytc) into the cytoplasm to bind with apoptotic protease activator factor 1 (Apaf-1) to form apoptosomes, which activate the cascade of responses mediated by the caspase family proteins to induce apoptosis. MOMP also leads to the release of second mitochondria-derived activator of caspases (SMAC) and HtrA2 proteins, both of which inhibit the anti-apoptotic effects of the X-linked inhibitor of apoptosis protein (XIAP), thereby promoting caspase-independent apoptosis (Bock and Tait, 2020; Lee et al., 2022).

3.4.1 Apoptosis and myogenic differentiation

Apoptosis-related events (e.g., cytoskeletal reorganization (Qu et al., 1997), phosphatidylserine receptor expression (Hochreiter-Hufford et al., 2013)) are necessary for myogenic differentiation. However, either excessive or absent apoptosis affects myotube formation (Fernando et al., 2002), suggesting that the level of apoptosis must be tightly regulated during myogenic differentiation.

(1) Impact of Bcl-2 family-related members on myogenic differentiation

Rahman FA et al. (Rahman and Quadrilatero, 2023) pointed out that in the early stage of myogenic differentiation, the local anti-apoptotic protein Bcl-2 levels in mitochondria rapidly increase, which may be related to the increased resistance of myoblasts to stressors produced during the initial differentiation process. The mitochondrial Bcl-2 inhibitor of transcription 1 (Bit1) was shown to be an essential mediator of muscle differentiation. Bit1-null mice exhibit a smaller muscle cross-sectional area, and primary myoblasts isolated from this model mice, with barely detectable Bcl-2, instead show higher caspase-3 activity and premature onset of myogenic differentiation (Griffiths et al., 2015). In addition to Bit1, Bcl-2 levels are regulated by mitogen-activated protein kinase (MAPK) signaling, and its effect on Bcl-2 is associated with skeletal muscle regeneration. For example, upregulation of Bcl-2 expression induced by MAP kinase phosphatase 5 (MKP-5) inhibition promotes the survival of regenerating myofibers (Min et al., 2017; Rahman and Quadrilatero, 2023). Another Bcl-2 family protein, B-Cell Lymphoma-extra-large (Bcl-xL), whose overexpression has the same effect on muscle differentiation as knockdown of caspase-9, inhibits myoblast fusion (Murray et al., 2008). In addition, the pro-apoptotic BH3-only protein BCL2 binding component 3 (BBC3/PUMA) appears transiently elevated 1 day after differentiation of C2C12 cells, with a concomitant increase in P53 (Rahman and Quadrilatero, 2023). Another study (Harford et al., 2017) noted that both MyoD and P53 bind to the BBC3 promoter when stimulated by differentiation conditions, and silencing MyoD prevents binding from occurring. These data demonstrate a complex link between the three and support an important role for Bcl-2 family-related members

regulating mitochondrial apoptotic signaling during myogenic differentiation for effective differentiation and myofiber regeneration.

(2) Impact of the caspase family on myogenic differentiation

Early work found that activation of caspase-3 was required for myoblast differentiation. Primary myoblasts isolated from caspase-3 null mice show normal proliferative capacity, however, after induction of differentiation, these cells continue to express cytokinin D1 (CCND1), resulting in an inability to exit the cell cycle and impaired differentiation (Fernando et al., 2002). Further subsequent studies demonstrated that caspase-3 activation during differentiation is caused by caspase-9 and found that knockdown of caspase-9 significantly affected caspase-3 activation and inhibited myoblast fusion (Murray et al., 2008). Cytc release is a key step in the activation of caspase-9, and indeed, myoblasts show Cytc release shortly after differentiation, accompanied by elevated caspase-9 activity (Rahman and Quadrilatero, 2023). C2C12 myoblasts after knockdown of Cytc using siRNA resulted in reduced apoptotic body formation, preventing caspase-9 and subsequent caspase-3 activation to reduce myotube formation (Dehkordi et al., 2020). Finally, caspase-2 and p21 have been found to be activated during the early stages of myogenic differentiation, which may underlie the proper cell cycle exit of myoblasts and the subsequent occurrence of differentiation (Boonstra et al., 2018).

In summary, myogenic differentiation is a highly dynamic and tightly coordinated process, with mitochondrial dynamic processes such as mitochondrial biogenesis, mitochondrial fission, fusion, mitophagy, and apoptosis running through the entire process of myogenic differentiation (Figure 2), which regulates the mass, structure, function and distribution of mitochondria. Myogenic differentiation coupled with metabolic reprogramming ultimately leads to an increase in mitochondrial mass and OXPHOS to support newly formed myotubes, which requires replacement of the original mitochondria of myoblasts (Rahman and Quadrilatero, 2021). Thus, mitochondrial fission and subsequent activation of mitophagy are critical processes in the early differentiation of myoblasts. Interestingly apoptosis activates mitophagy, which in turn inhibits apoptosis, thus maintaining the stability of myogenic differentiation (McMillan and Quadrilatero, 2014; Baechler et al., 2019; Jiang et al., 2021). After pre-existing mitochondria are removed, mitochondrial biogenesis and mitochondrial fusion drive the formation of a dense network of mitochondria to complement and sustain cellular energy metabolism (Sin et al., 2016; Rahman and Quadrilatero, 2021). All these results suggest that the individual stress responses during myogenic differentiation are not separate entities but an intricate network. In addition, it is worth noting that the mitochondrial dynamics processes associated with the above are regulated by Ca^{2+} signaling. For example, Ca^{2+} stimulates mitochondrial biogenesis (Yeh et al., 2005). Ca^{2+} can regulate mitochondrial fusion and fission homeostasis by mediating Drp1 phosphorylation or dephosphorylation (Cribbs and Strack, 2007; Cereghetti et al., 2008). Mitochondrial permeability transition pore (mPTP) opening is a crucial event in the induction of mitophagy and apoptosis, and Ca^{2+} overload is one of the key factors in inducing mPTP opening (Rimessi et al., 2013). Interestingly, the current study also found that Ca^{2+} and its associated signaling molecules are strongly associated with myogenic differentiation. Earlier studies have shown that myogenic differentiation is accompanied by transmembrane inward flow of extracellular Ca^{2+} and that lowering extracellular Ca^{2+} concentrations inhibits myoblast fusion (Adamo et al., 1976; Naro et al., 2003). Sun W et al. (Sun et al., 2017) proposed that intracellular Ca^{2+} may promote myogenic differentiation via the MLCK-MLC-myosin-actin pathway, a signaling pathway that mediates cytoskeletal dynamics. Meanwhile, some important molecules involved in the regulation of Ca^{2+} signaling, such as calcineurin, may be involved in the early process of myogenic differentiation by regulating nuclear factor of activated T cells 3(NFATc3) to promote MyHC expression (Delling et al., 2000); MyoG expression requires the activation of calmodulin-dependent protein kinase II (CaMII) (Terruzzi et al., 2017); S100 calcium binding protein B (S100B) is a chiral EF Ca^{2+}-binding protein that is downregulated in the early stages of myogenic differentiation as an inhibitor of myogenic differentiation, whereas in the late stages S100B expression is upregulated and reduces apoptosis through activation of NF-κB (Tubaro et al., 2011). It remains to be elucidated whether Ca^{2+} can be involved in the regulation of myogenic differentiation by influencing mitochondrial dynamics.

4 Conclusion and future perspectives

During myogenesis, myoblasts go through several important stages: first, rapid proliferation, followed by exit from the cell cycle, then myogenic differentiation and finally cell fusion to form multinucleated myofibers. Here, we highlight the impact of stress responses related to mitochondrial-nuclear interaction regulation signals and mitochondrial dynamics on myogenic differentiation (Table 2), and we argue that moderate stress signals are required to support myogenic differentiation. At the same time we can see that in the last decades there has been a rapid growth in the understanding of mitochondrial biogenesis, mitochondrial fusion and fission, mitophagy and apoptosis related to mitochondrial dynamics in myogenic differentiation, whereas there is still a lack of understanding of ISR, UPRmt related to the regulation of mitochondrial-nuclear interactions. For example, rapid dephosphorylation of eIF2α occurs early in differentiation and the ISR is inhibited (Zismanov et al., 2016), whereas ATF5 expression is elevated during the same period, suggesting to some extent that the UPRmt is activated (Fiorese et al., 2016), and whether this phenomenon could indicate that the activation of the UPRmt is not dependent on the ISR under certain conditions, and that this link has been pointed out in several previous studies (Münch and Harper, 2016; Forsström et al., 2019; Sutandy et al., 2023). In addition, as mentioned previously, ATF5 has a potential role in development and normal physiology, suggesting that the way in which ATF5 is activated may not be limited to stress onset.

TABLE 2 Mechanisms of regulation of myogenic differentiation by MSRs-related molecules.

Type	Molecule	Mechanism	PMID
ISR	ATF4	Influencing on myotube formation via c-Myc and MyoD	37273238
	CHOP	Regulation of MyoD gene transcription and protein expression	22242125
UPRmt	ClpP	Influencing mitochondrial morphology and respiration in myoblasts	26721594
		Activation of ISR to affect MyHC, MyoG protein translation	
	HtrA2	Activation of UPRmt to affect MyoG, Myosin protein translation	36233059
	LonP1	Regulation of mitochondrial network remodeling through the PINK1/PRKN-mediated mitophagy pathway	32936696
Mitochondrial biogenesis	PGC-1α	Triggering mitochondrial biogenesis	25375380
		Buffering the expression of genes involved in ROS/FOXO1-mediated mitophagy	
	NRF1	Collaborating with ERR alpha to mediate PGC-1β induced mitochondrial biogenesis and activation of cellular respiration	20561910
Mitochondrial fusion and fission	MFN2	Regulation of mitochondrial fusion in late myogenic differentiation	33749882
	OPA1	Influencing MyHC protein translation	25393477
	Drp1	Regulation of mitochondrial fission in early myogenic differentiation	23904108
Mitophagy	PINK1	Mediating mitophagy and affects MyoG protein transcription	25375380
	PRKN	Mediating mitophagy in skeletal muscle regeneration	33126429
	BNIP3	Influencing caspase-3 and caspase-9 activity and regulates apoptosis	30859901
Apoptosis	Bcl-2	Resistance to stress in the early stages of myogenic differentiation	35241367
	Bcl-xL	Influencing myoblast fusion	18957517
	Caspase-3	Influencing cell cycle progression	12177420
	Caspase-9	Influencing myoblast fusion	18957517
	Cytc	Influencing caspase-3 and caspase-9 activity	32366831
	Caspase-2	Regulating p21 induction at early stages of myogenic differentiation	28765049

10.3389/fcell.2024.1381417

Therefore, these outstanding issues still require our attention. Further, a common feature of MSRs and myogenic differentiation is that both require complex signaling cascades, suggesting that we also need to consider the role of organelles other than mitochondria in myogenic differentiation. Finally, it has been reported (Zismanov et al., 2016) that phosphorylation of eIF2α is a translational regulatory mechanism that regulates the quiescence and self-renewal of MuSCs, suggesting that myogenic differentiation is only one stage in the process of skeletal muscle regeneration and repair, and that the roles played by MSRs in the other stages of myogenesis need to be considered. These research gaps can be explored and analysed in depth in order to gain a comprehensive understanding of this knowledge and to provide theoretical support for the subsequent treatment of related muscle disorders.

Experimental animal studies have shown that some drugs can improve the disease phenotype by activating MSRs with significant efficacy. For example, nicotinamide riboside (NR), as a precursor of NAD+, can be involved in maintaining mitochondrial proteostasis in amyotrophic lateral sclerosis (ALS) mice by activating the UPRmt to attenuate the associated neurodegenerative pathology (Zhou et al., 2020); and rapamycin, by activating mitophagy, can restore muscular endurance and improve muscular function in mitochondrial myopathy model mice (Civiletto et al., 2018). Given that mitochondrial dysfunction is a common feature of aging and chronic muscular dystrophy-associated diseases, future research efforts could look for effective targets at the level of MSRs and open new directions for therapeutic means of treatment of related diseases.

Author contributions

FL: Conceptualization, Writing–original draft. LS: Conceptualization, Writing–original draft. YZ: Writing–review and editing. WG: Writing–review and editing. ZC: Methodology, Software, Writing–review and editing. YaL: Methodology, Software, Writing–review and editing. KT: Methodology, Software, Writing–review and editing. XH: Investigation, Resources, Writing–review and editing. RL: Investigation, Resources, Writing–review and editing. YL: Project administration, Supervision, Writing–review and editing. LuS: Project administration, Supervision, Writing–review and editing.

Funding

The author(s) declare that financial support was received for the research, authorship, and/or publication of this article. This work was supported by grants from National Natural Science Foundation of China (82102733), Jilin Provincial Research Foundation for the Development of Science and Technology Projects (20220505002ZP, 20220505029ZP, 20220303003SF), Science and Technology Research Project of Education Department of Jilin Province (JJKH20221055KJ), Jilin Provincial Research Foundation for Health Technology Innovation (2022JC080, 2023JC019).

Conflict of interest

The authors declare that the research was conducted in the absence of any commercial or financial relationships that could be construed as a potential conflict of interest.

Publisher's note

References

Adamo, S., Zani, B., Siracusa, G., and Molinaro, M. (1976). Expression of differentiative traits in the absence of cell fusion during myogenesis in culture. *Cell Differ.* 5, 53–67. doi:10.1016/0045-6039(76)90015-4

Alter, J., and Bengal, E. (2011). Stress-induced C/EBP homology protein (CHOP) represses MyoD transcription to delay myoblast differentiation. *PLoS One* 6, e29498. doi:10.1371/journal.pone.0029498

Anderson, N. S., and Haynes, C. M. (2020). Folding the mitochondrial UPR into the integrated stress response. *Trends Cell Biol.* 30, 428–439. doi:10.1016/j.tcb.2020.03.001

Baechler, B. L., Bloemberg, D., and Quadrilatero, J. (2019). Mitophagy regulates mitochondrial network signaling, oxidative stress, and apoptosis during myoblast differentiation. *Autophagy* 15, 1606–1619. doi:10.1080/15548627.2019.1591672

Baldelli, S., Aquilano, K., and Ciriolo, M. R. (2014). PGC-1α buffers ROS-mediated removal of mitochondria during myogenesis. *Cell Death Dis.* 5, e1515. doi:10.1038/cddis.2014.458

Barbieri, E., Battistelli, M., Casadei, L., Vallorani, L., Piccoli, G., Guescini, M., et al. (2011). Morphofunctional and biochemical approaches for studying mitochondrial changes during myoblasts differentiation. *J. Aging Res.* 2011, 845379. doi:10.4061/2011/845379

Barbieri, E., Guescini, M., Calcabrini, C., Vallorani, L., Diaz, A. R., Fimognari, C., et al. (2016). Creatine prevents the structural and functional damage to mitochondria in myogenic, oxidatively stressed C2C12 cells and restores their differentiation capacity. *Oxid. Med. Cell Longev.* 2016, 5152029. doi:10.1155/2016/5152029

Bock, F. J., and Tait, S. W. G. (2020). Mitochondria as multifaceted regulators of cell death. *Nat. Rev. Mol. Cell Biol.* 21, 85–100. doi:10.1038/s41580-019-0173-8

Boonstra, K., Bloemberg, D., and Quadrilatero, J. (2018). Caspase-2 is required for skeletal muscle differentiation and myogenesis. *Biochim. Biophys. Acta Mol. Cell Res.* 1865, 95–104. doi:10.1016/j.bbamcr.2017.07.016

Boukalova, S., Hubackova, S., Milosevic, M., Ezrova, Z., Neuzil, J., and Rohlena, J. (2020). Dihydroorotate dehydrogenase in oxidative phosphorylation and cancer. *Biochim. Biophys. Acta Mol. Basis Dis.* 1866, 165759. doi:10.1016/j.bbadis.2020.165759

Brearley, M. C., Li, C., Daniel, Z., Loughna, P. T., Parr, T., and Brameld, J. M. (2019). Changes in expression of serine biosynthesis and integrated stress response genes during myogenic differentiation of C2C12 cells. *Biochem. Biophys. Rep.* 20, 100694. doi:10.1016/j.bbrep.2019.100694

Bross, P., Andresen, B. S., Knudsen, I., Kruse, T. A., and Gregersen, N. (1995). Human ClpP protease: cDNA sequence, tissue-specific expression and chromosomal assignment of the gene. *FEBS Lett.* 377, 249–252. doi:10.1016/0014-5793(95)01353-9

Brown, H. M. G., Kuhns, M. M., Maxwell, Z., and Arriaga, E. A. (2021). Nonspecific binding correction for single-cell mass cytometric analysis of autophagy and myoblast differentiation. *Anal. Chem.* 93, 1401–1408. doi:10.1021/acs.analchem.0c03211

Brunk, C. F., and Yaffe, D. (1976). The reversible inhibition of myoblast fusion by ethidium bromide (EB). *Exp. Cell Res.* 99, 310–318. doi:10.1016/0014-4827(76)90588-7

Cereghetti, G. M., Stangherlin, A., Martins De Brito, O., Chang, C. R., Blackstone, C., Bernardi, P., et al. (2008). Dephosphorylation by calcineurin regulates translocation of

Drp1 to mitochondria. *Proc. Natl. Acad. Sci. U. S. A.* 105, 15803–15808. doi:10.1073/pnas.0808249105

Chabi, B., Hennani, H., Cortade, F., and Wrutniak-Cabello, C. (2021). Characterization of mitochondrial respiratory complexes involved in the regulation of myoblast differentiation. *Cell Biol. Int.* 45, 1676–1684. doi:10.1002/cbin.11602

Chan, D. C. (2020). Mitochondrial dynamics and its involvement in disease. *Annu. Rev. Pathol.* 15, 235–259. doi:10.1146/annurev-pathmechdis-012419-032711

Civiletto, G., Dogan, S. A., Cerutti, R., Fagiolari, G., Moggio, M., Lamperti, C., et al. (2018). Rapamycin rescues mitochondrial myopathy via coordinated activation of autophagy and lysosomal biogenesis. *EMBO Mol. Med.* 10, e8799. doi:10.15252/emmm.201708799

Cribbs, J. T., and Strack, S. (2007). Reversible phosphorylation of Drp1 by cyclic AMP-dependent protein kinase and calcineurin regulates mitochondrial fission and cell death. *EMBO Rep.* 8, 939–944. doi:10.1038/sj.embor.7401062

Deepa, S. S., Bhaskaran, S., Ranjit, R., Qaisar, R., Nair, B. C., Liu, Y., et al. (2016). Down-regulation of the mitochondrial matrix peptidase ClpP in muscle cells causes mitochondrial dysfunction and decreases cell proliferation. *Free Radic. Biol. Med.* 91, 281–292. doi:10.1016/j.freeradbiomed.2015.12.021

Dehkordi, M. H., Tashakor, A., O'connell, E., and Fearnhead, H. O. (2020). Apoptosome-dependent myotube formation involves activation of caspase-3 in differentiating myoblasts. *Cell Death Dis.* 11, 308. doi:10.1038/s41419-020-2502-4

Delling, U., Tureckova, J., Lim, H. W., De Windt, L. J., Rotwein, P., and Molkentin, J. D. (2000). A calcineurin-NFATc3-dependent pathway regulates skeletal muscle differentiation and slow myosin heavy-chain expression. *Mol. Cell Biol.* 20, 6600–6611. doi:10.1128/mcb.20.17.6600-6611.2000

De Palma, C., Falcone, S., Pisoni, S., Cipolat, S., Panzeri, C., Pambianco, S., et al. (2010). Nitric oxide inhibition of Drp1-mediated mitochondrial fission is critical for myogenic differentiation. *Cell Death Differ.* 17, 1684–1696. doi:10.1038/cdd.2010.48

Donnelly, N., Gorman, A. M., Gupta, S., and Samali, A. (2013). The eIF2α kinases: their structures and functions. *Cell Mol. Life Sci.* 70, 3493–3511. doi:10.1007/s00018-012-1252-6

Dumont, N. A., Bentzinger, C. F., Sincennes, M. C., and Rudnicki, M. A. (2015). Satellite cells and skeletal muscle regeneration. *Compr. Physiol.* 5, 1027–1059. doi:10.1002/cphy.c140068

Eckl, E. M., Ziegemann, O., Krumwiede, L., Fessler, E., and Jae, L. T. (2021). Sensing, signaling and surviving mitochondrial stress. *Cell Mol. Life Sci.* 78, 5925–5951. doi:10.1007/s00018-021-03887-7

English, A. M., Green, K. M., and Moon, S. L. (2022). A (dis)integrated stress response: genetic diseases of eIF2α regulators. *Wiley Interdiscip. Rev. RNA* 13, e1689. doi:10.1002/wrna.1689

Esteca, M. V., Severino, M. B., Silvestre, J. G., Palmeira Dos Santos, G., Tamborlin, L., Luchessi, A. D., et al. (2020). Loss of parkin results in altered muscle stem cell differentiation during regeneration. *Int. J. Mol. Sci.* 21, 8007. doi:10.3390/ijms21218007

Fernandez-Marcos, P. J., and Auwerx, J. (2011). Regulation of PGC-1α, a nodal regulator of mitochondrial biogenesis. *Am. J. Clin. Nutr.* 93, 884S–890S. doi:10.3945/ajcn.110.001917

Fernando, P., Kelly, J. F., Balazsi, K., Slack, R. S., and Megeney, L. A. (2002). Caspase 3 activity is required for skeletal muscle differentiation. *Proc. Natl. Acad. Sci. U. S. A.* 99, 11025–11030. doi:10.1073/pnas.162172899

Fiorese, C. J., Schulz, A. M., Lin, Y. F., Rosin, N., Pellegrino, M. W., and Haynes, C. M. (2016). The transcription factor ATF5 mediates a mammalian mitochondrial UPR. *Curr. Biol.* 26, 2037–2043. doi:10.1016/j.cub.2016.06.002

Forsström, S., Jackson, C. B., Carroll, C. J., Kuronen, M., Pirinen, E., Pradhan, S., et al. (2019). Fibroblast growth factor 21 drives dynamics of local and systemic stress responses in mitochondrial myopathy with mtDNA deletions. *Cell Metab.* 30, 1040–1054. doi:10.1016/j.cmet.2019.08.019

Fortini, P., Ferretti, C., Iorio, E., Cagnin, M., Garribba, L., Pietraforte, D., et al. (2016). The fine tuning of metabolism, autophagy and differentiation during *in vitro* myogenesis. *Cell Death Dis.* 7, e2168. doi:10.1038/cddis.2016.50

Fu, T., Xu, Z., Liu, L., Guo, Q., Wu, H., Liang, X., et al. (2018). Mitophagy directs muscle-adipose crosstalk to alleviate dietary obesity. *Cell Rep.* 23, 1357–1372. doi:10.1016/j.celrep.2018.03.127

Ganley, I. G., and Simonsen, A. (2022). Diversity of mitophagy pathways at a glance. *J. Cell Sci.* 135, jcs259748. doi:10.1242/jcs.259748

Garaeva, A. A., Kovaleva, I. E., Chumakov, P. M., and Evstafieva, A. G. (2016). Mitochondrial dysfunction induces SESN2 gene expression through Activating Transcription Factor 4. *Cell Cycle* 15, 64–71. doi:10.1080/15384101.2015.1120929

Griffiths, G. S., Doe, J., Jijiwa, M., Van Ry, P., Cruz, V., De La Vega, M., et al. (2015). Bit-1 is an essential regulator of myogenic differentiation. *J. Cell Sci.* 128, 1707–1717. doi:10.1242/jcs.158964

Guan, X., Yan, Q., Wang, D., Du, G., and Zhou, J. (2022). IGF-1 signaling regulates mitochondrial remodeling during myogenic differentiation. *Nutrients* 14, 1249. doi:10.3390/nu14061249

Gugliuzza, M. V., and Crist, C. (2022). Muscle stem cell adaptations to cellular and environmental stress. *Skelet. Muscle* 12, 5. doi:10.1186/s13395-022-00289-6

Guo, X., Aviles, G., Liu, Y., Tian, R., Unger, B. A., Lin, Y. T., et al. (2020). Mitochondrial stress is relayed to the cytosol by an OMA1-DELE1-HRI pathway. *Nature* 579, 427–432. doi:10.1038/s41586-020-2078-2

Harford, T. J., Kliment, G., Shukla, G. C., and Weyman, C. M. (2017). The muscle regulatory transcription factor MyoD participates with p53 to directly increase the expression of the pro-apoptotic Bcl2 family member PUMA. *Apoptosis* 22, 1532–1542. doi:10.1007/s10495-017-1423-x

He, S., Fu, T., Yu, Y., Liang, Q., Li, L., Liu, J., et al. (2021). LRG1 is an adipokine that mediates obesity-induced hepatosteatosis and insulin resistance. *J. Clin. Invest.* 131, e148545. doi:10.1172/JCI148545

Hey-Mogensen, M., Goncalves, R. L., Orr, A. L., and Brand, M. D. (2014). Production of superoxide/H2O2 by dihydroorotate dehydrogenase in rat skeletal muscle mitochondria. *Free Radic. Biol. Med.* 72, 149–155. doi:10.1016/j.freeradbiomed.2014.04.007

Hochreiter-Hufford, A. E., Lee, C. S., Kinchen, J. M., Sokolowski, J. D., Arandjelovic, S., Call, J. A., et al. (2013). Phosphatidylserine receptor Bai1 and apoptotic cells as new promoters of myoblast fusion. *Nature* 497, 263–267. doi:10.1038/nature12135

Huang, S., Wang, X., Yu, J., Tian, Y., Yang, C., Chen, Y., et al. (2020). LonP1 regulates mitochondrial network remodeling through the PINK1/Parkin pathway during myoblast differentiation. *Am. J. Physiol. Cell Physiol.* 319, C1020–c1028. doi:10.1152/ajpcell.00589.2019

Humphries, B. A., Cutter, A. C., Buschhaus, J. M., Chen, Y. C., Qyli, T., Palagama, D. S. W., et al. (2020). Enhanced mitochondrial fission suppresses signaling and metastasis in triple-negative breast cancer. *Breast Cancer Res.* 22, 60. doi:10.1186/s13058-020-01301-x

Jahnke, V. E., Sabido, O., and Freyssenet, D. (2009). Control of mitochondrial biogenesis, ROS level, and cytosolic Ca2+ concentration during the cell cycle and the onset of differentiation in L6E9 myoblasts. *Am. J. Physiol. Cell Physiol.* 296, C1185–C1194. doi:10.1152/ajpcell.00377.2008

Jiang, A., Guo, H., Wu, W., and Liu, H. (2021). The crosstalk between autophagy and apoptosis is necessary for myogenic differentiation. *J. Agric. Food Chem.* 69, 3942–3951. doi:10.1021/acs.jafc.1c00140

Jiang, T., Wang, Y., Wang, X., and Xu, J. (2022). CHCHD2 and CHCHD10: future therapeutic targets in cognitive disorder and motor neuron disorder. *Front. Neurosci.* 16, 988265. doi:10.3389/fnins.2022.988265

Khan, N. A., Nikkanen, J., Yatsuga, S., Jackson, C., Wang, L., Pradhan, S., et al. (2017). mTORC1 regulates mitochondrial integrated stress response and mitochondrial myopathy progression. *Cell Metab.* 26, 419–428. doi:10.1016/j.cmet.2017.07.007

Kim, B., Kim, J. S., Yoon, Y., Santiago, M. C., Brown, M. D., and Park, J. Y. (2013). Inhibition of Drp1-dependent mitochondrial division impairs myogenic differentiation. *Am. J. Physiol. Regul. Integr. Comp. Physiol.* 305, R927–R938. doi:10.1152/ajpregu.00502.2012

Kim, J. H., Choi, T. G., Park, S., Yun, H. R., Nguyen, N. N. Y., Jo, Y. H., et al. (2018). Mitochondrial ROS-derived PTEN oxidation activates PI3K pathway for mTOR-induced myogenic autophagy. *Cell Death Differ.* 25, 1921–1937. doi:10.1038/s41418-018-0165-9

Kraft, C. S., Lemoine, C. M., Lyons, C. N., Michaud, D., Mueller, C. R., and Moyes, C. D. (2006). Control of mitochondrial biogenesis during myogenesis. *Am. J. Physiol. Cell Physiol.* 290, C1119–C1127. doi:10.1152/ajpcell.00463.2005

Lampert, M. A., Orogo, A. M., Najor, R. H., Hammerling, B. C., Leon, L. J., Wang, B. J., et al. (2019). BNIP3L/NIX and FUNDC1-mediated mitophagy is required for mitochondrial network remodeling during cardiac progenitor cell differentiation. *Autophagy* 15, 1182–1198. doi:10.1080/15548627.2019.1580095

Lazarou, M., Sliter, D. A., Kane, L. A., Sarraf, S. A., Wang, C., Burman, J. L., et al. (2015). The ubiquitin kinase PINK1 recruits autophagy receptors to induce mitophagy. *Nature* 524, 309–314. doi:10.1038/nature14893

Leduc-Gaudet, J. P., Reynaud, O., Hussain, S. N., and Gouspillou, G. (2019). Parkin overexpression protects from ageing-related loss of muscle mass and strength. *J. Physiol.* 597, 1975–1991. doi:10.1113/JP277157

Lee, H., and Choi, S. J. (2018). Mild hyperthermia-induced myogenic differentiation in skeletal muscle cells: implications for local hyperthermic therapy for skeletal muscle injury. *Oxid. Med. Cell Longev.* 2018, 2393570. doi:10.1155/2018/2393570

Lee, Y. G., Park, D. H., and Chae, Y. C. (2022). Role of mitochondrial stress response in cancer progression. *Cells* 11, 771. doi:10.3390/cells11050771

Lemasters, J. J. (2005). Selective mitochondrial autophagy, or mitophagy, as a targeted defense against oxidative stress, mitochondrial dysfunction, and aging. *Rejuvenation Res.* 8, 3–5. doi:10.1089/rej.2005.8.3

Li, J., Shi, M., Liu, L., Wang, J., Zhu, M., and Chen, H. (2022). Tetrandrine inhibits skeletal muscle differentiation by blocking autophagic flux. *Int. J. Mol. Sci.* 23, 8148. doi:10.3390/ijms23158148

Li, X., Zhang, S., Zhang, Y., Liu, P., Li, M., Lu, Y., et al. (2021). Myoblast differentiation of C2C12 cell may related with oxidative stress. *Intractable Rare Dis. Res.* 10, 173–178. doi:10.5582/irdr.2021.01058

Li, Y., Li, J., Zhu, J., Sun, B., Branca, M., Tang, Y., et al. (2007). Decorin gene transfer promotes muscle cell differentiation and muscle regeneration. *Mol. Ther.* 15, 1616–1622. doi:10.1038/sj.mt.6300250

Licari, E., Sánchez-Del-Campo, L., and Falletta, P. (2021). The two faces of the Integrated Stress Response in cancer progression and therapeutic strategies. *Int. J. Biochem. Cell Biol.* 139, 106059. doi:10.1016/j.biocel.2021.106059

Luo, N., Yue, F., Jia, Z., Chen, J., Deng, Q., Zhao, Y., et al. (2021). Reduced electron transport chain complex I protein abundance and function in Mfn2-deficient myogenic progenitors lead to oxidative stress and mitochondria swelling. *Faseb J.* 35, e21426. doi:10.1096/fj.202002464R

Luo, W., Chen, J., Li, L., Ren, X., Cheng, T., Lu, S., et al. (2019). c-Myc inhibits myoblast differentiation and promotes myoblast proliferation and muscle fibre hypertrophy by regulating the expression of its target genes, miRNAs and lincRNAs. *Cell Death Differ.* 26, 426–442. doi:10.1038/s41418-018-0129-0

Martinus, R. D., Garth, G. P., Webster, T. L., Cartwright, P., Naylor, D. J., Høj, P. B., et al. (1996). Selective induction of mitochondrial chaperones in response to loss of the mitochondrial genome. *Eur. J. Biochem.* 240, 98–103. doi:10.1111/j.1432-1033.1996.0098h.x

Mcardle, A., Broome, C. S., Kayani, A. C., Tully, M. D., Close, G. L., Vasilaki, A., et al. (2006). HSF expression in skeletal muscle during myogenesis: implications for failed regeneration in old mice. *Exp. Gerontol.* 41, 497–500. doi:10.1016/j.exger.2006.02.002

Mcmillan, E. M., and Quadrilatero, J. (2014). Autophagy is required and protects against apoptosis during myoblast differentiation. *Biochem. J.* 462, 267–277. doi:10.1042/BJ20140312

Melber, A., and Haynes, C. M. (2018). UPR(mt) regulation and output: a stress response mediated by mitochondrial-nuclear communication. *Cell Res.* 28, 281–295. doi:10.1038/cr.2018.16

Memme, J. M., Sanfrancesco, V. C., and Hood, D. A. (2023). Activating transcription factor 4 regulates mitochondrial content, morphology, and function in differentiating skeletal muscle myotubes. *Am. J. Physiol. Cell Physiol.* 325, C224–c242. doi:10.1152/ajpcell.00080.2023

Meyer, P., Notarnicola, C., Meli, A. C., Matecki, S., Hugon, G., Salvador, J., et al. (2021). Skeletal ryanodine receptors are involved in impaired myogenic differentiation in Duchenne muscular dystrophy patients. *Int. J. Mol. Sci.* 22, 12985. doi:10.3390/ijms222312985

Min, K., Lawan, A., and Bennett, A. M. (2017). Loss of MKP-5 promotes myofiber survival by activating STAT3/Bcl-2 signaling during regenerative myogenesis. *Skelet. Muscle* 7, 21. doi:10.1186/s13395-017-0137-7

Miret-Casals, L., Sebastián, D., Brea, J., Rico-Leo, E. M., Palacín, M., Fernández-Salguero, P. M., et al. (2018). Identification of new activators of mitochondrial fusion reveals a link between mitochondrial morphology and pyrimidine metabolism. *Cell Chem. Biol.* 25, 268–278. doi:10.1016/j.chembiol.2017.12.001

Morgan, J. E., and Partridge, T. A. (2003). Muscle satellite cells. *Int. J. Biochem. Cell Biol.* 35, 1151–1156. doi:10.1016/s1357-2725(03)00042-6

Münch, C., and Harper, J. W. (2016). Mitochondrial unfolded protein response controls matrix pre-RNA processing and translation. *Nature* 534, 710–713. doi:10.1038/nature18302

Murray, T. V., Mcmahon, J. M., Howley, B. A., Stanley, A., Ritter, T., Mohr, A., et al. (2008). A non-apoptotic role for caspase-9 in muscle differentiation. *J. Cell Sci.* 121, 3786–3793. doi:10.1242/jcs.024547

Naro, F., De Arcangelis, V., Coletti, D., Molinaro, M., Zani, B., Vassanelli, S., et al. (2003). Increase in cytosolic Ca2+ induced by elevation of extracellular Ca2+ in skeletal myogenic cells. *Am. J. Physiol. Cell Physiol.* 284, C969–C976. doi:10.1152/ajpcell.00237.2002

Niu, W., Wang, H., Wang, B., Mao, X., and Du, M. (2021). Resveratrol improves muscle regeneration in obese mice through enhancing mitochondrial biogenesis. *J. Nutr. Biochem.* 98, 108804. doi:10.1016/j.jnutbio.2021.108804

O'malley, J., Kumar, R., Inigo, J., Yadava, N., and Chandra, D. (2020). Mitochondrial stress response and cancer. *Trends Cancer* 6, 688–701. doi:10.1016/j.trecan.2020.04.009

Peker, N., Donipadi, V., Sharma, M., Mcfarlane, C., and Kambadur, R. (2018). Loss of Parkin impairs mitochondrial function and leads to muscle atrophy. *Am. J. Physiol. Cell Physiol.* 315, C164–c185. doi:10.1152/ajpcell.00064.2017

Picard, M., and Shirihai, O. S. (2022). Mitochondrial signal transduction. *Cell Metab.* 34, 1620–1653. doi:10.1016/j.cmet.2022.10.008

Picca, A., Calvani, R., Coelho-Junior, H. J., and Marzetti, E. (2021). Cell death and inflammation: the role of mitochondria in health and disease. *Cells* 10, 537. doi:10.3390/cells10030537

Piochi, L. F., Machado, I. F., Palmeira, C. M., and Rolo, A. P. (2021). Sestrin2 and mitochondrial quality control: potential impact in myogenic differentiation. *Ageing Res. Rev.* 67, 101309. doi:10.1016/j.arr.2021.101309

Qu, G., Yan, H., and Strauch, A. R. (1997). Actin isoform utilization during differentiation and remodeling of BC3H1 myogenic cells. *J. Cell Biochem.* 67, 514–527. doi:10.1002/(sici)1097-4644(19971215)67:4<514::aid-jcb9>3.3.co;2-i

Rahman, F. A., and Quadrilatero, J. (2021). Mitochondrial network remodeling: an important feature of myogenesis and skeletal muscle regeneration. *Cell Mol. Life Sci.* 78, 4653–4675. doi:10.1007/s00018-021-03807-9

Rahman, F. A., and Quadrilatero, J. (2023). Mitochondrial apoptotic signaling involvement in remodeling during myogenesis and skeletal muscle atrophy. *Semin. Cell Dev. Biol.* 143, 66–74. doi:10.1016/j.semcdb.2022.01.011

Rainbolt, T. K., Atanassova, N., Genereux, J. C., and Wiseman, R. L. (2013). Stress-regulated translational attenuation adapts mitochondrial protein import through Tim17A degradation. *Cell Metab.* 18, 908–919. doi:10.1016/j.cmet.2013.11.006

Relaix, F., and Zammit, P. S. (2012). Satellite cells are essential for skeletal muscle regeneration: the cell on the edge returns centre stage. *Development* 139, 2845–2856. doi:10.1242/dev.069088

Remels, A. H., Langen, R. C., Schrauwen, P., Schaart, G., Schols, A. M., and Gosker, H. R. (2010). Regulation of mitochondrial biogenesis during myogenesis. *Mol. Cell Endocrinol.* 315, 113–120. doi:10.1016/j.mce.2009.09.029

Riar, A. K., Burstein, S. R., Palomo, G. M., Arreguin, A., Manfredi, G., and Germain, D. (2017). Sex specific activation of the ERα axis of the mitochondrial UPR (UPRmt) in the G93A-SOD1 mouse model of familial ALS. *Hum. Mol. Genet.* 26, 1318–1327. doi:10.1093/hmg/ddx049

Rimessi, A., Bonora, M., Marchi, S., Patergnani, S., Marobbio, C. M., Lasorsa, F. M., et al. (2013). Perturbed mitochondrial Ca2+ signals as causes or consequences of mitophagy induction. *Autophagy* 9, 1677–1686. doi:10.4161/auto.24795

Roca-Portoles, A., and Tait, S. W. G. (2021). Mitochondrial quality control: from molecule to organelle. *Cell Mol. Life Sci.* 78, 3853–3866. doi:10.1007/s00018-021-03775-0

Rosa, N., Speelman-Rooms, F., Parys, J. B., and Bultynck, G. (2022). Modulation of Ca(2+) signaling by antiapoptotic Bcl-2 versus Bcl-xL: from molecular mechanisms to relevance for cancer cell survival. *Biochim. Biophys. Acta Rev. Cancer* 1877, 188791. doi:10.1016/j.bbcan.2022.188791

Santopolo, S., Riccio, A., Rossi, A., and Santoro, M. G. (2021). The proteostasis guardian HSF1 directs the transcription of its paralog and interactor HSF2 during proteasome dysfunction. *Cell Mol. Life Sci.* 78, 1113–1129. doi:10.1007/s00018-020-03568-x

Scarpulla, R. C. (2008). Transcriptional paradigms in mammalian mitochondrial biogenesis and function. *Physiol. Rev.* 88, 611–638. doi:10.1152/physrev.00025.2007

Sears, T. K., and Angelastro, J. M. (2017). The transcription factor ATF5: role in cellular differentiation, stress responses, and cancer. *Oncotarget* 8, 84595–84609. doi:10.18632/oncotarget.21102

Seyer, P., Grandemange, S., Rochard, P., Busson, M., Pessemesse, L., Casas, F., et al. (2011). P43-dependent mitochondrial activity regulates myoblast differentiation and slow myosin isoform expression by control of Calcineurin expression. *Exp. Cell Res.* 317, 2059–2071. doi:10.1016/j.yexcr.2011.05.020

Shammas, M. K., Huang, X., Wu, B. P., Fessler, E., Song, I. Y., Randolph, N. P., et al. (2022). OMA1 mediates local and global stress responses against protein misfolding in CHCHD10 mitochondrial myopathy. *J. Clin. Invest.* 132, e157504. doi:10.1172/JCI157504

Shao, D., Liu, Y., Liu, X., Zhu, L., Cui, Y., Cui, A., et al. (2010). PGC-1 beta-regulated mitochondrial biogenesis and function in myotubes is mediated by NRF-1 and ERR alpha. *Mitochondrion* 10, 516–527. doi:10.1016/j.mito.2010.05.012

Sin, J., Andres, A. M., Taylor, D. J., Weston, T., Hiraumi, Y., Stotland, A., et al. (2016). Mitophagy is required for mitochondrial biogenesis and myogenic differentiation of C2C12 myoblasts. *Autophagy* 12, 369–380. doi:10.1080/15548627.2015.1115172

Sun, H., Shen, L., Zhang, P., Lin, F., Ma, J., Wu, Y., et al. (2022). Inhibition of high-temperature requirement protein A2 protease activity represses myogenic differentiation via UPRmt. *Int. J. Mol. Sci.* 23, 11761. doi:10.3390/ijms231911761

Sun, K., Jing, X., Guo, J., Yao, X., and Guo, F. (2021). Mitophagy in degenerative joint diseases. *Autophagy* 17, 2082–2092. doi:10.1080/15548627.2020.1822097

Sun, W., He, T., Qin, C., Qiu, K., Zhang, X., Luo, Y., et al. (2017). A potential regulatory network underlying distinct fate commitment of myogenic and adipogenic cells in skeletal muscle. *Sci. Rep.* 7, 44133. doi:10.1038/srep44133

Sutandy, F. X. R., Gößner, I., Tascher, G., and Münch, C. (2023). A cytosolic surveillance mechanism activates the mitochondrial UPR. *Nature* 618, 849–854. doi:10.1038/s41586-023-06142-0

Terruzzi, I., Montesano, A., Senesi, P., Vacante, F., Benedini, S., and Luzi, L. (2017). Ranolazine promotes muscle differentiation and reduces oxidative stress in C2C12 skeletal muscle cells. *Endocrine* 58, 33–45. doi:10.1007/s12020-016-1181-5

Thakur, S. S., Swiderski, K., Chhen, V. L., James, J. L., Cranna, N. J., Islam, A. M. T., et al. (2020). HSP70 drives myoblast fusion during C2C12 myogenic differentiation. *Biol. Open* 9, bio053918. doi:10.1242/bio.053918

Tubaro, C., Arcuri, C., Giambanco, I., and Donato, R. (2011). S100B in myoblasts regulates the transition from activation to quiescence and from quiescence to activation and reduces apoptosis. *Biochim. Biophys. Acta* 1813, 1092–1104. doi:10.1016/j.bbamcr.2010.11.015

Vertel, B. M., and Fischman, D. A. (1977). Mitochondrial development during myogenesis. *Dev. Biol.* 58, 356–371. doi:10.1016/0012-1606(77)90097-5

Wagatsuma, A., Kotake, N., and Yamada, S. (2011). Muscle regeneration occurs to coincide with mitochondrial biogenesis. *Mol. Cell Biochem.* 349, 139–147. doi:10.1007/s11010-010-0668-2

Wagatsuma, A., and Sakuma, K. (2013). Mitochondria as a potential regulator of myogenesis. *ScientificWorldJournal* 2013, 593267. doi:10.1155/2013/593267

Walsh, K., and Perlman, H. (1997). Cell cycle exit upon myogenic differentiation. *Curr. Opin. Genet. Dev.* 7, 597–602. doi:10.1016/s0959-437x(97)80005-6

Wang, X., Li, H., Zheng, A., Yang, L., Liu, J., Chen, C., et al. (2014). Mitochondrial dysfunction-associated OPA1 cleavage contributes to muscle degeneration: preventative effect of hydroxytyrosol acetate. *Cell Death Dis.* 5, e1521. doi:10.1038/cddis.2014.473

Washington, T. A., Haynie, W. S., Schrems, E. R., Perry, R. A., Jr., Brown, L. A., Williams, B. M., et al. (2022). Effects of PGC-1α overexpression on the myogenic response during skeletal muscle regeneration. *Sports Med. Health Sci.* 4, 198–208. doi:10.1016/j.smhs.2022.06.005

Yao, C. H., Wang, R., Wang, Y., Kung, C. P., Weber, J. D., and Patti, G. J. (2019). Mitochondrial fusion supports increased oxidative phosphorylation during cell proliferation. *Elife* 8, e41351. doi:10.7554/eLife.41351

Yeh, T. S., Ho, J. D., Yang, V. W., Tzeng, C. R., and Hsieh, R. H. (2005). Calcium stimulates mitochondrial biogenesis in human granulosa cells. *Ann. N. Y. Acad. Sci.* 1042, 157–162. doi:10.1196/annals.1338.017

You, C. L., Lee, S. J., Lee, J., Vuong, T. A., Lee, H. Y., Jeong, S. Y., et al. (2023). Inonotus obliquus upregulates muscle regeneration and augments function through muscle oxidative metabolism. *Int. J. Biol. Sci.* 19, 4898–4914. doi:10.7150/ijbs.84970

Zammit, P. S. (2017). Function of the myogenic regulatory factors Myf5, MyoD, Myogenin and MRF4 in skeletal muscle, satellite cells and regenerative myogenesis. *Semin. Cell Dev. Biol.* 72, 19–32. doi:10.1016/j.semcdb.2017.11.011

Zhou, Q., Zhu, L., Qiu, W., Liu, Y., Yang, F., Chen, W., et al. (2020). Nicotinamide riboside enhances mitochondrial proteostasis and adult neurogenesis through activation of mitochondrial unfolded protein response signaling in the brain of ALS SOD1(g93a) mice. *Int. J. Biol. Sci.* 16, 284–297. doi:10.7150/ijbs.38487

Zhu, L., Zhou, Q., He, L., and Chen, L. (2021). Mitochondrial unfolded protein response: an emerging pathway in human diseases. *Free Radic. Biol. Med.* 163, 125–134. doi:10.1016/j.freeradbiomed.2020.12.013

Zismanov, V., Chichkov, V., Colangelo, V., Jamet, S., Wang, S., Syme, A., et al. (2016). Phosphorylation of eIF2α is a translational control mechanism regulating muscle stem cell quiescence and self-renewal. *Cell Stem Cell* 18, 79–90. doi:10.1016/j.stem.2015.09.020

frontiers | Frontiers in Cell and Developmental Biology

TYPE Methods
PUBLISHED 14 May 2024
DOI 10.3389/fcell.2024.1346778

OPEN ACCESS

EDITED BY
Elena Levantini,
National Research Council (CNR), Italy

REVIEWED BY
Qian Peter Su,
University of Technology Sydney, Australia
Marco Tigano,
Thomas Jefferson University, United States

*CORRESPONDENCE
Michelle Giarmarco,
mgmarco@uw.edu

RECEIVED 29 November 2023
ACCEPTED 12 April 2024
PUBLISHED 14 May 2024

CITATION
Giarmarco M, Seto J, Brock D and Brockerhoff S (2024), Spatial detection of mitochondrial DNA and RNA in tissues.
Front. Cell Dev. Biol. 12:1346778.
doi: 10.3389/fcell.2024.1346778

Spatial detection of mitochondrial DNA and RNA in tissues

Michelle Giarmarco[1]*, Jordan Seto[1,2], Daniel Brock[2] and Susan Brockerhoff[1,2]

[1]Department of Ophthalmology, University of Washington, Seattle, WA, United States, [2]Department of Biochemistry, University of Washington, Seattle, WA, United States

Background: Mitochondrial health has gained attention in a number of diseases, both as an indicator of disease state and as a potential therapeutic target. The quality and amount of mitochondrial DNA (mtDNA) and RNA (mtRNA) can be important indicators of mitochondrial and cell health, but are difficult to measure in complex tissues.

Methods: mtDNA and mtRNA in zebrafish retina samples were fluorescently labeled using RNAscope™ *in situ* hybridization, then mitochondria were stained using immunohistochemistry. Pretreatment with RNase was used for validation. Confocal images were collected and analyzed, and relative amounts of mtDNA and mtRNA were reported. Findings regarding mtDNA were confirmed using qPCR.

Results: Signals from probes detecting mtDNA and mtRNA were localized to mitochondria, and were differentially sensitive to RNase. This labeling strategy allows for quantification of relative mtDNA and mtRNA levels in individual cells. As a demonstration of the method in a complex tissue, single photoreceptors in zebrafish retina were analyzed for mtDNA and mtRNA content. An increase in mtRNA but not mtDNA coincides with proliferation of mitochondria at night in cones. A similar trend was measured in rods.

Discussion: Mitochondrial gene expression is an important component of cell adaptations to disease, stress, or aging. This method enables the study of mtDNA and mtRNA in single cells of an intact, complex tissue. The protocol presented here uses commercially-available tools, and is adaptable to a range of species and tissue types.

KEYWORDS

mitochondria, mtDNA, mtRNA, spatial biology, multiplex imaging, zebrafish, RNAscope, photoreceptor

1 Introduction

Mitochondria, organelles typically associated with energy production, are vital components of nearly all cells. In recent decades new mitochondrial roles have been uncovered, including initiation of cell death (Wang and Youle, 2009), maintenance of calcium (Rizzuto et al., 2012) and redox homeostases (Willems et al., 2015), metabolism of lipids (Houten and Wanders, 2010), and even guiding light in the eye (Ball et al., 2022). They have intricate relationships with the endoplasmic reticulum (Rowland and Voeltz, 2012) that are crucial to the function of neurons and other cells (Wu et al., 2017). Mitochondria are highly dynamic, moving along cytoskeletal networks (Barnhart, 2016), undergoing replication and quality control via fission and fusion (Youle and van der Bliek,

2012; Ni et al., 2015), and sometimes being ejected from cells (Nakajima et al., 2008; Lyamzaev et al., 2022).

Owing to their bacterial symbiont origin, mitochondria possess heterogeneous populations of mitochondrial DNA (mtDNA) that are distinct from genomic DNA (gDNA). The mitochondrial genome is a compact plasmid, with less than 17,000 base pairs encoding 13 critical components of the electron transport chain, plus mitochondrial ribosomal and transfer RNAs needed for translation (Mercer et al., 2011). mtDNA is transcribed into mitochondrial RNA (mtRNA) using a dedicated mtDNA polymerase, and mtRNA is translated into proteins using mitochondrial ribosomes. The remaining >99% of mitochondrial proteins are encoded by gDNA and imported.

Mitochondrial diseases arise from mutations in gDNA that affect mitochondrial proteins, or from mutations to mtDNA itself (Gorman et al., 2016). mtDNA mutations can be difficult to characterize due to the unique maternal inheritance of mitochondria and resulting heteroplasmy (St John et al., 2010). Additionally, certain diseases and aging can lead to aberrant mtDNA levels and mitochondrial dysfunction (Filograna et al., 2021; Sanchez-Contreras and Kennedy, 2022). Despite the importance of mtDNA homeostasis for cells, few tools exist for spatially quantifying mtDNA copy number and/or mtRNA amounts in specific cells of a complex tissue.

We employed *in situ* hybridization (ISH) using RNAscope™ probes (Wang et al., 2012) designed to report either mtDNA, or mtDNA and mtRNA. The strategy is similar to a published chromogenic assay (Chen et al., 2020), but allows for higher-resolution 3-D imaging and simultaneous protein detection using immunohistochemistry (IHC). As a proof of principle, we used this method to explore mtDNA and mtRNA levels in cone and rod photoreceptors during day and night in zebrafish. At night mtRNA but not mtDNA levels increase in both photoreceptor types, which corresponds to increases in mitochondrial number and activity in cones (Giarmarco et al., 2020). This method is adaptable to many species and tissue types; paired with super-resolution imaging and AI-assisted analysis it can quantitatively report mtDNA and mtRNA in individual cells of a complex tissue.

2 Materials and equipment

2.1 Methods

2.1.1 Animals

Research was authorized by the University of Washington Institutional Animal Care and Use Committee. Wild-type AB *Danio rerio* were raised under standard conditions in the UW SLU Aquatics facility on a 14h/10 h light/dark cycle, with lights on at 9 a.m. Male and female fish were euthanized over an ice bath, followed by cervical dislocation and enucleation. For the 11 p.m. timepoint euthanasia and dissections were performed under infrared light with night vision goggles.

2.1.2 Tissue preparation

For histology, eyes were collected at 9 a.m. and 11 p.m. (4 animals per timepoint), pierced several times across the cornea with a needle, and the vitreous cavity was flushed with 4% paraformaldehyde fixative in phosphate buffered solution (PBS). Following overnight immersion in fixative at 4°C, eyes were rinsed in PBS, then bleached with 10% H_2O_2 in PBS overnight at 37°C to clarify the pigmented epithelium. Eyes were cryoprotected in 20% sucrose, the anterior halves dissected away, and eyecups were embedded and frozen in OCT cryomolds. Eyecups were cryosectioned at 20 µm onto slides that contained one section from each timepoint for parallel staining and analysis; slides were stored at −20°C.

For bulk genomic analysis, eyes were collected at 9 a.m. and 11 p.m. (4-5 animals per timepoint), and the retinas were isolated in PBS. Retinas were snap frozen in microfuge tubes over liquid nitrogen and stored at −80°C until DNA extraction.

2.1.3 Probe design

Three commercially-available ACD RNAscope™ probes were used. As a positive control, Dr-polr2a-C3 reported mRNA transcripts from a nuclear-encoded zebrafish housekeeping gene. As a negative control, 3-plex DapB reported transcripts from a bacterial gene. To explore mtDNA and mtRNA we used probes against the mitochondrial gene MT-ND5, which encodes a highly-conserved subunit of respiratory complex I and was identified by the manufacturer as a good candidate reporter. The "coding" probe Dr-MT-ND5 contains sequences antisense to the MT-ND5 gene, binding to regions of the noncoding (sense) mtDNA strand, and to MT-ND5 mtRNA transcripts.

To report mtDNA, we employed a strategy similar to one reported for chromogenic RNAscope™ with paraffin-embedded samples (Chen et al., 2020). The "noncoding" probe Dr-MT-ND5-sense-C3 was custom designed to contain sense sequences of the same mitochondrial gene; it binds regions of the coding (antisense) mtDNA strand. Antisense mtRNA transcripts from the noncoding strand of mtDNA are typically degraded (Pietras et al., 2018; Jedynak-Slyvka et al., 2021), so this probe reports primarily mtDNA.

2.1.4 *In situ* hybridization with RNAscope™

Sections were treated with the RNAscope™ Fluorescent Multiplex v2 kit. The standard protocol for fixed frozen sections was used including pretreatment, probe hybridization and fluorescent labelling, with the following modifications: 1) Target retrieval was reduced to 5 min 2) Protease III digestion was reduced to 15 min 3) Probe and dye concentrations were optimized to best visualize single molecules (see Table 2). 4) Following the final wash, sections were not mounted and instead immediately underwent IHC. Incubations were conducted in staining chambers in a standard incubator. MT-ND5 probes were conjugated to the fluorescent dye Opal™ 520 diluted in RNAscope™ TSA buffer. Polr2a (C3) and DapB (C2) control probes were conjugated to Opal™ 520 and Opal™ 570, respectively.

2.1.5 Enzymatic validation of probes

To verify specificity of mtDNA and mtRNA detection with the MT-ND5 probes, an additional incubation in either PBS or RNase A was performed. Following post-protease water washes and just prior to probe hybridization, sections were incubated 30 min at 37°C in either PBS or 50 µg/mL RNase A in PBS, followed by 3 water washes. This was followed by standard probe hybridization, fluorescent

TABLE 1 Materials and equipment. Primary antibodies suitable for multiplexing IHC with RNAscope™ in cryosections.

Tissue species	Structure labeled	Antigen	Supplier	Catalog #	RRID	IHC dilution
Any	Transgenic GFP	GFP	Abcam	ab13970	RRID:AB_300798	1:5,000
Zebrafish	Mitochondria	MTCO1	Abcam	ab14705	RRID:AB_2084810	1:1,000
Zebrafish	Mitochondria	Citrate synthetase	Abcam	ab96600	RRID:AB_10678258	1:500
Macaque	Neuron cytosol	Calbindin	Sigma-Aldrich	C8666	RRID:AB_10013380	1:1,000
Macaque	Synapses	GAD6	Iowa Hybridoma Bank	GAD-6	RRID:AB_528264	1:1,000
Human	Tight junctions	ZO-1	ThermoFisher	40–2,200	RRID:AB_2533456	1:100
Human	Collagen	COLVI	Abcam	ab6588	RRID:AB_305585	1:250
Human	Plasma membrane	CD46	Bio-Rad	MCA2113	RRID:AB_323983	1:100

labelling, and IHC. Additional validation strategies are outlined in the Section 3.

2.1.6 Immunohistochemistry

Following RNAscope™, sections underwent IHC using a primary antibody against MTCO1 (a subunit of respiratory complex IV) to report mitochondrial volume. Sections were washed 3 times with PBS, blocked 1 h at room temperature (RT) with blocking buffer, and incubated overnight at RT with anti-MTCO1 diluted in blocking buffer. They were then washed 3 times with PBS, incubated 2 h at RT with Alexa Fluor™ 633-conjugated secondary antibodies and DAPI counterstain, washed 3 times with PBS, and mounted with Vectashield and a coverslip. Table 1 lists primary antibodies used in this study, along with others the authors have found to be compatible for multiplexing IHC with RNAscope™.

2.1.7 Imaging and image processing

Imaging was conducted using a Leica SP8 confocal microscope with a ×63 oil objective to capture single Z-stacks and Z-stack montages. LAS-X software was used for acquisition, and images were deconvolved using Leica Lightning in adaptive mode. Images were processed in ImageJ, where mitochondrial clusters of individual rods and short-wavelength cones were identified based on morphology and position in the retina (cyan and yellow boxes in Figure 2A). Single clusters were cropped out for quantification using the MTCO1 mitochondrial channel as a mask. Confocal images presented are maximum intensity projections over 12 µm tissue depth.

2.1.8 Quantification of probe signals

Mitochondrial clusters of rod photoreceptors were found to have well-resolved individual RNAscope™ MT-ND5 puncta. Single cluster Z-stacks (n = 3 cells per condition) were analyzed using the 3D Objects Counter plugin in ImageJ to report the number of puncta per cluster. MT-ND5 puntca in cone clusters were poorly resolved in areas due to very dense packing of mitochondria. Single cluster Z-stacks (n = 30 cells per standard timepoint, n = 12 cells per timepoint for RNase validation) were analyzed using the 3D Objects Counter plugin in ImageJ to instead report total puncta volume relative to overall mitochondrial volume measured using the MTCO1 channel. For both rods and cones, analysis was conducted blind to sample condition and timepoint. Mann-Whitney statistical tests were performed using Microsoft Excel with the Real Statistics resource pack.

2.1.9 DNA extraction and quantification using qPCR

DNA was isolated from frozen retinas (n = 3-4 animals per timepoint, each with three technical replicates) using an AllPrep DNA/RNA Mini Kit, then quality checked via spectrophotometer. mtDNA:gDNA ratios were determined using the qPCR $2^{-\Delta\Delta CT}$ method (Livak and Schmittgen, 2001) relative to the 9 a.m. timepoint. Mitochondrial-encoded NADH dehydrogenase 1 (*mt-nd1*) served as the mtDNA target and *polg1* was the nuclear-encoded DNA target, a strategy reported previously in zebrafish (Artuso et al., 2012). Primer sequences for these targets are listed in Table 2. qPCR CT values were generated using extracted DNA on the 7500 Fast Real-Time PCR System and SYBR Green Real-Time PCR Master Mix. The number of mtDNA copies per cell was determined according to the following equation (Artuso et al., 2012):

$$mtDNA\,copies = \frac{(number\,of\,mtDNA\,copies)}{\frac{(number\,of\,allele\,of\,nDNA)}{2}}$$

3 Results

3.1 Experimental design

The mitochondrial genome consists of a "heavy" coding strand, and a complementary "light" noncoding strand. During transcription mtRNA is generated from both strands; sense transcripts from the coding strand are processed and translated into proteins, transfer RNAs, and ribosomal RNAs (Pietras et al., 2018; Jedynak-Slyvka et al., 2021). mtRNA transcripts from the noncoding strand are typically degraded, except for a few transfer RNAs and one protein (Chomyn et al., 1986; Mercer et al., 2011).

Figure 1A depicts the strategy for separately labelling mtDNA and mtRNA transcripts using two RNAscope™ probes against each strand of the mitochondrial gene MT-ND5. For consistency in this manuscript, the "coding" MT-ND5 probe sequence is antisense, binding both mtRNA transcripts and the mtDNA light strand. The "noncoding" MT-ND5 probe sequence is sense, binding primarily to the mtDNA heavy strand.

TABLE 2 Materials and Equipment.

Item	Source	Notes, concentrations
Phosphate buffered solution (PBS)	in-house	0.14 M phosphate buffer in water, pH 7.4
16% paraformaldehyde solution	ThermoFisher, #043368.9M	4% in PBS
30% hydrogen peroxide solution	MilliporeSigma, #HX0640	10% in PBS
20% sucrose solution	in-house	20% w/v sucrose in PBS
Optimal Cutting Temperature (OCT) compound	VWR, #4583	
Cryomolds (10 mm × 10 mm x 5 mm)	VWR, #4565	
SuperFrost Plus Gold slides	ThermoFisher, #15-188-48	
Cryostat	Leica Biosystems, #CM1850	
Hybridization Incubator	Robbins Scientific, #310	
Slide moisture chamber, black	Newcomer Supply, #68432A	
Probe Dr-polr2a-C3	ACD Bio, #559921	1:50 in probe diluent
Probe 3-plex DapB	ACD Bio, #320871	neat
Probe Dr-MT-ND5	ACD Bio, #574591	0.5X in probe diluent
Probe Dr-MT-ND5-sense-C3	ACD Bio, #1204141	1:75 in probe diluent
Probe diluent	ACD Bio, #300041	
Fluorescent Multiplex v2 kit	ACD Bio, #323100	
TSA buffer	ACD Bio, #322809	
Opal™ 520 dye	Akoya Biosciences, #FP1487001KT	1:1,000 for polr2a probe; 1:1,800 for MT-ND5 probes in TSA buffer
Opal™ 570 dye	Akoya Biosciences, #FP1488001KT	1:1,000 for DapB probe in TSA buffer
Monarch RNase A	New England Biolabs, #T3018-2	50 µg/mL (1:400) in PBS
Blocking buffer	in-house	5% normal donkey serum, 1 mg/mL bovine serum albumin, 1% Triton X-100 in PBS
Mouse anti-MTCO1	Abcam, #ab14705; RRID:AB_2084810	1:1,000 in blocking buffer
Goat anti-mouse IgG, Alexa Fluor™ 633 conjugate	ThermoFisher, #A21053	1:500 in blocking buffer
DAPI	Invitrogen, #D1306	1:1,000 in blocking buffer
Vectashield Vibrance	Vector labs, #H1700	
Leica SP8 confocal microscope with LAS-X	Leica Microsystems	
FIJI (ImageJ)	https://fiji.sc/ (Schindelin et al., 2012)	
3D Objects Counter Plugin	https://imagej.net/plugins/3d-objects-counter (Bolte and Cordelieres, 2006)	
AllPrep DNA/RNA Mini Kit	Qiagen, #80204	
NanoDrop™ spectrophotometer	ThermoFisher, #ND-2000C	
Fast Real-Time PCR System	Applied Biosystems, #7500	
DEPC-treated water	ThermoFisher, # R0601	
Zebrafish polg1 primer set	Integrated DNA Technologies	(F) GAGAGCGTCTATAAGGAGTAC
		(R) GAGCTCATCAGAAACAGGACT
Zebrafish *mt-nd1* primer set	Integrated DNA Technologies	(F) AGCCTACGCCGTACCAGTATT
		(R) GTTTCACGCCATCAGCTACTG

(Continued on following page)

TABLE 2 (*Continued*) Materials and Equipment.

Item	Source	Notes, concentrations
SYBR Green Real-Time PCR Master Mix (2X)	Applied Biosystems, # 4309155	1X in DEPC-treated water
Microsoft Excel with Real Statistics resource pack	Microsoft, Real Statistics	

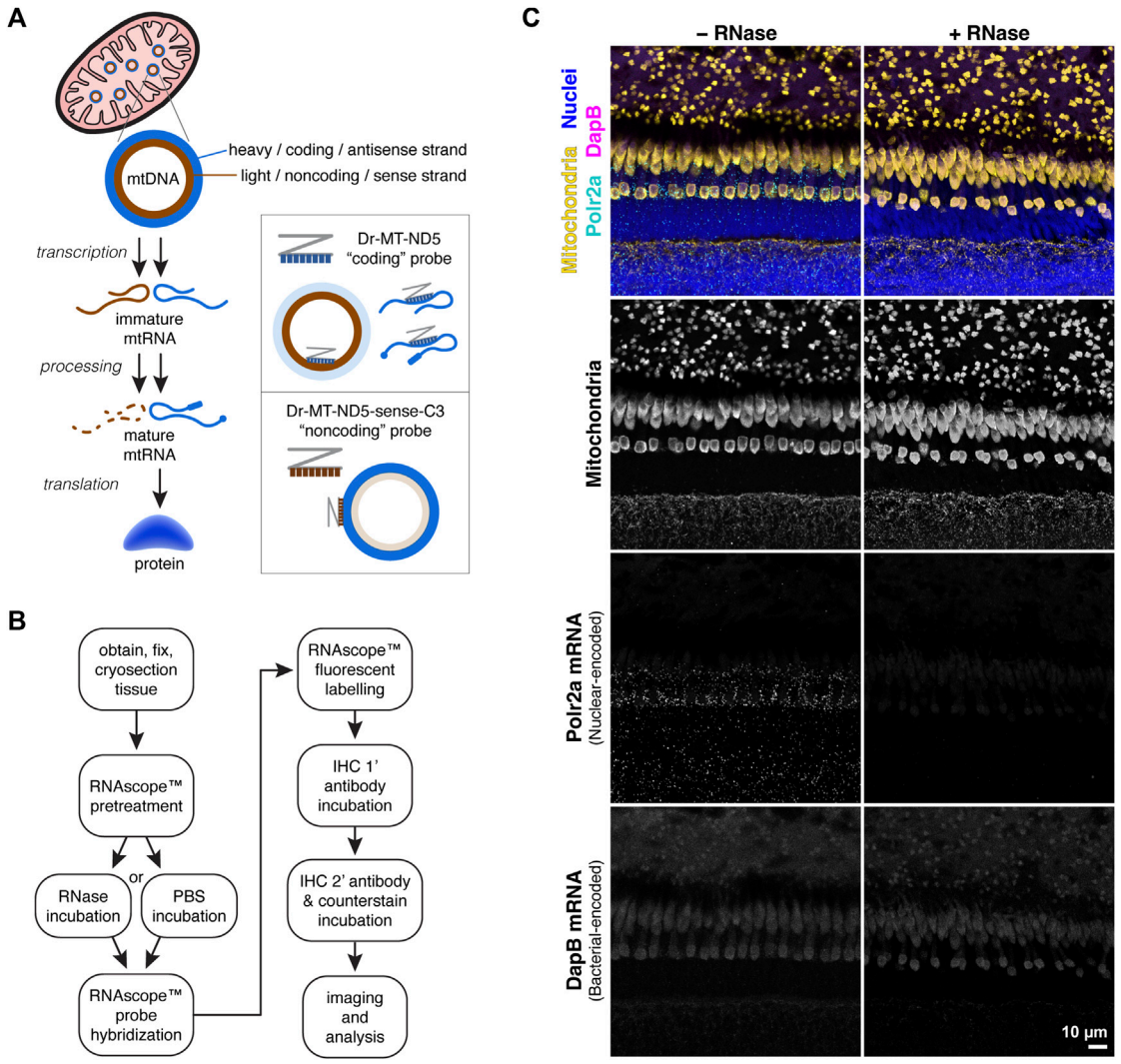

FIGURE 1
(A) Simplified schematic of protein synthesis from mtDNA. mtRNA transcripts from the mtDNA coding strand are processed and translated into protein; transcripts from the noncoding strand are typically degraded. Accordingly, the RNAscope™ Dr-MT-ND5 "coding" probe reports both mtRNA and mtDNA, while the "noncoding" probe reports primarily mtDNA. **(B)** Workflow for mtDNA and mtRNA detection using RNAscope™ and IHC. RNAscope™ steps were carried out using the manufacturer's protocol for the Fluorescent Multiplex v2 kit, with modifications listed in the methods section. **(C)** Images of zebrafish outer retina stained with a control probe against Polr2a nuclear-encoded mRNA, and a control probe against bacterial-encoded DapB mRNA. RNase treatment eliminates Polr2a mRNA signal.

3.2 Probe validation strategies

3.2.1 Enzymatic validation

To determine the relative contribution of RNA to probe signals, we employed an optional RNase incubation step prior to probe hybridization (Figure 1B). We used an RNAscope™ positive control probe against messenger RNA (mRNA) transcripts from the nuclear-encoded housekeeping gene Polr2a, and a negative control probe against mRNA transcripts from the bacterial gene DapB. In zebrafish retina sections, the Polr2a probe labeled puncta around nuclei that were absent with RNase pretreatment; no puncta were visible with the DapB probe (Figure 1C).

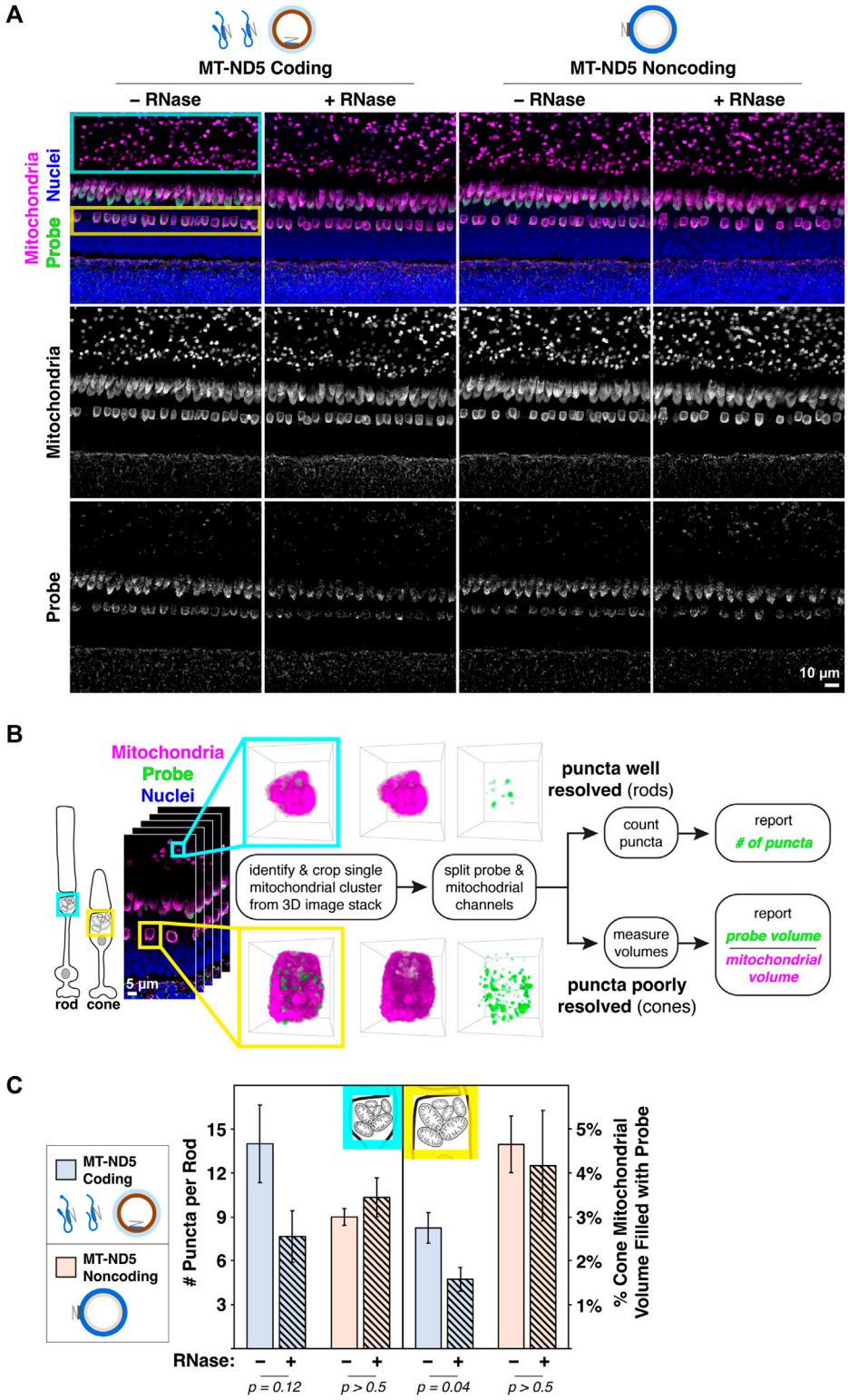

FIGURE 2
(A) Images of zebrafish outer retina showing signals from RNAscope™ MT-ND5 coding and noncoding probes. Cyan and yellow boxes indicate respective locations of rod and cone mitochondrial clusters used for quantification. RNase was used to determine signal contributions of RNA for each probe. All sections were counterstained for nuclei and mitochondria via IHC. Green–probe (ISH), magenta–mitochondria (IHC), blue–nuclei. **(B)** Workflow for quantification of MT-ND5 probe signals as either puncta counts or percent of mitochondrial volume. **(C)** Quantification of signals from coding and noncoding probes, including RNase conditions. Error bars represent standard error of the mean; *p* values determined using a Mann-Whitney test.

10.3389/fcell.2024.1346778

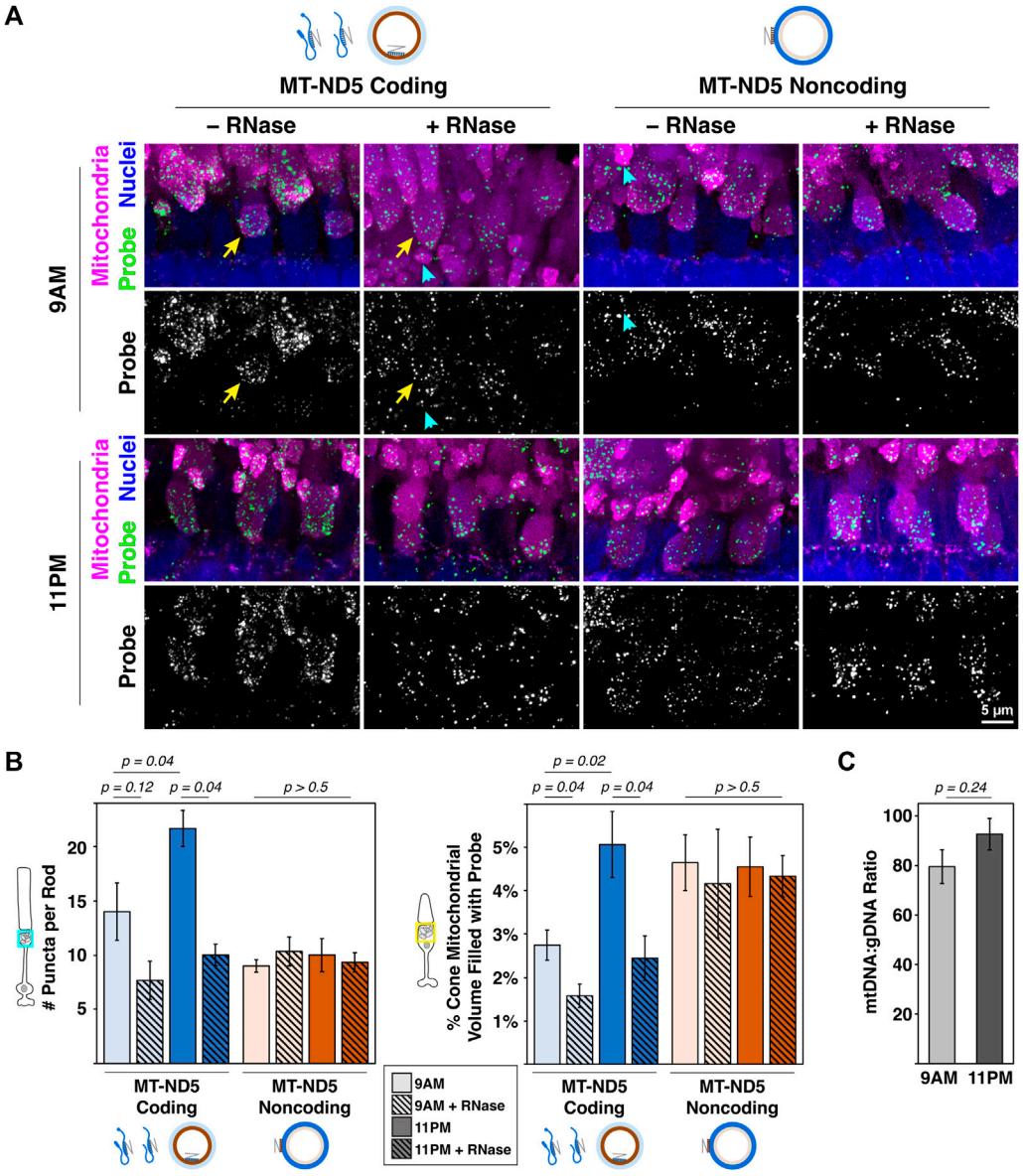

FIGURE 3
(A) Sample images of zebrafish photoreceptor mitochondrial clusters from 9 a.m. to 11 p.m. labeled with RNAscope™ MT-ND5 coding or noncoding probes. RNase was used to determine signal contributions of RNA for each probe. All sections were counterstained for nuclei and mitochondria via IHC. Cyan arrowheads and yellow arrows indicate examples of single rod and cone mitochondrial clusters used for quantification, respectively. Green–probe (ISH), magenta–mitochondria (IHC), blue–nuclei. **(B)** Quantification of signals from coding and noncoding probes at 9 a.m. and 11 p.m., including RNase conditions. **(C)** Ratios of mtDNA to gDNA measured using RT-qPCR from whole zebrafish retinas at 9 a.m. and 11 p.m.. For all graphs, error bars represent standard error of the mean; *p* values determined using a Mann-Whitney test.

Further enzymatic validation using DNase to digest mtDNA has been reported for paraffin sections (Chen et al., 2020). We attempted this repeatedly with fixed frozen retina sections but results were difficult to interpret, as DNases removed most of the RNA signal from the positive control mRNA probe. One explanation is that structural damage to the tissue from DNase is more severe in fixed frozen sections, causing RNA to float away before probe hybridization. This is an important control that could be successful in other tissues, but likely necessitates paraffin sections.

3.2.2 ISH and IHC multiplexing

To confirm that MT-ND5 probe signals were localized to mitochondria, we expanded the RNAscope™ procedure to include subsequent immunolabelling (Figure 1B). The pretreatment conditions required for RNAscope™ destroyed antigenicity of some primary antibody targets, while antigenicity was unaffected or improved for others. Table 1 lists primary antibodies we have used to successfully immunolabel various cell structures following ISH in zebrafish, macaque, or human tissue cryosections.

A primary antibody against MTCO1, a subunit of respiratory complex IV, displayed a robust mitochondrial staining pattern (Figure 1C, second row) following ISH that is typical of zebrafish retina stained using conventional IHC (Giarmarco et al., 2020). When ISH against MT-ND5 and IHC against MTCO1 were multiplexed, signals from coding and noncoding probes were confined to mitochondria (Figure 2A), demonstrating that the MT-ND5 probes are not binding off-target nuclear-encoded genes. Mitochondria in zebrafish photoreceptors are tightly packed and do not immunolabel uniformly (see U-shaped structures in Figure 1C, second row), but IHC is still useful for broad morphometrics like cluster size and outline.

Immunolabelling with antibodies against dsRNA or dsDNA is also useful for validation of mitochondrial probes. We did not employ this method in our samples because IHC quantification is confounded by limitations with antibody penetration. However, dual labeling with RNAscope™ and anti-dsRNA has been reported for cultured primate cells (Liu et al., 2018).

3.2.3 Bulk analysis

Given the difficulty using DNase as a control for RNAscope TM superscript on cryosections, bulk analysis using quantitative PCR (qPCR) can be used to confirm findings about mtDNA. By comparing the number of mitochondrial and nuclear genomes in a sample, mtDNA copy number per cell can be calculated (Artuso et al., 2012). While cell-specific information is lost, patterns in mtDNA copy numbers found using RNAscope TM superscript should be consistent with observations made using qPCR. We demonstrate validation using qPCR in a proof-of-principle experiment below (Figure 3C).

3.3 Quantification of mtDNA and mtRNA

As a demonstration of the multiplex labeling strategy, we sought to quantify mitochondrial RNAscope™ signals in photoreceptors of zebrafish retina, where mitochondria are concentrated in a dense cluster. We employed two strategies for quantification, outlined in Figure 2B.

For rods, quantification of MT-ND5 signals was straightforward. Individual puncta within a cluster were well resolved, and we used the 3D Object Counter plugin for ImageJ to report the number of puncta per cluster. For cones, quantification was limited by the dense packing of cone mitochondria, and the resolution of our microscope. Despite careful titration of MT-ND5 probes and their conjugated dyes, we could not reliably resolve individual puncta in all areas of a cluster. Instead, we used the 3D Objects Counter plugin for ImageJ to report probe volume as a percentage of overall cluster volume determined from IHC.

RNase pretreatment modestly reduced signal from the coding probe but not the noncoding probe (Figure 2C). Insensitivity of the noncoding probe to RNase confirms that it does not appreciably bind mtRNA.

3.4 Demonstration quantifying mtDNA and mtRNA in photoreceptors

Mitochondrial dynamics in rod photoreceptors are not well characterized, but cone clusters undergo daily remodeling. Their mitochondria are smaller and more numerous at night (Giarmarco et al., 2020) when energy demands are highest (Okawa et al., 2008), and it is not known how mtDNA and mtRNA change. In retina samples collected during the day (9 a.m.) and at night (11 p.m.), both MT-ND5 probes yielded robust signal in rod and cone mitochondrial clusters (Figure 3A). A subset of these samples was pretreated with RNase to determine the relative contribution of mtRNA to MT-ND5 signals.

Figure 3B summarizes the analyses of MT-ND5 coding and noncoding probe signals. Only the coding probe was significantly sensitive to RNase pretreatment (solid v. hashed bars), confirmation that the noncoding probe primarily reports mtDNA. In rods, the number of coding probe puncta increased 35% between 9 a.m. and 11 p.m., and noncoding puncta were not significantly different. A similar pattern was observed in cones, where volume of the coding probe increased 45% between 9 a.m. and 11 p.m., but noncoding probe volumes were unchanged.

Given the increase in mitochondrial number previously reported at night, we were surprised to find no change in mtDNA levels using the MT-ND5 noncoding probe. We further validated this finding by performing qPCR to report relative mtDNA copy number in whole retinal homogenates collected at 9 a.m. and 11 p.m.. Ratios of mtDNA:gDNA determined via qPCR were not significantly different between 9 a.m. and 11 p.m. (Figure 3C), consistent with observations made using RNAscope™.

Together this suggests that a burst of mitochondrial transcription, evidenced by increases in coding probe signal, could support a larger population of mitochondria at night in cones. Overall mtDNA levels remain unchanged, indicating that either existing mitochondrial genomes are simply divided among the growing population, and/or that some amount of mtDNA turnover is occurring. Alternately, it is possible that mtDNA levels rise at a timepoint that was not measured in this study.

4 Discussion

We present a method for spatial quantification of mtDNA and mtRNA in fixed frozen tissue sections. It employs a dual-probe strategy for RNAscope™ ISH similar to a published method in paraffin sections (Chen et al., 2020), coupled with IHC for unambiguous labeling of mitochondria. The protocol uses commercially-available reagents, can be carried out over 2–3 days, and is broadly adaptable to many species and tissues. It will enable researchers to characterize mitochondrial gene expression in single cells, and understand the mitochondrial adaptations that occur during disease, stress and aging.

Conventional methods for measuring mtDNA and mtRNA such as RT-qPCR often require tissue homogenization, which presents challenges to studying specific cells. In the example of the retina, photoreceptors are just part of a tissue comprised of around 100 cell types, making it difficult to discern their contribution to changes in mitochondrial gene expression above the retinal milieu. Recent advances in single-cell RNA sequencing have enabled the study of mtDNA in retinal cell subpopulations (Liu et al., 2022), but some neuron types are not represented. Further, tissue digestion and cell sorting conditions can induce stress-related changes to gene expression (Denisenko et al., 2020).

This method has several advantages over chromogenic ISH and bulk nucleotide analyses. In addition to preserving cells morphologically in their native microenvironment, rapid fixation of tissue for histology reduces risk of stress-related gene expression changes that occur during tissue dissociation. Multiplexing ISH with IHC enables counterstaining of mitochondria or other cell-identifying markers, making for unambiguous quantification of ISH signals. We found several primary antibodies suitable for ISH and IHC multiplexing (Table 1). Lastly, the high resolution afforded by confocal microscopy allows for visualization of single mtDNA or mtRNA molecules in 3-D, and subsequent quantification.

RNAscope™ is a versatile platform amenable to many species and tissue types, and the design of double Z probe sets enables accurate target labelling with virtually no off-target binding (Wang et al., 2012). We present a simple RNAscope™ application, but depending on the kit and sample, it can be used to visualize up to 48 targets. Its application in the study of mtDNA and mtRNA is somewhat recent but gaining popularity (Blumental-Perry et al., 2020; Lee et al., 2023; Sriram et al., 2024).

Following careful biostatistics-aided probe selection, additional validation steps are critical. Antibodies detecting mitochondrial proteins and dsDNA are useful to this end, and probes targeting several mitochondrial genes would also help validate results. In the case of the zebrafish MT-ND5 probes, RNase pretreatment confirmed that the coding probe reports mtDNA and mtRNA, while the noncoding probe reports primarily mtDNA. We attempted pretreatment with DNase as additional enzymatic validation, but it was not compatible with RNAscope™ on fixed frozen sections. We relied on qPCR comparing total amounts of gDNA and mtDNA as confirmation of our results.

In an example analysis of mtDNA and mtRNA in zebrafish photoreceptors, mtRNA levels increased 35%–45% between 9 a.m. and 11 p.m., a finding consistent with cone mitochondrial proliferation (Giarmarco et al., 2020) and increased photoreceptor energy consumption at night (Okawa et al., 2008). Interestingly mtDNA levels remained stable, highlighting the complicated nature of mitochondrial gene expression. It is possible that daily turnover of mitochondrial genomes keeps mtDNA levels stable, as cycles of mtRNA expression and degradation support changes to the mitochondrial population. This supports the idea that increases in cone mitochondrial number are driven primarily by increased gene expression, rather than a net increase in mtDNA copy number.

While our example analysis uncovered significant differences in mtRNA levels, there are limitations to quantification depending on the cell type and mitochondrial organization. In zebrafish rods, mitochondria are large and reside in a small cluster. mtDNA and mtRNA molecules were clearly resolved within rod clusters, making quantification straightforward. In contrast, cones have hundreds of smaller mitochondria concentrated in a dense cluster, and mtDNA and mtRNA molecules are very crowded. In such cases, it is important to titrate the concentrations of probe and fluorescent dye to best achieve individual puncta; even then we were unable to resolve individual puncta across the entire cone cluster. Reporting volume fractions was an effective strategy for demonstration of the method, however counts of individual puncta are most accurate. This could be achieved by utilizing super-resolution imaging (Liu and Rask-Andersen, 2022), and/or deploying machine learning analysis tools (Burkert et al., 2023).

Probe selection is an important consideration when using RNAscope™ to report mtDNA and mtRNA. We selected the MT-ND5 gene based on success with the commercially available MT-ND5 coding probe for zebrafish, and had the MT-ND5 noncoding probe custom designed by the manufacturer and their bioinformatics team. Because both probes target the same gene, they likely contain complementary sequences that would bind each other in solution when attempting to duplex both probes. Indeed, our attempts at duplexing coding and noncoding probes were difficult to interpret, despite tandem hybridization steps and labelling with spectrally separate dyes. To successfully duplex coding and noncoding probes on the same section, two different mitochondrial genes would need to be targeted.

Another factor to keep in mind when interpreting results from this method is probe affinity. In our example of zebrafish cones, 3-D electron microscopy in a previous study found ~180 mitochondria per cluster at 9 a.m. In a few instances where RNAscope™ mtDNA puncta in a cluster were resolved well enough for counting using 3-D segmentation and manual counting, we found roughly half that number of mtDNA molecules. While it is possible that some mitochondria in this system lack a genome, another explanation is that the probe did not bind every mitochondrial genome. Coding and noncoding probes may not have the same affinity for their target sequences, so it is important to include enzymatic validation, use several probes, and exercise caution when making direct numerical comparisons.

In conclusion, we have optimized a method of multiplexed ISH and IHC that can detect mtDNA and mtRNA at single molecule resolution. Using machine learning and super resolution imaging strategies, this method holds promise for precisely quantifying determinants of mitochondrial health, such as mtDNA copy number and gene expression. This spatial information can address new questions about mitochondrial biology at the level of an individual mitochondrion, in different locations within a cell or tissue, or in particular stages of the mitochondrial life cycle.

Data availability statement

The original contributions presented in the study are included in the article/Supplementary Material, further inquiries can be directed to the corresponding author.

Ethics statement

The animal study was approved by University of Washington Institutional Animal Care and Use Committee. The study was conducted in accordance with the local legislation and institutional requirements.

Author contributions

MG: Writing–original draft, Visualization, Validation, Supervision, Resources, Project administration, Methodology,

Investigation, Formal Analysis, Data curation, Conceptualization. JS: Writing–review and editing, Visualization, Validation, Methodology, Investigation, Formal Analysis, Data curation. DB: Data curation, Formal analysis, Investigation, Validation, Writing–review and editing. SB: Writing–review and editing, Supervision, Resources, Project administration, Methodology, Funding acquisition, Conceptualization.

Funding

The author(s) declare financial support was received for the research, authorship, and/or publication of this article. This work was supported by NIH NEI Grants P30EY001730 to Maureen Neitz, and R01EY026020 to SB.

Conflict of interest

The authors declare that the research was conducted in the absence of any commercial or financial relationships that could be construed as a potential conflict of interest.

Publisher's note

References

Artuso, L., Romano, A., Verri, T., Domenichini, A., Argenton, F., Santorelli, F. M., et al. (2012). Mitochondrial DNA metabolism in early development of zebrafish (*Danio rerio*). *Biochim. Biophys. Acta* 1817, 1002–1011. doi:10.1016/j.bbabio.2012.03.019

Ball, J. M., Chen, S., and Li, W. (2022). Mitochondria in cone photoreceptors act as microlenses to enhance photon delivery and confer directional sensitivity to light. *Sci. Adv.* 8 (9), eabn2070. doi:10.1126/sciadv.abn2070

Barnhart, E. L. (2016). Mechanics of mitochondrial motility in neurons. *Curr. Opin. Cell Biol.* 38, 90–99. doi:10.1016/j.ceb.2016.02.022

Blumental-Perry, A., Jobava, R., Bederman, I., Degar, A. J., Kenche, H., Guan, B. J., et al. (2020). Retrograde signaling by a mtDNA-encoded non-coding RNA preserves mitochondrial bioenergetics. *Commun. Biol.* 3 (1), 626. doi:10.1038/s42003-020-01322-4

Bolte, S., and Cordelieres, F. P. (2006). A guided tour into subcellular colocalization analysis in light microscopy. *J. Microsc.* 224 (Pt 3), 213–232. doi:10.1111/j.1365-2818.2006.01706.x

Burkert, N., Roy, S., Häusler, M., Wuttke, D., Müller, S., Wiemer, J., et al. (2023). Deep learning-based image analysis identifies a DAT-negative subpopulation of dopaminergic neurons in the lateral Substantia nigra. *Commun. Biol.* 6 (1), 1146. doi:10.1038/s42003-023-05441-6

Chen, J., Zheng, Q., Peiffer, L. B., Hicks, J. L., Haffner, M. C., Rosenberg, A. Z., et al. (2020). An *in situ* atlas of mitochondrial DNA in mammalian tissues reveals high content in stem and proliferative compartments. *Am. J. Pathol.* 190 (7), 1565–1579. doi:10.1016/j.ajpath.2020.03.018

Chomyn, A., Cleeter, M. W., Ragan, C. I., Riley, M., Doolittle, R. F., and Attardi, G. (1986). URF6, last unidentified reading frame of human mtDNA, codes for an NADH dehydrogenase subunit. *Science* 234 (4776), 614–618. doi:10.1126/science.3764430

Denisenko, E., Guo, B. B., Jones, M., Hou, R., de Kock, L., Lassmann, T., et al. (2020). Systematic assessment of tissue dissociation and storage biases in single-cell and single-nucleus RNA-seq workflows. *Genome Biol.* 21 (1), 130. doi:10.1186/s13059-020-02048-6

Filograna, R., Mennuni, M., Alsina, D., and Larsson, N. G. (2021). Mitochondrial DNA copy number in human disease: the more the better? *FEBS Lett.* 595 (8), 976–1002. doi:10.1002/1873-3468.14021

Giarmarco, M. M., Brock, D. C., Robbings, B. M., Cleghorn, W. M., Tsantilas, K. A., Kuch, K. C., et al. (2020). Daily mitochondrial dynamics in cone photoreceptors. *Proc. Natl. Acad. Sci. U. S. A.* 117 (46), 28816–28827. doi:10.1073/pnas.2007827117

Gorman, G. S., Chinnery, P. F., DiMauro, S., Hirano, M., Koga, Y., McFarland, R., et al. (2016). Mitochondrial diseases. *Nat. Rev. Dis. Prim.* 2, 16080. doi:10.1038/nrdp.2016.80

Houten, S. M., and Wanders, R. J. (2010). A general introduction to the biochemistry of mitochondrial fatty acid β-oxidation. *J. Inherit. Metab. Dis.* 33 (5), 469–477. doi:10.1007/s10545-010-9061-2

Jedynak-Slyvka, M., Jabczynska, A., and Szczesny, R. J. (2021). Human mitochondrial RNA processing and modifications: overview. *Int. J. Mol. Sci.* 22 (15), 7999. doi:10.3390/ijms22157999

Lee, W., Zamudio-Ochoa, A., Buchel, G., Podlesniy, P., Marti Gutierrez, N., Puigròs, M., et al. (2023). Molecular basis for maternal inheritance of human mitochondrial DNA. *Nat. Genet.* 55 (10), 1632–1639. doi:10.1038/s41588-023-01505-9

Liu, B., He, J., Zhong, L., Huang, L., Gong, B., Hu, J., et al. (2022). Single-cell transcriptome reveals diversity of Müller cells with different metabolic-mitochondrial signatures in normal and degenerated macula. *Front. Neurosci.* 16, 1079498. doi:10.3389/fnins.2022.1079498

Liu, J., Kline, B. A., Kenny, T. A., Smith, D. R., Soloveva, V., Beitzel, B., et al. (2018). A novel sheet-like virus particle array is a hallmark of Zika virus infection. *Emerg. Microbes Infect.* 7 (1), 69–11. doi:10.1038/s41426-018-0071-8

Liu, W., and Rask-Andersen, H. (2022). *GJB2* and *GJB6* gene transcripts in the human cochlea: a study using RNAscope, confocal, and super-resolution structured illumination microscopy. *Front. Mol. Neurosci.* 15, 973646. doi:10.3389/fnmol.2022.973646

Livak, K. J., and Schmittgen, T. D. (2001). Analysis of relative gene expression data using real-time quantitative PCR and the 2(-Delta Delta C(T)) Method. *Methods* 25, 402–408. doi:10.1006/meth.2001.1262

Lyamzaev, K. G., Zinovkin, R. A., and Chernyak, B. V. (2022). Extrusion of mitochondria: garbage clearance or cell-cell communication signals? *J. Cell Physiol.* 237 (5), 2345–2356. doi:10.1002/jcp.30711

Mercer, T. R., Neph, S., Dinger, M. E., Crawford, J., Smith, M. A., Shearwood, A. M., et al. (2011). The human mitochondrial transcriptome. *Cell* 146 (4), 645–658. doi:10.1016/j.cell.2011.06.051

Nakajima, A., Kurihara, H., Yagita, H., Okumura, K., and Nakano, H. (2008). Mitochondrial Extrusion through the cytoplasmic vacuoles during cell death. *J. Biol. Chem.* 283 (35), 24128–24135. doi:10.1074/jbc.M802996200

Ni, H. M., Williams, J. A., and Ding, W. X. (2015). Mitochondrial dynamics and mitochondrial quality control. *Redox Biol.* 4, 6–13. doi:10.1016/j.redox.2014.11.006

Okawa, H., Sampath, A. P., Laughlin, S. B., and Fain, G. L. (2008). ATP consumption by mammalian rod photoreceptors in darkness and in light. *Curr. Biol.* 18 (24), 1917–1921. doi:10.1016/j.cub.2008.10.029

Pietras, Z., Wojcik, M. A., Borowski, L. S., Szewczyk, M., Kulinski, T. M., Cysewski, D., et al. (2018). Dedicated surveillance mechanism controls G-quadruplex forming non-coding RNAs in human mitochondria. *Nat. Commun.* 9 (1), 2558. doi:10.1038/s41467-018-05007-9

Rizzuto, R., De Stefani, D., Raffaello, A., and Mammucari, C. (2012). Mitochondria as sensors and regulators of calcium signalling. *Nat. Rev. Mol. Cell Biol.* 13 (9), 566–578. doi:10.1038/nrm3412

Rowland, A. A., and Voeltz, G. K. (2012). Endoplasmic reticulum-mitochondria contacts: function of the junction. *Nat. Rev. Mol. Cell Biol.* 13 (10), 607–625. doi:10.1038/nrm3440

Sanchez-Contreras, M., and Kennedy, S. R. (2022). The complicated nature of somatic mtDNA mutations in aging. *Front. Aging* 2, 805126. doi:10.3389/fragi.2021.805126

Schindelin, J., Arganda-Carreras, I., Frise, E., Kaynig, V., Longair, M., Pietzsch, T., et al. (2012). Fiji: an open-source platform for biological-image analysis. *Nat. Methods* 9 (7), 676–682. doi:10.1038/nmeth.2019

Sriram, K., Qi, Z., Yuan, D., Malhi, N. K., Liu, X., Calandrelli, R., et al. (2024). Regulation of nuclear transcription by mitochondrial RNA in endothelial cells. *Elife* 13, e86204. doi:10.7554/eLife.86204

St John, J. C., Facucho-Oliveira, J., Jiang, Y., Kelly, R., and Salah, R. (2010). Mitochondrial DNA transmission, replication and inheritance: a journey from the gamete through the embryo and into offspring and embryonic stem cells. *Hum. Reprod. Update* 16 (5), 488–509. doi:10.1093/humupd/dmq002

Wang, C., and Youle, R. J. (2009). The role of mitochondria in apoptosis. *Annu. Rev. Genet.* 43, 95–118. doi:10.1146/annurev-genet-102108-134850

Wang, F., Flanagan, J., Su, N., Wang, L. C., Bui, S., Nielson, A., et al. (2012). RNAscope: a novel *in situ* RNA analysis platform for formalin-fixed, paraffin-embedded tissues. *J. Mol. Diagn* 14 (1), 22–29. doi:10.1016/j.jmoldx.2011.08.002

Willems, P. H., Rossignol, R., Dieteren, C. E., Murphy, M. P., and Koopman, W. J. (2015). Redox homeostasis and mitochondrial dynamics. *Cell Metab.* 22 (2), 207–218. doi:10.1016/j.cmet.2015.06.006

Wu, Y., Whiteus, C., Xu, C. S., Hayworth, K. J., Weinberg, R. J., Hess, H. F., et al. (2017). Contacts between the endoplasmic reticulum and other membranes in neurons. *Proc. Natl. Acad. Sci. U. S. A.* 114 (24), E4859–E4867. doi:10.1073/pnas.1701078114

Youle, R. J., and van der Bliek, A. M. (2012). Mitochondrial fission, fusion, and stress. *Science* 337 (6098), 1062–1065. doi:10.1126/science.1219855

Frontiers in
Cell and Developmental Biology

Explores the fundamental biological processes of life, covering intracellular and extracellular dynamics.

The world's most cited developmental biology journal, advancing our understanding of the fundamental processes of life. It explores a wide spectrum of cell and developmental biology, covering intracellular and extracellular dynamics.

Discover the latest Research Topics

See more →

Frontiers

Avenue du Tribunal-Fédéral 34
1005 Lausanne, Switzerland
frontiersin.org

Contact us

+41 (0)21 510 17 00
frontiersin.org/about/contact